NOVEL MOLECULAR TARGETS AND TREATMENTS FOR GASTROESOPHAGEAL CANCER, 3rd Edition

EDITED BY: Bin Li, Alfred King-yin Lam, Linhui Liang, Jianjun Xie and Wen Wen Xu

PUBLISHED IN: Frontiers in Oncology

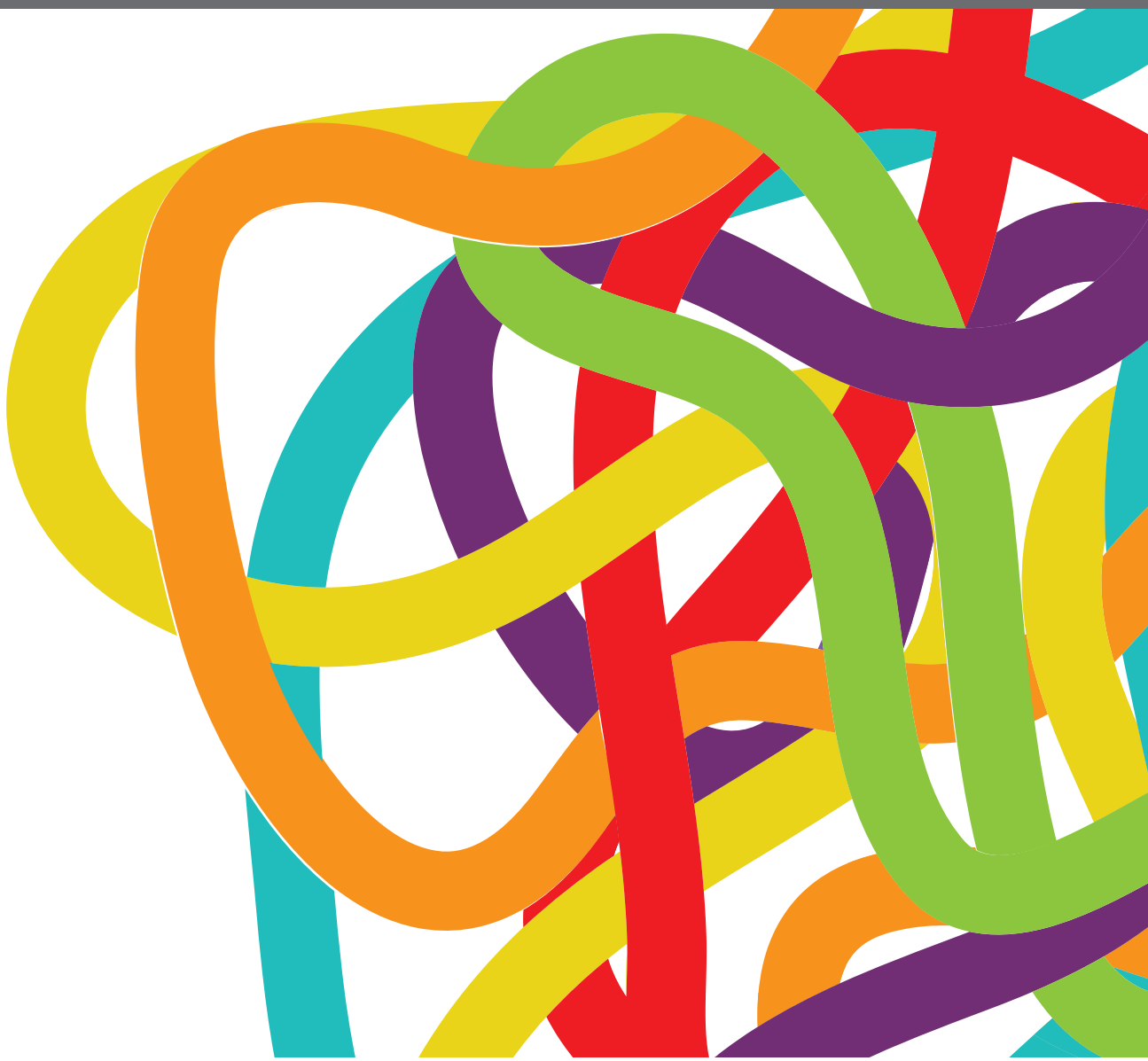

frontiers Research Topics

frontiers

ISSN 1664-8714
ISBN 978-2-8325-5508-8
DOI 10.3389/978-2-8325-5508-8

About Frontiers

Frontiers is more than just an open-access publisher of scholarly articles: it is a pioneering approach to the world of academia, radically improving the way scholarly research is managed. The grand vision of Frontiers is a world where all people have an equal opportunity to seek, share and generate knowledge. Frontiers provides immediate and permanent online open access to all its publications, but this alone is not enough to realize our grand goals.

Frontiers Journal Series

The Frontiers Journal Series is a multi-tier and interdisciplinary set of open-access, online journals, promising a paradigm shift from the current review, selection and dissemination processes in academic publishing. All Frontiers journals are driven by researchers for researchers; therefore, they constitute a service to the scholarly community. At the same time, the Frontiers Journal Series operates on a revolutionary invention, the tiered publishing system, initially addressing specific communities of scholars, and gradually climbing up to broader public understanding, thus serving the interests of the lay society, too.

Dedication to Quality

Each Frontiers article is a landmark of the highest quality, thanks to genuinely collaborative interactions between authors and review editors, who include some of the world's best academicians. Research must be certified by peers before entering a stream of knowledge that may eventually reach the public - and shape society; therefore, Frontiers only applies the most rigorous and unbiased reviews.
Frontiers revolutionizes research publishing by freely delivering the most outstanding research, evaluated with no bias from both the academic and social point of view. By applying the most advanced information technologies, Frontiers is catapulting scholarly publishing into a new generation.

What are Frontiers Research Topics?

Frontiers Research Topics are very popular trademarks of the Frontiers Journals Series: they are collections of at least ten articles, all centered on a particular subject. With their unique mix of varied contributions from Original Research to Review Articles, Frontiers Research Topics unify the most influential researchers, the latest key findings and historical advances in a hot research area! Find out more on how to host your own Frontiers Research Topic or contribute to one as an author by contacting the Frontiers Editorial Office: frontiersin.org/about/contact

NOVEL MOLECULAR TARGETS AND TREATMENTS FOR GASTROESOPHAGEAL CANCER, 3rd Edition

Topic Editors:
Bin Li, Jinan University, China
Alfred King-yin Lam, Griffith University, Australia
Linhui Liang, Fudan University, China
Jianjun Xie, Shantou University, China
Wen Wen Xu, Jinan University, China

Publisher's note: This is a 3rd edition due to an article retraction.

Citation: Li, B., Lam, A. K.-y., Liang, L., Xie, J., Xu, W. W., eds. (2024). Novel Molecular Targets and Treatments for Gastroesophageal Cancer, 3rd Edition. Lausanne: Frontiers Media SA. doi: 10.3389/978-2-8325-5508-8

Table of Contents

frontiers | Frontiers in Oncology

EDITORIAL
published: 13 May 2022
doi: 10.3389/fonc.2022.888861

Editorial: Novel Molecular Targets and Treatments for Gastroesophageal Cancer

Alfred King-yin Lam[1*], *Bin Li*[2*], *Linhui Liang*[3], *Jianjun Xie*[4] *and Wen Wen Xu*[5]

[1] School of Medicine & Dentistry and Menzies Health Institute Queensland, Griffith University, Gold Coast, QSL, Australia, [2] The Fifth Affiliated Hospital of Guangzhou Medical University, Guangzhou, China, [3] Fudan University Shanghai Cancer Center and Institutes of Biomedical Sciences, Shanghai Medical College, Fudan University, Shanghai, China, [4] Department of Biochemistry and Molecular Biology, Shantou University Medical College, Shantou, China, [5] Guangzhou Medical University, Guangzhou, China

Keywords: esophagus, stomach, gastroesophageal, adenocarcinoma, squamous cell carcinoma, genomics, target therapy, molecular markers

OPEN ACCESS

Edited and reviewed by:
Liang Qiao,
Westmead Institute for Medical Research, Australia

***Correspondence:**
Alfred King-yin Lam
a.lam@griffith.edu.au
Bin Li
libin2015@jnu.edu.cn

Specialty section:
This article was submitted to Gastrointestinal Cancers: Gastric & Esophageal Cancers, a section of the journal Frontiers in Oncology

Received: *03 March 2022*
Accepted: *29 March 2022*
Published: *13 May 2022*

Citation:
Lam AK, Li B, Liang L, Xie J and Xu WW (2022) Editorial: Novel Molecular Targets and Treatments for Gastroesophageal Cancer. Front. Oncol. 12:888861. doi: 10.3389/fonc.2022.888861

Editorial on the Research Topic

Novel Molecular Targets and Treatments for Gastroesophageal Cancer

In this Research Topic, we collected 20 papers under the title of "Novel Molecular Targets and Treatments for gastroesophageal Cancer" (Das et al., Power et al., Heng et al., Islam et al., Wang et al., Li et al., Zhang et al., Zhang et al., Deng et al., Bai et al., Lv et al., Guo et al., Chen et al., Luan et al., Jiang et al., Jafarzadeh and Soltani, Jin et al., Fang et al., Wang et al., Chen et al.). Cancers of the oesophagus and stomach account for 8.7% of new cases and 13.2% of new deaths of all sites worldwide (1). In the World Health Organization (WHO) classification of tumours, oesophageal cancer has two major histological types, namely squamous cell carcinoma (SCC) and adenocarcinoma (2). SCC is mostly noted in the upper and middle oesophagus and occurs mainly in high incidence regions such as in China, whereas adenocarcinoma is mostly in the lower oesophagus and oesophagogastric junction and is mostly in low incidence regions of high income and excess body weight. Recently, datasets reporting carcinoma of the oesophagus have been developed by the International Collaboration on Cancer Reporting (ICCR) (3, 4) to standardize the pathological reporting of cancer which allow a better base for research and improvement of management.

Among the papers focused on oesophageal cancer in this Research Topic, Das et al. review the therapeutic strategies against cancer stem cells, whereas Power et al. analyse immunotherapy approaches for oesophageal carcinomas. These papers open new avenues for innovative treatment of this cancer. The other papers are original studies based on SCCs from China, a high incidence area. Of these, Heng et al. studied the mechanisms and roles of camptothecin (anticancer agent) in oesophageal SCC cells. Islam et al. characterized the clinicopathological roles of molecular deregulation of *Endothelial PAS domain-containing protein 1 (EPAS1)* (code for an angiogenic factor) in 80 Hong Kong patients with oesophageal SCCs. In addition, the expression profiles of

microRNAs could be useful as prognostic, and predictive biomarkers in oesophageal carcinomas (5). Wang et al. highlight the potential molecular target roles of miR-17-5p and miR-443 in the treatment of oesophageal SCC.

Spindle cell SCC is an uncommon subtype of SCC (2, 6). Li et al. analysed one of the largest series (n=43) of this cancer subtype in Southern China and developed a risk stratification and personalized management model. In the same centre, Zhang et al. analysed the ABO blood type in blood samples from 2179 patients with oesophageal carcinomas revealing that blood types had independent prognostic roles. Lastly, Zhang et al. from Shanghai reported the tumour-suppressive effect of Chinese herbal monomer, fangchinoline on oesophageal SCC cells.

Gastric cancer, predominately adenocarcinoma, is more common than oesophageal cancer, ranking fifth for incidence and fourth for mortality globally (1). Dataset reporting of carcinoma of the stomach has also been developed by ICCR (7) to standardize the pathological reporting of gastric carcinoma. In this area, Deng et al. reviewed the potential clinical value of tetraspanins in the management of gastric carcinoma. In addition, Bai et al. reviewed the advances and markers of immunotherapy in the treatment of patients with gastric adenocarcinoma and oesophagogastric adenocarcinoma. Lv et al. from China studied the expression of programmed death-ligand 1(PDL-1; predictor for immunotherapy), *HER-2* (*human epidermal growth factor receptor 2*; predictor for anti-HER 2-antibody therapy), immune microenvironment, and clinical features in 120 gastric adenocarcinomas. They noted that *HER-2* status could predict the efficacy of immune checkpoint inhibitors and *HER-2* status combined with PD-L1 level could predict the prognosis of patients tithe gastric carcinomas.

At the DNA level, Guo et al. analysed blood samples from 640 gastric adenocarcinomas from Chinese patients as well as gastric carcinoma cell lines and showed that *tumour necrosis factor alpha-induced protein 2* (*TNFAIP2*) polymorphism (rs8126 TC genotype) had a high risk of gastric carcinoma in male, elderly patients who are Helicobacter pylori-negative, non-smoking, and non-drinking individuals.

Gene expressions were studied in gastric carcinomas to investigate mechanistic pathways as well as their potential for target therapies. Chen et al. reported the expression of the transcription factor regulation gene, *PLXNC1* (*transcriptional factor plexin C1*) in 111 gastric adenocarcinomas from Chinese patients and gastric carcinoma cell lines. The results showed that *PLXNC1* plays an oncogenic role in gastric adenocarcinoma and could act as a therapeutic target. Luan et al. studied the expression of the TOR signalling pathway regulator (TIPRL) in 230 gastric carcinomas from Chinese patients, revealing that it suppresses cell migration and invasion by regulating the AMPK/mTOR signalling pathway in cancer. In addition, in 74 Chinese patients with gastric carcinoma and cancer cells, Jiang et al. showed that expression of fibronectin type III domain containing 1 (FNDC1) promotes the invasiveness of gastric cancer *via* the Wnt/β-catenin signalling pathway and correlates with peritoneal metastasis and prognosis.

Non-coding RNAs may include microRNAs, long noncoding RNAs (IncRNAs), and circular RNAs (cirRNAs) (8). Jafarzadeh and Soltanil from Iran demonstrated that InCRNA LOC400043 inhibits gastric cancer progression by regulating the Wnt signalling pathway in 15 gastric carcinomas and cell lines. In addition, Jin et al. demonstrated in 31 cases of gastric carcinomas from China and cancer cell lines that cirRNA promotes metastases under a long-term hypoxic microenvironment.

Proteins in carcinoma could alter tumour microenvironments such as matrix and cancer cell adhesions. In this aspect, Fang et al. studied the junctional adhesion molecular-like protein in 63 gastric carcinomas from Chinese patients and noted that it promotes tumour progression and metastases *via* the p38 signalling pathway. Wang et al. showed that a high level of legumain, with critical roles in extracellular matrix degradation and modelling, was associated with worse prognosis and peritoneal metastases in 139 Chinese patients with gastric carcinoma. Furthermore, Chen et al. studied the expression of myeloid differentiation factor 88 (MyD88), an adaptor molecule in Toll-like signalling pathway recognizing Helicobacter pylori, in 102 proximal gastric adenocarcinomas from Chinese patients by immunohistochemistry. MyD88 expression correlates with tumour grade and NF-kB p105/p50 expression.

To conclude, the papers in this Research Topic summarize current and novel molecular targets and treatments for oesophageal cancer and gastric cancer. This will enrich our understanding of pathogenesis and treatment possibilities, leading to the potential improvement of clinical outcomes of cancer.

AUTHOR CONTRIBUTIONS

AL conceptualized, designed, and wrote the editorial. All the authors contributed and approved the submitted version.

REFERENCES

1. Sung H, Ferlay J, Siegel RL, Laversanne M, Soerjomataram I, Jemal A, et al. Global Cancer Statistics 2020: GLOBOCAN Estimates of Incidence and Mortality Worldwide for 36 Cancers in 185 Countries. *CA Cancer J Clin* (2021) 71:209–49. doi: 10.3322/caac.21660
2. Lam AK. Updates on World Health Organization Classification and Staging of Esophageal Tumors: Implications for Future Clinical Practice. *Hum Pathol* (2021) 108:100–12. doi: 10.1016/j.humpath.2020.10.015
3. Lam AK, Nagtegaal ID. Committee for the Development of the ICCR Dataset for Endoscopic Resection of the Esophagus and Esophagogastric Junction. Pathology Reporting of Esophagus Endoscopic Resections: Recommendations From the International Collaboration on Cancer Reporting. *Gastroenterology* (2022) 162:373–8. doi: 10.1053/j.gastro.2021.09.069
4. Lam AK, Bourke MJ, Chen R, Fiocca R, Fujishima F, Fujii S, et al. Dataset for the Reporting of Carcinoma of the Esophagus in Resection Specimens: Recommendations From the International Collaboration on Cancer Reporting. *Hum Pathol* (2021) 114:54–65. doi: 10.1016/j.humpath.2021.05.003
5. Islam F, Gopalan V, Lam AK. Roles of microRNAs in Esophageal Squamous Cell Carcinoma Pathogenesis. *Methods Mol Biol* (2020) 2129:241–57. doi: 10.1007/978-1-0716-0377-2_18

6. Lam KY, Law SY, Loke SL, Fok M, Ma LT. Double Sarcomatoid Carcinomas of the Oesophagus. *Pathol Res Pract* (1996) 192:604–9. doi: 10.1016/S0344-0338(96)80112-9
7. Shi C, Badgwell BD, Grabsch HI, Gibson MK, Hong SM, Kumarasinghe P, et al. Data Set for Reporting Carcinoma of the Stomach in Gastrectomy. *Arch Pathol Lab Med* (2022). doi: 10.5858/arpa.2021-0225-OA
8. Lee KT, Gopalan V, Lam AK. Roles of Long-Non-Coding RNAs in Cancer Therapy Through the PI3K/Akt Signalling Pathway. *Histol Histopathol* (2019) 34:593–609. doi: 10.14670/HH-18-081

Conflict of Interest: The authors declare that the research was conducted in the absence of any commercial or financial relationships that could be construed as a potential conflict of interest.

Publisher's Note: All claims expressed in this article are solely those of the authors and do not necessarily represent those of their affiliated organizations, or those of the publisher, the editors and the reviewers. Any product that may be evaluated in this article, or claim that may be made by its manufacturer, is not guaranteed or endorsed by the publisher.

frontiers in Oncology

ORIGINAL RESEARCH
published: 04 February 2020
doi: 10.3389/fonc.2020.00033

PLXNC1 Enhances Carcinogenesis Through Transcriptional Activation of IL6ST in Gastric Cancer

Jie Chen[1†], Haining Liu[2†], Jinggui Chen[1], Bo Sun[1], Jianghong Wu[1] and Chunyan Du[1*]*

[1] Department of Gastric Surgery, Fudan University Shanghai Cancer Center, Fudan University, Shanghai, China, [2] Department of Gastroenterology and Hepatology, Zhongshan Hospital, Fudan University, Shanghai, China

Background: Transcriptional factors (TFs) are responsible for orchestrating gene transcription during cancer progression. However, their roles in gastric cancer (GC) remain unclear.

Methods: We analyzed the differential expressions of TFs and, using GC cells and tissues, investigated plexin C1 (PLXNC1) RNA levels, as well as PLXNC1's clinical relevance and functional mechanisms. The molecular function of PLXNC1 was evaluated *in vitro* and *in vivo*. Kaplan-Meier curves and the log-rank test were used to analyze overall survival (OS) and disease-free survival (DFS).

Results: PLXNC1 was frequently up-regulated in GC and associated with poor prognosis. The expression level of PLXNC1 could serve as an independent biomarker to predict a patient's overall survival. Notably, knockdown of PLXNC1 significantly abolished GC cell proliferation, and migration, and overexpression of PLXNC1 accelerated carcinogenesis in GC. The gene set enrichment analysis (GSEA) indicated that high-expression of PLXNC1 was positively correlated with the activation of epithelial-mesenchymal transition (EMT), TNF-α, and IL-6/STAT3 signaling pathways. PLXNC1 promoted proliferation and migration of GC cells through transcriptional activation of the interleukin 6 signal transducer (IL6ST), which could rescue the malignant behavior of PLXNC1-deficient GC cells.

Conclusions: Our study demonstrated that the PLXNC1 plays an oncogenic role in GC patients. The PLXNC1-IL6ST axis represents a novel potential therapeutic target for GC.

Keywords: transcriptional factor, PLXNC1, IL6ST, gastric cancer, carcinogenesis

OPEN ACCESS

Edited by:
Bin Li,
Jinan University, China

Reviewed by:
Xu Yuqing,
Harbin Medical University, China
Chunjie Jiang,
University of Pennsylvania, United States

***Correspondence:**
Jianghong Wu
elite53@163.com
Chunyan Du
chunyanfudan@126.com

[†]These authors have contributed equally to this work

Specialty section:
This article was submitted to Gastrointestinal Cancers, a section of the journal Frontiers in Oncology

Received: *16 December 2019*
Accepted: *09 January 2020*
Published: *04 February 2020*

Citation:
Chen J, Liu H, Chen J, Sun B, Wu J and Du C (2020) PLXNC1 Enhances Carcinogenesis Through Transcriptional Activation of IL6ST in Gastric Cancer. Front. Oncol. 10:33. doi: 10.3389/fonc.2020.00033

INTRODUCTION

Gastric cancer (GC) is one of the most malignant and prevalent tumors, with poor prognosis worldwide (1, 2). Although clinical therapeutic methods and medical technology have improved (surgical resection and target drug therapy, for example), the 5 year survival rates of GC still remain dismal (3). Moreover, the molecular mechanism underlying gastrocarcinogenesis has not yet been completely elucidated. However, recently, genomic technology has become the essential methodology used by international organizations to discover the novel therapeutic targets in GC (4, 5). The Cancer Genome Atlas (TCGA) has carried out a systematic and multidimensional repertoire of genomic dysregulations, including gene expression,

gene-level-mutation, copy number variation, and clinical information for stomach adenocarcinoma (STAD). The open-source TCGA dataset provides a suitable repository for investigators to explore new methods for GC diagnosis, treatment, and prevention (6).

Transcriptional dysregulation is a hallmark of cancer (7). Transcription factors (TFs), chromatin regulators, and other co-factors jointly regulate this process. Master, signaling, and proliferation are the major classes of TFs, and could remodel chromatin status and manipulate the generation of addictive cancer transcripts (8). In GC, kruppel-like factor 5 (KLF5) and MYC proto-oncogene bHLH transcription factor (MYC) collectively regulate long intergenic non-protein coding RNA 346 (LINC00346), thus contributing to GC progression (9). Nevertheless, the roles of TFs and their regulated targets in GC remain elusive.

In this study, we examined the latest TF catalog, comprising 1,935 TF genes (10), and systematically analyzed their transcription profile in TCGA-STAD cohort to assess the roles of TFs in GC. We identified 419 up-regulated and 64 down-regulated TF genes in STAD paired tissues. Among the TFs identified, 189 targets showed a positive correlation with patient prognosis. Moreover, we found a transcriptional factor plexin C1 (PLXNC1), which was significantly up-regulated and correlated with poor outcomes in GC patients. Notably, the PLXNC1 promoted GC cell proliferation and metastasis by enhancing tumor-related signaling pathways and transcriptional activation of IL6ST. Our results demonstrated that the PLXNC1-IL6ST axis could be a promising therapeutic target in GC.

MATERIALS AND METHODS

Human Tissues and Follow-Up

Gastric cancer specimens and matched adjacent non-tumor tissues (NTs) from 111 patients were obtained from the Department of Gastric Surgery, Fudan University Shanghai Cancer Center, Fudan University (Shanghai, China) to analyze PLXNC1 mRNA levels. Upon resection, the tissue samples were snap-frozen in liquid nitrogen and stored at −80°C. Informed consent was acquired from all patients. The study was approved by the Ethics Committee of Shanghai Medical College of Fudan University.

Statistical Analysis

For comparisons of two groups, statistical significance for normally distributed variables were estimated using unpaired Students *t*-test, and non-normally distributed variables were analyzed by Mann-Whitney *U*-test (also called the Wilcoxon rank-sum test). The differentially expressed genes were analyzed from moderate students t-test using the *limma* package. The Kaplan-Meier method was used to generate survival curves for the two subgroups of the binomial variables, and the Log-rank (Mantel-Cox) test was used to determine the statistical significance of the differences between survival curves. The hazard ratios for uni- and multivariate analyses were calculated by the uni- and multivariate Cox proportional hazards regression model.

The diagnostic efficiency of PLXNC1 and CEA for patients' OS times was estimated using receiver operating characteristic (ROC) curves. From a comparison of two ROC curves and the areas under the curves (AUC), 95% confidence intervals were calculated, according to the DeLong method. All statistical analyses were carried out using the R language (version 3.5.2, https://www.r-project.org/). The statistical tests were two-sided, and a $P < 0.05$ was considered statistically significant. The following R packages were used in this study: "pROC," "rms," "survival," "clusterProfiler," and "pheatmap."

Cell Lines and Cell Culture

The human GC cell lines (HGC-27 and AGS) were purchased from the American Type Culture Collection (ATCC) (Manassas, VA, USA). The human embryonic kidney 293T (HEK-293T) cells were purchased from the Shanghai Cell Bank Type Culture Collection Committee (CBTCCC) (Shanghai, China). HGC-27 and AGS cells were cultured in RPMI1640 (Thermo Fisher Scientific, Waltham, MA, USA) and HEK-293T cells in DMEM (Gibco, Grand Island, NY, USA), supplemented with 10% fetal bovine serum (Gibco), 100 μg/ml penicillin (Gibco), and 100 μg/ml streptomycin (Gibco), at 37°C and 5% CO_2. Cells were treated with Mycoplasma-OUT (Genechem, Shanghai, China) for 1 week before a routine experiment and mycoplasma testing was performed by PCR.

RNA Extraction, Reverse Transcription, and qRT-PCR Analysis

Total RNA was extracted from GC or non-tumor tissues or cells using the TRIzol reagent (Invitrogen, Carlsbad, CA, USA). cDNA was synthesized using the PrimeScript RT Reagent Kit (TaKaRa, Shiga, Japan). The quantitative real-time polymerase chain reaction (qPCR) analyses were performed using SYBR Premix *Ex Taq II* assays (TaKaRa), determined using the QuantStudio 7 Flex sequence detection system (Thermo Fisher Scientific), and calculated and normalized to β-actin using the comparative CT method [$2^{-\Delta CT(\text{target gene}-\beta-\text{actin})}$]. The sequences of the target gene primers used are listed in **Table S1**; β-actin was used as an internal control.

RNA Interference

Small interfering RNA (siRNA) oligonucleotides targeting PLXNC1 were designed and synthesized by RiboBio (Guangzhou, China). Cells were transfected with siRNAs using the Lipofectamine RNAiMAX reagent (Invitrogen) at a final concentration of 50 nM. Cells were used for RNA extraction, proliferation, migration, and immunoblotting assays after transfection for 48 h. The sequences for the PLXNC1 siRNAs used are listed in **Table S1**.

Lentivirus Production and Transduction

The packaging plasmid psPAX2 and the VSV-G envelope plasmid pMD2.G (gifts from Dr. Didier Trono), coupled with PLXNC1, Cas9, GFP overexpression plasmids, or PLXNC1 sgRNAs plasmids, were transfected into HEK293T cells using Lipofectamine 2000 (Invitrogen). Lentiviral particles were harvested at 48 h after transfection, and GC cells were infected

with recombinant lentivirus plus 8 μg/mL polybrene (Sigma-Aldrich, St. Louis, MO, USA).

Colony Formation and Migration Assays

For the colony formation assay, 1.5×10^3 cells were seeded in a 6-well plate per well and incubated at 37°C for nearly 10 days. The number of colonies stained with 100% methanol containing 0.5% crystal violet (Sigma-Aldrich) was counted and analyzed. For cell migration assays, a total of 5×10^4 cells were suspended per well in the upper chamber (BD Biosciences, Franklin Lakes, NJ) with 200 μL of RPMI1640 [minus fetal bovine serum (FBS)] in a 24-well plate; 800 μL of RPMI1640, supplemented with 10% FBS, was added to the lower chamber. After 20 h of incubation, the chambers were fixed and stained with 100% methanol containing 0.5% crystal violet (Sigma-Aldrich) for 20 min, followed by imaging and counting under an inverted microscope (Olympus, Tokyo, Japan).

Xenograft in Nude Mice

PLXNC1 knockdown AGS cells and control cells were harvested and suspended in RPMI1640 without FBS. A total of 12 mice (male BALB/c-nu/nu, 6 weeks old) were randomly divided into two groups and subcutaneously injected in the lower back with 2×10^6 cells in 200 μL of RPMI1640 without FBS. The mice were sacrificed, and the tumors were dissected and weighed ∼5 weeks after injection. The mouse experiments were conducted using the Guide for the Care and Use of Laboratory Animals of Fudan University and approved by the Committee on the Ethics and Welfare of Laboratory Animal Science of Fudan University.

Chromatin Immunoprecipitation-Quantitative PCR (ChIP-qPCR)

AGS cells were cross-linked for about 10 min in 1% formaldehyde, quenched in glycine, re-suspended in ChIP lysis buffer (20 mM Tris-HCl pH 7.5, 150 mM NaCl, 1% NP-40, 0.02% SDS, 5 mM EDTA, proteinase inhibitor), sonicated, and centrifuged. The supernatant was collected and incubated with Flag antibody and Dynabeads® Protein G (Thermo Fisher Scientific). The beads complex was washed five times with ChIP lysis buffer, decrosslinked and digested with RNase A and proteinase K. DNA samples were collected using MinElute Reaction Cleanup Kit (Qiagen, Hilden, Germany). ChIP-qPCR was performed using the QuantStudio 7 Flex sequence detection system (Thermo Fisher Scientific). Primers are listed in **Table S1**.

Dual-Luciferase Assay

The dual-luciferase assay was conducted using the Dual-Luciferase Reporter Assay (promega). Briefly, AGS cells were transfected with luciferase, renilla, and PLXNC1-mixed siRNAs or negative control-siRNA. Cells were lysed, added with luciferase and renilla substrate, then measured after 24 h.

Western Blotting

Proteins were separated on 10% SDS-PAGE and transferred to a nitrocellulose membrane (Bio-Rad, Hercules, CA, USA). The membrane was blocked with 5% non-fat milk and incubated with primary antibodies, followed by horseradish peroxidase-conjugated secondary antibodies. The protein bands were visualized using enhanced chemiluminescence reagents (Thermo Fisher Scientific) and Tanon 5200 Chemiluminescent Imaging System (Tanon, Shanghai, China) detection. The antibodies used are offered in **Table S2**.

RESULTS

Transcription Factors Are Differentially Expressed With Clinical Significance in GC

We analyzed the expression profile of 1,935 TFs in TCGA-STAD cohort (370 samples) to explore the dysregulated levels and potential clinical significance of TFs in GC development. Twenty-seven paired tissue samples (tumor and adjacent tissues) were used to perform differential expression analysis. The results showed that 372 TFs were highly expressed in GC compared with para-cancerous samples, whereas 63 TFs were down-regulated in tumor tissues (FDR < 0.05, fold change > 1.3; **Figure 1A**; **Table S3**).

Analysis was first carried out to determine the correlation between these dysregulated TFs and OS, and to investigate the prognostic significance of TFs in GC. The clinical characteristics and whole TF expression profile (FPKM normalization) of 370 tumor samples were acquired for survival analyses. The samples were classified into two groups according to their optimal survival cut-off point for each TF, and the difference of accumulated survival curve was represented by Kaplan-Meier analysis (see Methods). The prognostic risk estimation of TFs was performed by the univariate cox proportional hazard model. Consequently, 29 down-regulated and 150 up-regulated TFs were significantly correlated with patient OS ($P < 0.05$; **Figure 1B**). Among them, 49 TFs showed a high risk for patient prognosis (hazard ratio > 1; highlighted in light red). Moreover, we completely analyzed the candidate-dysregulated TFs and their expression levels, hazard ratio, and correlation with tumor stages in TCGA-STAD cohort. Additionally, we investigated a possible correlation between clinical characteristics and PLXNC1 expression levels in TCGA -STAD patients, finding that GC patients with high PLXNC1 mRNA expression levels had a significant correlation with the tumor stage (**Figure 1C**). These results indicated that a group of TFs was dysregulated in GC, including PLXNC1, strongly correlating with clinical significance.

High Expression of PLXNC1 Predicts Poor Prognosis in GC

We carried out quantitative real-time polymerase chain reaction (qRT-PCR) on our internal GC cohort ($n = 111$) to reveal the differential expressions of PLXNC1 in GC tissues and paired non-tumorous tissues (NTs). Importantly, the PLXNC1 was significantly up-regulated in GC samples compared with NTs at mRNA level ($P < 0.001$; **Figure 2A**). Kaplan-Meier Survival analysis showed that GC patients with high PLXNC1 expression levels exhibited poor OS and disease-free survival

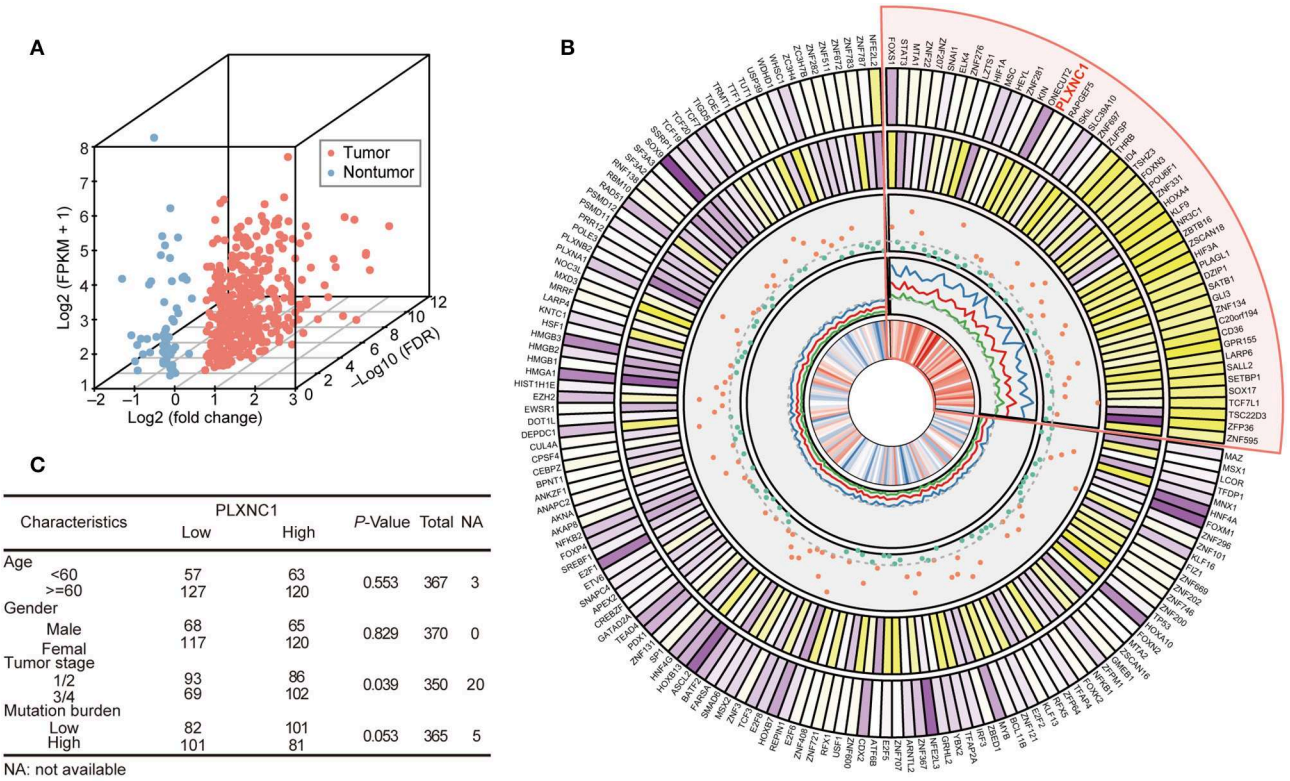

Characteristics	PLXNC1 Low	PLXNC1 High	*P*-Value	Total	NA
Age					
<60	57	63	0.553	367	3
>=60	127	120			
Gender					
Male	68	65	0.829	370	0
Femal	117	120			
Tumor stage					
1/2	93	86	0.039	350	20
3/4	69	102			
Mutation burden					
Low	82	101	0.053	365	5
High	101	81			

NA: not available

FIGURE 1 | Differentially expressed transcription factors predict a patient's overall survival in TCGA-STAD cohort. **(A)** Three-dimensional scatter plot generated from the differential expression profiles of TCGA-STAD 27 paired gastric tissue. **(B)** The circled diagram of differentially expressed TF genes in TCGA-STAD cohort. In the figure comprised of five tracks, the first track refers to the average expression level (log2 transfer) of TFs; the second track indicates the fold change of differential expression analysis of TFs in the STAD paired tissue dataset; the third track shows the *P*-value (–log10 transfer) of log-rank test for each TF; the fourth track represents the hazard ratio value of univariate-cox model (HR value and it's 95% CI (lower and upper) were both highlighted as red, blue, and green ligatures, respectively); the last track displays the correlation coefficients between tumor stage and TF expression level. The darker color indicates a higher quantitative value to distinguish TFs. The sector with light red shows the high-risk TFs, which indicate poorer outcomes for GC patients. **(C)** Correlation of clinicopathological features with tumor PLXNC1 expression level in TCGA-STAD cohort.

(DFS) ($P < 0.05$; **Figures 2B,C**). We applied multivariate analyses using the Cox proportional hazard regression model, comparing PLXNC1 expression values with other clinical factors (e.g., age, gender, tumor size, tumor stage, number of lymph node metastasis, recurrence status) as covariates, to investigate whether the expression levels of PLXNC1 were an independent prognostic factor in our internal GC cohort ($n = 111$). GC patients with a high expression level of PLXNC1 in tumors harbored a 2.66-fold high risk of death ($P < 0.05$, 95% CI, 1.20–5.90; **Figure 2D**).

We then investigated the effects of PLXNC1 on survival prediction by comparing it with the GC traditional diagnostic biomarker, carcinoembryonic antigen (CEA). For biopsy-proven GC patients, the expression levels of PLXNC1 and serum CEA levels (ng/ml) were used to construct a ROC curve which could evaluate the diagnostic efficiency of GC patient survival in our cohort. Consequently, PLXNC1 exhibited higher diagnostic efficacy than CEA for prediction of patient survival time ($P < 0.001$; **Figure 2E**). These results therefore showed that the PLXNC1 could serve as a promising prognostic biomarker for GC patients.

PLXNC1 Plays Oncogenic Roles in GC

We first designed two independent siRNAs targeting PLXNC1, in order to elucidate the molecular function of PLXNC1 in GC. Western blot analysis identified efficient siRNA-mediated knockdown of PLXNC1 in both HGC-27 and AGS gastric cell lines (**Figure S1A**). Knockdown of PLXNC1 significantly diminished GC cell proliferation and migration, as determined by colony formation and cell migration assays compared to cells treated with control siRNA (siNC) (**Figure 3A**). We then used lenti-clustered regularly interspaced short palindromic repeats (CRISPR) deletion systems to knockdown PLXNC1 (**Figure S1B**). Consistently, PLXNC1 knockdown in HGC-27 and AGS cells markedly abolished proliferation and migration (**Figure 3B**). We also constructed PLXNC1 overexpression lentivirus and found that overexpression of PLXNC1 in HGC-27 and AGS cells (**Figure S1C**) enhanced gastric cell proliferation and migration (**Figure 3C**). AGS cells infected with the PLXNC1 knockdown lentivirus and the control lentivirus were subcutaneously injected into the flanks of 6-week-old nude mice, then monitored for tumor growth for 5 weeks to further explore the effect of PLXNC1 on tumorigenicity.

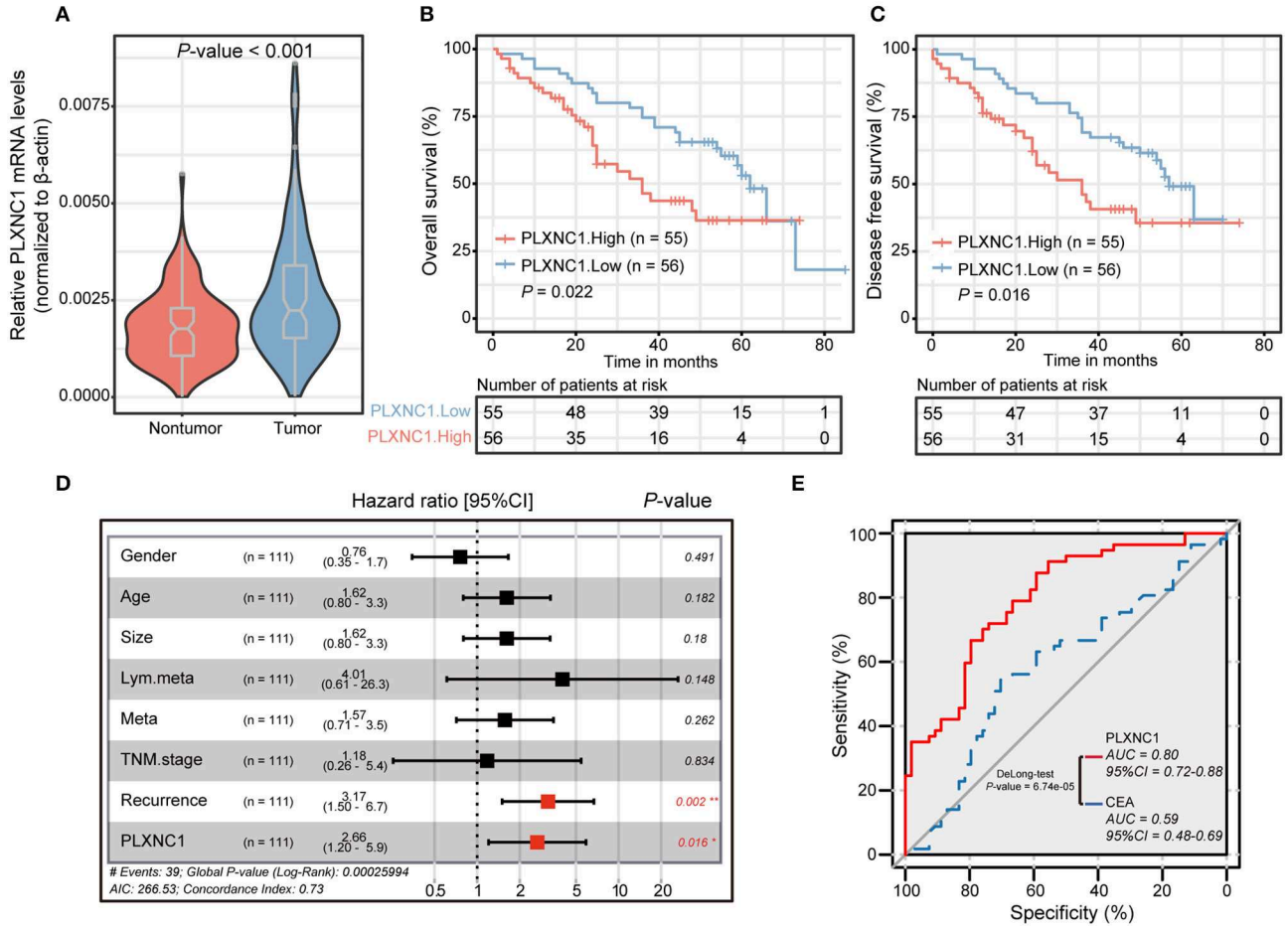

FIGURE 2 | PLXNC1 predicts prognosis in gastric cancer. **(A)** The differential expression level of PLXNC1 expressed in our 111 paired STAD tissues. **(B,C)** Kaplan–Meier curves of overall survival and disease-free survival in our internal 111 gastric patients, validated by PLXNC1 mRNA expression levels. **(D)** The results of multi-variate analyses using the Cox proportional hazard regression model for PLXNC1 mRNA levels and other clinical indices in our internal cohort. **(E)** The comparison of diagnostic efficacy of CEA and PLXNC1 mRNA levels for predicting the time period of tumor OS. *$P < 0.05$; **$P < 0.01$.

Importantly, knockdown of PLXNC1 protein expression decreased tumorigenicity (**Figure 3D**), as measured by the tumor weight (**Figure 3E**) and size (**Figure 3F**). In summary, these data suggest that PLXNC1 promoted carcinogenesis of GC both *in vitro* and *in vivo*.

PLXNC1 Activates Cancer-Associated Signatures in GC

We further explored the potential downstream targets and cancer-related signaling pathways controlled by PLXNC1. We first separated TCGA-STAD samples into two groups (high and low PLXNC1-expression level sub-groups) according to the PLXNC1 median value. Next, we performed the single-sample gene set enrichment method (ssGSEA) to evaluate the enrichment degree of 50 cancer hallmark gene signatures in whole 370 GC samples. Gene set enrichment scores for each sample were further clustered by hierarchical agglomerative clustering (Ward's linkage). The results demonstrated that the TNF-α, IL-6/STAT3 pathway, inflammatory response, epithelial-mesenchymal transition (EMT) signatures, and other signatures, were activated in the PLXNC1 high-expression group (**Figure 4A**). Moreover, Kyoto Encyclopedia of Genes and Genomes (KEGG) pathway analysis revealed that gene sets up-regulated in the high PLXNC1 sub-group were enriched with represented signatures involved in tumor development and progression, such as the JAK-STAT signaling pathway, ECM-receptor interaction, and cAMP signaling pathway (**Figure 4B**). We then used the GSEA to explore the cancer hallmark pathway enrichment with extract statistical results. The clusterprofiler package (11) was used to construct the GSEA plot of the cumulative curve, and the results showed the top five significant enrichment pathways with statistically significant signatures (enrichment score > 0, $P < 0.05$, **Figure 4C**). Routinely, we selected the significantly dysregulated genes in the aforementioned signaling pathways for validation. The qRT-PCR results showed that overexpression of PLXNC1 significantly enhanced the EMT, IL-6/STAT3, and inflammatory response-related genes such as IGFBP3, IL6ST,

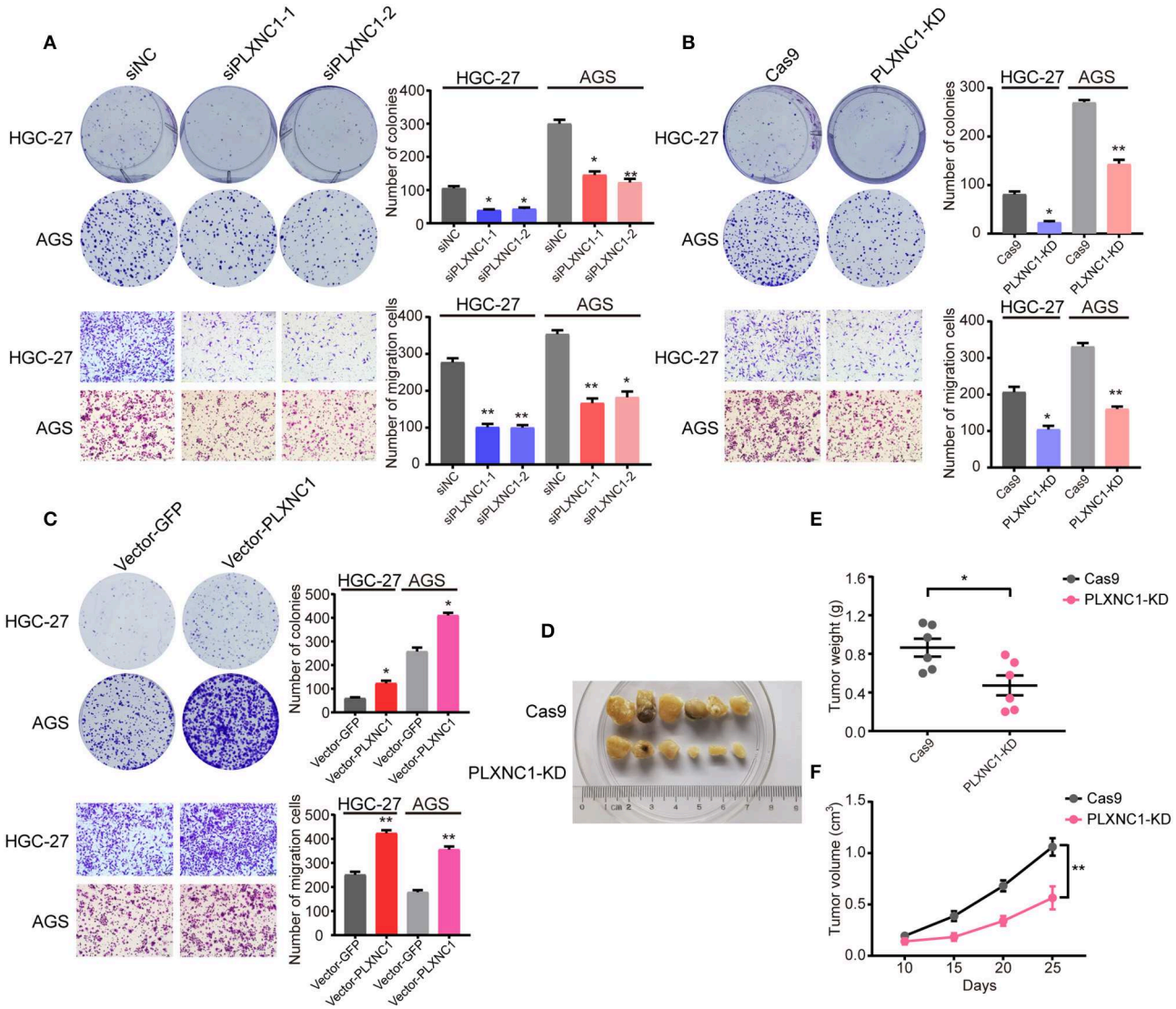

FIGURE 3 | PLXNC1 plays oncogenic roles in gastric cancer both *in vitro* and *in vivo*. **(A)** Colony formation assays (up) and Transwell migration assays (down) for HGC-27 and AGS cells transfected with PLXNC1 siRNAs or negative control (NC) siRNA. **(B)** Colony formation assays (up) and Transwell migration assays (down) for HGC-27 and AGS cells infected with the PLXNC1 knockdown-mixed sgRNAs or control sgRNA lentivirus. **(C)** Colony formation assays (up) and Transwell migration assays (down) for HGC-27 and AGS cells infected with PLXNC1 overexpression lentivirus or GFP control. **(D)** Xenograft tumors of Cas9 or PLXNC1 knockdown AGS cells in nude mice. **(E,F)** The knockdown of PLXNC1 reduces the **(E)** weight and **(F)** volume of xenograft tumors ($n = 6$ mice per group). Values represent the mean ± SEM, **(A–C)** $n = 3$ and **(D–F)** $n = 6$. $^*P < 0.05$; $^{**}P < 0.01$.

KIF1B, and FPR1 (**Figure 4D**). These results demonstrated that PLXNC1 accelerated the cancer development and progression by activating the cancerous signaling pathways in GC cells.

PLXNC1 Regulates IL6ST Expression at the DNA Level in GC Cells

IL-6/STAT3 has been identified as a crucial pathway to accelerate GC progression (12, 13). Our previous studies highlighted that PLXNC1 activates IL-6/STAT3 signaling pathway in GC cells; however, the direct downstream targets of PLXNC1 still remain unclear. We first analyzed the expressional correlation of genes in this pathway with PLXNC1, and found the mRNA expression of 35 genes was significantly correlated with PLXNC1 ($R \geq 0.4$), which elucidated the regulatory mechanism of PLXNC1 in the IL-6/STAT3 signaling pathway. Next, using the qRT-PCR method, we selected the top 20 genes in order to identify the potential regulation by PLXNC1, and found that knockdown of PLXNC1 could decrease the expression of genes such as CSF2RB (**Figure 5A**). Notably, knockdown of PLXNC1 could significantly diminish IL6ST mRNA levels (**Figures 5A,B**), while overexpression of PLXNC1 enhanced IL6ST mRNA levels (**Figure 4D**). These findings showed that IL6ST might be the direct downstream target of PLXNC1. IL6ST (also known

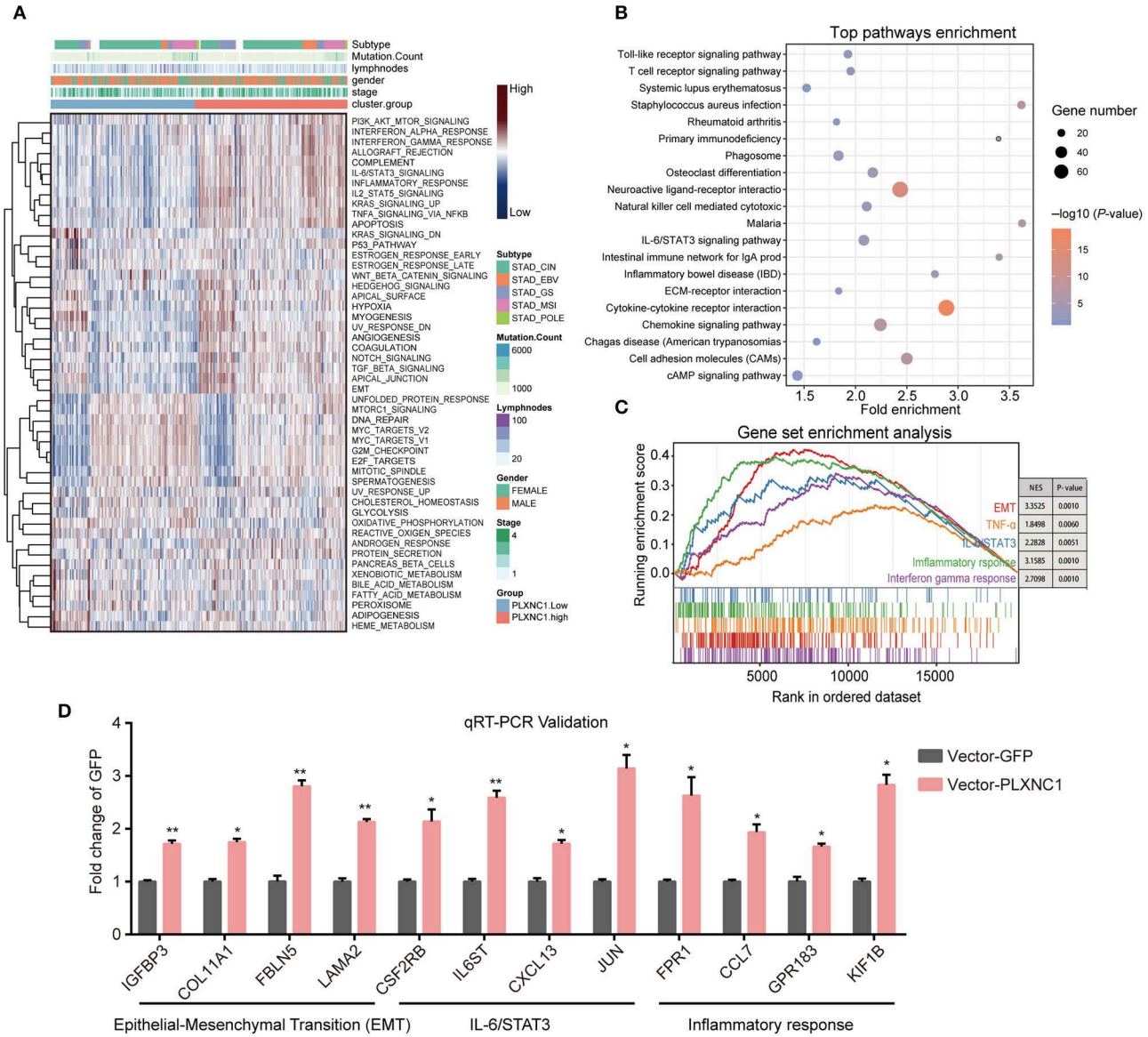

FIGURE 4 | PLXNC1 activates cancer-associated signatures in gastric cancer. **(A)** The heatmap of hierarchical clustering shows the enrichment score of cancer hallmark gene sets enriched in the PLXNC1 high/low expressed group based on single sample gene set enrichment analysis (GSEA) for TCGA-STAD cohort. **(B)** KEGG pathway analysis performed by the DAVID platform for PLXNC1 high-expressed group. The KEGG pathway with $P < 0.05$ is shown in a bubble plot. **(C)** GSEA of hallmark gene sets in high-level-group of PLXNC1. All transcripts were ranked by log2 (fold change) between two groups. Each run was performed with 500 permutations. Enrichment results with significant associations with PLXNC1 were shown. **(D)** The relative candidate cancer hallmark pathway gene mRNA expression infected with PLXNC1 or GFP overexpression lentivirus in AGS gastric cancer cells using qRT-PCR analysis. **(D)** Values represent the mean ± SEM, $n = 3$. $^{*}P < 0.05$; $^{**}P < 0.01$.

as GP130) controls the IL-6/STAT3 signaling pathway and accelerates gastric tumorigenesis (14, 15). We performed ChIP-qPCR and found PLXNC1 was enriched on the IL6ST promoter (**Figure 5C**), further identifying the expressional control of IL6ST by PLXNC1 under a DNA lever. The dual-luciferase reporter assay also showed that knockdown of PLXNC1 decreased IL6ST promoter activity (**Figure 5D**); PLXNC1 expression was highly correlated with LI6ST expression in TCGA-STAD samples (left) and our internal GC samples (right; **Figure 5E**). Importantly, overexpression of IL6ST could rescue PLXNC1-deficient GC cell proliferation and migration (**Figure 5F**). Collectively, this data suggests IL6ST as a downstream target of PLXNC1 in GC.

DISCUSSION

An increasing number of studies have revealed the crucial regulatory roles of TFs in the manipulation of tumor-specific,

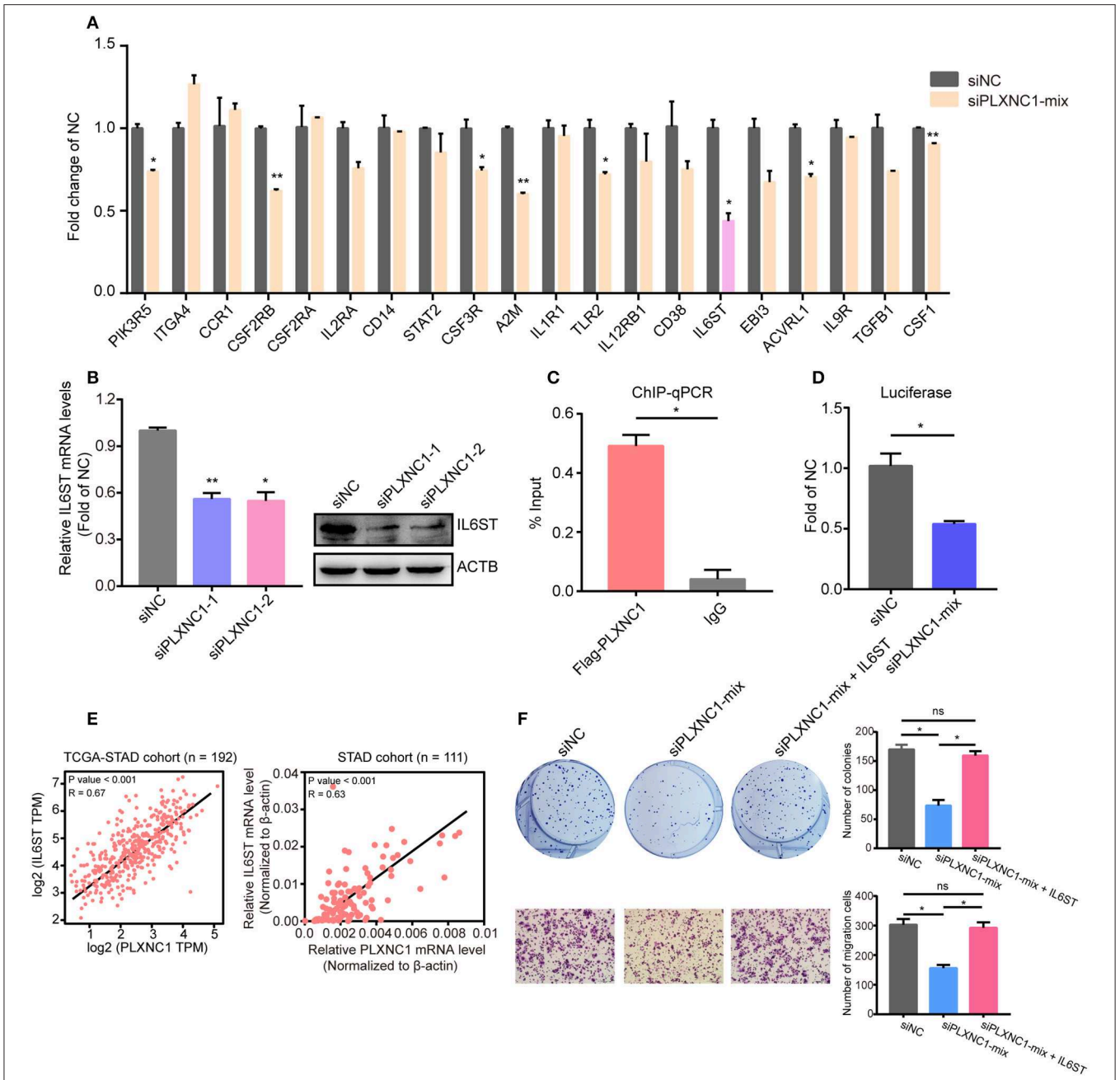

FIGURE 5 | PLXNC1 controls IL6ST expression at the DNA level. **(A)** The relative mRNA levels of the IL-6/STAT3 pathway genes in AGS cells transfected with PLXNC1-mixed siRNAs and negative control siRNA. **(B)** IL6ST mRNA levers and protein levels in AGS cells transfected with PLXNC1 siRNAs and negative control. **(C)** ChIP-qPCR revealed the enrichment of PLXNC1 in IL6ST promoter in AGS cells. **(D)** The IL6ST promoter activity transfected with PLXNC1-mixed siRNAs and negative control siRNA in AGS cells. **(E)** Expressional correlation of PLXNC1 and IL6ST in GC tissues. **(F)** Colony and migration assays of AGS cells transfected with PLXNC1-mixed siRNAs, PLXNC1-mixed siRNAs plus IL6ST overexpression plasmids, or negative control. **(A–D,F)** Values represent the mean ± SEM, $n = 3$. $^{*}P < 0.05$; $^{**}P < 0.01$.

addictive transcripts or cancer-related pathways, thus triggering carcinogenesis and promoting cancer development (16, 17). However, the complete function and clinical significance of TFs in GC remains unclear. In the present study, we systematically analyzed dysregulated TFs in GC and identified a critical role of transcriptional factor PLXNC1 in promoting GC progression, as well as the prognostic value of PLXNC1 in GC patients. We demonstrated that PLXNC1 was up-regulated in GC tissues, and GC patients with highly expressed PLXNC1 exhibited worse overall

survival. Further studies identified that PLXNC1 promoted GC proliferation *in vitro* and *in vivo*, as well as migration *in vitro* by activating tumor-related pathways such as the IL-6/STAT3 signaling pathway.

Plexin C1 was first discovered in the nervous system and has been found to be associated with neuronal cell adhesion (18). Recent evidence shows that PLXNC1 participates in many crucial biological or disease processes. In papillary thyroid cancer (PTC), miR-4500 functions as a tumor suppressor by decreasing PLXNC1 expression, and knockdown of PLXNC1 represses colony formation, proliferation, invasiveness, and enhances apoptosis in PTC cells (19). In liver cancer, PLXNC1 marks epithelial phenotype of liver cancer cells and is significantly up-regulated in liver cancer tissues, which suggests the important roles of PLXNC1 in liver cancer (20). In the present study, we first reported the molecular function and clinical significance of PLXNC1, which served as an oncogene in promoting GC progression. PLXNC1 not only enhanced GC cell proliferation but also increased migration. High expression of PLXNC1 manipulated IL6ST expression at the DNA level and activated tumor-related pathways such as the IL-6/STAT3 pathway. This finding is in accordance with recent studies that have reported that PLXNC1 promotes acute inflammation (21). However, the whole genomic binding sites of PLXNC1 in GC remain unclear and need to be elucidated in further studies. Additionally, which factors control PLXNC1 expression in GC should be studied in more depth.

CONCLUSION

Our study is the first to demonstrate that PLXNC1 is up-regulated and associated with poor survival in GC patients. PLXNC1 enhances the tumorigenesis and aggressiveness of GC cells through transcriptional activation of IL6ST and enhancement of the IL-6/STAT3 signaling pathway. These results reveal the crucial importance of PLXNC1 in GC progression, and suggest that the PLXNC1-IL6ST axis could be of potential value as a novel target of treatment for GC patients.

DATA AVAILABILITY STATEMENT

All datasets generated for this study are included in the article/**Supplementary Material**.

ETHICS STATEMENT

The studies involving human participants were reviewed and approved by the Ethics Committee of Shanghai Medical College of Fudan University. The patients/participants provided their written informed consent to participate in this study. The animal study was reviewed and approved by the mouse experiments were conducted using the Guide for the Care and Use of Laboratory Animals of Fudan University and approved by the Committee on the Ethics and Welfare of Laboratory Animal Science of Fudan University.

AUTHOR CONTRIBUTIONS

CD and JW designed the study. JieC and HL acquired the data. JieC, HL, CD, JinC, and BS performed the analysis of data. JieC, HL, and CD wrote the paper with comments from all authors.

FUNDING

This study was supported by grants from the National Natural Science Foundation of China (81702356).

ACKNOWLEDGMENTS

We are grateful for Dr. Didier Trono's gifts of the psPAX2 and pMD2.G lentivirus plasmids.

SUPPLEMENTARY MATERIAL

The Supplementary Material for this article can be found online at: https://www.frontiersin.org/articles/10.3389/fonc.2020.00033/full#supplementary-material

REFERENCES

1. Hu K, Wang S, Wang Z, Li L, Huang Z, Yu W, et al. Clinicopathological risk factors for gastric cancer: a retrospective cohort study in China. *BMJ Open.* (2019) 9:e030639. doi: 10.1136/bmjopen-2019-030639
2. Camargo MC, Figueiredo C, Machado JC. Review: gastric malignancies: basic aspects. *Helicobacter.* (2019) 24(Suppl. 1):e12642. doi: 10.1111/hel.12642
3. Siegel RL, Miller KD, Jemal A. Cancer statistics, 2019. *CA Cancer J Clin.* (2019) 69:7–34. doi: 10.3322/caac.21551
4. Roukos DH. Innovative genomic-based model for personalized treatment of gastric cancer: integrating current standards and new technologies. *Expert Rev Mol Diagn.* (2008) 8:29–39. doi: 10.1586/14737159.8.1.29
5. Cho JY. Molecular diagnosis for personalized target therapy in gastric cancer. *J Gastric Cancer.* (2013) 13:129–35. doi: 10.5230/jgc.2013.13.3.129
6. Tomczak K, Czerwinska P, Wiznerowicz M. The Cancer Genome Atlas (TCGA): an immeasurable source of knowledge. *Contemp Oncol.* (2015) 19:A68–77. doi: 10.5114/wo.2014.47136
7. Bradner JE, Hnisz D, Young RA. Transcriptional addiction in cancer. *Cell.* (2017) 168:629–43. doi: 10.1016/j.cell.2016.12.013
8. Bhagwat AS, Vakoc CR. Targeting transcription factors in cancer. *Trends Cancer.* (2015) 1:53–65. doi: 10.1016/j.trecan.2015.07.001
9. Xu TP, Ma P, Wang WY, Shuai Y, Wang YF, Yu T, et al. KLF5 and MYC modulated LINC00346 contributes to gastric cancer progression through acting as a competing endogeous RNA and indicates poor outcome. *Cell Death Differ.* (2019) 26:2179–93. doi: 10.1038/s41418-018-0236-y
10. Vaquerizas JM, Kummerfeld SK, Teichmann SA, Luscombe NM. A census of human transcription factors: function, expression, and evolution. *Nat Rev Genet.* (2009) 10:252–63. doi: 10.1038/nrg2538
11. Yu G, Wang LG, Han Y, He QY. clusterProfiler: an R package for comparing biological themes among gene clusters. *OMICS.* (2012) 16:284–7. doi: 10.1089/omi.2011.0118
12. Zhu Q, Zhang X, Zhang L, Li W, Wu H, Yuan X, et al. The IL-6-STAT3 axis mediates a reciprocal crosstalk between cancer-derived mesenchymal stem cells and neutrophils to synergistically prompt gastric cancer progression. *Cell Death Dis.* (2014) 5:e1295. doi: 10.1038/cddis.2014.263

13. Giraud AS, Menheniott TR, Judd LM. Targeting STAT3 in gastric cancer. *Expert Opin Ther Targets.* (2012) 16:889–901. doi: 10.1517/14728222.2012.709238
14. Hill DG, Yu L, Gao H, Balic JJ, West A, Oshima H, et al. Hyperactive gp130/STAT3-driven gastric tumourigenesis promotes submucosal tertiary lymphoid structure development. *Int J Cancer.* (2018) 143:167–78. doi: 10.1002/ijc.31298
15. Yu L, Wu D, Gao H, Balic JJ, Tsykin A, Han TS, et al. Clinical utility of a STAT3-regulated miRNA-200 family signature with prognostic potential in early gastric cancer. *Clin Cancer Res.* (2018) 24:1459–72. doi: 10.1158/1078-0432.CCR-17-2485
16. Kumar P, Mistri TK. Transcription factors in SOX family: potent regulators for cancer initiation and development in the human body. *Semin Cancer Biol.* (2019). doi: 10.1016/j.semcancer.2019.06.016. [Epub ahead of print].
17. Kent LN, Leone G. The broken cycle: E2F dysfunction in cancer. *Nat Rev Cancer.* (2019) 19:326–38. doi: 10.1038/s41568-019-0143-7
18. Ohta K, Mizutani A, Kawakami A, Murakami Y, Kasuya Y, Takagi S, et al. Plexin: a novel neuronal cell surface molecule that mediates cell adhesion via a homophilic binding mechanism in the presence of calcium ions. *Neuron.* (1995) 14:1189–99. doi: 10.1016/0896-6273(95)90266-X
19. Li R, Teng X, Zhu H, Han T, Liu Q. MiR-4500 regulates PLXNC1 and inhibits papillary thyroid cancer progression. *Horm Cancer.* (2019) 10:150–60. doi: 10.1007/s12672-019-00366-1
20. Odabas G, Cetin M, Turhal S, Baloglu H, Sayan AE, Yagci T. Plexin C1 marks liver cancer cells with epithelial phenotype and is overexpressed in hepatocellular carcinoma. *Can J Gastroenterol Hepatol.* (2018) 2018:4040787. doi: 10.1155/2018/4040787
21. Konig K, Marth L, Roissant J, Granja T, Jennewein C, Devanathan V, et al. The plexin C1 receptor promotes acute inflammation. *Eur J Immunol.* (2014) 44:2648–58. doi: 10.1002/eji.201343968

Conflict of Interest: The authors declare that the research was conducted in the absence of any commercial or financial relationships that could be construed as a potential conflict of interest.

frontiers in Oncology

ORIGINAL RESEARCH
published: 14 May 2020
doi: 10.3389/fonc.2020.00559

Expression and Significance of MyD88 in Patients With Gastric Cardia Cancer in a High-Incidence Area of China

Jingyao Chen[1†], Di Xia[1†], Muming Xu[2], Ruibing Su[1], Wenting Lin[1], Dan Guo[1], Guangcan Chen[3] and Shuhui Liu[1*]*

[1] Department of Pathology, Shantou University Medical College, Shantou, China, [2] Department of Abdominal Surgery, The Tumor Hospital of Shantou University Medical College, Shantou, China, [3] Department of Gastrointestinal Surgery, The First Affiliated Hospital of Shantou University Medical College, Shantou, China

OPEN ACCESS

Edited by:
Jianjun Xie,
Shantou University, China

Reviewed by:
Johan Nicolay Wiig,
Oslo University Hospital, Norway
Changting Meng,
Institute for Systems Biology (ISB), United States

***Correspondence:**
Guangcan Chen
515776718@qq.com
Shuhui Liu
liushuhuistu@126.com

[†] *These authors have contributed equally to this work*

Specialty section:
This article was submitted to Gastrointestinal Cancers, a section of the journal Frontiers in Oncology

Received: *18 January 2020*
Accepted: *27 March 2020*
Published: *14 May 2020*

Citation:
Chen J, Xia D, Xu M, Su R, Lin W, Guo D, Chen G and Liu S (2020) Expression and Significance of MyD88 in Patients With Gastric Cardia Cancer in a High-Incidence Area of China. Front. Oncol. 10:559. doi: 10.3389/fonc.2020.00559

Background: Gastric cardia cancer (GCC) arises in the area of the stomach adjoining the esophageal–gastric junction and has unique risk factors. It was suggested that the involvement of *Helicobacter pylori* is associated with GCC from high-risk population. Myeloid differentiation factor 88 (MyD88) is a crucial adaptor molecule in Toll-like signaling pathway recognizing *H. pylori*. Its role in GCC has not been elucidated yet. In this study, our purpose is to investigate the expression and significance of MyD88 in GCC tissue.

Methods: Expression of MyD88 and nuclear factor κB (NF-κB) p105/p50 and infection of *H. pylori* were detected by immunohistochemistry in gastric cardia tissue. The correlation of MyD88 expression to NF-κB p105/p50 expression, *H. pylori* infection, and clinicopathologic characteristics in gastric cardia tissue was analyzed. The involvement of MyD88 in patient prognosis was also analyzed.

Results: Our data showed that the expression of MyD88 elevated from normal mucosa to inflammation ($p = 0.071$). The expression of MyD88 was enhanced in GCC tissues by contrast to non-malignant cardia mucosa ($p = 0.025$). What's more, overexpression of MyD88 was detected in intestinal-type adenocarcinoma with inflammation. Patients with high MyD88 staining revealed a better differentiation ($p = 0.02$). MyD88 also positively correlated with NF-κB p105/p50 expression ($p = 0.012$) in cancer tissue. Expression of MyD88 was increased but not significantly in biopsies with *H. pylori* infection compared with non-infected biopsies. Multivariate analyses revealed lymph node metastasis but not MyD88 expression was an independent predictor for patient survival.

Conclusion: These findings provide pathological evidence that upregulating MyD88 and inducing inflammation might be involved in gastric cardia carcinogenesis in high-risk population. MyD88 plays a role in gastric cardia carcinogenesis with NF-κB pathway activation. Higher MyD88 expression is not a major prognostic determinant in GCC, but it may relate to the tumor cell differentiation.

Keywords: MyD88, *Helicobacter pylori*, gastric cardia cancer, cancer and inflammation, prognosis

Gastric cancer is a significant global health problem. It is one of the five most common malignancies and ranks after lung, breast, colorectal, and prostate cancer in 2012 (1). Geographically, 43% of total global cases occur in China (1). Gastric cancer is generally divided into two topographical categories: gastric cardia cancer (GCC) arising in the upper part of the stomach, where it connects to the esophageal, and non-GCC (NGCC) arising from rest part of the stomach. Gastric cardia cancer has unique epidemiology and risk factors different from NGCC. The incidence of GCC has been stable or increased, and the NGCC incidence decreased since the mid-1970s (1).

In China, the incidence of GCC differs on the basis of geographical situation and populations. Gastric cardia cancer has epidemiologic features of population and familial aggregation. The regions in China with high incidence rate of esophageal cancer also have high incidence of GCC, such as Linzhou (2) and Chaoshan area (3). Different from GCC, the incidence of NGCC is low in these areas. Risk factors of GCC are unclear and controversial. Studies of Caucasian populations suggested risk factors for GCC are similar to those for esophageal adenocarcinoma, including obesity, gastroesophageal reflux disease, and Barrett esophagus (1). *Helicobacter pylori* with positive test associated with NGCC is suggested inversely associated with GCC in Western countries. However, in high-risk settings, a positive association between *H. pylori* infection and gastric cancer was observed both for cardia and non-cardia cancers (4). Reports showed that the influence of gender, socioeconomic status, presence of intestinal metaplasia, and past alcohol intake also differ in GCC and NGCC (1). Considering the differences, more and more researches are addressing GCC and NGCC as separate diseases.

The Chaoshan GCC high-incidence area of east Guangdong province is the only coastal high-incidence area in China. From 1995 to 2004, previous epidemiological data revealed that the incidence of GCC was unusually high (34.81/100,000) on Nan'ao Island in the Chaoshan area (3). Our previous researches found that *H. pylori* infection accompanied with chronic inflammation may result in the carcinogenesis of GCC in Chaoshan region (5, 6).

Toll-like receptors (TLRs) may acquire oncogenic potential by initiating inflammatory pathways, which are essential for *H. pylori* recognition (5–7). The TLRs transmit signals through adaptor proteins. The first adaptor molecule of TLRs to be discovered is myeloid differentiation factor 88 (MyD88) (8). MyD88 is essential in regulating innate immune signals from members of the TLR and interleukin families. Toll-like receptors and interleukin 1 receptors can recognize microbes or endogenous ligands and then recruit MyD88, which can induce nuclear factor κB (NF-κB) activation (8–12). Previous study suggested that abnormal expression of MyD88 was closely associated with the development of tumor and resistance of drugs. In stomach, lung, liver, ovary cancer tissues, the expression of MyD88 was enhanced (8). However, the research data are contradictory. The effects of MyD88 in the development and progression of cancers are controversial (13, 14). MyD88-deficient mice models have shown MyD88 may either promote (10, 15–17) or suppress (18–20) tumor development. In colon cancer models, MyD88 showed contradictory roles even in the same cancer (21, 22).

Our previous study suggested that TLR4 plays a role in carcinogenesis of Chaoshan GCC (7). However, the expression of MyD88 in GCC and its effects on GCC development remain unknown. In the present study, we investigate the expression of MyD88 in gastric cardia tissue of different lesions from Chaoshan high-risk area and evaluate its correlation with *H. pylori* infection and NF-κB pathway activation.

MATERIALS AND METHODS

Study Patients

One hundred two gastric cardia carcinoma samples and 95 non-malignant gastric cardia mucosa were obtained from the Tumor Hospital and the First Affiliated Hospital of Shantou University Medical College in Chaoshan area. The inclusion criterion for GCC is the center of cancer within 2 cm below the gastroesophageal junction defined by the World Health Organization (23). Follow-up survey was conducted for survival status of 71 patients by mobile phone or personal interview. **Table 3** shows the clinicopathological features of the GCC patients. The median age was 62 years with range 40–78 years. Mean tumor diameter was 6 cm (range, 3–15 cm). In this study, we obtained all patients' informed consent and approval from the ethical review committees of the Medical College of Shantou University.

Immunohistochemistry

Formalin-fixed paraffin-embedded samples were sectioned at 4 μm and deparaffinized with xylene and rehydrated with graded ethanol, and then 3% hydrogen peroxide was used for preincubating for 10 min. Antigen retrieval was performed by heating for 20 min in microwave oven. Then, the sections were incubated with 10% normal goat serum to block/eliminate non-specific staining. Next, the tissues were incubated overnight at 4°C with the following antibodies: anti-MyD88 rabbit monoclonal antibody (ab133739; Abcam; Cambridge, MA, United States), anti–NF-κB p105/p50 rabbit monoclonal antibody (ab32360; Abcam; Cambridge, MA, United States), or anti-*H. pylori* rabbit polyclonal antibody (RAB-0064; Fuzhou Maixin Biotechnology; Fuzhou, Fujian Province, China). The tissues were incubated with the secondary antibody conjugated with horseradish peroxidase at 37°C for 30 min. Sections were counterstained with hematoxylin and mounted with glycerol gelatin. We used Olympus BX43 microscope (Olympus, Japan) and Olympus DP21 image management system (Olympus, Japan) to capture images.

Immunohistochemistry (IHC) staining score was evaluated by two experienced researchers in a blinded manner. The expression of MyD88 and NF-κB p105/p50 was rated (0–3) semiquantitatively according to the signal intensity (0 = no immunostaining, 1 = weak positive staining, 2 = moderate positive staining, 3 = strong positive staining) (24). We found intensity in different areas of the specimen was different. We observed the whole specimen and counted all positive and negative cells. Most sections with total number of cells varied

from 5,000 to 8,000. The value was calculated by multiplying the scores of staining intensity by the proportion of positive cells (0–100%).

All values were added to generate a final score ranging from 0 to 300 (25). *Helicobacter pylori* IHC–positive test showed *H. pylori* are brownish yellow, thick, and rod-like, and some of them are clumps (26).

Chronic Inflammation Grading

According to the updated Sydney System, chronic inflammation was measured by the presence of polymorphonuclear leukocytes alongside the mononuclear inflammatory infiltration. The normal gastric mucosa has fewer than 5 inflammatory cells in the lamina propria. Mild inflammation shows 5–30 inflammatory cells in the lamina propria per high-power field or the foveolae. More than 30 inflammatory cells per high-power field infiltrating mucosal layer was considered severe inflammation (27).

Statistical Analysis

Independent non-parametric *t*-tests for trend were used to evaluate increased or decreased MyD88 expression among groups. Spearman correlation was used to determine the correlation between MyD88 and NF-κB p105/p50. The risk factors for overall survival were tested by a Cox proportional hazards model with a stepwise forward procedure. All statistical analyses were performed by using SPSS v19 (SPSS, Chicago, IL, USA). $P < 0.05$ was considered statistically significant.

RESULTS

MyD88 Expression in Gastric Cardia Tissue

To detect the expression of MyD88 in nonmalignant tissue and GCC tissue, we performed MyD88 immunohistochemical staining in this retrospective cohort study. In **Table 1** and **Figure 1**, MyD88 expression in the different gastric cardia lesions is shown. Immunostaining of MyD88 protein was mainly found in the cytoplasm, which was consistent with published result (28). Among the non-malignant gastric cardia tissues, MyD88 expression was higher in inflamed epithelia than that in normal gastric cardia mucosa (**Figures 1A,B**), and the *p*-value was close to significant level, but did not differ between mild and severe inflammation. In 102 GCC cases, MyD88 expression was detectable in most of the cases 72/102 (70.59%). MyD88 expression was significantly higher in tumor tissue than that in non-malignant gastric cardia tissues ($p = 0.025$) (**Table 1**). Moreover, the stronger MyD88 staining was found in intestinal-type adenocarcinoma with severe inflammation than in diffuse-type cancer (**Figures 1C,D**).

Correlation Between MyD88 Expression and *H. pylori* Infection

MyD88 may play a role in gastric immunologic response to *H. pylori* (29, 30). We hypothesized that MyD88 expression correlates with *H. pylori* infection. At the beginning we tried to compare the MyD88 expression correlates with *H. pylori* infection in GCC tissue. However we found that most of the tumor tissue had necrosis and very few samples could found *H. pylori* by IHC. So we just used the non-GCC tissue to analyze *H. pylori* infection. We think that the results from non-malignant gastric cardia tissues can reflect the relationship between MyD88 expression and *H. pylori* infection. Thus, we use immunohistochemical staining to detect *H. pylori* infection in the non-malignant gastric cardia tissues. *Helicobacter pylori* was seen in the mucosa and gland epithelium tissues (**Figure 2A**). Expression of MyD88 was increased in biopsies with *H. pylori* infection compared with non-infected biopsies; however, the difference was not significant (**Table 1**, **Figure 2B**).

Correlation Between MyD88 Expression and NF-κB in GCC

MyD88 plays an important role in tumor immunity by regulating NF-κB–mediated functions (8, 31). We used an antibody that can recognize both p105 and p50 proteins to quantify NF-κB p105/p50 protein in the same cohort of samples. Immunohistochemical staining detected NF-κB p105/p50 in all non-malignant and malignant samples. Expression of NF-κB p105/p50 was higher in GCC ($n = 104$) than in non-malignant tissues ($n = 94$) ($p = 0.000$). Moreover, increased NF-κB p105/p50 staining in gastric cardia tissues was positively associated with overexpression of MyD88 expression ($p = 0.012$) (**Table 2**). The strongest immunostaining of NF-κB p105/p50 and MyD88 coexisted in tumors (**Figure 3**).

TABLE 1 | Immunohistochemical evaluation of MyD88 expression in different gastric cardia tissue.

Tissue feature		Case	MyD88 expression, percentage of positive cells (%)	Myd88 expression, median (IQR)	*P*-value
Tumor or non	GCC	102	38.93	55 (0, 110)	$p = 0.025^*$
	Non-GCC	95	26.45	30 (0, 70)	
H. pylori infection	Negative	63	24.1	20 (0, 60)	$p = 0.228$
	Positive	32	31.01	40 (0, 80)	
Inflammation	Normal	20	17.75	10 (0, 37.5)	$p = 0.071$
	Mild/severe	75	28.77	40 (0, 80)	

$^*p < 0.05$.

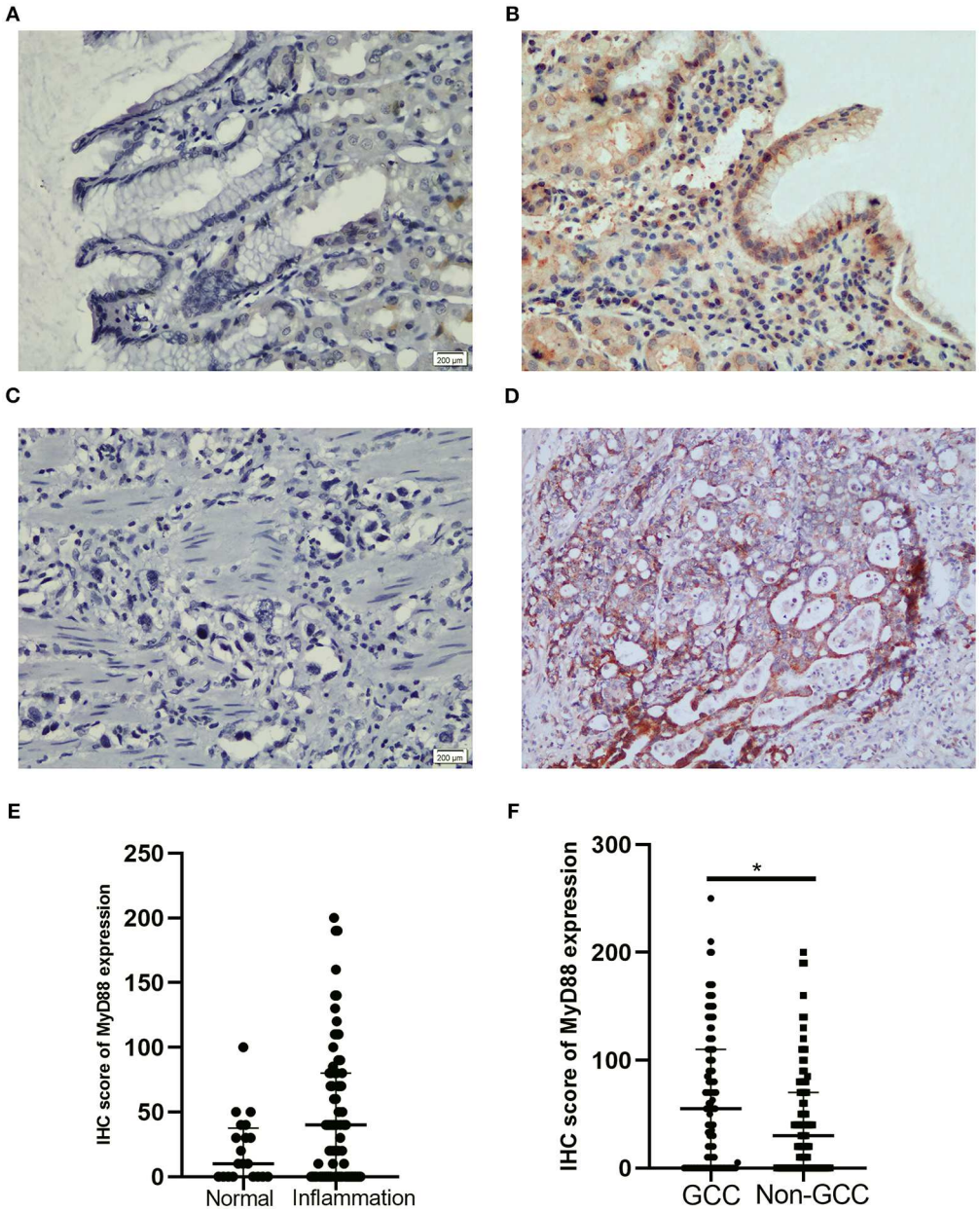

FIGURE 1 | Representative IHC staining for MyD88 in gastric cardia mucosae and gastric cardia cancer tissue. **(A)** No immunostaining in normal mucosae, **(B)** moderate positive staining in mucosae with inflammation, **(C)** negative MyD88 staining in poorly differentiated tumor, and **(D)** strong positive staining in intestinal-type adenocarcinoma. **(E)** Boxplot shows MyD88 expression was higher in the inflammation cases than normal tissues. **(F)** Boxplot shows MyD88 expression was significantly higher in the GCC cases compared to the non-malignant cases (*p < 0.05).

Clinical Significance of MyD88 Expression in Gastric Cardia Cancer Patients

We then analyze the relationship between MyD88 expression and clinicopathologic features of GCC patients including gender, size of the tumor, lymph node metastasis, histological grade, depth of tumor invasion, and TNM stage (**Table 3**).

Gastric cardia cancer tumors with higher MyD88 expression had higher histological grade ($p = 0.041$). There was no significant relationship between the expression of MyD88 and other clinical and pathological parameters in GCC.

All 70 patients followed were involved for survival analysis. On multivariable analysis, MyD88 did not correlate with survival in the GCC patients (overall survival, $p = 0.828$). Lymph node metastasis [hazard ratio (HR), 2.715; 95% confidence interval (CI), 1.348–5.468; $p = 0.005$] was independently associated with GCC patients' survival (**Table 4**).

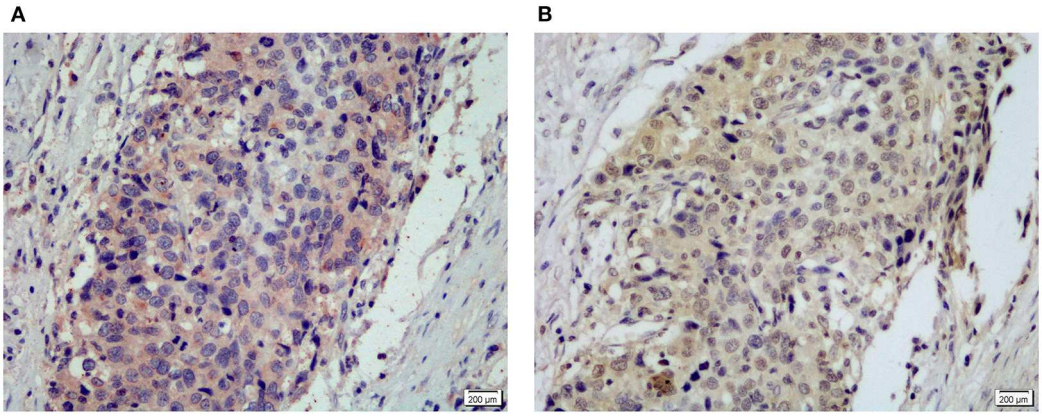

FIGURE 2 | Representative IHC staining for MyD88 **(A)** and NF-κB p50/105 **(B)** in the same gastric cardia cancer tissue.

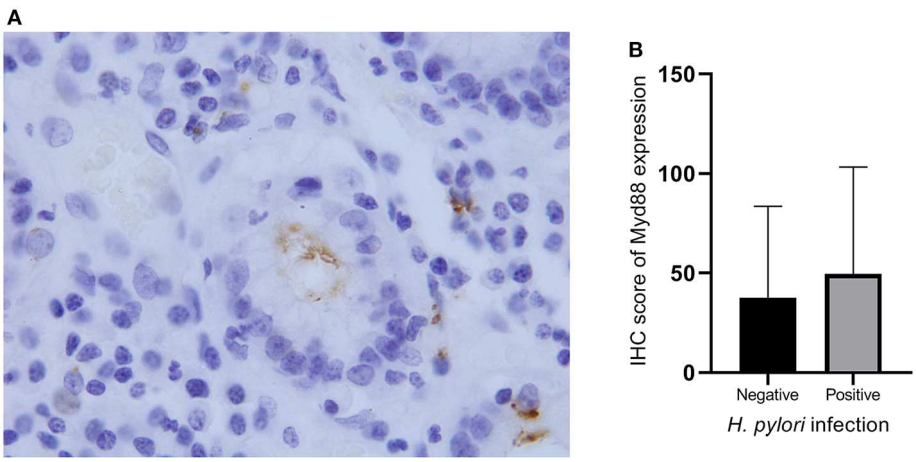

FIGURE 3 | *Helicobacter pylori* infection and MyD88 expression. **(A)** *Helicobacter pylori* infection was identified by IHC in gastric cardia glands. **(B)** Boxplot shows that MyD88 expression was higher in the severe *H. pylori* infection cases than the cases without *H. pylori* infection but not significantly.

TABLE 2 | Correlation of MyD88 and NF-κB p50/105 expression in gastric cardia cancer tissue.

		NF-κB p50/105 ($n = 102$)
MyD88 ($n = 102$)	Correlation	0.248
	P-value	0.012*

*$p < 0.05$.

DISCUSSION

The etiology of GCC is unclear. Previous reports showed that GCC is different from adenocarcinomas located in the lower esophagus or distal stomach in both epidemiology and biology (7). Gastric cardia cancer is defined as carcinoma in which the epicenter is ≤2 cm below the esophageal–gastric junction (32) in China. The highest regional rate of GCC was in Eastern/Southeastern Asia (1). The reason for a higher incidence of GCC in Chaoshan area in China is unknown. Given the differences between GCC and NGCC, in the present study, we considered GCC as a separate disease and reported for the first time in gastric cardia tissues the expression of MyD88 and its relationship with *H. pylori* infection and NF-κB p105/p50 expression. We observed that MyD88 expression gradually increased from normal tissue, gastric cardia inflammation, and carcinoma. A positive correlation between MyD88 and p105/p50 expression was detected. Thereby we provide pathological evidence that MyD88 expression is involved in gastric cardia tissue inflammation and carcinogenesis.

Lipopolysaccharide (LPS) is found in the outer membrane of *Helicobacter*, and it was reported that LPS could upregulate MyD88 expression. Few studies showed correlation between *H. pylori* and MyD88 expression in gastric cardia tissue. Here, we showed that MyD88 expression is higher in *H. pylori*–positive cases in comparison with *H. pylori*–negative cases, but the result was not significant. Several factors may contribute

TABLE 3 | The associations of MyD88 expression with clinicopathologic characteristics concerning 71 of the 102 GCC patients.

Features	MyD88 expression, percentage of positive cells (%)	MyD88 expression, median (IQR)	*P*-value
Gender			0.475
Male ($n = 63$)	43.26	70 (10, 120)	
Female ($n = 8$)	41.25	35 (2.5, 87.5)	
Age			0.934
≤62 ($n = 33$)	42	63 (0, 150)	
>62 ($n = 37$)	43.51	70 (20, 100)	
Size			0.803
<6 cm ($n = 36$)	42.94	66.5 (10, 135)	
≥6 cm ($n = 35$)	43.14	60 (0, 100)	
Tumor differentiation			0.02*
Well/moderately ($n = 39$)	53.23	70 (40, 130)	
Poorly ($n = 32$)	30.63	20 (0, 95)	
Lymph node metastasis			0.141
Yes ($n = 50$)	47.12	70 (27.5, 120)	
No ($n = 21$)	33.33	10 (0, 105)	
TNM stage			0.957
Stage 1–2 ($n = 12$)	45.83	70 (0, 112.5)	
Stage 3 ($n = 59$)	42.47	60 (10,120)	

*$p < 0.05$.

TABLE 4 | Multivariate analysis of factors associated with survival in GCC patients.

Variable	HR (95% CI)	*P*-value
Lymph node metastasis (yes vs. no)	2.715 (1.348–5.469)	0.005**
Age		0.219
Sex (male/female)		0.172
Histology (well/moderate vs. poor)		0.071
MyD88		0.828
Length		0.856
TNM (III vs. I/II)		0.428

**$p < 0.01$.

to lack of significant relationship between MyD88 expression and the *H. pylori* infection. One is the induction of endotoxin tolerance (33, 34). Lipopolysaccharide is the major component of *H. pylori*. Studies showed that after repeated challenge by LPS a reduced inflammatory response was observed, which is termed LPS tolerance. Lipopolysaccharide-induced tolerance can down-regulate the surface expression of the TLR4-MD2 complex, which might block MyD88-dependent pathways (35). We supposed that some of the patients with repeated *H. pylori* infection might reduce MyD88 expression. Second is that evidences suggest host genetics, environmental factors, and bacterial virulence factors might affect the ability of *H. pylori* to manipulate the immune response (33). These factors may contribute that some positive infection individuals show higher expression of MyD88 but not reach significant level. Third, pattern of MyD88 expression might not significantly change after the bacteria were eradicated. Michalkiewicz et al. (34) found that the involvement of *H. pylori* did not result in a significant upregulation of MyD88 mRNA expression when analyzing the expression of innate immunity components in the gastric mucosa among *H. pylori*–infected and uninfected children, which was consistent with our result.

Evidence showed that MyD88 can induce proinflammatory response and inflammation, which is regarded as the most important factor contributing to tumorigenesis (8, 21, 36). In the present study, MyD88 expression was evaluated from normal mucosa to inflammation and carcinoma restricted to gastric cardia tissue. MyD88 expression in normal cells differs in different tissue. Similar to the studies in gastric tissue (8, 37), our data indicated that the expression of MyD88 is low in normal gastric cardia tissue. MyD88 expression was increased during chronic inflammation. Echizen et al. (38) reported that depletion of MyD88 results in suppression of the inflammatory microenvironment in gastric tumors. These evidences indicated that MyD88 plays a role in increasing inflammation and changes innate immune activation between normal and mild inflammation. Gastric cardia cancer has the highest MyD88 expression and mainly in intestinal-type adenocarcinoma with inflammation. Gastric adenocarcinomas can be classified as the intestinal type and diffuse type according to the Lauren classification (39). Intestinal-type adenocarcinoma cells tend to form glands. Diffuse-type adenocarcinoma cells are poorly differentiated and tend to scatter throughout the stomach rather than form glands (40). Inflammatory cell infiltration was common in the intestinal-type adenocarcinoma in this study. We also showed that MyD88 expression was significantly higher in the well- and moderately differentiated tumors than in the poorly differentiated tumors, and most of the intestinal-type adenocarcinoma are well-differentiated. Studies reported that diffuse- and intestinal-type gastric carcinomas differ in risk factors, epidemiology, and distinct causal pathways (41–46). Our observation suggested that MyD88 pathway plays more important role in intestinal-type adenocarcinoma and might be responsible for the inflammatory response and carcinogenesis of this type of adenocarcinoma. The higher MyD88 expression in well-/moderately differentiated tumors comparing to poorly differentiated tumors might suggest that the MyD88 expression level is changing with the differentiation of cells. With the constant accumulation of different gene mutation and expression during tumor differentiation, MyD88 expression might be changing. We speculated that during tumor progression the antitumor role of MyD88 affects tumor differentiation to a certain degree resulting in well-/moderately differentiated tumors with higher MyD88 expression.

Reports have shown that MyD88 coupled with NF-κB contributes to carcinogenesis. Nuclear factor κB is the important signaling molecule downstream of MyD88 and data on how MyD88 deficiency affects carcinogenesis involved the role of NF-κB in cancer (21, 47). MyD88 is thought to mediate NF-κB activation and cytokine production (48, 49). Nuclear factor

κB is able to regulate inflammation, cell differentiation, and apoptosis and plays a role in tumorigenesis (50–54). Nuclear factor κB p105/p50 usually locates in the cytoplasm. Adverse stimuli can activate NF-κB pathway, and p50 translocates into the nucleus then changes cell signaling (55). In the present study, we demonstrated positive expression of p105/p50 both in the cytoplasm and nucleus of GCC cells. We found that MyD88 had significantly positive relationship with NF-κB p105/p50, suggesting that p105/p50 and MyD88 are both involved in GCC tumorigenesis.

Different from the study results in hepatocellular carcinoma and epithelial ovarian cancer in which recurrence rate was higher and recurrence-free survival and overall survival were poorer in patients with MyD88 overexpression (8), we showed that the expression of MyD88 did not correlate with survival of GCC patients. The role of MyD88 in cancer prognosis might differ in different cancers. Lymph node metastasis was independently associated with GCC patient survival.

Although some previous studies proved that MyD88 has protective effects in gastric carcinogenesis (56). Our results provide evidences about the contribution of MyD88 in the regulation of inflammation, carcinogenesis, and tumor differentiation in gastric cardia tissue. Enhanced MyD88 expression was closely related with the intestinal-type carcinomas with inflammatory cell infiltration. Furthermore, NF-κB p105/p50 showed positive relationship with MyD88 expression in GCC tissue. The lack of significance of MyD88 as a prognostic factor in GCC might be due to the complex role of MyD88 in cancer tissue, and we need further studies to provide evidences.

DATA AVAILABILITY STATEMENT

The datasets used and analyzed during the current study are available from the corresponding author on reasonable request.

ETHICS STATEMENT

The studies involving human participants were reviewed and approved by Ethical review committees of the Medical College of Shantou University. The patients/participants provided their written informed consent to participate in this study. Written informed consent was obtained from the individual(s) for the publication of any potentially identifiable images or data included in this article.

AUTHOR CONTRIBUTIONS

SL and GC designed the research study. JC, DX, WL, and DG conducted the experiments. GC and MX collected clinical data. SL, GC, and RS analyzed the data. SL wrote the manuscript with contribution from all authors. All authors read and approved the final version of the paper.

FUNDING

This work was supported by the Natural Science Foundation of China (Grant no. 81702717), the Natural Science Foundation of Guangdong Province (Grant no. 2014A030310139), and the Medical Science Foundation of Guangdong Province (Grant number A2019312).

REFERENCES

1. Colquhoun A, Arnold M, Ferlay J, Goodman KJ, Forman D, Soerjomataram I. Global patterns of cardia and non-cardia gastric cancer incidence in 2012. *Gut.* (2015) 64:1881–8. doi: 10.1136/gutjnl-2014-308915
2. Wang LD, Zheng S, Zheng ZY, Casson AG. Primary adenocarcinomas of lower esophagus, esophagogastric junction and gastric cardia: in special reference to China. *World J Gastroenterol.* (2003) 9:1156–64. doi: 10.3748/wjg.v9.i6.1156
3. Su M, Liu M, Tian DP, Li XY, Zhang GH, Yang HL, et al. Temporal trends of esophageal cancer during 1995-2004 in Nanao Island, an extremely high-risk area in China. *Eur J Epidemiol.* (2007) 22:43–8. doi: 10.1007/s10654-006-9086-x
4. Cavaleiro-Pinto M, Peleteiro B, Lunet N, Barros H. *Helicobacter pylori* infection and gastric cardia cancer: systematic review and meta-analysis. *Cancer Causes Control.* (2011) 22:375–87. doi: 10.1007/s10552-010-9707-2
5. Melit LE, Marginean CO, Marginean CD, Marginean MO. The relationship between toll-like receptors and *Helicobacter pylori*-related gastropathies: still a controversial topic. *J Immunol Res.* (2019) 2019:8197048. doi: 10.1155/2019/8197048
6. Nagashima H, Yamaoka Y. Importance of toll-like receptors in pro-inflammatory and anti-inflammatory responses by *Helicobacter pylori* infection. *Curr Top Microbiol Immunol.* (2019) 421:139–58. doi: 10.1007/978-3-030-15138-6_6
7. Chen G, Xu M, Chen J, Hong L, Lin W, Zhao S, et al. Clinicopathological features and increased expression of toll-like receptor 4 of gastric cardia cancer in a high-risk Chinese population. *J Immunol Res.* (2018) 2018:7132868. doi: 10.1155/2018/7132868
8. Liang B, Chen R, Wang T, Cao L, Liu Y, Yin F, et al. Myeloid differentiation factor 88 promotes growth and metastasis of human hepatocellular carcinoma. *Clin Cancer Res.* (2013) 19:2905–16. doi: 10.1158/1078-0432.CCR-12-1245
9. Anthoney N, Foldi I, Hidalgo A. Toll and toll-like receptor signalling in development. *Development.* (2018) 145:dev156018. doi: 10.1242/dev.156018
10. Maeda Y, Echizen K, Oshima H, Yu L, Sakulsak N, Hirose O, et al. Myeloid differentiation factor 88 signaling in bone marrow-derived cells promotes gastric tumorigenesis by generation of inflammatory microenvironment. *Cancer Prev Res.* (2016) 9:253–63. doi: 10.1158/1940-6207.CAPR-15-0315
11. Bajo M, Patel RR, Hedges DM, Varodayan FP, Vlkolinsky R, Davis TD, et al. Role of MyD88 in IL-1beta and ethanol modulation of GABAergic transmission in the central amygdala. *Brain Sci.* (2019) 9:361. doi: 10.3390/brainsci9120361
12. Wang L, Yu K, Zhang X, Yu S. Dual functional roles of the MyD88 signaling in colorectal cancer development. *Biomed Pharmacother.* (2018) 107:177–84. doi: 10.1016/j.biopha.2018.07.139
13. Pradere JP, Dapito DH, Schwabe RF. The yin and yang of toll-like receptors in cancer. *Oncogene.* (2014) 33:3485–95. doi: 10.1038/onc.2013.302
14. Lozano-Pope I, Sharma A, Matthias M, Doran KS, Obonyo M. Effect of myeloid differentiation primary response gene 88 on expression profiles of genes during the development and progression of helicobacter-induced gastric cancer. *BMC Cancer.* (2017) 17:133. doi: 10.1186/s12885-017-3114-y
15. Lee SH, Hu LL, Gonzalez-Navajas J, Seo GS, Shen C, Brick J, et al. ERK activation drives intestinal tumorigenesis in Apc(min/+) mice. *Nat Med.* (2010) 16:665–70. doi: 10.1038/nm.2143
16. Naugler WE, Sakurai T, Kim S, Maeda S, Kim K, Elsharkawy AM, et al. Gender disparity in liver cancer due to sex differences in MyD88-dependent IL-6 production. *Science.* (2007) 317:121–4. doi: 10.1126/science.1140485

17. Kennedy CL, Najdovska M, Tye H, McLeod L, Yu L, Jarnicki A, et al. Differential role of MyD88 and Mal/TIRAP in TLR2-mediated gastric tumourigenesis. *Oncogene.* (2014) 33:2540–6. doi: 10.1038/onc.2013.205
18. Banerjee A, Thamphiwatana S, Carmona EM, Rickman B, Doran KS, Obonyo M. Deficiency of the myeloid differentiation primary response molecule MyD88 leads to an early and rapid development of helicobacter-induced gastric malignancy. *Infect Immun.* (2014) 82:356–63. doi: 10.1128/IAI.01344-13
19. Garrett WS, Punit S, Gallini CA, Michaud M, Zhang D, Sigrist KS, et al. Colitis-associated colorectal cancer driven by T-bet deficiency in dendritic cells. *Cancer Cell.* (2009) 16:208–19. doi: 10.1016/j.ccr.2009.07.015
20. Ochi A, Nguyen AH, Bedrosian AS, Mushlin HM, Zarbakhsh S, Barilla R, et al. MyD88 inhibition amplifies dendritic cell capacity to promote pancreatic carcinogenesis via Th2 cells. *J Exp Med.* (2012) 209:1671–87. doi: 10.1084/jem.20111706
21. Salcedo R, Cataisson C, Hasan U, Yuspa SH, Trinchieri G. MyD88 and its divergent toll in carcinogenesis. *Trends Immunol.* (2013) 34:379–89. doi: 10.1016/j.it.2013.03.008
22. Salcedo R, Worschech A, Cardone M, Jones Y, Gyulai Z, Dai RM, et al. MyD88-mediated signaling prevents development of adenocarcinomas of the colon: role of interleukin 18. *J Exp Med.* (2010) 207:1625–36. doi: 10.1084/jem.20100199
23. Wen D, Shan B, Wang S, Zhang L, Wei L, Zhou W, et al. A positive family history of esophageal/gastric cardia cancer with gastric cardia adenocarcinoma is associated with a younger age at onset and more likely with another synchronous esophageal/gastric cardia cancer in a Chinese high-risk area. *Eur J Med Genet.* (2010) 53:250–5. doi: 10.1016/j.ejmg.2010.06.011
24. Jee H, Nam KT, Kwon HJ, Han SU, Kim DY. Altered expression and localization of connexin32 in human and murine gastric carcinogenesis. *Dig Dis Sci.* (2011) 56:1323–32. doi: 10.1007/s10620-010-1467-z
25. Xu Q, Xu Y, Pan B, Wu L, Ren X, Zhou Y, et al. TTK is a favorable prognostic biomarker for triple-negative breast cancer survival. *Oncotarget.* (2016) 7:81815–29. doi: 10.18632/oncotarget.13245
26. Liu LLD, Li C, Chen ZY. Comparison of three staining methods for detection of *Helicobacter pylori* in gastric biopsy specimens. *West China Medical J.* (2010) 25:80–1.
27. Zhang Y, Wang H, Bi C, Xiao Y, Liu Z. Expression of CDX2 in gastric cardia adenocarcinoma and its correlation with *H. pylori* and cell proliferation. *Oncotarget.* (2016) 7:54973–82. doi: 10.18632/oncotarget.10362
28. Yue Y, Zhou T, Gao Y, Zhang Z, Li L, Liu L, et al. High mobility group box 1/toll-like receptor 4/myeloid differentiation factor 88 signaling promotes progression of gastric cancer. *Tumour Biol.* (2017) 39:1010428317694312. doi: 10.1177/1010428317694312
29. Fulgione A, Di Matteo A, Contaldi F, Manco R, Ianniello F, Incerti G, et al. Epistatic interaction between MyD88 and TIRAP against *Helicobacter pylori*. *FEBS Lett.* (2016) 590:2127–37. doi: 10.1002/1873-3468.12252
30. Wang F, Mao Z, Liu D, Yu J, Wang Y, Ye W, et al. Overexpression of Tim-3 reduces *Helicobacter pylori*-associated inflammation through TLR4/NFkappaB signaling *in vitro*. *Mol Med Rep.* (2017) 15:3252–8. doi: 10.3892/mmr.2017.6346
31. Sakai J, Cammarota E, Wright JA, Cicuta P, Gottschalk RA, Li N, et al. Lipopolysaccharide-induced NF-κB nuclear translocation is primarily dependent on MyD88, but TNFα expression requires TRIF and MyD88. *Sci Rep.* (2017) 7:1428. doi: 10.1038/s41598-017-01600-y
32. Peng XB, Zhang CW, Chen ZF, Liang ZH, Ou ZX, Wei KR. Epidemiology of gastric cardia cancer in China. *Chin Arch Gen Surg.* (2014) 8:156–9.
33. Zaric SS, Coulter WA, Shelburne CE, Fulton CR, Zaric MS, Scott A, et al. Altered toll-like receptor 2-mediated endotoxin tolerance is related to diminished interferon beta production. *J Biol Chem.* (2011) 286:29492–500. doi: 10.1074/jbc.M111.252791
34. Michalkiewicz J, Helmin-Basa A, Grzywa R, Czerwionka-Szaflarska M, Szaflarska-Poplawska A, Mierzwa G, et al. Innate immunity components and cytokines in gastric mucosa in children with *Helicobacter pylori* infection. *Mediators Inflamm.* (2015) 2015:176726. doi: 10.1155/2015/176726
35. Sato S, Takeuchi O, Fujita T, Tomizawa H, Takeda K, Akira S. A variety of microbial components induce tolerance to lipopolysaccharide by differentially affecting MyD88-dependent and -independent pathways. *Int Immunol.* (2002) 14:783–91. doi: 10.1093/intimm/dxf046
36. Mantovani A, Allavena P, Sica A, Balkwill F. Cancer-related inflammation. *Nature.* (2008) 454:436–44. doi: 10.1038/nature07205
37. Je EM, Kim SS, Yoo NJ, Lee SH. Mutational and expressional analyses of MYD88 gene in common solid cancers. *Tumor.* (2012) 98:663–9. doi: 10.1700/1190.13209
38. Echizen K, Hirose O, Maeda Y, Oshima M. Inflammation in gastric cancer: interplay of the COX-2/prostaglandin E2 and Toll-like receptor/MyD88 pathways. *Cancer Sci.* (2016) 107:391–7. doi: 10.1111/cas.12901
39. Lauren P. The two histological main types of gastric carcinoma: diffuse and so-called intestinal-type carcinoma. An attempt at a histo-clinical classification. *Acta Pathol Microbiol Scand.* (1965) 64:31–49. doi: 10.1111/apm.1965.64.1.31
40. van der Woude CJ, Kleibeuker JH, Tiebosch ATGM, Homan M, Beuving A, Jansen PLM, et al. Diffuse and intestinal type gastric carcinomas differ in their expression of apoptosis related proteins. *J Clin Pathol.* (2003) 56:699–702. doi: 10.1136/jcp.56.9.699
41. Waldum HL, Fossmark R. Types of gastric carcinomas. *Int J Mol Sci.* (2018) 19:4109. doi: 10.3390/ijms19124109
42. Chen Y-C, Fang W-L, Wang R-F, Liu C-A, Yang M-H, Lo S-S, et al. Clinicopathological variation of lauren classification in gastric cancer. *Pathol Oncol Res.* (2016) 22:197–202. doi: 10.1007/s12253-015-9996-6
43. Yamazawa S, Ushiku T, Shinozaki-Ushiku A, Hayashi A, Iwasaki A, Abe H, et al. Gastric cancer with primitive enterocyte phenotype: an aggressive subgroup of intestinal-type adenocarcinoma. *Am J Surg Pathol.* (2017) 41:989–97. doi: 10.1097/PAS.0000000000000869
44. Correa P. Human gastric carcinogenesis: a multistep and multifactorial process–First American cancer society award lecture on cancer epidemiology and prevention. *Cancer Res.* (1992) 52:6735–40.
45. Henson DE, Dittus C, Younes M, Nguyen H, Albores-Saavedra J. Differential trends in the intestinal and diffuse types of gastric carcinoma in the United States, 1973-2000: increase in the signet ring cell type. *Arch Pathol Lab Med.* (2004) 128:765–70. doi: 10.1043/1543-2165(2004)128<765:DTITIA>2.0.CO;2
46. Shibata A, Longacre TA, Puligandla B, Parsonnet J, Habel LA. Histological classification of gastric adenocarcinoma for epidemiological research: concordance between pathologists. *Cancer Epidemiol Biomarkers Prev.* (2001) 10:75–8.
47. DiDonato JA, Mercurio F, Karin M. NF-κB and the link between inflammation and cancer. *Immunol Rev.* (2012) 246:379–400. doi: 10.1111/j.1600-065X.2012.01099.x
48. Shang L, Wang T, Tong D, Kang W, Liang Q, Ge S. Prolyl hydroxylases positively regulated LPS-induced inflammation in human gingival fibroblasts via TLR4/MyD88-mediated AKT/NF-κB and MAPK pathways. *Cell Prolif.* (2018) 51:e12516. doi: 10.1111/cpr.12516
49. Hirano H, Yoshioka T, Yunoue S, Fujio S, Yonezawa H, Niiro T, et al. TLR4, IL-6, IL-18, MyD88 and HMGB1 are highly expressed in intracranial inflammatory lesions and the IgG4/IgG ratio correlates with TLR4 and IL-6. *Neuropathology.* (2012) 32:628–37. doi: 10.1111/j.1440-1789.2012.01310.x
50. Taniguchi K, Karin M. NF-κB, inflammation, immunity and cancer: coming of age. *Nat Rev Immunol.* (2018) 18:309–24. doi: 10.1038/nri.2017.142
51. Markopoulos GS, Roupakia E, Tokamani M, Alabasi G, Sandaltzopoulos R, Marcu KB, et al. Roles of NF-κB Signaling in the regulation of miRNAs impacting on inflammation in cancer. *Biomedicines.* (2018) 6:40. doi: 10.3390/biomedicines6020040
52. Oeckinghaus A, Hayden MS, Ghosh S. Crosstalk in NF-κB signaling pathways. *Nat Immunol.* (2011) 12:695–708. doi: 10.1038/ni.2065
53. Siggers T, Chang AB, Teixeira A, Wong D, Williams KJ, Ahmed B, et al. Principles of dimer-specific gene regulation revealed by a comprehensive

characterization of NF-κB family DNA binding. *Nat Immunol.* (2011) 13:95–102. doi: 10.1038/ni.2151
54. Weng H, Deng Y, Xie Y, Liu H, Gong F. Expression and significance of HMGB1, TLR4 and NF-κB p65 in human epidermal tumors. *BMC cancer.* (2013) 13:311. doi: 10.1186/1471-2407-13-311
55. Xia S, Ji R, Zhan W. Long noncoding RNA papillary thyroid carcinoma susceptibility candidate 3 (PTCSC3) inhibits proliferation and invasion of glioma cells by suppressing the Wnt/β-catenin signaling pathway. *BMC Neurol.* (2017) 17:30. doi: 10.1186/s12883-017-0813-6
56. Banerjee A, Thamphiwatana S, Carmona EM, Rickman B, Doran KS, Obonyo M. Deficiency of the myeloid differentiation primary response molecule MyD88 leads to an early and rapid development of helicobacter-induced gastric malignancy. *Infect Immun.* (2014) 82:356–63. doi: 10.1128/IAI.01344-13

Conflict of Interest: The authors declare that the research was conducted in the absence of any commercial or financial relationships that could be construed as a potential conflict of interest.

The handling editor declared a shared affiliation, though no other collaboration, with the authors.

frontiers in Oncology

REVIEW
published: 04 June 2020
doi: 10.3389/fonc.2020.00891

The Cancer-Immune Set Point in Oesophageal Cancer

Robert Power[1,2], *Maeve A. Lowery*[1,2], *John V. Reynolds*[1,2] *and Margaret R. Dunne*[1,2]*

[1] Department of Surgery, Trinity College Dublin, Dublin, Ireland, [2] Trinity St. James Cancer Institute, Trinity College Dublin, Dublin, Ireland

Immunotherapy has achieved long-term disease control in a proportion of cancer patients, but determinants of clinical benefit remain unclear. A greater understanding of antitumor immunity on an individual basis is needed to facilitate a precision oncology approach. A conceptual framework called the "cancer-immune set point" has been proposed to describe the equilibrium between factors that promote or suppress anticancer immunity and can serve as a basis to understand the variability in clinical response to immune checkpoint blockade. Oesophageal cancer has a high mutational burden, develops from pre-existing chronic inflammatory lesions and is therefore anticipated to be sensitive to immune checkpoint inhibition. However, both tumour- and patient-specific factors including the immune microenvironment, the microbiome, obesity, and host genetics contribute to an immune set point that confers a lower-than-expected response to checkpoint blockade. Immunotherapy is therefore currently confined to latter lines of treatment of advanced disease, with no reliable predictive biomarker of response. In this review, we examine oesophageal cancer in the context of the cancer-immune set point, discuss factors that contribute to response to immunotherapeutic intervention, and propose areas requiring further investigation to improve treatment response.

Keywords: cancer immunology, immunotherapy, oesophageal cancer, immune checkpoint inhibitors, prognostic markers

OPEN ACCESS

Edited by:
Linhui Liang,
Fudan University, China

Reviewed by:
Francesco Caiazza,
University of California, San Francisco, United States
Shuji Ogino,
Dana–Farber Cancer Institute, United States

***Correspondence:**
Margaret R. Dunne
dunnem12@tcd.ie

Specialty section:
This article was submitted to Gastrointestinal Cancers, a section of the journal Frontiers in Oncology

Received: *30 March 2020*
Accepted: *06 May 2020*
Published: *04 June 2020*

Citation:
Power R, Lowery MA, Reynolds JV and Dunne MR (2020) The Cancer-Immune Set Point in Oesophageal Cancer. Front. Oncol. 10:891. doi: 10.3389/fonc.2020.00891

INTRODUCTION

Oesophageal cancer is the sixth most common cause of cancer-associated mortality worldwide and represents a major global health challenge (1). Oesophageal cancer is divided into squamous cell carcinoma (OSCC) and adenocarcinoma (OAC). The incidence of OAC has increased markedly in the western world within the last 40 years and is thought to arise from a multi-step inflammatory dysplastic transformation from the precursor lesion of Barrett's oesophagus (BO). Stomach acid and bile reflux and visceral obesity predispose individuals to both BO and OAC (2, 3). In contrast, OSCC accounts for 90% of oesophageal cancer worldwide and tobacco or alcohol consumption are the main risk factors (4, 5). As 5-year survival rates are <20% for these cancers (6) and systemic therapy confers a response in only a minority of patients, alternative treatment options are urgently needed (7, 8).

Several regulatory pathways, so-called "immune checkpoints" involved in immune homeostasis are hijacked by cancer cells as a means of evading the host immune response (**Figure 1**). The first to be targeted was cytotoxic T lymphocyte antigen 4 (CTLA4), expressed constitutively by regulatory T (T_{reg}) cells, and by activated T cells. CTLA4 inhibits T cell activation by binding to costimulatory molecules CD80/CD86 on antigen-presenting cells or tumour cells (9). Inhibition

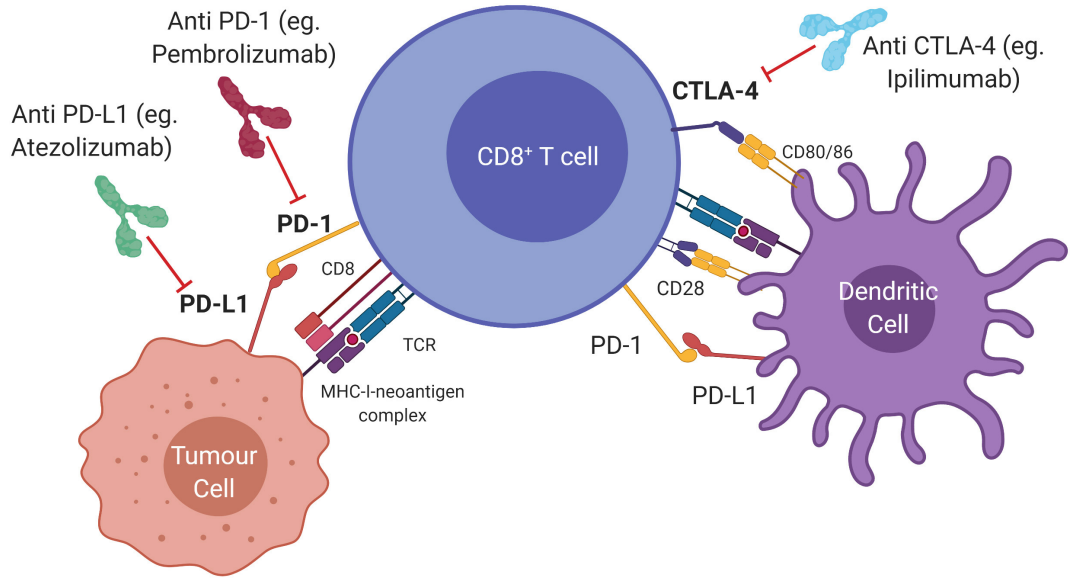

FIGURE 1 | Immune checkpoints and therapeutic targets in the anti-tumour immune response. Cytotoxic T lymphocyte antigen 4 (CTLA4) is a ligand expressed by T cells which prevents T cell activation and can be blocked by Ipilimumab (anti CTLA4). Activated T cells express programmed cell death protein 1 (PD1) which transmits an inhibitory signal that attenuates cytolytic activity when bound to programmed death ligand 1 (PDL1). Monoclonal antibodies that interfere with the PD1/PDL1 interaction (anti PDL1; anti PD1) allow re-invigoration of T cells.

of this pathway by antibody ligation, also known as immune checkpoint inhibition (ICI), has led to major clinical advances in the treatment of advanced melanoma (10). Programmed cell death-ligand 1 (PDL1, encoded by *CD274*) and 2 (PDL2, encoded by *PDCD1LG2*) are expressed by antigen presenting cells and some tumours, and bind to programmed cell death protein 1 (PD1, encoded by *PDCD1*) on effector T cells (11). This generates an inhibitory signal, resulting in attenuated cytotoxic activity. Administration of a monoclonal antibody that blocks the PDL1/PD1 interaction allows reinvigoration of inactivated T cells (12). This approach has led to durable clinical responses in melanoma, non-small-cell lung cancer (NSCLC), head and neck squamous cell carcinoma (HNSCC), renal cell carcinoma and urothelial carcinoma (13–16). Combination approaches incorporating both PD1/PDL1 and CTLA4 blockade, have seen clinical approval in mismatch-repair deficient colorectal cancer, renal cell carcinoma, and hepatocellular carcinoma (17–19).

The rationale to utilise immunotherapy for oesophageal cancer treatment stems from a recognised link with precursor chronic inflammatory lesions and a high mutational burden, suggesting an activated immune response which could be exploited for therapeutic benefit (20). However, as will be discussed in this review, the impact of immunotherapy on patient outcomes in oesophageal cancer to date has been limited (21). An improved understanding of the immune landscape of oesophageal cancer is therefore urgently required to develop effective immunotherapeutic strategies and to select patients likely to benefit from treatment. To conceptualise the myriad of factors that determine a favourable clinical response, a "cancer-immune set point" has been proposed; reflecting the equilibrium between factors that promote or suppress anticancer immunity and a threshold that must be overcome to generate an effective immune response to a tumour (22). A patient with a low set point responds to immunotherapy easily, while the converse is true in patients with a high set point. The immune set point of an individual is determined by tumour specific factors such as tumour genome, precursor lesions and the tumour microenvironment (TME), alongside the external factors of obesity, host genetics, viral infection, and the human microbiome. This review aims to evaluate what is known about each of these factors in the setting of oesophageal cancer, in order to better understand ways in which immunotherapeutic strategies can be improved.

THE CANCER-IMMUNE SET POINT

The Tumour Genome

The overall mutational burden of a tumour increases the probability that some mutations are immunogenic and can be presented as neoepitopes on major histocompatibility class I (MHC-I) molecules. This stimulates a $CD8^+$ T cell response and favourably affects the immune set point. This can be assessed clinically by measuring tumour mutational burden (TMB), defined as the number of asynchronous mutations per mega-base pair (mut/Mbp) which has been correlated to response to immune checkpoint inhibition (ICI) in a variety of tumour types, including oesophageal and gastric cancer (23). Relative to other malignancies, OAC has a relatively high mutational burden at 9.9 mut/Mbp, which is ranked 5th of 30 tumour types in terms of mutational burden, malignant melanoma, and NSCLC being

the first and second, respectively (24, 25). The Cancer Genome Atlas (TCGA) found that chromosomal instability was a cardinal genomic feature of OAC and shared with gastric cancer (26). Whole genome sequencing of 129 OAC samples, as part of the International Cancer Genome Consortium (ICGC), established 3 subgroups based on mutational signatures. The "mutagenic" subgroup displayed the highest TMB, neoantigen burden, and $CD8^+$ tumour infiltrating lymphocyte (TIL) density which may lead to an increased response to ICI (27). More recently, a combined multi-omic characterisation of 551 OAC samples has revealed a three-way association between hypermutation, activation of the *Wnt* pathway (associated with T cell exclusion from tumour parenchyma) and loss of immune signalling genes such as *B2M* (β2 microglobulin, a component of MHC-I) (28, 29). Hypermutation is associated with higher immune activity, while *Wnt* dysregulation and loss of *B2M* is associated with immune escape (30). This provides an acquired mechanism through which OAC may prevent immune surveillance induced by a high mutational burden, potentially offering an explanation for the observed lack of response to checkpoint inhibition.

Specific genomic alterations may also influence the immune set point, independent of overall mutational burden. Amplifications of receptor tyrosine kinases are frequent events in OAC, accounting for 32% of cases which display amplification of *ERBB2* (encoding the HER2 receptor) (26). HER2-positive breast cancer is associated with a distinctive immune landscape (31). Like breast cancer, HER2-positive OAC can be targeted by trastuzumab which could potentially modify the immune set point by antibody-dependant cellular cytotoxicity (32). Adding trastuzumab to standard chemotherapy in patients with metastatic gastroesophageal adenocarcinomas with HER2 overexpression showed a higher objective response rate and a significant increase in overall survival (33). However, tumour heterogeneity has been proposed as a barrier to success of HER2 targeted treatments in the gastroesophageal setting, unlike breast cancer (34). Other common driver mutations, including *TP53* and *KRAS* can promote PD-L1 expression, immune evasion, and immunosuppressive remodelling of the microenvironment in mouse models of pancreatic cancer (35, 36). In a study of resected OAC samples *KRAS* amplifications were a poor prognostic marker (37). Interestingly, amplifications in *PIK3CA*, present in just 5% of cases, correlated with a T cell rich inflammatory microenvironment and were associated with increased survival. There is a need to further characterise the genomic correlates of immune cell infiltration in oesophageal cancer, as has been carried out in colorectal cancer (38), to fully evaluate the impact of these driver mutations on the immune set point.

The genomic landscape of OSCC is distinct from OAC with upregulation of the *Wnt*, *SOX2*, and *TP63* pathways. The latter two genes are required for squamous epithelial differentiation which may explain a similar mutation signature to head and neck SCC (26, 39). OSCC also has a lower mutational burden than OAC; one cohort ($n = 62$) of tumours displayed a mean TMB of 3.9 mut/Mbp (40). In a direct comparison between the two subtypes, 3% of OSCC tumours were TMB-high (>17 mutations/Mbp) compared to 8% of OAC. However, a higher proportion of these same OSCC samples expressed PDL1 (41 vs. 9%) which suggests that the higher TMB of OAC does not necessarily correspond to increased PDL1 expression (41). In summary, the two subtypes of oesophageal cancer are genomically distinct, and this differential mutational burden contributes to divergent immune set points.

The Immune Landscape of Precursor Lesions

Despite differences in genetic drivers of disease, both types of oesophageal cancer share a background in chronic tumourigenic inflammation. OAC in particular is an exemplar model of inflammation-driven cancer, arising from a background of BO metaplasia, driven by chronic reflux, and characterised by intense inflammatory immune cell infiltration, summarised in **Figure 2**. Cytokine profiling and more recent T cell immunophenotypic studies have associated reflux oesophagitis with a predominantly T helper type 1 (TH_1) type cytokine profile, predominated by IFN-γ and interleukin 2 (IL2) expression, whereas BO displays a humoral-type TH_2 profile, associated with immunosuppression (42–45). Supporting this, a recent single-cell flow analysis found a shift from T cell to B cell predominance as normal tissue progresses to BO specialised intestinal metaplasia (46). This TH_2 polarisation drives upregulation of epithelial PDL2 in models of BO and OAC, suggesting that cytokine profile can indirectly induce T cell exhaustion (47). During this malignant progression, dendritic cells are rendered tolerogenic, promoting T_{reg} cell formation, and tumour progression (48). At the end of this sequence, OAC is associated with a mixed TH_1 and TH_2 profile, impaired T cell trafficking, and reduced levels of effector T cells (**Figure 2**) (49). Together, these data indicate that inflammation is a key initiator of the metaplasia-dysplasia-carcinoma sequence, but an immunosuppressive phenotype, potentially an adaptive response to inflammatory stress, enables transformation to OAC.

An Immunosuppressive Tumour Microenvironment

The mass of cells surrounding cancerous cells is often reprogrammed to induce a pro-tumorigenic milieu, known as the tumour microenvironment (TME) (**Figure 3**) (50, 51). Some elements of the immune environment can promote anticancer immunity, including conventional $CD8^+$ cytotoxic and $CD4^+$ helper T cells, and unconventional lymphocyte subsets with potent tumour-killing ability, such as natural killer (NK) cells (52), gamma-delta (γδ) T cells (53), and mucosa associated invariant T (MAIT) cells (54). Tumours exhibiting high levels of lymphocytic infiltration are referred to as "hot" tumours, those without "cold," and tumours with intermediate or ineffective infiltration are referred to as "altered" (55). $CD8^+$ TILs are observed in OAC tissue microarrays, and high levels at the tumour centre have been reported to be positive prognostic indicators (56–58). CD4 helper T cells, although not prognostic alone, have been recently shown to play an essential role in assisting CD8 T cell anti-tumour responses in many cancer types (59). Interestingly, elevated expression of the CD4 T cell antigen presentation molecule, HLA-DR, was noted to be an

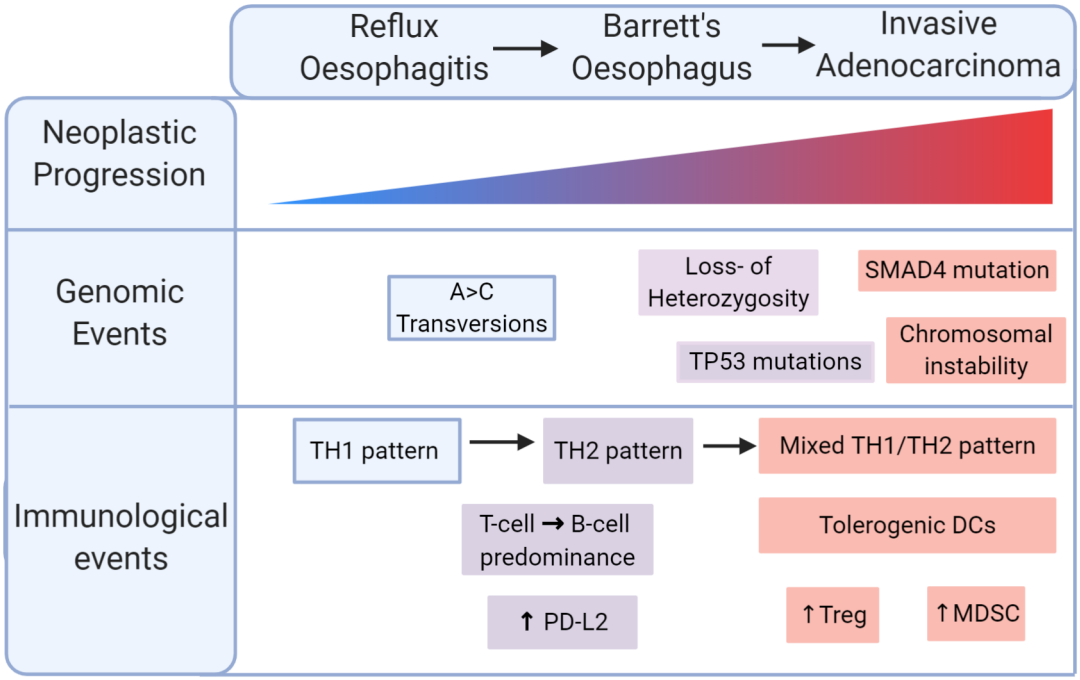

FIGURE 2 | Immunological progression in the malignant transformation to oesophageal adenocarcinoma (OAC). Reflux oesophagitis is accompanied by a TH_1 pattern of inflammation which shifts to a TH_2 pattern in Barrett's oesophagus. Malignant transformation is marked by a mixed TH_1/TH_2 pattern with tolerogenic dendritic cells (DCs), regulatory T (Treg) cells, myeloid derived suppressor cells (MDSCs).

independent favourable prognostic indicator in OAC (60) and other gastrointestinal tumour types, further highlighting the importance of CD4 T cells involvement in antitumour responses. A large molecular profiling study on 18,000 tumours across 39 malignancies including oesophageal cancer showed that γδ T cells and a MAIT cell associated gene *KLRB1* ranked as the most favourable markers of overall survival (61), highlighting a more important role for unconventional lymphocytes as mediators of antitumor immunity than previously thought. Lymphocyte activation state was also shown to affect immune cell prognostic ability. MAIT cells comprise a portion of $CD8^+$ TILs in OAC tumours and display a diminished effector capacity (62). NK cells are also potent antitumor effectors, but intra-tumoral NK cells display markers of exhaustion in OAC. These cytotoxic cells may be abundant in the immunogenic environment of ICGC-mutagenic OAC (27), suggesting an intact immune response that could be potentiated by PD1 blockade, or potentially by other novel means of therapeutic targeting.

Other constituents of the TME promote a pro-tumour milieu. Cancer-associated fibroblasts secrete extracellular matrix proteins and chemokines, excluding $CD8^+$ T cells from the tumour parenchyma (63). The vast majority (93%) of OAC tumours contain cancer-associated fibroblasts which interfere with T cell receptor signalling and leukocyte trafficking, conferring a poor prognosis (64). While "classically" activated M_1-macrophages have antitumor qualities, "alternatively" polarised M_2-macrophages produce immunosuppressive growth factors and cytokines that drive progression from BO to OAC (65, 66). Myeloid-derived suppressor cells (MDSCs, defined by $CD11b^+Gr1^+$ coexpression), and $FoxP3^+$ T_{reg} cells restrict antitumor $CD8^+$ T cell cytotoxicity and are recruited by TH_2 cytokines in the tolerogenic milieu of OAC (67, 68). T_{reg} cell abundance in resected OAC samples is linked with advanced stage and poor response to treatment (69–71). Populations of these tolerogenic cells may be prominent in the non-mutagenic ICGC subsets of OAC and contribute to a non-T cell inflamed immune profile.

In OSCC, there is an abundance of effector T cells and NK cells adjacent to cancer cells (72). Around 40% of OSCC tumours display high (>10%) levels of TILs, suggesting an intermediate level of immune infiltration. Similar to OAC, levels of $CD8^+$ TILs are a favourable prognostic factor in OSCC (73) but a large subset are confined to the stroma (74). Interestingly, high levels of stromal $CD8^+$ TILs are a stronger prognostic factor than intratumoural TILs in both early and late stage OSCC, suggesting that effector function is not limited by their location. The presence of M_2-polarised tumour associated macrophages is associated with angiogenesis, PDL1 expression, and poor prognosis in resected OSCC samples (75, 76). Like OAC, populations of MDSCs and CAFs restrict $CD8^+$ T cell function in OSCC and may reduce efficacy of PD1 blockade (64, 77). Infiltrating $FoxP3^+$ T_{reg} cells are also seen in OSCC but are not an independent predictor of survival. Levels of FoxP3 TILs solely correlates with effector $CD8/4^+$ levels, implying a less potent suppressive role in OSCC. Tumour cell PDL1 expression (>1%; the percentage of viable tumour cells that stain

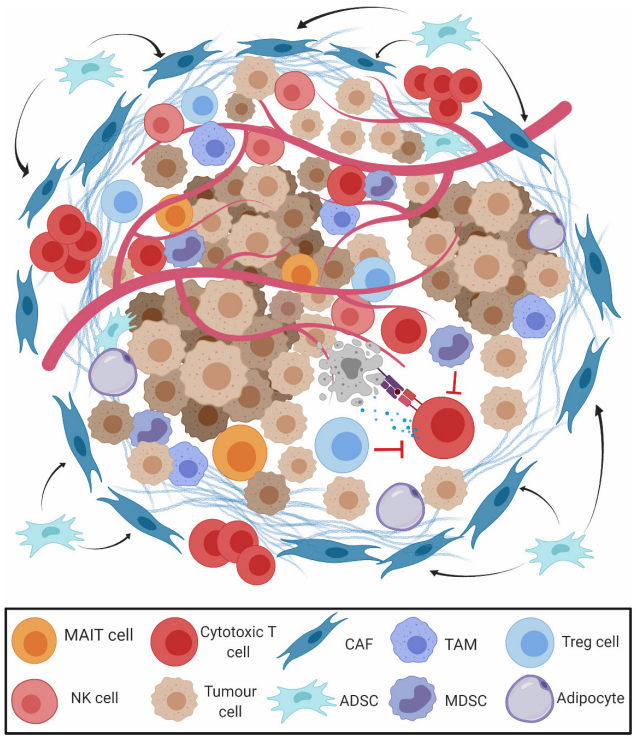

FIGURE 3 | The tumour microenvironment (TME) in oesophageal adenocarcinoma. The presence of M2-polarised tumour-associated-macrophages (TAM), regulatory T cells (Treg), and myeloid derived suppressor cells (MDSCs) restrict the action of cytotoxic $CD8^+$ T cells (CD8 T cells), natural killer (NK) cells, and mucosa associated invariant T (MAIT) cells. Cancer associated fibroblasts (CAFs) and adipocytes derived stem cells (ADSCs) secrete extracellular matrix (ECM) and prevent migration of effector T cells to the tumour parenchyma.

for PDL1 by immunohistochemistry) in OSCC is around 48%, compared to 23% in OAC (78, 79), potentially contributing to T cell exhaustion in the TME. The intermediate TIL infiltration, presence of suppressive cell populations, and immune checkpoint expression is typical of an altered-immunosuppressed tumour profile; suggesting different components of the TME shape the immune landscape of OAC and OSCC.

This distinction between hot, altered, and cold tumours is useful but overly simplifies the complex cancer-immune equilibrium to solely a T cell mediated response. Like many biological characteristics, the immune contexture of oesophageal cancer exists on a patient-specific continuum, and a broader view of anticancer immunity is therefore required. For example, high expression of B cells follicular helper T cell (T_{FH}) markers correlate with survival in colorectal cancer (80). T_{FH} cells secrete CXCL13 which supports organisation of B cells into compartments known as tertiary lymphoid structures (TLS) (81). "Mature" TLS can promote anti-tumour immunity through antibody dependant cellular cytotoxicity and antigen presentation (82, 83) while "immature" TLS may suppress T cell dependant immunity by expressing IL10 and PDL1 (84). Presence of mature TLS in tumours can predict response to immunotherapy in melanoma, sarcoma, and renal cell carcinoma (85–87). More recently, type 2 innate lymphoid cells (ILC2s) have emerged as tissue specific enhancers of anti-cancer immunity and amplify the efficacy of PD1 blockade in pancreatic cancer (88). Evaluating the role of these emerging elements of anti-tumour immunity in oesophageal cancer could describe a more nuanced picture, expanding the immune microenvironment beyond the dichotomy of "hot" and "cold."

The Gut and Tumour Microbiome

There is growing evidence that the diversity and content of the human microbiome is a component of an individual's inherent immune profile. Preclinical studies have long suggested that the response to anti-PD1/PDL1 therapy is contingent on an intact gut microbiome, and this is supported by recent research in melanoma, NSCLC and colorectal cancer patients (89, 90). In these studies, patients that responded to ICI had increased microbial diversity, increased microbial anabolic activity, high levels of *Faecalibacterium* and low levels of *Bacteroidales* in their gut microbiome. Increased $CD8^+$ TILs, higher levels of circulating effector T cells and a preserved cytokine response to PD1 blockade were found in patients with a putative favourable microbiome, suggesting that the gut microbiome influences antitumor immunity (91, 92). The gut microbiota can stimulate chemokine production in human colorectal tumours to influence TIL recruitment, shifting the immune set point (93). Furthermore, 11 low-abundance strains of human commensal bacteria were found to induce interferon-γ producing $CD8^+$ T cells in the intestine, and colonisation enhances efficacy of ICI in mouse models of colorectal cancer (94). In addition to the gut microbiome, the tumour microbiome has also been found to impact the immune setpoint in pancreatic cancer (95). Long term survivors had higher tumour microbiome diversity which shaped a favourable immune microenvironment, with augmented recruitment and activation of T cells.

Of interest, the eradication of *Helicobacter pylori* has been epidemiologically associated with an increase in OAC development, as has gastroesophageal reflux disease (GERD), and both conditions may alter the distal oesophageal microbiome (96–98). Indeed, oesophageal microbial diversity is altered in progression from BO to OAC (99). Microbiome phenotyping of OAC patients revealed a high abundance of *Fusobacterium nucleatum,* relative to normal oesophageal tissue (100, 101). These tumour samples were associated with a high degree of immune infiltration, and upregulation of MHC class II on intratumoral antigen-presenting cells following anti-PD1 therapy (100). In tandem, antibiotic use is associated with a lack of response to PD1 blockade in OSCC along with other cancers, which has been hypothesised to be mediated by intestinal dysbiosis (102).

In NSCLC and melanoma, faecal microbiota transplant (FMT) from human ICI responders improved response to ICI in mice, raising a possibility of a microbiome based therapeutic intervention (91, 92). A pilot study that subjected three ICI-refractory melanoma patients to FMT from ICI-responders has reported preliminary results (103). FMT increased intratumoural $CD8^+$ TILs in recipients, and this translated into a clinical

and radiological response in two of three patients. A similar trial is currently ongoing in oesophageal cancer (NCT04130763). There is a need to further understand the immunomodulatory role of the microbiome in non-T-cell inflamed tumours such as oesophageal cancer, since there may be potential here to discover novel treatment targets or adjuvants, which may ultimately predict and improve clinical response to ICI.

Obesity

Obesity has a multifaceted effect on the immune system and is beginning to be appreciated as a determinant of the cancer-immune set point (104). Excess adiposity drives a state of chronic low-level inflammation, leading to increases in the number of adipose tissue-derived stem cells, fibroblasts, and extracellular matrix in the TME (105). Adipose tissue-derived stem cells exert an immunomodulatory role through suppression of NK cell, B cell, and cytokine responses (106) and contribute to interstitial fibrosis (107, 108). In preclinical models of obesity associated cancers, obesity increases levels of MDSCs, M2-polarised macrophages and tolerogenic dendritic cells in the TME (109, 110). Given the strong relationship between obesity and OAC development, OAC is uniquely poised as a model for understanding the interplay between obesity and anticancer immunity (111, 112). In obese OAC patients, effector T cells are found to preferentially migrate to the omentum and the liver rather than infiltrating OAC tumours (113, 114). This is mediated by the CX3CL1 chemokine and may contribute to the non-T-cell inflamed immune profile of OAC (115).

The role of obesity in the cancer-immune set point has clinical implications. The protective effect of mild obesity (30–34.9 kg/m^2) has also been noted in certain cancers, termed the "Obesity Paradox" (116), where obesity is associated with prolonged survival in melanoma and NSCLC patients treated with immunotherapy (117). This mechanism has been proposed to involve leptin signalling, which drives T cell exhaustion, increases PD1 expression and impairs effector capacity. This attenuates antitumor immunity and promotes tumour progression but concurrently increases sensitivity to PD1 blockade (118). This is paradoxical, as an impaired immune response would be expected to decrease the efficacy of immunotherapy. Obesity associated immune alterations also provide targets for therapy; M2 polarisation of macrophages can be prevented by specific inhibitors and apoptosis of obesity associated MDSC populations in the TME can be induced by liver X receptor-β (LXRβ) agonists (110, 119). A combinatorial approach to immunotherapy may be useful in obesity associated cancers, including OAC.

Host Genetics

Genetic variation in immune response genes has been hypothesised to contribute to the inherent immune profile of a tumour and the immune set point of a cancer patient (22). An expression quantitative trait loci (eQTL) analysis found that common germline genetic variants can influence immune gene expression in 24 cancer types. Oesophageal cancer was not part of this dataset. Expression of *ERAP2* (endoplasmic reticulum aminopeptidase 2), a pan-cancer gene associated with MHC-I antigen processing, predicted survival in bladder cancer patients receiving ICI therapy (120). A total of 103 germline gene signature QTLs were associated with immune cell abundance in the TME. This highlights that germline genetics are an underappreciated determinant of immune gene expression and immune cell infiltration, potentially providing a new means of stratifying patients for ICI treatment. Patient HLA genotype, particularly heterozygosity of HLA-I alleles (*HLA-A, HLA-B, HLA-C*) is associated with more efficient neoantigen presentation, and extended survival in melanoma patients treated with ICI (121). More recently, HLA evolutionarily divergence as measured by sequence divergence between HLA-I alleles was found to predict ICI response in NSCLC and melanoma (122). No studies have assessed HLA genotype in ICI outcomes in oesophageal cancer. Germline loss-of-function in the *TLR4* gene has been associated with lack of response to chemo- and radiotherapy in breast cancer patients, putatively due to an effect on T cell antigen priming (123). A similar effect has been described in the *P2RX7* purinergic receptor, which activates the *NLRP3* inflammasome to produce IL1β, essential in $CD8^+$ T cell priming (124). Immunogenic cell death involves release of ATP and HMGB1 which bind to *TLR4* and *P2RX7,* respectively, to promote tumour antigen presentation. However, in both subtypes of oesophageal cancer, loss-of-function in *TLR4* was unexpectedly associated with improved cancer-specific survival (71). Loss-of-function mutations in *P2XR7* were not associated with a survival difference but were associated with intratumoral T_{reg} cell infiltration (71). Most research has focused on the tumour as a genomic predictor of response to ICI while the host genome has been left relatively unexplored. Future work should further elucidate the effect of germline genetic variation on the cancer-immune set point in oesophageal cancer, as there is evidence that oesophageal cancer may have unique traits which may prove useful in predicting ICI responses.

Viral Infection

Tumours secondary to viral infection, such as Epstein Barr Virus (EBV), or Human Papilloma Virus (HPV) can also express neoantigens derived from viral open reading frames (125, 126). The "EBV associated" gastric cancer subset has increased PDL1 expression, immune cell signalling, *PIK3CA* mutations, and reliable response to ICI (127). HPV-associated oropharyngeal cancer is associated with increased PDL1 expression and durable responses to immunotherapy (15, 128). OAC may also be associated with EBV in 0–6% of cases (129–131), and although this link is less robust than with gastric cancer, EBV tumour testing may represent a potential predictive biomarker to ICI (132). HPV has also been associated with OSCC in numerous case studies, especially in Asian populations (131, 133) but this association may reflect the worldwide prevalence of HPV rather than a causal relationship (26, 134). Although specific viral antigens have not yet been identified as common predictive markers in either subtype of oesophageal cancer, direct administration of viral antigens has shown potential in boosting general anti-tumour immunity (135). In a recent study, intratumoral injection of an unadjuvanted influenza vaccine reduced growth in preclinical models of melanoma and NSCLC

and augmented PD1 blockade. Vaccination increased levels of tumour antigen-specific $CD8^+$ T cells and dendritic cells in the TME, effectively converting a tumour from immunologically "cold" to "hot." Data from 300 patients with lung cancer showed that those who received influenza vaccination had a longer overall survival time (136). This strategy presents a cost-effective way to potentially shift the immune set point and transform oesophageal cancer to a T cell inflamed phenotype. However, further study is required since it is also observed that vaccination may increase risk for adverse immune events in cancer patients receiving ICI therapy (137).

Wider Environmental Factors

Immunity in humans can also be influenced by wider environmental exposures including drug intake, sun exposure, diet, and smoking. Chronic statin therapy, for example, is associated with altered response to the influenza vaccine in older people (138). Decreased exposure to sunlight is associated with increased serum levels of IL6 and C-reactive protein (139). This may be linked to vitamin D metabolism, as the *VDR* (vitamin D receptor) has differential seasonal expression (139). Vitamin D-*VDR* activation suppresses Wnt signalling and promotes anti-tumour immunity in melanoma (140), and expression of an enzyme that degrades vitamin D (*CYP24*) is a poor prognostic marker in OSCC (141), suggesting that vitamin D may be a link between diet, sun exposure and immunity. The incidence of both NSCLC and OSCC is associated with tobacco consumption and the carcinogenic effects of smoking confers a unique mutational signature (24). This signature is associated with response to PD1 blockade in NSCLC (142). In OSCC, however, smoking status was not associated with TIL frequency or PDL1 expression (143), suggesting a less robust relationship between smoking and anti-cancer immunity.

The molecular pathological epidemiology (MPE) framework can help integrate these complex dietary, lifestyle, environmental, and microbiome factors with multi-omic data to create a complete picture of the immune set point in oesophageal cancer (144). Such an approach has associated high levels of plasma 25-hydroxyl vitamin D with a lower risk of colorectal cancer with an intense T cell infiltrate (145). MPE approaches can also integrate microbiome data with immune phenotypes; *Fusobacterium Nucleatum* colonisation is associated with less immune infiltration in human colorectal tumours and may impair NK cell cytotoxicity (146, 147). This MPE framework can be used to evaluate the relationship between microbiome, environmental factors and immunity in oesophageal cancer, which can further aid understanding of an individual's immune set point.

IMMUNOTHERAPY TRIALS IN OESOPHAGEAL CANCER

Multiple clinical trials have evaluated PD1/PDL1 blockade, both alone and in combination in patients with OAC (**Table 1**). Tumour expression of PDL1, as determined by the combined positive score (CPS; the number of PDL1 staining cells divided

TABLE 1 | Completed clinical trials of immunotherapy in oesophageal cancer.

Study	Phase	Disease setting	Prior lines	Intervention	Results
Doi et al. (148) (KEYNOTE 028)	Ib	Advanced OAC ($n = 27$) and OSCC ($n = 65$)	≥2	Pembrolizumab	ORR = 24/83 (30%)
Janjigian et al. (149) (CheckMate−032)	I/II	Advanced OAC ($n = 59$), GEJC ($n = 75$) and GC ($n = 19$)	≥2	Nivolumab + Ipilimumab vs. Nivolumab	ORR = 24 vs. 12% Median OS = 6.9 vs. 4.8 mo
Fuchs et al. (150) (KEYNOTE-059)	II	GEJC ($n = 133$) or GC ($n = 126$)	≥2	Pembrolizumab	ORR = 11.6% in PD-L1$^+$ patients, 15.5% in PD-L1$^-$ patients
Shitara et al. (151) (KEYNOTE-061)	III	Advanced GEJC ($n = 89$) or GC ($n = 207$)	1	Pembrolizumab vs. Paclitaxel	Median OS 9.1 vs. 8.3 mo (HR: 0.82; $p = 0.0421$)
Shah et al. (152) (KEYNOTE-180)	II	Advanced OAC ($n = 58$) and OSCC ($n = 63$)	≥2	Pembrolizumab vs. Placebo	ORR = 12/21 (9.9%)
Janjigian et al. (153) (NCT0295453)	II	HER2+ advanced gastroesophageal adenocarcinoma ($n = 24$)	None	pembrolizumab, trastuzumab plus chemotherapy	ORR = 20/24 (83%) Median PFS = 11.4 mo
Kudo et al. (154)	II	Advanced OSCC ($n = 64$)	1	Nivolumab	ORR = 11/64 (17%)
Kang et al. (155) (ATTRACTION-2)	III	Advanced GEJC or GC	≥2	Nivolumab vs. placebo	Median OS 5.3 vs. 4.14 mo (HR = 0.63, $p < 0.0001$)
Kato et al. (78) (ATTRACTION-3)	III	Advanced OSCC ($n = 419$)	1	Nivolumab vs. Investigator's choice of chemotherapy	Median OS 10.9 vs. 8.4 mo (HR: 0.77 $p = 0.019$)
Kojima et. al. (156) (KEYNOTE-181)	III	Advanced OAC ($n = 227$) and OSCC ($n = 401$)	1	Pembrolizumab vs. Investigators choice of chemotherapy	Median OS 9.3 vs. 6.7 mo (HR: 0.69, $p = 0.0074$) No difference in ITT group

OAC, oesophageal adenocarcinoma; OSCC, oesophageal squamous cell carcinoma; GEJC, gastroesophageal junction carcinoma; ORR, objective response rate; OS, overall survival; PFS, Progression-free survival; HR, hazard ratio; ITT, intention-to-treat; mo, month.

by the total number of viable tumour cells, multiplied by 100) has been used to select and stratify patients on ICI trials (157). Early trials have established the safety of the anti-PD1 agents pembrolizumab and nivolumab in the chemorefractory setting. The phase 1/2 CHECKMATE-032 study investigated the role of nivolumab and/or ipilimumab in oesophageal and gastric cancer and included 26 patients with OAC (149). It found an objective response rate (ORR) of 24% in patients treated with nivolumab and ipilimumab, and this was 31% in patients with PDL1 positive (>1%) tumours. The ATTRACTION-2, phase III study, found that nivolumab improved overall survival (OS; 5.2 vs. 4.1 months, $p < 0.0001$) in heavily pretreated gastric (GC) or gastroesophageal junction cancer (GEJC). A limitation of this trial was that it only enrolled Asian patients, which have been shown to have a different tumour immune signatures, and better outcomes in GEJC clinical trials compared to non-Asian patients (158). In the KEYNOTE-059 phase II study of pembrolizumab in previously treated GC or GEJC, the ORR was 11.6%, with a longer median duration of response in $PDL1^+$ patients (16.3 vs. 6.9 months) (150). Based on these results, the FDA granted approval of pembrolizumab in recurrent GC or GEJC that overexpresses PDL1. In the phase 3 KEYNOTE-181 trial, pembrolizumab as second-line therapy for advanced oesophageal cancer (OAC/OSCC) did not improve OS in the whole population, compared to chemotherapy, but did improve survival for patients with strong expression of PDL1 (CPS $\geq$10) (156).

The phase Ib KEYNOTE-028 study evaluated the safety of pembrolizumab in PDL1 positive oesophageal cancer, the majority (65/92; 78%) of which were OSCC (148). The ORR was 30% and response was correlated to an interferon-γ gene expression signature. In KEYNOTE-181, a trend was observed favouring responses in patients with OSCC (156). This, along with the results of KEYNOTE-180 led to the FDA approval of pembrolizumab in metastatic OSCC with a CPS $\geq$10 after $\geq$1 line of therapy. Nivolumab was also evaluated in chemorefractory OSCC in a phase II trial, showing a modest ORR (17%) but manageable toxicity (154). More recently, the ATTRACTION-3 phase III study investigated the use of nivolumab in the second line treatment of advanced OSCC (78). Patients in the Nivolumab arm had a prolonged OS (10.9 vs. 8.4 months, $p = 0.019$), and less toxicity compared to chemotherapy regardless of PDL1 status. However, most (96%) patients were of Asian ethnicity, potentially limiting applicability to wider patient populations.

Future Combination Approaches

Combining immunotherapy with chemotherapy, radiotherapy or targeted therapy is currently being investigated to boost the modest response rate of oesophageal cancer to ICI. The precise delivery of radiotherapy and the resulting induction of immunogenic cell death may convert a tumour into an *in-situ* vaccine through the release of damage-associated molecular patterns (DAMPs) (157). Calreticulin, ATP and HMGB1 are all DAMPs released by radiation-induced cell death that promote efficient neoantigen processing by antigen presenting cells and priming of $CD8^+$ T cells (159). DNA released following radiation-induced cell damage can stimulate the cGAS-STING pathway, triggering type I interferon production (160, 161). Finally, radiotherapy can upregulate pre-existing neoantigen expression, and remodel the cellular composition of the TME (162). These effects enhance tumour immunogenicity and form the preclinical rationale of ongoing trials of ICI and chemoradiotherapy in resectable oesophageal cancer (NCT02735239).

There is also evidence that trastuzumab, a HER2 targeted therapy can have a synergistic effect with ICI. A phase II trial of 1st line pembrolizumab alongside trastuzumab and chemotherapy in $HER2^+$ OAC and GC found an encouraging ORR of 87% (153). This may be related to induction of immunogenic cell death by trastuzumab, releasing neoantigens, and stimulating a specific $CD8^+$ T cell response (163). This prompted the opening of the larger phase III KEYNOTE-811 trial (NCT03615326) which is currently recruiting patients. Cytotoxic chemotherapy can have genotoxic effects and general novel tumour neoantigens. Other cytotoxic agents (anthracyclines, cyclophosphamide, oxaliplatin, and taxanes) induce immunogenic cell death, increasing tumour adjuvanticity (164). This type of ICI combination is being investigated in the phase III KEYNOTE-590 study of pembrolizumab alongside 5-fluorouracil and cisplatin in the first line treatment of locally advanced/metastatic OAC and OSCC (165, 166).

CONCLUDING REMARKS

In spite of many preclinical and clinical studies, immunotherapy in oesophageal cancer currently remains confined to 2nd or 3rd line treatment of metastatic disease, with no unequivocal predictive biomarker available. These modest results are likely due to a high cancer-immune set point, where ICI is not sufficient to drive progression of the cancer immunity cycle. This is despite a high mutational burden in OAC, and an intermediate level of $CD8^+$ TILs in OSCC and OAC, suggesting an altered-immunosuppressed immune profile; where antitumor cytotoxicity is limited by soluble inhibitory mediators and suppressive cell populations in the TME (159). Less well-characterised aspects of the cancer immune set point in including obesity in OAC, and the microbiome in both subtypes, should be further explored as potential determinants of this immunosuppressive phenotype.

Although our knowledge of the individual components of the cancer-immune set point in oesophageal cancer has grown, the macroscopic picture is still poorly understood. We propose a systems biology approach integrating multi-omic tumour profiling with individual patient data to accurately predict antitumor immune responses. Optimally such an approach combines tumour genomics, immunohistochemistry, and peripheral blood assays to generate a "Cancer Immunogram" and integrate complex immune biomarkers (167). This paradigm has been applied in NSCLC, where whole-exome sequencing and RNA-seq separated 20 patients into personalised Immunograms (168), a proof-of-concept that such an approach may be clinically feasible. However, integrating these genome and immune based biomarkers with environmental exposures is needed to

fully account for interpatient variability in immunotherapy response. In this sense, the MPE framework may prove vital in evaluating the role of obesity, the microbiome and other external determinants of the immune set point in oesophageal tumours.

Conceptualising the cancer-immune set point provides clinicians and researchers with a crucial framework connecting the innumerate factors that determine response to immunotherapy. The immune landscape of oesophageal cancer is heterogeneous and is contingent on both patient- and tumour-specific variables. We anticipate that successful immuno-oncology drug development in oesophageal cancer will be dependent on leveraging knowledge of these factors to develop personalised treatment strategies, involving a combination of ICI and radiation or systemic therapy to elicit a T cell inflamed phenotype.

AUTHOR CONTRIBUTIONS

RP and MD wrote the first draft of this paper. All authors contributed to editing and preparation of the final draft.

FUNDING

MD funded by Health Research Board (grant: HRB-HRA-2015-1143).

ACKNOWLEDGMENTS

This paper was adapted from a thesis in the MSc in Molecular Medicine in Trinity College Dublin. Images were generated using BioRender (biorender.com).

REFERENCES

1. Arnold, Soerjomataram M, Ferlay IJ, Forman D. Global incidence of oesophageal cancer by histological subtype in 2012. *Gut*. (2015) 64:381–7. doi: 10.1136/gutjnl-2014-308124
2. Anderson LA, Watson RGP, Murphy SJ, Johnston BT, Comber H, Mc Guigan J, et al. risk factors for barrett's oesophagus and oesophageal adenocarcinoma: results from the FINBAR study. *World J Gastroenterol*. (2007) 13:1585–94. doi: 10.3748/wjg.v13.i10.1585
3. Quante, Bhagat M, Abrams G, Marache JA, Good F, Lee P, et al. Bile acid and inflammation activate gastric cardia stem cells in a mouse model of Barrett-like metaplasia. *Cancer Cell*. (2012) 21:36–51. doi: 10.1016/j.ccr.2011.12.004
4. Trivers KF, Sabatino SA, Stewart LS. Trends in esophageal cancer incidence by histology, United States, 1998-2003. *Int J Cancer*. (2008) 123:1422–8. doi: 10.1002/ijc.23691
5. Smyth EC, Lagergren J, Fitzgerald RC, Lordick F, Shah MA, Lagergren P, et al. Oesophageal cancer. *Nat Rev Dis Primers*. (2017) 3:17048. doi: 10.1038/nrdp.2017.48
6. Hur C, Miller M, Kong CY, Dowling EC, Nattinger KJ, Dunn M, et al. Trends in esophageal adenocarcinoma incidence and mortality. *Cancer*. (2013) 119:1149–58. doi: 10.1002/cncr.27834
7. Cunningham D, Allum WH, Stenning SP, Thompson JN, van de Velde CJ, Nicolson M, et al. Perioperative chemotherapy versus surgery alone for resectable gastroesophageal cancer. *N Engl J Med*. (2006) 355:11–20. doi: 10.1056/NEJMoa055531
8. Geh JI, Bond SJ, Bentzen SM, Glynne-Jones R. Systematic overview of preoperative (neoadjuvant) chemoradiotherapy trials in oesophageal cancer: evidence of a radiation and chemotherapy dose response. *Radiother Oncol*. (2006) 78:236–44. doi: 10.1016/j.radonc.2006.01.009
9. Leach DR, Krummel MF, Allison PJ. Enhancement of antitumor immunity by CTLA-4 blockade. *Science*. (1996) 271:1734–6. doi: 10.1126/science.271.5256.1734
10. Hodi FS, O'Day SJ, McDermott DF, Weber RW, Sosman JA, Haanen JB, et al. Improved survival with Ipilimumab in patients with metastatic Melanoma. *N Engl J Med*. (2010) 363:711–23. doi: 10.1056/NEJMoa1003466
11. Iwai Y, Ishida M, Tanaka Y, Okazaki TT, Honjo N. Involvement of PD-L1 on tumor cells in the escape from host immune system and tumor immunotherapy by PD-L1 blockade. *Proc Natl Acad Sci USA*. (2002) 99:12293–7. doi: 10.1073/pnas.192461099
12. Im SJ, Hashimoto M, Gerner MY, Lee J, Kissick HT, Burger MC, et al. Defining CD8+ T cells that provide the proliferative burst after PD-1 therapy. *Nature*. (2016) 537:417–21. doi: 10.1038/nature19330
13. Reck M, Rodriguez-Abreu D, Robinson AG, Hui R, Csoszi T, Fulop A, et al. Pembrolizumab versus chemotherapy for PD-L1-positive non-small-cell lung ccancer. *N Engl J Med*. (2016) 375:1823–33. doi: 10.1056/NEJMoa1606774
14. Robert C, Schachter J, Long GV, Arance A, Grob JJ, Mortier L, et al. Pembrolizumab versus ipilimumab in advanced Melanoma. *N Engl J Med*. (2015) 372:2521–32. doi: 10.1056/NEJMoa1503093
15. Ferris RL, Blumenschein G Jr, Fayette J, Guigay J, Colevas AD, Licitra L, et al. Nivolumab for recurrent squamous-cell Carcinoma of the head and neck. *N Engl J Med*. (2016) 375:1856–67. doi: 10.1056/NEJMoa1602252
16. Rini BI, Plimack ER, Stus V, Gafanov R, Hawkins R, Nosov D, et al. Pembrolizumab plus axitinib versus sunitinib for advanced renal-cell Carcinoma. *N Engl J Med*. (2019) 380:1116–27. doi: 10.1056/NEJMoa1816714
17. Yau T, Kang TK, Kim TY, El-Khoueiry AB, Santoro B, Sangro A, et al. Nivolumab (NIVO) + ipilimumab (IPI) combination therapy in patients (pts) with advanced hepatocellular carcinoma (aHCC): results from checkMate 040. *J Clin Oncol*. (2019) 37(Suppl. 15):4012. doi: 10.1200/JCO.2019.37.15_suppl.4012
18. Overman MJ, Lonardi S, Wong KYM, Lenz HJ, Gelsomino F, Aglietta M, et al. Durable clinical benefit with nivolumab plus ipilimumab in DNA mismatch repair-deficient/microsatellite instability-high metastatic colorectal cancer. *J Clin Oncol*. (2018) 36:773–9. doi: 10.1200/jco.2017.76.9901
19. Motzer RJ, Rini BI, McDermott DF, Arén Frontera O, Hammers HJ, Carducci MA, et al. Nivolumab plus ipilimumab versus sunitinib in first-line treatment for advanced renal cell carcinoma: extended follow-up of efficacy and safety results from a randomised, controlled, phase 3 trial. *Lancet Oncol*. (2019) 20:1370–85. doi: 10.1016/S1470-2045(19)30413-9
20. Alsina M, Moehler M, Lorenzen S. Immunotherapy of esophageal cancer: current status, many trials and innovative strategies. *Oncol Res Treat*. (2018) 41:266–71. doi: 10.1159/000488120
21. Kelly RJ. The emerging role of immunotherapy for esophageal cancer. *Curr Opin Gastroenterol*. (2019) 35:337–43. doi: 10.1097/MOG.0000000000000542
22. Chen DS, Mellman I. Elements of cancer immunity and the cancer-immune set point. *Nature*. (2017) 541:321–30. doi: 10.1038/nature21349
23. Samstein RM, Lee CH, Shoushtari AN, Hellmann MD, Shen R, Janjigian YY, et al. Tumor mutational load predicts survival after immunotherapy across multiple cancer types. *Nat Genet*. (2019) 51:202–6. doi: 10.1038/s41588-018-0312-8
24. Alexandrov LB, Nik-Zainal S, Wedge DC, Aparicio SA, Behjati AV, Bignell GR, et al. Signatures of mutational processes in human cancer. *Nature*. (2013) 500:415–21. doi: 10.1038/nature12477
25. Dulak AM, Stojanov P, Peng S, Lawrence MS, Fox C, Stewart C, et al. Exome and whole-genome sequencing of esophageal adenocarcinoma identifies recurrent driver events and mutational complexity. *Nat Genet*. (2013) 45:478–86. doi: 10.1038/ng.2591
26. Cancer Genome Atlas Research Network, Analysis Working Group, Asan University, BC Cancer Agency, Brigham and Women's Hospital, Broad Institute. Integrated genomic characterization of oesophageal carcinoma. *Nature*. (2017) 541:169–75. doi: 10.1038/nature20805

27. Secrier M, Li X, de Silva N, Eldridge MD, Contino G, Bornschein J, et al. Mutational signatures in esophageal adenocarcinoma define etiologically distinct subgroups with therapeutic relevance. *Nat Genet*. (2016) 48:1131–41. doi: 10.1038/ng.3659
28. Frankell AM, Jammula S, Li X, Contino G, Killcoyne S, Abbas S, et al. The landscape of selection in 551 esophageal adenocarcinomas defines genomic biomarkers for the clinic. *Nat Genet*. (2019) 51:506–16. doi: 10.1038/s41588-018-0331-5
29. Grasso CS, Giannakis M, Wells DK, Hamada T, Mu XJ, Quist M, et al. Genetic mechanisms of immune evasion in colorectal cancer. *Cancer Discov*. (2018) 8:730–49. doi: 10.1158/2159-8290.CD-17-1327
30. Sade-Feldman M, Jiao YJ, Chen JH, Rooney MS, Barzily-Rokni M, Eliane JP, et al. Resistance to checkpoint blockade therapy through inactivation of antigen presentation. *Nat Commun*. (2017) 8:1136. doi: 10.1038/s41467-017-01062-w
31. Krasniqi E, Barchiesi G, Pizzuti L, Mazzotta M, Venuti A, Maugeri-Sacca M, et al. Immunotherapy in HER2-positive breast cancer: state of the art and future perspectives. *J Hematol Oncol*. (2019) 12:111. doi: 10.1186/s13045-019-0798-2
32. Ayoub NM, Al-Shami KM, Yaghan JR. Immunotherapy for HER2-positive breast cancer: recent advances and combination therapeutic approaches. *Breast Cancer*. (2019) 11:53–69. doi: 10.2147/BCTT.S175360
33. Bang YJ, van Cutsem E, Feyereislova A, Chung HC, Shen L, Sawaki A, et al. Trastuzumab in combination with chemotherapy versus chemotherapy alone for treatment of HER2-positive advanced gastric or gastro-oesophageal junction cancer (ToGA): a phase 3, open-label, randomised controlled trial. *Lancet*. (2010) 376:687–97. doi: 10.1016/s0140-6736(10)61121-x
34. Zhao D, Klempner SJ, Chao J. Progress and challenges in HER2-positive gastroesophageal adenocarcinoma. *J Hematol Oncol*. (2019) 12:50. doi: 10.1186/s13045-019-0737-2
35. Hashimoto S, Furukawa S, Hashimoto A, Tsutaho A, Fukao A, Sakamura A, et al. ARF6 and AMAP1 are major targets of KRAS and TP53 mutations to promote invasion, PD-L1 dynamics, and immune evasion of pancreatic cancer. *Proc Natl Acad Sci USA*. (2019) 116:17450–9. doi: 10.1073/pnas.1901765116
36. Hou P, Kapoor A, Zhang Q, Li J, Wu CJ, Li J, et al. Tumor microenvironment remodeling enables bypass of oncogenic KRAS dependency in pancreatic cancer. *Cancer Discov*. (2020) doi: 10.1158/2159-8290.CD-19-0597. [Epub ahead of print].
37. Essakly A, Loeser H, Kraemer M, Alakus H, Chon SH, Zander T, et al. PIK3CA and KRAS Amplification in esophageal adenocarcinoma and their impact on the inflammatory tumor microenvironment and prognosis. *Transl Oncol*. (2020) 13:157–64. doi: 10.1016/j.tranon.2019.10.013
38. Giannakis M, Mu XJ, Shukla SA, Qian ZR, Cohen O, Nishihara R, et al. Genomic correlates of immune-cell infiltrates in colorectal carcinoma. *Cell Rep*. (2016) 15:857–65. doi: 10.1016/j.celrep.2016.03.075
39. Bass AJ, Watanabe H, Mermel CH, Yu S, Perner S, Verhaak RG, et al. SOX2 is an amplified lineage-survival oncogene in lung and esophageal squamous cell carcinomas. *Nat Genet*. (2009) 41:1238–42. doi: 10.1038/ng.465
40. Chen XX, Zhong Q, Liu Y, Yan SM, Chen ZH, Jin SZ, et al. Genomic comparison of esophageal squamous cell carcinoma and its precursor lesions by multi-region whole-exome sequencing. *Nat Commun*. (2017) 8:524. doi: 10.1038/s41467-017-00650-0
41. Salem ME, Puccini A, Xiu J, Raghavan D, Lenz HJ, Korn WM, et al. Comparative molecular analyses of esophageal squamous cell carcinoma, esophageal adenocarcinoma, gastric adenocarcinoma. *Oncologist*. (2018) 23:1319–27. doi: 10.1634/theoncologist.2018-0143
42. Fitzgerald RC, Onwuegbusi BA, Bajaj-Elliott M, Saeed IT, Burnham WR, Farthing MJR. Diversity in the oesophageal phenotypic response to gastro-oesophageal reflux: immunological determinants. *Gut*. (2002) 50:451–9. doi: 10.1136/gut.50.4.451
43. van Sandick JW, Boermeester MA, Gisbertz SS, ten Berge IJ, Out TA, van der Pouw Kraan TC, et al. Lymphocyte subsets and T(h)1/T(h)2 immune responses in patients with adenocarcinoma of the oesophagus or oesophagogastric junction: relation to pTNM stage and clinical outcome. *Cancer Immunol Immunother*. (2003) 52:617–24. doi: 10.1007/s00262-003-0406-7
44. O'Riordan JM, Abdel-latif MM, Ravi N, McNamara D, Byrne PJ, McDonald GS, et al. Reynolds: Proinflammatory cytokine and nuclear factor kappa-B expression along the inflammation-metaplasia-dysplasia-adenocarcinoma sequence in the esophagus. *Am J Gastroenterol*. (2005) 100:1257–64. doi: 10.1111/j.1572-0241.2005.41338.x
45. Kavanagh ME, Conroy MJ, Clarke NE, Gilmartin NT, O'Sullivan KE, Feighery R, et al. Impact of the inflammatory microenvironment on T-cell phenotype in the progression from reflux oesophagitis to Barrett oesophagus and oesophageal adenocarcinoma. *Cancer Lett*. (2016) 370:117–24. doi: 10.1016/j.canlet.2015.10.019
46. Sen M, Hahn F, Black TA, deMarshall M, Porter W, Snowden E, et al. Flow based single cell analysis of the immune landscape distinguishes Barrett's esophagus from adjacent normal tissue. *Oncotarget*. (2019) 10:3592–604. doi: 10.18632/oncotarget.26911
47. Derks, Nason KS, Liao, Stachler MD, Liu KX, Liu JB, et al. Epithelial PD-L2 expression marks barrett's esophagus and esophageal adenocarcinoma. *Cancer Immunol Res*. (2015) 3:1123–9. doi: 10.1158/2326-6066.CIR-15-0046
48. Somja J, Demoulin S, Roncarati P, Herfs M, Bletard N, Delvenne P, et al. dendritic cells in barrett's esophagus carcinogenesis: an inadequate microenvironment for antitumor immunity? *Am J Pathol*. (2013) 182:2168–79. doi: 10.1016/j.ajpath.2013.02.036
49. Kavanagh ME, Conroy MJ, Clarke NE, Gilmartin NT, Feighery, MacCarthy R, et al. Lysaght: Altered T cell migratory capacity in the progression from Barrett oesophagus to oesophageal adenocarcinoma. *Cancer Microenviron*. (2019) 12:57–66. doi: 10.1007/s12307-019-00220-6
50. Hanahan D, Coussens LM. Accessories to the crime: functions of cells recruited to the tumor microenvironment. *Cancer Cell*. (2012) 21:309–22. doi: 10.1016/j.ccr.2012.02.022
51. Balkwill FR, Capasso M, Hagemann T. The tumor microenvironment at a glance. *J Cell Sci*. (2012) 125:5591–6. doi: 10.1242/jcs.116392
52. Zheng Y, Li Y, Lian J, Yang H, Li F, Zhao S, et al. TNF-α-induced Tim-3 expression marks the dysfunction of infiltrating natural killer cells in human esophageal cancer. *J Transl Med*. (2019) 17:165. doi: 10.1186/s12967-019-1917-0
53. Thomas ML, Badwe RA, Deshpande RK, Samant UC, Chiplunkar VS. Role of adhesion molecules in recruitment of Vδ1 T cells from the peripheral blood to the tumor tissue of esophageal cancer patients. *Cancer Immunol Immunother*. (2001) 50:218–25. doi: 10.1007/s002620100190
54. Treiner E, Duban L, Moura IC, Hansen T, Gilfillan S, Lantz O. Mucosal-associated invariant T (MAIT) cells: an evolutionarily conserved T cell subset. *Microbes Infect*. (2005) 7:552–9. doi: 10.1016/j.micinf.2004.12.013
55. Camus M, Tosolini M, Mlecnik B, Pages F, Kirilovsky A, Berger A, et al. Coordination of intratumoral immune reaction and human colorectal cancer recurrence. *Cancer Res*. (2009) 69:2685–93. doi: 10.1158/0008-5472.can-08-2654
56. Stein AV, Dislich B, Blank A, Guldener L, Kroll D, Seiler CA, et al. High intratumoural but not peritumoural inflammatory host response is associated with better prognosis in primary resected oesophageal adenocarcinomas. *Pathology*. (2017) 49:30–7. doi: 10.1016/j.pathol.2016.10.005
57. McCormick Matthews LH, Noble F, Tod J, Jaynes E, Harris S, Primrose JN, et al. Systematic review and meta-analysis of immunohistochemical prognostic biomarkers in resected oesophageal adenocarcinoma. *Br J Cancer*. (2015) 113:107–18. doi: 10.1038/bjc.2015.179
58. Noble F, Mellows T, McCormick Matthews LH, Bateman AC, Harris S, Underwood TJ, et al. Tumour infiltrating lymphocytes correlate with improved survival in patients with oesophageal adenocarcinoma. *Cancer Immunol Immunother*. (2016) 65:651–62. doi: 10.1007/s00262-016-1826-5
59. Ostroumov D, Fekete-Drimusz N, Saborowski M, Kuhnel F, Woller N. CD4 and CD8 T lymphocyte interplay in controlling tumor growth. *Cell Mol Life Sci*. (2018) 75:689–713. doi: 10.1007/s00018-017-2686-7
60. Dunne MR, Michielsen AJ, O'Sullivan KE, Cathcart MC, Feighery R, Doyle B, et al. HLA-DR expression in tumor epithelium is an independent prognostic indicator in esophageal adenocarcinoma patients. *Cancer Immunol Immunother*. (2017) 66:841–50. doi: 10.1007/s00262-017-1983-1
61. Gentles AJ, Newman AM, Liu CL, Bratman SV, Feng W, Kim D, et al. The prognostic landscape of genes and infiltrating immune cells across human cancers. *Nat Med*. (2015) 21:938–945. doi: 10.1038/nm.3909

62. Melo AM, O'Brien AM, Phelan JJ, Kennedy SA, Wood NAW, Veerapen N, et al. Mucosal-associated invariant T cells display diminished effector capacity in oesophageal adenocarcinoma. *Front Immunol.* (2019) 10:1580. doi: 10.3389/fimmu.2019.01580
63. Underwood TJ, Hayden AL, Derouet M, Garcia E, Noble F, White MJ, et al. Cancer-associated fibroblasts predict poor outcome and promote periostin-dependent invasion in oesophageal adenocarcinoma. *J Pathol.* (2015) 235:466–77. doi: 10.1002/path.4467
64. Kato T, Noma K, Ohara T, Kashima H, Katsura Y, Sato H, et al. Cancer-associated fibroblasts affect intratumoral CD8+ and FoxP3+ T cells via IL6 in the tumor microenvironment. *Clin Cancer Res.* (2018) 24:4820–33. doi: 10.1158/1078-0432.CCR-18-0205
65. Colegio OR, Chu NQ, Szabo AL, Chu T, Rhebergen AM, Jairam V, et al. Functional polarization of tumour-associated macrophages by tumour-derived lactic acid. *Nature.* (2014) 513:559–63. doi: 10.1038/nature13490
66. Miyashita T, Tajima H, Shah FA, Oshima M, Makino I, Nakagawara H, et al. impact of inflammation–metaplasia–adenocarcinoma sequence and inflammatory microenvironment in esophageal carcinogenesis using surgical rat models. *Ann Surg Oncol.* (2014) 21:2012–9. doi: 10.1245/s10434-014-3537-5
67. Gabrilovich DI, Nagaraj S. Myeloid-derived suppressor cells as regulators of the immune system. *Nat Rev Immunol.* (2009) 9:162–74. doi: 10.1038/nri2506
68. Gao J, Wu Y, Su Z, Amoah Barnie P, Jiao Z, Bie Q, et al. Infiltration of alternatively activated macrophages in cancer tissue is associated with MDSC and Th2 polarization in patients with esophageal cancer. *PLoS ONE.* (2014) 9:e104453. doi: 10.1371/journal.pone.0104453
69. Ichihara F, Kono K, Takahashi A, Kawaida H, Sugai H, Fujii H. Increased populations of regulatory T cells in peripheral blood and tumor-infiltrating lymphocytes in patients with gastric and esophageal cancers. *Clin Cancer Res.* (2003) 9:4404.
70. Kono K, Kawaida H, Takahashi A, Sugai H, Mimura K, Miyagawa N, et al. CD4(+)CD25high regulatory T cells increase with tumor stage in patients with gastric and esophageal cancers. *Cancer Immunol Immunother.* (2006) 55:1064–71. doi: 10.1007/s00262-005-0092-8
71. Vacchelli E, Semeraro M, Enot DP, Chaba K, Poirier Colame V, Dartigues P, et al. Negative prognostic impact of regulatory T cell infiltration in surgically resected esophageal cancer post-radiochemotherapy. *Oncotarget.* (2015) 6:20840–50. doi: 10.18632/oncotarget.4428
72. Cho Y, Miyamoto M, Kato K, Fukunaga A, Shichinohe T, Kawarada Y, et al. CD4+ and CD8+ T cells cooperate to improve prognosis of patients with esophageal squamous cell carcinoma. *Cancer Res.* (2003) 63:1555–9.
73. Schumacher K, Haensch W, Roefzaad C, Schlag PM. Prognostic significance of activated CD8(+) T cell infiltrations within esophageal carcinomas. *Cancer Res.* (2001) 61:3932–6.
74. Jiang D, Liu Y, Wang H, Wang H, Song Q, Sujie A, et al. Tumour infiltrating lymphocytes correlate with improved survival in patients with esophageal squamous cell carcinoma. *Sci Rep.* (2017) 7:44823. doi: 10.1038/srep44823
75. Shigeoka M, Urakawa N, Nakamura T, Nishio M, Watajima T, Kuroda D, et al. Tumor associated macrophage expressing CD204 is associated with tumor aggressiveness of esophageal squamous cell carcinoma. *Cancer Sci.* (2013) 104:1112–9. doi: 10.1111/cas.12188
76. Yagi T, Baba Y, Koga Y, Uchihara T, Kiyozumi Y, Sawayama H, et al. Abstract 4742: role of tumor-associated macrophages in esophageal cancer: PD-L1 expression and prognosis. *Cancer Res.* (2018) 78(Suppl. 13):4742. doi: 10.1158/1538-7445.AM2018-4742
77. Chen X, Wang L, Li P, Song M, Qin G, Gao Q, et al. Zhang: Dual TGF-β and PD-1 blockade synergistically enhances MAGE-A3-specific CD8+ T cell response in esophageal squamous cell carcinoma. *Int J Cancer.* (2018) 143:2561–74. doi: 10.1002/ijc.31730
78. Kato K, Cho BC, Takahashi M, Okada M, Lin MC, Chin K, et al. Nivolumab versus chemotherapy in patients with advanced oesophageal squamous cell carcinoma refractory or intolerant to previous chemotherapy (ATTRACTION-3): a multicentre, randomised, open-label, phase 3 trial. *Lancet Oncol.* (2019) 20:1506–17. doi: 10.1016/S1470-2045(19)30626-6
79. Svensson MC, Borg, Zhang D, Hedner C, Nodin C, Uhlén B, et al. Jirström: Expression of PD-L1 and PD-1 in chemoradiotherapy-naïve esophageal and gastric adenocarcinoma: relationship with mismatch repair status and survival. *Front Oncol.* (2019) 9:136. doi: 10.3389/fonc.2019.00136
80. Bindea G, Mlecnik B, Tosolini M, Kirilovsky A, Waldner M, Obenauf AC, et al. Galon: Spatiotemporal dynamics of intratumoral immune cells reveal the immune landscape in human cancer. *Immunity.* (2013) 39:782–95. doi: 10.1016/j.immuni.2013.10.003
81. Sautès-Fridman C, Petitprez F, Calderaro J, Fridman WH. Tertiary lymphoid structures in the era of cancer immunotherapy. *Nat Rev Cancer.* (2019) 19:307–25. doi: 10.1038/s41568-019-0144-6
82. deFalco J, Harbell M, Manning-Bog A, Baia G, Scholz A, Millare B, et al. Non-progressing cancer patients have persistent B cell responses expressing shared antibody paratopes that target public tumor antigens. *Clin Immunol.* (2018) 187:37–45. doi: 10.1016/j.clim.2017.10.002
83. Bruno TC, Ebner PJ, Moore BL, Squalls OG, Waugh KA, Eruslanov EB, et al. Antigen-presenting intratumoral B cells affect CD4(+) TIL phenotypes in non-small cell lung cancer patients. *Cancer Immunol Res.* (2017) 5:898–907. doi: 10.1158/2326-6066.cir-17-0075
84. Shalapour S, Font-Burgada J, Di Caro G, Zhong Z, Sanchez-Lopez E, Dhar D, et al. Immunosuppressive plasma cells impede T-cell-dependent immunogenic chemotherapy. *Nature.* (2015) 521:94–8. doi: 10.1038/nature14395
85. Petitprez F, de Reyniès A, Keung EZ, Chen TW, Sun CM, Calderaro J, et al. B cells are associated with survival and immunotherapy response in sarcoma. *Nature.* (2020) 577:556–60. doi: 10.1038/s41586-019-1906-8
86. Cabrita R, Lauss M, Sanna A, Donia M, Skaarup Larsen M, Mitra S, et al. Tertiary lymphoid structures improve immunotherapy and survival in melanoma. *Nature.* (2020) 577:561–5. doi: 10.1038/s41586-019-1914-8
87. Helmink BA, Reddy SM, Gao J, Zhang S, Basar R, Thakur R, et al. B cells and tertiary lymphoid structures promote immunotherapy response. *Nature.* (2020) 577:549–55. doi: 10.1038/s41586-019-1922-8
88. Moral JA, Leung J, Rojas LA, Ruan J, Zhao J, Sethna Z, et al. ILC2s amplify PD-1 blockade by activating tissue-specific cancer immunity. *Nature.* (2020) 579:130–5. doi: 10.1038/s41586-020-2015-4
89. Iida N, Dzutsev A, Stewart CA, Smith L, Bouladoux N, Weingarten RA, et al. Commensal bacteria control cancer response to therapy by modulating the tumor microenvironment. *Science.* (2013) 342:967–70. doi: 10.1126/science.1240527
90. Sivan A, Corrales L, Hubert N, Williams JB, Aquino-Michaels K, Earley ZM, et al. Commensal bifidobacterium promotes antitumor immunity and facilitates anti-PD-L1 efficacy. *Science.* (2015) 350:1084–9. doi: 10.1126/science.aac4255
91. Gopalakrishnan V, Spencer CN, Nezi L, Reuben A, Andrews MC, Karpinets TV, et al. Gut microbiome modulates response to anti–PD-1 immunotherapy in melanoma patients. *Science.* (2018) 359:97–103. doi: 10.1126/science.aan4236
92. Routy B, Le Chatelier E, Derosa L, Duong CPM, Alou MT, Daillere R, et al. Gut microbiome influences efficacy of PD-1-based immunotherapy against epithelial tumors. *Science.* (2018) 359:91–7. doi: 10.1126/science.aan3706
93. Cremonesi E, Governa V, Garzon JFG, Mele V, Amicarella F, Muraro MG, et al. Gut microbiota modulate T cell trafficking into human colorectal cancer. *Gut.* (2018) 67:1984–94. doi: 10.1136/gutjnl-2016-313498
94. Tanoue T, Morita S, Plichta DR, Skelly AN, Suda W, Sugiura Y, et al. A defined commensal consortium elicits CD8 T cells and anti-cancer immunity. *Nature.* (2019) 565:600–5. doi: 10.1038/s41586-019-0878-z
95. Riquelme E, Zhang Y, Zhang L, Montiel M, Zoltan M, Dong W, et al. Tumor microbiome diversity and composition influence pancreatic cancer outcomes. *Cell.* (2019) 178:795–806.e12. doi: 10.1016/j.cell.2019.07.008
96. Islami F, Kamangar K. Helicobacter pylori and esophageal cancer risk: a meta-analysis. *Cancer Prev Res.* (2008) 1:329–38. doi: 10.1158/1940-6207.capr-08-0109
97. Nie S, Chen T, Yang X, Huai P, Lu M. Association of Helicobacter pylori infection with esophageal adenocarcinoma and squamous cell carcinoma: a meta-analysis. *Dis Esophagus.* (2014) 27:645–53. doi: 10.1111/dote.12194
98. Amir I, Konikoff FM, Oppenheim M, Gophna U, Half EE. Gastric microbiota is altered in oesophagitis and Barrett's oesophagus and further modified by proton pump inhibitors. *Environ Microbiol.* (2014) 16:2905–14. doi: 10.1111/1462-2920.12285

99. Snider EJ, Compres G, Freedberg DE, Khiabanian H, Nobel YR, Stump S, et al. Alterations to the esophageal microbiome associated with progression from barrett's esophagus to esophageal adenocarcinoma. *Cancer Epidemiol Biomarkers Prev*. (2019) 28:1687–93. doi: 10.1158/1055-9965.EPI-19-0008
100. Zhang C, Thakkar PV, Sharma P, Vennelaganti S, Betel D, Shah MA. Abstract 2826: understanding associations among local microbiome, immune response, and efficacy of immunotherapy in esophageal cancer. *Cancer Res*. (2019) 79(Suppl. 13):2826. doi: 10.1158/1538-7445.AM2019-2826
101. Yamamura K, Baba Y, Nakagawa S, Mima K, Miyake K, Nakamura K, et al. Human microbiome fusobacterium nucleatum in esophageal cancer tissue is associated with prognosis. *Clin Cancer Res*. (2016) 22:5574–81. doi: 10.1158/1078-0432.CCR-16-1786
102. Guo JC, Lin CC, Lin CY, Hsieh MS, Kuo HY, Lien MY, et al. Neutrophil-to-lymphocyte ratio and use of antibiotics associated with prognosis in esophageal squamous cell carcinoma patients receiving immune checkpoint inhibitors. *Anticancer Res*. (2019) 39:5675–82. doi: 10.21873/anticanres.13765
103. Baruch EN, Youngster I, Ortenberg R, Ben-Betzalel G, Katz LH, Lahat A, et al. Abstract CT042: fecal microbiota transplantation (FMT) and re-induction of anti-PD-1 therapy in refractory metastatic melanoma patients - preliminary results from a phase I clinical trial (NCT03353402). *Cancer Res*. (2019) 79(Suppl. 13):CT042. doi: 10.1158/1538-7445.AM2019-CT042
104. Chen DS, Mellman I. Oncology meets immunology: the cancer-immunity cycle. *Immunity*. (2013) 39:1–10. doi: 10.1016/j.immuni.2013.07.012
105. Incio J, Liu H, Suboj P, Chin SM, Chen IX, Pinter M, et al. Obesity-induced inflammation and desmoplasia promote pancreatic cancer progression and resistance to chemotherapy. *Cancer Discov*. (2016) 6:852–69. doi: 10.1158/2159-8290.CD-15-1177
106. Razmkhah M, Mansourabadi Z, Mohtasebi MS, Talei AR, Ghaderi A. Cancer and normal adipose-derived mesenchymal stem cells (ASCs): do they have differential effects on tumor and immune cells? *Cell Biol Int*. (2018) 42:334–43. doi: 10.1002/cbin.10905
107. Jotzu C, Alt E, Welte G, Li J, Hennessy BT, Devarajan E, et al. Adipose tissue-derived stem cells differentiate into carcinoma-associated fibroblast-like cells under the influence of tumor-derived factors. *Anal Cell Pathol*. (2010) 33:61–79. doi: 10.3233/acp-clo-2010-0535
108. Bochet L, Lehuede C, Dauvillier S, Wang YY, Dirat B, Laurent V, et al. Adipocyte-derived fibroblasts promote tumor progression and contribute to the desmoplastic reaction in breast cancer. *Cancer Res*. (2013) 73:5657–68. doi: 10.1158/0008-5472.can-13-0530
109. Wunderlich CM, Ackermann PJ, Ostermann AL, Adams-Quack P, Vogt MC, Tran M-Y, et al. Wunderlich: Obesity exacerbates colitis-associated cancer via IL-6-regulated macrophage polarisation and CCL-20/CCR-6-mediated lymphocyte recruitment. *Nat Commun*. (2018) 9:1646. doi: 10.1038/s41467-018-03773-0
110. Naik A, Monjazeb AM, Decock J. The obesity paradox in cancer, tumor immunology, and immunotherapy: potential therapeutic implications in triple negative breast cancer. *Front Immunol*. (2019) 10:1940. doi: 10.3389/fimmu.2019.01940
111. Renehan AG, Tyson M, Egger M, Heller RF, Zwahlen M. Body-mass index and incidence of cancer: a systematic review and meta-analysis of prospective observational studies. *Lancet*. (2008) 371:569–78. doi: 10.1016/s0140-6736(08)60269-x
112. Beddy P, Howard J, McMahon C, Knox M, de Blacam C, Ravi N, et al. Association of visceral adiposity with oesophageal and junctional adenocarcinomas. *Br J Surg*. (2010) 97:1028–34. doi: 10.1002/bjs.7100
113. Lysaght, Allott J EH, Donohoe CL, Howard JM, Pidgeon GP, Reynolds VJ. T lymphocyte activation in visceral adipose tissue of patients with oesophageal adenocarcinoma. *Br J Surg*. (2011) 98:964–74. doi: 10.1002/bjs.7498
114. Conroy MJ, Galvin KC, Doyle SL, Kavanagh ME, Mongan AM, Cannon A, et al. Parallel profiles of inflammatory and effector memory t cells in visceral fat and liver of obesity-associated cancer patients. *Inflammation*. (2016) 39:1729–36. doi: 10.1007/s10753-016-0407-2
115. Conroy MJ, Maher SG, Melo AM, Doyle SL, Foley, Reynolds JV, et al. Lysaght: Identifying a novel role for fractalkine (CX3CL1) in memory CD8(+) T cell accumulation in the omentum of obesity-associated cancer patients. *Front Immunol*. (2018) 9:1867. doi: 10.3389/fimmu.2018.01867
116. Albiges L, Hakimi AA, Xie W, McKay RR, Simantov R, Lin X, et al. Body mass index and metastatic renal cell carcinoma: clinical and biological correlations. *J Clin Oncol*. (2016) 34:3655–63. doi: 10.1200/JCO.2016.66.7311
117. McQuade JL, Daniel CR, Hess KR, Mak C, Wang DY, Rai RR, et al. Association of body-mass index and outcomes in patients with metastatic melanoma treated with targeted therapy, immunotherapy, or chemotherapy: a retrospective, multicohort analysis. *Lancet Oncol*. (2018) 19:310–22. doi: 10.1016/s1470-2045(18)30078-0
118. Wang Z, Aguilar EG, Luna JI, Dunai C, Khuat LT, Le CT, et al. Paradoxical effects of obesity on T cell function during tumor progression and PD-1 checkpoint blockade. *Nat Med*. (2019) 25:141–51. doi: 10.1038/s41591-018-0221-5
119. Tavazoie MF, Pollack I, Tanqueco R, Ostendorf BN, Reis BS, Gonsalves FC, et al. LXR/Apoe activation restricts innate immune suppression in cancer. *Cell*. (2018) 172:825-40.e18. doi: 10.1016/j.cell.2017.12.026
120. Lim YW, Chen-Harris H, Mayba O, Lianoglou S, Wuster A, Bhangale T, et al. Germline genetic polymorphisms influence tumor gene expression and immune cell infiltration. *Proc Natl Acad Sci USA*. (2018) 115:E11701–10. doi: 10.1073/pnas.1804506115
121. Chowell D, Morris LGT, Grigg CM, Weber JK, Samstein RM, Makarov, et al. Chan: Patient HLA class I genotype influences cancer response to checkpoint blockade immunotherapy. *Science*. (2018) 359:582. doi: 10.1126/science.aao4572
122. Chowell, Krishna D, Pierini C, Makarov F, Rizvi V, Kuo V, et al. Evolutionary divergence of HLA class I genotype impacts efficacy of cancer immunotherapy. *Nat Med*. (2019) 25:1715–20. doi: 10.1038/s41591-019-0639-4
123. Vacchelli E, Enot DP, Pietrocola F, Zitvogel L, Kroemer G. Impact of pattern recognition receptors on the prognosis of breast cancer patients undergoing adjuvant chemotherapy. *Cancer Res*. (2016) 76:3122–6. doi: 10.1158/0008-5472.CAN-16-0294
124. Ghiringhelli F, Apetoh F, Tesniere L, Aymeric A, Ma L, Ortiz Y, et al. Activation of the NLRP3 inflammasome in dendritic cells induces IL-1beta-dependent adaptive immunity against tumors. *Nat Med*. (2009) 15:1170–8. doi: 10.1038/nm.2028
125. Varn FS, Schaafsma E, Wang Y, Cheng C. Genomic characterization of six virus-associated cancers identifies changes in the tumor immune microenvironment and altered genetic programs. *Cancer Res*. (2018) 78:6413–23. doi: 10.1158/0008-5472.can-18-1342
126. Schumacher TN, Schreiber DR. Neoantigens in cancer immunotherapy. *Science*. (2015) 348:69–74. doi: 10.1126/science.aaa4971
127. CGAR Network. Comprehensive molecular characterization of gastric adenocarcinoma. *Nature*. (2014) 513:202–9. doi: 10.1038/nature13480
128. Seiwert TY, Burtness B, Mehra R, Weiss J, Berger R, Eder JP, et al. Safety and clinical activity of pembrolizumab for treatment of recurrent or metastatic squamous cell carcinoma of the head and neck (KEYNOTE-012): an open-label, multicentre, phase 1b trial. *Lancet Oncol*. (2016) 17:956–65. doi: 10.1016/s1470-2045(16)30066-3
129. Genitsch V, Novotny A, Seiler CA, Kröll D, Walch A, Langer R. Epstein-barr virus in gastro-esophageal adenocarcinomas - single center experiences in the context of current literature. *Front Oncol*. (2015) 5:73. doi: 10.3389/fonc.2015.00073
130. Hewitt LC, Inam IZ, Saito, Yoshikawa Y, Quaas T, Hoelscher A, et al. Epstein-Barr virus and mismatch repair deficiency status differ between oesophageal and gastric cancer: a large multi-centre study. *Eur J Cancer*. (2018) 94:104–14. doi: 10.1016/j.ejca.2018.02.014
131. Kunzmann AT, Graham S, McShane CM, Doyle J, Tommasino M, Johnston B, et al. The prevalence of viral agents in esophageal adenocarcinoma and Barrett's esophagus: a systematic review. *Eur J Gastroenterol Hepatol*. (2017) 29:817–25. doi: 10.1097/meg.0000000000000868
132. Kim ST, Cristescu R, Bass AJ, Kim KM, Odegaard JI, Kim K, et al. Comprehensive molecular characterization of clinical responses to PD-1 inhibition in metastatic gastric cancer. *Nat Med*. (2018) 24:1449–58. doi: 10.1038/s41591-018-0101-z
133. Mohammadpour B, Rouhi S, Khodabandehloo M, Moradi M. Prevalence and association of human papillomavirus with esophageal squamous cell carcinoma in iran: a systematic review and meta-analysis. *Iran J Public Health*. (2019) 48:1215–26.

134. Ludmir EB, Stephens SJ, Palta M, Willett CG, Czito GB. Human papillomavirus tumor infection in esophageal squamous cell carcinoma. *J Gastrointest Oncol*. (2015) 6:287–95. doi: 10.3978/j.issn.2078-6891.2015.001
135. Newman J, Chesson CB, Herzog NL, Bommareddy P, Aspromonte S, Pepe R, et al. Zloza: Intratumoral injection of the seasonal flu shot converts immunologically cold tumors to hot and serves as an immunotherapy for cancer. *Proc Natl Acad Sci USA*. (2020) 117:1119. doi: 10.1073/pnas.1904022116
136. Bersanelli M, Buti S, Banna GL, Giorgi UD, Cortellini A, Rebuzzi SE, et al. Impact of influenza syndrome and flu vaccine on survival of cancer patients during immunotherapy in the INVIDIa study. *Immunotherapy*. (2020) 12:151–9. doi: 10.2217/imt-2019-0180
137. Läubli H, Balmelli C, Kaufmann L, Stanczak M, Syedbasha M, Vogt D, et al. Influenza vaccination of cancer patients during PD-1 blockade induces serological protection but may raise the risk for immune-related adverse events. *J Immunother Cancer*. (2018) 6:40. doi: 10.1186/s40425-018-0353-7
138. Black S, Nicolay U, Del Giudice G, Rappuoli R. Influence of statins on influenza vaccine response in elderly individuals. *J Infect Dis*. (2016) 213:1224–8. doi: 10.1093/infdis/jiv456
139. Dopico XC, Evangelou M, Ferreira RC, Guo H, Pekalski ML, Smyth DJ, et al. Widespread seasonal gene expression reveals annual differences in human immunity and physiology. *Nat Commun.* (2015) 6:7000. doi: 10.1038/ncomms8000
140. Muralidhar S, Filia A, Nsengimana J, Pozniak J, Shea SJ, Diaz JMS, et al. Vitamin D-VDR signaling inhibits Wnt/β-catenin-mediated melanoma progression and promotes anti-tumor immunity. *Cancer Res.* (2019) 79:5986–5998. doi: 10.1158/0008-5472.CAN-18-3927
141. Mimori, Tanaka K, Yoshinaga Y, Masuda K, Yamashita T, Okamoto K, et al. Mori: Clinical significance of the overexpression of the candidate oncogene CYP24 in esophageal cancer. *Ann Oncol*. (2004) 15:236–41. doi: 10.1093/annonc/mdh056
142. Rizvi NA, Hellmann MD, Snyder A, Kvistborg P, Makarov V, Havel JJ, et al. Cancer immunology. Mutational landscape determines sensitivity to PD-1 blockade in non-small cell lung cancer. S*cience*. (2015) 348:124–8. doi: 10.1126/science.aaa1348
143. Hatogai K, Kitano S, Fujii S, Kojima T, Daiko H, Nomura S, et al. Comprehensive immunohistochemical analysis of tumor microenvironment immune status in esophageal squamous cell carcinoma. *Oncotarget*. (2016) 7:47252–64. doi: 10.18632/oncotarget.10055
144. Ogino S, Nowak JA, Hamada T, Milner DA, Nishihara R. Insights into pathogenic interactions among environment, host, and tumor at the crossroads of molecular pathology and epidemiology. *Ann Rev Pathol*. (2019) 14:83–103. doi: 10.1146/annurev-pathmechdis-012418-012818
145. Song M, Nishihara N, Wang M, Chan AT, Qian ZR, Inamura K, et al. Plasma 25-hydroxyvitamin D and colorectal cancer risk according to tumour immunity status. *Gut*. (2016) 65:296–304. doi: 10.1136/gutjnl-2014-308852
146. Mima K, Sukawa Y, Nishihara R, Qian ZR, Yamauchi M, Inamura K, et al. Fusobacterium nucleatum and t cells in colorectal carcinoma. *JAMA Oncol*. (2015) 1:653–61. doi: 10.1001/jamaoncol.2015.1377
147. Gur C, Ibrahim Y, Isaacson B, Yamin R, Abed J, Gamliel M, et al. Binding of the Fap2 protein of Fusobacterium nucleatum to human inhibitory receptor TIGIT protects tumors from immune cell attack. *Immunity*. (2015) 42:344–55. doi: 10.1016/j.immuni.2015.01.010
148. Doi T, Piha-Paul SA, Jalal SI, Saraf S, Lunceford J, Koshiji M, et al. Safety and antitumor activity of the anti–programmed death-1 antibody pembrolizumab in patients with advanced esophageal carcinoma. *J Clin Oncol*. (2017) 36:61–7. doi: 10.1200/JCO.2017.74.9846
149. Janjigian YY, Bendell J, Calvo E, Kim JW, Ascierto PA, Sharma P, et al. Checkmate-032 study: efficacy and safety of nivolumab and nivolumab plus ipilimumab in patients with metastatic esophagogastric cancer. *J Clin Oncol.* (2018) 36:2836–44. doi: 10.1200/JCO.2017.76.6212
150. Fuchs CS, Doi T, Jang RW, Muro K, Satoh T, Machado M, et al. Safety and efficacy of pembrolizumab monotherapy in patients with previously treated advanced gastric and gastroesophageal junction cancer: phase 2 clinical KEYNOTE-059 trial. *JAMA Oncol.* (2018) 4:e180013. doi: 10.1001/jamaoncol.2018.0013
151. Shitara K, Özgüroglu M, Bang YJ, Bartolomeo D, Mandalà M, Ryu MH, et al. Pembrolizumab versus paclitaxel for previously treated, advanced gastric or gastro-oesophageal junction cancer (KEYNOTE-061): a randomised, open-label, controlled, phase 3 trial. *Lancet*. (2018) 392:123–33. doi: 10.1016/S0140-6736(18)31257-1
152. Shah MA, Kojima T, Hochhauser D, Enzinger P, Raimbourg J, Hollebecque A, et al. Efficacy and safety of pembrolizumab for heavily pretreated patients with advanced, metastatic adenocarcinoma or squamous cell carcinoma of the esophagus: the phase 2 KEYNOTE-180 study. *JAMA Oncol*. (2019) 5:546–50. doi: 10.1001/jamaoncol.2018.5441
153. Janjigian YY, Maron SB, Chou JF, Gabler AR, Simmons MZ, Momtaz P, et al. First-line pembrolizumab (P), trastuzumab (T), capecitabine (C) and oxaliplatin (O) in HER2-positive metastatic esophagogastric adenocarcinoma. *J Clin Oncol*. (2019) 37(Suppl. 15):v253–324. doi: 10.1200/JCO.2019.37.15_suppl.4011
154. Kudo T, Hamamoto Y, Kato K, Ura T, Kojima T, Tsushima T, et al. Nivolumab treatment for oesophageal squamous-cell carcinoma: an open-label, multicentre, phase 2 trial. *Lancet Oncol*. (2017) 18:631–9. doi: 10.1016/s1470-2045(17)30181-x
155. Kang YK, Boku N, Satoh T, Ryu MH, Chao Y, Kato Y, et al. Nivolumab in patients with advanced gastric or gastro-oesophageal junction cancer refractory to, or intolerant of, at least two previous chemotherapy regimens (ONO-4538-12, ATTRACTION-2): a randomised, double-blind, placebo-controlled, phase 3 trial. *Lancet*. (2017) 390:2461–71. doi: 10.1016/S0140-6736(17)31827-5
156. Kojima T, Muro K, Francois E, Hsu C, Moriwaki H, Kim T-S, et al. Pembrolizumab versus chemotherapy as second-line therapy for advanced esophageal cancer: phase III KEYNOTE-181 study. *J Clin Oncol*. (2019) 37:2–2. doi: 10.1200/JCO.2019.37.4_suppl.2
157. Kulangara K, Zhang N, Corigliano E, Guerrero L, Waldroup S, Jaiswal D, et al. Emancipator: Clinical utility of the combined positive score for programmed death ligand-1 expression and the approval of pembrolizumab for treatment of gastric cancer. *Arch Pathol Lab Med*. (2019) 143:330–7. doi: 10.5858/arpa.2018-0043-OA
158. Smyth EC, Moehler M. Late-line treatment in metastatic gastric cancer: today and tomorrow. *Ther Adv Med Oncol.* (2019) 11:1758835919867522. doi: 10.1177/1758835919867522
159. Galon J, Bruni D. Approaches to treat immune hot, altered and cold tumours with combination immunotherapies. *Nat Rev Drug Discov*. (2019) 18:197–218. doi: 10.1038/s41573-018-0007-y
160. Deng L, Liang H, Xu M, Yang X, Burnette B, Arina A, et al. STING-dependent cytosolic DNA sensing promotes radiation-induced type I interferon-dependent antitumor immunity in immunogenic tumors. *Immunity*. (2014) 41:843–52. doi: 10.1016/j.immuni.2014.10.019
161. Woo SR, Fuertes MB, Corrales L, Spranger S, Furdyna MJ, Leung MY, et al. STING-dependent cytosolic DNA sensing mediates innate immune recognition of immunogenic tumors. *Immunity*. (2014) 41:830–42. doi: 10.1016/j.immuni.2014.10.017
162. McLaughlin M, Patin EC, Pedersen M, Wilkins A, Dillon MT, Melcher AA, et al. Harrington: Inflammatory microenvironment remodelling by tumour cells after radiotherapy. *Nat Rev Cancer*. (2020) 20:203–17. doi: 10.1038/s41568-020-0246-1
163. Andre F, Dieci MV, Dubsky P, Sotiriou C, Curigliano G, Denkert C, et al. Molecular pathways: involvement of immune pathways in the therapeutic response and outcome in breast cancer. *Clin Cancer Res*. (2013) 19:28–33. doi: 10.1158/1078-0432.ccr-11-2701
164. Vacchelli E, Ma Y, Baracco EE, Sistigu A, Enot DP, Pietrocola F, et al. Chemotherapy-induced antitumor immunity requires formyl peptide receptor 1. *Science*. (2015) 350:972–8. doi: 10.1126/science.aad0779
165. Kato K, Shah MA, Enzinger P, Bennouna J, Shen L, Adenis A, et al. KEYNOTE-590: phase III study of first-line chemotherapy with or without

pembrolizumab for advanced esophageal cancer. *Future Oncol*. (2019) 15:1057–66. doi: 10.2217/fon-2018-0609

166. Mamdani H, Schneider BJ, Abushahin LI, Birdas TJ, Kesler KA, Lee K, et al. Safety and efficacy of durvalumab following trimodality therapy for locally advanced esophageal and GEJ adenocarcinoma: early efficacy results from big ten cancer research consortium study. *J Clin Oncol*. (2019) 37(Suppl. 4):5. doi: 10.1200/JCO.2019.37.4_suppl.5
167. Blank CU, Haanen JB, Ribas A, Schumacher NT. Cancer mmunology. The "cancer immunogram". *Science*. (2016) 352:658–60. doi: 10.1126/science.aaf2834
168. Karasaki T, Nagayama K, Kuwano H, Nitadori JI, Sato M, Anraku M, et al. An immunogram for the cancer-immunity cycle: towards personalized immunotherapy of lung cancer. *J Thorac Oncol*. (2017) 12:791–803. doi: 10.1016/j.jtho.2017.01.005

Conflict of Interest: ML reports a Consulting/Advisory Role for Agios, Celgene, and Roche/Genentech.

The remaining authors declare that the research was conducted in the absence of any commercial or financial relationships that could be construed as a potential conflict of interest.

frontiers in Oncology

ORIGINAL RESEARCH
published: 03 July 2020
doi: 10.3389/fonc.2020.01062

TIPRL, a Novel Tumor Suppressor, Suppresses Cell Migration, and Invasion Through Regulating AMPK/mTOR Signaling Pathway in Gastric Cancer

Meng Luan[1,2†], *Shan-Shan Shi*[1,3†], *Duan-Bo Shi*[1,4], *Hai-Ting Liu*[1], *Ran-Ran Ma*[1,4], *Xiao-Qun Xu*[2], *Yu-Jing Sun*[1,4*] *and Peng Gao*[1,4*]

[1] *Key Laboratory for Experimental Teratology of Ministry of Education, Department of Pathology, School of Basic Medical Sciences, Cheeloo College of Medicine, Shandong University, Jinan, China,* [2] *Institute of Basic Medicine, Shandong Provincial Hospital Affiliated to Shandong First Medical University, Jinan, China,* [3] *Key Laboratory of Cardiovascular Proteomics of Shandong Province, Department of Geriatrics, Qilu Hospital of Shandong University, Jinan, China,* [4] *Department of Pathology, Qilu Hospital, Shandong University, Jinan, China*

OPEN ACCESS

Edited by:
Bin Li,
Jinan University, China

Reviewed by:
Xiaodi Zhao,
Fourth Military Medical University, China
Xu Zhang,
Jiangsu University, China

****Correspondence:***
Yu-Jing Sun
candysyj4@163.com
Peng Gao
gpzmq@sina.com

† These authors have contributed equally to this work

Specialty section:
This article was submitted to Gastrointestinal Cancers, a section of the journal Frontiers in Oncology

Received: *27 March 2020*
Accepted: *28 May 2020*
Published: *03 July 2020*

Citation:
Luan M, Shi S-S, Shi D-B, Liu H-T, Ma R-R, Xu X-Q, Sun Y-J and Gao P (2020) TIPRL, a Novel Tumor Suppressor, Suppresses Cell Migration, and Invasion Through Regulating AMPK/mTOR Signaling Pathway in Gastric Cancer. Front. Oncol. 10:1062. doi: 10.3389/fonc.2020.01062

Invasion and metastasis of gastric cancer after curative resection remain the most common lethal outcomes. However, our current understanding of the molecular mechanism underlying gastric cancer metastasis is far from complete. Herein, we identified TOR signaling pathway regulator (TIPRL) as a novel metastasis suppressor in gastric cancer through genome-wide gene expression profiling analysis using mRNA microarray. Decreased TIPRL expression was detected in clinical gastric cancer specimens, and low TIPRL expression was correlated with more-advanced TNM stage, distant metastasis, and poor clinical outcome. Moreover, TIPRL was identified as a direct target of miR-216a-5p and miR-383-5p. Functional study revealed that re-expression of TIPRL in gastric cancer cell lines suppressed their migratory and invasive capacities, whereas inverse effects were observed in TIPRL-deficient models. Mechanistically, TIPRL downstream effectors and signaling pathways were investigated using mRNA microarray. Gene expression profiling revealed that TIPRL could not modulate the downstream genes at transcriptional levels, thereby implying that the regulation might occur at the post-transcriptional levels. We further demonstrated that TIPRL induced phosphorylation/activation of AMPK, which in turn attenuated phosphorylation of mTOR, p70S6K, and 4E-BP1, thereby leading to inactivation of mTOR signaling and subsequent suppression of cell migration/invasion in gastric cancer. Taken together, TIPRL acts as a novel metastasis suppressor in gastric cancer, at least in part, through regulating AMPK/mTOR signaling, likely representing a promising target for new therapies in gastric cancer.

Keywords: TIPRL, gastric cancer, invasion, metastasis, AMPK/mTOR signaling

INTRODUCTION

Gastric cancer is an aggressive disease and the third highest cause of cancer-related mortality, with nearly 1,000,000 new cases occurring worldwide each year (1). Effective early diagnosis has led to prolonged survival. However, gastric cancer is typically diagnosed as advanced disease (2). Despite improving surgical and adjuvant therapies, the prognosis of patients with advanced gastric cancer remains dismal (3). The poor prognosis of patients with advanced gastric cancer is predominantly the result of the high rate of tumor metastasis and recurrence after curative resection (4, 5). Gastric cancer metastasis is a complex and multistep process involving multiple factors and genes (6, 7). However, our current understanding of the molecular mechanism underlying gastric cancer metastasis is far from complete. Much hope is focused on increasing our understanding of the signaling pathways and underlying biology involved in gastric cancer metastasis in order to develop new therapeutic options. Therefore, it is crucial to identify novel genes that govern gastric cancer metastasis and present predictive value for prognosis.

To identify novel candidates involved in gastric cancer metastasis, we used microarray based expression profiling of primary gastric cancer tissue samples with LNM (lymph node metastasis) and the samples without LNM. Using this high-throughput approach, we identified TIPRL (TOR signaling pathway regulator) as a novel candidate that was down-regulated in metastatic gastric cancer tissues through differential expression analysis.

TIPRL is an evolutionarily conserved protein which is identified as a homolog of yeast Tip41 (8). Unlike yeast TIP41, it has been shown that human TIPRL directly interacts with PP2A (Protein phosphatase 2A) and the PP2A-family phosphatases PP4 and PP6 (9, 10). It plays a key role in the ATM/ATR signaling pathway controlling DNA damage response and TOR (target of rapamycin) signaling through the regulation of PP2A (8, 9, 11). Recently, it has been reported that TIPRL is overexpressed in hepatocellular carcinoma, and that knockdown of TIPRL by small interfering RNA causes sustained activation of MKK7 (mitogen-activated protein kinase kinase 7) and JNK (c-Jun N-terminal kinase) by increasing MKK7 phosphorylation (12). This action of TIPRL appears to protect cancer cells from TRAIL (tumor necrosis factor-related apoptosis-inducing ligand)—induced apoptosis. However, detailed and mechanistic studies of the potential role of TIPRL in cancer invasion and metastasis are not available. Moreover, to date, no existing analyses have clarified the clinical and prognostic significance of TIPRL in human cancer, especially in gastric cancer. Therefore, in the current study, we investigated the gene expression, biological function, molecular mechanism and clinical significance of TIPRL in gastric cancer.

MATERIALS AND METHODS

Patients and Tissue Specimens

After obtaining informed consent, 190 cases of paraffin-embedded tissues and 40 cases of fresh gastric cancer tissues, along with the available clinicopathological and follow-up information, were collected from patients who underwent curative resection of gastric cancer at Qilu Hospital of Shandong University from 2007 to 2014. All fresh samples were dissected from surgically resected specimens by pathologists at Qilu Hospital of Shandong University, and immediately snap-frozen in liquid nitrogen for the subsequent experiments. Histopathological diagnosis of each gastric cancer tissue was performed by the Department of Pathology, Qilu Hospital of Shandong University, according to the World Health Organization (WHO) criteria. Clinicopathological staging was classified on the basis of AJCC classification. None of the patients with gastric cancer had received adjuvant treatment before curative resection.

Our study was ethically-approved by the Ethics Committee of Shandong University, China. All subjects had provided informed consent.

Gene Expression Microarray Analysis

Ten gastric cancer tissue samples (including 5 samples with LNM and 5 samples without LNM) with written informed consent were obtained. Total RNA from each gastric cancer tissue sample was isolated using TRIzol reagent (Invitrogen, Carlsbad, CA). After confirmation of RNA integrity and quantity, the RNA samples were analyzed at Kangchen Biotech (Kangchen, Shanghai, China) using Human LncRNA Array V2.0 (Arraystar, 8 × 60 K, Rockville, MD, USA) in accordance with the manufacturer's labeling, hybridization, scanning and normalization protocols. The criteria of significantly differentially expressed genes between the samples with LNM and the samples without LNM were a minimum of 2-fold absolute changes and a $P < 0.05$. More detailed information of the microarray data is available online via the NCBI's Gene Expression Omnibus (GEO) public database under the accession number GSE72307.

The mRNA expression profiles of MKN-45 cells treated with TIPRL overexpression plasmid or control were performed using the Human genome U133 Plus 2.0 Array (CapitalBio Corporation, Beijing, China). A fold change cutoff of 2.0 was set to identify differentially expressed mRNAs with biological significance between TIPRL-expressing MKN45 cells and empty vector controls.

RNA Isolation and Real-Time Quantitative PCR

Total RNA from gastric cancer tissue samples or treated cells in log-phase was separately prepared using TRIzol reagent (Invitrogen), and the quality of RNA was estimated by NanoDrop Spectrophotometric analysis (NanoDrop Technologies, USA). A final amount of one microgram of total RNA for each sample was reversed-transcribed into first-strand complementary DNA (cDNA) using Transcriptor First-Strand cDNA Synthesis Kit (Roche). Real-time quantitative PCR was conducted in triplicate on cDNA templates using SYBR Green master mixture (Roche, Germany) in a volume of 10 μL on HT7900 system (Applied Biosystems, USA), with GAPDH as endogenous control. Relative quantification of target mRNA expression was evaluated by using

the following equation $2^{-\Delta\Delta Ct}$. Primer sequences used in this assay are summarized in **Table S1**.

Immunohistochemistry

For immunohistochemistry *in situ*, paraffin-embedded gastric cancer specimens (4-μm-thick) were sequentially cut, deparaffinized, and rehydrated. The standard SP (streptavidin-peroxidase-biotin) method (SP-9000 kit, ZSGB-bio, Beijing, China) was employed for immunohistochemical staining with a heat-induced epitope retrieval step, and endogenous peroxidases were blocked. Subsequently, tissue samples were incubated with rabbit polyclonal anti-TIPRL (1:250, ab70795, Abcam) at 4°C overnight, followed by detection with appropriate secondary antibodies. After washing, sections were visualized using DAB chromogen and counterstaining was carried out with hematoxylin. Images of immunostained sections were photographed and scored under a light microscope (Olympus, Japan).

TIPRL expression was evaluated in a semiquantitative method. For each specimen, immunostaining score of TIPRL was measured using a histochemical score (H-score), which takes extent and intensity of TIPRL staining in consideration. The extent score was determined on the basis of the percentage of positive tumor cells (0–100). The intensity score was graded from 0 to 3 (0, negative; 1, weak; 2, moderate; 3, strong). The extent and intensity scores were multiplied to obtain the final H-score (range 0–300), which represented the expression level of TIPRL. ROC (receiver operating characteristic) curve analysis was carried out to select the optimal cut-off value for TIPRL on the basis of the highest Youden's index (sensitivity + specificity −1).

Cell Culture and Treatment

Two gastric cancer-derived cell lines, MKN45, and BGC823, were acquired from either the Shanghai Cancer Institute (Shanghai, China) or American Type Culture Collection (Manassas, VA, USA) and authenticated by DNA profiling. The gastric cancer-derived cell lines were maintained in RPMI-1640 medium (HyClone, Logan, UT, USA) with 10% fetal bovine serum (Gibco) under standard culture conditions, according to the recommended culture method.

For TIPRL overexpression, the human TIPRL (GenBank accession number NM_152902.5) coding sequence lacking the 3′UTR was constructed and subcloned into the mammalian expression vector [pcDNA3.1 (+) (pcDNA3.1 (+)-TIPRL] by Biosune Biotech (Shanghai, China). The TIPRL plasmid was transfected into cells using Turbofect transfection reagent (Thermo) following the manufacturer's protocols, whereas the empty plasmid [pcDNA3.1 (+)] was used as negative controls.

For TIPRL knockdown, small interfering RNA (siRNA) targeting human TIPRL (TIPRL siRNA, si-TIPRL, Targeting CTACAACAGATCATATAGA) and non-specific scrambled small interfering RNA were synthesized from Ribobio (Guangzhou, China). The siRNAs against human TIPRL were transfected into the gastric cancer cells at 50 nmol with X-tremeGENE transfection reagent (Roche, USA) according to the manufacturer's recommendations.

After transient transfection, the gastric cancer cells were incubated for 48 h before the subsequent functional assays were performed. Overexpression or knockdown of TIPRL was confirmed by western blot analysis.

Cell Viability and Proliferation Assay

The effect of TIPRL on cell viability was assessed by the MTS assay (Promega, USA). Treated and control gastric cancer cells were trypsinized, counted, and then plated in 96-well plates (∼4 × 10^3 transfected cells/well) in quintuplicate, in a final volume of 100 μL of complete medium. Cell viability was determined on days 1, 2, and 3 by examining the number of cells with MTS labeling reagent.

Cell proliferation was detected by the 5′Ethynyl-2′-deoxyuridine (EdU) incorporation assay (Ribobio, Guangzhou, China). Briefly, treated and control cells in log-phase were trypsinized and seeded onto 96-well plates in triplicate at a density of 1 × 10^4 cells/well the day before EdU incubation. After 12–24 h, EdU labeling solution (50 μmol) was added, and then treated and control cells were incubated for additional 2 h. After EdU incubating, cells were dyed with Apollo reaction cocktail and subsequently stained with 4′, 6-diamidino-2-phenylindole (DAPI). EdU positive cells were photographed and calculated with a fluorescence microscope (Olympus, Japan).

Apoptosis Assay

Apoptosis was assessed by flow cytometry, using an Annexin V-FITC/PI double stain Kit (BestBio, Shanghai, China) according to the standard protocols. Floating and trypsinized adherent cells were harvested at 48-h post-transfection. After washing with chilled PBS, unfixed tumor cells were resuspended in binding buffer and stained with Annexin-V-FITC and PI. The stained samples were immediately detected with a FACScan flow cytometer (Beckman-Coulter, Los Angeles, CA, USA) for early and late apoptosis analysis.

Cell Migration and Invasion Assays

The migratory and invasive potential of gastric cancer cells was assessed by using 24-well modified Boyden chambers (Corning, USA) with the polyethylene terephthalate membranes either uncoated or precoated with diluted Matrigel matrix (BD Biosciences, USA). After the appropriate treatments, MKN45 or BGC823 cell suspensions (1 × 10^5 cells/well) in 200 μL of serum-free medium were transferred and cultured in each upper insert. Meanwhile, medium containing 10% FBS (500 μL) was applied to the lower compartment to induce migration or invasion in 24-well plates. After 24 h, Non-migrating or non-invading cells on the upper chambers were removed, whereas cells that had migrated or invaded through the lower side of the inserts were fixed in paraformaldehyde, rinsed with distilled water, stained with crystal violet, counted, and photographed under an inverted microscope (Nikon, Japan).

Luciferase Assay

A fragment of human TIPRL-3′-UTR and the same fragment of TIPRL-3′-UTR with the miR-216a-5p/miR-383-5p putative binding site completely mutated was constructed by Biosune

Biotech (Shanghai, China) and separately inserted into a pmirGLO vector (Promega), to synthesize a series of wild-type TIPRL-3′-UTR vectors (WT 3′-UTR) and mutant-type TIPRL-3′-UTR vectors (MUT 3′-UTR). Cells were co-transfected with a mix containing miRNA mimics (20 nmol) or negative control (GenePharma Biotech, China) and wild-type TIPRL-3′-UTR vector (20 ng) or mutant-type TIPRL-3′-UTR vector using Turbofect transfection reagent (Thermo). Forty-eight hours after transfection, cell lysates were prepared, and then renilla and firefly luciferase signals were calculated using the Dual-Luciferase Reporter system (Promega).

PP2A Phosphatase Activity Assay

The MKN45 and BGC823 cells were transfected with TIPRL-expressing vector (pcDNA3.1 (±)-TIPRL), TIPRL siRNA, and the respective control vector. Samples from cells were prepared at 48-h post-transfection. The effect of TIPRL on PP2A activity was assessed by the phosphatase activity assay, using a PP2A Colorimetric Assay Kit (GENMED, Shanghai, China) in accordance with the manufacturer's protocols. Absorbance of each sample was measured at 660 nm using a microplate reader.

Western Blot Analysis

In brief, the pellets of treated cells were dissolved in prechilled RIPA cell lysis buffer (BestBio, Shanghai, China), supplemented with phosphatase-inhibitor (Roche) and protease-inhibitor (BestBio). The lysate was purified by centrifugation and then cell debris was removed. The supernatant was collected until analysis and protein concentration was quantified by using the Bradford assay (Beyotime Biotechnology, China). Total protein extracts (30 μg) was fractionated by electrophoresis in denaturing 10 or 14% SDS-PAGE and transferred to PVDF transfer membranes (Millipore). Non-specific binding sites were blocked and blots were incubated with commercially available antibodies overnight at 4°C. Commercial primary antibodies used were as follows: rabbit polyclonal anti-TIPRL (1:4,000, ab70795, Abcam), rabbit monoclonal anti-phospho-AMPK (1:5,000, ab133448, Abcam), rabbit monoclonal anti-AMPK (1:1,000, ab207442, Abcam), rabbit monoclonal anti-phospho-mTOR (1:5,000, ab109268, Abcam), rabbit monoclonal anti-mTOR (1:1,000, #2983, Cell Signaling), rabbit monoclonal anti-phospho-p70 S6 Kinase (1:1,000, #9234, Cell Signaling), rabbit polyclonal anti-p70 S6 Kinase (1:2000, 14485-1-AP, proteintech), rabbit monoclonal anti-phospho-4E-BP1 (1:1000, #2855, Cell Signaling), rabbit monoclonal anti-4E-BP1 (1:5,000, ab32024, Abcam), and rabbit polyclonal anti-β-actin (1:10,000, AP0060, Bioworld). Bound antibodies were detected and visualized using the chemiluminescent substrate (Millipore, USA).

Statistical Analysis

Results are analyzed as means ± SD from 3 representative independent experiments. Comparisons of continuous variables between two groups were carried out using Student's *t*-test. The correlation between the clinicopathologic categorical variables of patients with gastric cancer and TIPRL intensity scores was examined with the Chi-square test. Overall survival (OS) or disease-free survival (DFS) in relation to TIPRL expression was estimated by Kaplan-Meier method. Significance of differences between the low and high TIPRL expression groups was subsequently determined by applying log-rank test. Cox proportional hazards model was conducted to identify independent factors of survival. Statistical analysis and data plotting were conducted by using SPSS version 23.0 or GraphPad Prism 5. $P < 0.05$ was considered significant.

RESULTS

Genome-Wide Microarray Analysis Identified TIPRL as a Metastasis-Related Gene in Human Gastric Cancer

To identify novel gastric cancer-related candidates, genome-wide microarray was performed to compare the differential gene expression profiles of metastatic and non-metastatic cancer tissues of gastric cancer patients. Using stringent criteria, hundreds of differentially expressed genes were identified between metastatic and non-metastatic gastric cancer tissues (**Figure 1A**, $P < 0.05$ with >2-fold change, raw value >500; raw data accessible via GEO number: GSE72307). Based on the mining of microarray data, we focused on the novel genes, which have been poorly investigated and remained functionally uncharacterized in human cancer, especially in gastric cancer, because novel genes usually provide new insight into understanding human cancer. For this reason, TIPRL, SERINC3, COPS6, and SELM were chosen for further study (**Figure 1B**).

To further explore the microarray data, we evaluated the transcriptional levels of TIPRL, SERINC3, COPS6, and SELM in 40 frozen gastric tissues of gastric cancer patients by real-time PCR (**Figures 1C–F**). The statistical analysis revealed that TIPRL expression was significantly suppressed in metastatic compared with non-metastatic tissues, consistent with our microarray database (**Figure 1C**, $P = 0.0209$). Furthermore, data mining of the prognostic effect of TIPRL mRNA expression from Kaplan-Meier plotter (http://kmplot.com/) confirmed that lower TIPRL expression was associated with poor overall survival (OS), first progression survival (FP), and post-progression survival (PPS) in gastric cancer patients (**Figure 1G**, $P = 1.1e\text{-}5$, overall survival; **Figure 1H**, $P = 8.5e\text{-}5$, first progression survival; **Figure 1I**, $P = 1.7e\text{-}5$, post-progression survival). The data implied that an aberrant down-regulation of TIPRL might give rise to gastric cancer metastasis. Therefore, further investigations of TIPRL were instigated.

TIPRL Was Significantly Down-Regulated and Associated With Gastric Cancer Clinicopathologic Features

Expression of TIPRL was also investigated by immunohistochemistry (IHC) in 104 gastric cancer samples and 86 paired non-tumor samples. IHC assays showed that TIPRL was predominantly localized in the cytoplasm (**Figures 2A–C**). Similarly, assessment via IHC revealed that TIPRL protein expression was markedly down-regulated in gastric tumors

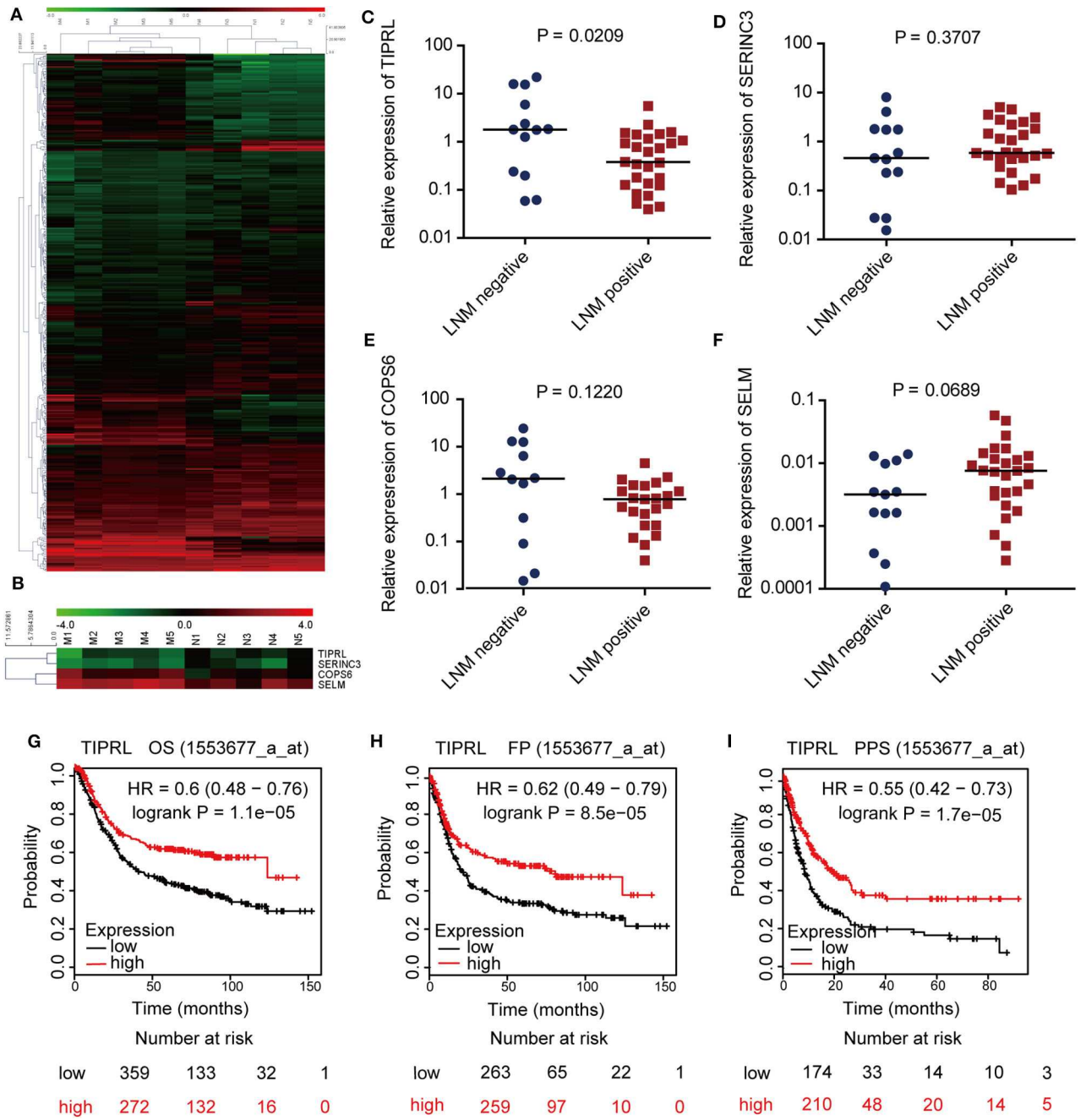

FIGURE 1 | Identification and expression evaluation of TIPRL as a metastasis-related gene in gastric cancer. **(A,B)** Microarray plots of metastatic tumors (M group) vs. non-metastatic tumors (*N* group) demonstrating a different expression profile. Hierarchical cluster analysis shows 372 genes are significantly altered in gastric cancer samples with or without lymphatic metastasis (**A**, $P < 0.05$ with >2-fold change, raw value >500). Four novel genes (TIPRL, SERINC3, COPS6, and SELM) are significantly differentially expressed in metastatic gastric cancer tissues compared with their counterparts **(B)**. Each column represents a sample; each row denotes the expression level of a single gene. Expression level is demonstrated by colors: Green, underexpressed genes; red, overexpressed genes. **(C–F)** The mRNA expression levels of TIPRL, but not SERINC3, COPS6, and SELM, were significantly lower in gastric cancer tissues with LNM (positive) than those without LNM (negative), as determined by RT-qPCR (*t*-test, $P = 0.0209$, $P = 0.3707$, $P = 0.1220$, and $P = 0.0689$, respectively). **(G–I)** Low mRNA expression of TIPRL was correlated with poor overall survival (**G**, $P = 1.1e\text{-}5$), first progression survival (**H**, $P = 8.5e\text{-}5$), and post-progression survival (**I**, $P = 1.7e\text{-}5$) in gastric cancer patients from Kaplan-Meier plotter (http://kmplot.com/).

compared with their normal counterparts (**Figures 2A,D,E**). Moreover, intensity of TIPRL staining was significantly decreased in the advanced stage (III+IV) group, compared to the early stage (I+II) group (**Figures 2B,F**, $P = 0.0467$, **Table 1**). More importantly, semiquantitative analysis also showed lower levels of TIPRL expression in the tumors with distant metastasis,

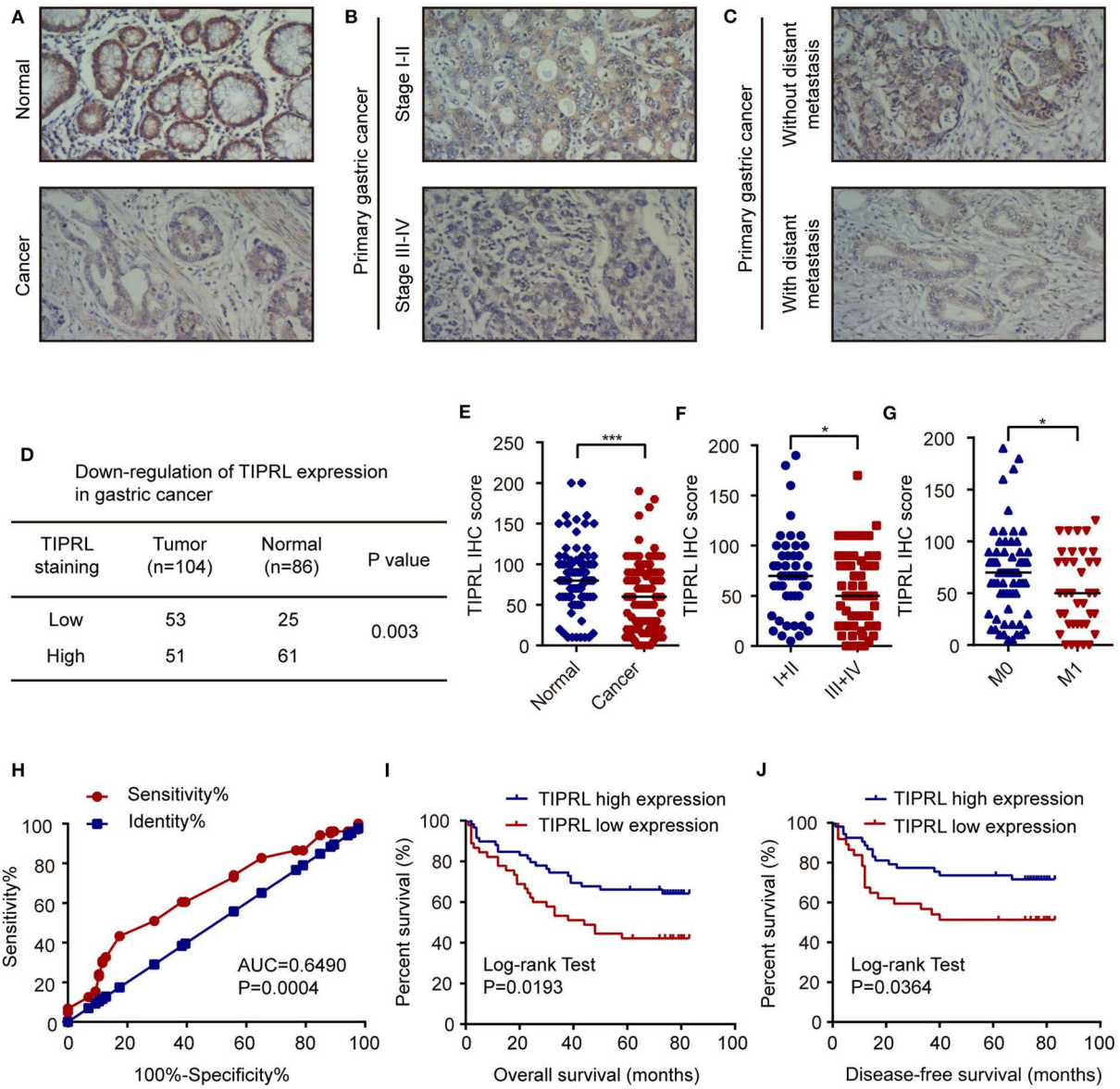

FIGURE 2 | Decrease of TIPRL expression correlates with a poor clinical outcome in gastric cancer. **(A–C)** Representative immunohistochemical staining for TIPRL expression in normal gastric tissues, gastric cancer with different TNM tumor stages (I-II vs. III-IV) and gastric tumors with or without distant metastasis (M0 vs. M1). Original magnification, × 100. **(D)** Statistical analysis of TIPRL expression in gastric cancer tissues. **(E)** Quantitative analysis of TIPRL staining indicated that staining intensity in gastric tumors was significantly lower than normal gastric mucosa (*t*-test, $^{***}P < 0.001$). **(F)** TIPRL expression was dramatically decreased in patients at advanced stages (III-IV), in contrast with those at earlier stages (I-II) (*t*-test, $^{*}P < 0.05$). **(G)** Analysis of TIPRL staining intensity also showed lower staining intensity in patient samples with distant metastasis (M1) compared to those without distant metastasis (M0) (*t*-test, $^{*}P < 0.05$). **(H)** The ROC curves demonstrated strong separation between normal and gastric cancer tissues [AUC = 0.6490, CI (95%): 0.5709–0.7270, $P = 0.0004$]. The sensitivity and specificity of TIPRL expression to distinguish normal from gastric cancer tissues were 43.27 and 82.56%, respectively. **(I,J)** Kaplan–Meier survival curves revealed that low intensity of TIPRL immunostaining strongly correlated with poor overall survival (**I**, log-rank test, $P = 0.0193$) and disease-free survival (**J**, log-rank test, $P = 0.0364$).

compared with those without distant metastasis (**Figures 2C,G**, $P = 0.0083$, **Table 1**).

Moreover, in receiver operator characteristic (ROC) curve analysis, which plots the area under the curve (AUC) to evaluate the diagnostic value of TIPRL in gastric cancer, clear separation was observed between normal and gastric cancer tissues, with an area of 0.6490 [**Figure 2H**, CI (95%): 0.5709–0.7270, $P = 0.0004$].

The correlation between protein expression of TIPRL and clinicopathologic features was further investigated using informative IHC data. The low and high levels of TIPRL expression in tissue samples were determined by ROC analysis, which demonstrated the optimal cut-off point of TIPRL is 55 (**Figure 2H**). After dichotomization based on the optimal cut-off value of TIPRL, low expression of TIPRL was positively

TABLE 1 | Correlation between TIPRL expression and clinicopathological features.

Variables	*n*	TIPRL expression		*P*-value
		Low	High	
Age (years)				
≤62	56	20	36	0.1139
>62	48	25	23	
Gender				
Male	24	11	13	0.8171
Female	80	34	46	
Tumor size (cm)				
≤5	55	22	33	0.5535
>5	49	23	26	
Clinical Stage				
I/II	47	15	32	0.0467*
III/IV	57	30	27	
Depth of Invasion (T)				
T1	4	0	4	0.1778
T2	60	27	33	
T3	35	14	21	
T4	4	3	1	
Missing	1	1	0	
Lymph Node Metastasis (LNM)				
Negative (N0)	34	13	21	0.6699
Positive (N1–N3)	64	28	36	
Missing	6	4	2	
Distant Metastasis (M)				
Negative (M0)	66	22	44	0.0083**
Positive (M1)	38	23	15	
Differentiation				
Well	1	0	1	0.1542
Moderate	38	13	25	
Poor	62	31	31	
Missing	3	1	2	
Prognosis				
Survival	57	19	38	0.0297*
Death	47	26	21	

*$P < 0.05$ and **$P < 0.01$.

correlated with advanced stages ($P = 0.0467$; **Table 1**), distant metastasis ($P = 0.0083$; **Table 1**), and poor prognosis ($P = 0.0297$; **Table 1**). However, TIPRL expression was not associated with age ($P = 0.1139$; **Table 1**), gender ($P = 0.8171$; **Table 1**), tumor size ($P = 0.5535$; **Table 1**), depth of invasion ($P = 0.1778$; **Table 1**), lymph node metastasis ($P = 0.6699$; **Table 1**), or tumor histological differentiation ($P = 0.1542$; **Table 1**). These data suggested that down-regulation of TIPRL might contribute to gastric cancer metastasis and progression.

Low TIPRL Expression Predicted Poor Prognosis in Gastric Cancer Patients

Kaplan-Meier analysis was conducted to assess the correlation of TIPRL expression with gastric cancer prognosis. The survival analysis revealed that low expression of TIPRL was significantly correlated with shorter overall survival (OS) and disease-free survival (DFS) (**Figures 2I,J**, $P = 0.0193$ and $P = 0.0364$, respectively, log-rank test). In univariate Cox regression analysis, expression of TIPRL was correlated with OS and DFS in gastric cancer after curative resection [OS: HR = 0.512, CI (95%): 0.288–0.910, $P = 0.023$; DFS: HR = 0.473, CI (95%): 0.240–0.993, $P = 0.031$, **Table 2**]. Apart from TIPRL expression, tumor TNM stage ($P = 0.000$ and $P = 0.000$, respectively), depth of invasion ($P = 0.001$ and $P = 0.006$, respectively), lymph node metastasis ($P = 0.000$ and $P = 0.002$, respectively), distant metastasis ($P = 0.000$ and $P = 0.000$, respectively), and tumor histological differentiation ($P = 0.017$ and $P = 0.004$, respectively) were also significant predictors of outcome. In addition, multivariate analysis also revealed that distant metastasis, as well as tumor histological differentiation, were independent predictors of OS ($P = 0.036$) and DFS ($P = 0.012$) in gastric cancer, respectively. In all, our findings strongly suggest that loss of TIPRL is associated with invasion, metastasis, and an increased risk of poor prognosis in gastric cancer.

Regulation of TIPRL by miR-216a-5p and miR-383-5p

Post-transcriptional regulation involving miRNAs may contribute to TIPRL expression. Based on a literature review of the candidate miRNAs' function, TargetScan (http://www.targetscan.org/) and microRNA.org (http://www.microrna.org/) analysis revealed that the TIPRL 3′-untranslated region (3′-UTR) contained cancer-related miRNAs-binding sites, including miR-216a-5p, miR-383-5p, miR-29a-3p, miR-29b-3sp, miR-29c-3p, miR-101-3p, miR-124-3p, miR-128-3p, miR-224-5p, miR-433-3p, miR-450a-5p, miR-506-3p, and miR-873-5p (**Figure 3A**). Next, Luciferase reporter assays were conducted to confirm the direct binding affinity between the candidate miRNAs and 3′-UTR of TIPRL. Both miR-216a-5p and miR-383-5p rather than the other 11 miRNAs dramatically impaired the luciferase activity of the wild-type reporter genes for TIPRL 3′-UTR in both MKN45 and BGC823 cells (**Figures 3B–D**), but there was no remarkable change in the relative luciferase activity in cells encompassing the mutant binding site of TIPRL (**Figure 3E**). Furthermore, Western blot analysis further confirmed that ectopic expression of either miR-216a-5p or miR-383-5p resulted in decreased protein expression of TIPRL in both MKN45 and BGC823 cells (**Figures 3F,G**). Our findings indicate that miR-216a-5p and miR-383-5p could directly recognize binding sites in TIPRL 3′-UTR, and TIPRL is down-regulated by miR-216a-5p and miR-383-5p in gastric cancer cells.

TIPRL Impaired Migratory and Invasive Capacities of Gastric Cancer Cells *in vitro*

To substantiate the possible role of TIPRL in regulating gastric cancer tumorigenesis and progression, we adopted gain-of-function and loss-of-function assays to investigate TIPRL function in gastric cancer. First, TIPRL expression vector or empty vector was transiently transfected into MKN45 and BGC823 cells. Conversely, we genetically decreased the expression of TIPRL in MKN45 and BGC823 cells with TIPRL-specific siRNAs. The up-regulation and knockdown of TIPRL

TABLE 2 | Univariate and multivariate analysis of OS and DFS in gastric cancer patients.

Variables	Univariate analysis			Multivariate analysis		
	HR	CI (95%)	*P*-value	HR	CI (95%)	*P*-value
Overall Survival						
TIPRL expression	0.512	0.288–0.910	0.023*	0.956	0.500–1.827	0.892
Clinical stage	4.693	2.890–7.619	0.000	2.207	0.842–5.788	0.108
Depth of invasion	2.120	1.377–3.263	0.001	0.831	0.468–1.476	0.528
Lymph node metastasis	5.320	2.083–13.586	0.000	1.675	0.584–4.808	0.337
Distant metastasis	20.918	9.495–46.082	0.000	5.957	1.125–31.543	0.036
Differentiation	2.165	1.147–4.084	0.017	2.13	0.962–4.719	0.062
Disease-Free Survival						
TIPRL expression	0.473	0.240–0.993	0.031*	1.036	0.489–2.195	0.926
Clinical stage	6.182	3.223–11.858	0.000	2.747	0.736–10.253	0.133
Depth of invasion	2.017	1.223–3.326	0.006	0.736	0.401–1.451	0.409
Lymph node metastasis	5.152	1.800–14.747	0.002	0.945	0.290–3.076	0.925
Distant metastasis	33.734	12.354–92.117	0.000	8.969	0.918–87.589	0.059
Differentiation	3.675	1.518–8.896	0.004	3.854	1.339–11.088	0.012

*HR, hazard ratio; CI, confidence interval. *P < 0.05.*

expression were evidenced by western blotting (**Figures 4A–D**). In addition, the effects of TIPRL on migration and invasion of gastric cancer cells were assessed by transwell assays. The ectopic expression of TIPRL markedly inhibited the migration capacities of MKN45 and BGC823 cells compared with respective empty vector-transfected MKN45 and BGC823 cells (**Figures 4E,F,I,K**). Matrigel invasion assay also revealed that the forced expression of TIPRL significantly reduced cell invasion in MKN45 and BGC823 cells (**Figures 4E,F,I,K**). Meanwhile, an inverse effect was observed in MKN45 and BGC823 cells with silencing TIPRL expression (**Figures 4G,H,J,L**). In concordance with the clinical and prognostic significance of TIPRL in gastric cancer patients, the above results illustrate that TIPRL is a critical regulator of migration and invasion in gastric cancer cells.

Effect of TIPRL on Cell Proliferation and Apoptosis of Gastric Cancer Cells

To investigate the effect of TIPRL on gastric cancer cell proliferation and survival, MTS, EdU, and cell apoptosis assays were performed. The exogenous expression of TIPRL could not have a considerable effect on cell viability in MKN45 and BGC823 cells, while a similar effect was observed in MKN45 and BGC823 with silencing TIPRL expression (**Figures 5A–D**). In keeping with this, ectopic expression of TIPRL or knockdown of TIPRL did not affect cell proliferation, as evidenced by EdU proliferation assay in MKN45 and BGC823 (**Figures 5E–H**). Additionally, apoptosis analysis by flow cytometry revealed that proportions of apoptotic cells were similar between TIPRL overexpressed or TIPRL siRNA cells and respective controls in both cell lines (**Figures 6A–H**).

TIPRL Suppressed Invasion and Migration Through Regulation of AMPK/mTOR Pathway

To explore the molecular mechanism underlying the anti-invasive function of TIPRL, gene expression in TIPRL and vector transfected MKN45 cells were analyzed using whole-genome mRNA microarray. Unexpectedly, compared with empty vector-transfected cells, only 4 down-regulated genes (IGFBP1, NDRG1, EIF4G2, and NBPF10; fold change $\geq$2), which were not metastasis-related gene in human cancer, were detected in the MKN45 cells overexpressing TIPRL, microarray analysis revealed that almost all the genes remained unaffected at the mRNA levels, suggesting that TIPRL may modulate the genes at the post-transcriptional levels (**Figure 7A**). In addition, no significant change at the mRNA levels was further validated using RT-qPCR by specific primers available from our laboratory (**Figures 7B–D**), supporting the reliability of the microarray analysis. Intriguingly, TIPRL has been identified as a pivotal inhibitory regulator of protein phosphatase 2A (PP2A) (9, 10), and PP2A contributes significantly to AMP-activated protein kinase (AMPK) inactivation by dephosphorylation (13). Based on the interaction between TIPRL and PP2A, we hypothesized that TIPRL might exert the inhibitory effect on cell migration/invasion through activating AMPK signaling by inhibition of PP2A. We further evaluated the effect of TIPRL on PP2A activity in MKN45 and BGC823 cells. Consistently, TIPRL overexpression significantly reduced PP2A activity, whereas TIPRL silencing dramatically increased PP2A activity (**Figure 7E**). As expected, Western blot analysis confirmed this hypothesis and indicated that in the TIPRL-transfected MKN45 and BGC823 cells, phosphorylation of AMPK was markedly increased, while silencing TIPRL induced the opposite effects (**Figures 7F,G**). Moreover, as AMPK/mTOR signaling affects tumor invasion and metastasis (14–16), the AMPK downstream effectors of mTOR, p70S6K, and 4E-BP1 were also examined. Accordingly, phosphorylation of mTOR, p70S6K, and 4E-BP1 was substantially decreased in TIPRL expressed cells. Meanwhile, siRNA-mediated knockdown of TIPRL led to the opposite changes (**Figures 7F,G**). Furthermore, the total protein levels of AMPK, mTOR, p70S6K, and 4E-BP1 were not significantly affected under

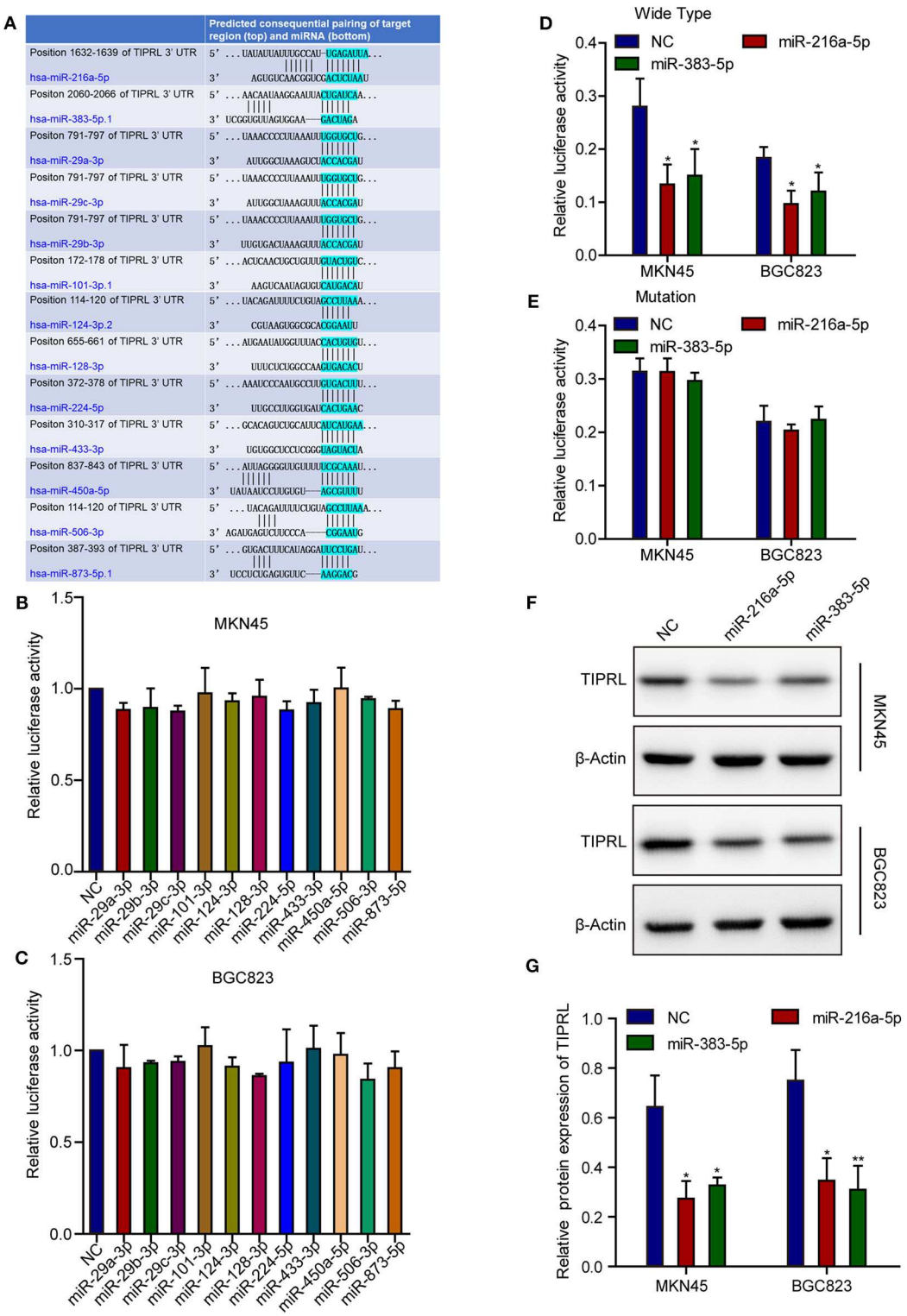

FIGURE 3 | MiR-216a-5p and miR-383-5p repress TIPRL expression through directly targeting its 3′-UTR. **(A)** Schematic illustration of the putative miRNAs binding sites in 3′-UTR of TIPRL. **(B–E)** The wild-type and mutant form of TIPRL 3′-UTR regions were fused with a luciferase reporter (pmirGLO) and luciferase reporter assay was performed. MiR-216a-5p/383-5p rather than other miRNAs significantly inhibited the luciferase activity of wild-type TIPRL 3′-UTR reporters in MKN45 and BGC823 cells (**B–D**, *t*-test, $^{*}P < 0.05$). Meanwhile, the luciferase responsiveness to miR-216a-5p/383-5p was abrogated by mutation of TIPRL 3′-UTR **(E)**. **(F,G)** Western blot analysis showed that up-regulated expression of miR-216a-5p/383-5p resulted in decreased protein expression of TIPRL. (*t*-test, $^{*}P < 0.05$; $^{**}P < 0.01$).

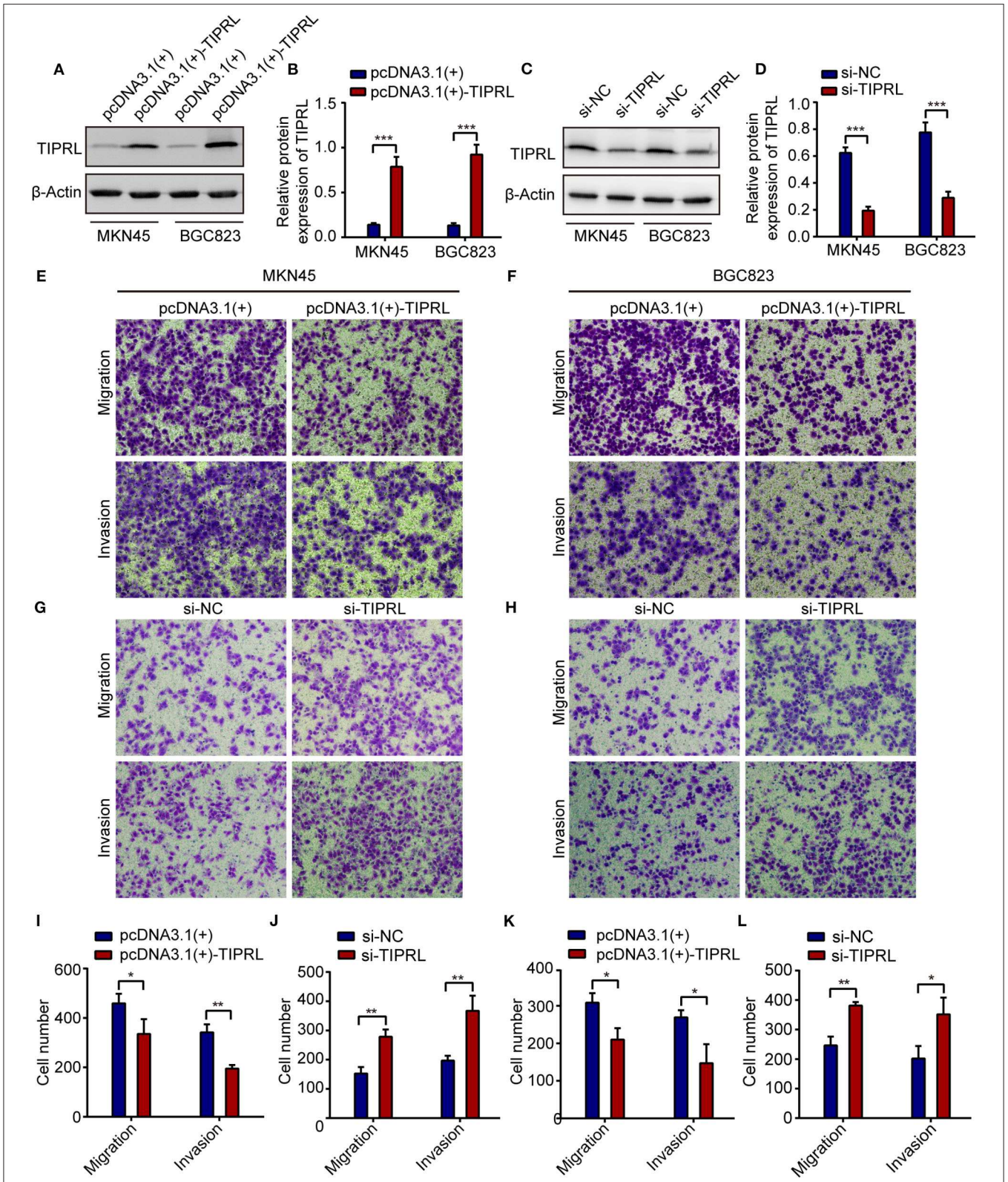

FIGURE 4 | TIPRL attenuates migration and invasion of gastric cancer cells. **(A–D)** The MKN45 and BGC823 cells were transfected with TIPRL-expressing vector [pcDNA3.1 (+)-TIPRL], TIPRL siRNA, and the respective control vector. The protein levels of TIPRL were examined by WB (***$P < 0.001$). **(E,F,I,K)** Expression of TIPRL inhibited the migration and invasion of MKN45 and BGC823 cells, as determined by transwell migration and matrigel invasion assays (*t*-test, *$P < 0.05$; **$P < 0.01$). **(G,H,J,L)** siRNA-mediated knockdown of TIPRL promoted the migration and invasion of MKN45 and BGC823 cells (*t*-test, *$P < 0.05$; **$P < 0.01$). All experiments were performed in triplicate. Error bars, SD.

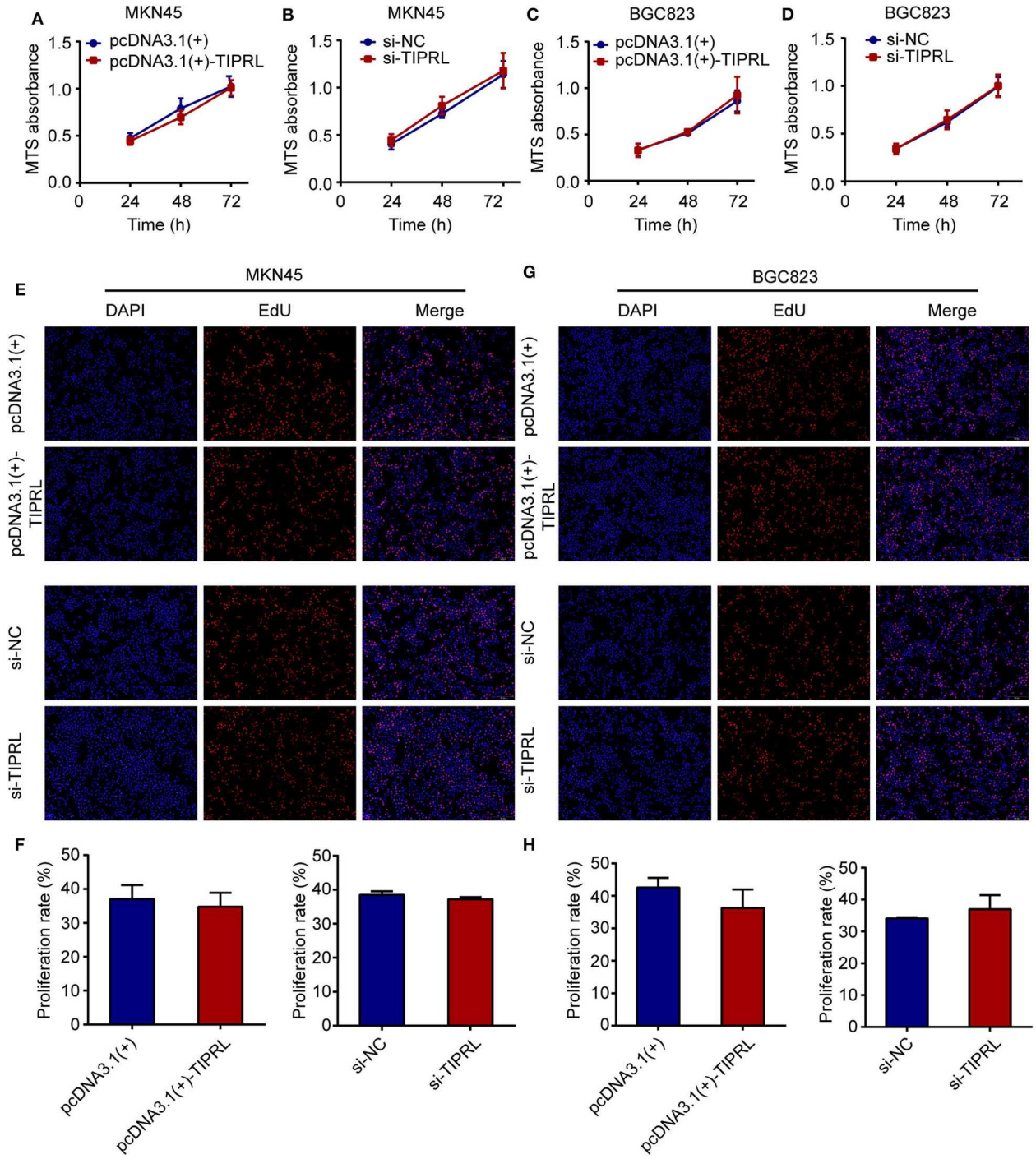

FIGURE 5 | Effect of TIPRL on cell proliferation in gastric cancer cells. **(A–D)** After transfection, cell viability was determined by MTS assay. The data showed that TIPRL had no effect on cell viability of MKN45 and BGC823 cells (*t*-test, $P > 0.05$). **(E–H)** EDU assays demonstrated that TIPRL did not influence the proliferation activities in MKN45 and BGC 823 cells (*t*-test, $P > 0.05$). All experiments were performed in triplicate. Error bars, SD.

either condition (**Figure 7F**). Thus, these results support our notion that TIPRL suppresses cell migration/invasion of gastric cancer through regulating AMPK/mTOR signaling pathway.

DISCUSSION

Invasion and metastasis of gastric cancer after curative resection remain the most common lethal outcomes with few efficacious

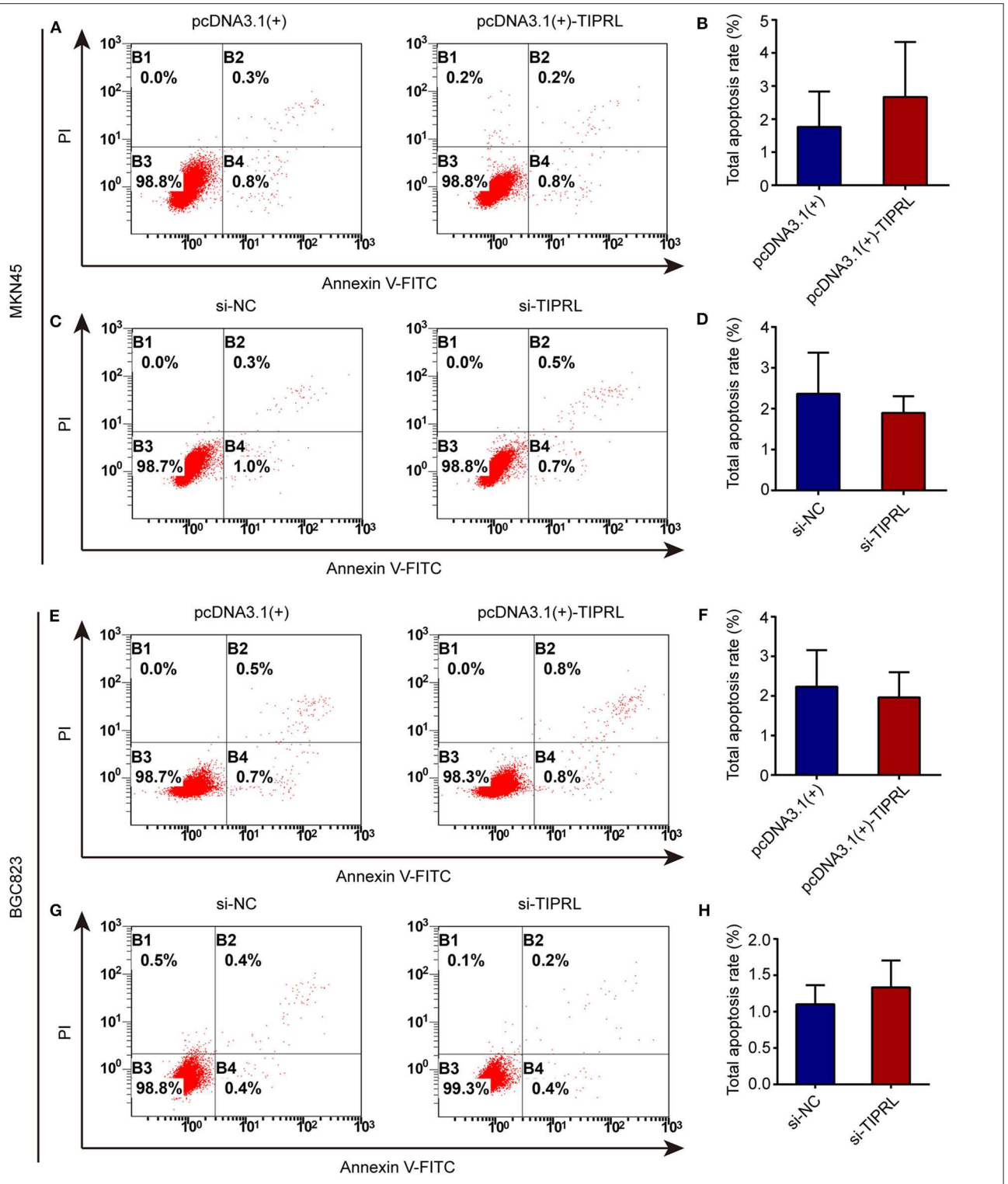

FIGURE 6 | Effect of TIPRL on cell apoptosis in gastric cancer cells. **(A–H)** Up-regulation or down-regulation of TIPRL expression could not induce apoptosis in both cell lines, as indicated by flow cytometry analysis following Annexin V-FITC/PI staining (*t*-test, $P > 0.05$). All experiments were performed in triplicate. Error bars, SD.

therapeutic options. Therefore, it is critical to understand the mechanisms underlying gastric cancer metastasis in order to discover novel effective therapeutic targets for clinical evaluation.

Using microarray analysis of metastatic and non-metastatic tumors, we identified TIPRL as a novel metastasis suppressor in gastric cancer through gene expression microarray. TIPRL

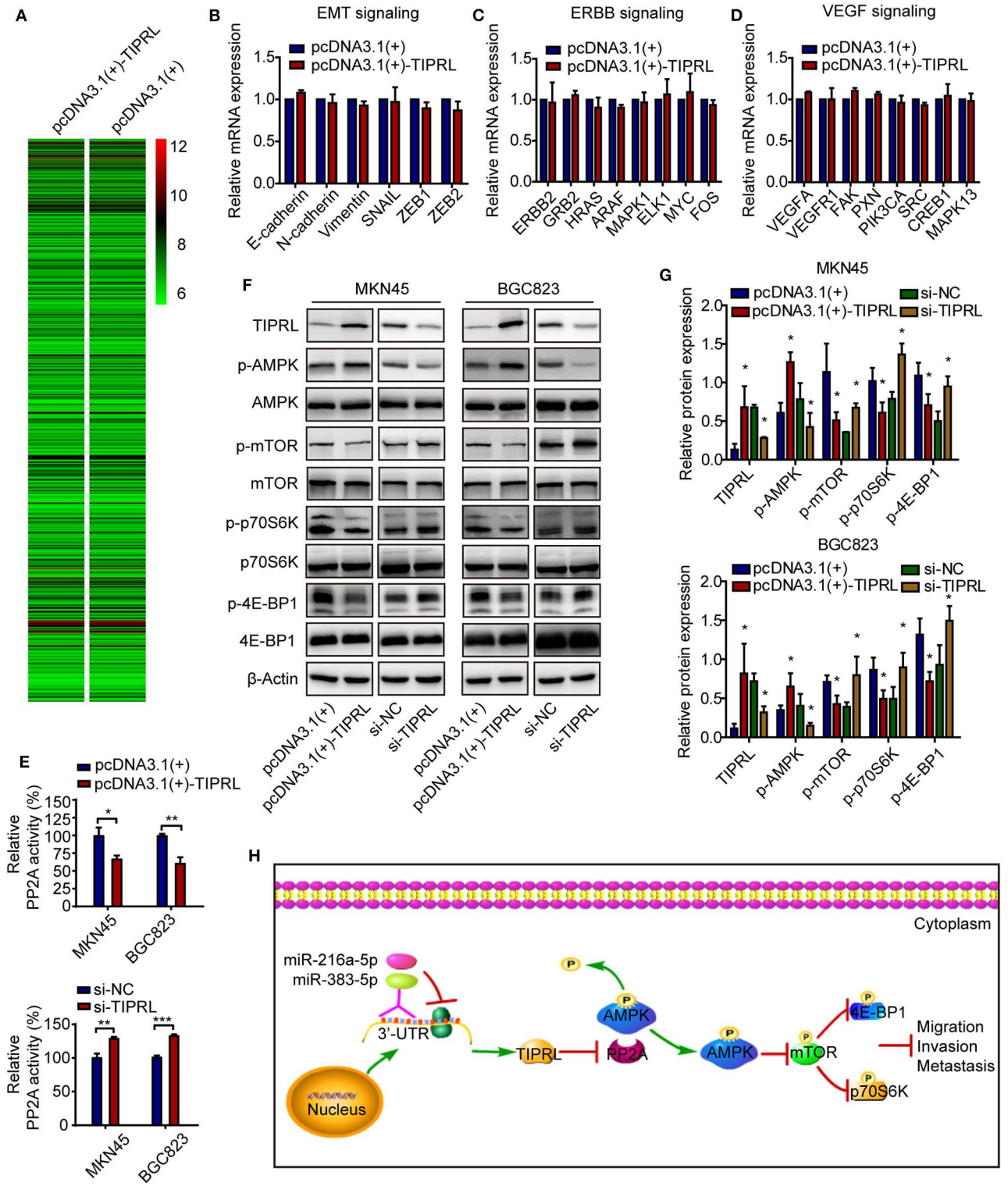

FIGURE 7 | TIPRL suppresses metastatic potential of gastric cancer via AMPK/mTOR signaling. **(A)** Microarray study on TIPRL-regulated genes. Hierarchical clustering of TIPRL-regulated genes on the basis of the expression patterns. Almost no change was observed at the mRNA levels between TIPRL overexpression and control cells. **(B–D)** Validation of the microarray analysis. No significant change at the mRNA expression levels of genes related to EMT, ERBB, and VEGF signaling pathways in MKN45 cells transfected with TIPRL overexpression and control vector was further validated using RT-qPCR. **(E)** PP2A activity analysis indicated that TIPRL resulted in inhibition of PP2A activity by PP2A activity assay (*t*-test, $^{*}P < 0.05$; $^{**}P < 0.01$; and $^{***}P < 0.001$). Overexpression of TIPRL significantly reduced PP2A activity in MKN45 and BGC823 cells. Conversely, an inverse effect was observed in MKN45 and BGC823 cells with silencing TIPRL expression.

(Continued)

FIGURE 7 | (F,G) Immunoblot results showed that up-regulated expression of TIPRL enhanced phosphorylation of AMPK (p-AMPK) and reduced phosphorylation of mTOR (p-mTOR), p70S6K (p-p70S6K), and 4E-BP1 (p-4E-BP1); Down-regulated expression of TIPRL led to the opposite changes (*t*-test, $^*P < 0.05$). The total protein levels of AMPK, mTOR, p70S6K, and 4E-BP1 did not change. **(H)** Schematic illustration of the molecular basis of TIPRL as a metastasis suppressor in gastric cancer. TIPRL, a target of miR-216a-5p/383-5p, facilitates AMPK phosphorylation via preventing the PP2A-dependent dephosphorylation and inactivation of AMPK, which in turn attenuates phosphorylation of mTOR and its downstream effectors p70S6K and 4E-BP1, leading to inactivation of mTOR signaling and subsequent suppression of invasion and metastasis of gastric cancer.

is a ubiquitously expressed protein which functions as a key inhibitory regulator of PP2A-like phosphatases, including PP2A, PP4, and PP6 (9, 10). Despite this, little is known about the functional and prognostic implications of TIPRL in cancer, particularly in tumor metastasis. Recently, a growing body of evidence supports an oncogenic role for PP2A-like enzymes. Upregulation of the catalytic subunit of PP2A predicts poor prognosis and promotes carcinogenesis through inhibition of p53 mediated apoptosis in hepatocellular cancer models (17, 18). In basal breast cancer, PP2A appears to act as a metastasis promoter by activating cofilin-1 (CFL-1) (19). In addition, PP4 has also been found to be overexpressed in numerous types of cancer (20–22) and inhibition of PP4 expression increases efficacy of cisplatin treatment (21). Given aforementioned studies and function of TIPRL, it is plausible to assume that TIPRL may be a potential tumor suppressor gene. Herein, we highlight a functional role for TIPRL in invasion and metastasis of gastric cancer.

The clinical relevance of TIPRL in gastric cancer was investigated in a large well-characterized clinical cohort. We showed that TIPRL was frequently decreased in gastric cancer tissues, relative to non-tumor tissues. Moreover, TIPRL expression was markedly down-regulated in primary tumor samples with distant metastasis, compared to those without distant metastasis. Importantly, IHC analysis of TIPRL in gastric cancer demonstrated a strong association between low expression of TIPRL and unfavorable clinicopathological variables such as more-advanced TNM stage and distant metastasis, suggesting that TIPRL down-regulation might facilitate a metastatic phenotype. Furthermore, significantly shortened overall survival and disease-free survival were observed in gastric cancer patients with low TIPRL expression compared with patients with high TIPRL expression. In keeping with our data, higher expression of TIPRL was associated with a favorable prognosis in gastric carcinoma patients according to analysis of publicly available data sets. These clinical data strongly suggested that TIPRL might be involved in the metastasis and progression of gastric cancer and serve as a novel useful prognostic biomarker.

Currently, regulatory mechanisms of TIPRL are not yet documented. MicroRNAs (miRNAs) play a pivotal role in tumorigenesis via negatively regulating target gene expression at the post-transcriptional level (23, 24). Using bioinformatics analysis and luciferase assay, we found that miR-216a-5p and miR-383-5p could directly regulate TIPRL expression through targeting the 3′-UTR of TIPRL. In recent years, accumulating evidence has demonstrated that miR-216a-5p and miR-383-5p are significantly elevated and function as oncogenic miRNAs in a variety of tumors (25–31). In particular, previous study have shown that miR-216a promotes invasion and metastasis in hepatocellular carcinoma through targeting TSLC1, PTEN, and SMAD7 (25–27), which is further confirmed in a variety of cell models (28–30). Moreover, it has been reported that miR-383 promotes cholangiocarcinoma cell invasion and proliferation by suppressing IRF1 (31). More importantly, in gastric cancer, miR-216a is significantly upregulated (32), and elevation of miR-216a would favor a worse clinical outcome (33). Additionally, elevated miR-216a-3p activates the NF-κB signaling pathway through targeting RUNX1, contributing to metastatic potential of gastric cancer (34). Here, our current study pointed out that miR-216a-5p/383-5p suppressed TIPRL expression, thus suggesting that elevation of miR-216a-5p/383-5p might contribute to aberrant down-regulation of TIPRL in gastric cancer. This study enriches our horizon of TIPRL regulation by miRNAs.

Our clinical data urged us to investigate the putative tumor-suppressive function of TIPRL in gastric cancer *in vitro*. Re-expression of TIPRL in MKN45 and BGC823 cells markedly suppressed the migration and invasion abilities; while the knockdown of TIPRL promoted migration and invasion of the gastric cancer cells *in vitro*. Both assays of forced and silenced expression of TIPRL revealed that TIPRL could suppress cell migration and invasion in gastric cancer, which are two crucial events during tumor metastasis (35), consistent with clinical observations. Moreover, previous report demonstrates that TIPRL prevents TRAIL-induced apoptosis through inactivation of MKK7-JNK signaling in hepatocellular carcinoma (12). However, in the current study, the apoptosis and proliferation of gastric cancer cells were not affected. Thus, the effects of TIPRL may be cell context-dependent. Collectively, these findings provide the first demonstration that TIPRL acts as a novel metastasis suppressor in gastric cancer.

We further elucidated the molecular basis by which TIPRL exerted the suppressive effect on cell migration and invasion in gastric cancer using mRNA microarray. Unexpectedly, it is noteworthy that TIPRL could not modulate the genes at transcriptional levels by the microarray and real-time PCR analysis, thereby implying that the regulation might occur at the post-transcriptional levels. Intriguingly, it is known that TIPRL has a well-established role as a crucial modulator to inactivate the phosphatase activity of PP2A (9, 10). PP2A, a major serine-threonine phosphatase, regulates a variety of kinase-driven intracellular signaling pathways by dephosphorylating many pivotal cellular molecules (36). The predominant form of PP2A inside cells contains a heterotrimer formed by catalytic (C), scaffolding (A), and regulatory (B) subunits (9). Structure-guided studies reveal that the butterfly-shaped TIPRL binds specifically to the PP2A catalytic subunit (C) and perturbs the phosphatase active site, resulting in phosphatase inactivation.

TIPRL also makes dynamic wobble contacts with scaffolding (A) subunit, leading to enhanced inactivation of disease-associated mutant PP2A. More importantly, TIPRL and latency chaperone, alpha4, coordinate to promote disassembly of PP2A complexes (10). Consistently, our study indicated that TIPRL negatively regulated PP2A activity in gastric cancer cells. Moreover, PP2A, an upstream phosphatase of AMPK (13), directly interacts with AMPK and negatively regulates AMPK activity by dephosphorylating Thr-172, a residue that is required for AMPK activation when phosphorylated (37). AMPK activity is also negatively regulates by calcium-mediated PR72-containing PP2A (38). Additionally, previous reports demonstrate that subunit A of PP2A co-immunoprecipitates with AMPK (39), leading to inactivation of AMPK activity in a glucose-dependent manner (39, 40). Furthermore, targeting PP2A by LB-100 (a novel PP2A inhibitor) activates AMPK to suppress colorectal cancer in *vitro* and *in vivo* (41). Unsurprisingly, PP2A also negatively regulates AMPK signaling by dephosphorylating and inactivating AMPK. Given the interaction between TIPRL and PP2A, we therefore postulated that TIPRL might potentiate AMPK signaling via preventing the PP2A-dependent dephosphorylation and inactivation of AMPK. As a critical cellular energy sensor, AMPK plays a central role in regulating cellular metabolism and energy homeostasis (42). Augmented AMPK activity also contributes to suppression of invasive and metastatic capacities of cancer cells (16, 43), which is a key process during tumor progression. As expected, overexpression of TIPRL induced strong phosphorylation and activation of AMPK in gastric cancer cells, whereas an inverse effect was observed in TIPRL-deficient cells. Therefore, the suppression of cell migration and invasion induced by TIPRL in gastric cancer might attribute, at least in part, to the TIPRL-mediated phosphorylation/activation of AMPK signaling. Concomitantly, compelling evidence indicates that AMPK activation has emerged as a pivotal negative regulator of mTOR and its downstream effectors (14, 44, 45), which intimately relates to tumor invasion and metastasis (15, 46–50). Accordingly, it is of interest to determine the effect of TIPRL on mTOR and its downstream effectors p70S6K and 4E-BP1. These data indicated that TIPRL could attenuate phosphorylation of mTOR, p70S6K, and 4E-BP1, thereby suppressing the mTOR signaling pathway. Together, our findings suggest that TIPRL may induce phosphorylation/activation of AMPK, which in turn attenuates the mTOR pathway, leading to inactivation of mTOR signaling and subsequent suppression of cell migration/invasion in gastric cancer.

To date, the role of TIPRL in cancer has been documented only in liver and lung cancer (12, 51, 52). In hepatocellular carcinoma samples and cell lines, TIPRL is overexpressed and prevents TRAIL-induced apoptosis through inactivation of MKK7-JNK signaling (12), thereby representing a potential biomarker for early liver cancer (51). In addition, TIPRL overexpression is found to induce autophagy and accelerate growth through the eIF2α-ATF4 pathway in non-small cell lung cancer (52). Given the previous reports, TIPRL is believed to be oncogenic. However, our study indeed suggested that TIPRL functioned as a metastasis suppressor in gastric cancer through regulating AMPK/mTOR signaling. This indicates that TIPRL may have strikingly distinct functional roles in tumorigenesis depending on the cellular context. For example, the dual role of p21 as a tumor suppressor and an oncogene in different types of cancer has been documented (53). Thus, our findings may lead to further studies of the effects of TIPRL in other cancers.

Taken together, the present study provides the first evidence that TIPRL, a target of miR-216a-5p/383-5p, is identified as a potential metastasis suppressor gene in gastric cancer. Clinically, loss of TIPRL expression in gastric cancer is a strong indicator of metastatic phenotype and poor clinical outcomes. TIPRL exerts its anti-invasive function through regulating AMPK/mTOR signaling pathway (**Figure 7H**). Thus, TIPRL may represent a prognostic biomarker and a promising target for new therapies in gastric cancer.

DATA AVAILABILITY STATEMENT

The datasets presented in this study can be found in online repositories. The names of the repository/repositories and accession number(s) can be found in the article/**Supplementary Material**.

ETHICS STATEMENT

The studies involving human participants were reviewed and approved by the Ethics Committee of Shandong University, China. The patients/participants provided their written informed consent to participate in this study.

AUTHOR CONTRIBUTIONS

PG designed and supervised the whole study and revised the manuscript. ML and S-SS performed the experiments and drafted the manuscript. D-BS, H-TL, and R-RM provided technical support and assisted with the experiments. X-QX and Y-JS conducted statistical analysis. All authors read and approved the final manuscript.

FUNDING

This study was supported by the National Natural Science Foundation of China (Grant Nos. 81872362 and 81672842) and the Taishan Scholars Program of Shandong Province (Grant No. ts201511096).

SUPPLEMENTARY MATERIAL

The Supplementary Material for this article can be found online at: https://www.frontiersin.org/articles/10.3389/fonc.2020.01062/full#supplementary-material

REFERENCES

1. Bray F, Ferlay J, Soerjomataram I, Siegel RL, Torre LA, Jemal A. Global cancer statistics 2018: GLOBOCAN estimates of incidence and mortality worldwide for 36 cancers in 185 countries. *CA Cancer J Clin*. (2018) 68:394–424. doi: 10.3322/caac.21492
2. Cervantes A, Roda D, Tarazona N, Rosello S, Perez-Fidalgo JA. Current questions for the treatment of advanced gastric cancer. *Cancer Treat Rev*. (2013) 39:60–7. doi: 10.1016/j.ctrv.2012.09.007
3. Camargo MC, Kim WH, Chiaravalli AM, Kim KM, Corvalan AH, Matsuo K, et al. Improved survival of gastric cancer with tumour epstein-Barr virus positivity: an international pooled analysis. *Gut*. (2014) 63:236–43. doi: 10.1136/gutjnl-2013-304531
4. Marrelli D, Roviello F, De Stefano A, Fotia G, Giliberto C, Garosi L, et al. Risk factors for liver metastases after curative surgical procedures for gastric cancer: a prospective study of 208 patients treated with surgical resection. *J Am Coll Surg*. (2004) 198:51–8. doi: 10.1016/j.jamcollsurg.2003.08.013
5. Yoo CH, Noh SH, Shin DW, Choi SH, Min JS. Recurrence following curative resection for gastric carcinoma. *Br J Surg*. (2000) 87:236–42. doi: 10.1046/j.1365-2168.2000.01360.x
6. Palmer TD, Ashby WJ, Lewis JD, Zijlstra A. Targeting tumor cell motility to prevent metastasis. *Adv Drug Deliv Rev*. (2011) 63:568–81. doi: 10.1016/j.addr.2011.04.008
7. Valastyan S, Weinberg RA. Tumor metastasis: molecular insights and evolving paradigms. *Cell*. (2011) 147:275–92. doi: 10.1016/j.cell.2011.09.024
8. Jacinto E, Guo B, Arndt KT, Schmelzle T, Hall MN. TIP41 interacts with TAP42 and negatively regulates the TOR signaling pathway. *Mol Cell*. (2001) 8:1017–26. doi: 10.1016/S1097-2765(01)00386-0
9. McConnell JL, Gomez RJ, McCorvey LR, Law BK, Wadzinski BE. Identification of a PP2A-interacting protein that functions as a negative regulator of phosphatase activity in the ATM/ATR signaling pathway. *Oncogene*. (2007) 26:6021–30. doi: 10.1038/sj.onc.1210406
10. Wu CG, Zheng A, Jiang L, Rowse M, Stanevich V, Chen H, et al. Methylation-regulated decommissioning of multimeric PP2A complexes. *Nat Commun*. (2017) 8:2272. doi: 10.1038/s41467-017-02405-3
11. Nakashima A, Tanimura-Ito K, Oshiro N, Eguchi S, Miyamoto T, Momonami A, et al. A positive role of mammalian Tip41-like protein, TIPRL, in the amino-acid dependent mTORC1-signaling pathway through interaction with PP2A. *FEBS Lett*. (2013) 587:2924–9. doi: 10.1016/j.febslet.2013.07.027
12. Song IS, Jun SY, Na HJ, Kim HT, Jung SY, Ha GH, et al. Inhibition of MKK7-JNK by the TOR signaling pathway regulator-like protein contributes to resistance of HCC cells to TRAIL-induced apoptosis. *Gastroenterology*. (2012) 143:1341–51. doi: 10.1053/j.gastro.2012.07.103
13. Gao X, Zhao L, Liu S, Li Y, Xia S, Chen D, et al. gamma-6-Phosphogluconolactone, a byproduct of the oxidative pentose phosphate pathway, contributes to AMPK activation through inhibition of PP2A. *Mol Cell*. (2019) 76:857–71 e9. doi: 10.1016/j.molcel.2019.09.007
14. Inoki K, Kim J, Guan KL. AMPK and mTOR in cellular energy homeostasis and drug targets. *Annual Rev Pharmacol Toxicol*. (2012) 52:381–400. doi: 10.1146/annurev-pharmtox-010611-134537
15. Murugan AK. mTOR: role in cancer, metastasis and drug resistance. *Semin Cancer Biol*. (2019) 59:92–111. doi: 10.1016/j.semcancer.2019.07.003
16. Yan Y, Tsukamoto O, Nakano A, Kato H, Kioka H, Ito N, et al. Augmented AMPK activity inhibits cell migration by phosphorylating the novel substrate Pdlim5. *Nature Commun*. (2015) 6:6137. doi: 10.1038/ncomms7137
17. Duong FH, Dill MT, Matter MS, Makowska Z, Calabrese D, Dietsche T, et al. Protein phosphatase 2A promotes hepatocellular carcinogenesis in the diethylnitrosamine mouse model through inhibition of p53. *Carcinogenesis*. (2014) 35:114–22. doi: 10.1093/carcin/bgt258
18. Gong SJ, Feng XJ, Song WH, Chen JM, Wang SM, Xing DJ, et al. Upregulation of PP2Ac predicts poor prognosis and contributes to aggressiveness in hepatocellular carcinoma. *Cancer Biol Ther*. (2016) 17:151–62. doi: 10.1080/15384047.2015.1121345
19. Quintela-Fandino M, Arpaia E, Brenner D, Goh T, Yeung FA, Blaser H, et al. HUNK suppresses metastasis of basal type breast cancers by disrupting the interaction between PP2A and cofilin-1. *Proc Natl Acad Sci USA*. (2010) 107:2622–7. doi: 10.1073/pnas.0914492107
20. Li X, Liang L, Huang L, Ma X, Li D, Cai S. High expression of protein phosphatase 4 is associated with the aggressive malignant behavior of colorectal carcinoma. *Mol Cancer*. (2015) 14:95. doi: 10.1186/s12943-015-0356-7
21. Wang B, Zhao A, Sun L, Zhong X, Zhong J, Wang H, et al. Protein phosphatase PP4 is overexpressed in human breast and lung tumors. *Cell Res*. (2008) 18:974–7. doi: 10.1038/cr.2008.274
22. Weng S, Wang H, Chen W, Katz MH, Chatterjee D, Lee JE, et al. Overexpression of protein phosphatase 4 correlates with poor prognosis in patients with stage II pancreatic ductal adenocarcinoma. *Cancer Epidemiol Biomarkers Prev*. (2012) 21:1336–43. doi: 10.1158/1055-9965.EPI-12-0223
23. Wu W. MicroRNA: potential targets for the development of novel drugs? *Drugs R D*. (2010) 10:1–8. doi: 10.2165/11537800-000000000-00000
24. Zhang H, Li Y, Lai M. The microRNA network and tumor metastasis. *Oncogene*. (2010) 29:937–48. doi: 10.1038/onc.2009.406
25. Chen PJ, Yeh SH, Liu WH, Lin CC, Huang HC, Chen CL, et al. Androgen pathway stimulates microRNA-216a transcription to suppress the tumor suppressor in lung cancer-1 gene in early hepatocarcinogenesis. *Hepatology*. (2012) 56:632–43. doi: 10.1002/hep.25695
26. Xia H, Ooi LL, Hui KM. MicroRNA-216a/217-induced epithelial-mesenchymal transition targets PTEN and SMAD7 to promote drug resistance and recurrence of liver cancer. *Hepatology*. (2013) 58:629–41. doi: 10.1002/hep.26369
27. Bai J, Yao B, Wang L, Sun L, Chen T, Liu R, et al. lncRNA A1BG-AS1 suppresses proliferation and invasion of hepatocellular carcinoma cells by targeting miR-216a-5p. *J Cell Biochem*. (2019) 120:10310–22. doi: 10.1002/jcb.28315
28. Chen P, Quan J, Jin L, Lin C, Xu W, Xu J, et al. miR-216a-5p acts as an oncogene in renal cell carcinoma. *Exp Ther Med*. (2018) 15:4039–46. doi: 10.3892/etm.2018.5881
29. Liu H, Pan Y, Han X, Liu J, Li R. MicroRNA-216a promotes the metastasis and epithelial-mesenchymal transition of ovarian cancer by suppressing the PTEN/AKT pathway. *OncoTargets Ther*. (2017) 10:2701–9. doi: 10.2147/OTT.S114318
30. Miyazaki T, Ikeda K, Sato W, Horie-Inoue K, Okamoto K, Inoue S. MicroRNA library-based functional screening identified androgen-sensitive miR-216a as a player in bicalutamide resistance in prostate cancer. *J Clin Med*. (2015) 4:1853–65. doi: 10.3390/jcm4101853
31. Wan P, Chi X, Du Q, Luo J, Cui X, Dong K, et al. miR-383 promotes cholangiocarcinoma cell proliferation, migration, and invasion through targeting IRF1. *J Cell Biochem*. (2018) 119:9720–9. doi: 10.1002/jcb.27286
32. Zhang Z, Xue H, Dong Y, Zhang J, Pan Y, Shi L, et al. GKN2 promotes oxidative stress-induced gastric cancer cell apoptosis via the Hsc70 pathway. *J Exp Clin Cancer Res*. (2019) 38:338. doi: 10.1186/s13046-019-1336-3
33. Guo J, Li Y, Duan H, Yuan L. LncRNA TUBA4B functions as a competitive endogenous RNA to inhibit gastric cancer progression by elevating PTEN via sponging miR-214 and miR-216a/b. *Cancer Cell Int*. (2019) 19:156. doi: 10.1186/s12935-019-0879-x
34. Wu Y, Zhang J, Zheng Y, Ma C, Liu XE, Sun X. miR-216a-3p inhibits the proliferation, migration, and invasion of human gastric cancer cells via targeting RUNX1 and activating the NF-kappaβ signaling pathway. *Oncol Res*. (2018) 26:157–71. doi: 10.3727/096504017X15031557924150
35. Friedl P, Wolf K. Tumour-cell invasion and migration: diversity and escape mechanisms. *Nat Rev Cancer*. (2003) 3:362–74. doi: 10.1038/nrc1075
36. Seshacharyulu P, Pandey P, Datta K, Batra SK. Phosphatase: PP2A structural importance, regulation and its aberrant expression in cancer. *Cancer Lett*. (2013) 335:9–18. doi: 10.1016/j.canlet.2013.02.036
37. Joseph BK, Liu HY, Francisco J, Pandya D, Donigan M, Gallo-Ebert C, et al. Inhibition of AMP kinase by the protein phosphatase 2A heterotrimer, PP2APpp2r2d. *J Biol Chem*. (2015) 290:10588–98. doi: 10.1074/jbc.M114.626259
38. Park S, Scheffler TL, Rossie SS, Gerrard DE. AMPK activity is regulated by calcium-mediated protein phosphatase 2A activity. *Cell calcium*. (2013) 53:217–23. doi: 10.1016/j.ceca.2012.12.001
39. Gimeno-Alcaniz JV, Sanz P. Glucose and type 2A protein phosphatase regulate the interaction between catalytic and regulatory subunits of AMP-activated protein kinase. *J Mol Biol*. (2003) 333:201–9. doi: 10.1016/j.jmb.2003.08.022

40. Ravnskjaer K, Boergesen M, Dalgaard LT, Mandrup S. Glucose-induced repression of PPARalpha gene expression in pancreatic beta-cells involves PP2A activation and AMPK inactivation. *J Mol Endocrinol*. (2006) 36:289–99. doi: 10.1677/jme.1.01965
41. Dai C, Zhang X, Xie D, Tang P, Li C, Zuo Y, et al. Targeting PP2A activates AMPK signaling to inhibit colorectal cancer cells. *Oncotarget*. (2017) 8:95810–23. doi: 10.18632/oncotarget.21336
42. Carling D, Mayer FV, Sanders MJ, Gamblin SJ. AMP-activated protein kinase: nature's energy sensor. *Nat Chem Biol*. (2011) 7:512–8. doi: 10.1038/nchembio.610
43. Schaffer BE, Levin RS, Hertz NT, Maures TJ, Schoof ML, Hollstein PE, et al. Identification of AMPK phosphorylation sites reveals a network of proteins involved in cell invasion and facilitates large-scale substrate prediction. *Cell Metab*. (2015) 22:907–21. doi: 10.1016/j.cmet.2015.09.009
44. Avivar-Valderas A, Bobrovnikova-Marjon E, Alan Diehl J, Bardeesy N, Debnath J, Aguirre-Ghiso JA. Regulation of autophagy during ECM detachment is linked to a selective inhibition of mTORC1 by PERK. *Oncogene*. (2013) 32:4932–40. doi: 10.1038/onc.2012.512
45. van Veelen W, Korsse SE, van de Laar L, Peppelenbosch MP. The long and winding road to rational treatment of cancer associated with LKB1/AMPK/TSC/mTORC1 signaling. *Oncogene*. (2011) 30:2289–303. doi: 10.1038/onc.2010.630
46. Gulhati P, Bowen KA, Liu J, Stevens PD, Rychahou PG, Chen M, et al. mTORC1 and mTORC2 regulate EMT, motility, and metastasis of colorectal cancer via RhoA and Rac1 signaling pathways. *Cancer Research*. (2011) 71:3246–56. doi: 10.1158/0008-5472.CAN-10-4058
47. Liu L, Chen L, Chung J, Huang S. Rapamycin inhibits F-actin reorganization and phosphorylation of focal adhesion proteins. *Oncogene*. (2008) 27:4998–5010. doi: 10.1038/onc.2008.137
48. Liu L, Li F, Cardelli JA, Martin KA, Blenis J, Huang S. Rapamycin inhibits cell motility by suppression of mTOR-mediated S6K1 and 4E-BP1 pathways. *Oncogene*. (2006) 25:7029–40. doi: 10.1038/sj.onc.1209691
49. Pon YL, Zhou HY, Cheung AN, Ngan HY, Wong AS. p70 S6 kinase promotes epithelial to mesenchymal transition through snail induction in ovarian cancer cells. *Cancer Res*. (2008) 68:6524–32. doi: 10.1158/0008-5472.CAN-07-6302
50. Wan X, Mendoza A, Khanna C, Helman LJ. Rapamycin inhibits ezrin-mediated metastatic behavior in a murine model of osteosarcoma. *Cancer Res*. (2005) 65:2406–11. doi: 10.1158/0008-5472.CAN-04-3135
51. Jun SY, Jeon SJ, Yoon JY, Lee JJ, Yoon HR, Choi MH, et al. The positive correlation of TIPRL with LC3 and CD133 contributes to cancer aggressiveness: potential biomarkers for early liver cancer. *Sci Rep*. (2019) 9:16802. doi: 10.1038/s41598-019-53191-5
52. Jeon SJ, Ahn JH, Halder D, Cho HS, Lim JH, Jun SY, et al. TIPRL potentiates survival of lung cancer by inducing autophagy through the eIF2alpha-ATF4 pathway. *Cell Death Dis*. (2019) 10:959. doi: 10.1038/s41419-019-2190-0
53. Abbas T, Dutta A. p21 in cancer: intricate networks and multiple activities. *Nat Rev Cancer*. (2009) 9:400–14. doi: 10.1038/nrc2657

Conflict of Interest: The authors declare that the research was conducted in the absence of any commercial or financial relationships that could be construed as a potential conflict of interest.

frontiers in Oncology

ORIGINAL RESEARCH
published: 16 July 2020
doi: 10.3389/fonc.2020.00966

High Level of Legumain Was Correlated With Worse Prognosis and Peritoneal Metastasis in Gastric Cancer Patients

Yan Wang[1†], Shilong Zhang[2†], Haiwei Wang[3], Yuehong Cui[1], Zhiming Wang[1], Xi Cheng[1], Wei Li[1], Jun Hou[4], Yuan Ji[4] and Tianshu Liu[1,5]*

[1] Department of Medical Oncology, Zhongshan Hospital, Fudan University, Shanghai, China, [2] Minhang Hospital, Fudan University, Shanghai, China, [3] Maternity and Children's Hospital of Fujian Province, Fujian Medical University, Fuzhou, China, [4] Department of Pathology, Zhongshan Hospital, Fudan University, Shanghai, China, [5] Center of Evidence-Based Medicine, Fudan University, Shanghai, China

OPEN ACCESS

Edited by:
Jianjun Xie,
Shantou University, China

Reviewed by:
Midie Xu,
Fudan University Shanghai Cancer Center, China
Zehua Bian,
Affiliated Hospital of Jiangnan University, China

***Correspondence:**
Tianshu Liu
liu.tianshu@zs-hospital.sh.cn

[†]These authors have contributed equally to this work

Specialty section:
This article was submitted to Gastrointestinal Cancers, a section of the journal Frontiers in Oncology

Received: *17 March 2020*
Accepted: *15 May 2020*
Published: *16 July 2020*

Citation:
Wang Y, Zhang S, Wang H, Cui Y, Wang Z, Cheng X, Li W, Hou J, Ji Y and Liu T (2020) High Level of Legumain Was Correlated With Worse Prognosis and Peritoneal Metastasis in Gastric Cancer Patients. Front. Oncol. 10:966. doi: 10.3389/fonc.2020.00966

Background: Accumulating evidence has demonstrated that legumain (LGMN) is abnormally expressed in several malignancies and functions as an oncogene. However, the association between LGMN and gastric cancer (GC) has not yet been fully elucidated. In this study, we performed a comprehensive analysis of the role of LGMN in clinicopathologic characteristics and survival of GC patients.

Methods: The study had two patient cohorts, The Cancer Genome Atlas (TCGA) cohort and the Zhongshan Hospital cohort, both of which were used to analyze the role of LGMN in GC samples. The relationship between LGMN and clinicopathologic characteristics was determined by the Chi-square test and logistic regression analysis. The Kaplan–Meier method and Cox proportional hazards regression analysis were conducted to investigate the prognostic role of LGMN in GC patients. Moreover, a nomogram was constructed based on the factors that were independently associated with peritoneal metastasis. Finally, the gene set enrichment analysis (GSEA) was conducted to explore the underlying pathways through which LGMN was involved in GC progression.

Results: The mRNA and protein levels of LGMN were significantly upregulated in GC tissues, especially for diffuse-type GC. High level of LGMN was independently associated with poor prognosis in both TCGA and Zhongshan cohorts. Further analysis showed that increased protein level of LGMN was related to peritoneal metastasis in GC patients. In a nomogram model, the LGMN expression could help predict the possibility of peritoneal metastasis in GC patients. LGMN was a strong determinant for prediction of peritoneal metastasis. GC patients with high LGMN expression tended to have worse survival together with more frequent diffuse-type tumors and increased risk of peritoneal metastasis. The GSEA results showed that focal adhesion, ecm receptor interaction, cell adhesion molecules cams, TGF-β signaling pathway, JAK-STAT signaling pathway, gap junction, etc. were differentially enriched in the phenotype with high LGMN expression.

Conclusion: LGMN was an independent prognostic factor for OS in GC patients. Increased expression of LGMN was significantly associated with peritoneal metastasis. The nomogram based on LGMN might guide the clinical decisions for patients with GC.

Keywords: gastric cancer, peritoneal metastasis, legumain, survival, nomogram

INTRODUCTION

Gastric cancer (GC) is one of the common malignant tumors threatening human health, causing ∼1,033,701 new cases and 782,685 deaths worldwide in 2018 (1). According to Lauren's classification system, GC has three types, intestinal type, diffuse type, and mixed type, of which the diffuse type tends to be more invasive. Peritoneal metastasis accounts to nearly 50% of death in GC patients (2, 3). Interestingly, peritoneal metastasis is more commonly observed in diffuse-type GC than other types (4–6), which may contribute to their worse survival. Although considerable advances have been made in the management of GC, such as chemotherapy, targeted therapy, and immunotherapy, the 5-year overall survival (OS) of GC patients with peritoneal metastasis remains dismal (7, 8). However, the molecular biomarkers and mechanisms underlying peritoneal metastasis have not been well-established in GC patients. Therefore, it is essential to identify novel molecular biomarkers for early diagnosis, prevention, and targeted therapy for GC patients.

Legumain (LGMN), also known as asparagine endopeptidase, is a cysteine endopeptidase of the asparaginyl endopeptidase family, showing high specificity for hydrolysis of asparaginyl bonds (9). It belongs to the peptidase family C13, which expresses both on surface and intracellularly (10). LGMN promotes activation of zymogen gelatinase A through cleaving pro-gelatinase A, which is considered to play a critical role in extracellular matrix degradation and remodeling, thereby facilitating cell migration and invasion (11–13). Our recent study has demonstrated that LGMN is expressed at elevated levels in diffuse GC cell lines and contributes critically to

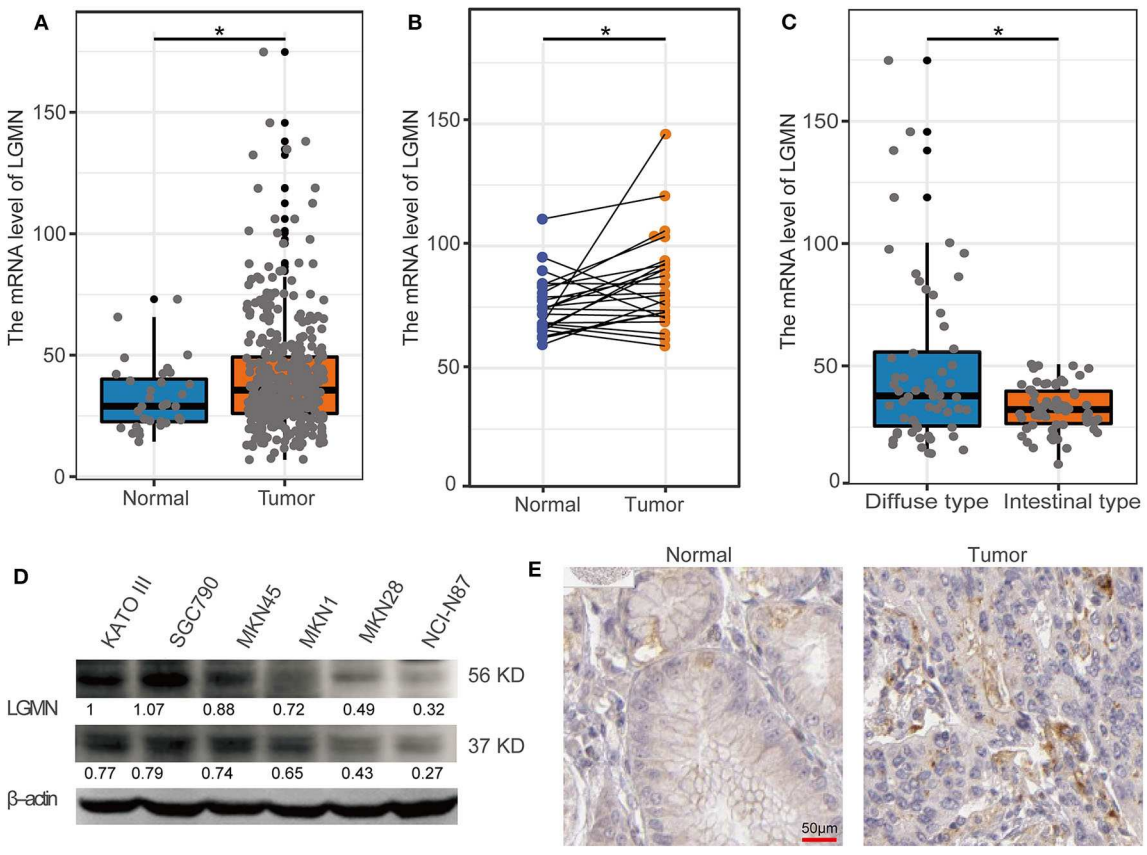

FIGURE 1 | The level of LGMN in GG based on TCGA database, Western blot, and HPA database. **(A)** LGMN expression level in GC tissues relative to corresponding normal gastric tissue from the TCGA database. **(B)** Comparison of LGMN expression in 24 matched GC tissues and normal tissues. **(C)** Comparison of LGMN expression between diffuse-type GC and intestinal-type GC from the TCGA database. **(D)** Comparison of LGMN expression between diffuse-type GC and intestinal-type GC in different cell lines by Western blot. **(E)** Representative images of protein expression detected by immunohistochemistry of LGMN were detected in GC and normal tissues from the HPA database. *$P < 0.05$.

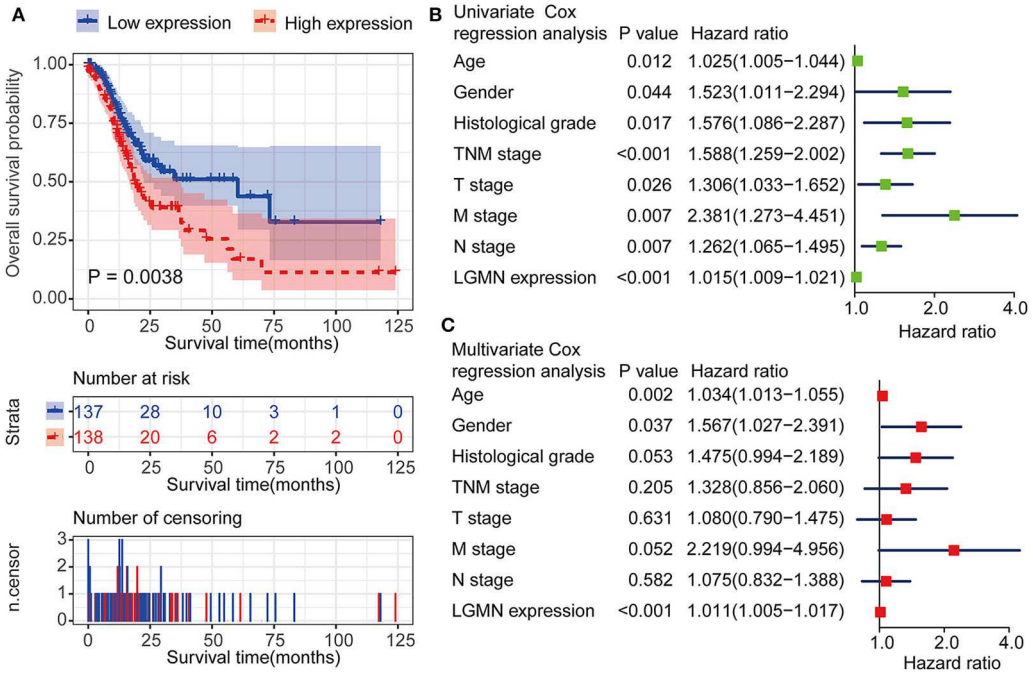

FIGURE 2 | LGMN expression was an independent prognostic factor associated with OS in the GC patients from the TCGA cohort. **(A)** Kaplan–Meier survival analysis between GC patients in the high- and low-expression group of LGMN. **(B)** Univariate Cox proportional hazards regression analyses of overall survival in GC patients. The green squares on the transverse lines represent the HR, and the blue transverse lines represent 95% CI. **(C)** Multivariate Cox proportional hazards regression analyses of overall survival in GC patients. The red squares on the transverse lines represent the HR, and the blue transverse lines represent 95% CI.

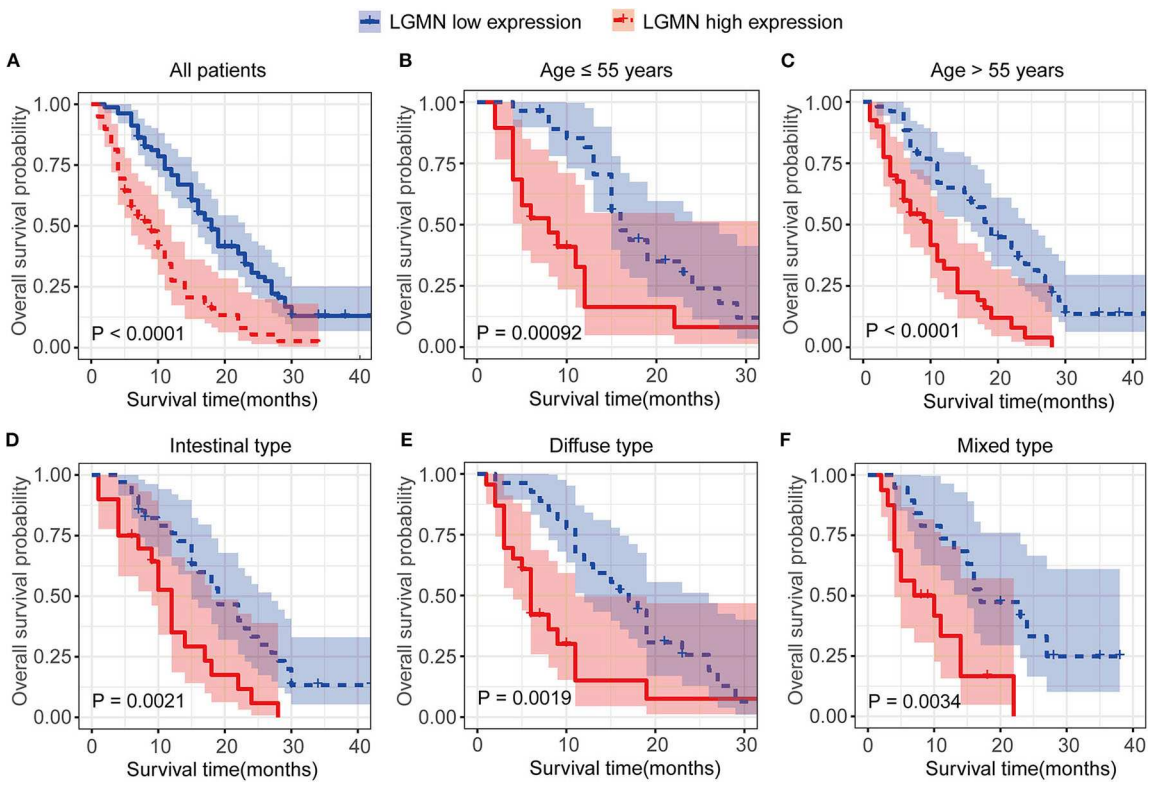

FIGURE 3 | Kaplan–Meier survival analyses of GC patients from the TCGA cohort. **(A)** The Kaplan–Meier curves for all patients set. **(B)** The Kaplan–Meier curves for age ≥ 55 years subgroup. **(C)** The Kaplan–Meier curves for age <55 years subgroup. **(D)** The Kaplan–Meier curves for the intestinal-type subgroup. **(E)** The Kaplan–Meier curves for the diffuse-type subgroup. **(F)** The Kaplan–Meier curves for the mixed-type subgroup.

the invasion and metastasis phenotype through epithelial–mesenchymal transition in diffuse GC (14). Previous studies have shown that higher LGMN level is associated with poor prognosis of multiple cancers including breast cancer (15), colorectal cancer (16), and prostate cancer (17). However, the exact relationship of LGMN expression and clinicopathologic signature, especially peritoneal metastasis, in GC patients remains poorly characterized. To our best knowledge, there is no literature reporting on a clinicopathologic signature to improve the diagnosis and prediction of peritoneal metastasis in GC patients.

Therefore, this study aimed to investigate the expression pattern of LGMN in GC tissue from the Zhongshan hospital cohort and to use bioinformatics data from The Cancer Genome Atlas (TCGA) to explore the role of LGMN as a clinicopathological and prognostic biomarker for patients with GC. Moreover, the nomogram integrating LGMN expression and clinical clinicopathologic characteristics was also established to predict peritoneal metastasis for GC patients.

MATERIALS AND METHODS

Extraction of Clinical and mRNA Expression Data From TCGA Cohort

The mRNAs expression data and corresponding clinicopathologic information of GC patients were downloaded from the TCGA database (up to January 1, 2019). The included clinical characteristics were age, gender, pathologic grade, tumor stage, survival time, and vital status. Patients were excluded if they had incomplete survival information or their survival time was 0 days. The baseline characteristics of GC patients in the TCGA cohort are summarized in **Supplement Table 1**.

Patients in the Zhongshan Hospital

A total of 139 patients who were diagnosed with advanced GC at the Department of Medical Oncology, Zhongshan Hospital, Fudan University, Shanghai, China, from January 2009 and June 2016 were included in our analysis. Inclusion criteria for the eligible patients were listed as follows: (a) histologically proven gastric adenocarcinoma; (b) no previous anticancer treatment; (c) signs of distant metastasis; (d) completed clinicopathological and follow-up information. Written informed consent from all patients was obtained with the approval of the Ethics Committee of Zhongshan Hospital. The primary outcome is OS, which was censored at the last follow-up record (December 31, 2017). The baseline characteristics of GC patients in the Zhongshan cohort are summarized in **Supplement Table 2**.

IHC Staining and Evaluation of IHC Intensity

Immunohistochemistry was performed on tissue microarray (TMA) according to the standard biotin–streptavidin–peroxidase method (18). The polyclonal goat anti-human LGMN antibody (#AF2199, R & D Systems, USA) in a 1:300 dilution was used for IHC staining. The IHC results were analyzed by two independent pathologists who were blinded to the clinical characteristics. Staining intensity for LGMN was scored as 0 (0%), 1 (<10%), 2 (10–50%), and 3 (>50%), depending on the percentage of positive-stained cells. In subsequent statistical analysis, specimens with a score of ≤2 were grouped as low LGMN expression, while a score of 3 was grouped as high LGMN expression. The specimens would be reexamined by both pathologists under a multihead microscope in case of a discrepancy in scoring.

Western Blot

The GC cell lines were maintained in RPMI 1640 containing 10% FB. Cellular protein was extracted using a protein extraction kit, according to the manufacturer's instructions (#WLA019, Wanleibio, China). Proteins were separated using 6% SDS-PAGE gel electrophoresis and then transferred to PVDF membranes. The membranes were blocked in 5% non-fat dry milk in Tris-buffered saline (pH 7.5) for an hour at 37°C. Membranes were incubated overnight at 4°C with anti-human LGMN antibody as IHC described above, then followed by the horseradish peroxidase conjugated secondary antibody for 1 h at room temperature. Signals were detected using enhanced chemiluminescence reagents (Pierce, Rockford, IL, USA).

TABLE 1 | Univariate and multivariate Cox proportional hazards regression analysis of the overall survival in GC patients from the Zhongshan cohort.

Variables	Overall survival			
	Univariate analysis	*P*-value	Multivariate analysis	*P*-value
Age				
≤55	Reference		/	
>55	1.18 (0.81–1.71)	0.379	/	/
Gender				
Male	Reference		/	
Female	1.04 (0.71–1.53)	0.841	/	/
Tumor site				
Cardia	Reference		Reference	
Corpus	1.46 (0.84–2.44)	0.184	1.21 (0.71–2.07)	0.481
Antrum	3.48 (1.15–10.52)	0.027	0.91 (0.29–2.83)	0.874
Lauren type				
Intestinal type	Reference		/	/
Diffuse type	1.39 (0.90–2.12)	0.134	/	/
Mixed type	1.06 (0.65–1.72)	0.812	/	/
Historical grade				
G1/G2	Reference		/	/
G3/G4	1.21 (0.78–1.86)	0.397	/	/
Her2 status				
Negative	Reference		/	
Positive	1.03 (0.61–1.73)	0.918	/	/
Tumor recurrence				
No	Reference		Reference	
Yes	1.78 (1.21–2.61)	0.003	0.68 (0.45–1.02)	0.059
LGMN expression				
Low	Reference		Reference	
High	2.78 (1.89–4.09)	<0.001	2.51 (1.68–3.76)	<0.001

GSEA Enrichment

The gene set enrichment analysis (GSEA) created a list of all genes connected with the expression of the LGMN. Then, the samples were categorized as the high- and low-LGMN phenotypes to elucidate the potential biological function utilizing GSEA software GSEA v2.2.2 (19). The annotated gene sets c2.cp.kegg.v7.0.symbols.gmt in the MSigDB Collection were utilized as the reference gene sets. The nominal *P*-value and normalized enrichment score (NES) were used to sort the pathways enriched in each phenotype. Gene sets with nominal $P < 0.05$ and FDR < 0.25 were considered statistically significant.

Statistical Analysis

The relationship between LGMN expression and clinicopathological characteristics was analyzed with Chi-square test and logistic regression. The Kaplan–Meier method and log-rank test were used to perform survival analysis. Univariate and multivariate Cox proportional hazards regression analysis were used to evaluate whether LGMN could be an independent prognostic factor in GC. We used the "rms" R package to plot the nomogram for peritoneal metastasis prediction among GC patients. Receiver operating characteristics (ROC) curve was used to evaluate the performance of nomogram in peritoneal metastasis prediction among GC patients. Decision curve analysis (DCA) was introduced to assess the clinical utility of this nomogram (20). DCA is a novel analytical technique that integrates all clinical consequences of a decision and then quantifies the clinical utility of a predictive model (21). All analyses were conducted using R software (version 3.5.1). $P < 0.05$ was considered to be statistically significant.

RESULTS

The Level of LGMN Was Upregulated in GC, Especially for Diffuse-Type GC

First, the TCGA database was used to examine the differential expression levels of LGMN mRNA between GC and normal gastric tissue. The LGMN mRNA expression level was

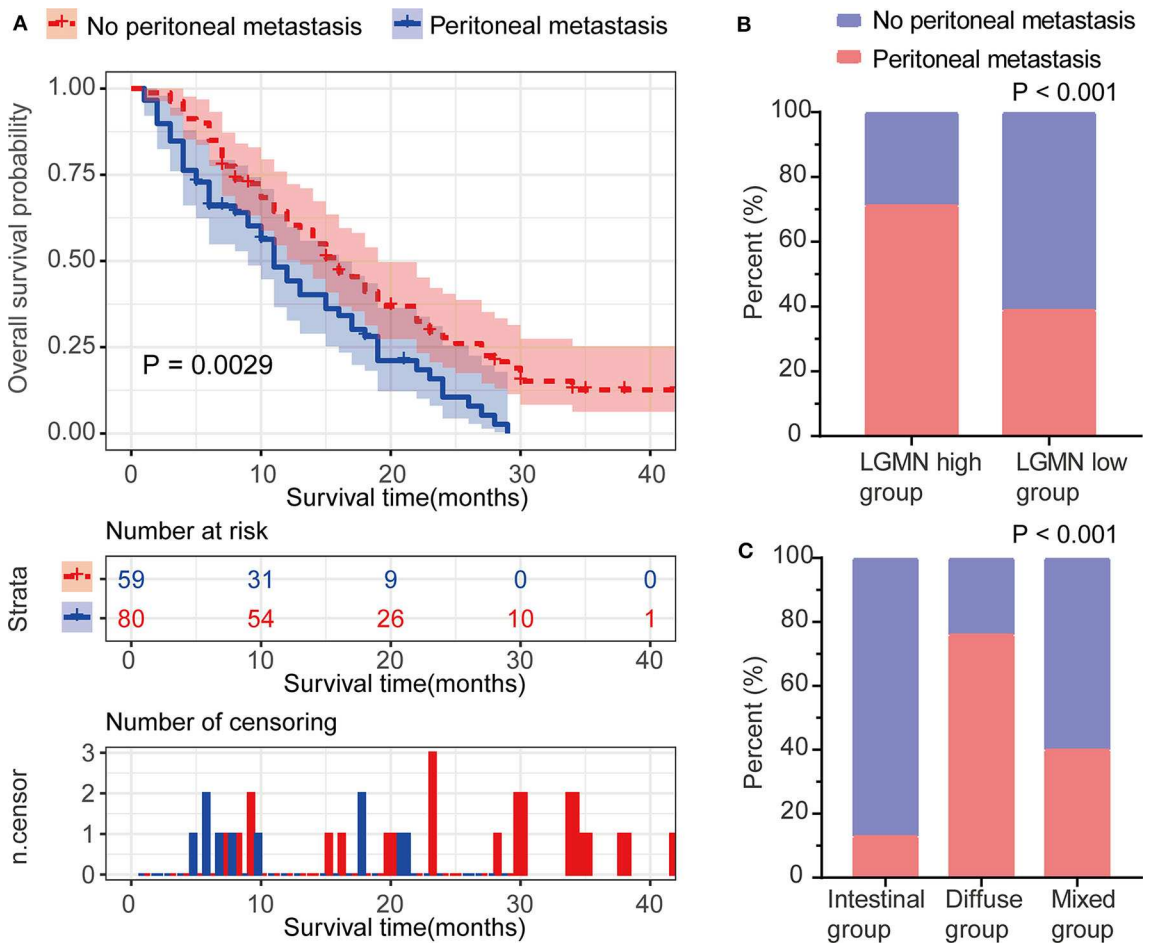

FIGURE 4 | The association between LGMN and peritoneal metastasis in GC patients from the Zhongshan cohort. **(A)** The Kaplan–Meier survival analyses of peritoneal metastasis in GC patients. **(B)** The percentage of peritoneal metastasis in high/low LGMN level of GC tissues was compared. **(C)** The Lauren type in GC patients with and without peritoneal metastasis was compared.

significantly higher in GC tissues than in normal tissues ($P < 0.05$, **Figure 1A**). Additionally, paired analysis of LGMN mRNA expression in 24 matched GC tissues and normal tissues demonstrated that LGMN mRNA expression was significantly increased in tumor tissues compared with normal tissues ($P < 0.05$, **Figure 1B**). Interestingly, we found that the mRNA levels of LGMN were higher in diffuse-type GC compared with intestinal-type GC ($P < 0.05$, **Figure 1C**). To further confirm this result, we performed Western blot to compare the LGMN expression in three cell lines of diffuse-type GC (KATO III, SGC790, and MKN45) between three cell lines of intestinal-type GC (MKN1, MKN28, and NCI-N87). The Western blot results demonstrated that diffuse-type cells showed a higher expression of LGMN compared with the intestinal-type GC (**Figure 1D**). Additionally, representative images from the Human Protein Atlas (HPA) database demonstrated that LGMN protein expression was higher in GC tissues compared with normal gastric tissues (**Figure 1E**).

TABLE 2 | Chi-square tests for patients stratified by peritoneal metastasis status from the Zhongshan cohort.

Variables	Peritoneal metastasis status		*P*-value
	Metastasis (%)	Without metastasis (%)	
	59(42.5)	80 (57.5)	
Gender			<0.001
Male	26 (44.1)	61 (76.2)	
Female	33 (55.9)	19 (23.8)	
Age			0.099
≤55	25 (42.4)	22 (27.5)	
>55	34 (57.6)	58 (72.5)	
Tumor site			0.004
Cardia	4 (6.8)	19 (23.8)	
Corpus	55 (93.2)	57 (71.2)	
Antrum	0 (0.0)	4 (5.0)	
Lauren type			<0.001
Intestinal type	7 (11.90)	47 (58.8)	
Diffuse type	38 (64.4)	12 (15.0)	
Mixed type	14 (23.7)	21 (26.2)	
LGMN expression			<0.001
High	36 (61.0)	23 (28.7)	
Low	23 (39.0)	57 (71.3)	
Histological grade			0.096
G1/G2	9 (15.3)	23 (28.8)	
G3/G4	50 (84.7)	57 (71.2)	
Her2 status			0.109
Positive	4 (6.8)	14 (17.5)	
Negative	55 (93.2)	66 (82.5)	
Tumor recurrence			0.083
Yes	29 (49.2)	48 (60.0)	
No	30 (50.8)	32 (40.0)	
Surgery			0.669
Done	34 (57.6)	42 (52.5)	
Not done	25 (42.4)	38 (47.5)	
Chemotherapy			0.102
Done	54 (91.5)	64 (80.0)	
Not done	5 (8.5)	16 (20.0)	

LGMN Was an Independently Prognostic Factor in GC Patients

In the TCGA database, GC patients were divided into the high-expression group and the low-expression group using median value as a cutoff (35.62). The Kaplan–Meier analysis showed that the GC patients with high mRNA level of LGMN had an unfavorable OS, and the median OS for the high LGMN group and the low LGMN group was 18.47, and 34.77 months, respectively ($P = 0.0038$) (**Figure 2A**). In the Cox proportional hazards regression analysis, we discovered that GC patients with high mRNA level of LGMN or high histological grade (G3/4) were at significantly high risk of death. GC patients with a higher age or distant metastasis were also at high risk of death (**Figure 2B**). After adjustment for age, gender, tumor stage, and histological grade, to our surprise, high mRNA level of LGMN remained associated with high risk of death in GC patients (HR, 1.011; 95% CI, 1.005–1.017; $P < 0.001$, **Figure 2C**).

We next ask whether the prognostic value of LGMN persisted in the protein level. TMA derived from 139 GC patients in the Zhongshan cohort was used. In univariate Cox proportional hazards regression analysis, GC patients with high LGMN expression had a significantly lower 1-year OS than those with low LGMN expression (27.54 vs. 70. 90%, $P < 0.0001$) (**Figure 3A**, **Table 1**). In addition, tumor site ($P = 0.027$) and recurrence ($P = 0.003$) were also significantly associated with OS. Multivariate Cox proportional hazards regression analysis was performed using all of the significant variables in the univariate analysis. The results from the multivariate analysis

TABLE 3 | LGMN expression associated with peritoneal metastasis in GC patients from the Zhongshan cohort.

Variables	Logistic regression		
	OR in peritoneal metastasis	95% CI of OR	*P*-value
Age (≤55 vs. >55)	0.771	0.294–2.029	0.596
Gender (male vs. female)	4.633	1.835–12.449	0.001
Tumor site (cardia vs. corpus)	1.558	0.421–6.328	0.514
(Cardia vs. antrum)	10.584	0.764–152.882	0.071
Lauren type (intestinal vs. diffuse type)	19.461	5.312– 87.653	<0.001
(Intestinal vs. mixed type)	2.736	0.808–9.771	0.109
Histological grade (G1/G2 vs. G3/G4)	0.916	0.221–4.198	0.889
Her2 status (negative vs. positive)	0.533	0.107–2.846	0.443
LGMN expression (low vs. high)	3.941	1.558–10.770	0.005
Tumor recurrence(no vs. yes)	2.046	0.831–5.197	0.123

showed that LGMN expression was a significantly independent prognostic factor for OS ($P < 0.001$). Of note, high expression level of LGMN might double the risk of death among GC patients (HR, 2.51; 95% CI, 1.68–3.76; $P < 0.001$) (**Table 1**). We further conducted a subgroup analysis for evaluating the effect of LGMN expression on OS based on two risk factors, namely, age and Lauren type. We found that high expression of LGMN continued to contribute to a worse survival even in each subgroup stratified by age (**Figures 3B,C**) and Lauren type (**Figures 3D–F**).

Increased Protein Level of LGMN Was Related to Peritoneal Metastasis in GC Patients

Peritoneal metastasis is one of the most common causes of death in GC patients. In the Zhongshan cohort, we observed that patients with peritoneal metastasis had a significantly increased risk of death in GC (**Figure 4A**). Meanwhile, using the median expression score as the cutoff point, we tested the probability of peritoneal metastasis in the low LGMN and high LGMN expression groups using Chi-square test (**Table 2**). In total,

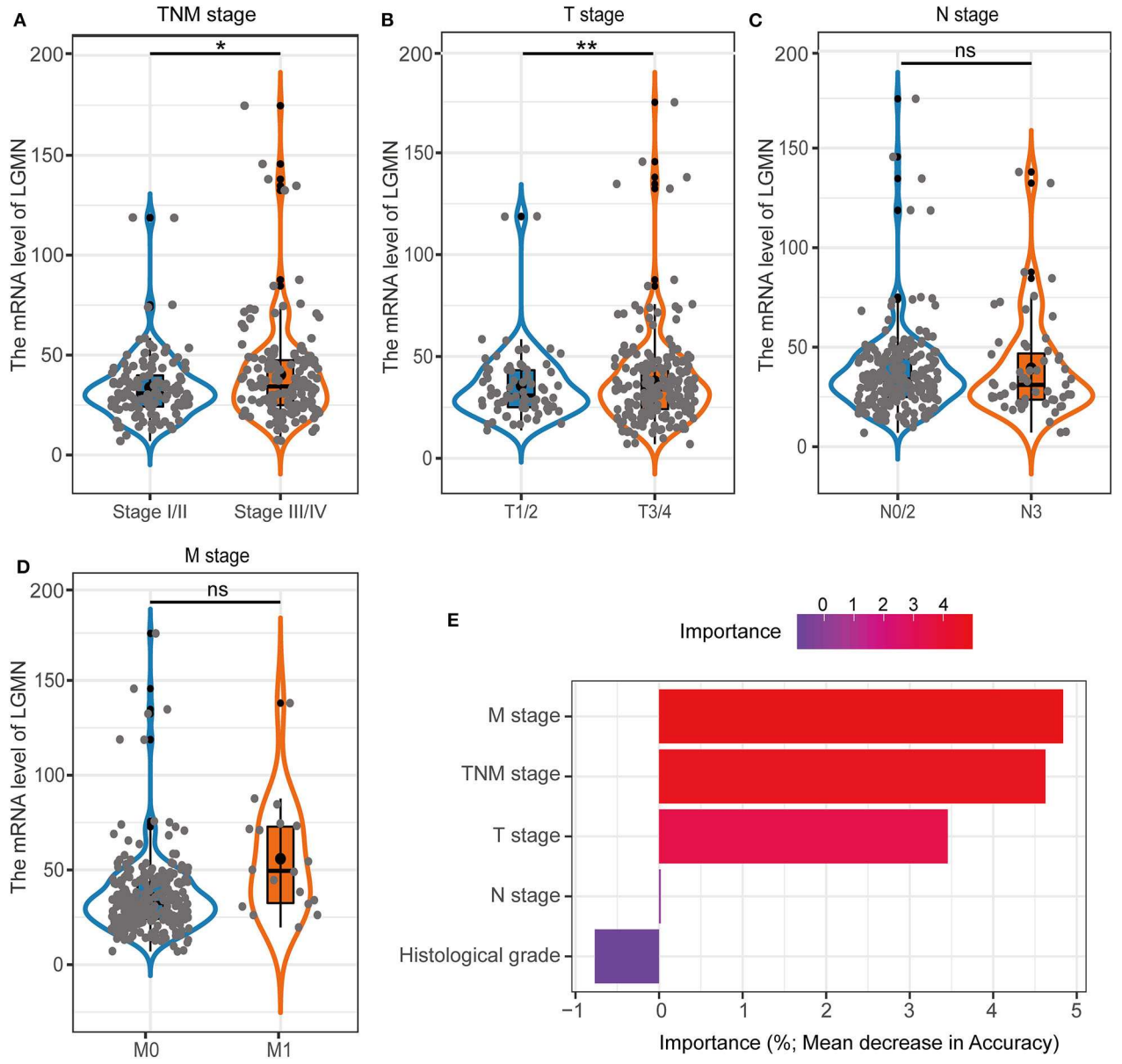

FIGURE 5 | The association with LGMN expression and clinicopathologic characteristics including **(A)** TNM stage, **(B)** M stage, **(C)** T stage, and **(D)** N stage in the TCGA cohort. **(E)** M stage contributed most to classification between high LGMN and low LGMN patients by RandomForest in the TCGA cohort. *$P < 0.05$, **$P < 0.01$, ns, no significance.

71.25% patients with high LGMN expression had peritoneal metastasis, but only 38.98% patients with low LGMN expression had metastasis (Chi-square test, $P < 0.001$; **Figure 4B**). At the same time, patients with diffuse-type GC tended to suffer from peritoneal metastasis compared to those patients with intestinal GC and those with mixed GC ($P < 0.001$; **Figure 4C**). These results were further confirmed by logistic regression analysis (**Table 3**). Additionally, we found that female patients were more likely to progress to peritoneal metastasis (OR = 4.633; 95% CI, 1.835–12.449; $P = 0.001$).

In the TCGA cohort, we first investigated the LGMN mRNA levels in different tumor stages. We found that the LGMN expression was much higher ($P < 0.05$) in GC patients with stage III/IV compared to GC patients with tumor stage I/II (**Figure 5A**). Interestingly, similar results were obtained in the M stage, as LGMN expression was associated with high M stage (**Figure 5B**). However, with the increased T or N stage, the LGMN expression was not further increased (**Figures 5C,D**). These results indicated that high expression of LGMN might contribute to advanced tumor stage mainly through promoting distant metastasis. Furthermore, we performed unsupervised RandomForest classification analysis to validate our result, which determined that the M stage contributes most to discrimination between high LGMN and low LGMN samples (**Figure 5E**). Since the TCGA database did not record the peritoneal metastasis status for GC patients, we failed to evaluate the role of LGMN mRNA played in the peritoneal metastasis. However, we found that the LGMN mRNA expression was much higher in diffuse GC patients compared to intestinal ones (**Figure 1C**), consistent with the observations in the Zhongshan cohort.

The Protein Level of LGMN, Combined With Lauren Type and Gender, Was Able to Better Predict Peritoneal Metastasis for GC Patients

The above results indicated that the level of LGMN, Lauren type, and gender might be related to peritoneal metastasis in GC patients. Therefore, a nomogram for prediction of peritoneal metastasis probabilities, which included LGMN, Lauren type, and gender were constructed (**Figure 6A**). ROC curve was used to analyze the power of LGMN and nomogram to discriminate between GC patients with or without peritoneal metastasis. According to the ROC analysis, the area under the curve (AUC) of the nomograms for probability based on LGMN and nomogram (**Figure 6B**) was 0.615 and 0.842, respectively, suggesting that this model can accurately predict

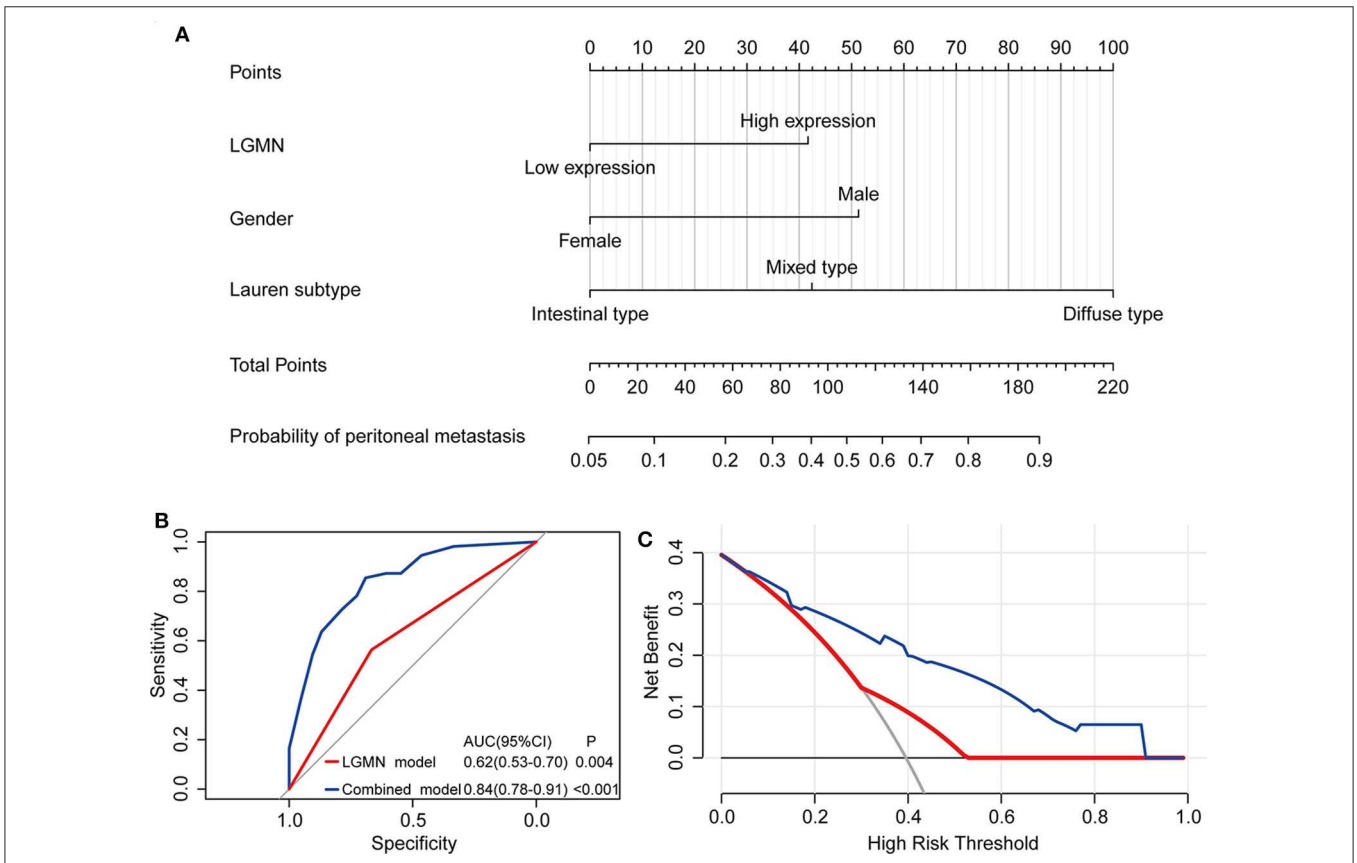

FIGURE 6 | The role of LGMN in predicting peritoneal metastasis in GC patients from the Zhongshan cohort. **(A)** Nomograms for predicting peritoneal metastasis. **(B)** ROC analyses of the nomogram for peritoneal metastasis prediction. **(C)** DCA for assessment of the clinical utility of the nomogram.

the possibility of potential peritoneal metastasis among GC patients. After addressing the accuracy, DCA was introduced to evaluate the clinical utility of this nomogram. **Figure 6C** showed that the established nomogram had high potential for clinical application.

The Potential Molecular Mechanisms Mediated by LGMN in GC

Since LGMN was upregulated and an independent prognostic factor was associated with OS in both cohorts, we were eager to explore the underlying mechanisms by which LGMN is involved in GC progression. Next, GSEA was performed between patients with low or high LGMN mRNA expression based on the TCGA cohort. Based on the NESs, the several significantly enriched signaling pathways were selected (**Figures 7A–F**). The focal adhesion, ecm receptor interaction, cell adhesion molecules cams, TGF-β signaling pathway, JAK-STAT signaling pathway, gap junction, etc. were differentially enriched in phenotypes with high LGMN expression. The top 20 enriched signaling pathways were summarized in **Table 4**. In conclusion, functional enrichment analysis results showed that LGMN might play a significant role in GC progression and biological progress.

DISCUSSION

Although LGMN has been confirmed to be highly expressed in several types of solid tumors (15–17), its expression level and potential clinical implications in GC, which were the focus of the current study, have not been well-defined. This study represented the first comprehensive and detailed analysis of LGMN in GC patients from the TCGA database and our institute to investigate its association with clinicopathologic characteristics, survival, function, and expression difference. By analyzing GC patients from the TCGA cohort and the Zhongshan cohort, we demonstrated a notable association between high LGMN expression and poor survival in GC patients. Moreover, LGMN expression has also been demonstrated as an independent prognostic factor for OS, and higher LGMN levels in patients with peritoneal metastasis and diffuse-type GC were observed, which suggested that LGMN might play a vital role in the peritoneal metastasis of GC. Furthermore, LGMN could be integrated with acknowledged clinicopathological factors to construct a nomogram for peritoneal metastasis prediction.

Our recent study has demonstrated that LGMN is highly expressed in diffuse-type GC cell lines and enhances the malignant phenotype of diffuse-type GC, including proliferation,

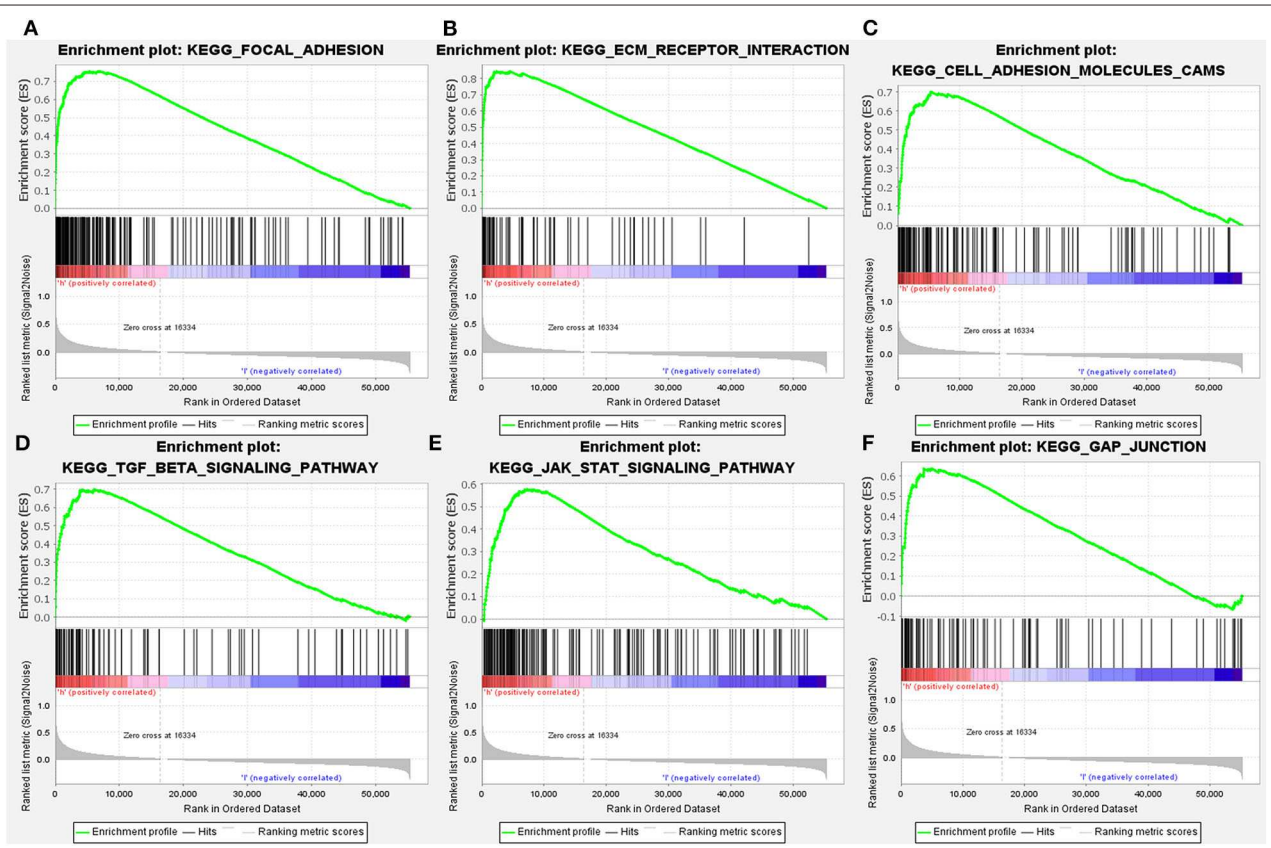

FIGURE 7 | GSEA analyses of KEGG signaling pathways activated in GC patients with high expression of LGMN compared with the ones with low expression. **(A)** Focal adhesion, **(B)** ecm receptor interaction, **(C)** cell adhesion molecules cams, **(D)** TGF-β signaling pathway, **(E)** JAK-STAT signaling pathway, and **(F)** gap junction were differentially enriched when LGMN overexpressed.

TABLE 4 | Gene sets enriched in the high-expression phenotype of GC patients from the TCGA cohort.

Name	ES	NES	NOM *P*-value	FDR *Q*-value
KEGG_FOCAL_ADHESION	0.76	2.57	0.00	0.00
KEGG_ECM_RECEPTOR_INTERACTION	0.85	2.50	0.00	0.00
KEGG_DILATED_CARDIOMYOPATHY	0.72	2.39	0.00	0.00
KEGG_HYPERTROPHIC_CARDIOMYOPATHY_HCM	0.71	2.39	0.00	0.00
KEGG_CYTOKINE_CYTOKINE_RECEPTOR_INTERACTION	0.64	2.39	0.00	0.00
KEGG_HEDGEHOG_SIGNALING_PATHWAY	0.73	2.34	0.00	0.00
KEGG_PATHWAYS_IN_CANCER	0.63	2.33	0.00	0.00
KEGG_TGF_BETA_SIGNALING_PATHWAY	0.70	2.32	0.00	0.00
KEGG_REGULATION_OF_ACTIN_CYTOSKELETON	0.61	2.32	0.00	8.32E−05
KEGG_AXON_GUIDANCE	0.64	2.27	0.00	1.46E−04
KEGG_GAP_JUNCTION	0.64	2.26	0.00	1.33E−04
KEGG_CELL_ADHESION_MOLECULES_CAMS	0.70	2.25	0.00	1.67E−04
KEGG_BASAL_CELL_CARCINOMA	0.71	2.25	0.00	1.55E−04
KEGG_MELANOMA	0.64	2.23	0.00	1.45E−04
KEGG_HEMATOPOIETIC_CELL_LINEAGE	0.71	2.23	0.00	1.36E−04
KEGG_CALCIUM_SIGNALING_PATHWAY	0.58	2.20	0.00	2.16E−04
KEGG_GLYCOSAMINOGLYCAN_DEGRADATION	0.77	2.19	0.00	4.45E−04
KEGG_MAPK_SIGNALING_PATHWAY	0.57	2.19	0.00	4.21E−04
KEGG_JAK_STAT_SIGNALING_PATHWAY	0.58	2.16	0.00	5.42E−04
KEGG_RENAL_CELL_CARCINOMA	0.65	2.15	0.00	6.43E−04

NES, normalized enrichment score; NOM, nominal; FDR, false discovery rate.

invasion, as well as metastasis (14). However, its clinical implications for GC patients have not been investigated. Additionally, although Li et al. have reported the relationship of overexpression of LGMN and poor prognosis of GC (22), the exact correlation of LGMN and peritoneal metastasis in GC is still unknown. Peritoneal metastasis, as the most critical determinant of death in GC patients (2), is difficult to discriminate from advanced GC preoperatively (23). In most cases, peritoneal metastasis may remain asymptomatic for a remarkably long period of time and therefore is typically diagnosed intraoperatively, which does not benefit surgeons in determining the optimal therapeutic strategy (23). Operative diagnostic methods such as staging microscopy have emerged as a standard method for discrimination of peritoneal metastasis among GC patients (24, 25). Nevertheless, these methods have an invasive nature, are time-consuming, are expensive, and result in complications including intra-abdominal organ iatrogenic damages, hemorrhage, as well as infections (26). Recently, the main non-invasive diagnostic methods for peritoneal metastasis are imaging examinations, such as computed tomography (CT), positron emission tomography–computed tomography (PET-CT), and magnetic resonance imaging (MRI); however, all of them lack diagnostic accuracy for early micrometastatic lesions (27, 28).

In recent years, researches had undertaken efforts to develop several biomarkers in identifying GC patients with peritoneal metastasis (29–31). However, most of them mainly focus on the clinicopathological parameters and ignore the components of genetic characteristics, which also play a critical role in peritoneal metastasis (32). It is reasonable to combine clinicopathological parameters and gene expression for better prediction and clinical application. In the Zhongshan cohort, we tested the probability of peritoneal metastasis between GC patients with low and high LGMN expression. We found that patients with high LGMN expression had increased risks of peritoneal metastasis compared to those with low LGMN expression. The poor prognosis of patients with high LGMN expression might derive from higher rate of peritoneal metastasis. Hence, a nomogram was constructed by integrating Lauren type, gender, and LGMN expression. Notably, this nomogram indicated that LGMN was a strong determinant for peritoneal metastasis prediction. In addition, the nomogram showed satisfactory performance, as indicated by ROC curves and DCA. The nomogram might be useful for patient counseling and individualized clinical decision-making as it helps predict the possibility that GC patients will encounter peritoneal metastasis.

There are also several limitations about our present study. First, as a retrospective study, it has several inherent limitations, such as selection bias confounding factors and missing data, which might provide inaccurate conclusions (33). Therefore, to further confirm our results, a prospective study with large samples might be needed. Second, the Zhongshan cohort consisted of GC patients who undertook previous surgery; hence, the limited sample size might weaken the power of LGMN as a biomarker for detecting peritoneal metastasis. In addition, as we used the TCGA cohort as well as a clinical cohort for analysis, the clinicopathological factors and expression profiles were different between cohorts. Third, although the biologic effect including invasion and migration has been demonstrated in our recent publication (14), this study failed to explore the underlying mechanisms of the signaling pathways involved in GC, but a GSEA was performed. Further studies are required to investigate the mechanisms responsible for the regulation of LGMN and its role in peritoneal metastasis in GC, which would provide insights into its roles in other malignancies. Nevertheless, we have provided strong evidence indicating that LGMN is overexpressed in GC and is associated with a poor survival for GC patients. What is more, our data suggested that LGMN might be of a critical role in the progression of peritoneal metastasis and could be integrated with the acknowledged clinicopathological factors to predict the possibility of peritoneal metastasis, which might guide the clinical management.

In conclusion, to the best of our knowledge, this is the first comprehensive analysis of expression pattern and clinicopathological implications of LGMN in GC. This study demonstrated that higher levels of LGMN mRNA and protein were observed in GC compared to their adjacent tissues. LGMN expression was an independent prognostic factor associated with OS. Moreover, higher LGMN levels tended

to be observed patients with diffuse-type GC and peritoneal metastasis. Furthermore, a nomogram for peritoneal metastasis prediction was constructed by Lauren type, gender, and LGMN expression, which show satisfactory performance and clinical utility, which might guide patient counseling and clinical decision-making.

DATA AVAILABILITY STATEMENT

Publicly available datasets were analyzed in this study, these can be found in the Cancer Genome Atlas (https://portal.gdc.cancer.gov/). The raw data supporting the conclusions of this article will be made available by the authors, without undue reservation, to any qualified researcher.

ETHICS STATEMENT

The studies involving human participants were reviewed and approved by the Ethics Committee of Zhongshan Hospital, Fudan University. The patients/participants provided their written informed consent to participate in this study.

AUTHOR CONTRIBUTIONS

YW and TL contributed to the conception, design, and drafting of the manuscript. YC, ZW, XC, and WL obtained ethical approval and contributed to the preparation of the dataset. YW, SZ, and HW carried out the statistical analysis. TL, YJ, YW, and SZ contributed with a critical revision of the manuscript. All authors contributed to the article and approved the submitted version.

FUNDING

This work was supported by the Shanghai Science and Technology Committee (15411961900).

SUPPLEMENTARY MATERIAL

The Supplementary Material for this article can be found online at: https://www.frontiersin.org/articles/10.3389/fonc.2020.00966/full#supplementary-material

REFERENCES

1. Bray F, Ferlay J, Soerjomataram I, Siegel RL, Torre LA, Jemal, et al. Global cancer statistics 2018: GLOBOCAN estimates of incidence and mortality worldwide for 36 cancers in 185 countries. *CA Cancer J Clin.* (2018) 68:394–424. doi: 10.3322/caac.21492
2. Thomassen I, van Gestel YR, van Ramshorst B, Luyer MD, Bosscha K, Nienhuijs SW, et al. Peritoneal carcinomatosis of gastric origin: a population-based study on incidence, survival and risk factors. *Int J Cancer.* (2014) 134:622–8. doi: 10.1002/ijc.28373
3. Lee IS, Yook JH, Kim TH, Kim HS, Kim KC, Oh ST, et al. Prognostic factors and recurrence pattern in node-negative advanced gastric cancer. *Eur J Surg Oncol.* (2013) 39:136–40. doi: 10.1016/j.ejso.2012.10.008
4. Bringeland EA, Wasmuth HH, Mjones P, Myklebust TA, Gronbech JE. A population-based study on incidence rates, Lauren distribution, stage distribution, treatment, and long-term outcomes for gastric adenocarcinoma in central Norway 2001-2011. *Acta Oncol.* (2017) 56:39–45. doi: 10.1080/0284186X.2016.1227086
5. Chen YC, Fang WL, Wang RF, Liu CA, Yang MH, Lo SS, et al. Clinicopathological variation of lauren classification in gastric cancer. *Pathol Oncol Res.* (2016) 22:197–202. doi: 10.1007/s12253-015-9996-6
6. Qiu MZ, Cai MY, Zhang DS, Wang ZQ, Wang DS, Li YH, et al. Clinicopathological characteristics and prognostic analysis of Lauren classification in gastric adenocarcinoma in China. *J Transl Med.* (2013) 11:58. doi: 10.1186/1479-5876-11-58
7. Pyo JH, Ahn S, Lee H, Min BH, Lee JH, Shim SG, et al. Clinicopathological features and prognosis of mixed-type t1a gastric cancer based on Lauren's classification. *Ann Surg Oncol.* (2016) 23:784–91. doi: 10.1245/s10434-016-5549-9
8. Lee JH, Chang KK, Yoon C, Tang LH, Strong VE, Yoon SS. Lauren histologic type is the most important factor associated with pattern of recurrence following resection of gastric adenocarcinoma. *Ann Surg.* (2018) 267:105–13. doi: 10.1097/SLA.0000000000002040
9. Dall E, Brandstetter H. Mechanistic and structural studies on legumain explain its zymogenicity, distinct activation pathways, and regulation. *Proc Natl Acad Sci USA.* (2013) 110:10940–5. doi: 10.1073/pnas.1300686110
10. Dall E, Brandstetter H. Structure and function of legumain in health and disease. *Biochimie.* (2016) 122:126–50. doi: 10.1016/j.biochi.2015.09.022
11. Chen JM, Fortunato M, Stevens RA, Barrett AJ. Activation of progelatinase A by mammalian legumain, a recently discovered cysteine proteinase. *Biol Chem.* (2001) 382:777–83. doi: 10.1515/bchm.2001.382.5.777
12. Mai J, Finley RL Jr, Waisman DM, Sloane BF. Human procathepsin B interacts with the annexin II tetramer on the surface of tumor cells. *J Biol Chem.* (2000) 275:12806–12. doi: 10.1074/jbc.275.17.12806
13. Stern L, Perry R, Ofek P, Many A, Shabat D, Satchi-Fainaro R, et al. A novel antitumor prodrug platform designed to be cleaved by the endoprotease legumain. *Bioconjug Chem.* (2009) 20:500–10. doi: 10.1021/bc800448u
14. Cui Y, Wang Y, Li H, Li Q, Yu Y, Xu X, et al. Asparaginyl endopeptidase promotes the invasion and metastasis of gastric cancer through modulating epithelial-to-mesenchymal transition and analysis of their phosphorylation signaling pathways. *Oncotarget.* (2016) 7:34356–70. doi: 10.18632/oncotarget.8879
15. Gawenda J, Traub F, Luck HJ, Kreipe H, von Wasielewski R. Legumain expression as a prognostic factor in breast cancer patients. *Breast Cancer Res Treat.* (2007) 102:1–6. doi: 10.1007/s10549-006-9311-z
16. Murthy RV, Arbman G, Gao J, Roodman GD, Sun XF. Legumain expression in relation to clinicopathologic and biological variables in colorectal cancer. *Clin Cancer Res.* (2005) 11:2293–9. doi: 10.1158/1078-0432.CCR-04-1642
17. Ohno Y, Nakashima J, Izumi M, Ohori M, Hashimoto T, Tachibana, et al. Association of legumain expression pattern with prostate cancer invasiveness and aggressiveness. *World J Urol.* (2013) 31:359–64. doi: 10.1007/s00345-012-0977-z
18. Kampf C, Olsson I, Ryberg U, Sjostedt E, Ponten, F. Production of tissue microarrays, immunohistochemistry staining and digitalization within the human protein atlas. *J Vis Exp.* (2012) 31:3620. doi: 10.3791/3620
19. Subramanian A, Tamayo P, Mootha VK, Mukherjee S, Ebert BL, Gillette MA, et al. Gene set enrichment analysis: a knowledge-based approach for interpreting genome-wide expression profiles. *Proc Natl Acad Sci USA.* (2005) 102:15545–50. doi: 10.1073/pnas.0506580102
20. Zhang S, Wang X, Li Z, Wang W, Wang L. Score for the overall survival probability of patients with first-diagnosed distantly metastatic cervical cancer: a novel nomogram-based risk assessment system. *Front Oncol.* (2019) 9:1106. doi: 10.3389/fonc.2019.01106
21. Vickers AJ, Elkin EB. Decision curve analysis: a novel method for evaluating prediction models. *Med Decis Making.* (2006) 26:565–74. doi: 10.1177/0272989X06295361

22. Li N, Liu Q, Su Q, Wei C, Lan B, Wang J, et al. Effects of legumain as a potential prognostic factor on gastric cancers. *Med Oncol.* (2013) 30:621. doi: 10.1007/s12032-013-0621-9
23. Glockzin G, Piso P. Current status future directions in gastric cancer with peritoneal dissemination. *Surg Oncol Clin N Am.* (2012) 21:625–33. doi: 10.1016/j.soc.2012.07.002
24. Ramos RF, Scalon FM, Scalon MM, Dias DI. Staging laparoscopy in gastric cancer to detect peritoneal metastases: a systematic review and meta-analysis. *Eur J Surg Oncol.* (2016) 42:1315–21. doi: 10.1016/j.ejso.2016.06.401
25. Hu YF, Deng ZW, Liu H, Mou TY, Chen T, Lu X, et al. Staging laparoscopy improves treatment decision-making for advanced gastric cancer. *World J Gastroenterol.* (2016) 22:1859–68. doi: 10.3748/wjg.v22.i5.1859
26. Rausei S, Ruspi L, Mangano A, Lianos GD, Galli F, Boni L, et al. Advantages of staging laparoscopy in gastric cancer: they are so obvious that they are not evident. *Future Oncol.* (2015) 11:369–72. doi: 10.2217/fon.14.283
27. Wang Z, Chen JQ. Imaging in assessing hepatic and peritoneal metastases of gastric cancer: a systematic review. *BMC Gastroenterol.* (2011) 11:19. doi: 10.1186/1471-230X-11-19
28. Li ZY, Tang L, Li ZM, Li YL, Fu J, Zhang Y, et al. Four-point computed tomography scores for evaluation of occult peritoneal metastasis in patients with gastric cancer: a region-to-region comparison with staging laparoscopy. *Ann Surg Oncol.* (2020) 27:1103–9. doi: 10.1245/s10434-019-07812-y
29. Sawaki K, Kanda M, Miwa T, Umeda S, Tanaka H, Tanaka C, et al. Troponin I2 as a specific biomarker for prediction of peritoneal metastasis in gastric cancer. *Ann Surg Oncol.* (2018) 25:2083–90. doi: 10.1245/s10434-018-6480-z
30. Nakanishi K, Kanda M, Umeda S, Tanaka C, Kobayashi D, Hayashi M, et al. The levels of SYT13 and CEA mRNAs in peritoneal lavages predict the peritoneal recurrence of gastric cancer. *Gastric Cancer.* (2019) 22:1143–52. doi: 10.1007/s10120-019-00967-3
31. Qin R, Yang Y, Qin W, Han J, Chen H, Zhao J, et al. The value of serum immunoglobulin G glycome in the preoperative discrimination of peritoneal metastasis from advanced gastric cancer. *J Cancer.* (2019) 10:2811–21. doi: 10.7150/jca.31380
32. Zhang S, Zang D, Cheng Y, Li Z, Yang B, Guo T, et al. Identification of key gene and pathways for the prediction of peritoneal metastasis of gastric cancer by co-expression analysis. *J Cancer.* (2020) 11:3041–51. doi: 10.7150/jca.39645
33. Zhang SL, Wang ZM, Wang WR, Wang X, Zhou YH. Novel nomograms individually predict the survival of patients with soft tissue sarcomas after surgery. *Cancer Manag Res.* (2019) 11:3215–25. doi: 10.2147/CMAR.S195123

Conflict of Interest: The authors declare that the research was conducted in the absence of any commercial or financial relationships that could be construed as a potential conflict of interest.

frontiers in Oncology

REVIEW
published: 21 July 2020
doi: 10.3389/fonc.2020.00912

Novel Frontiers of Treatment for Advanced Gastric or Gastroesophageal Junction Cancer (GC/GEJC): Will Immunotherapy Be a Future Direction?

Rilan Bai[1], *Naifei Chen*[1], *Tingting Liang*[1], *Lingyu Li*[1], *Zheng Lv*[1], *Xiaomin Lv*[2]* and *Jiuwei Cui*[1]*

[1] Cancer Center, The First Hospital of Jilin University, Changchun, China, [2] Department of Neurology, The First Hospital of Jilin University, Changchun, China

Considering the limited progress of chemotherapy and targeted therapy in improving the generally disappointing outcomes of advanced gastric or gastroesophageal junction cancer (GC/GEJC), immunotherapies have been gradually developed and advanced into novel frontiers of treatment for advanced GC/GEJC. Nevertheless, the response to immunotherapy was not always satisfactory, and the emergence of resistance was unavoidable. These factors prompt the development of different combination therapies and predictive and prognostic biomarkers of efficacy to improve the outcomes of patients with advanced GC/GEJC and to overcome drug resistance. This article discusses the advances of immune monotherapy, multiple current and ongoing clinical trials of immune combination therapy, immune-related adverse events, and various biomarkers in GC/GEJC.

Keywords: gastric or gastroesophageal junction cancer, immunotherapy, combination therapy, immune related adverse events, biomarkers

OPEN ACCESS

Edited by:
Linhui Liang,
Fudan University, China

Reviewed by:
Yuan Yin,
Affiliated Hospital of Jiangnan University, China
Midie Xu,
Fudan University Shanghai Cancer Center, China

***Correspondence:**
Xiaomin Lv
781685620@qq.com
Jiuwei Cui
cuijw@jlu.edu.cn

Specialty section:
This article was submitted to Gastrointestinal Cancers, a section of the journal Frontiers in Oncology

Received: *09 March 2020*
Accepted: *11 May 2020*
Published: *21 July 2020*

Citation:
Bai R, Chen N, Liang T, Li L, Lv Z, Lv X and Cui J (2020) Novel Frontiers of Treatment for Advanced Gastric or Gastroesophageal Junction Cancer (GC/GEJC): Will Immunotherapy Be a Future Direction? Front. Oncol. 10:912. doi: 10.3389/fonc.2020.00912

Gastric or gastroesophageal junction cancer (GC/GEJC) is the third most common cause of cancer deaths worldwide, and the incidence ranks fifth, 63% of which show locally advanced or metastatic disease (1). Considering the limited progress of traditional therapy, like chemotherapy and anti-Human epidermal growth factor receptor-2 (HER-2) therapy in improving the generally disappointing outcomes (2), and the genetic complexity and heterogeneity of GC/GEJC, immunotherapies have gradually been developed and advanced into novel frontiers of treatment for advanced GC/GEJC, entirely revolutionizing the therapeutic landscape in the last 10 years. Nowadays, a number of clinical trials with immunotherapies have been conducted or are ongoing. These clinical trials involve cancer vaccines [such as, dendritic cell (DC) vaccine, melanoma-associated antigen 3 (MAGE-3) peptide vaccine], adoptive cell therapies [such as cytokine-induced killer (CIK) cells, DC-CIK, chimeric antigen receptor (CAR)-T cell therapy], and immune checkpoint inhibitor (ICI) therapies. Some of these therapies have been approved for the treatment of advanced GC/GEJC, indicating the expanding range and potential of immunotherapy applications. Although the response obtained from immunotherapy in patients with GC/GEJC adenocarcinoma is only 10–20%, and the potential of drug resistance and rapid disease progression is likely, the exploration of mechanisms of resistance to immunotherapy, of effective immune combination therapy strategies, and of predictive and prognostic biomarkers is essential for issues in oncology. This article discusses advances of immune monotherapy, multiple current and

ongoing clinical trials of immune combination therapy, immune-related adverse events (irAEs), and various biomarkers in GC/GEJC.

RATIONALE FOR THE USE OF IMMUNOTHERAPY IN THE TREATMENT OF GC/GEJC

Landmark analyses by the Cancer Genome Atlas (TCGA) in 2014 proposed classifications based on comprehensive genomic profiling for four subtypes of gastric cancer (GC) (3): Epstein–Barr virus (EBV, 8%) infection, microsatellite instability (MSI) (22%), genomic stability (20%), and chromosomal instability (CIN) (50%). The EBV subtype GC is characterized by a high incidence of DNA hypermethylation and amplification of CD274 [encoding programmed death-ligand 1 (PD-L1)] and PGD1LG2 (encoding PD-L2). An increased expression of PD-L1/2 that were evaluated in mRNA from EBV-positive GCs in the TCGA cohort characterizes their immune profile, which is known to have prominent stromal lymphoid infiltrates and a high density of tumor infiltrating lymphocytes (TILs), establishing a balance between host immune evasion mediated by PD-L1/2 overexpression and host immune responses (4). Therefore, the EBV subtype is a promising choice for ICI therapy in GC. The ongoing phase II/III clinical trials **(NCT02488759** and **Checkmate-358)** are also evaluating the efficacy of nivolumab in EBV-positive GC. Chronic EBV infection can trigger Th1 antiviral responses which lead to antitumor responses, such as the induction of IFN-γ production (3). The MSI subtype GC has high mutation load, TILs, and neoantigen presentation of DCs and macrophages (3). Therefore, EBV-positive and MSI phenotype GCs display unique immune characteristics that may be suitable targets for immunotherapy (5–7). A comprehensive analysis of the molecular characteristics of 295 gastric adenocarcinomas shows that about 34% of GCs show a relatively high mutation load, including MSI-H (8). In addition, the level of TILs and a high expression of CD3, CD8, and C45RO in patients with GC have a certain predictive value of patient prognosis. Patients with TILs highly expressing a combination of these three markers showed a longer overall survival (OS) than those with low expression (9), suggesting that GC might be a better target disease for ICIs.

Abbreviations: ACT, adoptive cell therapy; CAR, chimeric antigen receptor; CEA, carcinoembryonic antigen; CIK, cytokine-induced killer; CIN, chromosomal instability; CTA, cancer-testis antigen; CTLA-4, cytotoxic T-lymphocyte-associated protein 4; CPS, combined positive score; DC, dendritic cell; DCR, disease control rate; DFS, disease free survival; dMMR, mismatch repair deficiency; EBV, Epstein-Barr virus; EAAL, expanded activated autologous lymphocyte; EpCAM, epithelial cell adhesion molecule; FDA, Food and Drug Administration; FGFR, Fibroblast growth factor receptor; 5-FU, 5-fluorouracil; GC, gastric cancer; GC/GEJC, gastric or gastroesophageal junction cancer; GITR, glucocorticoid-induced tumor necrosis factor receptor–related protein; G17DT, gastrin-17 diphtheria toxoid; HSP, heat shock proteins; HER-2, Human epidermal growth factor receptor-2; HLA, human leukocyte antigen; ICI, immune checkpoint inhibitor; IDO-1, indoleamine 2,3-dioxygenase; irAEs, immune-related adverse events; LAG3, lymphocyte activation gene 3; MSI, microsatellite instability; MAGE-3, melanoma-associated antigen 3; MMP9, matrix metalloproteinase 9; NK, natural killer; OS, overall survival; ORR, objective response rate; PFS, progression free survival; PD-1, programmed death-1; PD-L1, programmed death-ligand 1; SD, stable disease; TTP, time to progression; TRAE, treatment related adverse event; TCGA, the Cancer Genome Atlas; TMB, tumor mutation burden; TIL, tumor infiltrating lymphocyte; TIM3, T cell immunolobulin and mucin-con-taining protein-3; VEGFR, vascular endothelial growth factor receptor.

CLINICAL ADVANCES OF IMMUNE MONOTHERAPY IN GC/GEJC

Cancer Vaccines

Cancer vaccines take advantage of antigens associated with tumor cells such as proteins overexpressed in tumor cells, cancer-testis antigens (CTAs), protein products of oncogenes, and heat-shock protein complexes (10), which may be recognized as foreign by the host adaptive immune system and trigger antitumor immune responses (11). MAGE-3 peptide vaccine acted as an adjuvant and was used to enhance an antitumor immune response resulting in a successful regression of tumor growth in a mouse model of GC (12). HER-2^+ cancer is an example where overexpressed proteins have been exploited for vaccination (12, 13). DCs, stimulated with HER-2 peptides, which were capable of inducing antitumor immunity against HER-2^+ GC, were developed as vaccines, and were evaluated in a phase I trial (13). NY-ESO-1 is a CTA expressed in gastroesophageal neoplasms. A phase I trial assessed the efficacy of NY-ESO-1 vaccine in tumors where 9 out of 10 patients with gastroesophageal cancer had an enhanced antibody response, and all patients had an increase in antigen-responsive CD4 and CD8 T cells (14). A peptide vaccine consisting of three different human leukocyte antigen (HLA)-A24-conjugated CTAs was assessed in a phase II clinical trial following promising phase I trial results (15). In cancer cells, heat shock proteins (HSP), acting as tumor rejection antigens, can form protein complexes with various deranged intracellular proteins and induce $CD4^+$ and $CD8^+$ T cell responses, suggesting that vaccines against HSP will play a role in immunotherapy for GC (16).

Adoptive Cell Therapies

Adoptive cell therapies (ACTs) may use autologous lymphocytes that have been isolated from the tumor itself or from the blood and manipulated *in vitro* to enhance their activity by expressing particular T-cell receptors or CARs against target antigens (17). CAR-T GC patients received immunotherapy with EAALs that were stimulated by the IL-2 or anti-CD3 inhibitor. As a result, significantly longer OS was observed in the treatment group (18, 19). In GC, CAR-T therapy against four major antigens is currently being tested in clinical trials. First, HER-2 gene amplification has been reported in 1/3 of GCs. A trial of anti-HER-2 CAR-T therapy aiming to study the adverse effects in patients with advanced HER-2^+ GC/GEC is ongoing **(NCT02713984).** Next, carcinoembryonic antigen (CEA) is overexpressed in gastrointestinal tumors where its overexpression indicates poor prognosis in GC (20). A trial investigating the efficacy of anti-CEA CAR-T cell therapy in advanced CEA^+GC has been initiated **(NCT02349724)**. Third, anti-MUC1 CAR-T cells are also being studied in patients with

advanced MUC1$^+$ GC/GEC **(NCT02617134)**. Finally, CAR-T therapy against epithelial cell adhesion molecule (EpCAM) is under trial **(NCT03013712)**. These trials are currently recruiting patients, and data on the antitumor efficacy and survival time of CAR-T cells in patients with advanced GC/GEC will be collected. However, available clinical trial data suggest that GC patients respond poorly to ACTs and there are insufficient ongoing trials assessing ACTs, reflecting the disappointing results. The reason for their poor response rate may be the induction of immune tolerance in adoptive cells. Therefore, combination therapies targeting multiple mechanisms of tumor-mediated immunomodulatory may need to be developed to overcome the poor efficacy seen in ACTs alone.

ICI Monotherapy in GC/GEJC

Recently, immunotherapy with antibodies that inhibit PD-1/PD-L1 interaction has emerged as a new treatment option in the field of GC. Following the results from the Phase Ib Keynote012 study (21) and from the phase II Keynote-059 cohort 1 (22), the U.S. Food and Drug Administration (FDA) has approved pembrolizumab for third-line treatment of PD-L1$^+$ [combined positive score (CPS) $\geq$ 1%] recurrent or metastatic GC/GEJC adenocarcinoma (22–25). However, the phase III Keynote-061 study (26) did not show significant survival benefits when pembrolizumab was used as a second-line treatment for PD-L1$^+$ advanced GC, but improvement of OS, better efficacy, and fewer treatment related adverse events (TRAEs) were found in patients with ECOG 0, PD-L1 CPS $\geq$ 10, or MSI-H. Subsequently, phase III Keynote-062 (27) showed survival benefits in patients with PD-L1$^+$, especially in PD-L1 CPS $\geq$ 10, making pembrolizumab possible as a first-line treatment. As for nivolumab, based on the results of the Phase III ATTRACTION-02 study (28), many regions approved nivolumab for the treatment of unresectable advanced or recurrent GC that progresses after chemotherapy, regardless of PD-L1 expression. Subsequent results in the Phase I/II Checkmate-032 study also confirmed survival benefit with nivolumab in the third-line setting (29). Due to the encouraging results from the JAVELIN Phase I trial (30) with avelumab, two randomized controlled phase 3 trials for avelumab are currently underway: JAVELIN 300 **(NCT02625623)** (31, 32) and JAVELIN 100 **(NCT02625610)** (33, 34). Disappointingly, the results of the JAVELIN 300 trial recently failed to reach its primary endpoint OS in order to consider avelumab as a third-line treatment option for advanced GC/GEJC adenocarcinoma that did not test for PD-L1. On the other hand, JAVELIN 100 is ongoing. Overall, there are still many trials being conducted to explore the effectiveness of immune monotherapy in GC. The Keynote 063 trial **(NCT03019588)** is comparing the efficacy of treatment with pembrolizumab vs. paclitaxel in Asian PD-L1$^+$ patients with advanced GC who did not respond to any combination treatment containing a fluoropyrimidine and platinum agent. The ongoing phase II/III clinical trials **(NCT02488759** and **Checkmate-358)** are also evaluating the efficacy of nivolumab in EBV-positive GC. As for other PD-L1 inhibitors, for example, a phase Ib/II study in patients with advanced GC/GEJC is currently underway to test the role of durvalumab and tremelimumab as a second- or third-line single-agent and combination therapy **(NCT02340975)** (35).

At present, the anti-cytotoxic T-lymphocyte-associated protein 4 (CTLA-4) antibody, ipilimumab, did not reach the expected endpoint of improved progression free survival (PFS) and OS in advanced GC/GEJC adenocarcinoma (NCT01585987) (36). A phase II trial investigated tremelimumab as a second-line treatment in patients with metastatic gastric and esophageal adenocarcinoma. The objective response rate (ORR) was only 5%, but there was a clinical benefit with evidence of stable disease (SD) in 4 of the 18 patients enrolled, and one patient showed a durable response, obtaining 32.7 months of treatment (37). Currently, the efficacy of CTLA-4 inhibitor monotherapy is not clear, thus they are only used in clinical trials in combination with other agents, such as programmed death-1 (PD-1)/PD-L1 inhibitors.

The summary of ICI monotherapies in GC/GEJC is described in **Table 1**. Despite many encouraging results, most patients remain unresponsive to immunotherapy, manifesting primary resistance, or the emergence of an acquired resistance phenomena in initial responders after a period of treatment. Our understanding of the mechanisms of tumor resistance to immunotherapy involving tumor-intrinsic factors (such as lack of tumor antigen expression, loss of HLA expression, and alterations of signaling pathways) and tumor-extrinsic factors (such as local tumor microenvironment like immunosuppressive cells and molecules, and host-related factors like age, gender, intestinal flora) continue to expand and deepen (38), but the issue of tumor resistance remains complex and difficult to overcome. Therefore, multiple studies of immunotherapy in combination with other treatments are underway.

CLINICAL ADVANCES OF IMMUNOTHERAPY IN COMBINATION WITH OTHER THERAPIES IN GC/GEJC

Considering the poor efficacy of immunotherapy as a single agent, as well as the complex mechanisms of drug resistance, it is necessary to carry out a variety of immunotherapy-combined regimens to improve the efficacy and reduce or overcome the drug resistance of advanced GC. Current combination strategies include different immunotherapy with chemotherapy, anti-HER-2-targeted therapy, anti-angiogenesis therapy, and immunotherapy.

Immunotherapy in Combination With Chemotherapy

Cancer Vaccine Combined With Chemotherapy

DC vaccines have been used to stimulate immunity in the treatment of cancer patients. In a phase II study with metastatic or unresectable GC/GEJ adenocarcinoma, the treatment of gastrin-17 diphtheria toxoid (G17DT) vaccine combined with chemotherapy [cisplatin þ 5-fluorouracil (5-FU)] resulted in a long time to progression (TTP) and longer OS in 69% of patients (39). A study of vascular endothelial growth factor receptor (VEGFR) 1 and 2 vaccine combined with S-1/cisplatin in metastatic or recurrent gastric adenocarcinoma showed its usefulness with an ORR and disease control rate (DCR) of 55 and 100%, an OS of up to 14.2 months, and a 1- and 2-year

TABLE 1 | The summary of ICI monotherapies in GC/GEJC.

Agent	Clinical trial	Line	Phase	Outcomes	Significance
Pembrolizumab	Keynote012	Terminal-line	Phase Ib	Safe and effective in PD-L1+ advanced GC	FDA approves pembrolizumab for third-line treatment of PD-L1+ (CPS ≥ 1%) recurrent or metastatic GC/GEJC adenocarcinoma.
	Keynote-059	Third-line	Phase II	PD-L1+ patients had higher response rates than negative patients	
	Keynote-061	Second-line	Phase III	Did not show significant survival benefits in mOS and mPFS of PD-L1+ advanced GC	Improvement of OS, better efficacy, and fewer TRAEs were found in patients with PD-L1 CPS ≥ 10 and MSI-H.
	Keynote-062	First-line	Phase III	Had survival benefits in patients with PD-L1+, especially in PD-L1 CPS ≥ 10	It makes pembrolizumab possible as a first-line treatment
	Keynote 063	Second-line	Phase III	Ongoing	–
Nivolumab	ATTRACTION-02	Third-line	Phase III	All patients could benefit from OS regardless of PD-L1 expression	Many regions approve nivolumab for the treatment of unresectable advanced or recurrent GC regardless of PD-L1 expression
	Checkmate-032	Third-line	Phase I/II	Had potential advantages over chemotherapy	–
	NCT02488759, Checkmate-358	–	Phase II/III	Ongoing	–
Avelumab	JAVELIN	First-line or second-line	Phase I	ORR, DCR, mPFS, and mOS had improved.	Encouraging results facilitate phase III studies
	JAVELIN 300	Third-line	Phase III	Failed to reach its primary endpoint OS recently	–
	JAVELIN 100	First-line maintenance	Phase III	Ongoing	–
Durvalumab and tremelimumab	NCT 02340975	Second- or third-line	Phase Ib/II	Ongoing	–
Ipilimumab	NCT01585987	First-line	Phase II	Did not reach expected endpoint of improved PFS and OS	Currently, the efficacy of CTLA-4 inhibitor monotherapy is not clear

ICI, immune checkpoint inhibitor; DCR, disease control rate; FDA, Food and Drug Administration; GC, gastric cancer; GC/GEJC, gastric or gastroesophageal junction cancer; OS, overall survival; ORR, objective response rate; PFS, progression free survival; PD-L1, programmed death-ligand 1; CPS, combined positive score; TRAEs, treatment related adverse events; MSI-H, microsatellite instability-high; CTLA-4, cytotoxic T-lymphocyte-associated protein 4.

survival of 68.2 and 25.9% (40). The lack of antigenicity and the failure to provide adequate co-stimulation, as well as the inactivation of T cells against tumors, are likely leading to the poor efficacy of cancer vaccines (41). A clinical trial evaluated the outcome of patients that received vaccine plus chemotherapy or chemotherapy alone. Disease free survival (DFS) was higher in the group that received vaccination (HSP gp96 vaccination) ($p = 0.045$), and 2-year OS was 81.9 vs. 67.9% ($p = 0.123$) in the vaccination plus chemotherapy and chemotherapy alone groups, respectively (42). Moreover, due to the characteristic of HLA being restricted, RNA vaccines become a novel option in cancer immunotherapy and are therefore safer and well-tolerated by cancer patients (43). As such, there are an increasing number of researchers giving attention to RNA vaccines.

Adoptive Cell Therapies Combined With Chemotherapy

A study evaluated ACT with TILs in stage IV GC patients divided into chemotherapy-only or ACT plus chemotherapy groups. The combination group showed a higher OS and 50% survival rates compared to the chemotherapy group (11.5 vs. 8.3 months). However, the survival benefit was not associated with OR in this trial (44). Another clinical trial evaluated the efficacy of ACT (cells cultured with cytokines and anti-CD3) plus chemotherapy in 151 stage III/IV GC patients in the adjuvant setting. Although 5-year OS was not significantly different, the 5-year DFS was significantly increased in the combination group (28.3% vs. 10.4%) (45). The investigators used autologous natural killer (NK) cells, γδ T cells, and CIK cells in combination with chemotherapy to treat patients with advanced GC and found that the combination group had better prognosis and tolerability, and lower disease recurrence rate than the group treated with chemotherapy alone (46). The results of a meta-analysis of chemotherapy combined with DC-CIK for advanced GC showed that the DCR, ORR, and quality of life were significantly higher in the combination group; in addition, the levels of CD3, CD4, CD3, CD56, IFN-γ, and IL-12 related to immune function detected in the blood were significantly higher than those in the chemotherapy-alone group (47). The existing clinical trial data suggest that the responses of GC to ACTs are encouraging, but there are an inadequate number of ongoing clinical trials.

ICIs Combined With Chemotherapy

Keynote-059 cohort 2 and cohort 3 (48) studied the first-line treatment of advanced GC with pembrolizumab alone or in combination with chemotherapy. Cohort 2 showed that the results of the combination group were significantly better than those for monotherapy, especially in the PD-L1$^+$ group.

Cohort 3 included only PD-L1$^+$ patients, with an overall ORR of 26%, DCR of 36%, mPFS of 3.3 months, and mOS of 20.7 months. The interim data of the ATTRACTION-04 trial (49) showed that ORR of patients receiving nivolumab/SOX or nivolumab/CapeOX ware 57.1 and 76.5%, respectively. Furthermore, the mOS was not reached in both groups, and most of grade $\geq$ 3 TRAEs were common side effects of chemotherapy, as expected for follow-up results. Thus, the combined use of ICIs and chemotherapy in GC preliminarily showed better effect than that of monotherapy, and adverse events were mainly related to chemotherapy and were tolerable, which promote the development of multiple large, phase III clinical trials to assess its efficacy more effectively and accurately. The ongoing phase 3 trial evaluating combination chemotherapy with checkpoint inhibitors as a first-line treatment in PD-L1$^+$/HER-2$^-$ advanced GC is Keynote-062 **(NCT02494583)**, which is divided into three groups, pembrolizumab, pembrolizumab in combination with cisplatin/5-FU, and cisplatin/5-FU alone. The Phase III Checkmate-649 study with a larger sample size is exploring the efficacy and safety of nivolumab combined with XELOX or FOLFOX chemotherapy vs. first-line chemotherapy alone for advanced GC/GEJC **(NCT02872116)**. The phase II Keynote-659 trial is evaluating the safety and efficacy of pembrolizumab combined with chemotherapy as a first-line treatment for advanced GC **(NCT03382600)**. At present, the efficacy of immunotherapy combined with chemotherapy in the treatment of GC still needs to be evaluated continuously. In the future, we should fully consider the particularity of the immune microenvironment of GC and explore new combination therapy strategies.

Immunotherapy in Combination With Antiangiogenic Agents

Preclinical studies suggest that VEGF inhibited by antiangiogenic agents has immunomodulatory activity, which provides a rationale for their use with ICIs (50). In a study of pembrolizumab combined with ramucirumab (anti-VEGFR-2) in gastroesophageal cancer, ORR and OS of PD-L1$^+$ patients were 9% and 14.9 months, respectively, while the results of patients who were PD-L1– were only 6% and 5.2 months (51). A phase I trial in 69 patients with advanced GC/GEJC studied the efficacy and safety of pembrolizumab plus ramucirumab as first-line and second-line or later subgroups. The results showed that ORR was 14 and 7%, and grade $\geq$ 3 TRAEs were 39 and 27%, respectively (52), supporting the additive for ramucirumab to ICIs. Other ongoing trials of ICIs plus antiangiogenic agents include trials of atezolizumab plus bevacizumab with or without chemotherapy **(NCT01633970)**, nivolumab plus ramucirumab **(NCT02999295)**, pembrolizumab plus ramucirumab **(NCT02443324)**, and durvalumab plus ramucirumab **(NCT02572687)**.

Immunotherapy in Combination With Anti-HER-2 Antibody and Chemotherapy

Currently, the first-line standard treatment for advanced HER-2$^+$ advanced GC/GEJC adenocarcinoma is trastuzumab combined with chemotherapy. HER-2 overexpression has been shown to suppress the immune response within the tumor microenvironment. Inhibition of HER-2 can promote T cell activation and transport, enhance NK cells to produce IFN-γ, and enhance the ADCC effect. Thus, combination therapy of an anti-HER-2 monoclonal antibody and a PD-1/PD-L1 inhibitor may have synergistic effects (53). In patients with HER-2$^+$ metastatic EG cancer, first-line treatment with the combination of pembrolizumab and trastuzumab plus chemotherapy showed encouraging clinical activity (54). A phase II clinical trial is ongoing to evaluate the effectiveness and tolerability of pembrolizumab in combination with HER-2 antibody margetuximab **(NCT02689284)** and trastuzumab **(NCT02901301)** (55). The phase III Keynote-811 study exploring the effect of adding pembrolizumab to chemotherapy and trastuzumab is still in its enrollment phase **(NCT036153260)**. A phase I/II trial involving various cancers including GC with the treatment of NK cells plus trastuzumab is in its recruitment phase **(NCT02030561)**.

Dual Immunotherapy Combined Strategies

Preclinical data showed that blocking both PD-1 and CTLA-4 signal transduction can increase IFN-γ production by lymphocytes, increase the expression of CD4/CD8 on TILs, and reduce Tregs in tumors to increase antitumor activity. The Checkmate-032 study (56) explored the efficacy of nivolumab alone or in combination with ipilimumab (different dosage) in second- and third-line treatments of advanced GC/GEJC in the Western population. Although both ORR and mOS were the best in the N1 + I3 (nivolumab 1 mg/kg + ipilimumab 3 mg/kg Q3W) group, its side effects cannot be ignored. 47% grade 3/4 irAEs were observed in the nivolumab/ipilimumab group of the phase III CheckMate 649 study **(NCT03215706),** making it difficult to combine this regimen with chemotherapy. Thus, the main obstacle and limitation of the immunotherapy-combined treatment of GC is the increased high frequency and severity of irAEs (57). Almost all patients (93%) had irAEs after concurrent combination therapy with anti-PD-1 and anti-CTLA-4, with grade 3 or 4 irAEs increasing (50%). In melanoma trials, high-grade irAEs were 21% with anti-PD-1 monotherapy (nivolumab), 28% with anti-CTLA-4 monotherapy, and 59% with the combination of anti-CTLA-4 and anti-PD-1 (58). IrAEs usually involve the gastrointestinal tract, lungs, skin, endocrine glands, and liver and less frequently involved central nervous system and cardiovascular, musculoskeletal, and hematological systems. Still, a phase I/IIb study of durvalumab in combination with tremelimumab for gastric adenocarcinoma is ongoing to explore in depth **(NCT02340975)**.

Immunotherapy in Combination With Other Therapeutic Strategies

In addition to CTLA-4 and PD-1/PD-L1, inhibitors of other immune checkpoint proteins [T cell immunolobulin and mucin-con-taining protein-3 (TIM3), lymphocyte activation gene 3 (LAG3)], co-stimulatory receptors expressed on T cells [glucocorticoid-induced tumor necrosis factor receptor–related protein (GITR), OX40, 4-1BB], enzymes indoleamine 2,3-dioxygenase (IDO-1), etc. (59) may synergize with anti–PD-1/PD-L1 inhibitors to generate a more robust antitumor immune response. Trials examining these strategies in EG

cancer and various other cancers include nivolumab plus BMS-986016 (anti–LAG-3; **NCT01968109**) and pembrolizumab plus epacadostat (IDO-1 inhibitor; **NCT02178722 and NCT03196232)**. In addition, the FRACTION-GC study is assessing nivolumab plus LAG-3 inhibitor (BMS-986016) or ipilimumab specifically in patients with advanced GC **(NCT02935634)**. The therapeutic regimen of anti–GITR agent (INCAGN01876) and nivolumab combined with or without ipilimumab is being investigated in advanced tumors with a cohort of patients with advanced GC/GEJC **(NCT03126110)**. In addition, matrix metalloproteinase 9 (MMP9) is a protein that is overexpressed in many solid tumors. It could remodel the extracellular matrix and is related to the recruitment of angiogenesis and myeloid suppressor cells and regulatory T cells. A trial is investigating a combination of nivolumab and MMP9 inhibitor GS-5745 in patients with unresected or relapsed GC/GEJC adenocarcinoma **(NCT02864381)**. Furthermore, phase I/II trials of ICIs plus other molecules like INCB054828, a pan-inhibitor of Fibroblast growth factor receptor (FGFR) types 1, 2, and 3, are ongoing **(NCT02393248)**. Another trial is studying a combination of pembrolizumab and CRS-207, a live attenuated *Listeria monocytogenes* vaccine genetically engineered to overexpress mesothelin for patients with advanced GC/GEJC **(NCT03122548)**.

Ongoing trials of novel combination therapies not mentioned above are listed in **Table 2**.

IDENTIFYING PROGNOSTIC AND PREDICTIVE BIOMARKERS FOR IMMUNOTHERAPY IN GC/GEJC

Currently, PD-1/PD-L1 inhibitors are approved as a third-line treatment for PD-L1^{+} and MSI-H refractory metastatic gastroesophageal cancer (25). However, from the research data, regardless of PD-L1 expression levels, the ORR of immunotherapy applied to end-line treatment for GC is less than 20%. With such low ORR, it is necessary to explore predictive biomarkers in the future to identify patients who would benefit from immunotherapy for gastroesophageal cancer.

TABLE 2 | Ongoing trials of novel combination therapies.

Clinical Trials.gov identifier	Intervention used	Phase	Estimated sample size	Population	Primary endpoints
NCT02335411	Pembrolizumab (treatment naïve) OR pembrolizumab (previously treated) OR P+ cisplatin+ 5-FU+ capecitabine (treatment naïve); 1 line or more	Phase II	316	Advanced gastric and GEJ cancer	Adverse events; discontinuing study due to AE;ORR
NCT02318901	Pembrolizumab OR P+ ado-trastuzumab etamine OR P+ cetuximab	Phase Ib/II	90	Patients with advanced cancer (one cohort for patients with unresectable HER-2+ gastric or GEJ cancers)	Recommended phase 2 dose of trastuzumab with pembrolizumab
NCT02658214	Durvalumab+ 5-FU+ oxaliplatin + leucovorin; 1 line	Phase I	60	Cohort 5 for advanced GC/GEC	Safety/tolerability of first line therapy; Incidence of adverse events
NCT02746796	ONO-4538+ SOX (Part 1) ONO-4538+ Cape OX (Part 1) ONO-4538+ Chemo group (Part 2)→ either SOX or Cape OX Placebo+ Chemo group (Part 2); 1 line	Phase II	680	Unresectable advanced or recurrent gastric and GEJ cancer	PFS;OS
NCT02572687	MEDI4736 in combination with ramucirumab	Phase I	114	Locally advanced and unresectable or metastatic gastrointestinal or thoracic malignancies including gastric or GEJ adenocarcinoma	DLTs
NCT02268825	MK-3475 (pembrolizumab) in combination with mFOLFOX6	Phase I/IIa	128	Various advanced gastrointestinal Cancers	Safety of combination of FOLFOX and MK-3475
NCT02903914	INCB001158 (CB-1158) alone or in combination with Pembrolizumab (advanced/metastatic gastric and GEJ cancer that have never received prior checkpoint inhibitor therapy)	Phase I/II	424	Various advanced/metastatic solid tumors including GC	Safety, pharmacokinetics; biomarkers and tumor response.
AIO-STO-0217 (NCT03409848)	(nivolumab + trastuzumab) in combination with FOLFOX vs. ipilimumab; 1 line	Phase II	Recruiting	Previously untreated HER-2+ locally advanced or metastatic esophagogastric adenocarcinoma.	OS

DLTs, dose-limiting toxicity; 5-FU, 5-fluorouracil; GC, gastric cancer; GEJ, gastric or gastroesophageal junction; GC/GEJC, gastric or gastroesophageal junction cancer; ORR, objective response rate; AE, adverse event; OS, overall survival; PFS, progression free survival; HER-2, Human epidermal growth factor receptor-2.

At present, PD-L1 expression and MSI-H/mismatch repair deficiency (dMMR) have been recognized and have become common markers for predicting efficacy in the clinical setting (25), but there still exist many limitations in the effective and accurate evaluation of patient efficacy and prognosis. EBV infection, tumor mutation burden (TMB), and the search for new biomarkers are currently potential research directions. There has been a greater understanding of the complex dynamics of the immune signaling necessary for antitumor responses. As such, the application of multiple immunomarkers to evaluate immune gene expression profiles, comprehensive immune scores, and tumor microenvironment phenotypes have entered into the forefront of biomarker analyses, providing insights into the molecular characteristics of response to immunotherapy and greater specificity in predicting efficacy. The two important biomarkers are detailed below.

PD-L1 Expression

Studies have shown that PD-L1 is expressed in 30–65% invasive GCs and is related to the depth of tumor invasion, lymph node metastasis, distant metastasis, tumor size, EBV infection, etc., which is a negative marker of prognosis (60–62). Currently, FDA has an approved PD-L1-positive expression as a biomarker for third-line treatment of pembrolizumab in gastric cancer (24), and many regions had approved nivolumab for the treatment of unresectable advanced or recurrent GC regardless of PD-L1 expression. In addition, the correlation between PD-L1 expression and efficacy of nivolumab appears to be related to race. In the ATTRACTION-2 phase III study (28) in the Asian population, ORR of nivolumab monotherapy was 11% and 12-month OS rate increased to 27%, and this survival benefit was not related to PD-L1 expression, while in the CheckMate-032 study (56) in Western patients, the ORR rate in PD-L1$^+$ tumors was significantly higher than in negative tumors (27 vs. 12%). At present, the PD-L1 level as a predictive biomarker for anti-PD-1/PD-L1 therapy in clinical trials still has many problems. For example, the definition of PD-L1$^+$GC/GEJC is based on a comprehensive positive score, including the expression on tumor cells, lymphocytes, and macrophages, which is different from the definition in lung cancer (25); there is still no consensus on the cutoff value of PD-L1-positive expression, and the expression of PD-L1 was affected by many factors such as standardization of measurement methods, antitumor therapy, and immune response of the host.

Tumor Mutation Load

TMB is a powerful predictor of response to ICIs in multiple tumor types. Clinically, next-generation sequencing can be used to capture the TMB of malignant tumors. Li et al. (63) used the Foundation One platform for sequencing and defined high TMB as >20 mut/Mb, which was found only accounting for 5% of 1,485 cases of GC. An earlier report by Licitra et al. (64) suggested that TMB $\geq$ 14 mut/Mb would benefit more from immunotherapy (2-year OS rate was 15 vs. 60%, $p = 0.094$). However, the proportion of patients with this high TMB subset was small (6/55), 4 of which were dMMR tumors. The follow-up report of the IMPACT team on gastroesophageal cancer seems to indicate that a cutoff value of >9.7 mut/Mb of TMB represents the top quartile of 40 patients treated with ICIs, which is more relevant to clinical benefit (mOS is 16.8 vs. 6.62 months, $p = 0.058$) (65). Therefore, further research is needed to determine if there is an ideal cutoff value of TMB and evaluate the predictive efficacy of TMB in GC.

SAFETY OF IMMUNOTHERAPY IN GC/GEJC

Because of their immunological mechanism of action, adverse effects of immunotherapies are distinctive from those of conventional chemotherapies. Overall, the safety of immunotherapy in GC/GEJC was better than that of chemotherapy (grade 3–5 TRAE was 35 vs. 14%) (26). Cancer vaccines are associated with minimal toxicities. Common adverse effects are similar to those associated with vaccination against pathogens such as induration, fatigue, fever, and chills (15). For ACTs, the adverse effect profiles are less well-defined with major AEs including on-target off-tumor toxicities similar to those observed in autoimmune diseases, which result from the sharing of antigens between tumor and healthy cells. In general, ACTs are associated with a benign AE profile that ranges from mild to moderate constitutional symptoms in GC. As for checkpoint inhibitor therapies, the side effects are roughly similar with about 10–20% of grade 3 or higher, involving fatigue, pruritis, arthralgias, diarrhea, and elevated aminotransferases (66). Also due to the activated effects of preexisting autoreactive T cells and B cells, these therapies can lead to dermatitis, pneumonitis, colitis, and hepatitis as well as endocrinopathies (67), with pneumonia and colitis being the most common grade 3 irAEs in GC patients. Immunotherapy can also lead to more severe complications as a result of their immune-related effects. For example, neurotoxicity (linked to the release of IL-2) and cytokine release syndrome (linked to the release of IL-6, IFN-γ, and TNF-α) induced by ACTs are potentially fatal if not diagnosed in a timely manner. Compared to PD-1/PD-L1 monotherapy, anti-CTLA-4 antibodies, and combined regimens have a higher incidence of TRAEs (68). Further research and better characterization are needed as serious and fatal toxicities have been reported with the use of immunotherapy in other cancers.

SUMMARY AND OUTLOOK

In recent years, immunotherapies involving cancer vaccines, adoptive cell therapies, and ICI therapies have gradually been developed and advanced into novel frontiers of treatment for advanced GC/GEJC, revolutionizing the therapeutic landscape. The development of immune combination therapies, identification of irAEs, and search for more robust predictive biomarkers are essential for improving the treatment efficacy of patients with advanced GC/GEJC and overcoming the drug resistance problem.

There are still many challenges in immunotherapy of advanced GC/GEJC, which are also future directions that need

in-depth study. Firstly, in which stage of advanced tumors should we use immunotherapy in earlier lines or after disease progression with more than two lines of therapy? We look forward to the ongoing phase III trials and wait with hope for their results. Two studies carried out in our study center have confirmed the efficacy of immunotherapy combined with chemotherapy in the treatment of stage III GC (69, 70), suggesting that the clinical application of immunotherapy may be expanded to early-stage GC. Moreover, considering that only a minority of patients with ICIs can achieve a durable response, multimodal treatment strategies in addition to combination therapy should be developed to improve patient clinical outcomes and overcome the development of resistance. Insights into specific molecular subtypes and genomic alterations could prompt the development of more precise novel therapies in the future. Secondly, the complex resistance mechanisms to immunotherapy are still not well-understood. The gradual elucidation and in-depth exploration of new immune resistance mechanisms contribute to the discovery of new therapeutic targets and continue to expand the scope of clinical applications of cancer immunotherapy. Additionally, more studies are needed to confirm predictive and prognostic biomarkers to immunotherapy agents in GC. However, due to the complexity of the antitumor immune response and tumor heterogeneity among different patients, there are currently no suitable wide and uniform biomarkers to predict clinical benefits. Nevertheless, this exploration can help screen immunotherapy-dominant populations, develop personalized precise diagnosis and treatment programs, predict the efficacy of treatment, and adjust the treatment regimen in a timely manner. Finally, the toxicities and tolerability of these new combinations, especially dual immunotherapy-combined strategy, are important issues to be managed in these trials. In future studies, exploring biomarkers of irAEs is an area that should be focused, which relies on the constant revelation of their mechanisms. Predictors associated with irAEs should be comprehensively analyzed and identified and reduce the incidence and severity of irAEs through early intervention, or timely detection and treatment, which facilitates the continuous optimization of clinical decision-making and patient care and the achievement of maximum clinical benefit.

In conclusion, much progress has been achieved in the treatment of advanced GC/GEJC over the past decade. With the recent molecular and biologic exploration, we have recognized that GC is a group of distinct molecular entities rather than a single disease. It is unquestionable that this field is moving to more precise medicine, and constant accomplishments will transform the management of advanced GC/GEJC in the clinical setting in the near future.

AUTHOR CONTRIBUTIONS

RB reviewed the literature, analyzed, and wrote the paper. NC, TL, LL, and ZL consulted the literature, reviewed, and modified the article. XL and JC put forward valuable comments on the article, reviewed, and edited it. All authors read and approved the final manuscript.

FUNDING

The authors are supported by the National Key R&D Program of China (No. 2016YFC1303800), the Innovation Project of Health and Technology in Jilin Province (No. 2017J064), the 13th Five-Year Science and Technology Project of Jilin Provincial Education Department (JJKH20190020KJ), Jilin Provincial Science and Technology Department Science, and Technology Development Plan Project Jilin Provincial Key Laboratory Project (20180101009JC).

REFERENCES

1. Bray F, Ferlay J, Soerjomataram I, Siegel RL, Torre LA, Jemal A. Global cancer statistics 2018: GLOBOCAN estimates of incidence and mortality worldwide for 36 cancers in 185 countries. *CA Cancer J Clin*. (2018) 68:394–424. doi: 10.3322/caac.21492
2. Bilici A. Treatment options in patients with metastatic gastric cancer: current status and future perspectives. *World J Gastroenterol*. (2014) 20:3905–15. doi: 10.3748/wjg.v20.i14.3905
3. The Cancer Genome Atlas Research Network. Comprehensive molecular characterization of gastric adenocarcinoma. *Nature*. (2014) 513:202–9. doi: 10.1038/nature13480
4. Naseem M, Barzi A, Brezden-Masley C, Puccini A, Berger MD, Tokunaga R, et al. Outlooks on Epstein-Barr virus associated gastric cancer. *Cancer Treat Rev*. (2018) 66:15–22. doi: 10.1016/j.ctrv.2018.03.006
5. Zhang L, Qiu M, Jin Y, Ji J, Li B, Wang X, et al. Programmed cell death ligand 1 (PD-L1) expression on gastric cancer and its relationship with clinicopathologic factors. *Int J Clin Exp Pathol*. (2015) 8:11084–91.
6. Kang BW, Kim JG, Lee IH, Bae HI, Seo AN. Clinical significance of tumor-infiltrating lymphocytes for gastric cancer in the era of immunology. *World J Gastrointest Oncol*. (2017) 9:293–9. doi: 10.4251/wjgo.v9.i7.293
7. Kang BW, Seo AN, Yoon S, Bae HI, Jeon SW, Kwon OK, et al. Prognostic value of tumor-infiltrating lymphocytes in Epstein-Barr virus-associated gastric cancer. *Ann Oncol*. (2016) 27:494–501. doi: 10.1093/annonc/mdv610
8. Lawrence MS, Stojanov P, Polak P, Kryukov GV, Cibulskis K, Sivachenko A, et al. Mutational heterogeneity in cancer and the search for new cancer-associated genes. *Nature*. (2013) 499:214–8. doi: 10.1038/nature12213
9. Lee HE, Chae SW, Lee YJ, Kim MA, Lee HS, Lee BL, et al. Prognostic implications of type and density of tumour-infiltrating lymphocytes in gastric cancer. *Br J Cancer*. (2008) 99:1704–11. doi: 10.1038/sj.bjc.6604738
10. Bruggen PVD, Zhang Y, Chaux P, Stroobant V, Panichelli C, Schultz ES, et al. Tumor-specific shared antigenic peptides recognized by human T cells. *Immunol Rev*. (2002) 188:51–64. doi: 10.1034/j.1600-065X.2002.18806.x
11. Klein G. The strange road to the tumor-specific transplantation antigens (TSTAs). *Cancer Immun*. (2001) 1:6.
12. Yang J, Li ZH, Zhou JJ, Chen RF, Chang LZ, Zhou QB. Preparation and antitumor effects of nanovaccines with MAGE-3 peptides in transplanted gastric cancer in mice. *Chin J Cancer*. (2010) 29:359–64. doi: 10.5732/cjc.009.10541
13. Kono K, Takahashi A, Sugai H, Fujii H, Matsumoto Y. Dendritic cells pulsed with HER-2/neu-derived peptides can induce specific T-cell responses in patients with gastric cancer. *Clin Cancer Res*. (2002) 8:3394–400. doi: 10.1093/carcin/23.11.1963

14. Kakimi K, Isobe M, Uenaka A, Wada H, Sato E, Doki Y, et al. A phase I study of vaccination with NY-ESO-1f peptide mixed with Picibanil OK-432 and Montanide ISA-51 in patients with cancers expressing the NY-ESO-1 antigen. *Int J Cancer*. (2011) 129:2836–46. doi: 10.1002/ijc.25955
15. Kono K, Mizukami Y, Daigo Y, Takano A, Masuda K, Yoshida K, et al. Vaccination with multiple peptides derived from novel cancer-testis antigens can induce specific T-cell responses and clinical responses in advanced esophageal cancer. *Cancer Sci*. (2009) 100:1502–9. doi: 10.1111/j.1349-7006.2009.01200.x
16. Wood C, Srivastava P, Bukowski R, Lacombe L, Gorelov AI, Gorelov S, et al. An adjuvant autologous therapeutic vaccine (HSPPC-96; vitespen) versus observation alone for patients at high risk of recurrence after nephrectomy for renal cell carcinoma: a multicentre, open-label, randomised phase III trial. *Lancet*. (2008) 372:145–54. doi: 10.1016/S0140-6736(08)60697-2
17. Yeku O, Li X, Brentjens RJ. Adoptive T-Cell Therapy for Solid Tumors. American Society of Clinical Oncology educational book. *Am Soc Clin Oncol*. (2017) 37:193–204. doi: 10.1200/EDBK_180328
18. Guo-Qing Z. Prolonged overall survival in gastric cancer patients after adoptive immunotherapy. *World J Gastroenterol*. (2015) 21:2777–85. doi: 10.3748/wjg.v21.i9.2777
19. Ahmed N, Brawley VS, Hegde M, Robertson C, Ghazi A, Gerken C, et al. Human epidermal growth factor receptor 2 (HER2) -specific chimeric antigen receptor-modified T cells for the immunotherapy of HER2-positive sarcoma. *J Clin Oncol*. (2015) 33:1688–96. doi: 10.1200/JCO.2014.58.0225
20. Kai D, Li Y, Bing H, Hao W, Hong Z, Chengwei T, et al. The prognostic significance of pretreatment serum CEA levels in gastric cancer: a meta-analysis including 14651 patients. *PLoS ONE*. (2015) 10:e0124151. doi: 10.1371/journal.pone.0124151
21. Muro K, Chung HC, Shankaran V, Geva R, Catenacci D, Gupta S, et al. Pembrolizumab for patients with PD-L1-positive advanced gastric cancer (KEYNOTE-012): a multicentre, open-label, phase 1b trial. *Lancet Oncol*. (2016) 17:717–26. doi: 10.1016/S1470-2045(16)00175-3
22. Fuchs CS, Doi T, Jang RW, Muro K, Satoh T, Machado M, et al. Safety and efficacy of pembrolizumab monotherapy in patients with previously treated advanced gastric and gastroesophageal junction cancer: phase 2 clinical KEYNOTE-059 trial. *JAMA Oncol*. (2018) 4:e180013. doi: 10.1001/jamaoncol.2018.0013
23. Le DT, Durham JN, Smith KN, Wang H, Bartlett BR, Aulakh LK, et al. Mismatch repair deficiency predicts response of solid tumors to PD-1 blockade. *Science*. (2017) 357:409–13. doi: 10.1126/science.aan6733
24. Chen TT. Milestone survival: a potential intermediate endpoint for immune checkpoint inhibitors. *J Natl Cancer Inst*. (2015) 107:djv156. doi: 10.1093/jnci/djv156
25. Gandara DR, Shames DS, Schleifman E, Zou W, Sandler A, Ballinger M, et al. 1295OBlood-based biomarkers for cancer immunotherapy: Tumor mutational burden in blood (bTMB) is associated with improved atezolizumab (atezo) efficacy in 2L+ NSCLC (POPLAR and OAK). *Ann Oncol*. (2017) 28(Suppl_5):v460–96. doi: 10.1093/annonc/mdx380
26. Shitara K, Özgüroglu M, Bang Y-J, Di Bartolomeo M, Mandalà M, Ryu M-H, et al. Pembrolizumab versus paclitaxel for previously treated, advanced gastric or gastro-oesophageal junction cancer (KEYNOTE-061): a randomised, open-label, controlled, phase 3 trial. *Lancet*. (2018) 392:123–33. doi: 10.1016/S0140-6736(18)31257-1
27. Tabernero J, Bang YJ, Fuchs CS, Ohtsu A, Kher U, Lam B, et al. KEYNOTE-062: Phase III study of pembrolizumab (MK-3475) alone or in combination with chemotherapy versus chemotherapy alone as first-line therapy for advanced gastric or gastroesophageal junction (GEJ) adenocarcinoma. *J Clin Oncol*. (2016) 34(Suppl_4):tps185. doi: 10.1200/jco.2016.34.4_suppl.tps185
28. Kang YK, Boku N, Satoh T, Ryu MH, Chao Y, Kato K, et al. Nivolumab in patients with advanced gastric or gastro-oesophageal junction cancer refractory to, or intolerant of, at least two previous chemotherapy regimens (ONO-4538-12, ATTRACTION-2): a randomised, double-blind, placebo-controlled, phase 3 trial. *Lancet*. (2017) 390:2461–71. doi: 10.1016/S0140-6736(17)31827-5
29. Janjigian YY, Bendell J, Calvo E, Kim JW, Ascierto PA, Sharma P, et al. CheckMate-032 study: efficacy and safety of nivolumab and nivolumab plus ipilimumab in patients with metastatic esophagogastric cancer. *J Clin Oncol*. (2018) 36:2836–44. doi: 10.1200/JCO.2017.76.6212
30. Chung HC, Arkenau H-T, Lee J, Rha SY, Oh D-Y, Wyrwicz L, et al. Avelumab (anti-PD-L1) as first-line switch-maintenance or second-line therapy in patients with advanced gastric or gastroesophageal junction cancer: phase 1b results from the JAVELIN Solid Tumor trial. *J Immunother Cancer*. (2019) 7:30. doi: 10.1186/s40425-019-0508-1
31. Bang YJ, Ruiz EY, Van Cutsem E, Lee KW, Wyrwicz L, Schenker M, et al. Phase III, randomised trial of avelumab versus physician's choice of chemotherapy as third-line treatment of patients with advanced gastric or gastro-oesophageal junction cancer: primary analysis of JAVELIN Gastric 300. *Ann Oncol*. (2018) 29:2052–60. doi: 10.1093/annonc/mdy264
32. Eric VC, Lucjan W, Keun-Wook L, Fortunato C, Rosine G, Julien T, et al. P-282JAVELIN Gastric 300: Phase 3 trial of avelumab (anti-PD-L1 antibody) + best supportive care (BSC) vs BSC ± chemotherapy as third-line treatment for advanced gastric or gastroesophageal junction cancer. *Ann Oncol*. (2016) 27(Suppl. 2):ii82. doi: 10.1093/annonc/mdw199.272
33. Moehler MH, Taieb J, Gurtler JS, Xiong H, Zhang J, Cuillerot JM, et al. Maintenance therapy with avelumab (MSB0010718C; anti-PD-L1) vs continuation of first-line chemotherapy in patients with unresectable, locally advanced or metastatic gastric cancer: The phase 3 JAVELIN Gastric 100 trial. *J Clin Oncol*. (2016) 34(Suppl_15):tps4134. doi: 10.1200/JCO.2016.34.15_suppl.TPS4134
34. Julien T, Maria DB, Antonio C, Jayne G, Deborah W, Huiling X, et al. P-281JAVELIN Gastric 100: Phase 3 trial of avelumab (anti-PD-L1 antibody) maintenance therapy vs continuation of first-line chemotherapy in patients with unresectable, locally advanced or metastatic gastric or gastroesophageal junction cancer. *Ann Oncol*. (2016) 27(Suppl. 2):ii81–2. doi: 10.1093/annonc/mdw199.271
35. Kelly RJ, Chung K, Gu Y, Steele KE, Rebelatto MC, Robbins PB, et al. Phase Ib/II study to evaluate the safety and antitumor activity of durvalumab (MEDI4736) and tremelimumab as monotherapy or in combination, in patients with recurrent or metastatic gastric/gastroesophageal junction adenocarcinoma. *J Immunother Cancer*. (2015) 3(Suppl. 2):P157. doi: 10.1186/2051-1426-3-S2-P157
36. Moehler MH, Cho JY, Kim YH, Kim JW, Bartolomeo MD, Ajani JA, et al. A randomized, open-label, two-arm phase II trial comparing the efficacy of sequential ipilimumab (ipi) versus best supportive care (BSC) following first-line (1L) chemotherapy in patients with unresectable, locally advanced/metastatic (A/M) gastric or gast. *J Clin Oncol*. (2016) 34(Suppl_15):4011. doi: 10.1200/JCO.2016.34.15_suppl.4011
37. Pereira CG, Gimenez-Xavier P, Pros E, Pajares MJ, Sanchez-Cespedes M. Genomic profiling of patient-derived xenografts for lung cancer identifies b2m inactivation impairing immunorecognition. *Clin Cancer Res*. (2016) 23:3203–13. doi: 10.1158/1078-0432.CCR-16-1946-T
38. Sharma P, Hu-Lieskovan S, Wargo JA, Ribas A. Primary, adaptive, and acquired resistance to cancer immunotherapy. *Cell*. (2017) 168:707–23. doi: 10.1016/j.cell.2017.01.017
39. Ajani JA, Hecht JR, Ho L, Baker J, Oortgiesen M, Eduljee A, et al. An open-label, multinational, multicenter study of G17DT vaccination combined with cisplatin and 5-fluorouracil in patients with untreated, advanced gastric or gastroesophageal cancer: the GC4 study. *Cancer*. (2006) 106:1908–16. doi: 10.1002/cncr.21814
40. Masuzawa T, Fujiwara Y, Okada K, Nakamura A, Takiguchi S, Nakajima K, et al. Phase I/II study of S-1 plus cisplatin combined with peptide vaccines for human vascular endothelial growth factor receptor 1 and 2 in patients with advanced gastric cancer. *Int J Oncol*. (2012) 41:1297–304. doi: 10.3892/ijo.2012.1573
41. Melero I, Gaudernack G, Gerritsen W, Huber C, Parmiani G, Scholl S, et al. Therapeutic vaccines for cancer: an overview of clinical trials. *Nat Rev Clin Oncol*. (2014) 11:509–24. doi: 10.1038/nrclinonc.2014.111
42. Zhang K, Peng Z, Huang X, Qiao Z, Wang X, Wang N, et al. Phase II trial of adjuvant immunotherapy with autologous tumor-derived Gp96 vaccination in patients with gastric cancer. *J Cancer*. (2017) 8:1826–32. doi: 10.7150/jca.18946
43. Ulmer JB, Mason PW, Geall A, Mandl CW. RNA-based vaccines. *Vaccine*. (2012) 30:4414–8. doi: 10.1016/j.vaccine.2012.04.060

44. Kono K, Takahashi A, Ichihara F, Amemiya H, Iizuka H, Fujii H, et al. Prognostic significance of adoptive immunotherapy with tumor-associated lymphocytes in patients with advanced gastric cancer: a randomized trial. *Clin Cancer Res*. (2002) 8:1767–71. doi: 10.1093/carcin/23.6.1089
45. Shi L, Zhou Q, Wu J, Ji M, Li G, Jiang J, et al. Efficacy of adjuvant immunotherapy with cytokine-induced killer cells in patients with locally advanced gastric cancer. *Cancer Immunol Immunother*. (2012) 61:2251–9. doi: 10.1007/s00262-012-1289-2
46. Zhao H, Fan Y, Li H, Yu J, Liu L, Cao S, et al. Immunotherapy with cytokine-induced killer cells as an adjuvant treatment for advanced gastric carcinoma: a retrospective study of 165 patients. *Cancer Biother Radiopharm*. (2013) 28:303–9. doi: 10.1089/cbr.2012.1306
47. Zhang L, Mu Y, Zhang A, Xie J, Chen S, Xu F, et al. Cytokine-induced killer cells/dendritic cells-cytokine induced killer cells immunotherapy combined with chemotherapy for treatment of colorectal cancer in China: a meta-analysis of 29 trials involving 2,610 patients. *Oncotarget*. (2017) 8:45164–77. doi: 10.18632/oncotarget.16665
48. Chang CH, Curtis JD, Maggi LB Jr, Faubert B, Villarino AV, O'Sullivan D, et al. Posttranscriptional control of T cell effector function by aerobic glycolysis. *Cell*. (2013) 153:1239–51. doi: 10.1016/j.cell.2013.05.016
49. Boku N, Ryu MH, Kato K, Chung HC, Minashi K, Lee KW, et al. Safety and efficacy of nivolumab in combination with S-1/capecitabine plus oxaliplatin in patients with previously untreated, unresectable, advanced, or recurrent gastric/gastroesophageal junction cancer: interim results of a randomized, phase II trial (ATTRACTION-4). *Ann Oncol*. (2019) 30:250–8. doi: 10.1093/annonc/mdy540
50. Lapeyre-Prost A, Terme M, Pernot S, Pointet AL, Voron T, Tartour E, et al. Immunomodulatory activity of VEGF in cancer. *Int Rev Cell Mol Biol*. (2017) 330:295–342. doi: 10.1016/bs.ircmb.2016.09.007
51. Apetoh L, Ghiringhelli F, Tesniere A, Criollo A, C, Lidereau R, Mariette C, et al. The interaction between HMGB1 and TLR4 dictates the outcome of anticancer chemotherapy and radiotherapy. *Immunol Rev*. (2010) 220:47–59. doi: 10.1111/j.1600-065X.2007.00573.x
52. Gibson MK, Li Y, Murphy B, Hussain MH, DeConti RC, Ensley J, et al. Randomized phase III evaluation of cisplatin plus fluorouracil versus cisplatin plus paclitaxel in advanced head and neck cancer (E1395): an intergroup trial of the Eastern Cooperative Oncology Group. *J Clin Oncol*. (2005) 23:3562–7. doi: 10.1200/JCO.2005.01.057
53. Vanneman M, Dranoff G. Combining immunotherapy and targeted therapies in cancer treatment. *Nat Rev Cancer*. (2012) 12:237–51. doi: 10.1038/nrc3237
54. Ying GS, Heitjan DF. Weibull prediction of event times in clinical trials. *Pharm Stat*. (2008) 7:107–20. doi: 10.1002/pst.271
55. Yoshida S, Kaibara A, Ishibashi N, Shirouzu K. Glutamine supplementation in cancer patients. *Nutrition*. (2001) 17:766–8. doi: 10.1016/S0899-9007(01)00629-3
56. Mickaël M, Isabelle M, Abdul Qader S, Sandy A, Yuting M, Patrizia P, et al. Autophagy-dependent anticancer immune responses induced by chemotherapeutic agents in mice. *Autophagy*. (2012) 334:1573–7. doi: 10.1126/science.1208347
57. Antonia SJ, Lopez-Martin JA, Bendell J, Ott PA, Taylor M, Eder JP, et al. Nivolumab alone and nivolumab plus ipilimumab in recurrent small-cell lung cancer (CheckMate 032): a multicentre, open-label, phase 1/2 trial. *Lancet Oncol*. (2016) 17:883–95. doi: 10.1016/S1470-2045(16)30098-5
58. Wolchok JD, Chiarion-Sileni V, Gonzalez R, Rutkowski P, Grob JJ, Cowey CL, et al. Overall survival with combined nivolumab and ipilimumab in advanced melanoma. *N Engl J Med*. (2017) 377:1345–56. doi: 10.1056/NEJMoa1709684
59. Chen DS, Mellman I. Oncology meets immunology: the cancer-immunity cycle. *Immunity*. (2013) 39:1–10. doi: 10.1016/j.immuni.2013.07.012
60. Geng Y, Wang H, Lu C, Li Q, Xu B, Jiang J, et al. Expression of costimulatory molecules B7-H1, B7-H4 and Foxp3+ Tregs in gastric cancer and its clinical significance. *Int J Clin Oncol*. (2015) 20:273–81. doi: 10.1007/s10147-014-0701-7
61. Böger C, Behrens H-M, Mathiak M, Krüger S, Kalthoff H, Röcken C. PD-L1 is an independent prognostic predictor in gastric cancer of Western patients. *Oncotarget*. (2016) 7:24269–83. doi: 10.18632/oncotarget.8169
62. Derks S, Liao X, Chiaravalli AM, Xu X, Camargo MC, Solcia E, et al. Abundant PD-L1 expression in Epstein-Barr Virus-infected gastric cancers. *Oncotarget*. (2016) 7:32925–32. doi: 10.18632/oncotarget.9076
63. Li Y, Bai O, Cui J, Li W. Genetic polymorphisms in the DNA repair gene, XRCC1 associate with non-Hodgkin lymphoma susceptibility: a systematic review and meta-analysis. *Eur J Med Genet*. (2016) 59:91–103. doi: 10.1016/j.ejmg.2015.12.011
64. Licitra L, Locati LD, Bossi P. Optimizing approaches to head and neck cancer. Metastatic head and neck cancer: new options. *Ann Oncol*. (2008) 19(Suppl. 7):vii200–3. doi: 10.1093/annonc/mdn456
65. Janjigian YY, Sanchez-Vega F, Jonsson P, Chatila WK, Hechtman JF, Ku GY, et al. Genetic predictors of response to systemic therapy in esophagogastric cancer. *Cancer Discov*. (2018) 8:49–58. doi: 10.1158/2159-8290.CD-17-0787
66. Taieb J, Moehler M, Boku N, Ajani JA, Yañez Ruiz E, Ryu M-H, et al. Evolution of checkpoint inhibitors for the treatment of metastatic gastric cancers: Current status and future perspectives. *Cancer Treat Rev*. (2018) 66:104–13. doi: 10.1016/j.ctrv.2018.04.004
67. Kottschade LA. Incidence and management of immune-related adverse events in patients undergoing treatment with immune checkpoint inhibitors. *Currt Oncol Rep*. (2018) 20:24. doi: 10.1007/s11912-018-0671-4
68. Postow MA. Managing immune checkpoint-blocking antibody side effects. *Am Soc Clin Oncol Educ Book*. (2015) 2015:76–83. doi: 10.14694/EdBook_AM.2015.35.76
69. Wang Y, Wang C, Xiao H, Niu C, Wu H, Jin H, et al. Adjuvant treatment combining cellular immunotherapy with chemotherapy improves the clinical outcome of patients with stage II/III gastric cancer. *Cancer Med*. (2017) 6:45–53. doi: 10.1002/cam4.942
70. Cui J, Li L, Wang C, Jin H, Yao C, Wang Y, et al. Combined cellular immunotherapy and chemotherapy improves clinical outcome in patients with gastric carcinoma. *Cytotherapy*. (2015) 17:979–88. doi: 10.1016/j.jcyt.2015.03.605

Conflict of Interest: The authors declare that the research was conducted in the absence of any commercial or financial relationships that could be construed as a potential conflict of interest.

frontiers in Oncology

ORIGINAL RESEARCH
published: 24 July 2020
doi: 10.3389/fonc.2020.01127

Correlation Between TNFAIP2 Gene Polymorphism and Prediction/Prognosis for Gastric Cancer and Its Effect on TNFAIP2 Protein Expression

Fang Guo[1,2], *Qian Xu*[1,3,4], *Zhi Lv*[1,3,4], *Han-Xi Ding*[1,3,4], *Li-Ping Sun*[1,3,4], *Zhen-Dong Zheng*[2] *and Yuan Yuan*[1,3,4]*

[1] *Tumor Etiology and Screening Department of Cancer Institute and General Surgery, The First Hospital of China Medical University, Shenyang, China,* [2] *Department of Oncology, PLA Cancer Center, General Hospital of Northern Theater Command, Shenyang, China,* [3] *Key Laboratory of Cancer Etiology and Prevention in Liaoning Education Department, The First Hospital of China Medical University, Shenyang, China,* [4] *Key Laboratory of GI Cancer Etiology and Prevention in Liaoning Province, The First Hospital of China Medical University, Shenyang, China*

OPEN ACCESS

Edited by:
Bin Li,
Jinan University, China

Reviewed by:
Pim Johan Koelink,
Amsterdam University Medical Center, Netherlands
Manpreet Kaur,
Guru Nanak Dev University, India

****Correspondence:***
Yuan Yuan
yuanyuan@cmu.edu.cn

Specialty section:
This article was submitted to Gastrointestinal Cancers, a section of the journal Frontiers in Oncology

Received: *14 December 2019*
Accepted: *04 June 2020*
Published: *24 July 2020*

Citation:
Guo F, Xu Q, Lv Z, Ding H-X, Sun L-P, Zheng Z-D and Yuan Y (2020) Correlation Between TNFAIP2 Gene Polymorphism and Prediction/Prognosis for Gastric Cancer and Its Effect on TNFAIP2 Protein Expression. Front. Oncol. 10:1127. doi: 10.3389/fonc.2020.01127

Objective: TNFAIP2 is a novel gene induced by TNF-α and participates in inflammatory reaction and tumor angiogenesis. This study aims to understand the correlation between TNFAIP2 gene polymorphism and prediction as well as prognosis of gastric cancer (GC) in a Chinese population.

Methods: One thousand two hundred seventy-nine cases were enrolled, including 640 GC and 639 non-cancer cases. The functional tagSNPs of the TNFAIP2 gene were screened by Haploview software and NIH Snpinfo website. Human whole-blood genomic DNA was extracted by phenol chloroform method and analyzed by KASP SNP typing and sequencing method. ELISA was used to determine the expression of TNFAIP2 protein in serum samples. The miRNAs bound to TNFAIP2 3′ UTR rs8126 were predicted by MirSNP and TargetScan database. SPSS 22.0 software was used for statistical analysis, and $P < 0.05$ showed statistical difference.

Results: Four functional TNFAIP2 tagSNPs were found by bioinformatics analysis. TNFAIP2 rs8126 T>C polymorphism increased GC risk, and the risk in TC genotype cases was higher than that in TT genotype cases ($P = 0.001$, OR = 1.557). In the dominant model, the TNFAIP2 rs8126 polymorphic carrier was 1.419 times higher ($P = 0.007$). TNFAIP2 rs710100 C>T polymorphism, TNFAIP2 rs3759571 G>A polymorphism, and TNFAIP2 rs3759573 A>G polymorphism were not correlated with GC risk. In the subgroup analysis, TNFAIP2 rs8126 TC genotype cases had a higher GC risk in male, aged 60 years or older, *Helicobacter pylori*-negative, non-smoking, and non-drinking. However, there was no correlation between TNFAIP2 SNPs and GC prognosis. The TNFAIP2 protein concentration in GC patients was significantly different from that in healthy persons ($P = 0.029$), but it was not associated with GC prognosis. The high or low expression of TNFAIP2 protein had no significant difference with gender, age, *H. pylori* infection, smoking, and drinking in GC patients. The serum TNFAIP2 protein expression

in rs8126 TT genotype carriers was significantly higher than that in rs8126 CC genotype carriers ($P < 0.001$).

Conclusion: TNFAIP2 3′ UTR rs8126 T>C polymorphism was associated with GC risk in a Chinese population, especially in cases with males aged 60 years or older, *H. pylori* negative, non-smoking and non-drinking. Compared with healthy persons, serum TNFAIP2 protein expression was higher in Chinese GC patients, and TNFAIP2 3′ UTR rs8126 T>C polymorphism might affect TNFAIP2 protein expression.

Keywords: gastric cancer, TNFAIP2, SNP, prediction, prognosis

INTRODUCTION

Gastric cancer (GC) is considered to be one of the most common malignant tumors in the world (1). It is usually asymptomatic or has mild symptoms in the early days but is prone to recurrence and metastasis due to tumor specificity and heterogeneity (2–4). In China, GC has become the second leading cause of cancer-related death, and the situation of disease prevention is extremely grim (5–7). So far, the pathogenesis of GC has not been completely clarified. Many etiological studies have found that some factors are closely related to GC, including environment, diet, microorganism, family inheritance, and physicochemical and genetic changes, especially specific oncogenes and tumor suppressor genes (8–10). In recent years, the Human Genome Atlas Project has provided a theoretical basis for exploring the correlation between genetic changes and malignant tumors. In nature, gene polymorphism is one of the most common forms of gene changes, and it can reflect the differences of biological activity between different individuals (11). The studies on gene polymorphism can lay an important foundation of molecular biology for revealing the mechanism of malignant tumors, and they have important roles in clarifying tumor susceptibility and predicting the development trend of tumors. Single nucleotide polymorphism (SNP), as the most common type of human genetic variation, is an important part of the research on gene polymorphism and can be used to explore the mechanism of tumor generation (12, 13).

Tumor necrosis factor alpha-induced protein 2 (TNFAIP2), also known as B94 and EXOC3L3, is a member of tumor necrosis factor alpha-induced proteins (TNFAIPs). It is located on human chromosome 14q32.32 and contains 14 exons, which has a genomic DNA span of 13.45 kDa and can encode a protein with 654 amino acids and a molecular weight of 72.6 kDa. TNFAIP2 interacts with EXOC1, EXOC2, EXOC4, EXOC7, and EXOC8 and participates in the formation and the development of human organs (14). It may also be involved in various biological processes such as angiogenesis, cell differentiation, bone marrow tissue generation, and spermatogenesis, and its main function is to regulate inflammation and angiogenesis (15). In *in vitro* studies, TNFAIP2 is believed to have differential expression during angiogenesis (16). In addition, TNFAIP2 also regulates the apoptosis of tumor cells and is considered to be a target gene for retinoic acid in acute promyelocytic leukemia (17). Previous studies have reported that functional TNFAIP2 SNPs, mainly located in the 3′ non-coding region (3′ UTR), may regulate gene expression by modifying the binding ability of miRNA to target genes and eventually lead to the differences in disease susceptibility. Recently, some studies have confirmed the relationship between TNFAIP2 SNPs and malignant tumors such as head and neck squamous cell carcinoma (SCCHN) and esophageal squamous cell carcinoma (ESCC), which is beneficial for screening high-risk groups and predicting outcomes of tumors (14, 15, 18, 19).

However, the correlation between TNFAIP2 gene polymorphism and prediction or prognosis of GC is rarely reported, especially in Asian or Chinese populations. At present, only one study from an American population reported that, compared with TT + TC genotype, the TNFAIP2 3′ UTR rs8126 CC genotype significantly increased GC risk, especially in the drinking population (14).

This study aims to understand the correlation between TNFAIP2 gene polymorphism and prediction or prognosis of GC in a Chinese population, explore the effect of TNFAIP2 gene polymorphism on the expression of TNFAIP2 protein, and attempt to provide a theoretical basis for molecular target prediction, disease diagnosis, and individualized treatment of GC.

MATERIALS AND METHODS

Study Participants

This was a case–control study from multiple medical centers in Liaoning Province, northern China, and 640 patients with GC and 639 non-GC cases were enrolled between December 1997 and December 2013. The inclusion criteria included the following: all participants had a clear pathological diagnosis and typing by electronic gastroscopy. The exclusion criteria included the following: (A) The participants had a major organ dysfunction; (B) The participants had autoimmune diseases; (C) The participants had other malignant tumors; and (D) The participants had infectious diseases. The fasting venous blood and serum of all participants were isolated and saved under the condition of 20°C below zero. The epidemiological information and the clinicopathological parameters of the cases were recorded, and the GC patients were followed up by telephone every 6 months. The main follow-up contents were overall survival, and the deadline for data collection was June 30,

2017 (**Figure 1**). This study was approved by the ethics committee of the First Affiliated Hospital of China Medical University [No. (2015)77], and all participants had signed the informed consent.

Functional TagSNP Selection

The functional tagSNPs of the TNFAIP2 gene were screened by Haploview software and NIH Snpinfo website (https://snpinfo.niehs.nih.gov/). The F-SNP website (http://compbio.cs.queensu.ca/F-SNP/) and the NIH Snpinfo website were used to predict the functional tagSNPs, respectively. The parameters were set as: Chinese Han population, minimum allele frequency >5%, and frequency distribution $r^2 > 0.8$ (**Supplementary Figures 1**, **2**).

Genotyping

Human whole-blood genomic DNA was extracted by phenol chloroform method and analyzed by KASP SNP typing and sequencing method. In the Sequenom MassARRAY platform (Sequenom, San Diego, CA, USA), SNP genotyping was performed by Bio Miao Biological Technology (Beijing, China). In addition, we randomly selected 10% of the samples for repeated analysis and found that the consistency rate of all the duplicated samples was 100%.

Detection of Serum TNFAIP2 Protein and *H. pylori*-IgG by ELISA

Enzyme-linked immunosorbent assay (ELISA) was used to determine the expression of the TNFAIP2 protein in the serum samples. Double-antibody sandwich method was used for ELISA, and the ELISA kit was purchased from Shanghai Enzyme-linked Biotechnology Co., Ltd. The absorbance (OD value) was measured by Multiskan Ascent (Thermo Labsystems, USA) at 450 nm, and the TNFAIP2 concentration was calculated by a standard curve. Serum *H. pylori*-IgG titer was also detected by ELISA (*Helicobacter pylori* IgG kit; Biohit, Helsinki, Finland), and the details were described in our published study (20).

Statistical Analysis

SPSS 20.0 software (SPSS Inc., Chicago, IL, USA) was used for statistical analysis. Firstly, we tested the normal distribution for units of measurement. If it conformed to the normal distribution, *T*-test could be used for statistical analysis. If it did not conform to the normal distribution, non-parametric test should be used for statistical analysis. The counting units were statistically analyzed by chi-square test. Multivariate logistic regression model was used to compare TNFAIP2 SNPs genotypes between the GC group and the non-GC group, and OR value

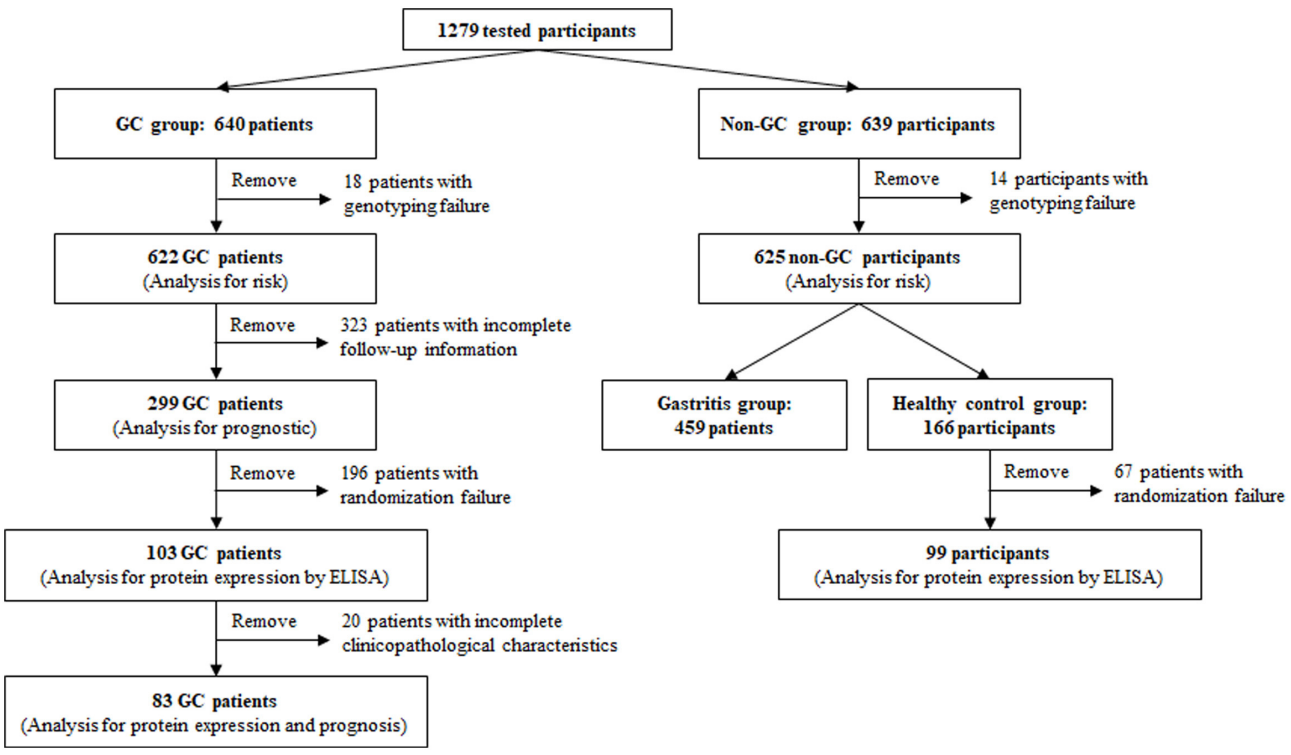

FIGURE 1 | Participants' disposition. Human whole-blood genomic DNA tests were performed on 1,279 participants in this study, including 640 gastric cancer (GC) patients and 639 non-GC participants. Due to genotyping failure on some participants, the analysis of correlation between TNFAIP2 TagSNPs and GC risk was performed on 1,247 eligible participants, including 622 GC patients and 625 non-GC participants. Due to incomplete follow-up information, the analysis of correlation between TNFAIP2 TagSNPs and GC prognosis was performed on 299 GC patients. The analysis of TNFAIP2 protein expression and GC risk and prognosis was performed on 202 participants randomly selected from the GC group and the healthy control group, including 103 GC patients and 99 healthy persons. Due to incomplete clinicopathological characteristics, only 83 GC patients were enrolled in the analysis of correlation between serum TNFAIP2 protein expression and GC prognosis.

TABLE 1 | The basic characteristics of the study participants.

Basic characteristics	Gastric cancer (*n*, %)	Control (*n*, %)	*P*-value
Gender	*n* = 622	*n* = 625	0.381
Male	443 (71.2)	459 (73.4)	
Female	179 (28.8)	166 (26.6)	
Age (years)	*n* = 622	*n* = 625	0.195
Mean ± SD	59.26 ± 11.40	58.53 ± 8.17	
Median	59	58	
Range	26–87	26–89	
H. pylori infection*	*n* = 622	*n* = 625	**<0.001**
Positive	314 (50.5)	106 (17.0)	
Negative	308 (49.5)	519 (83.0)	
Smoking	*n* = 247	*n* = 361	0.359
Yes	98 (39.7)	130 (36.0)	
No	149 (60.3)	231 (64.0)	
Drinking	*n* = 247	*n* = 359	0.058
Yes	80 (32.4)	91 (25.3)	
No	167 (67.6)	268 (74.7)	

**SPSS 20.0 random number generator was used to supplement the H. pylori infection status of 122 cases, whose H. pylori was unknown, so as to facilitate the subsequent statistical analysis. Bold Value indicate the data is statistically significant differences (P < 0.05).*

and confidence interval (95% CI) were calculated to represent the relative risk. Logistic regression model was used to evaluate the interaction relationship between TNFAIP2 SNPs and *H. pylori* infection, smoking, and drinking. Adjusting for gender and age, a full-factor model was used to calculate the *P*-value of the interaction relationship between TNFAIP2 SNPs genotypes and *H. pylori* infection, smoking, and drinking. Cox proportional risk model was used for univariate and multivariate analysis to calculate the relationship between the clinical parameters and the prognosis of GC patients. $P < 0.05$ was considered as statistically significant.

RESULTS

The Basic Characteristics of Study Participants

In this study, 1,247 qualified peripheral blood samples were analyzed for gene polymorphism, including 622 cases in the GC group and 625 cases in the non-GC group. Age and sex were matched in both groups. The mean age in the GC group and in the non-GC group was 59.26 ± 11.4 (26–87) and 58.53 ± 8.17 (26–89), respectively. The difference in *H. pylori* infection between the two groups was statistically significant ($P < 0.001$), but there were no significant differences in smoking and drinking (**Table 1**).

Functional TagSNPs Selected

Haploview software and NIH Snpinfo website were used to screen for functional tagSNPs, respectively. We found four functional TNFAIP2 SNPs and used them as candidate SNPs for further genotyping and statistical analysis, including miRNA binding sites (rs8126 and rs710100) and transcription factor binding sites (rs3759571 and rs3759573).

The Correlation Between TNFAIP2 TagSNPs and GC Risk in General Population

A total of 1,247 samples were included to analyze the correlation between TNFAIP2 SNPs and GC risk. The wild and the mutant bases of SNPs were defined by searching the NCBI website. TNFAIP2 SNPs were classified by KASP SNP typing and sequencing as follows: wild type, heterozygous type, mutant type, dominant model, and recessive model. The differences of TNFAIP2 SNPs between the GC group and the non-GC group were compared, and the correlation between TNFAIP2 SNPs and GC risk was analyzed. The results showed that TNFAIP2 rs8126 T>C polymorphism was associated with GC risk in general populations, and the risk in TC genotype cases was higher than that in TT genotype cases ($P = 0.001$, OR = 1.557). In the dominant model, the GC risk in TNFAIP2 rs8126 polymorphic carriers was 1.419 times higher ($P = 0.007$). However, TNFAIP2 rs710100 C>T polymorphism, TNFAIP2 rs3759571 G>A polymorphism, and TNFAIP2 rs3759573 A>G polymorphism were not associated with GC risk. In particular, TNFAIP2 rs3759573 A>G polymorphism was not consistent with Hardy–Weinberg's genetic linkage balance ($P_{HWE} < 0.05$) and was excluded in the subsequent analysis (**Table 2**).

The Correlation Between TNFAIP2 TagSNPs and GC Risk in Subgroup Population

In the subgroup analysis, we found that, in male subjects, TNFAIP2 rs8126 TC genotype cases were associated with a higher GC risk than TT genotype cases ($P = 0.005$, OR = 1.573), and GC risk was 1.443 times higher in TNFAIP2 rs8126 polymorphic carriers in the dominant model ($P = 0.018$). In subjects aged over 60 years, TNFAIP2 rs8126 TC genotype cases had a higher GC risk than TT genotype cases ($P = 0.005$, OR = 1.816), and GC risk was 1.693 times higher in TNFAIP2 rs8126 polymorphic carriers in the dominant model ($P = 0.010$). In subjects younger than 60 years old, TNFAIP2 rs8126 TC genotype cases had a higher GC risk than TT genotype cases ($P = 0.049$, OR = 1.440). In subjects without *H. pylori* infection, TNFAIP2 rs8126 TC genotype cases had a higher GC risk than TT genotype cases ($P = 0.006$, OR = 1.560), and GC risk was 1.440 times higher in TNFAIP2 rs8126 polymorphic carriers in the dominant model ($P = 0.017$). In non-smoking subjects, TNFAIP2 rs8126 TC genotype cases had a higher GC risk than TT genotype cases ($P = 0.038$, OR = 1.701), and GC risk was 1.643 times higher in TNFAIP2 rs8126 polymorphic carriers in the dominant model ($P = 0.038$). In non-drinking subjects, TNFAIP2 rs8126 TC genotype cases had a higher GC risk than TT genotype cases ($P = 0.045$, OR = 1.630) (**Table 3**).

The Interaction Effects Between TNFAIP2 TagSNPs and Environmental Factors on GC Risk

The interaction effects between TNFAIP2 SNPs (rs8126, rs710100, and rs3759571) and environmental factors (*H. pylori* infection, smoking, and drinking) on GC risk

TABLE 2 | The correlation between TNFAIP2 TagSNPs and gastric cancer (GC) risk in the general population.

TNFAIP2 SNPs	GC (%)	Control (%)	*P*-value*	OR* (95% CI)
rs8126	$n = 1125$			
	$n = 587$	$n = 538$		
TT	272 (46.4)	205 (38.1)		1 (Ref)
TC	235 (40.0)	270 (50.2)	**0.001**	**1.557 (1.188–2.041)**
CC	80 (13.6)	63 (11.7)	0.901	1.026 (0.685–1.536)
CC + TC vs. TT			**0.007**	**1.419 (1.099–1.832)**
CC vs. TC + TT			0.298	0.818 (0.561–1.194)
P_{HWE}		0.067		
rs710100	$n = 1115$			
	$n = 543$	$n = 572$		
CC	217 (40.0)	214 (37.4)		1 (Ref)
CT	251 (46.2)	285 (49.8)	0.545	0.920 (0.701–1.206)
TT	75 (13.8)	73 (12.8)	0.545	1.131 (0.156–0.332)
TT + CT vs. CC			0.805	0.968 (0.747–1.254)
TT vs. CT + CC			0.329	1.202 (0.831–1.738)
P_{HWE}		0.145		
rs3759571				
	$n = 578$	$n = 584$		
GG	239 (41.3)	230 (39.4)		1 (Ref)
GA	268 (46.4)	278 (47.6)	0.597	0.931 (0.715–1.213)
AA	71 (12.3)	76 (13.0)	0.926	0.981 (0.662–1.455)
AA + GA vs. GG			0.672	0.947 (0.736–1.218)
AA vs. GA + GG			0.882	1.028 (0.711–1.488)
P_{HWE}		0.575		
rs3759573				
	$n = 529$	$n = 554$		
AA	179 (33.8)	184 (33.2)		1 (Ref)
AG	291 (55.0)	302 (54.5)	0.858	1.026 (0.774–1.361)
GG	59 (11.2)	68 (12.3)	0.778	0.941 (0.614–1.440)
GG + AG vs. AA			0.918	1.014 (0.773–1.331)
GG vs. AG + AA			0.766	0.942 (0.633–1.400)
P_{HWE}		**0.001**[#]		

*Adjusted for gender, age, and H. pylori infection.

#The results were inconsistent with Hardy–Weinberg genetic linkage equilibrium. Bold Values indicate the data is statistically significant differences ($P < 0.05$).

were analyzed, and the results showed that there was no significant correlation between them ($P_{interaction} > 0.05$; **Table 4**).

The Correlation Between TNFAIP2 TagSNPs and GC Prognosis

Prognostic analysis was performed in 299 GC patients who had complete survival follow-up data. We found that GC prognosis was correlated with Borrmann classification, depth of invasion, growth pattern, lymphatic vessel invasion, lymph node metastasis, and TNM stage (**Table 5**). Both univariate analysis and multivariate analysis showed no statistical differences between TNFAIP2 SNPs and GC prognosis ($P > 0.05$), suggesting that TNFAIP2 SNPs had nothing to do with GC prognosis in this group (**Table 6**). In the subgroup analysis, TNFAIP2 rs8126 polymorphism was stratified by gender, age, and *H. pylori* infection, and no correlation was found between TNFAIP2 rs8126 polymorphism and GC prognosis ($P > 0.05$) (**Table 7**).

Serum TNFAIP2 Protein Expression Between GC Patients and Healthy Persons

ELISA was performed on 202 serum samples randomly selected from the GC group and the healthy control group, including 103 GC patients and 99 healthy persons. There was no statistical difference in age, gender, and TNFAIP2 rs8126 genotypes between the two groups. The average age of the GC group and the healthy control group was 56.57 ± 7.656 (29–67) years old and 54.45 ± 7.737 (43–81) years old, respectively. The TNFAIP2 protein concentration in GC patients was significantly different from that in healthy persons ($P = 0.029$; **Table 8**).

TABLE 3 | The correlation between TNFAIP2 TagSNPs and gastric cancer (GC) risk in the subgroup population.

Parameters	Genotype	GC vs. control	*P*-value*	OR (95%)
rs8126				
Gender#		*n* = 587 vs. 538		
Male	TT	195/149		
	TC	171/201	**0.005**	**1.573 (1.143–2.164)**
	CC	55/45	0.841	1.051 (0.648–1.703)
	CC + TC vs. TT		**0.018**	**1.443 1.066–(1.954)**
	CC vs. TC + TT		0.407	0.825 (0.524–1.300)
Female	TT	77/56		
	TC	64/69	0.116	1.510 (0.903–2.525)
	CC	25/18	0.866	1.067 (0.500–2.275)
	CC + TC vs. TT		0.193	1.374 (0.852–2.216)
	CC vs. TC + TT		0.642	0.849 (0.425–1.694)
Age (years)		*n* = 587 vs. 538		
≥60	TT	129/74		
	TC	126/124	**0.005**	**1.816 (1.195–2.758)**
	CC	34/25	0.493	1.257 (0.653–2.420)
	CC + TC vs. TT		**0.010**	**1.693 (1.135–2.526)**
	CC vs. TC + TT		0.718	0.895 (0.488–1.638)
<60	TT	143/131		
	TC	109/146	**0.049**	**1.440 (1.002–2.069)**
	CC	46/38	0.788	0.931 (0.551–1.572)
	CC + TC vs. TT		0.138	1.292 (0.921–1.811)
	CC vs. TC + TT		0.321	0.780 (0.477–1.274)
H. pylori infection#		*n* = 587 vs. 538		
Positive	TT	137/35		
	TC	121/46	0.084	1.569 (0.941–2.618)
	CC	41/9	0.757	0.879 (0.386–1.997)
	CC + TC vs. TT		0.186	1.391 (0.853–2.266)
	CC vs. TC + TT		0.361	0.698 (0.322–1.511)
Negative	TT	135/170		
	TC	114/224	**0.006**	**1.560 (1.133–2.147)**
	CC	39/54	0.693	1.099 (0.687–1.759)
	CC + TC vs. TT		**0.017**	**1.440 (1.067–1.944)**
	CC vs. TC + TT		0.563	0.878 (0.564–1.365)
Smoking		*n* = 246 vs. 314		
Yes	TT	47/44		
	TC	34/62	0.182	1.556 (0.813–2.979)
	CC	16/10	0.615	0.770 (0.277–2.135)
	CC + TC vs. TT		0.377	1.318 (0.715–2.432)
	CC vs. TC + TT		0.232	0.560 (0.216–1.450)
No	TT	76/74		
	TC	56/99	**0.038**	**1.701 (1.030–2.809)**
	CC	17/25	0.298	1.501 (0.699–3.227)
	CC + TC vs. TT		**0.038**	**1.643 (1.027–2.627)**
	CC vs. TC + TT		0.750	1.123 (0.549–2.298)
Drinking		*n* = 246 vs. 311		
Yes	TT	39/30		
	TC	29/43	0.089	1.831 (0.913–3.674)
	CC	12/6	0.579	0.718 (0.222–2.317)
	CC + TC vs. TT		0.216	1.518 (0.784–2.940)
	CC vs. TC + TT		0.233	0.515 (0.174–1.531)

(Continued)

TABLE 3 | Continued

Parameters	Genotype	GC vs. control	*P*-value*	OR (95%)
No	TT	84/87		
	TC	61/117	**0.045**	**1.630 (1.010–2.629)**
	CC	21/28	0.524	1.258 (0.620–2.552)
	CC + TC vs. TT		0.065	1.524 (0.974–2.384)
	CC vs. TC + TT		0.873	0.947 (0.485–1.851)
rs710100		*n* = 543 vs. 572		
Gender#				
Male	CC	151/166		
	CT	182/209	0.913	0.982 (0.713–1.352)
	TT	49/52	0.649	1.119 (0.689–1.816)
	TT + CT vs. CC		0.950	1.010 (0.744–1.371)
	TT vs. CT + CC		0.567	1.140 (0.728–1.787)
Female	CC	66/48		
	CT	69/76	0.251	0.738 (0.440–1.239)
	TT	26/21	0.877	1.060 (0.505–2.228)
	TT + CT vs. CC		0.427	0.818 (0.499–1.342)
	TT vs. CT + CC		0.439	1.298 (0.670–2.512)
Age (years)		*n* = 543 vs. 572		
≥60	CC	106/78		
	CT	131/131	0.373	0.827 (0.544–1.257)
	TT	33/24	0.461	1.290 (0.656–2.536)
	TT + CT vs. CC		0.581	0.892 (0.594–1.339)
	TT vs. CT + CC		0.274	1.410 (0.761–2.612)
<60	CC	111/136		
	CT	120/154	0.860	0.968 (0.673–1.391)
	TT	42/49	0.787	1.074 (0.641–1.800)
	TT + CT vs. CC		0.999	1.000 (0.710–1.409)
	TT vs. CT + CC		0.608	1.131 (0.706–1.812)
H. pylori infection#		*n* = 543 vs. 572		
Positive	CC	112/47		
	CT	124/44	0.536	1.168 (0.714–1.910)
	TT	36/7	0.080	2.227 (0.908–5.462)
	TT + CT vs. CC		0.258	1.313 (0.819–2.104)
	TT vs. CT + CC		0.104	2.031 (0.865–4.768)
Negative	CC	105/167		
	CT	127/241	0.272	0.833 (0.601–1.155)
	TT	39/66	0.676	0.905 (0.566–1.446)
	TT + CT vs. CC		0.313	0.853 (0.625–1.162)
	TT vs. CT + CC		0.945	1.015 (0.661–1.560)
Smoking		*n* = 228 vs. 337		
Yes	CC	37/48		
	CT	40/66	0.451	0.785 (0.418–1.474)
	TT	13/10	0.387	1.619 (0.543–4.823)
	TT + CT vs. CC		0.732	0.899 (0.490–1.651)
	TT vs. CT + CC		0.179	1.944 (0.737–5.125)
No	CC	61/82		
	CT	60/101	0.851	1.049 (0.635–1.735)
	TT	17/30	0.914	1.042 (0.492–2.210)
	TT + CT vs. CC		0.840	1.050 (0.652–1.693)
	TT vs. CT + CC		0.974	1.011 (0.505–2.025)
Drinking		*n* = 228 vs. 335		

(Continued)

TABLE 3 | Continued

Parameters	Genotype	GC vs. control	*P*-value*	OR (95%)
Yes	CC	30/35		
	CT	34/46	0.570	0.820 (0.413–1.626)
	TT	10/5	0.354	1.826 (0.511–6.529)
	TT + CT vs. CC		0.825	0.928 (0.478–1.802)
	TT vs. CT + CC		0.178	2.238 (0.693–7.226)
No	CC	68/94		
	CT	66/120	0.947	0.984 (0.611–1.585)
	TT	20/35	0.892	1.050 (0.519–2.125)
	TT + CT vs. CC		0.965	1.010 (0.641–1.591)
	TT vs. CT + CC		0.879	1.052 (0.549–2.014)
rs3759571				
Gender#		*n* = 578 vs. 584		
Male	GG	163/172		
	GA	201/201	0.751	1.052 (0.769–1.438)
	AA	47/56	0.844	0.953 (0.592–1.534)
	AA + GA vs. GG		0.822	1.035 (0.768–1.395)
	AA vs. GA + GG		0.778	0.938 (0.601–1.463)
Female	GG	76/58		
	GA	67/77	0.128	0.678 (0.411–1.119)
	AA	24/20	0.848	0.930 (0.446–1.941)
	AA + GA vs. GG		0.218	0.743 (0.462–1.193)
	AA vs. GA + GG		0.620	1.188 (0.601–2.349)
Age (years)		*n* = 578 vs. 584		
≥60	GG	113/86		
	GA	141/121	0.408	0.841 (0.557–1.268)
	AA	28/31	0.353	0.735 (0.385–1.406)
	AA + GA vs. GG		0.324	0.819 (0.551–1.218)
	AA vs. GA + GG		0.528	0.823 (0.449–1.507)
<60	GG	126/144		
	GA	127/157	0.771	0.949 (0.667–1.349)
	AA	43/45	0.663	1.122 (0.668–1.884)
	AA + GA vs. GG		0.966	0.993 (0.712–1.385)
	AA vs. GA + GG		0.491	1.183 (0.733–1.907)
H. pylori infection#		*n* = 578 vs. 584		
Positive	GG	119/46		
	GA	140/44	0.510	1.178 (0.723–1.919)
	AA	34/8	0.249	1.656 (0.703–3.903)
	AA + GA vs. GG		0.338	1.256 (0.788–2.003)
	AA vs. GA + GG		0.306	1.530 (0.678–3.451)
Negative	GG	120/184		
	GA	128/234	0.279	0.840 (0.613–1.152)
	AA	37/68	0.425	0.828 (0.521–1.317)
	AA + GA vs. GG		0.253	0.840 (0.623–1.132)
	AA vs. GA + GG		0.676	0.912 (0.593–1.403)
Smoking		*n* = 236 vs. 350		
Yes	GG	42/50		
	GA	41/62	0.659	0.869 (0.465–1.624)
	AA	14/15	0.730	1.183 (0.456–3.070)
	AA + GA vs. GG		0.803	0.927 (0.511–1.680)
	AA vs. GA + GG		0.625	1.243 (0.519–2.978)

(Continued)

TABLE 3 | Continued

Parameters	Genotype	GC vs. control	*P*-value*	OR (95%)
No	GG	62/88		
	GA	63/107	0.746	0.922 (0.565–1.506)
	AA	14/28	0.564	0.798 (0.371–1.716)
	AA + GA vs. GG		0.666	0.902 (0.565–1.440)
	AA vs. GA + GG		0.706	0.867 (0.413–1.819)
Drinking		*n* = 236 vs. 350		
Yes	GG	29/38		
	GA	38/46	0.736	1.125 (0.568–2.227)
	AA	10/5	0.200	2.225 (0.655–7.561)
	AA + GA vs. GG		0.535	1.230 (0.640–2.365)
	AA vs. GA + GG		0.236	2.039 (0.628–6.625)
No	GG	75/100		
	GA	66/121	0.261	0.765 (0.480–1.220)
	AA	18/38	0.244	0.664 (0.334–1.321)
	AA + GA vs. GG		0.194	0.746 (0.479–1.161)
	AA vs. GA + GG		0.481	0.788 (0.407–1.527)

**Adjusted for gender, age, and H. pylori infection.*

#Adjusted for two other factors besides self. Bold Values indicate the data is statistically significant differences (P < 0.05).

TABLE 4 | The interaction effects between TNFAIP2 TagSNPs and environmental factors on gastric cancer (GC) risk.

SNP genotype	*H. pylori* infection		Smoking		Drinking	
	Positive	Negative	Yes	No	Yes	No
rs8126	*n* = 389	*n* = 736	*n* = 213	*n* = 347	*n* = 159	*n* = 398
TT						
GC/control (CON)	137/35	135/170	47/44	76/74	39/30	84/87
OR (95% CI)	4.858 (3.527–6.692)	1 (Ref)	0.338 (0.201–0.567)	1 (Ref)	0.282(0.170–0.468)	1 (Ref)
TC + CC						
GC/CON	162/55	153/278	50/72	72/127	41/49	82/145
OR (95% CI)	2.975(1.807–4.898)	0.432(0.293–0.635)	0.412(0.211–0.805)	1.012(0.683–1.501)	0.729(0.362–1.471)	1.144(0.750–1.747)
	$P_{interaction}$ = 0.788		$P_{interaction}$ = 0.793		$P_{interaction}$ = 0.823	
	OR = 0.925 (0.524–1.632)		OR = 0.910 (0.451–1.836)		OR = 0.918(0.432–1.950)	
rs710100	*n* = 370	*n* = 745	*n* = 214	*n* = 351	*n* = 160	*n* = 403
CC						
GC/CON	112/47	105/167	37/48	61/82	30/35	68/94
OR (95% CI)	3.790 (2.493–5.763)	1 (Ref)	1.036 (0.603–1.782)	1 (Ref)	1.185(0.664–2.114)	1 (Ref)
TC + TT						
GC/CON	160/51	166/307	53/76	77/131	44/51	86/155
OR (95% CI)	4.990 (3.349–7.434)	0.860 (0.632–1.171)	0.937 (0.579–1.519)	0.790 (0.512–1.220)	1.193(0.716–1.986)	0.767(0.510–1.154)
	$P_{interaction}$ = 0.119		$P_{interaction}$ = 0.827		$P_{interaction}$ = 0.604	
	OR = 1.560 (0.892–2.728)		OR = 1.082 (0.532–2.201)		OR = 1.222 (0.572–2.612)	
rs3759571	*n* = 391	*n* = 771	*n* = 224	*n* = 362	*n* = 166	*n* = 418
GG						
GC/CON	119/46	120/184	42/50	62/88	29/38	75/100
OR (95% CI)	3.967 (2.631–5.981)	1 (Ref)	1.192 (0.706–2.012)	1 (Ref)	1.018(0.576–1.797)	1(Ref)
GA + AA						
GC/CON	174/52	165/302	55/77	77/135	48/51	84/159
OR (95% CI)	5.131 (3.488–7.546)	0.838 (0.622–1.129)	1.014 (0.631–1.630)	0.810 (0.527–1.243)	1.225(0.765–2.059)	0.704(0.472–1.050)
	$P_{interaction}$ = 0.123		$P_{interaction}$ = 0.944		$P_{interaction}$ = 0.156	
	OR = 1.540 (0.890–2.666)		OR = 1.025 (0.513–2.048)		OR = 1.715 (0.815–3.610)	

TABLE 5 | The correlation between basic characteristics and gastric cancer (GC) prognosis.

Basic characteristics	GC patients	Death	Median survival time (mean)	*P*-value
Total	$n = 299$	$n = 124$		
Gender				0.097
Male	219	92	79.0[a]	
Female	80	32	54.1[b]	
Age (years)				0.553
≥60	141	61	58.0[a]	
<60	158	63	79.0[a]	
H. pylori infection				0.334
Positive	157	61	56.7[b]	
Negative	142	63	58.0[a]	
Smoking				0.718
Yes	98	41	79.0[a]	
No	149	64	52.9[b]	
Drinking				0.703
Yes	80	35	79.0[a]	
No	167	70	53.6[b]	
Family history				0.570
Yes	33	13	68.0[a]	
No	210	93	79.0[a]	
Borrmann classification				**<0.001**
Borrmann I–II	69	22	64.8[b]	
Borrmann III–IV	199	98	47.0[a]	
Lauren classification				0.594
Intestinal type	109	43	56.2[b]	
Diffuse type	189	81	79.0[a]	
Site of primary lesions				
Corpus	81	34	52.0[b]	0.513
Fundus	31	9	64.1[b]	
Antrum/angle	123	54	79.0[a]	
Growth pattern				**0.035**
Infiltrative	136	67	40.0[a]	
Intermediate/expanding	106	35	61.8[b]	
Depth of invasion				**<0.001**
T1/T2	130	22	75.3[b]	
T3/T4	169	102	29.0[a]	
TNM stage				**0.001**
I–II	85	22	65.2[b]	
III–IV	214	102	57.0[a]	
Lymph node metastasis				**<0.001**
Positive	178	102	35.0[a]	
Negative	121	22	70.1[b]	
Lymphatic vessel invasion				**<0.001**
Positive	34	24	31.0[a]	
Negative	182	62	59.3[b]	
Blood vessel invasion				0.061
Positive	23	14	20.0[a]	
Negative	193	72	57.8[b]	

[a]*Median survival time.*

[b]*Mean survival time. Bold Values indicate the data is statistically significant differences ($P < 0.05$).*

The Correlation Between Serum TNFAIP2 Protein Expression and Clinicopathological Parameters in GC Patients

According to median TNFAIP2 protein concentration, 103 GC patients were divided into high-expression group and low-expression group, and the correlation between TNFAIP2 protein expression and clinicopathological parameters in GC patients was analyzed. We found that a high or a low expression of TNFAIP2 protein had no significant difference with gender, age, *H. pylori* infection, smoking, and drinking (**Table 9**).

The Correlation Between Serum TNFAIP2 Protein Expression and GC Prognosis

A total of 83 cases with complete clinical data and survival data were selected from 103 GC patients. The basic characteristics of the patients included gender, age, *H. pylori* infection, smoking, drinking, family history, Borrmann classification, Lauren classification, site of primary lesions, growth pattern, depth of invasion, TNM stage, and lymph node metastasis. We found significant differences in depth of invasion ($P < 0.001$) and lymph node metastasis ($P = 0.002$; **Table 10**). According to serum TNFAIP2 protein concentration, the univariate analysis showed that TNFAIP2 protein expression was not significantly correlated with GC prognosis ($P = 0.798$; hazard ratio, HR = 1.090). The multivariate analysis with depth of invasion and lymph node metastasis as covariables confirmed that there was no significant difference in GC prognosis between the two groups ($P = 0.339$; HR = 1.387). The results suggested that serum TNFAIP2 protein expression was not associated with the prognosis of GC patients in this group (**Table 11**).

The Correlation Between TNFAIP2 3′ UTR rs8126 T>C Polymorphism and TNFAIP2 Protein Expression

The correlation between TNFAIP2 3′ UTR rs8126 T>C polymorphism and TNFAIP2 protein expression was analyzed by different polymorphism genotypes in 103 GC patients, and we found that TNFAIP2 protein expression in rs8126 TT genotype carriers was significantly higher than that in rs8126 CC genotype carriers ($P < 0.001$) (**Table 12**).

DISCUSSION

TNFAIP2 is a novel gene induced by TNF-α and can regulate inflammatory and tumor angiogenesis (21). In recent years, studies have found that SNPs in mRNA 3′ UTR may impact the miRNA-mediated expression and regulation of oncogenes and tumor suppressors and confirmed that TNFAIP2 3′ UTR SNPs are correlated with risk of multiple malignancies, especially that TNFAIP2 3′ UTR rs8126 polymorphism may affect TNFAIP2 expression in GC, SCCHN, and ESCC by disturbing the binding of miR-184 with TNFAIP2 mRNA (14, 18, 19). However, only one study reports the correlation between TNFAIP2 SNPs and GC risk in the American population (14), and the correlation between TNFAIP2 SNPs and GC prognosis has not been reported until now, especially in Asian or Chinese populations.

TABLE 6 | The correlation between TNFAIP2 SNPs and gastric cancer (GC) prognosis in the general analysis.

TNFAIP2 SNPs	GC	Death	Median survival time (mean)	Univariate analysis		Multivariate analysis	
				P-value	HR (95% CI)	*P*-value*	HR (95% CI)
rs8126	$n = 287$	$n = 120$					
TT	137	58	56.4[b]				
TC	109	44	79.0[a]	0.840	0.960 (0.649–1.421)	0.501	1.147 (0.770–1.707)
CC	41	18	68.0[a]	0.840	1.056 (0.622–1.792)	0.399	1.262 (0.735–2.165)
CC + TC vs. TT				0.932	1.008 (0.843–1.205)	0.408	1.166 (0.811–1.676)
CC vs. TC + TT				0.793	0.967 (0.753–1.242)	0.588	1.151 (0.692–1.915)
rs710100	$n = 263$	$n = 111$					
CC	110	49	68.0[a]				
TC	114	46	79.0[a]	0.468	1.161 (0.776–1.736)	0.349	0.824 (0.549–1.236)
TT	39	16	68.0[a]	0.513	1.099 (0.829–1.457)	0.638	0.871 (0.489–1.550)
TC + TT vs. CC				0.394	1.085 (0.899–1.309)	0.329	0.828 (0.567–1.209)
TT vs. CC + TC				0.643	1.065 (0.817–1.388)	0.713	0.904 (0.528–1.547)
rs3759571	$n = 275$	$n = 113$					
GG	113	45	58.2[b]				
GA	124	53	79.0[a]	0.685	0.921 (0.619–1.370)	0.803	0.950 (0.635–1.421)
AA	38	15	55.1[b]	0.951	1.009 (0.753–1.352)	0.325	0.739 (0.405–1.349)
GA + GG vs. AA				0.772	0.973 (0.806–1.174)	0.599	0.902 (0.614–1.324)
GG vs. GA + AA				0.780	1.039 (0.792–1.364)	0.335	0.762 (0.438–1.324)

Borrmann classification, TNM staging, lymph node metastasis, and depth of invasion were taken as covariables.

[a]*Median survival time.*

[b]*Mean survival time.*

This is the first study about TNFAIP2 SNPs in Chinese Han population, and this explored the correlation between TNFAIP2 SNPs and prediction as well as the prognosis of GC in a large sample population and its effect on TNFAIP2 protein expression. By analyzing TNFAIPS SNP genotyping of 1,247 samples, we found that the GC risk in TNFAIP2 rs8126 TC genotype cases was higher than that in TT genotype cases ($P = 0.001$, OR = 1.557), and the GC risk in polymorphic carriers of TNFAIP2 rs8126 was increased to 1.419 times in the dominant model ($P = 0.007$). These results were consistent with the American study and confirmed the correlation between TNFAIP2 rs8126 polymorphism and GC risk (14). In the subgroup analysis, we found that cases with TNFAIP2 rs8126 TC genotype had a higher GC risk in males, aged 60 years or older, *H. pylori* negative, non-smoking, and non-drinking. These results suggested that TNFAIP2 rs8126 T>C polymorphism was an important factor in predicting GC risk, and it is beneficial to the discovery and the diagnosis of early gastric cancer.

This study is the first to report the interaction effects between *H. pylori* infection and TNFAIP2 SNPs on GC risk. *H. pylori* infection is currently considered to be one of the environmental factors closely related to the risk and prognosis of GC (22, 23). Clarifying the interaction effects between TNFAIP2 SNPs and *H. pylori* infection is conducive to revealing the influence of key environmental factors on GC risk. Our results showed that there was no interaction between *H. pylori* infection and TNFAIP2 SNPs (rs8126, rs710100, and rs3759571) ($P_{\text{interaction}} > 0.05$), suggesting that the interaction effects between *H. pylori* infection and TNFAIP2 SNPs could not affect GC risk in this group, and no other similar results had been reported so far. In addition, we analyzed the interaction effects between smoking and drinking and TNFAIP2 SNPs on GC risk and found that there was no interaction between smoking and drinking and TNFAIP2 SNPs on GC risk ($P_{\text{interaction}} > 0.05$). This result was different from that of the American population (14), which may be related to differences in race, dietary habits and diet, and type and content of alcohol between Chinese and Americans.

This study also revealed the correlation between TNFAIP2 SNPs and GC prognosis in a Chinese population for the first time. Both univariate and multivariate analyses in the general population and in the subgroup suggested that TNFAIP2 rs8126 T>C polymorphism, TNFAIP2 rs3759571 G>A polymorphism, and TNFAIP2 rs3759573 A>G polymorphism were not related to GC prognosis. These results were not entirely consistent with those reported in other tumors. For example, TNFAIP2 was an independent prognostic factor for nasopharyngeal carcinoma (24) and TNFAIP2 3′ UTR rs8126 may shorten the survival time of patients with septic shock (16).

At the same time, the serum of 202 participants was tested by ELISA to explore differences in TNFAIP2 protein expression between GC patients and healthy persons. We found that the TNFAIP2 protein concentration in GC patients was significantly higher than that in healthy persons, suggesting that the TNFAIP2 protein may be more highly expressed in GC patients. However, the clinicopathological parameters such as gender, age, *H. pylori* infection, smoking, and drinking in GC patients did not affect serum TNFAIP2 protein expression. In addition, we analyzed the correlation between basic characteristics and survival in GC

TABLE 7 | The correlation between TNFAIP2 rs8126 polymorphism and gastric cancer (GC) prognosis in the subgroup analysis.

Parameters	Genotype	GC	Death	Median survival time (mean)	Univariate analysis		Multivariate analysis	
					P-value	HR (95% CI)	*P*-value*	HR (95% CI)
rs8126		$n = 287$	$n = 120$					
Gender								
Male	TT	103	44	56.3[b]				
	TC	79	32	79.0[a]	0.843	0.955 (0.606–1.506)	0.488	1.177 (0.743–1.864)
	CC	29	13	68.0[a]	0.961	1.016 (0.547–1.886)	0.795	1.087 (0.579–2.039)
	CC + TC vs. TT				0.892	0.972 (0.641–1.472)	0.499	1.156 (0.760–1.758)
	CC vs. TC + TT				0.912	1.034 (0.574–1.862)	0.948	1.020 (0.562–1.850)
Female	TT	34	14	50.4[b]				
	TC	30	12	51.8[b]	0.943	1.029 (0.476–2.225)	0.762	1.132 (0.506–2.532)
	CC	12	5	54.3[b]	0.700	1.223 (0.439–3.405)	0.081	2.729 (0.883–8.431)
	CC + TC vs. TT				0.846	1.073 (0.529–2.177)	0.522	1.275 (0.606–2.679)
	CC vs. TC + TT				0.719	1.192 (0.457–3.112)	0.278	1.733 (0.641–4.681)
Age (years)		$n = 287$	$n = 120$					
≥60	TT	65	29	58.0[a]				
	TC	51	23	57.0[a]	0.925	1.027 (0.593–1.776)	0.506	1.210 (0.690–2.124)
	CC	20	7	58.9[b]	0.400	0.701 (0.307–1.603)	0.570	0.783 (0.336–1.823)
	CC + TC vs. TT				0.765	0.925 (0.555–1.543)	0.788	1.074 (0.638–1.809)
	CC vs. TC + TT				0.371	0.697 (0.317–1.536)	0.446	0.732 (0.329–1.632)
<60	TT	72	29	53.8[b]				
	TC	58	21	79.0[a]	0.673	0.886 (0.505–1.554)	0.968	1.012 (0.570–1.797)
	CC	21	11	68.0[a]	0.332	1.410 (0.704–2.826)	0.147	1.690 (0.832–3.435)
	CC + TC vs. TT				0.961	1.013 (0.612–1.674)	0.501	1.192 (0.715–1.985)
	CC vs. TC + TT				0.224	1.501 (0.780–2.888)	0.152	1.628 (0.836–3.170)
H. pylori infection		$n = 287$	$n = 120$					
Positive	TT	76	29	56.7[b]				
	TC	56	23	79.0[a]	0.660	1.131 (0.654–1.956)	0.108	1.583 (0.904–2.772)
	CC	20	6	63.1[b]	0.437	0.705 (0.292–1.700)	0.549	0.760 (0.309–1.865)
	CC + TC vs. TT				0.999	1.000 (0.597–1.673)	0.294	1.329 (0.781–2.261)
	CC vs. TC + TT				0.338	0.661 (0.284–1.542)	0.345	0.662 (0.282–1.557)
Negative	TT	61	29	58.0[a]				
	TC	53	21	54.1[b]	0.427	0.796 (0.454–1.397)	0.488	0.816 (0.460–1.450)
	CC	21	12	29.0[a]	0.361	1.369 (0.698–2.686)	0.101	1.792 (0.893–3.595)
	CC + TC vs. TT				0.779	0.931 (0.565–1.534)	0.902	0.969 (0.586–1.604)
	CC vs. TC + TT				0.196	1.516 (0.807–2.850)	0.080	1.794 (0.932–3.454)

**Borrmann classification, TNM staging, lymph node metastasis, and depth of invasion were taken as covariables.*

[a]*Median survival time.*

[b]*Mean survival time.*

patients and found that GC patients with T1/T2 invasion depth and no lymph node metastasis had a better prognosis, but both the univariate analysis and the multivariate analysis showed that TNFAIP2 protein expression was not significantly correlated with GC prognosis, suggesting that serum TNFAIP2 protein expression was not associated with GC prognosis.

In the last part, we revealed the correlation between TNFAIP2 3′ UTR rs8126 T>C polymorphism and TNFAIP2 protein expression. As far as we know, 3′ UTR consisted of cis-/trans elements and may affect mRNA translation, stability, and subcellular localization. In malignant tumors, the reprogramming of 3′ UTRs mainly included cleavage, polyadenylation, chromosomal rearrangements, hormone-regulated 3′ UTR processing, point mutations, and polymorphisms (25). Therefore, abnormal gene expression caused by reprogramming nucleotides in 3'UTRs might be one of the important factors leading to the occurrence and the progression of tumors. rs8126 was located in the 3′ UTR of the TNFAIP2 gene sequence. A previous study showed that the rs8126 genetic variant was significantly associated with increased ESCC risk in a Chinese population (19). In this paper, our results showed that the serum TNFAIP2 protein expression in rs8126 TT genotype carriers was significantly higher than that in rs8126 CC genotype carriers, and it was suggested that TNFAIP2 3′ UTR rs8126 T>C polymorphism could affect serum TNFAIP2 protein expression. Our data also validated the previous hypothesis that

TABLE 8 | Serum TNFAIP2 protein expression between gastric cancer (GC) patients and healthy persons.

Basic characteristics	GC (*n*, %)	Control (*n*, %)	*P*
Total	*n* = 103	*n* = 99	
Gender			0.085
Male	78 (75.7)	64 (64.6)	
Female	25 (24.3)	35 (35.4)	
Age (years)			
Mean ± SD	56.57 ± 7.656	54.45 ± 7.737	0.052
Median	58	53	
Range	29–67	43–81	
TNFAIP2 concentration (ng/ml)			**0.029***
Median (QR)	14.82 (19.56)	14.32 (2.85)	
Range	8.10–204.05	1.28–49.09	
TNFAIP2 rs8126 genotypes			0.941
TT	48 (46.6)	38 (38.4)	
TC	45 (43.7)	50 (50.5)	
CC	10 (9.7)	11 (11.1)	

**Non-parametric test. Bold Value indicate the data is statistically significant differences (P < 0.05).*

TABLE 9 | The correlation between serum TNFAIP2 protein expression and clinicopathological parameters in gastric cancer (GC) patients.

Clinicopathological parameters	TNFAIP2 protein expression in GC patients		*P*
	High expression concentration ≥ 14.82ng/ml (*n*, %)	Low expression concentration < 14.82 ng/ml (*n*, %)	
Total	*n* = 51	*n* = 52	
Gender	*n* = 51	*n* = 52	0.274
Male	41 (80.4)	37 (71.2)	
Female	10 (19.6)	15 (28.8)	
Age (years)	*n* = 51	*n* = 52	0.716
Mean ± SD	56.29 ± 8.008	56.85 ± 7.363	
Median	58	58	
Range	29–67	30–67	
H. pylori infection	*n* = 51	*n* = 52	0.754
Positive	21 (41.2)	23 (44.2)	
Negative	30 (58.8)	29 (55.8)	
Smoking	*n* = 42	*n* = 41	0.198
Yes	18 (42.9)	12 (29.3)	
No	24 (57.1)	29 (70.7)	
Drinking	*n* = 42	*n* = 41	0.261
Yes	15 (35.7)	10 (24.4)	
No	27 (64.3)	31 (75.6)	

TABLE 10 | The correlation between basic characteristics and survival in gastric cancer (GC) patients.

Basic characteristics	GC patients	Death	Median survival time (mean)	*P*-value
Total	***n* = 35**	***n* = 48**		
Gender				0.592
Male	28 (80.0)	36 (75.0)	40.8[b]	
Female	7 (20.0)	12 (25.0)	53.0[b]	
Age (years)				0.384
≥60	23 (65.7)	27 (56.2)	53.0[a]	
<60	12 (34.3)	21 (43.8)	46.0[b]	
H. pylori infection				0.328
Positive	13 (37.1)	23 (47.9)	42.4[b]	
Negative	22 (62.9)	25 (52.1)	30.0[a]	
Smoking				0.763
Yes	12 (34.3)	18 (37.5)	39.1[b]	
No	23 (65.7)	30 (62.5)	53.0[a]	
Drinking				0.793
Yes	10 (28.6)	15 (31.2)	39.2[b]	
No	25 (71.4)	33 (68.8)	53.0[a]	
Family history				1.000*
Yes	2 (5.7)	4 (8.3)	36.8[b]	
No	33 (94.3)	44 (91.7)	42.0[b]	
Borrmann classification				0.448*
Borrmann I–II	4 (11.4)	3 (6.2)	29.0[a]	
Borrmann III–IV	31 (88.6)	45 (93.8)	42.6[b]	
Lauren classification				0.719
Intestinal type	13 (37.1)	16 (33.3)	46.0[a]	
Diffuse type	22 (62.9)	32 (66.7)	39.3[b]	
Site of primary lesions				
Corpus	13 (37.1)	14 (29.2)	32.0[a]	0.189
Fundus	1 (2.9)	7 (14.6)	49.9[b]	
Antrum/angle	21 (60.0)	27 (56.2)	38.5[b]	
Growth pattern				0.621
Infiltrative	26 (81.2)	36 (76.6)	41.8[b]	
Intermediate/expanding	6 (18.8)	11 (23.4)	42.3[b]	
Depth of invasion				**<0.001**
T1/T2	3 (8.6)	24 (50.0)	53.7[b]	
T3/T4	32 (91.4)	24 (50.0)	24.0[a]	
TNM stage				0.456
I–II	7 (20.0)	13 (27.1)	42.8[b]	
III–IV	28 (80.0)	35 (72.9)	53.0[a]	
Lymph node metastasis				**0.002**
Positive	28 (80.0)	22 (45.8)	26.0[a]	
Negative	7 (20.0)	26 (54.2)	48.4[b]	

[a]*Median survival time.*
[b]*Mean survival time.*
**Fisher's exact test. Bold Values indicate the data is statistically significant differences (P < 0.05).*

functional genetic variants in 3′ UTR of gene might influence miRNA-mediated expression and regulation of mRNA.

As far as we know, this study has the largest sample size about TNFAIP2 SNPs in a Chinese Han population until now, and the study is the first to reveal the correlation between TNFAIP2 SNPs and GC risk, prognosis, and related risk factors in Chinese people. In addition, this is the first report on the correlation between serum TNFAIP2 protein expression and GC risk and prognosis. However, there are some limitations in this paper. For example, due to the lack of statistical data on previous treatment history, therapeutic effect, concomitant diseases, and other prognostic

TABLE 11 | The correlation between serum TNFAIP2 protein expression and gastric cancer (GC) prognosis.

TNFAIP2 protein concentration	GC	Death	Median survival time (mean)	Univariate analysis		Multivariate analysis	
				P-value	HR (95% CI)	*P**	HR (95% CI)
	$n = 83$	$n = 48$		0.798	1.090 (0.562–2.116)	0.339	1.387 (0.710–2.710)
High expression concentration ≥ 14.82 ng/ml	42	24	53.0[a]				
Low expression concentration < 14.82 ng/ml	41	24	43.0[b]				

*Depth of invasion and lymph node metastasis were taken as covariables.
[a]Median survival time.
[b]Mean survival time.

TABLE 12 | The correlation between TNFAIP2 3′ UTR rs8126 T > C polymorphism and TNFAIP2 protein expression.

Basic characteristics	TNFAIP2 3′ UTR rs8126 T > C polymorphism			*P*
	TT	TC	CC	
Total	$n = 48$	$n = 45$	$n = 10$	
TNFAIP2 protein concentration (ng/ml)*				**<0.001**
Median (QR)	22.72 (34.26)	13.06 (4.13)	13.24 (12.50)	
Range	8.10–204.05	9.10–142.9	10.48–48.11	

**Nonparametric test. Bold Value indicate the data is statistically significant differences (P < 0.05).*

factors, these might affect the reliability of partial results, and the above results needed to be verified by further studies.

To sum up, TNFAIP2 3′ UTR rs8126 T>C polymorphism is associated with GC risk in a Chinese population, especially in cases with males, aged 60 years or older, *H. pylori*-negative, non-smoking, and non-drinking. However, there was no correlation between TNFAIP2 SNPs and GC prognosis. Compared with healthy persons, serum TNFAIP2 protein expression was higher in GC patients, but it was not associated with GC prognosis. In addition, TNFAIP2 3′ UTR rs8126 T>C polymorphism might affect serum TNFAIP2 protein expression, and the mechanism remains to be further explored.

DATA AVAILABILITY STATEMENT

The datasets presented in this study can be found in online repositories. The names of the repository/repositories and accession number(s) can be found below: dbSNP (https://www.ncbi.nlm.nih.gov/snp/—ss2137544092, ss3984446983, ss3984446984, and ss3984446985).

ETHICS STATEMENT

The studies involving human participants were reviewed and approved by Medical Science Research Ethics Committee of the First Affiliated Hospital of China Medical University. The patients/participants provided their written informed consent to participate in this study.

AUTHOR CONTRIBUTIONS

YY and FG: conceived and designed the experiments. FG: performed the experiments. FG, QX, ZL, H-XD, Z-DZ, and L-PS: collected the samples and analyzed the data. YY: contributed reagents, materials, and analysis tools. FG and YY: wrote and revised the paper. All authors: read and approved the final manuscript.

FUNDING

This study was funded partly by grants from the National Key R&D Program of China (Grant #2018YFC1311600).

SUPPLEMENTARY MATERIAL

The Supplementary Material for this article can be found online at: https://www.frontiersin.org/articles/10.3389/fonc.2020.01127/full#supplementary-material

Supplementary Figure 1 | Linkage disequilibrium diagram on TNFAIP2 tagSNPs by Haploview software. The tagSNPs of the TNFAIP2 gene were screened by Haploview software and F-SNP website was used to predict the function of tagSNPs. The parameters were set as Chinese Han population; minimum allele frequency >5%; frequency distribution $r^2 > 0.8$. This linkage disequilibrium diagram showed that rs2234130, rs710100, rs146514706, and rs1132339 were tagSNPs of the TNFAIP2 gene, and the alleles of rs2234130 included rs8126, rs3759571, rs3759573, rs2234130, rs749206, rs4369588, rs2234143, rs8176365, rs2234131, rs2403128, rs944000, rs1887940, rs2234133, rs4283165, and rs11160713.

Supplementary Figure 2 | Prediction diagram on TNFAIP2 tagSNPs by the NIH Snpinfo website. The functional tagSNPs of the TNFAIP2 gene were predicted by the NIH Snpinfo website. The parameters were set as Chinese Han population; minimum allele frequency >5%; frequency distribution $r^2 > 0.8$. This prediction diagram showed that rs1887940 and rs710100 were tagSNPs of the TNFAIP2 gene, and the alleles of rs1887940 included rs8126, rs1887940, rs2234130, and rs749206.

REFERENCES

1. Bray F, Ferlay J, Soerjomataram I, Siegel RL, Torre LA, Jemal A. Global cancer statistics 2018: GLOBOCAN estimates of incidence and mortality worldwide for 36 cancers in 185 countries. *CA Cancer J Clin.* (2018) 68:394–424. doi: 10.3322/caac.21492
2. Ferlay J, Colombet M, Soerjomataram I, Dyba T, Randi G, Bettio M, et al. Cancer incidence and mortality patterns in Europe: estimates for 40 countries and 25 major cancers in 2018. *Eur J Cancer.* (2018) 103:356–87. doi: 10.1016/j.ejca.2018.07.005
3. GBD 2017 Causes of Death Collaborators. Global, regional, and national age-sex-specific mortality for 282 causes of death in 195 countries and territories, 1980-2017: a systematic analysis for the Global Burden of Disease Study 2017. *Lancet*. (2018). 392:1736–88. doi: 10.1016/S0140-6736(18)32203-7
4. Balakrishnan M, George R, Sharma A, Graham DY. Changing trends in stomach cancer throughout the world. *Curr Gastroenterol Rep.* (2017) 19:36. doi: 10.1007/s11894-017-0575-8
5. Chen W, Zheng R, Baade PD, Zhang S, Zeng H, Bray F, et al. Cancer statistics in China, 2015. *CA Cancer J Clin.* (2016) 66:115–32. doi: 10.3322/caac.21338
6. Feng RM, Zong YN, Cao SM, Xu RH. Current cancer situation in China: good or bad news from the 2018 Global Cancer Statistics? *Cancer Commun.* (2019) 39:22. doi: 10.1186/s40880-019-0368-6
7. Yang L, Zheng R, Wang N, Yuan Y, Liu S, Li H, et al. Incidence and mortality of stomach cancer in China, 2014. *Chin J Cancer Res.* (2018) 30:291–8. doi: 10.21147/j.issn.1000-9604.2018.03.01
8. Karimi P, Islami F, Anandasabapathy S, Freedman ND, Kamangar F. Gastric cancer: descriptive epidemiology, risk factors, screening, and prevention. *Cancer Epidemiol Biomarkers Prev.* (2014) 23:700–13. doi: 10.1158/1055-9965.EPI-13-1057
9. Russo A, Li P, Strong VE. Differences in the multimodal treatment of gastric cancer: East versus west. *J Surg Oncol.* (2017) 115:603–14. doi: 10.1002/jso.24517
10. Yoshida T, Yamaguchi T, Maekawa S, Takano S, Kuno T, Tanaka K, et al. Identification of early genetic changes in well-differentiated intramucosal gastric carcinoma by target deep sequencing. *Gastric Cancer.* (2019) 22:742–50. doi: 10.1007/s10120-019-00926-y
11. Zou J, Wu D, Li T, Wang X, Liu Y, Tan S. Association of PD-L1 gene rs4143815 C>G polymorphism and human cancer susceptibility: a systematic review and meta-analysis. *Pathol Res Pract.* (2019) 215:229–34. doi: 10.1016/j.prp.2018.12.002
12. Shaw V, Bullock K, Greenhalf W. Single-nucleotide polymorphism to associate cancer risk. *Methods Mol Biol.* (2016) 1381:93–110. doi: 10.1007/978-1-4939-3204-7_6
13. Laytragoon-Lewin N, Cederblad L, Andersson BÅ, Olin M, Nilsson M, Rutqvist LE, et al. Single-nucleotide polymorphisms and cancer risk, tumor recurrence, or survival of head and neck cancer patients. *Oncology.* (2017) 92:161–9. doi: 10.1159/000452278
14. Xu Y, Ma H, Yu H, Liu Z, Wang LE, Tan D, et al. The miR-184 binding-site rs8126 T>C polymorphism in TNFAIP2 is associated with risk of gastric cancer. *PLoS One.* (2013) 8:e64973. doi: 10.1371/journal.pone.0064973
15. Jia L, Zhou Z, Liang H, Wu J, Shi P, Li F, et al. KLF5 promotes breast cancer proliferation, migration and invasion in part by upregulating the transcription of TNFAIP2. *Oncogene.* (2016) 35:2040–51. doi: 10.1038/onc.2015.263
16. Thair SA, Topchiy E, Boyd JH, Cirstea M, Wang C, Nakada TA, et al. TNFAIP2 Inhibits Early TNFα-induced NF-κB signaling and decreases survival in septic shock patients. *J Innate Immun.* (2016) 8:57–66. doi: 10.1159/000437330
17. Rusiniak ME, Yu M, Ross DT, Tolhurst EC, Slack JL. Identification of B94 (TNFAIP2) as a potential retinoic acid target gene in acute promyelocytic leukemia. *Cancer Res.* (2000) 60:1824–9.
18. Liu Z, Wei S, Ma H, Zhao M, Myers JN, Weber RS, et al. A functional variant at the miR-184 binding site in TNFAIP2 and risk of squamous cell carcinoma of the head and neck. *Carcinogenesis.* (2011) 32:1668–74. doi: 10.1093/carcin/bgr209
19. Zhang J, Yu H, Zhang Y, Zhang X, Zheng G, Gao Y, et al. A functional TNFAIP2 3'-UTR rs8126 genetic polymorphism contributes to risk of esophageal squamous cell carcinoma. *PLoS One.* (2014) 9:e109318. doi: 10.1371/journal.pone.0109318
20. Gong YH, Sun LP, Jin SG, Yuan Y. Comparative study of serology and histology based detection of Helicobacter pylori infections: a large population-based study of 7,241 subjects from China. *Eur J Clin Microbiol Infect Dis.* (2010) 29:907–11. doi: 10.1007/s10096-010-0944-9
21. Jia L, Shi Y, Wen Y, Li W, Feng J, Chen C. The roles of TNFAIP2 in cancers and infectious diseases. *J Cell Mol Med.* (2018) 22:5188–95. doi: 10.1111/jcmm.13822
22. Alfarouk KO, Bashir AHH, Aljarbou AN, Ramadan AM, Muddathir AK, AlHoufie STS, et al. The possible role of *Helicobacter pylori* in gastric cancer and its management. *Front Oncol.* (2019) 9:75. doi: 10.3389/fonc.2019.00075
23. Huang J, Hang JJ, Qin XR, Huang J, Wang XY. Interaction of *H.* pylori with toll-like receptor 2-196 to−174 ins/del polymorphism is associated with gastric cancer susceptibility in southern China. *Int J Clin Oncol.* (2019) 24:494–500. doi: 10.1007/s10147-018-1379-z
24. Chen LC, Chen CC, Liang Y, Tsang NM, Chang YS, Hsueh C, et al. A novel role for TNFAIP2: its correlation with invasion and metastasis in nasopharyngeal carcinoma. *Mod Pathol.* (2011) 24:175–84. doi: 10.1038/modpathol.2010.193
25. Li J, Lu X. The emerging roles of 3′ untranslated regions in cancer. *Cancer Lett.* (2013) 337:22–5. doi: 10.1016/j.canlet.2013.05.034

Conflict of Interest: The authors declare that the research was conducted in the absence of any commercial or financial relationships that could be construed as a potential conflict of interest.

frontiers in Oncology

ORIGINAL RESEARCH
published: 13 August 2020
doi: 10.3389/fonc.2020.01612

CircHIPK3 Promotes Metastasis of Gastric Cancer *via* miR-653-5p/miR-338-3p-NRP1 Axis Under a Long-Term Hypoxic Microenvironment

Yue Jin[1,2,3,4†], Xiaofang Che[1,2,3,4†], Xiujuan Qu[1,2,3,4], Xin Li[5], Wenqing Lu[1,2,3,4], Jie Wu[1,2,3,4], Yizhe Wang[1,2,3,4], Kezuo Hou[1,2,3,4], Ce Li[1,2,3,4], Xiaojie Zhang[1,2,3,4], Jianping Zhou[5] and Yunpeng Liu[1,2,3,4*]*

[1] Department of Medical Oncology, The First Hospital of China Medical University, Shenyang, China, [2] Key Laboratory of Anticancer Drugs and Biotherapy of Liaoning Province, The First Hospital of China Medical University, Shenyang, China, [3] Liaoning Province Clinical Research Center for Cancer, Shenyang, China, [4] Key Laboratory of Precision Diagnosis and Treatment of Gastrointestinal Tumors, Ministry of Education, Shenyang, China, [5] Department of Gastrointestinal Surgery, The First Hospital of China Medical University, Shenyang, China

As a vital feature of the microenvironment, hypoxia, especially long-term hypoxia, is known to promote metastasis and lead to poor prognosis in solid tumors. Circular RNAs (circRNAs) participate in important processes of cell proliferation and metastasis in cancers. However, the contribution of circRNAs to metastasis under long-term hypoxia is obscure. In this study, we aim to explore specific functions of circHIPK3 in long-term hypoxia-promoting metastasis of gastric cancer (GC). The hypoxic resistant gastric cancer (HRGC) cell lines we established previously, which were tolerant to 2% O_2 conditions, were used as the long-term hypoxia model. We found that circHIPK3 was upregulated by HIF-2α in HRGC cells, and circHIPK3 facilitated the migration and invasion ability of HRGC cells. Further investigation proved that circHIPK3 promoted metastasis of HRGC cells directly by interacting with miR-653-5p and miR-338-3p to relieve the suppression of neuropilin 1 (NRP1), resulting in the activation of downstream ERK and AKT pathways. Our study identified oncogene functions of circHIPK3 under a long-term hypoxic microenvironment and the possibility of using circHIPK3 as a potential biomarker of long-term hypoxia in GC. In conclusion, circHIPK3 could promote GC metastasis via the miR-653-5p/miR-338-3p-NRP1 axis under a long-term hypoxic microenvironment.

Keywords: circHIPK3, long-term hypoxic microenvironment, HIF-2α, gastric cancer, metastasis

Abbreviations: GC, gastric cancer; HIF, hypoxia-inducible factor; HRGC, hypoxic resistant gastric cancer; KD, knockdown; NC, negative control; NRP1, neuropilin 1; PVDF, polyvinylidene difluoride; qRT-PCR, quantitative real-time PCR; TCGA, the Cancer Genome Atlas.

OPEN ACCESS

Edited by:
Bin Li,
Jinan University, China

Reviewed by:
Kenji Takahashi,
Asahikawa Medical University, Japan
Peng Gao,
Shandong University, China

****Correspondence:***
Jianping Zhou
zjphama@163.com
Yunpeng Liu
ypliu@cmu.edu.cn

† These authors have contributed equally to this work

Specialty section:
This article was submitted to Gastrointestinal Cancers, a section of the journal Frontiers in Oncology

Received: *06 May 2020*
Accepted: *24 July 2020*
Published: *13 August 2020*

Citation:
Jin Y, Che X, Qu X, Li X, Lu W, Wu J, Wang Y, Hou K, Li C, Zhang X, Zhou J and Liu Y (2020) CircHIPK3 Promotes Metastasis of Gastric Cancer via miR-653-5p/miR-338-3p-NRP1 Axis Under a Long-Term Hypoxic Microenvironment. Front. Oncol. 10:1612. doi: 10.3389/fonc.2020.01612

INTRODUCTION

Gastric cancer is a kind of global malignant tumor, especially in developing countries including China. In China, GC ranks as the fifth most common cancer and the third-ranked leading cause of cancer-related death (1). Even though tremendous advances have been made in diagnosis and treatment strategies in recent years, the prognosis of GC patients remains poor on account of its high relapse and metastatic rates (2). Therefore, exploring novel molecular mechanisms underlying metastasis would provide potential target candidates for prognosis improvement in GC.

Hypoxia, an important microenvironment feature in solid tumors, can promote distant metastasis (3, 4). In a hypoxic microenvironment, hypoxia-inducible factors (HIFs) are upregulated due to the stabilization of HIF-α subunits and play a vital role in tumor progression including angiogenesis, metabolic reprogramming, invasion, and resistance to radiation therapy or chemotherapy (5). Hundreds of genes including VEGFA, Glut1, KLF8, ITGβ1 and etc., transcribed by HIFs are reported to promote metastasis and result in poor prognosis of GC (6–9). However, most of these studies are based on acute hypoxia treatment, while the actual condition inside solid tumors is chronic or cycling hypoxia, which deserves greater concern (10, 11). However, to date, few studies have been focused on long-term hypoxia-promoting tumor metastasis. The limited studies related to long-term hypoxia of tumors reported that slug promoted metastasis of prostate cancer under chronic hypoxia (12); miR-191 induced by chronic hypoxia promoted cell migration in NSCLC (13). Due to the discovery more novel important functions of non-coding RNAs (ncRNAs) including miRNAs, LncRNAs, and circRNAs, participating in tumor progression, we pay special attention in the present work to the role of hypoxia microenvironment-related ncRNAs in GC. In our previous study, we established HRGC cell lines to stimulate the real situation of a long-term hypoxic microenvironment, and found that LncRNA UCA1 was upregulated and promoted the migration of GC cells through the miR-7-5p/EGFR axis under a long-term hypoxic microenvironment (14). However, the biological functions of another subtype of ncRNAs—circRNAs involved in long-term hypoxia-promoting metastatic process of GC remain largely unknown.

Circular RNA (circRNA) is a class of single-strand endogenous ncRNAs formed by 3′ and 5′ joining to form a covalently closed continuous loop (15, 16). Accumulating evidence has shown that circRNAs are essential in the development of various diseases, especially cancers (17). Many circRNAs are reported to play a vital role in tumor metastasis. For example, circNSD2 promoted metastasis of colorectal cancer by targeting miR-199b-5p-mediated DDR1 and JAG1 signaling (18); circPRMT5 promoted metastasis of urothelial carcinoma through sponging with miR-30c (19). However, none of them are related to long-term hypoxia-promoting metastasis. CircHIPK3, an identified circular RNA of 1099 bp in length, is reported to have significant promotional effects on the progression of various cancers including lung cancer, colorectal cancer, and glioma (20–22). However, its function in GC remains ambiguous. It was reported that circHIPK3 could promote proliferation and migration in GC indicating its oncogenic role, while circHIPK3 was downregulated in GC tissues compared to para-carcinoma tissues indicating its tumor-suppressing role (23, 24). The different roles might be due to the strong heterogeneity of GC resulting in the inconsistent effect of circHIPK3 in different specimens. Therefore, the role of circHIPK3 in GC remains to be further studied in detail. Considering that hypoxia might be a crucial reason leading to GC heterogeneity, we aimed to explore the functions and molecular mechanisms of circHIPK3 on long-term hypoxia-promoting metastasis of GC.

In this study, we demonstrated that circHIPK3 was increased under long-term hypoxic microenvironment and could promote metastasis through the miR-653-5p/miR-338-3p-NRP1 axis in GC. These findings elucidated a new mechanism of hypoxia-induced metastasis in GC and revealed the possibility of using circHIPK3 as a new biomarker for long-term hypoxia.

MATERIALS AND METHODS

Patient Tissue Samples

Thirty-one GC patients without therapy before surgery between 2018 to 2019 were enrolled in our study. All the GC and adjacent normal tissues were obtained from operation excision specimens of GC patients in the First Hospital of China Medical University (Shenyang, China). Tissues were promptly frozen in liquid nitrogen and then stored at −80°C. The research was approved by the Ethics Committee of the First Hospital of China Medical University (No. 2019-24-2), and all procedures were conducted according to ethical principles.

Cell Culture

Human gastric cancer cell lines MGC803 (TCHu84) and BGC823 (TCHu11) were purchased from the Chinese Academy of Sciences (Shanghai, China). These cells were cultured with RPMI-1640 medium containing 10% heat-inactivated fetal bovine serum (FBS) and 1% penicillin-streptomycin. The two long-term HRGC cell lines, MGC803/Hypo and BGC823/Hypo, established from MGC803 and BGC823 in our laboratory (14), were cultured with DMEM containing 10% FBS and 1% penicillin-streptomycin under 2% O_2 concentration. All the cells were cultured in a 5% CO_2 humidified incubator at 37°C.

Reagents and Antibodies

AKT (#9272), phosphorylated (p)-AKT (#9271), p-ERK (#4370), and NRP1 (#3725) antibodies were obtained from Cell Signaling Technology (Danvers, United States). β-actin (sc-47778) and ERK (sc-514302) antibodies were obtained from Santa Cruz Biotechnology (Santa Cruz, United States).

RNA Isolation and Quantitative Real-Time PCR

Total RNA was isolated with Trizol reagent (Invitrogen, United States) and quantified by measuring the absorbance at 260 nm by nanodrop 2000 (Thermo Fisher Scientific, United States). The reverse transcription reagents were all

purchased from TaKaRa (Shiga, Japan). The PrimeScript™ RT reagent Kit (Takara, Japan) was used for mRNA reverse transcription and the One Step PrimeScript® miRNA cDNA Synthesis Kit (Takara, Japan) was used for miRNA reverse transcription. Quantitative real-time PCR was carried out with SYBR Premix Ex Taq II (TaKaRa) and detected using Applied Biosystems® 7500 Real-Time PCR Systems (Thermo Fisher Scientific, United States). 1000 ng RNA was used for cDNA Synthesis and 40 ng cDNA was used for qRT-PCR. The internal control for mRNA and circRNA was 18S and the internal control for miRNA was U6. The *n*-fold change of the RNA expression was calculated using the $2^{-\Delta\Delta Ct}$ method. All primer sequences are listed in **Supplementary Table S1**.

Transfection

The specific siRNAs targeted to circHIPK3 and NRP1, miR-653-5p and miR-338-3p mimics or inhibitors, and their corresponding NC, were compounded by JTS Scientific (Wuhan, China). CircHIPK3 overexpression plasmid (pCD25-circHIPK3-GFP) was designed and constructed by Geneseed Biotech Co. (Guangzhou, China). HRGC cells or their parent GC cells (1.0×10^5) were transfected with 0.1 μM siRNAs, 0.1 μM miRNA mimics/0.15 μM inhibitors, or 1 mg/L plasmids using jetPRIME® Transfection Reagent according to manufacturer's instructions. The sequences of all siRNAs or mimics/inhibitors are shown in **Supplementary Table S1**.

Transwell Migration and Invasion Assay

Transwell chambers (Corning, NY, United States) were plated into a 24-well plate. For migration assay, 2×10^4 cells were plated within 200 μL serum-free medium onto the upper chamber and 500 μL medium with 10% FBS was added to the lower chamber. After incubating for 24 h, the chambers were fixed with methanol and then stained with Wright-Giemsa dye. The stained cells were counted and analyzed statistically. For invasion assay, except for pre-coating the chamber with 50 μL diluted-matrigel before the cells were plated onto the upper chamber, other steps were as outlined for the aforementioned migration assay.

Western Blot Assay

All treated cells were lyzed by 1% Triton lysis buffer. After quantification, the protein samples were mixed with 3 × loading buffer. The prepared samples were separated by SDS-polyacrylamide gel electrophoresis and then transferred onto PVDF membranes (Millipore, United States). Next, the PVDF membranes were blocked with 5% skimmed milk in TBST buffer, and then incubated with the primary antibodies overnight at 4°C. The following day, the membranes were incubated with the secondary antibodies. Finally, the membranes were examined with enhanced chemiluminescence reagent and visualized using the Electrophoresis Gel Imaging Analysis System (DNR Bio-Imaging Systems, Israel).

RNA Immunoprecipitation

RNA immunoprecipitation (RIP) assays were executed by the Magna RIP RNA-Binding Protein Immunoprecipitation Kit (Millipore, Burlington, MA, United States) according to manufacturer's protocols. HRGC cells were lysed in lysis buffer and then incubated with RIP immunoprecipitation buffer which contained magnetic beads pre-incubated with the anti-AGO2 and anti-IgG (Millipore, United States). RNA was purified from RNA-protein complex and detected by qRT-PCR.

Luciferase Reporter Assay

Hypoxic resistant gastric cancer cells (to a total number of 2.5×10^4) were co-transfected with pmirGLO-circHIPK3-WT and pmirGLO-circHIPK3-MUT (RiboBio, Guangzhou, China) or pmirGLO-NRP1-WT and pmirGLO-NRP1-MUT (OBIO, Shanghai, China) and miR-NC or miR-653-5p or miR-338-3p mimics (JTS Scientific, Wuhan, China). Twenty-four hours later, the luciferase activity of cell lysates was examined by a Dual Luciferase Reporter System (Promega, United States).

RNA Pull Down Assay

Biotinylated-circHIPK3 and control probes were synthesized by RiboBio (Guangzhou, China). A total of 1.0×10^7 HRGC cells were washed by cold PBS, and then lysed and sonicated. The biotinylated-circHIPK3 and control probes were used for incubation with C-1 magnetic beads (Life Technologies) at 25°C for 2 h. The cell lysate was incubated with the biotinylated-circHIPK3 or control probe at 4°C overnight. Then the beads were washed by buffer and miRNAs were extracted using Trizol reagent and analyzed by qRT-PCR assay. The sequence of circHIPK3 probe was biotin-5′-ACTTGTGAGGCCATACCTGT AGTACCGAGATT-3′; the sequence of control probe was biotin-5′-CGACTTTGGCTTGTTCTGGCCTGCATGACTGTTGAAA TGT- 3′.

Statistical Analysis

The data are all shown as mean ± SD with three independent experiments. An unpaired Student's *t*-test was used to analyze the statistical differences between two groups and p-value < 0.05 was regarded as indicative of significance.

RESULTS

CircHIPK3 Was Upregulated by HIF-2α in HRGC Cells

Firstly, the migration and invasion capability, and HIF-1α and HIF-2α protein, two important hypoxia-related markers in HRGC cells were compared with those in their parent GC cells. As a result, the migration and invasion ability of HRGC cells was notably enhanced, and HIF-2α was remarkably upregulated whereas HIF-1α was merely slightly upregulated in HRGC cells, which was similar to the findings of our previous research (14) (**Figures 1A–C**). Then, circHIPK3 expression levels in HRGC cells and their parent GC cells were examined by qRT-PCR analysis, and the result showed that circHIPK3 expression in HRGC cells was notably upregulated more than 5-fold over that in their parent GC cells, while the expression of linear HIPK3 mRNA was practically unchanged under the long-term hypoxic microenvironment (**Figures 1D,E**). To explore whether

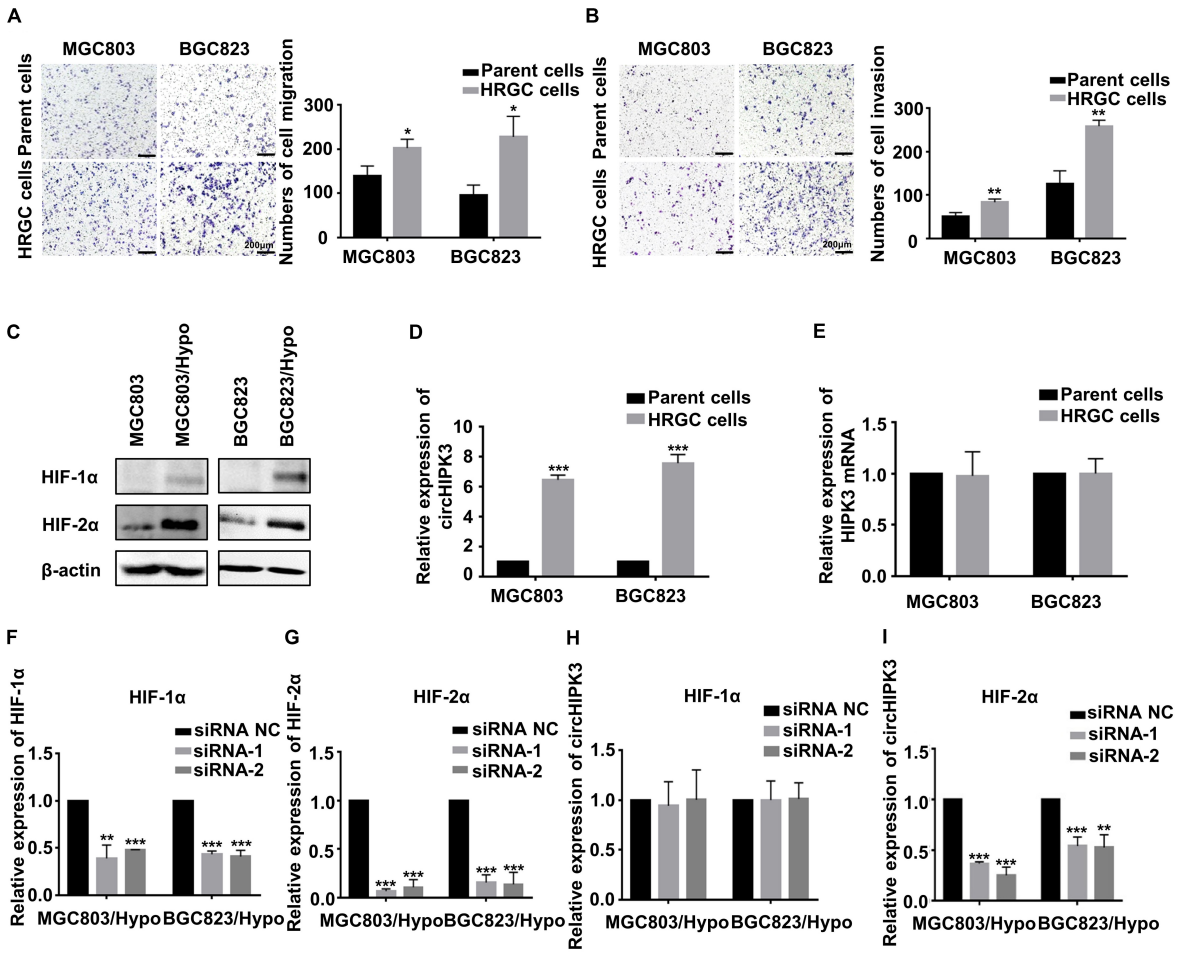

FIGURE 1 | CircHIPK3 was upregulated by HIF-2α in HRGC cells. **(A,B)** The migration and invasion ability of HRGC cells and their parent GC cells was examined by transwell assay (original magnification, 100×). The columns on the right are quantified by counting three fields, and presented as the mean ± standard deviation. $^{*}p < 0.05$, $^{**}p < 0.01$. **(C)** The protein expression of HIF-1α and HIF-2α in HRGC cells compared with their parent GC cells was detected by western blot. β-actin was used as an internal control. **(D,E)** The relative expression of circHIPK3 and linear HIPK3 mRNA in HRGC cells and their parent GC cells was detected by qRT-PCR. **(F,G)** The knockdown efficiency of HIF-1α or HIF-2α in HRGC cells was detected by qRT-PCR. **(H,I)** The relative expression of circHIPK3 in HRGC cells after transfected with HIF-1α or HIF-2α siRNAs was detected by qRT-PCR. Data are presented as the mean ± SD of three independent experiments. $^{*}p < 0.05$, $^{**}p < 0.01$, $^{***}p < 0.001$. 18S was used as an internal control for all qRT-PCR experiments.

HIF-1α or HIF-2α is involved in hypoxia-induced circHIPK3 upregulation, HIF-1α and HIF-2α were knocked down. The result of qRT-PCR showed that HIF-2α knockdown (KD) but not HIF-1α KD decreased the expression of circHIPK3 in HRGC cells, indicating that HIF-2α mainly contributed to circHIPK3 upregulation in GC under a long-term hypoxic microenvironment (**Figures 1F–I**).

CircHIPK3 Promoted Migration and Invasion of HRGC Cells

To identify whether circHIPK3 is involved in long-term hypoxia-promoting metastasis of GC cells, circHIPK3 was transiently knocked down with nearly no expression change in parent gene HIPK3 (**Figures 2A–C**), and transwell assays were then performed. It was shown that circHIPK3-KD significantly restrained the migration and invasion capability of both MGC803/Hypo and BGC823/Hypo cells (**Figures 2D,E**). On the contrary, when overexpressing circHIPK3 in MGC803 and BGC823 cells to imitate a long-term hypoxic microenvironment (**Figure 2F**), the migration and invasion ability was significantly increased (**Figures 2G,H**). All of these results indicated that circHIPK3 promoted GC metastasis under a long-term hypoxic microenvironment.

CircHIPK3 Promoted Migration and Invasion of HRGC Cells by Sponging With miR-653-5p and miR-338-3p

It is known that the cellular localization of circRNAs was closely related to their functions. Therefore, to clarify the molecular mechanism of action of circHIPK3 on long-term hypoxia-promoting metastasis, the expression of circHIPK3 in nucleus and cytoplasm was examined separately by qRT-PCR assay. The

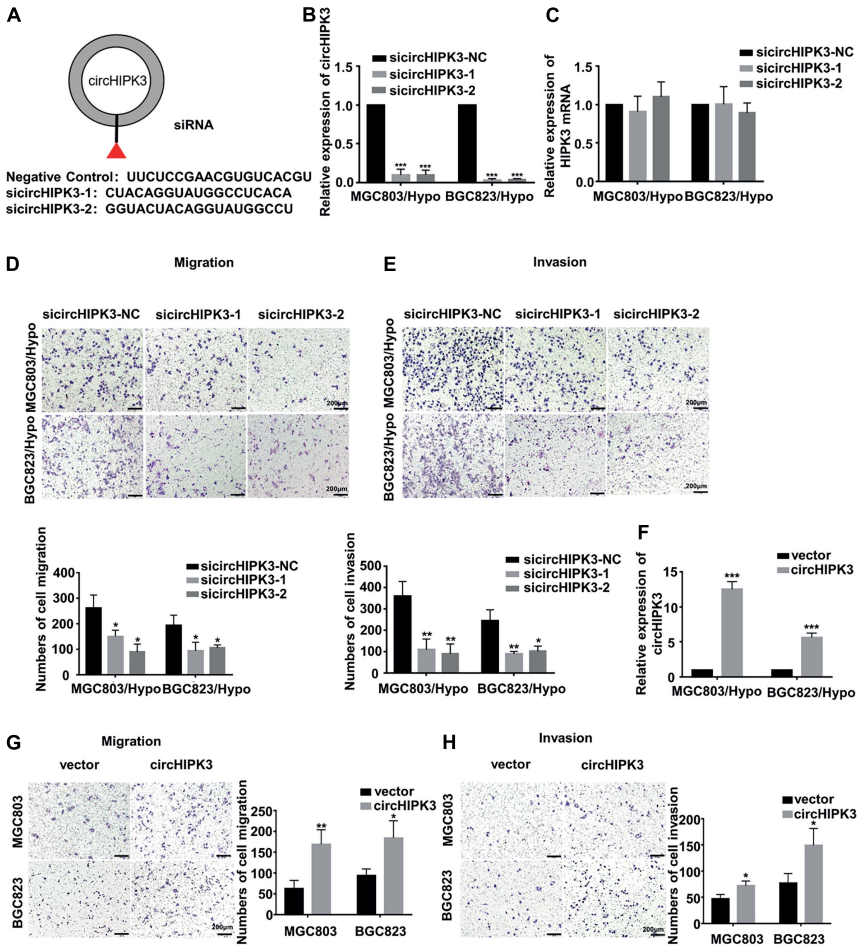

FIGURE 2 | CircHIPK3 promoted migration and invasion of HRGC cells. **(A)** The sequence of two siRNAs targeted to back-splicing site of circHIPK3 and the negative control siRNA. **(B,C)** The relative expression of circHIPK3 and linear HIPK3 mRNA in HRGC cells after transfected with negative control siRNA (siNC) or circHIPK3 siRNAs was detected by qRT-PCR. 18S was used as an internal control. **(D,E)** The migration and invasion ability of HRGC cells after transfected with siNC or circHIPK3 siRNAs was examined by transwell assay (original magnification, 100×). The columns on the down panels are quantified by counting 3 fields, and presented as the mean ± standard deviation. $^{*}p < 0.05$, $^{**}p < 0.01$, $^{***}p < 0.001$. **(F)** The overexpression efficiency of circHIPK3 in MGC803 and BGC823 cells was detected by qRT-PCR. 18S was used as an internal control. **(G,H)** The migration and invasion ability of MGC803 and BGC823 cells after transfected with circHIPK3 overexpression plasmids and empty vectors was examined by transwell assay (original magnification, 100×). The columns on the right are quantified by counting three fields, and presented as the mean ± standard deviation. $^{*}p < 0.05$, $^{**}p < 0.01$, $^{***}p < 0.001$. Data are presented as the mean ± SD of three independent experiments. $^{*}p < 0.05$, $^{**}p < 0.01$, $^{***}p < 0.001$.

result demonstrated that circHIPK3 was principally enriched in the cytoplasm (**Figure 3A**), indicating its feasibility as a miRNA sponge function. Next, underlying targeted miRNAs of circHIPK3 were predicted using three databases: circBank[1], Circular RNA Interactome[2] and StarBase V2.0[3]. As a result, two miRNAs (miR-653-5p and miR-338-3p) with more than four binding sites with circHIPK3, were predicted on all three websites (**Supplementary Figure S1A**). Then, the sponging relationship between circHIPK3 and miR-653-5p or miR-338-3p was verified in HRGC cells. The result revealed that miR-653-5p and miR-338-3p in HRGC cells were both lower than that in their parent GC cells (**Figure 3B**). Considering Argonaute2 (AGO2) protein, binding with circRNAs and miRNAs, is the core of RNA-induced silencing complex (RISC), an RIP assay was performed to confirm that anti-AGO2 could enrich more circHIPK3, miR-653-5p, and miR-338-3p molecules compared to anti-IgG under a long-term hypoxic microenvironment (**Supplementary Figure S1B** and **Figure 3C**). Furthermore, miR-653-5p and miR-338-3p mimics significantly reduced the luciferase activity of wild-type circHIPK3 but not mutant-type circHIPK3 (**Supplementary Figure S1C** and **Figure 3D**). Meanwhile, RNA pull down assay was performed to confirm that miR-653-5p and miR-338-3p could be significantly pulled down by biotinylated probe of circHIPK3 compared to control (**Figure 3E**). Finally, circHIPK3-KD1 enhanced miR-653-5p and miR-338-3p expression, whereas miR-653-5p and miR-338-3p

[1]http://www.circbank.cn/

[2]https://circinteractome.nia.nih.gov/

[3]http://starbase.sysu.edu.cn/

mimics attenuated circHIPK3 expression, respectively, in HRGC cells (**Supplementary Figure S1D** and **Figure 3F**). These results therefore revealed that circHIPK3 could directly combine to miR-653-5p and miR-338-3p in GC under a long-term hypoxic microenvironment.

Next, the function of miR-653-5p and miR-338-3p in the metastatic process of HRGC cells was investigated. As a result, miR-653-5p and miR-338-3p mimics significantly restrained migration and invasion capability in HRGC cells (**Figures 3G,H**), indicating the metastatic inhibiting function of these miRNAs. The further to prove the involvement of miR-653-5p and miR-338-3p in circHIPK3-induced metastasis, circHIP3-KD1 and miRNA inhibitors were co-transfected into HRGC cells. As shown in **Figure 3I**, circHIPK3-KD-inhibiting migration was partially reversed by miR-653-5p or miR-338-3p inhibitors in HRGC cells, further illustrating that circHIPK3 could promote GC metastasis by directly interacting with miR-653-5p and miR-338-3p in GC under a long-term hypoxic microenvironment.

CircHIPK3 Promoted Migration and Invasion of HRGC Cells via the miR-653-5p/miR-338-3p-NRP1 Axis

To find the target gene of miR-653-5p and miR-338-3p, the miRanda[4] and TargetScan databases[5] were applied to predict the common target gene for these two miRNAs. Neuropilin 1 (NRP1), which was known to be involved in metastatic process of cancers, was selected. Dual luciferase reporter assay demonstrated that miR-653-5p and miR-338-3p mimics significantly reduced the luciferase activity of wild-type NRP1 but not mutant-type NRP1, indicating miR-653-5p and miR-338-3p could directly bind to NRP1 (**Figure 4A**). For further verification, NRP1 expression levels were examined in HRGC cells and parent GC cells, and the result confirmed that NRP1 was upregulated in HRGC cells (**Figure 4B**). Furthermore, it was shown that the mimics of miR-653-5p and miR-338-3p, as same as circHIPK3-KD, reduced NRP1 expression in MGC803/Hypo and BGC823/Hypo (**Figures 4C–F**). In addition, circHIPK3-KD1-downregulated NRP1 expression was also partially reversed by co-transfection with miR-653-5p or miR-338-3p inhibitors (**Figures 4G,H**). Therefore, these data indicated that circHIPK3 upregulated NRP1 expression by sponging with miR-653-5p and miR-338-3p in GC under a long-term hypoxic microenvironment.

CircHIPK3 Promoted Migration and Invasion of HRGC Cells via the NRP1-ERK/AKT Pathway

The involvement of NRP1 in the metastatic process of HRGC cells was also investigated. The result showed that NRP1-KD not only significantly suppressed the migration and invasion capability of HRGC cells (**Figures 5A–C**), but also decreased the phosphorylation level of ERK and AKT, in downstream pathways of NRP1 (**Figure 5D**). A similar result was also obtained using circHIPK3-KD (**Figure 5E**). The results showed that circHIPK3 could promote migration and invasion via the NRP1-ERK/AKT pathway in HRGC cells. Moreover, the clinical significance of NRP1 was further analyzed using the following on-line databases: GEPIA[6], Kaplan-Meier Plotter[7], and TCGA[8]. The result of GEPIA website showed that NRP1 expression significantly increased in GC tissues compared to the adjacent normal tissues (**Figure 5F**). The Kaplan-Meier Plotter website showed that the overall survival (OS) of GC patients with NPR1-high expression was shorter than that with NPR1-low expression. The GEPIA website and TCGA data analyzed by best cut-off also showed the similar results (**Figure 5G**), indicating that NRP1 was a poor prognostic biomarker for GC. Taken together, these data demonstrated that circHIPK3-upregulated NRP1 could promote GC metastasis via the ERK/AKT pathway and may lead to poor prognosis of GC patients.

Verification of the CircHIPK3-miR-653-5p/miR-338-3p-NRP1 Axis in GC Tissues

The further to confirm the role of the circHIPK3-miR-653-5p/miR-338-3p-NRP1 axis in GC, qRT-PCR was conducted on GC tissues and adjacent normal tissues of 31 GC patients. The results confirmed that circHIPK3 and NRP1 expression was increased, whereas miR-653-5p and miR-338-3p expression was reduced in GC tissues compared with that in adjacent normal tissues (**Figures 6A–C**); HIF-2α levels were shown to be positively correlated with circHIPK3 levels in GC tissues (**Figure 6D**); moreover, circHIPK3 mRNA levels were positively correlated with NRP1 mRNA levels (**Figure 6E**). Therefore, all these data further proved that circHIPK3 was upregulated by HIF-2α and functioned by constructing the ceRNA network with miR-653-5p/miR-338-3-NRP1 under a long-term hypoxic microenvironment in GC.

DISCUSSION

In this study, we found that circHIPK3, upregulated by HIF-2α, could promote migration and invasion of HRGC cells via the miR-653-5p/miR-338-3p-NPR1 axis, indicating that circHIPK3 participated in metastatic promotion of GC under a long-term hypoxic microenvironment.

Hypoxia, an important typical characteristic of solid malignant tumors, often leads to poor prognosis of cancer by contributing to metastasis. Hypoxia can be divided into acute hypoxia and chronic hypoxia based on the dynamics of oxygen deprivation: the real status of the hypoxic microenvironment inside solid tumors is closer to chronic hypoxia, or so-called long-term hypoxia, rather than acute hypoxia (25). The HRGC cell lines in this study established in our laboratory previously have been shown to be a good model for long-term

[4]http://www.microrna.org/microrna/home.do

[5]http://www.targetscan.org/vert_72/

[6]http://gepia.cancer-pku.cn/detail.php

[7]http://kmplot.com/analysis/

[8]https://portal.gdc.cancer.gov

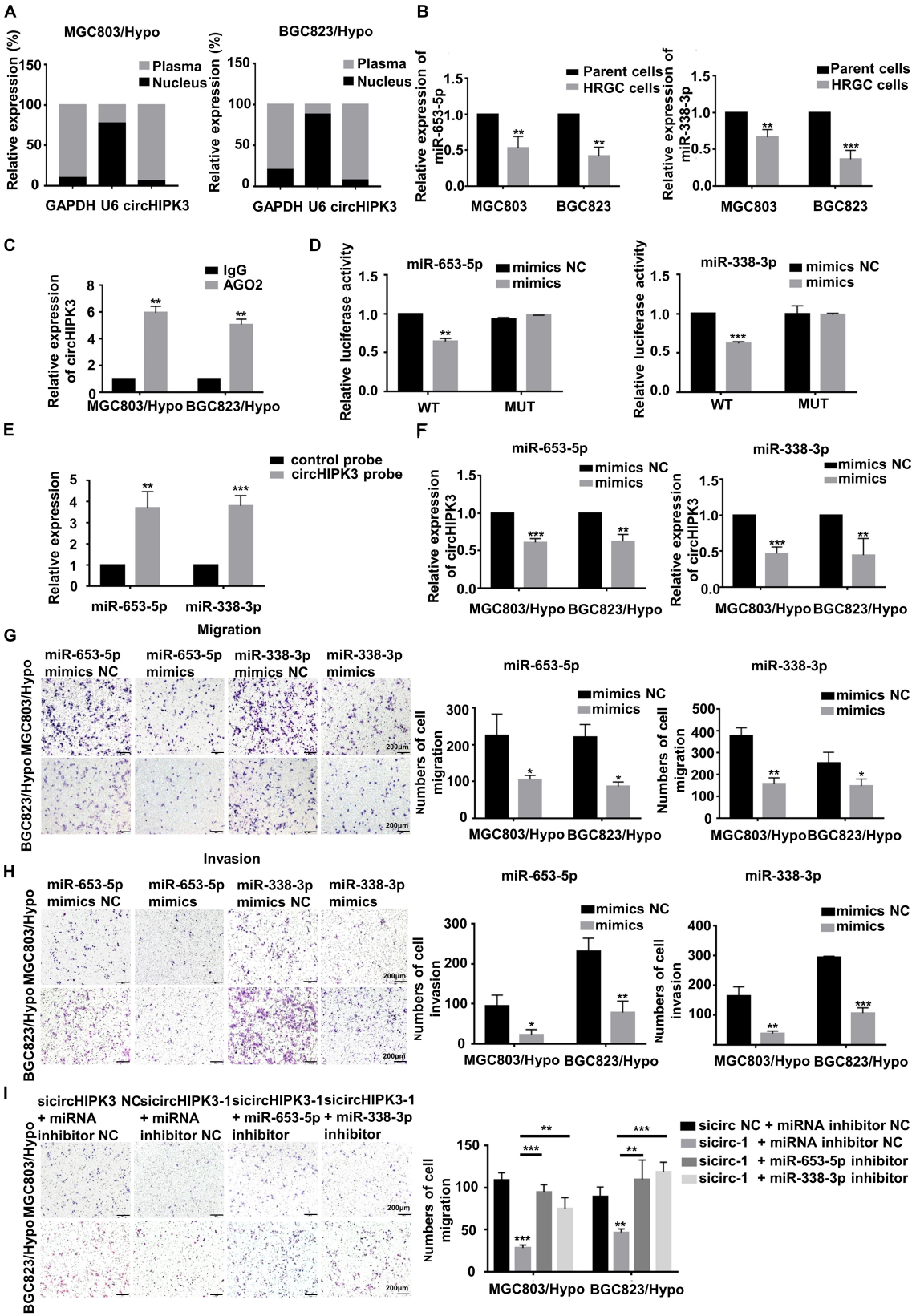

FIGURE 3 | Continued

FIGURE 3 | CircHIPK3 promoted migration and invasion of HRGC cells by sponging with miR-653-5p and miR-338-3p. **(A)** The distribution proportion of circHIPK3 in nucleus and cytoplasma of HRGC cells was detected by qRT-PCR. GAPDH and U6 were used as internal controls. **(B)** The relative expression of miR-653-5p and miR-338-3p in HRGC cells compared with their parent GC cells was detected by qRT-PCR. U6 was used as an internal control. **(C)** The relative expression of circHIPK3 combined with AGO2 was examined by Anti-AGO2 RIP assay. IgG was used as a negative control. **(D)** The luciferase activities of HRGC cells after co-transfected with luciferase reporter vectors circHIPK3-WT or circHIPK3-Mut and miR-653-5p or miR-338-3p mimics or miR-NC were examined. **(E)** The relative expression of miR-653-5p or miR-338-3p pulled down by circHIPK3 probe was detected by qRT-PCR. **(F)** The relative expression of circHIPK3 after transfected with miR-NC and miR-653-5p or miR-338-3p mimics. 18S was used as an internal control. **(G,H)** The migration and invasion ability of HRGC cells after transfected with miR-NC and miR-653-5p or miR-338-3p mimics was examined by transwell assay (original magnification, 100×). The columns on the right are quantified by counting 3 fields, and presented as the mean ± standard deviation. $^{*}p < 0.05$, $^{**}p < 0.01$, $^{***}p < 0.001$. **(I)** The migration ability of HRGC cells after co-transfected with siNC or circHIPK3 siRNAs and miR-NC or miR-653-5p or miR-338-3p inhibitor was examined by transwell assay (original magnification, 100×). The columns on the right are quantified by counting 3 fields, and presented as the mean ± standard deviation. $^{*}p < 0.05$, $^{**}p < 0.01$, $^{***}p < 0.001$. Data are presented as the mean ± SD of three independent experiments. $^{*}p < 0.05$, $^{**}p < 0.01$, $^{***}p < 0.001$.

hypoxia-related research in GC. Using these HRGC cells, we have revealed that LncRNA—UCA1 was upregulated, and promoted the migration of HRGC cells through the miR-7-5p/EGFR axis under long-term hypoxia (14). Now, we have further demonstrated that circRNA—circHIPK3 was also increased in HRGC cells and promoted GC metastasis under a long-term hypoxic microenvironment. CircHIPK3, a classical circular RNA involved in cancer development, appeared to play opposite roles in different cancers. CircHIPK3 promoted proliferation, metastasis, and chemotherapy resistance in lung cancer, colorectal cancer, and prostate cancer, whereas it suppressed cell proliferation, migration, and invasion in osteosarcoma (20, 21, 26, 27). However, only three studies on circHIPK3 were reported in GC, and the conclusions were still contradictory. The contradiction might be due to the strong heterogeneity of GC resulting in the inconsistent effect of circHIPK3 in different specimens. In our study, we found that overexpression of circHIPK3 in normoxia could promote metastasis of GC and the expression of circHIPK3 increased in GC tissues compared with that in adjacent normal tissues, indicating circHIPK3 might play an oncogenic role in GC. Our findings that circHIPK3 was upregulated in HRGC cells and promoted GC metastasis, might reflect the heterogeneity of GC because of hypoxia, and partially explain the different roles of circHIPK3 in GC as evinced by our result and previous studies. Certainly, many other factors, such as the number of samples, sampling quality, tumor cell content, storage conditions and time, RNA extraction, qRT-PCR and etc., may also lead to this contradictory conclusion. In the future, more GC samples are needed to collect further to investigate the definite roles of circHIPK3 in GC.

Hypoxia-inducible factors are the key transcriptional regulatory factors of many target genes in hypoxia (28). It is known that HIF-1α exhibits stable expression and plays the main transcriptional role in acute hypoxia, while HIF-2α is also stable but mainly functions in chronic hypoxia (25). Although HIF-1α and HIF-2α could both promote target gene transcription by combining with the HRE promoter region, their target genes are not completely consistent (29–31). For example, HE4 and RIT1 can only be transcriptionally regulated by HIF-1α, while LncNEAT1 and PTPMT1 can only be transcriptionally regulated by HIF-2α (32–35). In this study, HIF-2α-KD, but not HIF-1α-KD, decreased circHIPK3 expression, and the strong positive correlation was verified between HIF-2α and circHIPK3 in GC samples, indicating that circHIPK3 is a novel target of HIF-2α. Certainly, it still remains unclear whether circHIPK3 is directly upregulated by HIF-2α transcription or is upregulated by another HIF-2α target gene. Further study is warranted in the future.

The localization of circRNAs is essential to their function, and a non-negligible function of circRNAs distributed in cytoplasma is working as sponges by binding with miRNAs (36, 37). CircRNAs can not only sponge with multiple miRNAs but also sponge with the same miRNA at several binding sites. The more miRNAs bound by one kind of circRNAs, the stronger functions of circRNAs in cells. The most typical representative circRNA is ciRS-7, which exists at over 70 binding sites of miR-7 and promotes cancer progression in esophageal squamous cell carcinoma and non-small cell lung cancer (38, 39). In our research, we found that circHIPK3 was principally enriched in cytoplasm of HRGC cells and could combine to miR-653-5p and miR-338-3p with four binding sites, respectively, suggesting the importance of the role of circHIPK3. Besides, qRT-PCR results revealed that the levels of miR-653-5p and miR-338-3p were decreased in HRGC cells, and both of these miRNAs could restrain the migration and invasion of HRGC cells, which was similar to previous research findings indicating that miR-653-5p could suppress growth and invasion in non-small cell lung cancer, and miR-338-3p could suppress tumor progression in colorectal cancer and breast cancer (40–42). Therefore, our research proved that circHIPK3 had an essential effect in facilitating GC metastasis by sponging with miR-653-5p and miR-338-3p under a long-term hypoxic microenvironment.

Neuropilin 1 is a kind of non-tyrosine kinase transmembrane glycoprotein known as a co-receptor of VEGF (43). It was reported that NRP1 could play important role in tumor progression by promoting angiogenesis, proliferation, metastasis, and drug resistance in several different types of cancers (44–47). In this study, based on the result predicted by bioinformatics analysis that NRP1 has stable binding sites with miR-653-5p and miR-338-3p, NRP1 was selected as the common downstream target gene, and the result proved miR-653-5p and miR-338-3p mimics downregulated NRP1 expression, further confirmed this prediction. Although the

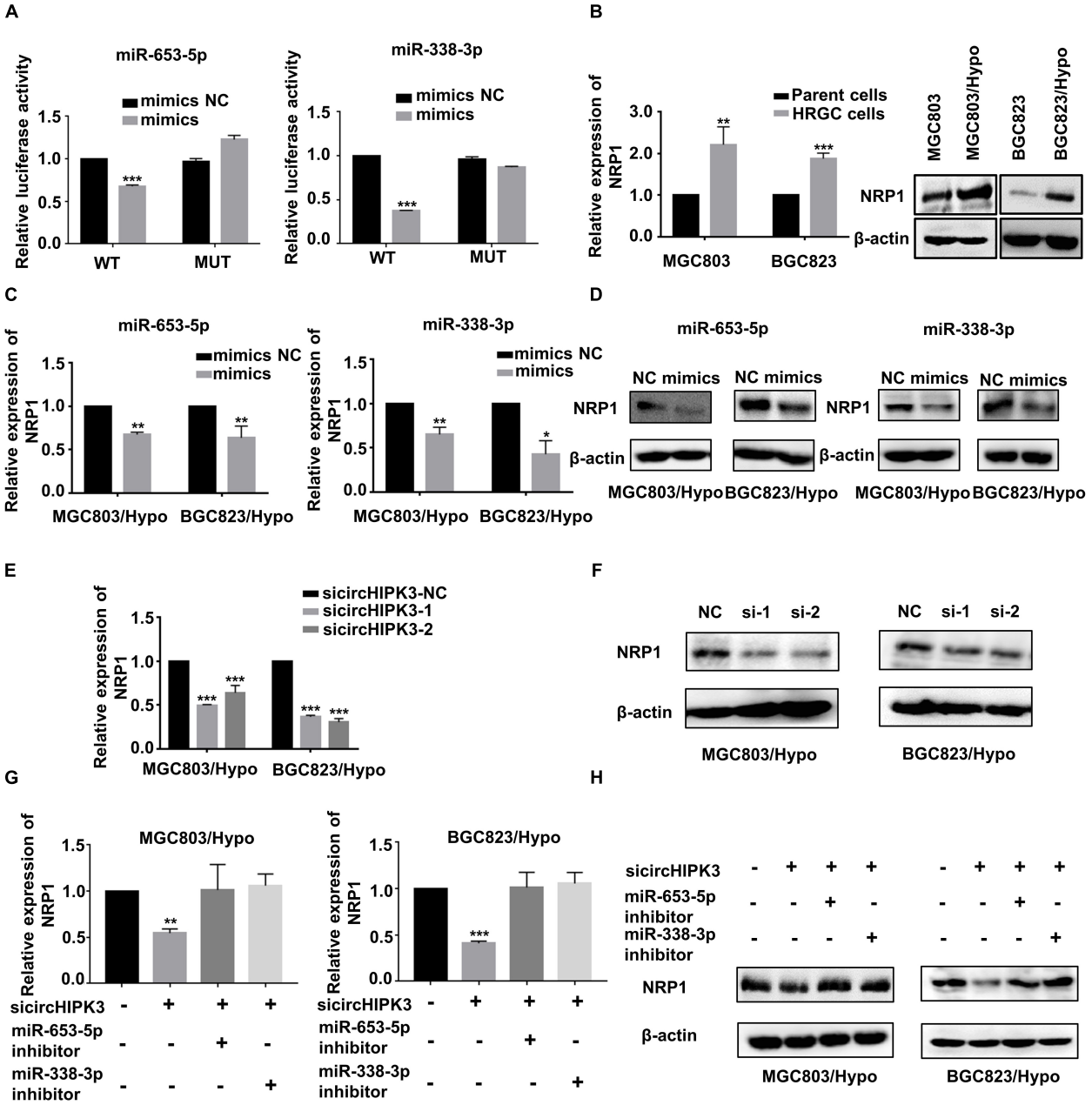

FIGURE 4 | CircHIPK3 promoted migration and invasion of HRGC cells via the miR-653-5p/miR-338-3p-NRP1 axis. **(A)** The luciferase activities of HRGC cells after co-transfected with luciferase reporter vectors NRP1-WT or NRP1-Mut and miR-653-5p or miR-338-3p mimics or miR-NC were examined. **(B)** The relative mRNA and protein expression of NRP1 in HRGC cells compared with their parent GC cells was detected by qRT-PCR and western blot. **(C,D)** The relative mRNA and protein expression of NRP1 in HRGC cells after transfected with miR-NC and miR-653-5p or miR-338-3p mimics was detected by qRT-PCR and western blot. **(E,F)** The relative mRNA and protein expression of NRP1 in HRGC cells after transfected with siNC or circHIPK3 siRNAs was detected by qRT-PCR and western blot. **(G,H)** The relative mRNA and protein expression of NRP1 in HRGC cells after co-transfected with siNC or circHIPK3 siRNAs and miR-NC or miR-653-5p or miR-338-3p inhibitor was detected by western blot. Data are presented as the mean ± SD of three independent experiments. $^{*}p < 0.05$, $^{**}p < 0.01$, $^{***}p < 0.001$. 18S was used as an internal control for all qRT-PCR experiments. β-actin was used as an internal control for all western blot assays.

study of NRP1 in GC remained limited, it was reported that the high expression of NRP1 due to hypomethylation was co-expressed with PDGFRB and was significantly correlated with tumor malignant phenotypes with poor prognosis (48). Similarly, we also found that NRP1-KD restrained the migration and invasion capability of HRGC cells, and NRP1 was involved in circHIPK3 promotion of HRGC metastasis by the sponging with miR-653-5p and miR-338-3p, suggesting the metastatic promotion role of NRP1 in GC under a long-term hypoxic microenvironment.

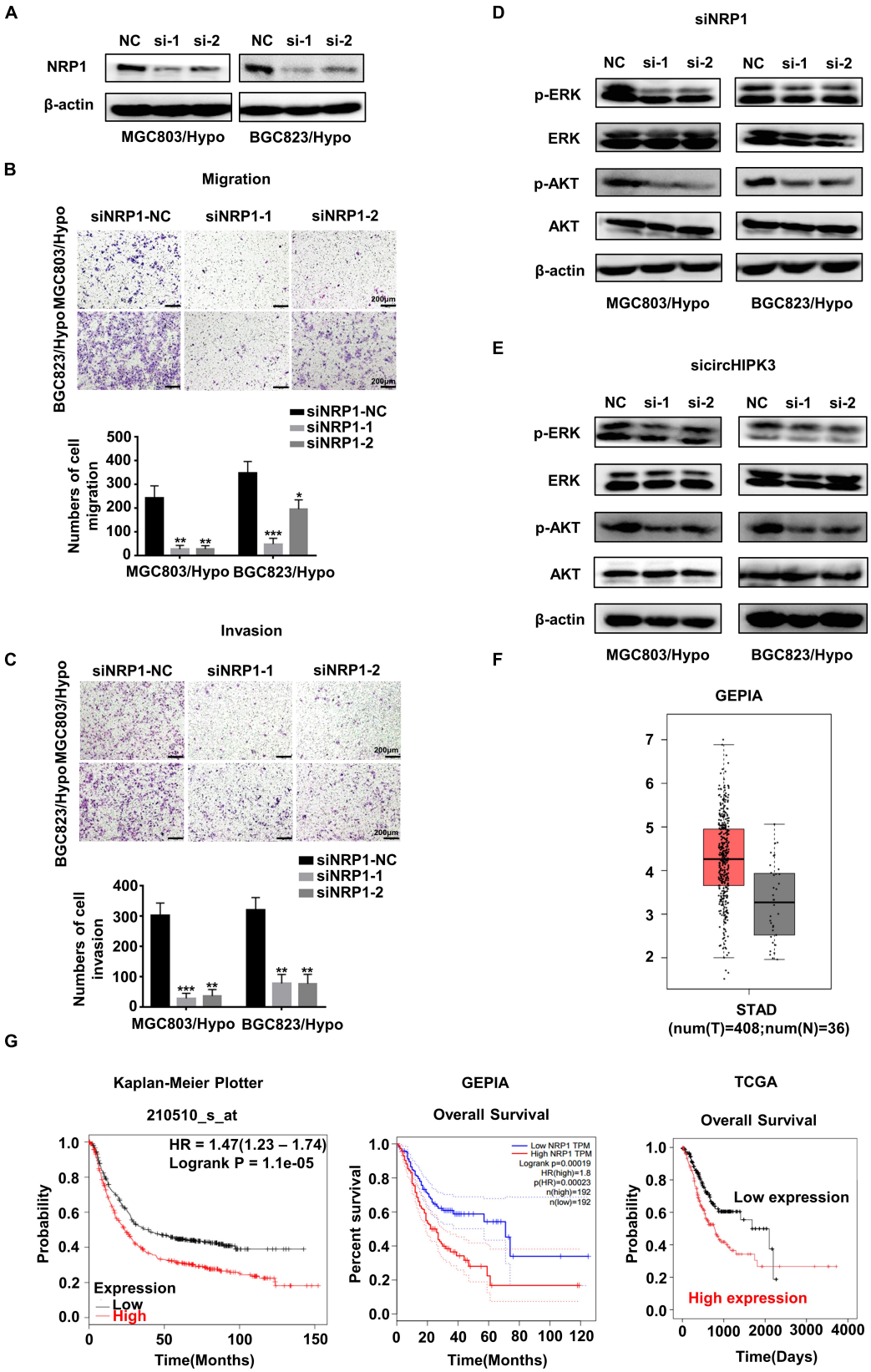

FIGURE 5 | Continued

FIGURE 5 | CircHIPK3 promoted migration and invasion of HRGC cells via the NRP1-ERK/AKT pathway. **(A)** The knockdown efficiency of NRP1 in HRGC cells was detected by western blot. **(B,C)** The migration and invasion ability of HRGC cells after transfected with siNC or NRP1 siRNAs was examined by transwell assay (original magnification, 100×). The columns on the down panels are quantified by counting 3 fields, and presented as the mean ± standard deviation. $^{*}p < 0.05$, $^{**}p < 0.01$, $^{***}p < 0.001$. **(D)** The downstream pathway proteins in HRGC cells after transfected with siNC or NRP1 siRNAs were detected by western blot. **(E)** The same downstream pathway proteins as **(D)** in HRGC cells after transfected with siNC or circHIPK3 siRNAs were detected by western blot. **(F)** The relative expression of NRP1 in GC tissues and adjacent normal tissues was analyzed by GEPIA database. **(G)** The overall survival of GC patients with NRP1-high expression or NRP1-low expression was analyzed by GEPIA, Kaplan-Meier Plotter and TCGA databases. Data are presented as the mean ± SD of three independent experiments. β-actin was used as an internal control for all western blot assays.

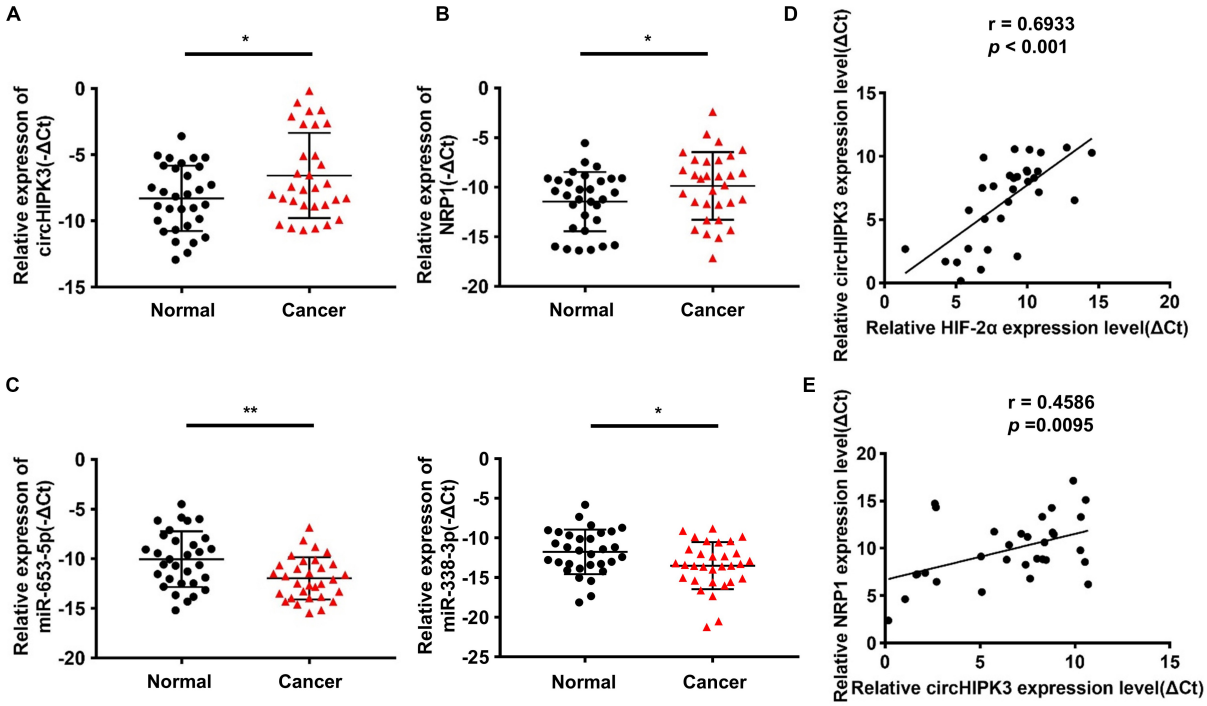

FIGURE 6 | Verification of the circHIPK3-miR-653-5p/miR-338-3p-NRP1 axis in GC tissues. **(A,B)** The relative expression of circHIPK3 and NRP1 in 31 pairs of GC tissues and adjacent non-tumor tissues of patients was detected by qRT-PCR. **(C)** The relative expression of miR-653-3p and miR-338-3p in 31 pairs of GC tissues and adjacent non-tumor tissues of patients was detected by qRT-PCR. **(D)** The correlation between HIF-2α and circHIPK3 expression in GC tissues was analyzed by Pearson correlation analysis. **(E)** The correlation between circHIPK3 and NRP1 expression in GC tissues was analyzed by Pearson correlation analysis. $^{*}p < 0.05$, $^{**}p < 0.01$.

As it is known that NRP1 could activate the MAPK and AKT pathways by binding to VEGF, we also detected the possible downstream pathway of NRP1 in HRGC cells, and found that either NRP1-KD or circHIPK3-KD reduced the expression of *p*-ERK and *p*-AKT, suggesting that NRP1 upregulated by circHIPK3 promoted GC metastasis by activating ERK and AKT pathways in a long-term hypoxic microenvironment (49).

The circRNA-miRNA-mRNA ceRNA network analyzed in this research is composed of circHIPK3, miR-653-5p, and miR-338-3p, each of which have four binding sites with circHIPK3, and NRP1, which is the common target gene of the two miRNAs. Therefore, long-term hypoxia-upregulated circHIPK3 significantly promoted GC metastasis via construction of a stable ceRNA network with miR-653-5p/miR-338-3-NRP1, indicating the important functions of circHIPK3 in GC metastasis under a long-term hypoxic microenvironment. In our study, the stable ceRNA network was also verified in GC tissues and obtained similar results with that in GC cells. However, due to limited GC samples, it needs to be verified in larger scale samples in the future. Certainly, other mechanisms of circHIPK3 except for the ceRNA function under a long-term hypoxic microenvironment of GC also needs the further exploration.

In summary, our study demonstrated that circHIPK3 upregulated by HIF-2α could facilitate the migration and invasion of GC cells via the miR-653-5p/miR-338-3p-NRP1 axis under a long-term hypoxic microenvironment (the mechanism is shown in diagrammatic form in **Figure 7**. These findings revealed a new mechanism of long-term hypoxia-promoting metastasis in GC and showed that circHIPK3 might be a long-term

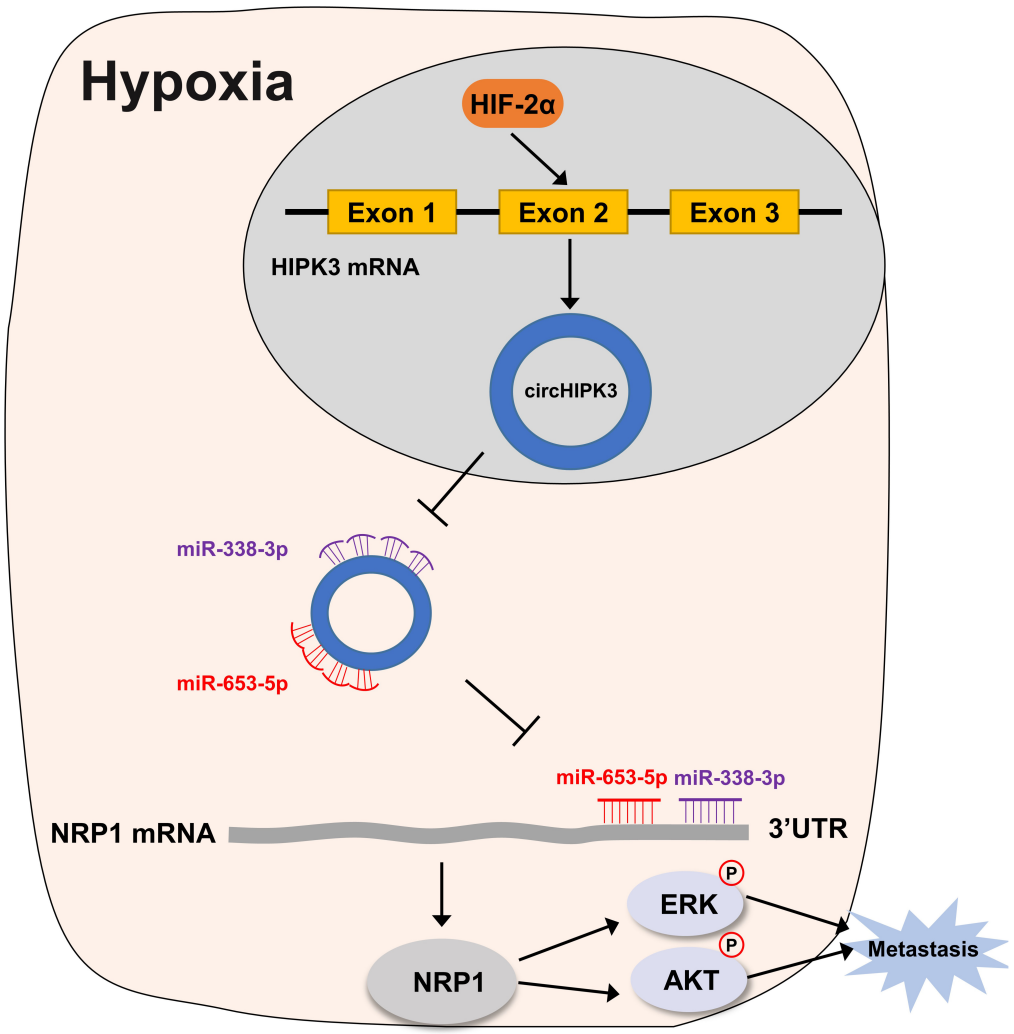

FIGURE 7 | Working model for circHIPK3 in HRGC cells. Under a long-term hypoxic microenvironment of gastric cancer, circHIPK3 was upregulated by HIF-2α; then circHIPK3 upregulated NRP1 by sponging with miR-653-3p and miR-338-3p followed by relieving the transcriptional suppress of NRP1; finally, NRP1 promoted metastasis by activating ERK and AKT pathway.

hypoxic biomarker and a potential prognostic biomarker for GC patients in the future.

DATA AVAILABILITY STATEMENT

All datasets presented in this study are included in the article/**Supplementary Material**.

ETHICS STATEMENT

The studies involving human participants were reviewed and approved by the Ethics Committee of the First Hospital of China Medical University. The patients/participants provided their written informed consent to participate in this study.

AUTHOR CONTRIBUTIONS

YL and XC designed the research study. YJ did the majority of the experiment and wrote the manuscript. WL and YW analyzed the data. XQ, KH, JW, CL, and XZ conducted the experimental guidance. JZ and XL contributed essential samples. YL, JZ, and XC revised the manuscript. All authors reviewed and approved the final manuscript.

FUNDING

This study was supported by the National Natural Science Foundation of China (No. 81972751), the Technological Special Project of Liaoning Province of China (2019020176-JH1/103), the Science and Technology Plan Project of Liaoning Province (No. 2013225585), the Key Research and

Development Program of Liaoning Province (2018225060), and Science and Technology Plan Project of Shenyang City (19-112-4-099).

ACKNOWLEDGMENTS

The authors would like to acknowledge the Key Laboratory of Precision Diagnosis and Treatment of Gastrointestinal Tumors, Ministry of Education (China Medical University, Shenyang, China) for providing the space and equipment for conducting the experiments.

SUPPLEMENTARY MATERIAL

The Supplementary Material for this article can be found online at: https://www.frontiersin.org/articles/10.3389/fonc.2020.01612/full#supplementary-material

REFERENCES

1. Bray F, Ferlay J, Soerjomataram I, Siegel RL, Torre LA, Jemal A. Global cancer statistics 2018: GLOBOCAN estimates of incidence and mortality worldwide for 36 cancers in 185 countries. *CA Cancer J Clin*. (2018) 68:394–424. doi: 10.3322/caac.21492
2. Chen W, Zheng R, Baade PD, Zhang S, Zeng H, Bray F, et al. Cancer statistics in China, 2015. *CA Cancer J Clin*. (2016) 66:115–32. doi: 10.3322/caac.21338
3. Wilson WR, Hay MP. Targeting hypoxia in cancer therapy. *Nat Rev Cancer*. (2011) 11:393–410. doi: 10.1038/nrc3064
4. Chang Q, Jurisica I, Do T, Hedley DW. Hypoxia predicts aggressive growth and spontaneous metastasis formation from orthotopically grown primary xenografts of human pancreatic cancer. *Cancer Res*. (2011) 71:3110–20. doi: 10.1158/0008-5472.CAN-10-4049
5. Rankin EB, Giaccia AJ. Hypoxic control of metastasis. *Science*. (2016) 352:175–80. doi: 10.1126/science.aaf4405
6. Zhang J, Xu J, Dong Y, Huang B. Down-regulation of HIF-1alpha inhibits the proliferation, migration, and invasion of gastric cancer by inhibiting PI3K/AKT pathway and VEGF expression. *Biosci Rep*. (2018) 38:BSR20180741. doi: 10.1042/BSR20180741
7. Hao LS, Liu Q, Tian C, Zhang DX, Wang B, Zhou DX, et al. Correlation and expression analysis of hypoxia-inducible factor 1alpha, glucose transporter 1 and lactate dehydrogenase 5 in human gastric cancer. *Oncol Lett*. (2019) 18:1431–41. doi: 10.3892/ol.2019.10457
8. Liu N, Wang Y, Zhou Y, Pang H, Zhou J, Qian P, et al. Kruppel-like factor 8 involved in hypoxia promotes the invasion and metastasis of gastric cancer via epithelial to mesenchymal transition. *Oncol Rep*. (2014) 32:2397–404. doi: 10.3892/or.2014.3495
9. Xu Y, Jin X, Huang Y, Dong J, Wang H, Wang X, et al. Inhibition of peritoneal metastasis of human gastric cancer cells by dextran sulphate through the reduction in HIF-1alpha and ITGbeta1 expression. *Oncol Rep*. (2016) 35:2624–34. doi: 10.3892/or.2016.4693
10. Span PN, Bussink J. Biology of hypoxia. *Semin Nucl Med*. (2015) 45:101–9. doi: 10.1053/j.semnuclmed.2014.10.002
11. Horsman MR, Vaupel P. Pathophysiological basis for the formation of the tumor microenvironment. *Front Oncol*. (2016) 6:66. doi: 10.3389/fonc.2016.00066
12. Iwasaki K, Ninomiya R, Shin T, Nomura T, Kajiwara T, Hijiya N, et al. Chronic hypoxia-induced slug promotes invasive behavior of prostate cancer cells by activating expression of ephrin-B1. *Cancer Sci*. (2018) 109:3159–70. doi: 10.1111/cas.13754
13. Zhao J, Qiao C, Ding Z, Sheng Y, Li X, Yang Y, et al. A novel pathway in NSCLC cells : miR-191, targeting NFIA, is induced by chronic hypoxia, and promotes cell proliferation and migration. *Mol Med Rep*. (2017) 15:1319–25. doi: 10.3892/mmr.2017.6100
14. Yang Z, Shi X, Li C, Wang X, Hou K, Li Z, et al. Long non-coding RNA UCA1 upregulation promotes the migration of hypoxia-resistant gastric cancer cells through the miR-7-5p/EGFR axis. *Exp Cell Res*. (2018) 368:194–201. doi: 10.1016/j.yexcr.2018.04.030
15. Wilusz JE, Sharp PA. A circuitous route to noncoding RNA. *Science*. (2013) 340:440–1. doi: 10.1126/science.1238522
16. Chen LL, Yang L. Regulation of circRNA biogenesis. *RNA Biol*. (2015) 12:381–8. doi: 10.1080/15476286.2015.1020271
17. Wang Y, Mo Y, Gong Z, Yang X, Yang M, Zhang S, et al. Circular RNAs in human cancer. *Mol Cancer*. (2017) 16:25. doi: 10.1186/s12943-017-0598-7
18. Chen L, Zhi Z, Wang L, Zhao Y, Deng M, Liu Y, et al. NSD2 circular RNA promotes metastasis of colorectal cancer by targeting miR-199b-5p-mediated DDR1 and JAG1 signalling. *J Pathol*. (2019) 248:103–15. doi: 10.1002/path.5238
19. Chen X, Chen R, Wei W, Li Y, Feng Z, Tan L, et al. PRMT5 circular RNA promotes metastasis of urothelial carcinoma of the bladder through sponging miR-30c to induce epithelial-mesenchymal transition. *Clin Cancer Res*. (2018) 24:6319–30. doi: 10.1158/1078-0432.CCR-18-1270
20. Yu H, Chen Y, Jiang P. Circular RNA HIPK3 exerts oncogenic properties through suppression of miR-124 in lung cancer. *Biochem Biophys Res Commun*. (2018) 506:455–62. doi: 10.1016/j.bbrc.2018.10.087
21. Zeng K, Chen X, Xu M, Liu X, Hu X, Xu T, et al. CircHIPK3 promotes colorectal cancer growth and metastasis by sponging miR-7. *Cell Death Dis*. (2018) 9:417. doi: 10.1038/s41419-018-0454-8
22. Hu D, Zhang Y. Circular RNA HIPK3 promotes glioma progression by binding to miR-124-3p. *Gene*. (2019) 690:81–9. doi: 10.1016/j.gene.2018.11.073
23. Liu W, Xu Q. Upregulation of circHIPK3 promotes the progression of gastric cancer via Wnt β-catenin pathway and indicates a poor prognosis. *Eur Rev Med. Pharmacol Sci*. (2019) 23:7905–12. doi: 10.26355/eurrev_201909_19004
24. Ghasemi S, Emadi-Baygi M, Nikpour P. Down-regulation of circular RNA ITCH and circHIPK3 in gastric cancer tissues. *Turk J Med Sci*. (2019) 49:687–95. doi: 10.3906/sag-1806-50
25. Saxena K, Jolly MK. Acute vs. Chronic vs. Cyclic Hypoxia: their differential dynamics, molecular mechanisms, and effects on tumor progression. *Biomolecules*. (2019) 9:E339. doi: 10.3390/biom9080339
26. Chen D, Lu X, Yang F, Xing N. Circular RNA circHIPK3 promotes cell proliferation and invasion of prostate cancer by sponging miR-193a-3p and regulating MCL1 expression. *Cancer Manag Res*. (2019) 11:1415–23. doi: 10.2147/CMAR.S190669
27. Xiao-Long M, Kun-Peng Z, Chun-Lin Z. Circular RNA circ_HIPK3 is down-regulated and suppresses cell proliferation, migration and invasion in osteosarcoma. *J Cancer*. (2018) 9:1856–62. doi: 10.7150/jca.24619
28. Majmundar A, Wong W, Simon M. Hypoxia-inducible factors and the response to hypoxic stress. *Mol Cell*. (2010) 40:294–309. doi: 10.1016/j.molcel
29. Rankin EB, Giaccia AJ. The role of hypoxia-inducible factors in tumorigenesis. *Cell Death Differ*. (2008) 15:678–85. doi: 10.1038/cdd.2008.21
30. Zhao J, Du F, Shen G, Zheng F, Xu B. The role of hypoxia-inducible factor-2 in digestive system cancers. *Cell Death Dis*. (2015) 6:e1600. doi: 10.1038/cddis.2014.565
31. Nagaraju GP, Bramhachari PV, Raghu G, El-Rayes BF. Hypoxia inducible factor-1alpha: its role in colorectal carcinogenesis and metastasis. *Cancer Lett*. (2015) 366:11–8. doi: 10.1016/j.canlet.2015.06.005
32. Peng C, Liu G, Huang K, Zheng Q, Li Y, Yu C. Hypoxia-induced upregulation of HE4 is responsible for resistance to radiation therapy of gastric cancer. *Mol Ther Oncolytics*. (2019) 12:49–55. doi: 10.1016/j.omto.2018.11.004
33. Song Z, Liu T, Chen J, Ge C, Zhao F, Zhu M, et al. HIF-1α-induced RIT1 promotes liver cancer growth and metastasis and its deficiency increases sensitivity to sorafenib. *Cancer Lett*. (2019) 460:96–107. doi: 10.1016/j.canlet.2019.06.016
34. Choudhry H, Albukhari A, Morotti M, Haider S, Moralli D, Smythies J, et al. Tumor hypoxia induces nuclear paraspeckle formation through HIF-2alpha

dependent transcriptional activation of NEAT1 leading to cancer cell survival. *Oncogene*. (2015) 34:4482–90. doi: 10.1038/onc.2014.378
35. Xu QQ, Xiao FJ, Sun HY, Shi XF, Wang H, Yang YF, et al. Ptpmt1 induced by HIF-2alpha regulates the proliferation and glucose metabolism in erythroleukemia cells. *Biochem Biophys Res Commun*. (2016) 471:459–65. doi: 10.1016/j.bbrc.2016.02.053
36. Salmena L, Poliseno L, Tay Y, Kats L, Pandolfi PP. A ceRNA hypothesis: the rosetta stone of a hidden RNA language? *Cell*. (2011) 146:353–8. doi: 10.1016/j.cell.2011.07.014
37. Hansen T, Jensen T, Clausen B, Bramsen J, Finsen B, Damgaard C, et al. Natural RNA circles function as efficient microRNA sponges. *Nature*. (2013) 495:384–8. doi: 10.1038/nature11993
38. Zhang X, Yang D, Wei Y. Overexpressed CDR1as functions as an oncogene to promote the tumor progression via miR-7 in non-small-cell lung cancer. *Onco Targets Ther*. (2018) 11:3979–87. doi: 10.2147/OTT.S158316
39. Li RC, Ke S, Meng FK, Lu J, Zou XJ, He ZG, et al. CiRS-7 promotes growth and metastasis of esophageal squamous cell carcinoma via regulation of miR-7/HOXB13. *Cell Death Dis*. (2018) 9:838. doi: 10.1038/s41419-018-0852-y
40. Han W, Wang L, Zhang L, Wang Y, Li Y. Circular RNA circ-RAD23B promotes cell growth and invasion by miR-593-3p/CCND2 and miR-653-5p/TIAM1 pathways in non-small cell lung cancer. *Biochem Biophys Res Commun*. (2019) 510:462–6. doi: 10.1016/j.bbrc.2019.01.131
41. Zou T, Duan J, Liang J, Shi H, Zhen T, Li H, et al. miR-338-3p suppresses colorectal cancer proliferation and progression by inhibiting MACC1. *Int J Clin Exp Pathol*. (2018) 11:2256–67.
42. Jin Y, Zhao M, Xie Q, Zhang H, Wang Q, Ma Q. MicroRNA-338-3p functions as tumor suppressor in breast cancer by targeting SOX4. *Int J Oncol*. (2015) 47:1594–602. doi: 10.3892/ijo.2015.3114
43. Gu C, Limberg BJ, Whitaker GB, Perman B, Leahy DJ, Rosenbaum JS, et al. Characterization of neuropilin-1 structural features that confer binding to semaphorin 3A and vascular endothelial growth factor 165. *J Biol Chem*. (2002) 277:18069–76. doi: 10.1074/jbc.M201681200
44. Wu Y, Chen Y, Jao Y, Hsieh I, Chang K, Hong T. miR-320 regulates tumor angiogenesis driven by vascular endothelial cells in oral cancer by silencing neuropilin 1. *Angiogenesis*. (2014) 17:247–60. doi: 10.1007/s10456-013-9394-1
45. Zhang L, Xing Y, Gao Q, Sun X, Zhang D, Cao G. Combination of NRP1-mediated iRGD with 5-fluorouracil suppresses proliferation, migration and invasion of gastric cancer cells. *Biomed Pharmacother*. (2017) 93:1136–43. doi: 10.1016/j.biopha.2017.06.103
46. Al-Shareef H, Hiraoka S, Tanaka N, Shogen Y, Lee A, Bakhshishayan S, et al. Use of NRP1, a novel biomarker, along with VEGF-C, VEGFR-3, CCR7 and SEMA3E, to predict lymph node metastasis in squamous cell carcinoma of the tongue. *Oncol Rep*. (2016) 36:2444–54. doi: 10.3892/or.2016.5116
47. Rizzolio S, Cagnoni G, Battistini C, Bonelli S, Isella C, Van GJ, et al. Neuropilin-1 upregulation elicits adaptive resistance to oncogene-targeted therapies. *J Clin Invest*. (2018) 128:3976–90. doi: 10.1172/JCI99257DS1
48. Wang G, Shi B, Fu Y, Zhao S, Qu K, Guo Q, et al. Hypomethylated gene NRP1 is co-expressed with PDGFRB and associated with poor overall survival in gastric cancer patients. *Biomed Pharmacother*. (2019) 111:1334–41. doi: 10.1016/j.biopha.2019.01.023
49. Akagi M, Kawaguchi M, Liu W, McCarty M, Takeda A, Fan F, et al. Induction of neuropilin-1 and vascular endothelial growth factor by epidermal growth factor in human gastric cancer cells. *Br J Cancer*. (2003) 88:796–802. doi: 10.1038/sj.bjc.6600811

Conflict of Interest: The authors declare that the research was conducted in the absence of any commercial or financial relationships that could be construed as a potential conflict of interest.

frontiers in Oncology

CORRECTION
published: 12 November 2021
doi: 10.3389/fonc.2021.783320

Corrigendum: CircHIPK3 Promotes Metastasis of Gastric Cancer *via* miR-653-5p/miR-338-3p-NRP1 Axis Under a Long-Term Hypoxic Microenvironment

Yue Jin[1,2,3,4†], *Xiaofang Che*[1,2,3,4†], *Xiujuan Qu*[1,2,3,4], *Xin Li*[5], *Wenqing Lu*[1,2,3,4], *Jie Wu*[1,2,3,4], *Yizhe Wang*[1,2,3,4], *Kezuo Hou*[1,2,3,4], *Ce Li*[1,2,3,4], *Xiaojie Zhang*[1,2,3,4], *Jianping Zhou*[5*] *and Yunpeng Liu*[1,2,3,4*]

[1] Department of Medical Oncology, The First Hospital of China Medical University, Shenyang, China, [2] Key Laboratory of Anticancer Drugs and Biotherapy of Liaoning Province, The First Hospital of China Medical University, Shenyang, China, [3] Liaoning Province Clinical Research Center for Cancer, Shenyang, China, [4] Key Laboratory of Precision Diagnosis and Treatment of Gastrointestinal Tumors, Ministry of Education, Shenyang, China, [5] Department of Gastrointestinal Surgery, The First Hospital of China Medical University, Shenyang, China

OPEN ACCESS

Edited and reviewed by:
Bin Li,
Jinan University, China

***Correspondence:**
Jianping Zhou
zjphama@163.com
Yunpeng Liu
ypliu@cmu.edu.cn

[†]These authors have contributed equally to this work

Specialty section:
This article was submitted to Gastrointestinal Cancers, a section of the journal Frontiers in Oncology

Received: 29 September 2021
Accepted: 29 October 2021
Published: 12 November 2021

Citation:
Jin Y, Che X, Qu X, Li X, Lu W, Wu J, Wang Y, Hou K, Li C, Zhang X, Zhou J and Liu Y (2021) Corrigendum: CircHIPK3 Promotes Metastasis of Gastric Cancer via miR-653-5p/miR-338-3p-NRP1 Axis Under a Long-Term Hypoxic Microenvironment. Front. Oncol. 11:783320. doi: 10.3389/fonc.2021.783320

Keywords: CircHIPK3, long-term hypoxic microenvironment, HIF-2α, gastric cancer, metastasis

A Corrigendum on

CircHIPK3 Promotes Metastasis of Gastric Cancer via miR-653-5p/miR-338-3p-NRP1 Axis Under a Long-Term Hypoxic Microenvironment

By Jin Y, Che X, Qu X, Li X, Lu W, Wu J, Wang Y, Hou K, Li C, Zhang X, Zhou J and Liu Y (2020). Front. Oncol. *10:1612. doi: 10.3389/fonc.2020.01612*

In the original article, there was a mistake in **Figure 2D** as published. The picture of migration of sicircHIPK3 in BGC823/Hypo cells in **Figure 2D** was misused. The corrected **Figure 2** appears below.

The authors apologize for this error and state that this does not change the scientific conclusions of the article in any way. The original article has been updated.

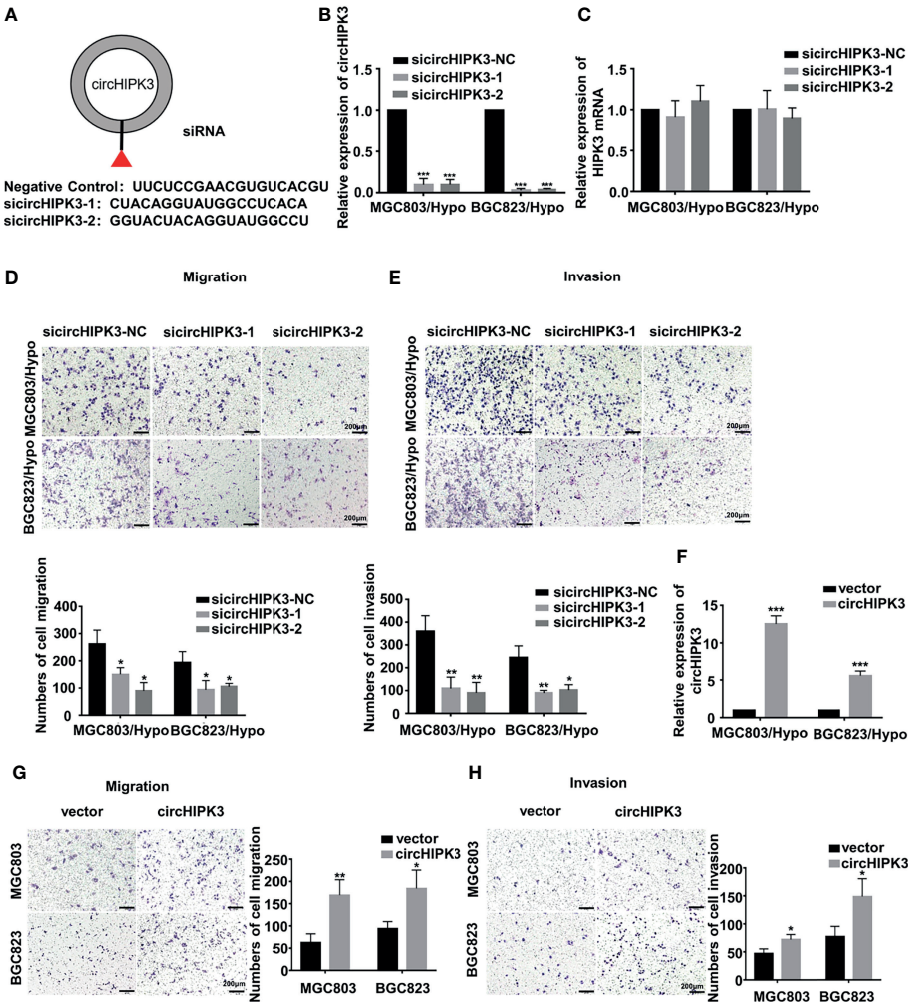

FIGURE 2 | CircHIPK3 promoted migration and invasion of HRGC cells. **(A)** The sequence of two siRNAs targeted to back-splicing site of circHIPK3 and the negative control siRNA. **(B, C)** The relative expression of circHIPK3 and linear HIPK3 mRNA in HRGC cells after transfected with negative control siRNA (siNC) or circHIPK3 siRNAs was detected by qRT-PCR. 18S was used as an internal control. **(D, E)** The migration and invasion ability of HRGC cells after transfected with siNC or circHIPK3 siRNAs was examined by transwell assay (original magnification, 100×). The columns on the down panels are quantified by counting 3 fields, and presented as the mean ± standard deviation. *p < 0.05, **p < 0.01, ***p < 0.001. **(F)** The overexpression efficiency of circHIPK3 in MGC803 and BGC823 cells was detected by qRT-PCR. 18S was used as an internal control. **(G, H)** The migration and invasion ability of MGC803 and BGC823 cells after transfected with circHIPK3 overexpression plasmids and empty vectors was examined by transwell assay (original magnification, 100×). The columns on the right are quantified by counting three fields, and presented as the mean ± standard deviation. *p < 0.05, **p < 0.01, ***p < 0.001. Data are presented as the mean ± SD of three independent experiments. *p < 0.05, **p < 0.01, ***p < 0.001.

frontiers in Oncology

ORIGINAL RESEARCH
published: 11 September 2020
doi: 10.3389/fonc.2020.01534

Molecular Deregulation of *EPAS1* in the Pathogenesis of Esophageal Squamous Cell Carcinoma

Farhadul Islam[1,2], *Vinod Gopalan*[3], *Simon Law*[4], *Alfred K. Lam*[3]* *and Suja Pillai*[1]*

[1] School of Biomedical Sciences, Faculty of Medicine, University of Queensland, Brisbane, QLD, Australia, [2] Department of Biochemistry and Molecular Biology, University of Rajshahi, Rajshahi, Bangladesh, [3] School of Medicine, Griffith University, Gold Coast Campus, Gold Coast, QLD, Australia, [4] Department of Surgery, University of Hong Kong, Hong Kong, China

Endothelial PAS domain-containing protein 1 (EPAS1) is an angiogenic factor and its implications have been reported in many cancers but not in esophageal squamous cell carcinoma (ESCC). Herein, we aim to examine the genetic and molecular alterations, clinical implications, and functional roles of *EPAS1* in ESCC. High-resolution melt-curve analysis and Sanger sequencing were used to detect mutations in *EPAS1* sequence. *EPAS1* DNA number changes and mRNA expressions were analyzed by polymerase chain reaction. *in vitro* functional assays were used to study the impact of EPAS1 on cellular behaviors. Overall, 7.5% (n = 6/80) of patients with ESCC had mutations in *EPAS1*, and eight novel variants (c.1084C>T, c.1099C>A, c.1145_1145delT, c.1093C>G, c.1121T>G, c.1137_1137delG, c.1135_1136insT, and c.1091_1092insT) were detected. Among these mutations, four were frameshift (V382Gfs*12, A381Lfs*13, K379lfs*6, and K364Nfs*12) mutations and showed the potential of non–sense-mediated mRNA decay (NMD) in computational analysis. The majority of patients showed molecular deregulation of *EPAS1* [45% (n = 36/80) DNA amplification, 42.5% (n = 34/80) DNA deletion, as well as 53.7% (n = 43/80) high mRNA expression, 20% (n = 16/80) low mRNA expression]. These alterations of *EPAS1* were associated with tumor location and T stages. Patients with stage III ESCC having *EPAS1* DNA amplification had poorer survival rates in comparison to *EPAS1* DNA deletion (p = 0.04). In addition, suppression of *EPAS1* in ESCC cells showed reduced proliferation, wound healing, migration, and invasion in comparison to that of control cells. Thus, the molecular and functional studies implied that *EPAS1* plays crucial roles in the pathogenesis of ESCC and has the potential to be used as a prognostic marker and as a therapeutic target.

Keywords: ESCC, EPAS1, cancer prognosis, cancer genetics, mutations

OPEN ACCESS

Edited by:
Muzafar Ahmad Macha,
Central University of Kashmir, India

Reviewed by:
Nissar Ahmad Wani,
Central University of Kashmir, India
Rinu Sharma,
Guru Gobind Singh Indraprastha University, India

***Correspondence:**
Alfred K. Lam
a.lam@griffith.edu.au
Suja Pillai
s.pillai@uq.edu.au

Specialty section:
This article was submitted to Gastrointestinal Cancers, a section of the journal Frontiers in Oncology

Received: *18 April 2020*
Accepted: *17 July 2020*
Published: *11 September 2020*

Citation:
Islam F, Gopalan V, Law S, Lam AK and Pillai S (2020) Molecular Deregulation of EPAS1 in the Pathogenesis of Esophageal Squamous Cell Carcinoma. Front. Oncol. 10:1534. doi: 10.3389/fonc.2020.01534

INTRODUCTION

Hypoxia-inducible factor 1 (HIF1) is an oxygen-sensitive transcription factor consisting of heterodimer of α and β subunits (1). The functional HIF1 is composed of constitutively expressed β subunit and an oxygen-sensitive subunit HIF1α or its isomers HIF2α and HIF3α. These HIF1α isomers are encoded by the *HIF1A*, *endothelial PAS domain-containing protein 1* (*EPAS1*), and *HIF3A* genes, respectively (2). In hypoxia, HIF1 recognizes the hypoxia response element

and regulates the expression of many genes associated with cell proliferation, growth, survival, angiogenesis, and iron and glucose metabolism (1, 3).

HIF2α, an angiogenic factor encoded by *EPAS1* gene, is involved in many physiological and pathological processes, including ferroptosis, endochondral and intramembranous ossification, and Pacak-Zhuang syndrome (4–6). Dysregulation of ferroptosis, a form of regulated cell death, characterized by excessive accumulation of iron and lipid peroxidation, is associated with several diseases such as cancer, neurodegeneration, and ischemia–reperfusion injury (6, 7). Accordingly, it was reported that expression of EPAS1 is associated with pathogenesis, progression, and prognosis of different cancers, including non–small cell lung carcinoma (8), renal cell carcinoma (9), hepatocellular carcinoma (10), neuroblastoma (11), pheochromocytoma (12), glioma (13), and colorectal carcinoma (14). For example, in colorectal carcinoma, EPAS1 protein expression inversely correlated with higher tumor grade and plasma mRNA level of EPAS1 expression and is associated with poor patients' survival and advanced pathological stages (15, 16).

Mutations in the coding sequence of *EPAS1* has been identified in several pathophysiological conditions in human, including congenital heart disease, erythrocytosis, and Lynch syndrome (17–20). In addition, various tumors, e.g., paraganglioma (21), pheochromocytoma (12), and pancreatic adenocarcinoma (22), showed mutations in *EPAS1* sequences. To the best of our knowledge, mutations and their impacts with clinicopathological parameters in patients with ESCC have not been reported in the literature. Also, the molecular deregulations of *EPAS1* and their cellular impact in ESCC have never been studied. Therefore, the present study aims to screen mutations in *EPAS1* sequence in patients with ESCC and their association with clinical and pathological parameters. Furthermore, the EPAS1 DNA number changes, mRNA expression, their correlation with clinical factors, and functional implications of EPAS1 in ESCC cells were investigated in the present study.

MATERIALS AND METHODS

Patients and Clinicopathological Parameters

The clinical samples used in this study were collected from patients who had a surgical resection for primary ESCC. The samples were recruited with no selection bias. Those cancers from patients who underwent preoperative chemoradiotherapy and/or with poor histology were excluded in the present study. Ethic approval was obtained from Griffith University (MED/19/08/HREC) for the present study. The specimens were received fresh after the operation. The age and gender of the patients were noted. In each case, the location and the size of the carcinoma were examined and recorded in fresh. The nonneoplastic esophageal tissues were prospectively collected from the nonneoplastic esophageal mucosa at the proximal resection margin (act as controls) during the operation of the patients with ESCC at the same time of collection of the ESCC tumor tissues. Samples were also collected in 10% buffered formalin and processed in formalin. For each selected sample, tissues were sectioned using a microtome (Leica Biosystems Inc., Buffalo Grove, IL, USA) and stained by hematoxylin–eosin staining for histological analysis by an anatomical pathologist (A.K.L.). The other portion of the resected specimen was fixed in formalin, processed in paraffin, and examined pathologically by the same anatomical pathologist (A.K.L.) using a standard protocol (23). Histological types and grades of selected ESCCs were assessed based on the current World Health Organization histological typing of esophageal tumors prior to analysis (24). Pathological staging was identified according to the current Cancer Staging Manual of the American Joint Committee on Cancer (25).

In this study, 80 patients (67 men, 13 women) with resections of primary ESCC were recruited. In addition, 33 nonneoplastic tissues from esophagus were collected to use as controls. The mean age of the 80 patients with ESCC was 63 years (ranging from 39 to 83 years), and the sizes of the tumors ranged from 5 to 120 mm (mean = 50 mm). The majority of patients (66%, $n = 53/80$) included in this study had stage III ESCCs. In addition, 75% (60/80) of the patients with ESCC had lymph node metastasis at the time of surgery, and 6% (5/80) had distant metastasis at presentation.

In this study, the follow-up period was defined as the interval between the date of surgery for ESCC and the date of death or closing date of the study. The actuarial survival rate of the patients was calculated from the date of surgical resection of the ESCC to the date of death or last follow-up. A schematic summary of the flow of the experiments used in the current study is shown in **Figure 1**.

Cell Culture

Five ESCC cancer cell lines (KYSE70, KYSE150, KYSE450, KYSE520, and HKESC-1) and one nonneoplastic keratinocyte (HaCaT) were used in the present study. All the cells were maintained as previously described (26, 27).

Extraction of DNA and RNA

A microtome (Leica Biosystems) was used to section (10 μm) tissues for RNA and DNA extraction. Sections that contained a representative cancer area (made up >70% of the volume of the samples) were used for extraction. DNA was extracted and purified using Qiagen DNeasy Blood & Tissue kits (Qiagen Pty. Ltd., Hilden, Germany) following the manufacturer's guidelines. DNA from cultured cells was extracted with the same kits. In addition, RNA was extracted from the tissue sections and cultured cells using miRNeasy Mini kits (Qiagen) according to the manufacturer's protocol. The purity of the extracted DNA and RNA was checked with optical density using a NanoDrop spectrophotometer. The extracted DNA and RNA were stored at −20°C for further analysis.

High-Resolution Melt Curve Analysis

Genomic DNAs extracted from 80 cancers and 30 noncancer tissues were used to screen possible mutations in *EPAS1* sequence by high-resolution melt (HRM) analysis. Rotor-Gene Q detection system (Qiagen) was used for amplifying target sequences, followed by HRM curve analyzed using Rotor-Gene

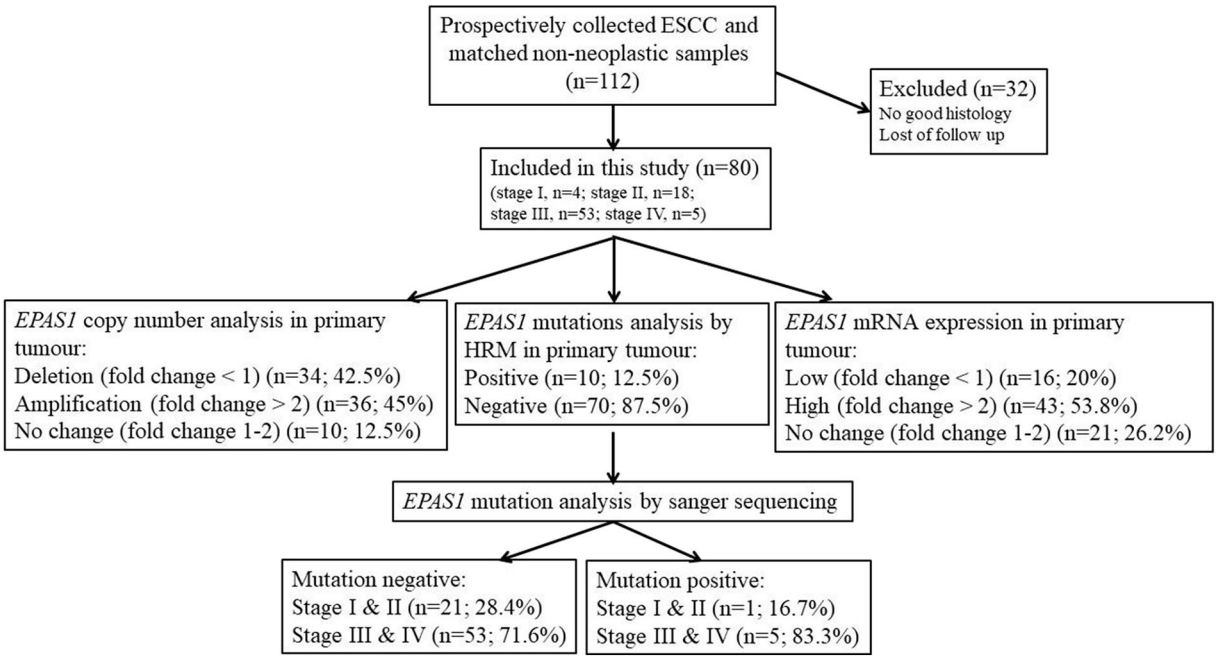

FIGURE 1 | Schematic representation of the methodological flow used for clinical samples analysis in the present study. Tissue samples with poor histology and loss of follow-up were excluded in the present study. Among the samples, 45% showed *EPAS1* DNA amplification, whereas 42.5% showed *EPAS1* DNA deletion. The rest of the samples (12.5%) showed no changes in *EPAS1* DNA. In addition, 53.8% of samples showed high *EPAS1* mRNA expression, and 16.2% of samples showed low *EPAS1* mRNA expression, whereas 20% of samples did not show any changes in *EPAS1* mRNA expression. Furthermore, 12.5% of samples showed *EPAS1* mutations, and 87.5% of samples were mutation negative in the present study.

ScreenClust HRM Software. The *EPAS1* sequence was amplified via polymerase chain reaction (PCR) in a total reaction volume of 10 μL comprising 5 μL of 2Xsensimix HRM master mix, 1 μL of 30 ng/μL genomic DNA, diethylpyrocarbonate (DEPC, RNase-free) treated water 2 and 1 μL of each forward and reverse *EPAS1* primer. The thermal cycling protocol was the same as published previously (28). The melt curve data were generated by increasing the temperature from 65 to 85°C for all assays, with a temperature increase rate of 0.05°C/s and recording fluorescence. All the samples were run in triplicates and included a negative (no template) control.

Purification of PCR Products and Sanger Sequencing Analysis

The variants detected in HRM analysis were further confirmed via checking with Sanger sequencing for identifying the mutations in *EPAS1* sequence. Briefly, after HRM analysis, PCR products from mutant samples were purified using NucleoSpin® Gel and PCR Clean-up kit (Macherey- Nagel, Bethlehem, PA, USA) according to the manufacturer's protocols. Then, the purified PCR products were sequenced using Big Dye Terminator Chemistry version 3.1 (Applied Biosystems, Foster City, CA, USA) under standardized cycling PCR conditions. The generated data were analyzed at the Australian Genome Research Facility using a 3730xl Capillary sequencer (Applied Biosystems). The sequences were analyzed with Sequence Scanner 2 software (Applied Biosystems).

In silico Analysis

The Ensembl transcript ID ENST00000263734 was used as input when required by a method. In this study, all the variants were analyzed using freely available bioinformatics tools such as Mutation Taster with NCBI 37 and Ensembl 69 database release (29), PROVEAN (protein variation effect analyzer), and SIFT (sorting intolerant from tolerant) to evaluate the consequences of the identified mutations. In addition, results were compared with ExAc and 1000 Genomes variant databases to check the single-nucleotide polymorphism. In the current study, the cutoff value for PROVEAN and SIFT analysis was used as −2.5 and 0.05, respectively, for predicting the pathogenic/nonpathogenic variants.

Quantitative Real-Time PCR (qPCR) Analysis

DNA copy number changes of *EPAS1* in ESCC ($n = 80$) and noncancerous ($n = 30$) tissues were examined using QuantStudio 6 Flex Real-Time PCR System (Thermo Fisher Scientific, Waltham, MA, USA). Briefly, quantitative PCR (qPCR) was performed in a total volume of 20 μL reaction mixture containing 10 μL of DyNAmo Flash SYBR Green Master Mix (Bio-Rad, Gladesville, New South Wales, Australia), 1.5 μL of each 5 μmol/L forward and reverse primer, 3 μL of DNA at 50 ng/μL, and 4 μL of 0.1% DEPC-treated water as previously described (30).

For qPCR, first-strand cDNA was generated using DyNAmo™ cDNA Synthesis Kits (Qiagen) as previously

described (31). EPAS1 mRNA expression changes in ESCC samples were examined using QuantStudio 6 Flex Real-Time PCR System (Thermo Fisher Scientific). In short, qPCR was performed in a total volume of 20 μL reaction mixture containing 10 μL of DyNAmo Flash SYBR Green Master Mix (Bio-Rad), 1.5 μL of each 5 μmol/L forward and reverse primer, 1 μL of cDNA at 50 ng/μL, and 4 μL of 0.1% DEPC-treated water as previously described (30). The amplification efficiencies were normalized to that of multiple housekeeping genes, including β-actin, 18s, and glyceraldehyde 3-phosphate dehydrogenase (GAPDH). GAPDH and β-actin were selected based on consistent results. Results were presented as a ratio of expression (expression of *EPAS1* normalized by internal control *GAPDH* and *β-actin* expression) in ESCC tissue samples and cells. Fold changes were calculated according to a previously published protocol (32), and a fold change of more than 2 was considered as high *EPAS1* expression or amplification, a fold change of 1.0–2.0 was considered as no change, and a fold change of <1.0 was considered as low *EPAS1* expression or deletion.

Transfection of ESCC Cells With *EPAS1* siRNA Silencer and Scramble siRNA

KYSE70 and KYSE150 ESCC cells were seeded approximately at 2×10^4 cells/cm^2 into 24-well plate in the growth media (26). After 24 h of initial seeding, cells were transfected with *EPAS1* siRNA silencer (Qiagen) ($KYSE70^{-EPAS1}$ and $KYSE150^{-EPAS1}$) at 15-nM concentrations and with scramble siRNA (Qiagen) ($KYSE70^{+Scr}$ and $KYSE150^{+Scr}$) at 10-nM concentrations according to the manufacturer's guidelines. Briefly, 3 μL of the transfection reagent, Hiperfect (Qiagen), was added to the siRNAs and incubate for 5 min at room temperature to form the complexes. Then, cells were treated with the complex and used for functional assays. Cells treated with scrambled siRNA ($KYSE70^{+Scr}$ and $KYSE150^{+Scr}$) and transfection reagents (Hiperfect) alone ($KYSE70^{wildtype}$ and $KYSE150^{wildtype}$) were used as controls in the present study.

Western Blot Analysis

Total proteins were extracted from the cultured cells with lysis buffer (Bio-Rad) and quantitation by bovine serum albumin method. Afterward, total protein (30 μg) was separated by 15% sodium dodecyl sulfate–polyacrylamide gel electrophoresis (Bio-Rad) and transferred to polyvinylidene fluoride membranes (Bio-Rad) using Turbo Trans-blot transfer system (Bio-Rad). Then, the membrane was incubated with mouse monoclonal EPAS1 and GAPDH antibody (1:1,000) at 4°C overnight with gentle shaking. The membrane was then incubated with anti–mouse secondary antibody (1:2,000) at room temperature for 2 h. Finally, the blots were developed to detect protein bands according to the published protocol (33).

Cell Proliferation Assay

To examine the effect of EPAS1 on the proliferation of ESCC, cell proliferation assay was performed using cell counting kit-8 (CCK-8) (Sigma-Aldrich, St Louis, MO, USA) (34). Briefly, KYSE70 and KYSE150 cells were seeded in a flat-bottom 96-well plate at 1 × 104 cells/well. After 24 h of initial seeding, cells were treated with EPAS1 siRNA silencer and scramble siRNA as previously described (34). Then, the proliferation rate of EPAS1 siRNA-treated and controls cells was determined on days 0 to 3 with CCK-8 following manufacturer guidelines.

Colony Formation Assay

To determine the effect of EPAS1 manipulation on clonogenic capacity of ESCC, equal numbers (∼1,000) of cells (KYSE70 and KYSE150) were seeded in six-well plates and were then transfected with EPAS1 siRNA and scramble siRNA. Cells were grown (for 14–16 days) at 37°C in 5% carbon dioxide and saturation humidity until microscopic clones were noted in the plate. After that, the media was discarded, and cells were washed with a phosphate-buffered saline solution. The cells were then fixed with 70% cold ethanol for 15 min at room temperature. Subsequently, the clones were stained with crystal violet (0.5%) for 2 h at room temperature and washed with tap water. Finally, after being air-dried, images of the plates were taken, and clone formation rates were calculated as previously described (26).

Wound Healing Assay

To examine the effect of EPAS1 on the capacity of cells of ESCC to migrate for repairing, the scratch wound healing assay were used as previously reported (35). In short, KYSE70 and KYSE150 cells were grown in the medium until 70–80% confluence as a monolayer, and scratches were made using a 200-μL pipette tip across the center of culture plates. The cells were later treated with EPAS1 siRNA and scramble siRNA (control siRNA) and incubated for analysis of the migration of cells to heal the wound. Images were taken to monitor the changes among the cells type on days 0 to 2, and wound areas on different days of all cell types were recorded.

Invasion Assay

To investigate the silencing effect of EPAS1 on ESCC cells' *in vitro* cell penetration/invasion to a barrier, CultreCoat® 96-well basement membrane extract (BME)–coated cell invasion assay (Trevigen Inc., Gaithersburg, MD, USA) kit with basement membrane components was used following the protocol previously published (36). In brief, KYSE70 and KYSE150 cells were cultured to 80% confluence and passaged to a serum-free medium for 24 h. Then, the serum-starved cells were collected, and 50 μL (1×10^6/mL) of cell suspension was added to each well of 96-well top chamber. After that, the transfection complex consisting of EPAS1 siRNA and Hiperfect transfection reagent (Qiagen) was added to the top chamber to transfect the cells. Similarly, scramble siRNA and transfection reagent (Hiperfect) was added in wells to be used as control. Then, the complete growth media was added to the bottom chamber of the assay kit and incubated at 37°C in 5% carbon dioxide incubator for 48 h. After incubation, 100-μL cell dissociation solution/calcein AM was added to the bottom chamber, which allows internalization of calcein AM to the cells, and intracellular esterase cleaves it to produce calcein (a bright fluorophore). Finally, the fluorescence generated by the invaded cells was used to quantitate the number of invasive cells in each group with POLARstar Omega

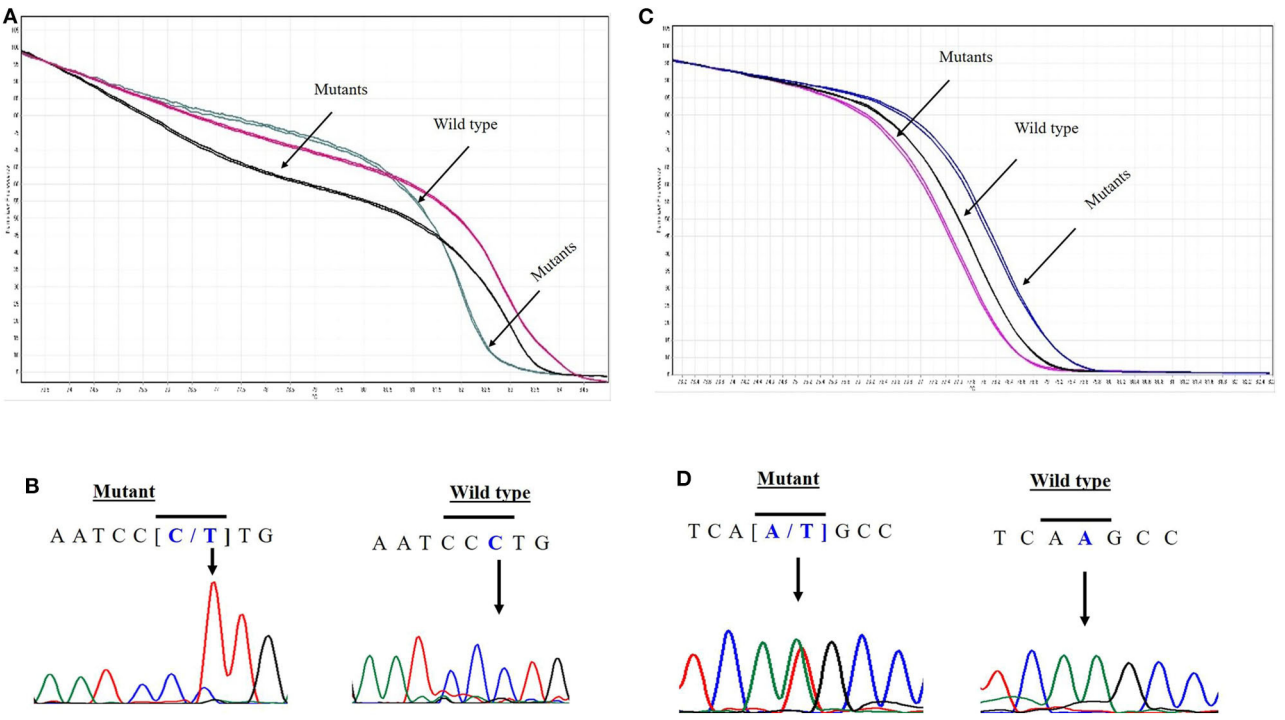

FIGURE 2 | Novel variants in *EPAS1* detected in ESCC tissues. Comparison of HRM curve analysis and Sanger sequencing of the variants identified in patients with ESCC. Representative HRM curve **(A)** and chromatograph **(B)** for the synonymous mutation c.1084C>T (L362L). Representative HRM curve **(C)** and chromatograph **(D)** for the frameshift variant c.1091_1092insT (K364Nfs*12).

multimode microplate reader (BMGLABTECH, Mornington, Victoria, Australia).

Statistical Analysis

Comparisons between variable groups were analyzed using the χ^2 test, likelihood ratio, and Fisher exact test. All the data were entered into a computer database, and the statistical analysis was executed using the Statistical Package for Social Sciences for Windows (version 25.0; IBM SPSS Inc., New York, NY, USA). Survival analysis was tested using Kaplan–Meier method. Results are shown as mean ± SD (standard deviation), and the significance level was taken at $p < 0.05$. $^{*}p < 0.05$, $^{**}p < 0.01$, and $^{***}p < 0.001$.

RESULTS

Identification of Novel *EPAS1* Mutations in ESCC Tissue Samples

EPAS1 mutant variants were detected in tissues based on the distinctive melting curve of HRM analysis and then confirmed with Sanger sequencing (**Figure 2**). In the present study, 7.5% ($n = 6$) of 80 patients had mutations in *EPAS1* sequence. There were eight variants (c.1084C>T, c.1099C>A, c.1145_1145delT, c.1093C>G, c.1121T>G, c.1137_1137delG, c.1135_1136insT, and c.1091_1092insT) identified in the coding region of *EPAS1* (**Table 1**). Among these mutations, four were frameshift (V382Gfs*12, A381Lfs*13, K379Ifs*6, and K364Nfs*12) mutations. No mutant variant was detected in noncancerous control tissues.

The consequences of nucleotides, as well as amino acid changes on protein features and functions, were predicted by computational analysis (**Table 1**). All the variants identified in the present study in *EPAS1* were predicted as deleterious or damaging on the functionality of EPAS1 protein in ESCC (**Table 1**). In addition, the detected variants are novel as the identified variants were not found in the ExAc and 1000 Genomes variant databases or in the PubMed database.

The associations of the *EPAS1* mutations with clinicopathological factors are summarized in **Table 2**. Clinicopathological factors such as site, size, differentiation, and pathological stages were not associated with *EPAS1* mutations. Mutations in *EPAS1* sequence correlated with patient's age ($p = 0.02$) and the presence of metastatic carcinoma in lymph node ($p = 0.05$). Overall, 10% ($n = 6/60$) of ESCCs with metastatic carcinoma in the lymph node had *EPAS1* mutations, whereas no mutation was detected in ESCC without lymph node metastasis.

EPAS1 DNA Changes and mRNA Deregulation in ESCC

In the present study, 45% ($n = 36$) of the 80 ESCC samples showed *EPAS1* DNA amplification, whereas 42.5% ($n = 34$) showed deletion in comparison to the noncancer tissue samples

TABLE 1 | Mutations detected in the sequence of *EPAS1* in esophageal squamous cell carcinoma.

Sample ID	Copy No. Change	mRNA expression	DNA change	Amino acid changes	Effect on protein features	*In silico* prediction		
						Mutation taster	*PROVEAN*	*SIFT*
P1	Amplification	High	c.1084C>T cDNA.1594C>T g.82922C>T	No	Protein features (might be) affected	Diseases causing	Neutral	Tolerated
P13	Amplification	High	c.1099C>A cDNA.1609C>A g.82937C>A	L367M	Amino acid sequence changed NMD	Diseases causing	Neutral Deleterious	Tolerated Deleterious
			c.1145_1145delT cDNA.1655_1655delT g.82983_82983delT	V382Gfs*12	Amino acid sequence changed Frameshift protein features (might be) affected			
P22	Deletion	No change	c.1093C>G cDNA.1603C>G g.82931C>G	P365A	Amino acid sequence changed	Diseases causing	Deleterious	Damaging
			c.1099C>A cDNA.1609C>A g.82937C>A	L367M	Amino acid sequence changed NMD			
			c.1145_1145delT cDNA.1655_1655delT g.82983_82983delT	V382Gfs*12	Amino acid sequence changed Frameshift protein features (might be) affected			
P29	Amplification	High	c.1099C>A cDNA.1609C>A g.82937C>A	L367M	Amino acid sequence changed Amino acid sequence changed	Diseases causing	Deleterious	Damaging
			c.1121T>G cDNA.1631T>G g.82959T>G	F374C				
			c.1137_1137delG cDNA.1647_1647delG g.82975_82975delG	A381Lfs*13	NMD amino acid sequence changed frameshift protein features (might be) affected splice site changes			
P78	Amplification	High	c.1135_1136insT cDNA.1645_1646insT g.82973_82974insT	K379Ifs*6	NMD Amino acid sequence changed Frameshift Protein features (might be) affected Splice site changes	Diseases causing	Deleterious	Damaging
			c.1099C>A cDNA.1609C>A g.82937C>A	L367M	Amino acid sequence changed			
P103	Deletion	Low	c.1091_1092insT cDNA.1601_1602insT g.82929_82930insT	K364Nfs*12	NMD Amino acid sequence changed Frameshift Protein features (might be) affected Splice site changes	Diseases causing	Deleterious	Damaging

NMD, nonsense-mediated mRNA decay.

(**Table 3**). The rest of the samples (12.5%; $n = 10$) did not exhibit any changes in *EPAS1* DNA copies (**Table 3**). The distribution of *EPAS1* DNA in cancer and noncancer tissue samples is shown in **Figure 3A**. A significantly higher *EPAS1* DNA expression was noted in cancer samples (1.706 ± 0.209) when compared with noncancerous (0.569 ± 0.078) samples.

The associations of *EPAS1* DNA changes with clinicopathological parameters of the patients with ESCC are presented in **Table 3**. We observed that *EPAS1* DNA amplification significantly ($p < 0.05$) correlated with the tumor site and pathological stages in patients with ESCC. ESCCs located at the lower portion of the esophagus had significantly more *EPAS1* DNA amplification in comparison to those from the upper or middle part of the esophagus (63.0 vs. 35.8%; $p = 0.03$). Higher frequency of patients with ESCC having tumor stage I and IV showed *EPAS1* DNA amplification, whereas the majority of the patients with ESCC having tumor stages II and III showed *EPAS1* DNA deletion ($p = 0.02$).

TABLE 2 | Correlation of *EPAS1* mutations with clinicopathological features of patients with esophageal squamous cell carcinoma.

Features	Number	Negative	Positive	P-value
Total patients		80	74 (92.5%)	6 (7.5%)
Sex				
Male	67 (83.8%)	62 (92.5%)	5 (7.5%)	0.66
Female	13 (16.2%)	12 (92.3%)	1 (7.7%)	
Age				
≤60	54 (67.5%)	48 (88.9%)	6 (11.1%)	**0.02**
>60	26 (32.5%)	26 (100%)	0 (0%)	
Site				
Upper or middle	53 (66.3%)	50 (94.3%)	3 (5.7%)	0.32
Lower	27 (33.7%)	24 (88.9 %)	3 (11.1%)	
Size (cm)				
≤6	31 (38.7%)	29 (93.5%)	2 (6.5%)	0.57
>6	49 (61.3%)	45 (91.8%)	4 (8.2%)	
Differentiation				
Well	24 (30.0%)	23 (95.8%)	1 (4.2%)	0.65
Moderate	39 (48.8%)	36 (93.3%)	3 (7.7%)	
Poor	17 (21.2%)	15 (88.2%)	2 (11.8%)	
T-stages				
I & II	6 (7.5%)	5 (83.3%)	1 (16.7%)	0.38
III & IV	74 (92.5%)	69 (93.2%)	5 (6.8%)	
Lymph-node metastasis				
Presence	60 (75.0%)	54 (90.0%)	6 (10.0%)	**0.05**
Absence	20 (25.0%)	20 (100%)	0 (0.0%)	
Distant metastasis				
Yes	5 (6.3%)	4 (80.0%)	1 (20.0%)	0.33
No	75 (93.7%)	70 (93.3%)	5 (6.7%)	
Stage				
I & II	22 (27.5%)	21 (95.5%)	1 (4.5%)	0.47
III & IV	58 (72.5%)	53 (91.4%)	5 (8.6%)	

Bold values indicates p-value of 0.05 or below.

TABLE 3 | Correlation of *EPAS1* DNA variations with clinicopathological features of patients with esophageal squamous cell carcinoma.

Features	Number	Amplification	Deletion	No change	P-value
Total patients	80	36 (45.0%)	34 (42.5%)	10 (12.5%)	–
Sex					
Male	67 (83.8%)	33 (49.3%)	26 (38.8%)	8 (11.9%)	0.19
Female	13 (16.2%)	3 (23.1%)	8 (61.5%)	2 (15.4%)	
Age					
≤60	54 (67.5%)	22 (40.7%)	25 (46.3%)	7 (13.0%)	0.53
>60	26 (32.5%)	14 (53.9%)	9 (34.6%)	3 (11.5%)	
Site					
Upper or middle	53 (66.3%)	19 (35.8%)	25 (47.2%)	9 (17.0%)	**0.03**
Lower	27 (33.7%)	17 (63.0 %)	9 (33.3%)	1 (3.7%)	
Size (cm)					
≤6	31 (38.7%)	12 (38.7%)	12 (38.7%)	7 (22.6%)	0.09
>6	49 (61.3%)	24 (49.0%)	22 (44.9%)	3 (6.1%)	
Differentiation					
Well	24 (30.0%)	12 (50.0%)	9 (37.5%)	3 (12.5%)	0.89
Moderate	39 (48.8%)	18 (46.2%)	16 (41.0%)	5 (12.8%)	
Poor	17 (21.2%)	6 (35.2%)	9 (53.0%)	2 (11.8%)	
T-stages					
I	3 (3.8%)	2 (66.7%)	1 (33.3%)	–	**0.02**
II	3 (3.8%)	1 (33.3%)	2 (66.7%)	–	
III	53 (66.2%)	21 (39.6%)	28 (52.8%)	4 (7.6%)	
IV	21 (26.2%)	12 (57.1%)	3 (14.3%)	6 (28.6%)	
Lymph-node metastasis					
Presence	60 (75.0%)	29 (48.3%)	22 (36.7%)	9 (15.0%)	0.14
Absence	20 (25.0%)	7 (35.0%)	12 (60.0%)	1 (5.0%)	
Distant metastasis					
Yes	5 (6.3%)	2 (40.0%)	3 (60.0%)	-	0.43
No	75 (93.7%)	34 (45.3%)	31 (41.3%)	10 (13.4%)	
Stage					
I & II	22 (27.5%)	8 (36.4%)	13 (59.1%)	1 (4.5%)	0.12
III & IV	58 (72.5%)	28 (48.3%)	21 (36.2%)	9 (15.5%)	

Bold values indicates p-value of 0.05 or below.

The expressions of *EPAS1* mRNA in cancer and nonneoplastic tissue samples were presented in **Figure 3B**. The distribution of *EPAS1* mRNA expression in cancer tissues was significantly (1.656 ± 0.193 vs. 0.573 ± 0.078; $p < 0.05$) higher when compared with nonneoplastic tissue samples (**Figure 3B**). In addition, the mRNA expression ratio of *EPAS1* was significantly higher in cancer in comparison to those in noncancer tissue samples (1.656 ± 0.12 vs. 0.573 ± 0.07; $p < 0.001$). Among the patients' samples used in this study, 53.7% ($n = 43/80$) had higher *EPAS1* mRNA expression, whereas the remaining 20% ($n = 16/80$) exhibited *EPAS1* mRNA lower expression. The rest of the samples ($n = 21/80$; 26.3%) had no changes in *EPAS1* mRNA expression (**Table 4**). The association of *EPAS1* mRNA expression and the clinicopathological parameters of patients with ESCC were analyzed (**Table 4**). It was noted that *EPAS1* mRNA expression was not associated with the clinical–pathological parameters of patients with ESCC (**Table 4**; $p > 0.05$).

The number of *EPAS1* DNA in cancer cells is presented in **Figure 3C**. *EPAS1* DNA numbers (1.4 ± 0.07, 2.10 ± 0.10, 2.41 ± 0.12) in ESCC cancer cell lines KYSE70, KYSE450 and HKESC-1, respectively, are higher when compared with that of nonneoplastic keratinocyte HaCaT (1.01 ± 0.05) cells (**Figure 3C**). Similarly, the mRNA expression of *EPAS1* cancer cells (KYSE70, KYSE450, and HKESC-1) is significantly higher (1.98 ± 0.09, 2.24 ± 0.11, 2.45 ± 0.12, respectively) than noncancerous HaCaT (1.2 ± 0.06) cells (**Figure 3D**). However, KYSE520 and KYSE150 did not show any significant difference in *EPAS1* DNA number and mRNA expression when compared with nonneoplastic keratinocyte HaCaT cells (**Figures 3C,D**).

Association of *EPAS1* Molecular Deregulation With Patient's Survival

Finally, the prognostic significance of *EPAS1* in patients with ESCC was analyzed. The median overall follow-up of patients with ESCC used in this study was 60 months and the survival rates correlated with the pathological stages of cancer ($p = 0.0001$). Patients with ESCCs harboring mutations in *EPAS1* sequence have poorer survival rates than the patients without *EPAS1* mutations (570.89 ± 205.02 vs. $2{,}097.15 \pm 332.09$ days; $p = 0.46$) (**Figure 4A**). Patients with ESCC having *EPAS1* DNA

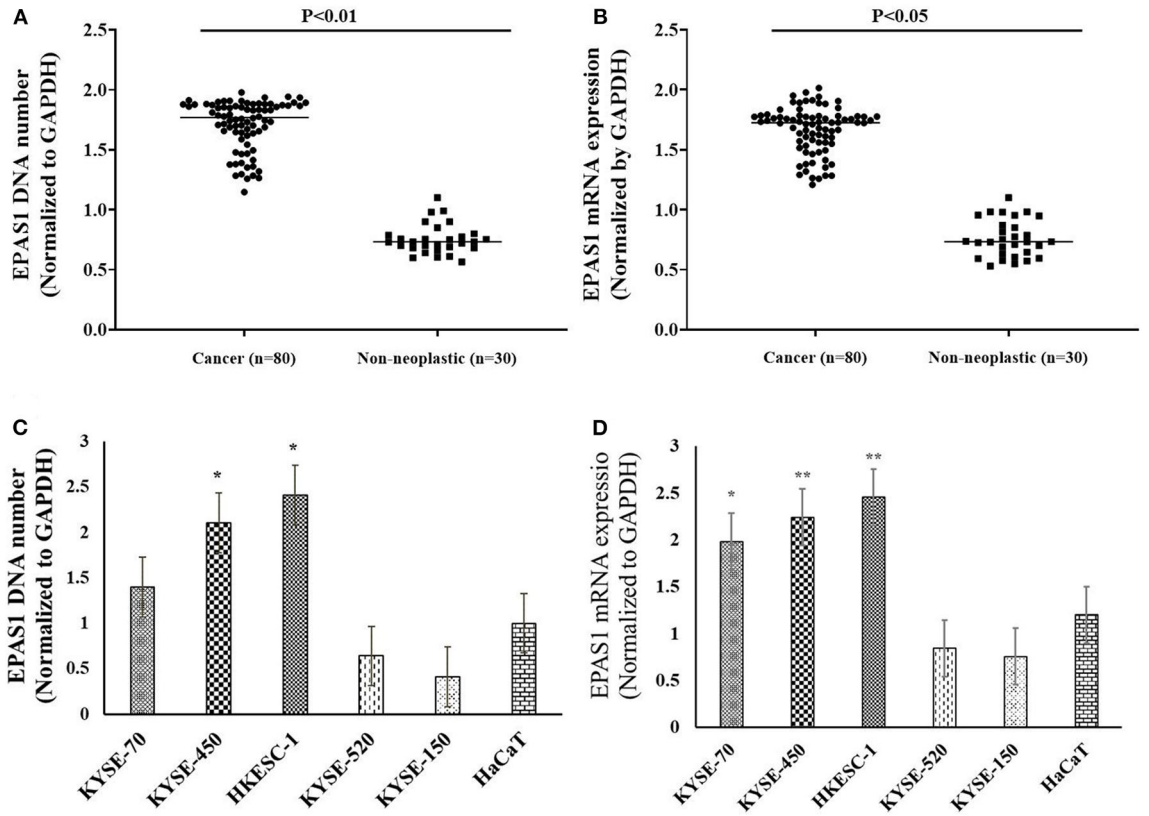

FIGURE 3 | *EPAS1* DNA number and mRNA expression profile in patients with ESCC and cell lines. **(A)** Patients with ESCC exhibited significant amplifications of *EPAS1* DNA when compared with noncancerous samples ($p < 0.01$). **(B)** Similarly, a significant overexpression of *EPAS1* mRNA in ESCC was noted in comparison to that of noncancerous tissues ($p < 0.05$). **(C)** Cell lines showed higher or lower *EPAS1* DNA number when compared to that of noncancerous keratinocyte (HaCaT) cells. **(D)** Higher or lower *EPAS1* mRNA was noted in ESCC cancer cells when compared with nonneoplastic HaCaT cells. Results are shown as mean ± SD, and significance level was taken at $p < 0.05$. *$p < 0.05$, and **$p < 0.01$.

number amplification showed short survival when compared with that of *EPAS1* DNA deletion (1,568.62 ± 515.31 vs. 2,239.18 ± 489.48 days; $p = 0.2$), although the difference in survival time between the groups did not reach statistical significance (**Figure 4B**). On the other hand, the survival of patients with stage III ESCC having *EPAS1* DNA amplification showed a significant reduction in patient survival compared to those of stages III patients with *EPAS1* DNA deletion (873.79 ± 576.85 vs. 1,936.63 ± 622.19 days, $p = 0.04$) (**Figure 4C**).

Association of *EPAS1* Mutations, DNA Alteration, and mRNA Expression in Patients With ESCC

The relationships of *EPAS1* mutations, DNA number, and mRNA expression in patients with ESCC were analyzed (**Figure 5**). ESCCs bearing *EPAS1* mutations showed significantly higher DNA number (1.736 ± 0.241 vs. 1.701 ± 0.204) in comparison to those without the mutation (**Figure 5A**). Similarly, ESCC with *EPAS1* mutations exhibited significant overexpression (1.741 ± 0.084 vs. 1.564 ± 0.192) of *EPAS1* mRNA level when compared with those without the mutation (**Figure 5B**).

A statistically significant positive correlation was noted between *EPAS1* DNA number amplification and mRNA overexpression ($r = 0.468$; $p = 0.01$, Fisher exact test). In addition, 84% (30/36) of ESCCs having *EPAS1* DNA amplification had overexpression of *EPAS1* mRNA level. Similarly, *EPAS1* mRNA downregulation was noted in 59% ($n = 20$) of the 34 ESCCs with *EPAS1* DNA deletion (**Figure 5C**). Moreover, *EPAS1* mRNA expression changes notably with the changes of *EPAS1* DNA variations in ESCC (**Figure 5D**). In addition, The *EPAS1* mRNA expression changes were also correlated with *EPAS1* DNA copy number variations in ESCC ($p = 0.05$).

Suppression of *EPAS1* Decreases the Proliferation and Colony Formation Capacity of Colon Cancer Cells

The effects of EPAS1 manipulation on ESCC cell proliferation, invasion, and migration were examined followed by *EPAS1* silencing using *EPAS1* siRNA. For cell proliferation, viable cells from KYSE70^{-EPAS1}, KYSE150^{-EPAS1}, KYSE70^{+Scr}, KYSE150^{+Scr}, KYSE70^{wildtype}, and KYSE150^{wildtype} cell groups were measured on days 0–3. EPAS1 suppressive cells, KYSE70^{-EPAS1} and KYSE150^{-EPAS1}, showed a significant decrease in cell proliferation when compared with

TABLE 4 | Correlation of *EPAS1* mRNA expression with clinicopathological features of patients with esophageal squamous cell carcinoma.

Features	Number	High	Low	No change	P-value
Total patients	80	43 (53.7%)	16 (20.0%)	21 (26.3%)	–
Sex					
Male	67 (83.8%)	39 (58.2%)	13 (19.4%)	15 (22.4%)	0.14
Female	13 (16.2%)	4 (30.8%)	3 (23.1%)	6 (46.1%)	
Age					
≤60	54 (67.5%)	31 (57.4%)	10 (18.5%)	13 (24.1%)	0.63
>60	26 (32.5%)	12 (46.2%)	6 (23.1%)	8 (30.7%)	
Site					
Upper or middle	53 (66.3%)	26 (49.1%)	12 (22.6%)	15 (28.3%)	0.48
Lower	27 (33.7%)	17 (63.0 %)	4 (14.8%)	6 (22.2%)	
Size (cm)					
≤6	31 (38.7%)	13 (41.9%)	7 (22.6%)	11 (35.5%)	0.21
>6	49 (61.3%)	30 (61.2%)	9 (18.4%)	10 (20.4%)	
Differentiation					
Well	24 (30.0%)	15 (62.5%)	4 (16.7%)	5 (20.8%)	0.75
Moderate	39 (48.8%)	21 (53.8%)	8 (20.5%)	10 (25.7%)	
Poor	17 (21.2%)	7 (41.2%)	4 (23.5%)	6 (35.3%)	
T-stages					
I & II	6 (7.5%)	2 (33.3%)	1 (16.7%)	3 (50.0%)	0.38
III & IV	74 (92.5%)	41 (55.4%)	15 (20.3%)	18 (24.3%)	
Lymph-node metastasis					
Presence	60 (75.0%)	34 (56.6%)	13 (21.7%)	13 (21.7%)	0.26
Absence	20 (25.0%)	9 (45.0%)	3 (15.0%)	8 (40.0%)	
Distant metastasis					
Yes	5 (6.3%)	2 (40.0%)	1 (20.0%)	2 (40.0%)	0.75
No	75 (93.7%)	41 (54.7%)	15 (20.0%)	19 (25.3%)	
Stage					
I & II	22 (27.5%)	11 (50.0%)	3 (13.6%)	8 (36.4%)	0.39
III & IV	58 (72.5%)	32 (55.2%)	13 (22.4%)	13 (22.4%)	

control groups ($KYSE70^{+Scr}$, $KYSE150^{+Scr}$, $KYSE70^{wildtype}$, and $KYSE150^{wildtype}$), respectively (**Figures 6A,B**). For example, significant [46.50% ($p < 0.05$), 49.78% ($p < 0.01$), and 53.41% ($p < 0.001$)] inhibitions of $KYSE70^{-EPAS1}$ cells proliferation were noted on days 1, 2, and 3, respectively, in comparison to that of $KYSE70^{+Scr}$ cells (**Figure 6A**). Similar results were noted in the case of $KYSE150^{-EPAS1}$, exhibiting 39.06%, 40.99% ($p < 0.05$), and 59.72% ($p < 0.001$) inhibition on days 1, 2, and 3, respectively, in comparison to that of $KYSE150^{+Scr}$ cells (**Figure 6B**).

Silencing of EPAS1 caused a significant reduction of clonogenic capacity of ESCC cells ($KYSE70^{-EPAS1}$ and $KYSE150^{-EPAS1}$) in comparison to the controls ($KYSE70^{+Scr}$ and $KYSE150^{+Scr}$) and nontransfected wild-type ($KYSE70^{wildtype}$ and $KYSE150^{wildtype}$) ESCC cells (**Figures 6C,D**). A 55.85% reduction of colony formation in $KYSE70^{-EPAS1}$ was observed in comparison to the control $KYSE70^{+Scr}$ cells (**Figure 6C**; $p < 0.01$). Similarly, 43.32% reduction in colony formation capacity was noted by the $KYSE150^{-EPAS1}$ cells when compared to that of $KYSE150^{+Scr}$ control cells (**Figure 6D**; $p < 0.05$).

Silencing of EPAS1 Reduced Wound Healing, Migration, and Invasion of ESCC Cells

The ESCC cells with reduced EPAS1 expression ($KYSE70^{-EPAS1}$ and $KYSE150^{-EPAS1}$) cells showed significant ($p < 0.01$) reduction in wound healing, invasion, and migration capacity when compared with the control and nontransfected wild-type cancer cells (**Figure 7**). $KYSE70^{-EPAS1}$ and $KYSE150^{-EPAS1}$ ESCC cells had lower cell migration potential than the controls ($KYSE70^{+Scr}$ and $KYSE150^{+Scr}$) and wild-type ($KYSE70^{wildtype}$ and $KYSE150^{wildtype}$) cells as they healed the created scratch slowly when compared to their counterpart (**Figures 7A,B**). $KYSE70^{-EPAS1}$ and $KYSE150^{-EPAS1}$ cells took more time in healing the wounds, whereas nontreated and control cells took less time to heal the wounds. Similarly, $KYSE70^{-EPAS1}$ and $KYSE150^{-EPAS1}$ had reduced barrier penetration and migration potential in BME-coated invasion chamber when compared with control and nontreated cancer cells (**Figures 7C,D**). The relative fluorescence unit (which is proportional to the BME-barrier invading cells) from $KYSE70^{-EPAS1}$ and $KYSE150^{-EPAS1}$ cells was significantly less in comparison to

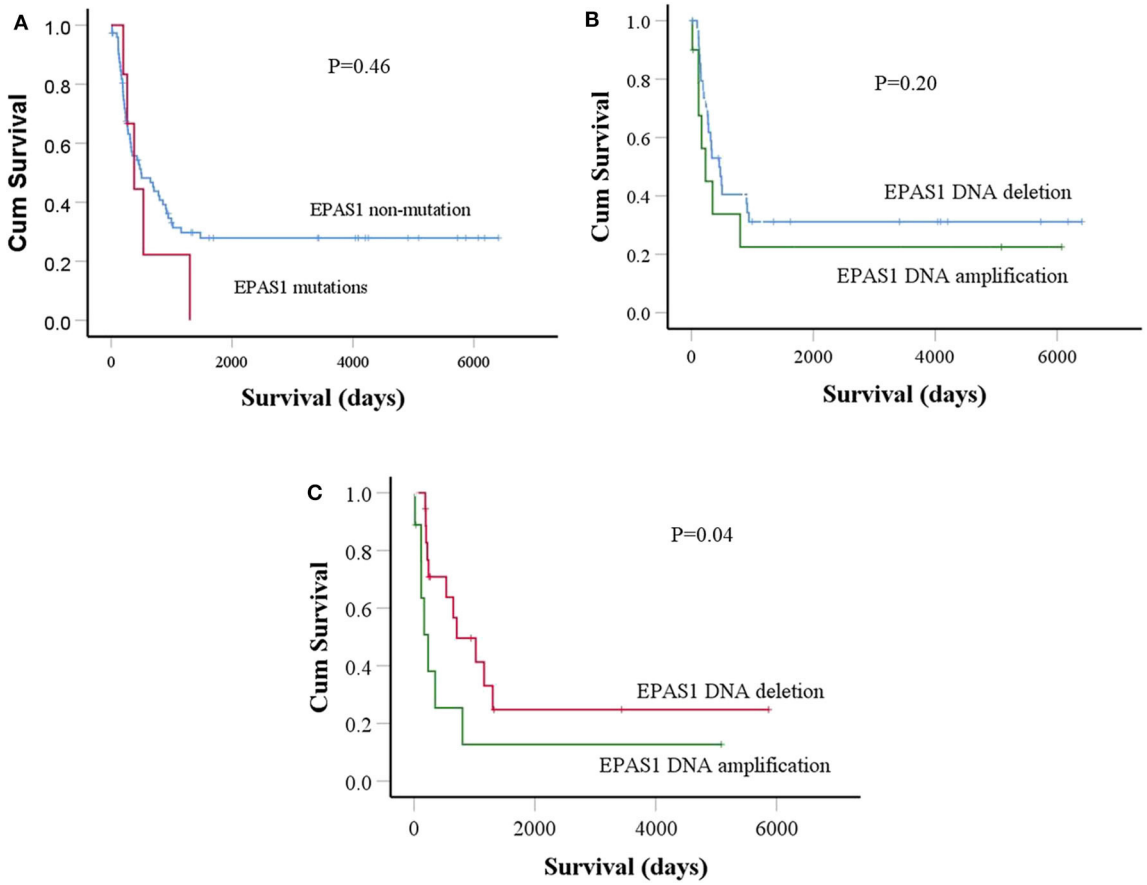

FIGURE 4 | Prognostic significance of *EPAS1* dysregulation in ESCC. **(A)** The trends of *EPAS1*-mutated positive patients had shorter survival rates compared to the nonmutated patients. However, the difference did not reach statistical significance level ($p = 0.46$). **(B)** Patients with *EPAS1* DNA amplification had poorer survival than *EPAS1* DNA deletion ($p = 0.20$). **(C)** In stage III patients with ESCC, the survival rates of patients having *EPAS1* DNA amplification is significantly poor when compared to that of *EPAS1* DNA deletion ($p = 0.04$).

that of KYSE70^{+Scr} and KYSE150^{+Scr} and KYSE70^{wildtype} and KYSE150^{wildtype} cells. KYSE70^{-EPAS1} cells showed 50% reduction of invasion and migration when compared to that of KYSE70^{+Scr} cells (**Figure 7C**; $p < 0.05$), whereas KYSE150^{-EPAS1} cells exhibited 55.32% reduction of invasion and migration in comparison to that of KYSE150^{+Scr} cells (**Figure 7D**; $p < 0.01$).

DISCUSSION

This study reported the molecular dysregulation, its clinical significance, and functional insights of *EPAS1* in the pathogenesis of ESCC. The results implied that *EPAS1* plays an important role in carcinogenesis of ESCC through regulation of cellular proliferation, migration, and invasion and thus acts as an oncogene.

Mutations of *EPAS1* has been identified in various cancers such as in paraganglioma (21), pheochromocytoma (12), and pancreatic carcinomas (22). In addition, data analysis from the International Cancer Genome Consortium (ICGC) revealed that mutations in *EPAS1* are common in many human malignancies, including esophageal cancer (adenocarcinoma) (https://dcc.icgc.org/). It was shown that 23.72% ($n = 97/409$) of patients with esophageal adenocarcinoma had somatic mutations in *EPAS1*. However, there are no data available regarding the mutational status of *EPAS1* in ESCC in the ICGC database. In the present study, we have detected *EPAS1* mutations in 7.5% ($n = 6/80$) patients with ESCC. The computational analysis revealed that the variants identified in the current study are novel and could have the potential to affect the functionality of the protein. The four frameshift variants (V382Gfs*12, A381Lfs*13, K379Ifs*6, and K364Nfs*12) may cause NMD, resulting in strongly truncated nonfunctional protein production. However, further functional studies with these variants are needed to confirm their roles in generating NMD or truncated protein product. The other variants (c.1099C>A, c.1093C>G, c.1121T>G, and c.1091A>T) may cause a change in the primary structure of the protein and may lead nonfunctional/overfunctional protein as they showed deleterious/diseases causing effects on protein in computational prediction. Therefore, further studies are warranted to validate the functional implications of the variants identified in the present study.

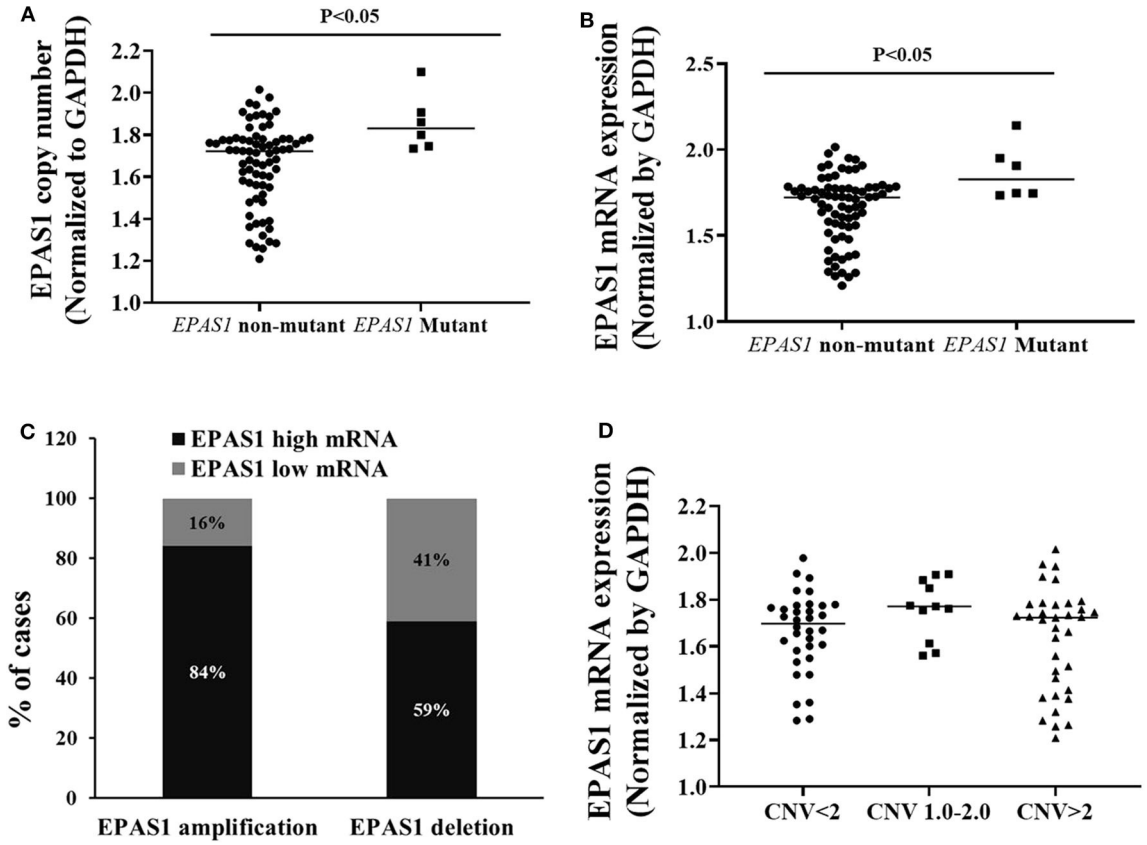

FIGURE 5 | Relationship of *EPAS1* molecular dysregulation in ESCC. **(A)** *EPAS1*-mutated samples showed significant amplification of DNA number in comparison to that of nonmutated samples ($p < 0.05$). **(B)** Similarly, *EPAS1*-mutated samples exhibited significant higher expression (mRNA) when compared to that of nonmutated tissue samples ($p < 0.05$). **(C)** Association of *EPAS1* DNA number changes and mRNA expression. RT-qPCR analysis revealed that *EPAS1* DNA number amplification significantly correlated with mRNA overexpression ($p < 0.01$). A 84% patients having *EPAS1* DNA amplification showed mRNA overexpression whereas 59% patients with *EPAS1* DNA deletion showed mRNA overexpression. **(D)** Distribution of *EPAS1* mRNA expression vs. *EPAS1* DNA number in patients with ESCC. Patients with DNA number greater 2 showed higher mRNA expression and DNA number <2 showed lower *EPAS1* mRNA expression.

This is the first study reporting *EPAS1* mutations in patients with ESCC and their clinical implications. The association of *EPAS1* mutations with the presence of lymph node metastasis indicates that mutations in *EPAS1* sequence could be predictive makers for lymph node metastasis. Also, younger patients (≤60 years old) are predicted to be more likely to harbor *EPAS1* mutations. In addition, the trends of poorer survival rates (mutant = 570 days vs. nonmutant = 2,097 days) of patients with ESCC having *EPAS1* mutations could help to predict the clinical outcome of these patients. However, the difference did not reach statistical significance, maybe due to the low number ($n = 6$) of positive populations.

DNA copy number alterations and dysregulated expression of genes are common in human cancers and are being used as biomarkers of the disease (37). Dysregulation of *EPAS1* is associated with the carcinogenesis of different types of cancers such as lung carcinoma (8), renal cell carcinoma (9), hepatocellular carcinoma (10), neuroblastoma (11), pheochromocytoma (12), glioma (13), and colorectal adenocarcinoma (14). Tumor-promoting oncogenic roles of *EPAS1* was noted in the pathogenesis of lung carcinoma, renal cell carcinoma, liver neuroblastoma, pheochromocytoma, and so on (8–12), whereas other studies reported the tumor-suppressive properties in the pathogenesis of glioma, colorectal carcinoma, and neuroblastoma (13, 14, 38). For example, EPAS1 expression is associated with a better outcome of patients with neuroblastoma and low-risk tumors (38). In this study, amplification or deletion of *EPAS1* DNA number (87.5%; $n = 70/80$) followed by mRNA higher or lower expression (73.7%; $n = 59/80$) in tissue samples indicates its regulatory roles in progression of ESCC. Several studies also noted higher or lowered expression of *EPAS1* both in mRNA and protein levels in patients with other cancers (14–16, 39). The present study for the first time reported the deregulation of *EPAS1* in ESCCs, which are in consistence with other studies.

The association of *EPAS1* DNA number amplification or deletion with tumor site and tumor stages indicated the heterogeneous nature of ESCC. The biological aggressiveness, surgical accessibility, and molecular makeup of ESCC from

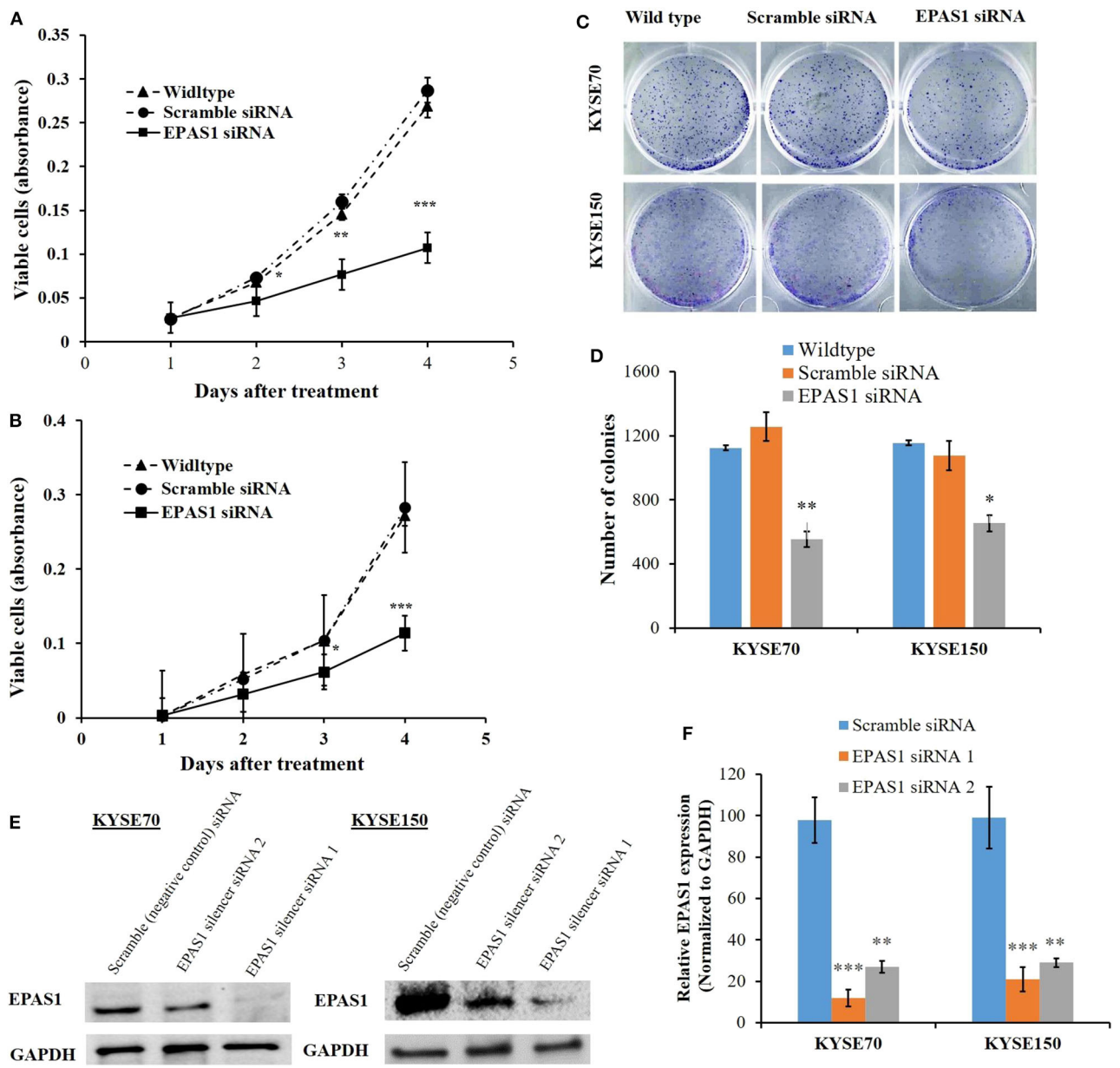

FIGURE 6 | EPAS1 suppression inhibited ESCC cells proliferation and colony formation. *in vitro* suppression of EPAS1 using siRNA in KYSE70 **(A)** and KYSE150 **(B)** cells caused significant reduction in proliferation at different time points when compared with untreated and scramble control cell groups. In addition, silencing of EPAS1 induced significant reduction of colony formation capacity KYSE70 **(C)** and KYSE150 **(D)** cells in comparison to that of control groups. **(E)** Expression of EPAS1 protein in KYSE70 and KYSE150 cells followed by siRNA treatment. **(F)** Relative expression of EPAS1 in KYSE70 and KYSE150 cells followed. EPAS1 siRNA1 ans siRNA2 significantly inhibited the expression of EPAS1 in KYSE70 and KYSE150 cells. Results are shown as mean ± SD and significance level was taken at $p < 0.05$. $^{*}p < 0.05$, $^{**}p < 0.01$, and $^{***}p < 0.001$.

different sites of the esophagus, upper site (proximal), and the middle/lower site (distal) are different (40). Thus, it is not surprising that *EPAS1* DNA number is different in these two portions of the esophagus. In addition, the genetic and epigenetic makeup of different tumor stages is different (40). Thus, ESCC of different T stages showed a different level of *EPAS1* DNA number in the present study. Finally, the poorer survival rates of patients with stage III ESCC having *EPAS1* DNA amplification implied the prognostic significance of *EPAS1* in ESCC (**Figure 4C**). Therefore, *EPAS1* DNA changes could have the potential to be used as a prognostic marker for patients with ESCC.

DNA copy number aberrations are frequent acquired changes in cancers, which lead to abnormal expression of genes and play crucial roles in pathogenesis and progression of ESCC (40, 41). The correlation of *EPAS1* DNA number

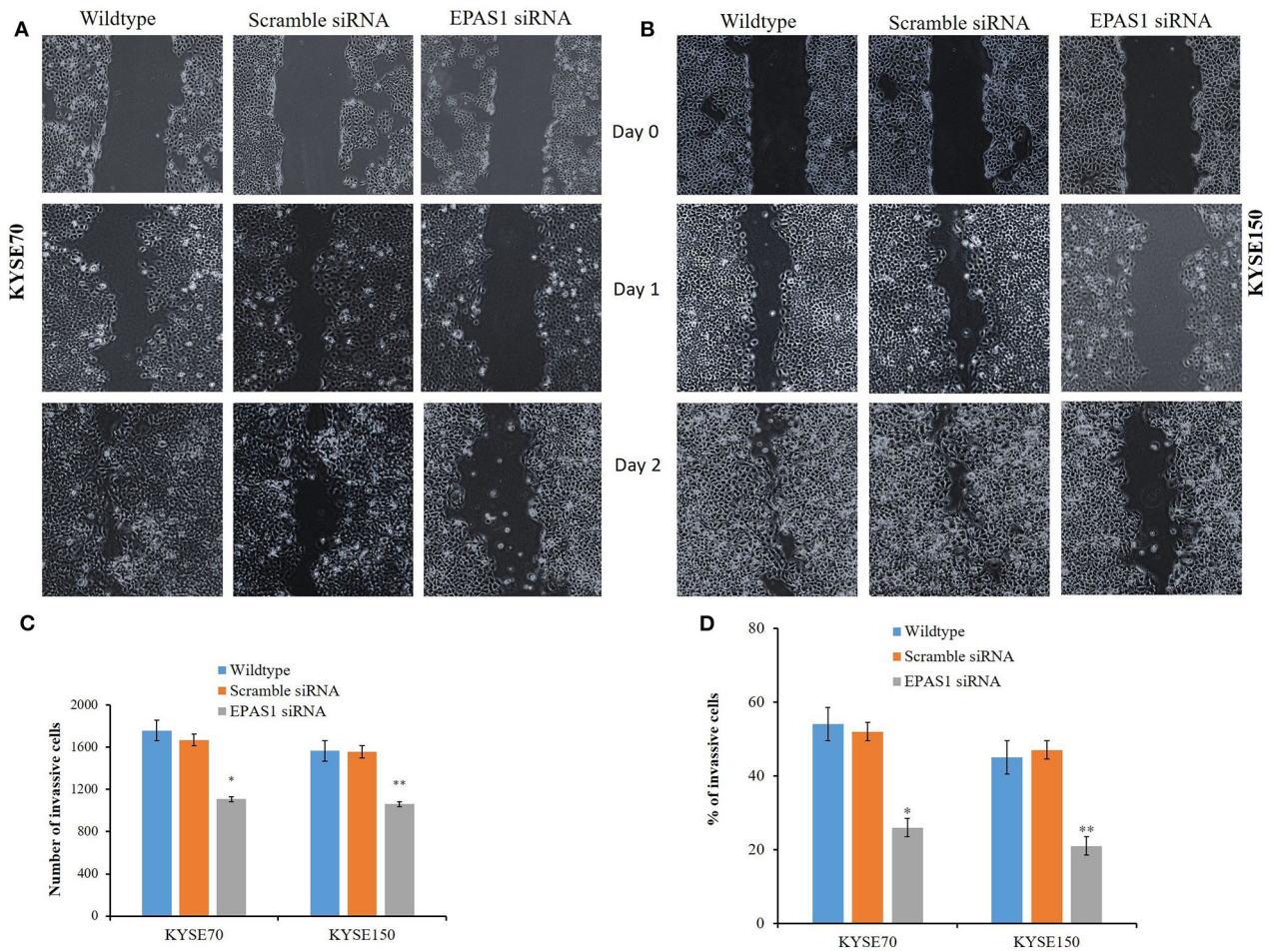

FIGURE 7 | Silencing of EPAS1 causes reduction of wound healing, invasion and migration of ESCC cells. Silencing of EPAS1 causes inhibition of wound healing of ESCC cells as suppression of EPAS1 induced reduction of migration capacity of KYSE70 **(A)** and KYSE150 **(B)** cells, thereby healing the wound more slowly in comparison to that of untreated wild type and scramble control cells. Similarly, a significantly reduced population of KYSE70 **(C)** and KYSE150 **(D)** cells exhibited invasion and migration followed by suppression of *EPAS1* when compared to that of untreated or scramble control cells. Results are shown as mean ± SD, and significance level was taken at $p < 0.05$. $^{*}p < 0.05$ and $^{**}p < 0.01$.

amplification and increased mRNA expression in ESCC in the present study indicated that hypoxic tumor niche induces alterations of *EPAS1*, which in turn can promote carcinogenesis. Furthermore, DNA amplification and higher mRNA expression in ESCC harboring mutations indicated the concerted aberration of *EPAS1* in ESCC. Thus, the molecular dysregulation of *EPAS1* detected in the present study could stimulate carcinogenesis.

The functional roles of *EPAS1* in ESCC have been studied, followed by siRNA-mediated silencing in ESCC cells. A significant reduction of cancer cell proliferation and colony formation capacity in comparison to that of untreated wild-type and scramble control groups were noted (**Figure 6**). The findings of the present study are in concurrence with previous reports on various types of cancers, including clear cell renal cell carcinoma, pancreatic adenocarcinoma, and breast carcinoma (9, 42, 43). Silencing of *EPAS1* via siRNA induced reduced cell proliferation, increased apoptosis, and generated smaller tumor in a mouse model of pancreatic carcinoma (43), whereas inhibition of EPAS1 with a small molecular target (PT2399) causes tumor regression in a preclinical mouse model of primary and metastatic clear cell renal cell carcinoma (9). Our results and available information in the literature implied that *EPAS1* could be a potential target for developing effective therapeutics for better management of patients with cancer. However, some other studies reported tumor inhibitory functionality of EPAS1 in various cancer models (38, 44). For example, treatment with EPAS1 inhibitors did not block *in vitro* neuroblastoma cell proliferation or xenograft growth in the mouse model (38). Furthermore, HIF-2α inhibited *in vivo* growth of cells from high-grade soft tissue sarcomas. Loss of HIF-2α promoted proliferation of sarcoma and increased calcium and mTORC1 signaling in undifferentiated pleomorphic sarcoma and dedifferentiated liposarcoma (44).

EPAS1 promotes angiogenesis in mouse models by inducing both vascular endothelial growth factor and its receptor Fms related tyrosine kinase 1 expression in endothelial cells (45). Furthermore, suppression of *EPAS1* using shRNA in breast carcinoma cells reduced the cellular growth and inhibited angiogenesis (42). Inconsistent with the previous study, we noted that silencing of *EPAS1* inhibited the wound healing and migration capacity when compared to that of untreated and scramble control groups of ESCC cells. Similarly, suppression of *EPAS1* showed a significant reduction in barrier penetration and invasion, indicating its lower metastatic potential in comparison to that of control ESCC cells. Thus, the therapeutic strategies targeting EPAS1 could have the potential for effective inhibition of cancer cell growth, migration, and invasion.

To conclude, the present study for the first time detected multiple novel *EPAS1* mutations in ESCC. These mutations may contribute to the altered expression and/or structural and functional changes of the gene, which in turn could play an essential role in the pathogenesis of the disease. In addition, the association of molecular dysregulation in DNA number, mRNA expression, and mutations in ESCC along the clinical significance of the gene has provided critical insights of tumor-promoting properties of EPAS1 in the pathogenesis of ESCC. Therefore, the results of this study will enrich the current understanding of *EPAS1* in directing carcinogenesis of ESCC, as well as opening new opportunities for the development of novel therapeutic strategies against cancer.

DATA AVAILABILITY STATEMENT

The raw data supporting the conclusions of this article will be made available by the authors, without undue reservation.

ETHICS STATEMENT

The studies involving human participants were reviewed and approved by Ethical approval for this work has been obtained from the Griffith University Human Research Ethics Committee (MED/19/08/HREC). The patients/participants provided their written informed consent to participate in this study.

AUTHOR CONTRIBUTIONS

FI carried out most of the experiments and draft the manuscript. VG plan the project and revised the manuscript. SL manage the clinical data. AL analyze the clinical data and revised the manuscript. SP supervise and collect the funding for the project. All authors contributed to the article and approved the submitted version.

FUNDING

The project was supported by the new staff start-up funding, Faculty of Medicine, The University of Queensland, Queensland, Australia.

REFERENCES

1. Ke Q, Costa M. Hypoxia-inducible factor-1 (HIF-1). *Mol Pharmacol*. (2006) 70:1469–80. doi: 10.1124/mol.106.027029
2. Jokilehto T, Jaakkola PM. The role of HIF prolyl hydroxylases in tumour growth. *J Cell Mol Med*. (2010) 14:758–70. doi: 10.1111/j.1582-4934.2010.01030.x
3. Webb JD, Coleman ML, Pugh CW. Hypoxia, hypoxia-inducible factors (HIF), HIF hydroxylases and oxygen sensing. *Cell Mol Life Sci*. (2009) 66:3539–54. doi: 10.1007/s00018-009-0147-7
4. Dmitriev PM, Wang H, Rosenblum JS, Prodanov T, Cui J, Pappo AS, et al. Vascular changes in the retina and choroid of patients with EPAS1 gain-of-function mutation syndrome. *JAMA Ophthalmol*. (2019) 138:148–55. doi: 10.1001/jamaophthalmol.2019.5244
5. Rosenblum JS, Maggio D, Pang Y, Nazari MA, Gonzales MK, Lechan RM, et al. Chiari malformation type 1 in EPAS1-associated syndrome. *Int J Mol Sci*. (2019) 20:2819. doi: 10.3390/ijms20112819
6. Dai C, Chen X, Li J, Comish P, Kang R, Tang D. Transcription factors in ferroptotic cell death. *Cancer Gene Ther*. (2020). doi: 10.1038/s41417-020-0170-2
7. Bebber CM, Müller F, Prieto Clemente L, Weber J, von Karstedt S. Ferroptosis in Cancer Cell Biology. *Cancers*. (2020) 12:164. doi: 10.3390/cancers12010164
8. Putra AC, Eguchi H, Lee KL, Yamane Y, Gustine E, Isobe T, et al. The A Allele at rs13419896 of EPAS1 is associated with enhanced expression and poor prognosis for non-small cell lung cancer. *PLoS ONE*. (2015) 10:e0134496. doi: 10.1371/journal.pone.0134496
9. Cho H, Du X, Rizzi JP, Liberzon E, Chakraborty AA, Gao W, et al. On-target efficacy of a HIF-2α antagonist in preclinical kidney cancer models. *Nature*. (2016) 539:107–11. doi: 10.1038/nature19795
10. Sena JA, Wang L, Heasley LE, Hu CJ. Hypoxia regulates alternative splicing of HIF and non-HIF target genes. *Mol Cancer Res*. (2014) 12:1233–43. doi: 10.1158/1541-7786.MCR-14-0149
11. Favier J, Lapointe S, Maliba R, Sirois MG. HIF2 alpha reduces growth rate but promotes angiogenesis in a mouse model of neuroblastoma. *BMC Cancer*. (2007) 7:139. doi: 10.1186/1471-2407-7-139
12. Welander J, Andreasson A, Brauckhoff M, Bäckdahl M, Larsson C, Gimm O, et al. Frequent EPAS1/HIF2α exons 9 and 12 mutations in non-familial pheochromocytoma. *Endocr Relat Cancer*. (2014) 21:495–504. doi: 10.1530/ERC-13-0384
13. Acker T, Diez-Juan A, Aragones J, Tjwa M, Brusselmans K, Moons L, et al. Genetic evidence for a tumor suppressor role of HIF-2alpha. *Cancer Cell*. (2005) 8:131–41. doi: 10.1016/j.ccr.2005.07.003
14. Rawłuszko-Wieczorek AA, Horbacka K, Krokowicz P, Misztal M, Jagodziński PP. Prognostic potential of DNA methylation and transcript levels of HIF1A and EPAS1 in colorectal cancer. *Mol Cancer Res*. (2014) 12:1112–27. doi: 10.1158/1541-7786.MCR-14-0054
15. Baba Y, Nosho K, Shima K, Irahara N, Chan AT, Meyerhardt JA, et al. HIF1A overexpression is associated with poor p ognosis in a cohort of 731 colorectal cancers. *Am J Pathol*. (2010) 176:2292–301. doi: 10.2353/ajpath.2010.090972
16. Mohammed N, Rodriguez M, Garcia V, Garcia JM, Dominguez G, Peña C, et al. EPAS1 mRNA in plasma from colorectal cancer patients is associated with poor outcome in advanced stages. *Oncol Lett*. (2011) 2:719–24. doi: 10.3892/ol.2011.294
17. Comino-Méndez I, de Cubas AA, Bernal C, Álvarez-Escolá C, Sánchez-Malo C, Ramírez-Tortosa CL, et al. Tumoral EPAS1 (HIF2A) mutations explain sporadic pheochromocytoma and paraganglioma in the absence of erythrocytosis. *Hum Mol Genet*. (2013) 22:2169–76. doi: 10.1093/hmg/ddt069
18. Alaikov T, Ivanova M, Shivarov V. EPAS1 p.M535T mutation in a Bulgarian family with congenital erythrocytosis. *Hematology*. (2016) 21:619–22. doi: 10.1080/10245332.2016.1192394
19. Pan H, Chen Q, Qi S, Li T, Liu B, Liu S, et al. Mutations in EPAS1 in congenital heart disease in Tibetans. *Biosci Rep*. (2018) 38:BSR20181389. doi: 10.1042/BSR20181389

20. Salo-Mullen EE, Lynn PB, Wang L, Walsh M, Gopalan A, Shia J, et al. Contiguous gene deletion of chromosome 2p16.3-p21 as a cause of Lynch syndrome. *Fam Cancer*. (2018) 17:71–7. doi: 10.1007/s10689-017-0006-x
21. Yang C, Hong CS, Prchal JT, Balint MT, Pacak K, Zhuang Z. Somatic mosaicism of EPAS1 mutations in the syndrome of paraganglioma and somatostatinoma associated with polycythemia. *Hum Genome Var*. (2015) 2:15053. doi: 10.1038/hgv.2015.53
22. Zhang Q, Lou Y, Zhang J, Fu Q, Wei T, Sun X, et al. Hypoxia-inducible factor-2α promotes tumor progression and has crosstalk with Wnt/β-catenin signaling in pancreatic cancer. *Mol Cancer*. (2017) 16:119. doi: 10.1186/s12943-017-0689-5
23. Lam AK. Application of pathological staging in esophageal squamous cell carcinoma. *Methods Mol Biol*. (2020) 2129:19–31. doi: 10.1007/978-1-0716-0377-2_3
24. Brown IS, Fujii S, Kawachi H, Lam AK, Saito T. Chapter 2: Oesophageal squamous cell carcinoma NOS. In: Odze RD, Lam AK, Ochiai A, Washington MK, editors. *WHO Classification of Tumours*. 5th ed. Lyon: IARC Press (2019). p. P48–53.
25. Lam AK. Macroscopic Examination of surgical specimen of esophageal squamous cell carcinoma. *Methods Mol Biol*. (2020) 2129:33–46. doi: 10.1007/978-1-0716-0377-2_4
26. Islam F, Gopalan V, Law S, Tang JC, Lam AK. FAM134B promotes esophageal squamous cell carcinoma *in vitro* and its correlations with clinicopathologic features. *Hum Pathol*. (2019) 87:1–10. doi: 10.1016/j.humpath.2018.11.033
27. Islam F, Gopalan V, Lam AK. *In vitro* assays of biological aggressiveness of esophageal squamous cell carcinoma. *Methods Mol Biol*. (2020) 2129:161–75. doi: 10.1007/978-1-0716-0377-2_13
28. Islam F, Gopalan V, Wahab R, Lee KT, Haque MH, Mamoori A, et al. Novel FAM134B mutations and their clinicopathological significance in colorectal cancer. *Hum Genet*. (2017) 136:321–37. doi: 10.1007/s00439-017-1760-4
29. Schwarz JM, Cooper DN, Schuelke M, Seelow D. MutationTaster2: mutation prediction for the deep-sequencing age. *Nat Methods*. (2014) 11:361–2. doi: 10.1038/nmeth.2890
30. Kasem K, Gopalan V, Salajegheh A, Lu CT, Smith RA, Lam AK. JK1 (FAM134B) gene and colorectal cancer: a pilot study on the gene copy number alterations and correlations with clinicopathological parameters. *Exp Mol Pathol*. (2014) 97:31–6. doi: 10.1016/j.yexmp.2014.05.001
31. Gopalan V, Islam F, Pillai S, Tang JC, Tong DK, Law S, et al. Overexpression of microRNA-1288 in oesophageal squamous cell carcinoma. *Exp Cell Res*. (2016) 348:146–54. doi: 10.1016/j.yexcr.2016.09.010
32. Islam F, Gopalan V, Law S, Tang JC, Chan KW, Lam AK. MiR-498 in esophageal squamous cell carcinoma: clinicopathological impacts and functional interactions. *Hum Pathol*. (2017) 62:141–51. doi: 10.1016/j.humpath.2017.01.014
33. Islam F, Gopalan V, Lam AK, Kabir SR. Pea lectin inhibits cell growth by inducing apoptosis in SW480 and SW48 cell lines. *Int J Biol Macromol*. (2018) 117:1050–7. doi: 10.1016/j.ijbiomac.2018.06.021
34. Islam F, Gopalan V, Vider J, Lu CT, Lam AK. MiR-142-5p act as an oncogenic microRNA in colorectal cancer: clinicopathological and functional insights. *Exp Mol Pathol*. (2018) 104:98–107. doi: 10.1016/j.yexmp.2018.01.006
35. Maroof H, Islam F, Dong L, Ajjikuttira P, Gopalan V, McMillan NAJ, et al. Liposomal delivery of miR-34b-5p induced cancer cell death in thyroid carcinoma. *Cells*. (2018) 7:E265. doi: 10.3390/cells7120265
36. Qallandar OB, Ebrahimi F, Islam F, Wahab R, Qiao B, Reher P, et al. Bone invasive properties of oral squamous cell carcinoma and its interactions with alveolar bone cells: an *in vitro* study. *Curr Cancer Drug Targets*. (2019) 19:631–40. doi: 10.2174/1568009618666181102144317
37. Myllykangas S, Himberg J, Böhling T, Nagy B, Hollmén J, Knuutila S. DNA copy number amplification profiling of human neoplasms. *Oncogene*. (2006) 25:7324–32. doi: 10.1038/sj.onc.1209717
38. Westerlund I, Shi Y, Holmberg J. EPAS1/HIF2α correlates with features of low-risk neuroblastoma and with adrenal chromaffin cell differentiation during sympathoadrenal development. *Biochem Biophys Res Commun*. (2019) 508:1233–9. doi: 10.1016/j.bbrc.2018.12.076
39. Imamura T, Kikuchi H, Herraiz MT, Park DY, Mizukami Y, Mino-Kenduson M, et al. HIF-1alpha and HIF-2alpha have divergent roles in colon cancer. *Int J Cancer*. (2009) 124:763–71. doi: 10.1002/ijc.24032
40. Lam AKY. Molecular biology of esophageal squamous cell carcinoma. *Crit Rev Oncol Hematol*. (2000) 33:71–90. doi: 10.1016/S1040-8428(99)00054-2
41. Baba Y, Watanabe M, Murata A, Shigaki H, Miyake K, Ishimoto T, et al. LINE-1 hypomethylation, DNA copy number alterations, and CDK6 amplification in esophageal squamous cell carcinoma. *Clin Cancer Res*. (2014) 20:1114–24. doi: 10.1158/1078-0432.CCR-13-1645
42. Cui J, Duan B, Zhao X, Chen Y, Sun S, Deng W, et al. MBD3 mediates epigenetic regulation on EPAS1 promoter in cancer. *Tumour Biol*. (2016) 37:13455–67. doi: 10.1007/s13277-016-5237-1
43. Pan X, Zhu Q, Sun Y, Li L, Zhu Y, Zhao Z, et al. PLGA/poloxamer nanoparticles loaded with EPAS1 siRNA for the treatment of pancreatic cancer *in vitro* and *in vivo*. *Int J Mol Med*. (2015) 35:995–1002. doi: 10.3892/ijmm.2015.2096
44. Nakazawa MS, Eisinger-Mathason TS, Sadri N, Ochocki JD, Gade TPF, Amin RK, et al. Epigenetic re-expression of HIF-2α suppresses soft tissue sarcoma growth. *Nat Commun*. (2016) 7:10539. doi: 10.1038/ncomms10539
45. Takeda N, Maemura K, Imai Y, Harada T, Kawanami D, Nojiri T, et al. Endothelial PAS domain protein 1 gene promotes angiogenesis through the transactivation of both vascular endothelial growth factor and its receptor, Flt-1. *Circ Res*. (2004) 95:146. doi: 10.1161/01.RES.0000134920.10128.b4

Conflict of Interest: The authors declare that the research was conducted in the absence of any commercial or financial relationships that could be construed as a potential conflict of interest.

frontiers in Oncology

ORIGINAL RESEARCH
published: 18 December 2020
doi: 10.3389/fonc.2020.586084

Prognostic Role of ABO Blood Type in Operable Esophageal Cancer: Analysis of 2179 Southern Chinese Patients

Shuishen Zhang[1†], Minghan Jia[2†], Xiaoli Cai[3†], Weixiong Yang[1], Shufen Liao[4], Zhenguo Liu[1], Jing Wen[5,6], Kongjia Luo[5,6,7*] and Chao Cheng[1*]*

[1] Department of Thoracic Surgery, The First Affiliated Hospital, Sun Yat-sen University, Guangzhou, China, [2] Department of Breast Cancer, Guangdong Provincial People's Hospital Cancer Center, Guangdong Academy of Medical Sciences, Guangzhou, China, [3] Department of Medical Ultrasonics, First Affiliated Hospital of Jinan University, Guangzhou, China, [4] Operating room of the First Affiliated Hospital of Sun Yat-sen University, Guangzhou, China, [5] Guangdong Esophageal Cancer Institute, Guangzhou, China, [6] Department of Thoracic Oncology, Sun Yat-sen University Cancer Center, Guangzhou, China, [7] State Key Laboratory of Oncology in South China, Collaborative Innovation Center for Cancer Medicine, Sun Yat-sen University Cancer Center, Guangzhou, China

OPEN ACCESS

Edited by:
Jianjun Xie,
Shantou University, China

Reviewed by:
Signe Friesland,
Karolinska University Hospital, Sweden
Kai Wu,
University of Michigan, United States

***Correspondence:**
Chao Cheng
chengch3@mail.sysu.edu.cn
Kongjia Luo
luokj@sysucc.org.cn
Jing Wen
wenjing@sysucc.org.cn

[†]These authors have contributed equally to this work and share first authorship

Specialty section:
This article was submitted to Gastrointestinal Cancers, a section of the journal Frontiers in Oncology

Received: 22 July 2020
Accepted: 17 November 2020
Published: 18 December 2020

Citation:
Zhang S, Jia M, Cai X, Yang W, Liao S, Liu Z, Wen J, Luo K and Cheng C (2020) Prognostic Role of ABO Blood Type in Operable Esophageal Cancer: Analysis of 2179 Southern Chinese Patients. Front. Oncol. 10:586084. doi: 10.3389/fonc.2020.586084

Background: The prognostic value of ABO blood types is not well clarified for esophageal carcinoma (EC). This study attempted to elucidate the associations between different ABO blood types and disease-free survival (DFS) and overall survival (OS) of EC.

Methods: This study was a retrospective review of the records of 2179 patients with EC who received surgery from December 2000 to December 2008. The prognostic impact of ABO blood group on DFS and OS were estimated using the Kaplan-Meier method and cox proportional hazard models.

Results: Univariate analyses found significant differences in DFS and OS among the four blood types. Multivariate analyses showed ABO blood type independently predicted DFS (P=0.001) and OS (P=0.002). Furthermore, patients with non-B blood types had a significantly shorter DFS (HR=1.22, 95%CI:1.07–1.38, P=0.002) and OS (HR=1.22, 95%CI:1.07–1.38, P=0.003) than patients with blood type B, and patients with non-O blood types had a significantly better DFS (HR=0.86, 95%CI:0.77–0.96, P=0.006) and OS (HR=0.86, 95%CI:0.77–0.96, P=0.007) than patients with blood type O. Subgroup analyses found that blood type B had a better DFS and OS than non-B in patients who were male, younger, early pathological stages and had squamous-cell carcinomas (ESCC). Blood type O had a worse DFS and OS than non-O in patients who were male, younger, and had ESCC (P<0.05).

Conclusions: The results demonstrate that ABO blood group is an independent prognostic factor of survival, and that type B predicts a favorable prognosis, whereas type O predicts an unfavorable prognosis for survival in patients with EC, especially those with ESCC.

Keywords: esophageal cancer, ABO blood group, survival, prognostic factor, large cohort

INTRODUCTION

Esophageal cancer (EC), which is predominantly squamous cell carcinoma, is the fourth leading cause of cancer-related deaths in China (1, 2). Despite decades of improvements in surgical techniques and the incorporation of multiple therapeutic approaches, 5-year overall survival (OS) of EC is still less than 40% (3, 4). Therefore, it is of great important to find new prognostic factors to identify high risk patients.

ABO blood group has recently been established to be an independent prognostic factor of survival in several malignancies (5–9). Moreover, ABO blood group was identified to be associated with the risk of esophageal cancer (9–12). Nevertheless, ABO blood group has not yet been demonstrated to independently predict survival of esophageal cancer in previous studies (13–17). Some studies have found no significant association between ABO blood group and survival (13, 14), whereas others indicate ABO blood group had significantly different survival, but not independently associated with prognosis for all patients (16). What's worse, there is no general consensus on the prognostic value of each ABO blood type in esophageal cancer (16, 17). A Chinese study by Qin et al. showed that blood type AB was not associated with OS for all patients, but was independently associated with worse OS compared to non-AB in patients with lymph node-negative (16). The other study, only including 181 Japanese patients, reported that patients with blood type B had a significantly better OS than those with non-B. However, blood type B was not an independent prognostic factor after adjusting by covariates (17). Hence, the role of each ABO blood type in predicting prognosis remains uncertain. In addition, ABO genes have been found to be distributed differently among socioeconomic groups (18) and geographic areas (12).

Therefore, we studied a large cohort of southern Chinese patients to clarify the prognostic value of ABO blood group and each ABO blood type for esophageal cancer.

MATERIALS AND METHODS

Patient Selection

We identified consecutive patients with esophageal cancer who underwent surgical resection at Sun Yat-sen University Cancer Center from December 2000 to December 2008. This database was analyzed in our previous studies (19, 20). We included patients based on the following criteria: histologically confirmed esophageal cancer; cancer of thoracic esophagus or esophagogastric junction; Karnofsky performance score of ≥ 90; received esophagectomy. Patients were excluded from the study based on the following criteria: history of other cancer; prior neoadjuvant therapy; died in the perioperative period; and lack of information on ABO blood type. Esophagectomy was performed with standard or extended dissection of the thoracic and abdominal lymph nodes (21). Pathologic stage was retrospectively determined according to the 7th edition of the American Joint Committee on Cancer staging system. All the patients provided written informed consent for their information to be stored and used in the hospital database. The study was approved by independent ethics committees at Sun Yat-sen University Cancer Center.

Abbreviations: EC, esophageal cancer; OS, overall survival; DFS, disease free survival; ESCC, esophageal squamous cell cancer; CEA, carcinoembryonic antigen; SCCA, squamous cell carcinoma antigen.

Clinicopathological Factors

Clinicopathological factors associated with survival were collected from the patients' medical records. The factors included ABO blood group, age, gender, smoking, alcohol consumption, histopathology, surgical procedure, radicality of surgery, postoperative adjuvant therapy, preoperative comorbidity (e.g., cardiovascular diseases and diabetes), differentiation, tumor location, pathological (p) T stage, pathological (p) N stage, level of pretreatment serum carcinoembryonic antigen (CEA), and squamous cell carcinoma antigen (SCCA).

As the definitions in our previous study, patients who had smoked more than 100 cigarettes in their lifetime are defined as smokers, those who had the habit and stopped the habit more than 1 year before the time of admission in hospital are defined as former smokers (22). We calculated alcohol drinks in the way described previously (23). Patients were routinely requested to report their lifetime history of drinking, including status, frequency, average consumption amount, and type of alcohol, at the time of admission. The same as described in previous study (24), former drinkers were defined as those who had the habit and stopped the habit more than 1 year before the time of admission in hospital; current drinkers were defined as those who had the habit at the time of admission in hospital or stopped the habit within 1 year before the time of admission in hospital.

Postoperative adjuvant therapy is usually recommended for patients with LNs metastasis. Treatment options were selected based on the tumor stage, doctor's opinion, patient's performance status, and patient's desire. Generally, adjuvant therapy was started at 4–8 week after operation. In this study, 37 patients received postoperative chemoradiotherapy, 92 patients received postoperative radiotherapy and 243 patients received adjuvant chemotherapy.

Pretreatment serum CEA and SCCA were measured as a standard procedure in all patients on the day of admission.

Follow-Up

All patients received standardized follow-up at 3-month intervals for the first 2 years after surgery, at 6-month intervals during the 3rd year, and annually thereafter. Follow-up time was calculated from the date of surgery to the event or the date of last contact, with follow-up continuing until June 2013. The median follow-up time was 32.1 months. The primary endpoint was OS, which was calculated from the time of surgery to the time of death from any cause. The second endpoint was disease free survival (DFS). DFS was calculated from the time of surgery to the first recurrence of index cancer or to all-cause death.

Statistical Analysis

The association between ABO blood group and clinicopathologic parameters was analyzed with the chi-square test or Fisher's exact test. Survival curves were calculated by the Kaplan–Meier

method and compared by log-rank tests. Multivariate analysis was performed using Cox's proportional hazards regression model with a forward stepwise procedure (the entry and removal probabilities were 0.05 and 0.10, respectively). We tested the proportional hazards assumption by the Shoenfeld residuals test to determine if the test was not statistically significant for each of the covariates, as well as the global test. Therefore, we could assume proportional hazards. A difference was considered significant if $P < 0.05$ (two-tailed). All statistical analyses were performed with SPSS 16.0 for Windows (SPSS Inc., Chicago, IL, USA).

RESULTS

Patient Characteristics

A total of 2179 consecutive patients with EC were included in the study. We excluded 231 patients, among them 88 patients with history of other cancers, 106 patients received neoadjuvant therapy, 4 patients died in the perioperative period and 33 patients with unknown ABO blood type. The clinicopathologic characteristics of the patients are shown in **Table 1**. The number of patients with blood types A, B, O and AB were 28.3%, 25.3%, 39.4%, and 8.0%, respectively. No significant difference was observed among the four ABO blood types with regard to histopathology, age, gender, smoking, alcohol consumption, surgical procedure, radicality of surgery, postoperative adjuvant therapy, differentiation, tumor location, pT category, or pN category (**Table 1**). Interestingly, there were significant differences among the four blood types in the proportions of pretreatment serum CEA elevation ($P < 0.001$) and serum SCCA elevation ($P < 0.001$). Patients with blood type O had higher proportions of serum CEA and SCCA elevation, whereas patients with blood type B had lower proportions of serum CEA and SCCA elevation than those with other blood groups (**Table 1**).

Univariate and Multivariate Analyses

The median time of follow-up was 32.1 months. Up to the last day of follow-up, 298 of the 551 patients with blood type B (54.1%) and 1018 of the 1628 patients with the other blood types (A, O, and AB) (62.5%) died. Univariate survival analysis showed a significant difference in DFS and OS among the four groups of patients with different blood types (P=0.005, **Table 2**, **Figure 1**). Additionally, patients with blood type B had significantly better DFS (P=0.001, **Figure 2A**) and OS (P=0.001, **Figure 2B**) than those with non-B blood types. Moreover, patients with blood type O had a significantly shorter DFS (P=0.027, **Figure 2C**) and OS (P=0.017, **Figure 2D**) compared to patients with non-O blood types. However, there was no significant difference in DFS or OS between patients with blood types A and non-A (P<0.05), or patients with blood types AB and non-AB (P<0.05). As shown in **Table 2**, male patients and patients with a smoking history, alcohol history, poor histologic differentiation, and advanced pathological stage were found to have a significantly shorter OS and DFS (P<0.05). However, no significant association was observed between histopathology, age, or tumor location and DFS or OS.

Adjusting for covariates including age, gender, smoking, alcohol, differentiation and pathological stage, the final multivariate survival analysis found that ABO blood group was an independent prognostic factor in operable esophageal cancer for DFS (P=0.001) and OS (P=0.002, **Table 3**), and patients with non-B blood types had significantly shorter DFS (HR=1.22, 95% CI=1.07–1.38, P=0.002) and OS (HR=1.22, 95% CI=1.07–1.38, P=0.003) compared to patients with B blood types. Furthermore, patients with non-O blood types had a better DFS (HR=0.86, 95% CI=0.77–0.96, P=0.006) and OS (HR=0.86, 95% CI=0.77–0.96, P=0.007) than those with blood type O.

Subgroup Analysis

Univariate survival analyses were stratified by histopathology, age, gender and TMN stage. The analyses revealed that the association of blood type B with longer DFS and OS was observed in male patients, younger patients, patients with esophageal squamous-cell carcinomas (ESCC), and patients in the early pathological stage (P<0.05, **Table 4**, **Figure 3A**). However, there was no significant association between blood type B and DFS or OS in patients who were female, old, had adenocarcinoma, or were in advanced pathological stages (III-IV) (**Table 4**, P>0.05). Moreover, the association between blood type O and shorter DFS and OS was observed in male patients, younger patients, and patients with ESCC (P<0.05, **Table 4**, **Figure 3B**). There was no significant association between blood type O and DFS or OS in patients who were female, old, had adenocarcinoma, or were in early or advanced pathological stages (**Table 4**, P>0.05).

DISCUSSION

The ABO blood group has been associated with the risk of esophageal cancer, but the prognostic value of ABO blood group and each ABO blood type has not been established because the studies have yielded conflicting results (13–17). The reasons for this may be the absence of large cohort clinical studies, the results varying by different geographic areas and ethnic groups, patients receiving neoadjuvant therapy enrolled in some of the studies, and potential confounding variables not controlled in some studies. Therefore, we studied 2179 patients from southern China who had esophageal cancer, without prior neoadjuvant therapy or a history of other cancers. In addition, potential confounding variables were balanced across ABO blood groups. To the best of our knowledge, our study is the first large cohort study to demonstrated that ABO blood group was an independent prognostic factor for DFS and OS in patients with esophageal cancer, which is in line with previous studies for other cancers (5, 6, 8).

The prognostic value of each ABO blood type has not been well clarified to date. Previous studies indicated that the ABO blood type was not an independently associated with prognosis of esophageal cancer (16, 17). One study showed that blood type AB was not associated with OS for all patients, but was

TABLE 1 | Clinicopathologic characteristics of 2179 patients with esophageal cancer.

Prognostic factor	Patients (%)N=2179	Blood group				*P* value
		BN = 551	AN = 617	ON = 859	ABN = 152	
Hp						0.142
ESCC	1898(87.1)	493(89.5)	540(87.5)	741(86.3)	124(81.6)	
EA	196(9.0)	42(7.6)	51(8.3)	85(9.9)	18(11.8)	
Others	85(3.9)	16(2.9)	26(4.2)	33(3.8)	10(6.6)	
Age						0.303
≤60 years	1316(60.4)	342(62.1)	374(60.6)	511(59.5)	86(56.6)	
>60 years	863(39.6)	208(37.9)	242(39.4)	347(40.5)	66(43.4)	
Gender						0.308
Females	497(22.8)	117(21.2)	158(25.6)	190(22.1)	32(21.1)	
Males	1682(77.2)	432(78.8)	459(74.4)	667(77.9)	120(78.9)	
Smoking						0.238
Never	781(35.8)	186(33.7)	232(37.6)	317(36.9)	46(30.3)	
Ever (former + current)	1398(63.7)	365(66.3)	385(62.4)	542(63.1)	106(69.7)	
Alcohol						0.580
Never	1494(68.5)	383(69.5)	411(66.6)	596(74.3)	104(69.4)	
Ever (former + current)	685(31.4)	168(30.5)	206(33.4)	263(25.7)	48(30.6)	
Surgical procedure						0.549
Left thoracic approach	1468(67.4)	391(71.0)	408(66.1)	565(65.8)	104(68.4)	
Right thoracic approach	657(30.1)	148(26.9)	192(31.1)	272(31.7)	45(29.6)	
Others	54(2.5)	12(2.1)	17(2.8)	22(2.5)	3(2.0)	
Radicality of surgery						0.715
R0	2009(92.2)	510(92.6)	571(92.5)	790(92.0)	138(90.8)	
R1	170(7.8)	41(7.4)	46(7.5)	69(8.0)	14(9.2)	
Postoperative adjuvant therapy						0.528
Yes	372(17.1)	87(15.8)	100(16.2)	159(18.5)	26(17.1)	
No	1807(82.9)	464(84.2)	517(83.8)	700(81.5)	126(82.9)	
Preoperative comorbidity						0.214
Yes	627(28.8)	142(25.7)	179(29.0)	255(29.7)	51(33.6)	
No	1552(71.2)	409(74.3)	438(71.0)	604(70.3)	101(66.4)	
Differentiation						0.383
G1	1474(67.6)	382(69.1)	427(69.2)	574(63.7)	92(60.5)	
G2-3	705(32.4)	170(30.9)	190(30.8)	285(36.3)	60(39.5)	
Tumor location						0.183
Upper	393(18.0)	105(19.1)	121(19.6)	149(17.3)	18(11.8)	
Middle	1137(52.2)	293(53.2)	321(52.0)	432(50.3)	91(60.0)	
Lower	453(20.8)	116(21.1)	126(20.4)	187(21.8)	24(15.8)	
EGJ	196(9.0)	37(6.6)	49(8.0)	91(10.6)	19(12.4)	
pT category						0.433
T1-2	667(30.6)	176(31.9)	186(30.1)	260(30.2)	45(29.6)	
T3-4	1512(69.4)	375(68.1)	431(69.9)	599(69.7)	107(70.4)	
pN category						0.346
N0	1113(51.1)	291(52.8)	333(54.0)	427(49.7)	62(40.8)	
N1-3	1066(48.9)	260(47.2)	284(46.0)	432(50.3)	90(59.2)	
Serum CEA						**<0.001**
Normal	1714(78.7)	470(85.3)	488(79.1)	632(73.6)	124(81.6)	
Elevated	465(21.3)	81(14.7)	129(20.9)	227(26.4)	28(18.4)	
Serum SCCA						**<0.001**
Normal	1681(77.1)	483(87.7)	493(79.9)	573(66.7)	132(86.8)	
Elevated	498(22.9)	68(12.3)	124(20.1)	286(33.3)	20(13.2)	

Hp, histopathology; ESCC, esophageal squamous cell carcinoma; EA, esophageal adenocarcinoma; EGJ, esophagogastric junction; G, grade; CEA, carcinoembryonic antigen; SCCA, squamous cell carcinoma antigen.

Bold values are statistically significant (P < 0.05).

independently associated with worse OS compared to non-AB in subgroup of patients with lymph node-negative (16). The other study including 181 patients showed that blood type B was not an independent prognostic factor in multivariate analysis (17). Thus, we examined the impact of each ABO blood type on survival and found that patients with non-B blood types had a 22% higher risk of disease progression and a 22% higher risk of death, compared to patients with blood type B. Moreover, patients with non-O blood types had a 14% lower risk of disease progression and a 14% lower risk of death than patients with blood type O. These findings suggested that blood type B is a favorable prognostic factor and blood type O is an adverse prognostic factor for survival in patients with esophageal cancer. However, blood type AB or A was not significantly associated with prognosis in our study. Therefore, our study is also first time to systematically demonstrate the role

TABLE 2 | Univariate survival analysis for overall survival and disease free survival in patients with esophageal cancer.

Prognostic factor	Disease-free survival (Months)			Overall survival (Months)		
	Mean	Median	*P* value	Mean	Median	*P* value
Hp			0.305			0.161
ESCC	71.6	27.7		77.0	36.7	
EA	53.8	23.8		57.8	31.2	
Others	62.9	32.0		70.4	40.3	
Age			0.558			**0.023**
≤60 years	73.1	27.1		79.7	38.5	
>60 years	66.4	27.8		70.2	35.0	
Gender			**<0.001**			**<0.001**
Females	82.2	39.2		89.2	54.8	
Males	66.3	25.6		71.5	34.3	
Smoking			**<0.001**			**<0.001**
Never	81.3	36.3		86.9	46.7	
Ever (former + current)	63.9	24.1		69.3	31.7	
Alcohol			**<0.001**			**<0.001**
Never	76.9	33.2		82.8	43.4	
Ever (former + current)	55.6	20.2		60.2	25.3	
ABO Blood group			**0.005**			**0.005**
A	70.3	28.2		75.9	37.6	
B	82.4	35.7		87.8	40.9	
O	62.2	26.0		66.4	33.0	
AB	53.6	25.1		59.3	31.4	
Blood type B			**0.001**			**0.001**
B	82.4	35.7		87.8	40.9	
Non-B	66.2	26.8		71.2	34.6	
Blood type O			**0.027**			**0.017**
O	62.2	22.6		66.4	33.0	
Non-O	74.7	25.1		80.6	38.8	
Blood type A			0.861			0.974
A	70.3	28.2		76.0	37.6	
Non-A	70.7	27.1		75.7	36.0	
Blood type AB			0.202			0.258
AB	53.6	25.1		59.3	31.4	
Non-AB	71.2	27.6		76.5	36.5	
Differentiation			**<0.001**			**<0.001**
G1	77.5	34.4		82.6	43.1	
G2-3	55.7	21.3		61.7	26.8	
Tumor location			0.404			0.196
Upper	62.3	29.6		66.1	40.3	
Middle	72.8	28.3		78.8	38.7	
Lower	67.5	25.0		72.9	32.7	
EGJ	43.5	25.1		47.1	34.3	
Pathological stage			**<0.001**			**<0.001**
Stage I–II	95.5	71.1		100.0	84.0	
Stage III–IV	39.7	15.8		45.8	20.8	

EGJ, esophagogastric junction; G, grade; HR, hazard ratio; 95% CI, 95% confidence interval.
Bold values are statistically significant (P < 0.05).

of each ABO blood type in predicting the prognosis of patients with esophageal cancer.

In addition, we found that in subgroup of patients with male, younger, esophageal squamous cell carcinomas, and early pathological stage (I-II), blood type B was associated with better DFS and OS compared to non-B. However, no significant association between blood type B and prognosis was observed in subgroup of patients who were female, old, had adenocarcinoma, or were in advanced pathological stages (III-IV). Moreover, the association between blood type O and worse DFS and OS was observed in subgroup of patients who were male, younger, and esophageal squamous cell carcinomas, but not in subgroup of patients who were female, old, had adenocarcinoma, or were in early or advanced pathological stages.

The mechanisms underlying the association between ABO blood group and the survival of patients with esophageal cancer are still unknown. It has been shown that the modified expression of blood group antigens on tumor cells may alter cell motility, resistance to apoptosis, and immune escape (25). In addition, the relationship between ABO group genotype and circulating levels of ICAM-1, E-selectin, p-selectin, and tumor necrosis factor-alpha were revealed (26–29), suggesting the blood antigens may play a role in the immune systemic response. However, no significant association between ABO blood group and the oncological characteristics, such as pathological T stage

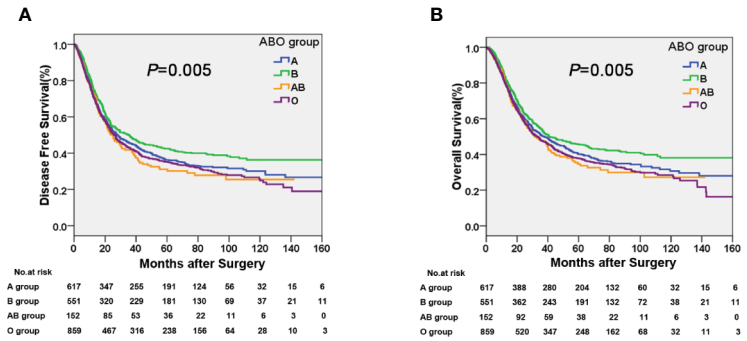

FIGURE 1 | Kaplan-Meier curves showing a significant difference in **(A)** disease free survival (DFS) and **(B)** overall survival (OS) among the four ABO blood groups.

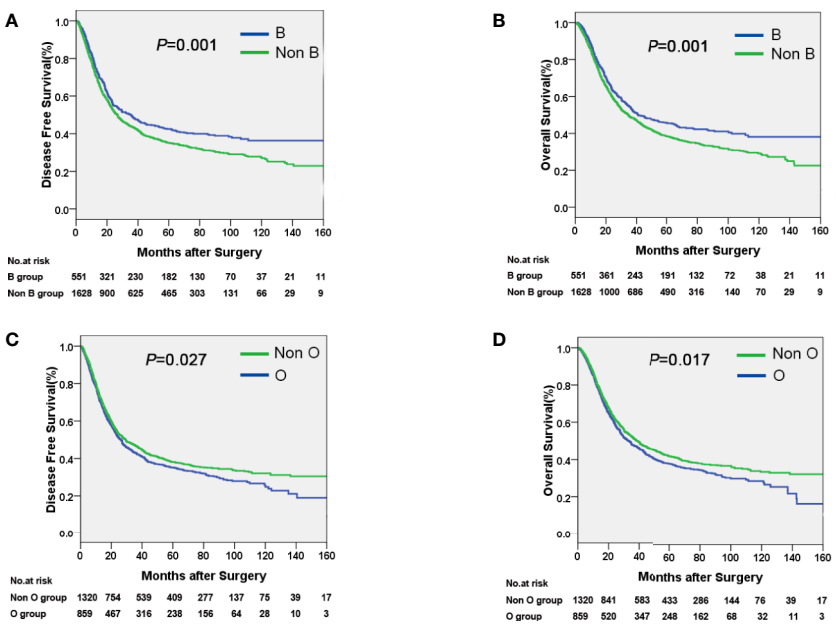

FIGURE 2 | Kaplan-Meier curves showing that patients with blood type B had a longer DFS **(A)** and OS **(B)** compared with non-B patients, and that patients with blood type O had a shorter DFS **(C)** and OS **(D)** compared with non-O patients.

or N stage was observed in our study. Interestingly, we found that ABO blood group was correlated with elevated serum CEA and SCCA. The proportion of tumors associated with elevated pretreatment serum CEA and SCCA was significantly higher in patients with blood type O than in patients with other blood types, while the proportion associated with elevated serum CEA and SCCA was significantly lower in patients with blood type B than in patients with other blood types. This finding indicates that ABO blood group might have biological significance as markers of the progression of human tumors. However, the association between ABO blood group and elevated serum CEA and SCCA was not observed in previous study with a small sample of patients in Japan (17). Thus, further basic researches are needed to elucidate the association between ABO blood group and the genetic and biological features of esophageal cancer.

Our study implicated that ABO blood group might serve as a useful biomarker to independently predict prognosis of patients with esophageal cancer, adjuvant therapy and close follow-up after surgery are more necessary as patients with blood type O were identified to have higher risk of recurrence and poorer prognosis than others. Moreover, our findings also suggest ABO blood type should be taken into account in the future clinical trial design in terms of prognosis in ESCC.

We acknowledge several limitations of this study. First, although our sample was large, our study was a single-institution retrospective study, which may have led to selection bias. Second, information on post-treatment recurrence was

TABLE 3 | Multivariate survival analysis for overall survival and disease free survival in patients with esophageal cancer.

Prognostic factor	Disease-free survival		Overall survival	
	HR(95%CI)	*P* value	HR(95%CI)	*P* value
Age	–	-	1.17(1.05-1.30)	0.006
Gender	0.99(0.84–1.19)	0.994	0.96(0.80–1.15)	0.965
Smoking	1.11(0.95–1.29)	0.210	1.11(0.98–1.27)	0.097
Alcohol	1.35(1.20–1.51)	**<0.001**	1.31(1.16–1.50)	**<0.001**
Blood group[a]	1.07(1.03–1.12)	**0.001**	1.25(1.12–1.41)	**0.002**
Blood type B[a]				
B	1.00		1.00	
Non-B	1.22(1.07–1.38)	**0.002**	1.22(1.07–1.38)	**0.003**
Blood type O[a]				
O	1.00		1.00	
Non-O	0.86(0.77–0.96)	**0.006**	0.86(0.77–0.96)	**0.007**
Differentiation	1.26(1.13–1.41)	**<0.001**	1.26(1.12–1.42)	**<0.001**
Pathological stage	2.46(2.20–2.75)	**<0.001**	2.43(2.17–2.72)	**<0.001**

HR, hazard ratio; 95% CI, 95% confidence interval.
Bold values are statistically significant (P < 0.05).
[a]*Blood group, blood type B and blood type, as one of covariates, were separately included in multivariate analysis, respectively.*

insufficient, which might affect the survival of patients. Third, there was the possibility of selection bias because patients with metastatic disease and those with unresectable EC were excluded. Fourth, the data of Rh blood group were not collected in this study due to the proportion of Rh negative in Chinese adults is quite low.

In conclusion, the ABO blood group is an independent prognostic factor for patients with esophageal cancer after

TABLE 4 | Subgroup analysis by blood type B for overall survival and disease free survival in patients with esophageal cancer.

Prognostic factor	Disease free Survival (Months)		Overall Survival (Months)	
	HR(95%CI)	*P*-value	HR(95%CI)	*P*-value
Hp				
ESCC				
Blood type B	1.27(1.11–1.45)	**<0.001**	1.26(1.10–1.45)	**0.001**
Blood type O	0.87(0.73–0.97)	**0.014**	0.86(0.77–0.97)	**0.014**
EA				
Blood type B	0.88(0.58–1.33)	0.534	1.00(0.66–1.54)	0.984
Blood type O	0.87(0.62–1.23)	0.430	0.93(0.66–1.33)	0.700
Others				
Blood type B	1.09(0.51–2.34)	0.816	1.12(0.50–2.50)	0.787
Blood type O	0.90(0.51–1.60)	0.728	0.83(0.46–1.49)	0.534
Age				
≤60 years				
Blood type B	1.37(1.16–1.62)	**<0.001**	1.39(1.17–1.65)	**<0.001**
Blood type O	0.78(0.68–0.90)	**<0.001**	0.76(0.66–0.88)	**<0.001**
>60 years				
Blood type B	1.06(0.88–1.29)	0.546	1.06(0.89–1.28)	0.585
Blood type O	1.07(0.90–1.27)	0.401	1.07(0.90–1.27)	0.428
Gender				
Females				
Blood type B	1.10(0.76–1.31)	0.997	0.99(0.75–1.31)	0.943
Blood type O	1.04(0.82–1.32)	0.762	1.07(0.83–1.37)	0.609
Males				
Blood type B	1.33(1.15–1.53)	**<0.001**	1.34(1.16–1.55)	**<0.001**
Blood type O	0.85(0.76–0.96)	**0.009**	0.84(0.74–0.94)	**0.004**
TNM stage				
Stage I–II				
Blood type B	1.45(1.19–1.76)	**<0.001**	1.47(1.20–1.80)	**<0.001**
Blood type O	0.97(0.74–1.02)	0.089	0.87(0.73–1.02)	0.094
Stage III–IV				
Blood type B	1.05(0.89–1.24)	0.570	1.05(0.89–1.24)	0.565
Blood type O	0.88(0.77–1.02)	0.091	0.86(0.75–1.01)	0.060

Hp, histopathology; ESCC, esophageal squamous cell carcinoma; EA, esophageal adenocarcinoma.
Bold values are statistically significant (P < 0.05).

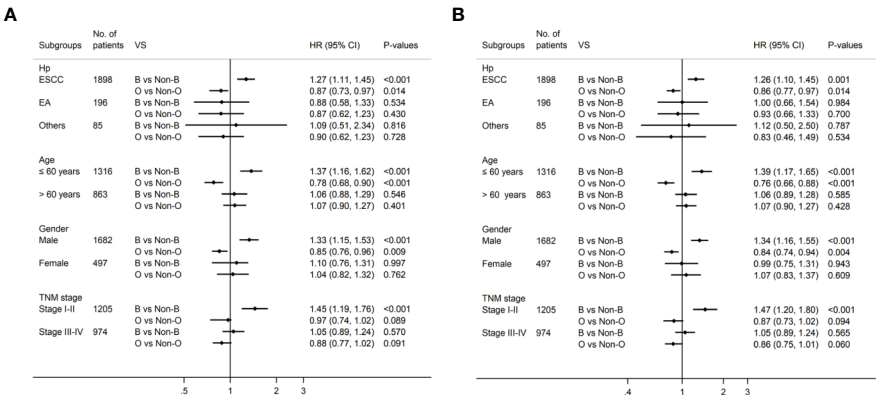

FIGURE 3 | Subgroup analysis by blood type B and blood type O for DFS **(A)** and OS **(B)** in patients with esophageal cancer.

esophagectomy. Blood type B is a favorable prognostic factor, whereas blood type O is an adverse prognostic factor for the survival in patients with esophageal cancer, especially those with ESCC. Further prospective studies of large cohorts of patients are necessary to confirm these results.

DATA AVAILABILITY STATEMENT

The raw data supporting the conclusions of this article will be made available by the authors, without undue reservation.

ETHICS STATEMENT

The study was approved by independent ethics committees at Sun Yat-sen University Cancer Center. All the patients provided written informed consent for their information to be stored and used in the hospital database.

AUTHOR CONTRIBUTIONS

Conception and design: SZ, JW, KL, CC. Development of methodology: SZ, MJ, XC. Acquisition of data (provided animals, acquired and managed patients, provided facilities, etc.): SZ, XC, WY. Analysis and interpretation of data (e.g., statistical analysis, biostatistics, computational analysis): SZ, MJ, ZL, SL. Writing, review, and/or revision of the manuscript: SZ, MJ, XC, WY, JW, KL, CC. Administrative, technical, or material support (i.e., reporting or organizing data, constructing databases): SZ. Study supervision: JW, KL, CC. All authors contributed to the article and approved the submitted version.

FUNDING

This study was supported by grants from the Science and Technology Planning Project of Guangdong Province, China (A2016042; to SZ), Wu Jieping Medical foundation (320.320.2730.1875; to SZ), National Science Foundation of China (Grant No. 81672356; to JW, Grant No.81572391 to CC), Guangzhou Science Technology and Innovation Commission (Grant No. 201610010127; to JW), and Guangdong Talents Special Support Program (Grant No. 201629038; to JW).

ACKNOWLEDGMENTS

We would like to thank the patients and family members who gave their consent to present data in this study.

REFERENCES

1. Bray F, Ferlay J, Soerjomataram I, Siegel RL, Torre LA, Jemal A. Global cancer statistics 2018: GLOBOCAN estimates of incidence and mortality worldwide for 36 cancers in 185 countries. *CA Cancer J Clin* (2018) 68:394–424. doi: 10.3322/caac.21492
2. Chen W, Zheng R, Baade PD, Zhang S, Zeng H, Bray F, et al. Cancer statistics in China, 2015. *CA Cancer J Clin* (2016) 66:115–32. doi: 10.3322/caac.21338
3. van Hagen P, Hulshof MC, van Lanschot JJ, Steyerberg EW, van Berge Henegouwen MI, Wijnhoven BP, et al. Preoperative chemoradiotherapy for esophageal or junctional cancer. *N Engl J Med* (2012) 366:2074–84. doi: 10.1056/NEJMoa1112088
4. Enzinger PC, Mayer RJ. Esophageal cancer. *N Engl J Med* (2003) 349:2241–52. doi: 10.1056/NEJMra035010
5. Rahbari NN, Bork U, Hinz U, Leo A, Kirchberg J, Koch M, et al. AB0 blood group and prognosis in patients with pancreatic cancer. *BMC Cancer* (2012) 12:319. doi: 10.1186/1471-2407-12-319
6. Cao X, Wen ZS, Sun YJ, Li Y, Zhang L, Han YJ. Prognostic value of ABO blood group in patients with surgically resected colon cancer. *Br J Cancer* (2014) 111:174–80. doi: 10.1038/bjc.2014.302

7. Xu YQ, Jiang TW, Cui YH, Zhao YL, Qiu LQ. Prognostic value of ABO blood group in patients with gastric cancer. *J Surg Res* (2016) 201:188–95. doi: 10.1016/j.jss.2015.10.039
8. Ouyang PY, Su Z, Mao YP, Liu Q, Xie FY. Prognostic value of ABO blood group in southern Chinese patients with established nasopharyngeal carcinoma. *Br J Cancer* (2013) 109:2462–6. doi: 10.1038/bjc.2013.559
9. Wang W, Liu L, Wang Z, Lu X, Wei M, Lin T, et al. ABO blood group and esophageal carcinoma risk: from a case-control study in Chinese population to meta-analysis. *Cancer Causes Control* (2014) 25:1369–77. doi: 10.1007/s10552-014-0442-y
10. Kumar N, Kapoor A, Kalwar A, Narayan S, Singhal MK, Kumar A, et al. Allele frequency of ABO blood group antigen and the risk of esophageal cancer. *BioMed Res Int* (2014) 2014:286810. doi: 10.1155/2014/286810
11. Gong Y, Yang YS, Zhang XM, Su M, Wang J, Han JD, et al. ABO blood type, diabetes and risk of gastrointestinal cancer in northern China. *World J Gastroenterol* (2012) 18:563–9. doi: 10.3748/wjg.v18.i6.563
12. Su M, Lu SM, Tian DP, Zhao H, Li XY, Li DR, et al. Relationship between ABO blood groups and carcinoma of esophagus and cardia in Chaoshan inhabitants of China. *World J Gastroenterol* (2001) 7:657–61. doi: 10.3748/wjg.v7.i5.657
13. Nozoe T, Ezaki T, Baba H, Kakeji Y, Maehara Y. Correlation of ABO blood group with clinicopathologic characteristics of patients with esophageal squamous cell carcinoma. *Dis Esophagus* (2004) 17:146–9. doi: 10.1111/j.1442-2050.2004.00392.x
14. Wang W, Liu L, Wang Z, Wei M, He Q, Ling T, et al. Impact of ABO blood group on the prognosis of patients undergoing surgery for esophageal cancer. *BMC Surg* (2015) 15:106. doi: 10.1186/s12893-015-0094-1
15. Fan G, Hu D, Zhang X, Peng F, Lin X, Chen G, et al. Interaction Between Prediabetes and the ABO Blood Types in Predicting Postsurgical Esophageal Squamous Cell Carcinoma-Specific Mortality: The FIESTA Study. *Front Oncol* (2018) 8:461. doi: 10.3389/fonc.2018.00461
16. Qin J, Wu SG, Sun JY, Lin HX, He ZY, Li Q. Effect of blood type on survival of Chinese patients with esophageal squamous cell carcinoma. *Onco Targets Ther* (2015) 8:947–53. doi: 10.2147/OTT.S81936
17. Shiratori F, Shimada H, Yajima S, Suzuki T, Oshima Y, Nanami T, et al. Relationship between ABO blood group and clinicopathological factors and their effect on the survival of Japanese patients with esophageal squamous cell carcinoma. *Surg Today* (2017) 47:959–65. doi: 10.1007/s00595-016-1459-5
18. Beardmore JA, Karimi-Booshehri F. ABO genes are differentially distributed in socio-economic groups in England. *Nature* (1983) 303:522–4. doi: 10.1038/303522a0
19. Zhang SS, Yang H, Luo KJ, Huang QY, Chen JY, Yang F, et al. The impact of body mass index on complication and survival in resected oesophageal cancer: a clinical-based cohort and meta-analysis. *Br J Cancer* (2013) 109:2894–903. doi: 10.1038/bjc.2013.666
20. Zou JY, Chen J, Xie X, Liu Z, Cai X, Liu Q, et al. Hepatitis B Virus Infection is a Prognostic Biomarker for Better Survival in Operable Esophageal Cancer: Analysis of 2,004 Patients from an Endemic Area in China. *Cancer Epidemiol Biomarkers Prev* (2019) 28:1028–35. doi: 10.1158/1055-9965.EPI-18-1095
21. Fujita H, Sueyoshi S, Tanaka T, Fujii T, Toh U, Mine T, et al. Optimal lymphadenectomy for squamous cell carcinoma in the thoracic esophagus: comparing the short- and long-term outcome among the four types of lymphadenectomy. *World J Surg* (2003) 27(5):571–9.
22. Zheng Y, Cao X, Wen J, Yang H, Luo K, Liu Q, et al. Smoking affects treatment outcome in patients with resected esophageal squamous cell carcinoma who received chemotherapy. *PLoS One* (2015) 10(4):e0123246. doi: 10.1371/journal.pone.0123246
23. Huang Q, Luo K, Yang H, Wen J, Zhang S, Li J, et al. Impact of alcohol consumption on survival in patients with esophageal carcinoma: a large cohort with long-term follow-up. *Cancer Sci* (2014) 105(12):1638–46. doi: 10.1111/cas.12552
24. Wu M, Zhao JK, Zhang ZF, Han RQ, Yang J, Zhou JY, et al. Smoking and alcohol drinking increased the risk of esophageal cancer among Chinese men but not women in a high-risk population. *Cancer Causes Control* (2011) 22(4):649–57. doi: 10.1007/s10552-011-9737-4
25. Le Pendu J, Marionneau S, Cailleau-Thomas A, Rocher J, Le Moullac-Vaidye B, Clement M. ABH and Lewis histo-blood group antigens in cancer. *Apmis* (2001) 109(1):9–31. doi: 10.1111/j.1600-0463.2001.tb00011.x
26. Paterson AD, Lopes-Virella MF, Waggott D, Boright AP, Hosseini SM, Carter RE, et al. Genome-Wide Association Identifies the ABO Blood Group as a Major Locus Associated With Serum Levels of Soluble E-Selectin. *Arterioscler Thromb Vasc Biol* (2009) 29(11):1958–U609. doi: 10.1161/ATVBAHA.109.192971
27. Pare G, Chasman DI, Kellogg M, Zee RYL, Rifai N, Badola S, et al. Novel Association of ABO Histo-Blood Group Antigen with Soluble ICAM-1: Results of a Genome-Wide Association Study of 6,578 Women. *PLoS Genet* (2008) 4(7):e1000118. doi: 10.1371/journal.pgen.1000118
28. Melzer D, Perry JRB, Hernandez D, Corsi A-M, Stevens K, Rafferty I, et al. A genome-wide association study identifies protein quantitative trait loci (pQTLs). *PLoS Genet* (2008) 4(5):e1000072. doi: 10.1371/journal.pgen.1000072
29. Barbalic M, Dupuis J, Dehghan A, Bis JC, Hoogeveen RC, Schnabel RB, et al. Large-scale genomic studies reveal central role of ABO in sP-selectin and sICAM-1 levels. *Hum Mol Genet* (2010) 19(9):1863–72. doi: 10.1093/hmg/ddq061

Conflict of Interest: The authors declare that the research was conducted in the absence of any commercial or financial relationships that could be construed as a potential conflict of interest.

frontiers in Oncology

ORIGINAL RESEARCH
published: 01 February 2021
doi: 10.3389/fonc.2020.580045

Expression of Human Epidermal Growth Factor Receptor-2 Status and Programmed Cell Death Protein-1 Ligand Is Associated With Prognosis in Gastric Cancer

*Huifang Lv[1], Junling Zhang[2], Keran Sun[1], Caiyun Nie[1], Beibei Chen[1], Jianzheng Wang[1], Weifeng Xu[1], Saiqi Wang[1], Yingjun Liu[3] and Xiaobing Chen[1]**

[1] Department of Oncology, The Affiliated Cancer Hospital of Zhengzhou University, Henan Cancer Hospital, Zhengzhou, China, [2] Medical Department, 3D Medicines Inc., Shanghai, China, [3] Department of Surgery, The Affiliated Cancer Hospital of Zhengzhou University, Henan Cancer Hospital, Zhengzhou, China

Background: PD-L1 and HER-2 are routine biomarkers for gastric cancer (GC). However, little research has been done to investigate the correlation among PD-L1, HER-2, immune microenvironment, and clinical features in GC.

Methods: Between January 2013 and May 2020, a total of 120 GC patients treated with chemotherapy were admitted to Henan Tumor Hospital. We retrospectively identified PD-L1, HER-2 level before chemotherapy and abstracted clinicopathologic features and treatment outcomes. Univariate and multivariate survival analyses were performed to assess the relationship between PD-L1/HER-2 levels and progression-free survival (PFS). The mRNA and tumor microenvironment of 343 patients with GC from The Cancer Genome Atlas (TCGA) were used to explore the underlying mechanism.

Results: We retrospectively analyzed 120 patients with gastric cancer, including 17 patients with HER-2 positive and 103 patients with HER-2 negative GC. The results showed that the expression of PD-L1 was closely correlated with HER-2 (P = 0.015). Patients with PD-L1/HER-2 positive obtained lower PFS compared to PD-L1/HER-2 negative (mPFS: 6.4 *vs*. 11.1 months, P = 0.014, mPFS: 5.3 *vs*. 11.1 months, P = 0.002, respectively), and the PD-L1 negative and HER-2 negative had the best PFS than other groups (P = 0.0008). In a multivariate model, PD-L1 status, HER-2 status, tumor location, and tumor differentiation remained independent prognostic indicators for PFS (P < 0.05). The results of database further analysis showed that the proportion of PD-L1+/CD8A+ in HER-2 negative patients was higher than that in HER-2 positive patients (37.6 *vs* 20.3%), while PD-L1−/CD8A− was significantly higher in HER-2 positive patients than HER-2 negative patients (57.8 *vs*. 28.8%). In addition, it showed that not only CD4+T cells, macrophages, and CD8+T cells, but also the associated inflammatory pathways such as IFN-γ/STAT1 were associated with HER-2.

Conclusion: HER-2 status could predict the efficacy of immune checkpoint inhibitors, and HER-2 status combined with PD-L1 level could predict the prognosis of GC patients.

Keywords: HER-2, PD-L1, prognosis, gastric cancer, CD8+T cells

OPEN ACCESS

Edited by:
Jianjun Xie,
Shantou University, China

Reviewed by:
Brian M. Olson,
Emory University, United States
Wang-Kai Fang,
Shantou University, China

****Correspondence:***
Xiaobing Chen
chenxbxh@126.com

Specialty section:
This article was submitted to Gastrointestinal Cancers, a section of the journal Frontiers in Oncology

Received: *04 July 2020*
Accepted: *14 December 2020*
Published: *01 February 2021*

Citation:
Lv H, Zhang J, Sun K, Nie C, Chen B, Wang J, Xu W, Wang S, Liu Y and Chen X (2021) Expression of Human Epidermal Growth Factor Receptor-2 Status and Programmed Cell Death Protein-1 Ligand Is Associated With Prognosis in Gastric Cancer. Front. Oncol. 10:580045. doi: 10.3389/fonc.2020.580045

INTRODUCTION

Gastric cancer (GC) is a common malignant tumor in the digestive tract, ranking the second in the global mortality rate of malignant tumors, and more than 50% of new cases are from developing countries (1). The 5-year overall survival rate of metastatic GC is only 5–20% (2). Human epidermal growth factor receptor-2 (*HER-2*, also known as ERBB2) is a transmembrane receptor tyrosine kinase, and *HER-2* expression is significantly up-regulated in approximately 6–23% GC tissues (3–5). Since trastuzumab combined with chemotherapy became the standard treatment for advanced GC with positive HER-2 (ToGA study), a significant increase was needed for HER-2 assessment for GC (6). In breast cancer, HER-2 amplification and overexpression are associated with low prognosis, high mortality, and high recurrence and metastasis (7–9). However, the prognostic value of HER-2 in GC remains controversial. Some studies have shown that HER-2 positive patients have a high survival rate (10–12). In addition, HER-2 positive patients are correlated with serous membrane infiltration, lymph node metastasis, disease stage, distant metastasis, and other clinicopathological characteristics (13, 14). Other studies have shown no correlation between *HER-2* expression and survival (15–17).

The interaction of programmed cell death protein-1 (PD-1) and its ligand (PD-L1) with immune cells and tumor cells limits the T-cell-mediated immune response (18). Immune checkpoint blocking of anti-PD-1 or anti-PD-L1 antibodies is the latest treatment for a variety of cancers, including non-small cell lung cancer (19–21), melanoma (22), bladder cancer (23), and kidney cancer (24). In early clinical studies, PD-1 inhibitors in the treatment of metastatic gastric cancer, such as pembrolizumab (25) and nivolumab (26), have been reported to have good efficacy. Current studies have shown that the expression level of PD-L1 in tumor tissue could be used to predict the efficacy of anti-PD-1 treatment (27); not only in patients with high expression of PD-L1 will it be effective, but also in patients with low expression of PD-L1. Therefore, it is essential to find the best biomarkers for GC in order to provide predictive information about the treatment response and ultimately improve the treatment outcome. The expression level of PD-L1 and the status of HER-2 are two important pathological characteristics of gastric cancer patients. Although some studies focused on the expression of PD-L1 and HER-2 in gastric cancer, the results of these studies are not consistent. Some researchers have found that expression of PD-L1, a potential biomarker for the immunotherapy response, was observed in HER-2 positive and negative patients to a similar extent, and its presence was not influenced by the HER-2 status (28). However, it has also been studied that the PD-L1 expression in GC is significantly correlated with HER2-negative status (29). Therefore, the relationship between HER-2 and PD-L1 state and what role the immune microenvironment plays in the prognosis of GC patients are still not clear.

In order to demonstrate the association between HER-2 and PD-L1 status, we analyzed the data from the largest available cohort of GC with both clinical and survival data. The immune microenvironment and PD-L1 mRNA from The Cancer Genome Atlas were also analyzed to explore the possible underlying mechanism.

MATERIALS AND METHODS

Study Design and Clinical Data Collection

We retrospectively reviewed 120 GC patients at the Affiliated Cancer Hospital of Zhengzhou University between January 2013 and May 2020. All patients were confirmed by two pathologists and the histological diagnoses were without discrepancy. Patients without any signs of distant metastasis preferably received neoadjuvant treatment, which was followed by surgical resection of the tumor. After an adjuvant chemotherapy period, routine control visits with computed tomography (CT) scans were performed. Patients with typical signs of distant metastasis underwent palliative chemotherapy. Biopsy or resection samples were used to detect PD-L1 and HER-2 expression. If the tumor was HER-2 positive, trastuzumab was added to the treatment schedule. Trastuzumab was administered by intravenous infusion at a dose of 8 mg/kg on day 1 of the first cycle, followed by 6 mg/kg every 3 weeks until progression of the disease, the occurrence of unacceptable toxicity, or the patient's refusal. After administration of two cycles of chemotherapy or trastuzumab containing treatment, the size of the tumor was investigated by CT imaging and assessed using the Response Evaluation Criteria in Solid Tumors version 1.1 (RECIST 1.1). The following clinical characteristics were abstracted: age, sex, HER-2 status, PD-L1 status, tumor differentiation degree, lauren classification, treatment. The follow-up information was conducted *via* medical records plus telephone interview, and the following information was obtained: disease-free survival (DFS) and progression free survival (PFS).

In addition, the PD-L1 mRNA data and immune microenvironment of 343 patients with gastric cancer (GC) were sourced from The Cancer Genome Atlas (TCGA) (www.cbioportal.org).

The study was approved by relevant regulatory and independent ethics committee of the Henan Tumor Hospital and done in accordance with the Declaration of Helsinki and the International Conference on Harmonization Good Clinical Practice guidelines.

Immunohistochemical Staining and Evaluation

Representative sections of each surgical tumor resection or biopsy specimens were stained with PD-L1 antibody (SP263, Ventana) and VENTANA HER-2/neu rabbit monoclonal antibody (Clone 4B5, Ventana). Omission of primary antibody and substitution by non-specific immunoglobins were used as negative controls. The immunoreactivity of PD-L1 was evaluated according to combined positive score (CPS). CPS was calculated by dividing the number of PD-L1 positive tumor cells, lymphocytes and histiocytes by the total number of vital tumor cells and then multiplying the result by 100. Specimens in which PD-L1 staining was observed in CPS >1 were considered PD-L1 positive. And CPS ≤1 was regarded as PD-L1 negative. IHC 3+ or IHC 2+ was defined as HER-2 positive.

Fluorescence In Situ Hybridization

When the result of IHC was 2+/3+, the amplification level of HER-2 was detected. PathVysion DNA Probe kit was used for

the analysis of FISH according to the manufacturer's protocol. The positive results from FISH were defined as a HER-2: CEP17 ratio ≥2.0. Examples of HER2 FISH positive and negative were shown in **Figures 1E, F**. According to the standards of the European Medicines Agency, HER-2 positive was defined as any case of IHC 3+ or IHC 2+ with a positive FISH result, while any case of IHC 0, IHC 1+ or IHC 2+ with a negative FISH result is considered HER-2 negative.

Statistical Analyses

Progression free survival (PFS) was defined as the time from the date of first line therapy administration to the progression of cancer, or death from any cause. PFS was calculated using the Kaplan–Meier method. Correlation analyses were performed using the two-sided chi-squared test or the Fisher exact test. Variables with significant *P* values or interest were included into multivariate logistic regression. For all analyses, *P* value <0.05 was considered to be statistically significant, and a confidence interval of 95% was used (95% CI). All statistical analyses were performed using SPSS22.0 software (SPSS, Inc., Chicago, IL, USA).

RESULTS

Patient Baseline Clinical Features

We retrospectively analyzed 120 patients with gastric cancer in our hospital, including 17 patients with HER-2 positive and 103 patients with HER-2 negative GC (**Table 1**). There were 32 patients with PD-L1 positive and 88 patients with PD-L1

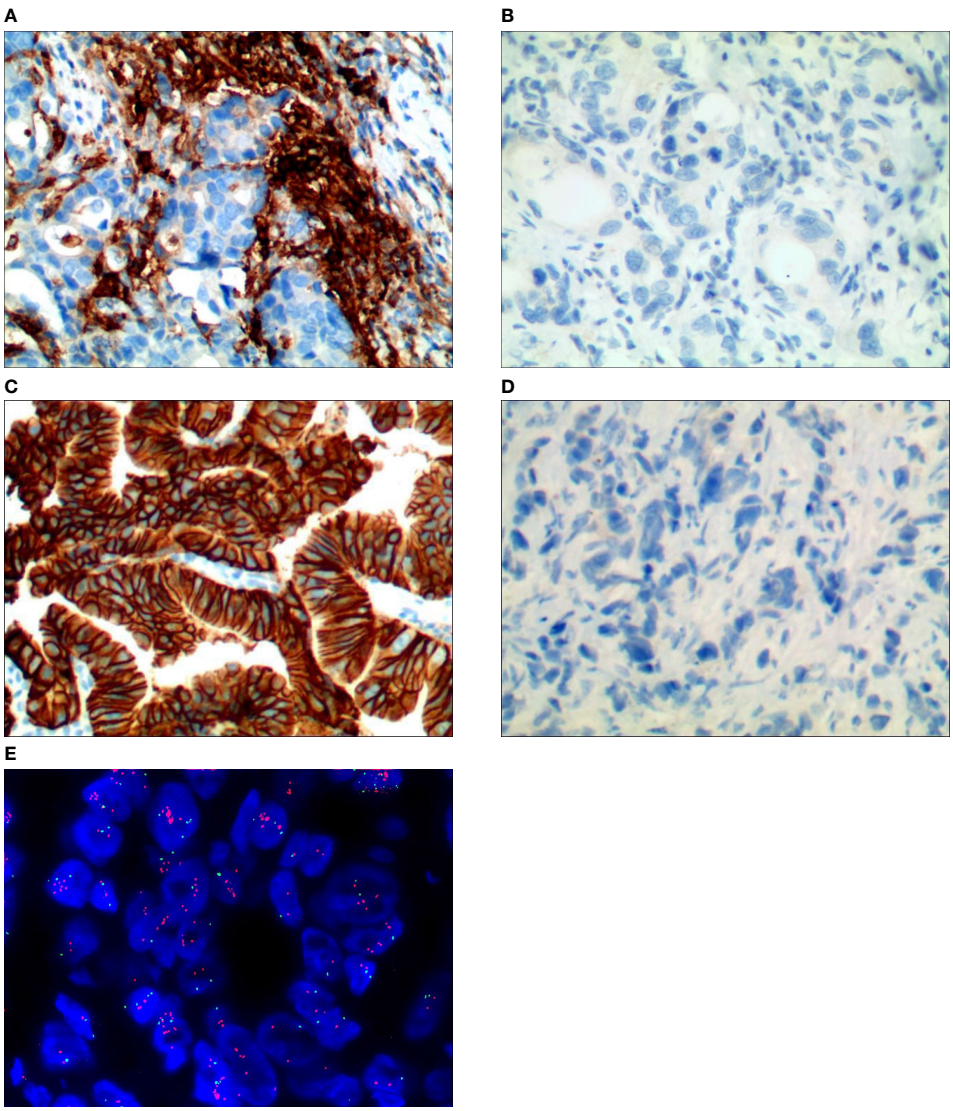

FIGURE 1 | Representative images of PD-L1 and HER-2 immunostaining/FISH results, **(A)** PD-L1 positive, **(B)** PD-L1 negative, **(C)** HER-2 positive by immunostaining, **(D)** HER-2 negative by immunostaining, **(E)** HER-2 positive by FISH.

negative (**Figure 1**). 57.5% were male and 42.5% GC patients were ≥60 years. The results showed that the expression of PD-L1 was closely correlated with HER-2 status, with statistical significance (P = 0.015, as shown in **Table 1**).

Association Between Programmed Cell Death Protein-1 Ligand/Human Epidermal Growth Factor Receptor-2 Status and Survival Outcomes

We analyzed whether PD-L1/HER-2 status was associated with the survival outcomes of chemotherapy in advanced GC. Patients with PD-L1 positive obtained lower PFS compared to PD-L1 negative (mPFS: 6.4 *vs.* 11.1 months, P = 0.014, **Figure 2A**). The similar results were in HER-2 negative (mPFS: 5.3 *vs.* 11.1 months, P = 0.002, **Figure 2B**). And the PD-L1 negative and HER-2 negative had the best PFS than the other groups (P = 0.0008, **Figure 2C**). In the present study, univariable analysis revealed significant association between poorer PFS and PD-L1 status, HER-2 status, tumor location in body, while there was no relation between PFS and age, sex, lauren classification and tumor differentiation (**Table 2**). In a multivariate model, PD-L1 status, HER-2 status, tumor location, and tumor differentiation remained independent prognostic indicators for PFS (**Table 1**, $P < 0.05$).

TABLE 1 | Clinicopathologic and baseline clinical features of gastric cancer patients.

Characteristics	PD-L1 Positive (n = 32)	PD-L1 Negative (n =88)	*P*
Sex			
Male	21	48	0.3039
Female	11	40	
Age			
≥60	14	37	>0.9999
<60	18	51	
Histological differentiation			
Moderate	7	17	0.7031
Poor	19	48	
NOS	6	23	
Lauren Classification			
Diffuse	4	18	0.1809
Intestinal	2	8	
Mixed	5	4	
Unknown	21	58	
Tumor Location			
Body	12	31	0.2573
Antrum	5	11	
Cardia, gastric fundus	15	36	
Unknown	0	10	
T stage (%)			
T1	0	4	0.336
T2	4	7	
T3	7	30	
T4	6	9	
Tx	15	38	
N stage (%)			
N0	4	13	0.8118
N1	2	6	
N2	2	12	
N3	8	18	
Nx	16	39	
M stage (%)			
M0	15	54	0.1476
M1	17	31	
Mx	0	3	
HER-2 status			
Positive.	9	8	0.0153
Negative	23	80	

Association Between Human Epidermal Growth Factor Receptor-2 Status and Programmed Cell Death Protein-1 Ligand mRNA Expression

In order to explore the mechanism of potential, we first analyzed whether HER-2 status was associated with the PD-L1 mRNA expression in GC. It showed that the expression of PD-L1 was higher in HER-2 negative GC, but decreased in HER-2 positive GC (**Figure 3**, $P < 0.0001$).

Association Between Programmed Cell Death Protein-1 Ligand Status and Tumor-Infiltrating Lymphocyte

tAccording to the classification of PD-L1 and TIL, tumors were divided into $PD\text{-}L1^{-}/TIL^{-}$, $PD\text{-}L1^{+}/TIL^{+}$, $PD\text{-}L1^{+}/TIL^{-}$ and $PD\text{-}L1^{-}/TIL^{+}$, among which $PD\text{-}L1^{+}/TIL^{+}$ was considered to be the most suitable state for immunotherapy (27). We further analyzed the effect of *HER-2* on the distribution of PD-L1/CD8A in TCGA data. In *HER-2* amplified patients, the proportions of $PD\text{-}L1^{+}/CD8A^{+}$, $PD\text{-}L1^{+}/CD8A^{-}$, $PD\text{-}L1^{-}/CD8A^{+}$ and $PD\text{-}L1^{-}/CD8A^{-}$ were 20.3, 12.5, 15.6, and 57.8%, respectively. The proportions of $PD\text{-}L1^{+}/CD8A^{+}$, $PD\text{-}L1^{+}/CD8A^{-}$, $PD\text{-}L1^{-}/CD8A^{+}$, and $PD\text{-}L1^{-}/CD8A^{-}$ in patients without HER-2 amplification were 37.6, 16.4, 17.2, and 28.8%, respectively (see **Figure 4**, $P < 0.001$). The results indicated that the ratio of $PD\text{-}L1^{+}/CD8A^{+}$ was significantly increased in patients without HER-2 amplification, while the ratio of $PD\text{-}L1^{-}/CD8A^{-}$ was the highest in patients with HER-2 amplification. This result further suggests that immunotherapy may be more effective for patients with HER2-negative GC, while patients with HER2-positive GC have a poorer prognosis, and combination therapy may be effective.

Association Between Human Epidermal Growth Factor Receptor-2 Status and Immune Cell Infiltration

In the following experiments, we attempted to explore the effect of HER-2 status on immune cell infiltration. Through deconvolution of 574 labeled gene expression values, the proportions of 22 kinds of immune cells in GC tissues in TCGA database were analyzed by CIBERSORT. The results showed that the proportion of resting state memory CD4+ T cells was the highest in GC samples, followed by macrophages. CD8+ T cells and memory B cells were highly expressed in the non-amplified HER-2 group, while resting state memory CD4+ T cells and M0 macrophages were highly expressed in the amplified HER-2 group (**Figures 5A, B**).

Pearson correlation analysis showed that there was no significant correlation among immune cells infiltration (**Figure 5B**). M1-type

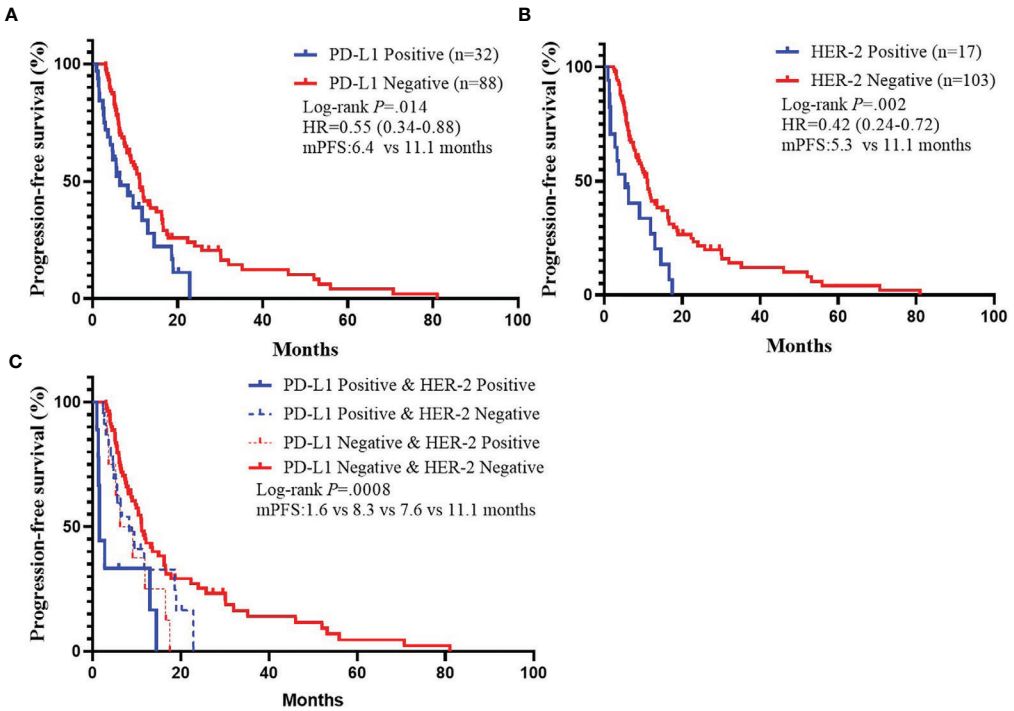

FIGURE 2 | Kaplan–Meier Estimates of Progression-Free Survival by PD-L1 Status or *HER-2* status. **(A)** Kaplan–Meier survival curves of PFS by PD-L1 status. **(B)** Kaplan–Meier survival curves of PFS by *HER-2* status. **(C)** Kaplan–Meier survival curves of PFS by PD-L1 and HER-2 status.

TABLE 2 | Univariate and multivariate analyses of progression-free survival.

Parameter	Univariate analysis			Multivariate analysis		
	HR	95% CI	*P*	HR	95% CI	*P*
Sex Male *vs* Female	0.769	0.509–1.162	0.213			
Age ≥ 60 *vs* <60	0.825	0.540–1.260	0.373			
Tumor differentiation Moderate *vs*. poorly	0.629	0.375–1.056	0.080	0.444	0.25–0.777	0.004
LAUREN Diffuse *vs* intestinal	0.928	0.522–1.649	0.799	2.009	1.257–3.210	0.004
Tumor location Body *vs* antrum	1.614	1.034–2.519	0.035			
PD-L1 status Negative *vs* Positive	0.547	0.339–0.883	0.014	0.596	0.364–0.975	0.039
HER-2 status Negative *vs* Positive	0.416	0.240–0.722	0.002	0.280	0.149–0.525	0.000

macrophages were moderately correlated with activated memory CD4+ T cells (r = 0.41), while resting memory CD4 + T cells were negatively correlated with CD8 + T cells (r = −0.41). The results showed that the proportion of resting CD4+ T cells in the immune microenvironment of HER-2 amplified patients was high, and the proportion of activated memory CD4+ T cells was low, suggesting that CD4+ T cells in the immune microenvironment were not activated, which reduced the flooding effect of CD8+ T cells in the immune microenvironment, leading to decreased infiltration of CD8+ T cells.

Association Between Human Epidermal Growth Factor Receptor-2 Status and Cytokines

By comparing HER-2 amplification and non-amplification groups, significant changes in some cytokines were found as

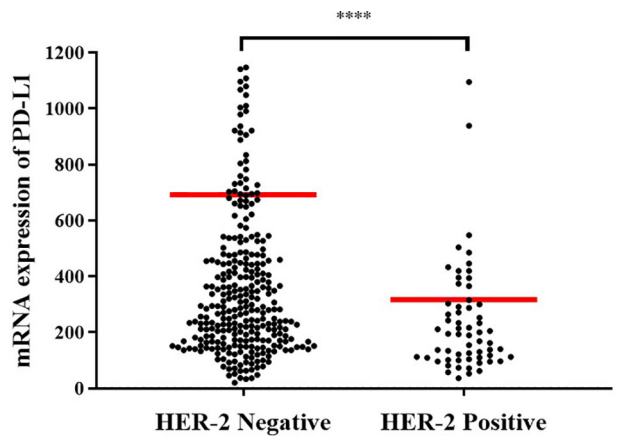

FIGURE 3 | Expression levels of PD-L1 mRNA in different *HER-2* gene states. *HER-2* amp represents *HER-2* amplification; *HER-2* non-amp indicates *HER-2* non-amplification. ****P < 0.0001.

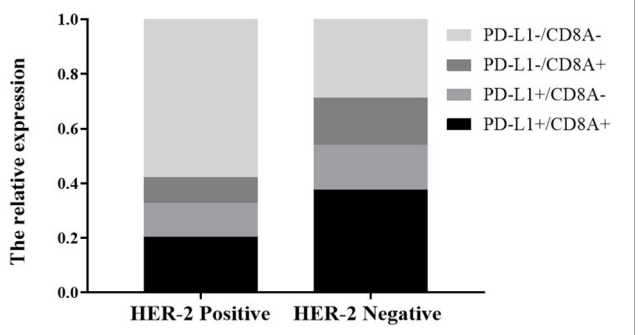

FIGURE 4 | Effect of *HER-2* status on tumor immune typing.

shown in **Figure 6A**, and INF-γ was significantly decreased. By using an online system (https://string-db.org/cgi/network.pl?taskId=lP6ij62YlPsZ), we found that the *STAT1* had a close reciprocal relationship with *IFN-γ*. Biological process analysis of cytokines showed that they are mainly involved in immune responsibility-related reactions (**Figure 6B**). At the same time, KEGG pathway analysis was also carried out, and it was found that antigen processing and presentation, natural killer cell mediated cytotoxicity and Toll-like receptor signaling pathway were included (**Figure 6D**). Therefore, we could find that HER-2 status is closely related to the immune response. Amplification of HER-2 may negatively regulate the immune response of GC and further affect the anti-tumor effect, which explains why immunotherapy for HER-2 positive GC patients is not effective.

DISCUSSION

As immunotherapy has ushered in a new era in the treatment of GC, PD-1 inhibitors have become the standard treatment for PD-L1 positive advanced GC, and further studies on immune-

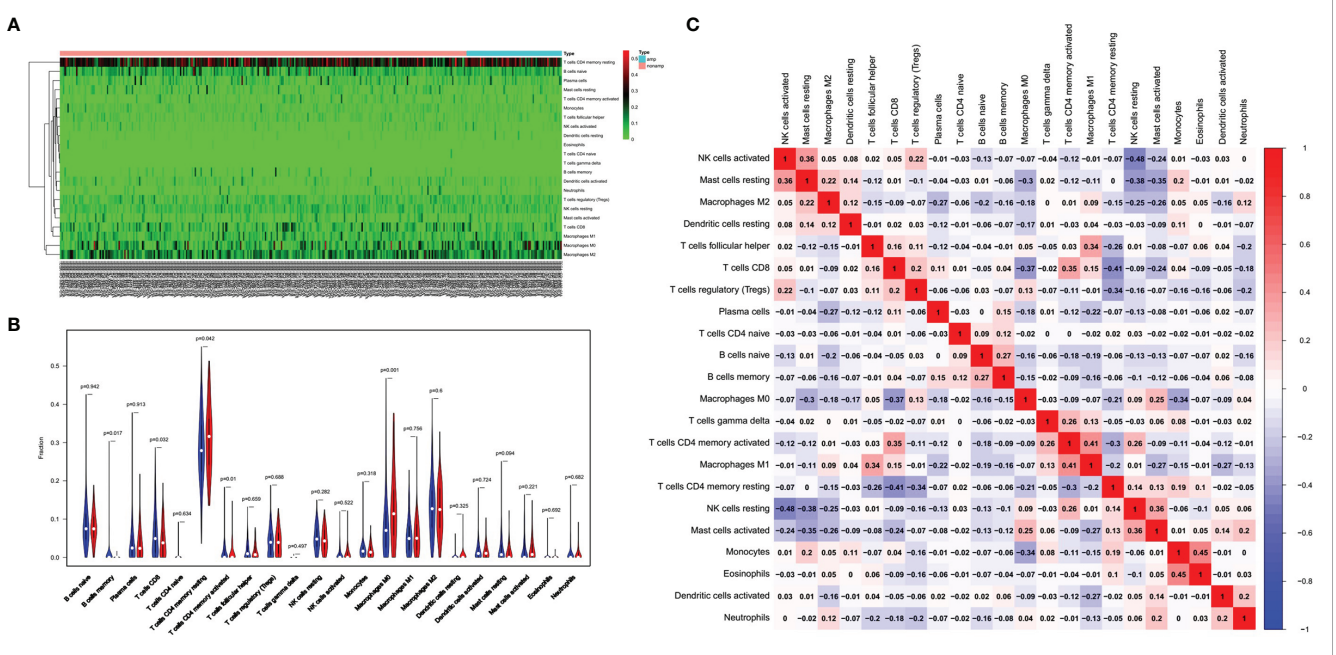

FIGURE 5 | Effects of HER-2 status and immune cell infiltration. **(A)** The heat map of immune cells in GC. **(B)** The proportion of 22 immune cells in GC. **(C)** The correlation between the immune cells infiltration in GC by Pearson analyzed.

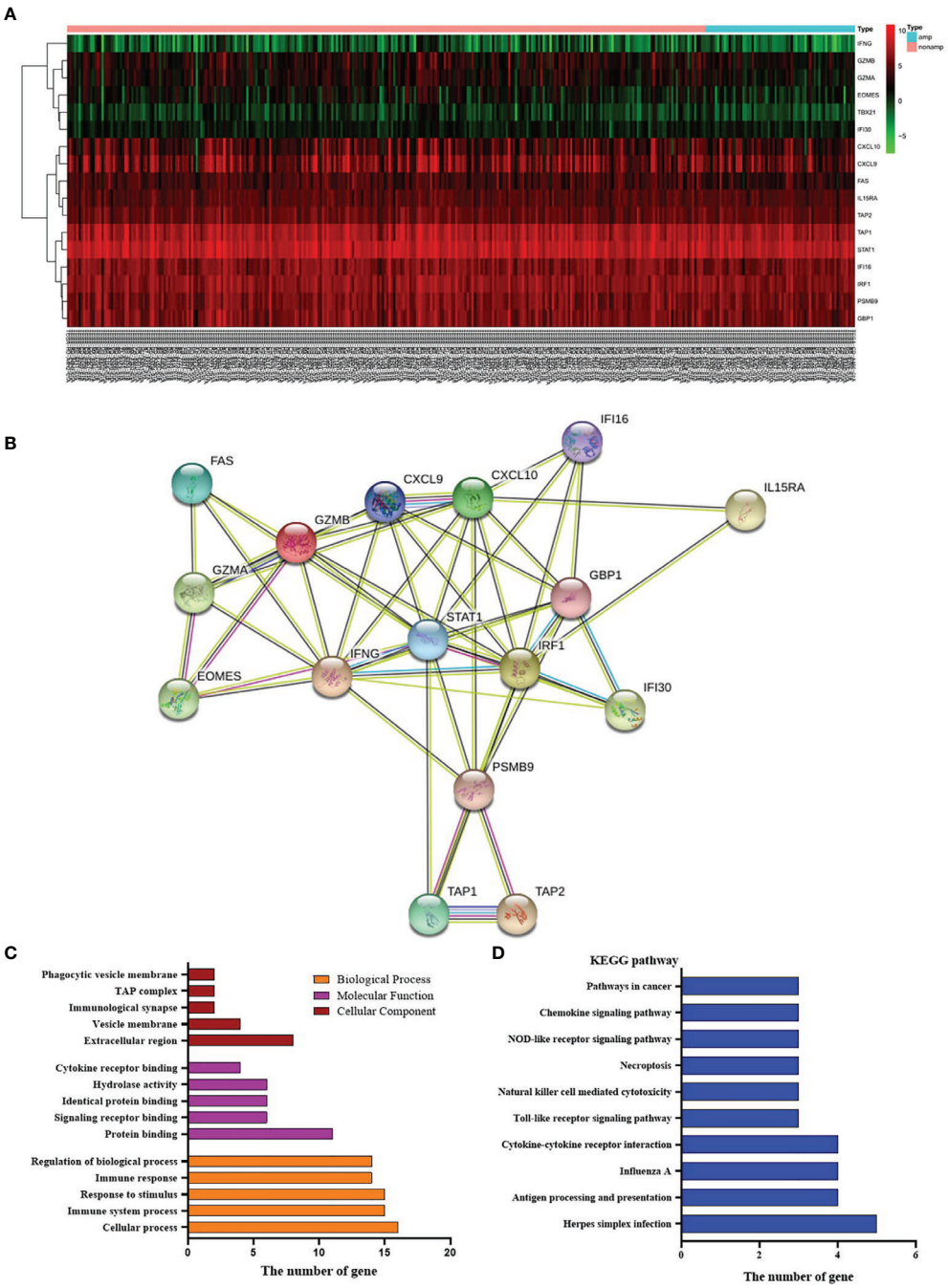

FIGURE 6 | Effects of *HER-2* status and cytokines. **(A)** The heat map of cytokines in GC. **(B)** Interaction mapping of different gene in *HER-2* Amp and non-amp group. **(C)** Gene distribution based on GO analysis. **(D)** KEGG pathway analysis of differential genes.

related biomarkers and their interactions with other cancer-related pathways are necessary. In our study, we investigated the potential correlation between HER-2 and PD-L1 expression and their relationship with clinical characteristics and prognosis in patients with GC.

Immunotherapy, especially immune checkpoint blockade, has become a promising cancer treatment. Immune checkpoint inhibitors, such as anti-PD-1 and anti-PD-L1, have been approved by the Food and Drug Administration (FDA) for the treatment of various types of cancer, resulting in durable tumor regression and prolonged survival (30, 31). It has also been shown that blocking PD-L1 could improve the immune function of tumor-specific effector T cells when interacting with target tumor cells *in vitro* (32). However, the relationship

between PD-L1 expression and prognosis in GC is still controversial. Some studies found that the prognosis of GC patients with PD-L1 positive was significantly improved (33). On the contrary, other researchers have shown that high PD-L1 expression was a significant poor prognostic factor (34). In this study, we found that positive PD-L1 in GC tissues was associated with poor prognosis of PFS. This finding is consistent with previous research results (35). A reasonable hypothesis for the poor clinical efficacy of PD-L1 positive tumors is that the up-regulation of PD-L1 in immune cells inactivates cytotoxic T lymphocytes (CTLs), leading to host immune evasion.

Interestingly, we also found that the expression of PD-L1 was higher in HER-2 negative GC, but decreased in HER-2 positive GC which might lead to a novel treatment strategy. As in the ToGA study, only HER-2 positive patients can benefit from anti-HER-2 drug (5). Anti-PD-1/PD-L1 immunotherapy might become a potentially new treatment for HER-2 negative patients. Whether HER-2 could be used independently as an indicator to evaluate the disease progression and prognosis of GC patients was still a big controversy. A retrospective study found that HER-2 was highly expressed in GC and closely related to poor quality of life and short survival, indicating that HER-2 has a certain potential value in prognosis assessment of GC (12). Other research results showed that the high expression of HER-2 in GC tissues was only negatively correlated with the degree of tumor differentiation, while there was no difference in the distribution of other pathological characteristics related data such as gender, age, tumor size (36), which were similarly with our study.

More literature indicates that tumor microenvironment plays a critical role in cancer progression and treatment response (37). Not only compositions, but also the number of T cells, associated macrophages, and associated inflammatory pathways influenced the immune response and chemotherapy benefit at diagnosis (38–40). Based on the existence of tumor-infiltrating lymphocytes (TILs) and PD-L1 expression, we know that PD-L1+CD8+ was adaptive immune resistance. In our study, the ratio of PD-L1+/CD8A+, CD8+T cells, and B cells were highly expressed in the non-amplified HER-2 group and CD4+T cells and macrophages M0 were highly expressed in the amplified HER-2 group. In addition, immune responsibility-related reactions of biological process and a significant decrease in IFN-γ were found in HER-2 negative GC. Those also highlight the potential role of tumor microenvironment in GC and explain the fact that HER-2 negative patients are more suitable for immunotherapy.

Taken together, PD-L1 positive in tumor cells is correlated with worse prognosis in GC patients and is correlated positively with HER-2 positive. Our findings suggest that tumors expressing higher levels of PD-L1 are more aggressive and that administration of adjuvant chemotherapy should be considered for patients with these tumors.

DATA AVAILABILITY STATEMENT

The original contributions presented in the study are included in the article/supplementary material, further inquiries can be directed to the corresponding author.

ETHICS STATEMENT

The study was approved by relevant regulatory and independent ethics committee of the Henan Tumor Hospital and done in accordance with the Declaration of Helsinki.

AUTHOR CONTRIBUTIONS

HL and XC designed the study. HL and JZ wrote the first draft of the manuscript. HL, KS, CN, BC, JW, WX, SW, and YL treated the patients and acquired data. HL and JZ analyzed the data. XC revised the manuscript. All authors contributed to the article and approved the submitted version.

FUNDING

We would like to thank the financial support from the National Natural Science Foundation of China (No. 81472714), 1000 Talents Program of Central plains (No. 204200510023), Science and Technique Foundation of Henan Province (No. 202102310413), Medical Science and Technique Foundation of Henan Province (Nos. 2018020486 and SB201901101) and State Key Laboratory of Esophageal Cancer Prevention & Treatment (No. Z2020000X).

REFERENCES

1. Torre LA, Bray F, Siegel RL, Ferlay J, Lortet-Tieulent J, Jemal A. Global Cancer Statistics 2012. *CA Cancer J Clin* (2015) 65(2):87–108. doi: 10.3322/caac.21262
2. Wagner AD, Syn NL, Moehler M, Grothe W, Yong WP, Tai B-C, et al. Chemotherapy for advanced gastric cancer. *Cochrane Database Syst Rev* (2017) 8(29):CD004064. doi: 10.1002/14651858.CD004064.pub4
3. Hsu J-T, Chen T-C, Tseng J-H, Chiu C-T, Liu K-H, Yeh C-N, et al. Impact of HER-2 overexpression/amplification on the prognosis of gastric cancer patients undergoing resection: a single-center study of 1,036 patients. *Oncologist* (2011) 16(12):1706–13. doi: 10.1634/theoncologist.2011-0199
4. Sheng WQ, Huang D, Ying JM, Lu N, Wu HM, Liu YH, et al. HER2 status in gastric cancers: a retrospective analysis from four Chinese representative clinical centers and assessment of its prognostic significance. *Ann Oncol* (2013) 24(9):2360–4. doi: 10.1093/annonc/mdt232
5. Bang YJ, Van Cutsem E, Feyereislova A, Chung HC, Shen L, Sawaki A, et al. Trastuzumab in combination with chemotherapy versus chemotherapy alone for treatment of HER2-positive advanced gastric or gastro-oesophageal junction cancer (ToGA): a phase 3, open-label, randomised controlled trial. *Lancet* (2010) 376(9742):687–97. doi: 10.1016/S0140-6736(10)61121-X
6. Kai K, Yoda Y, Kawaguchi A, Minesaki A, Iwasaki H, Aishima S, et al. Formalin fixation on HER-2 and PD-L1 expression in gastric cancer: A pilot

analysis using the same surgical specimens with different fixation times. *World J Clin Cases* (2019) 7(4):419–30. doi: 10.12998/wjcc.v7.i4.419
7. Seshadri R, Horsfall DJ, Firgaira F, McCaul K, Setlur V, Chalmers AH, et al. The relative prognostic significance of total cathepsin D and HER-2/neu oncogene amplification in breast cancer. The South Australian Breast Cancer Study Group. *Int J Cancer* (1994) 56(1):61–5. doi: 10.1002/ijc.2910560112
8. Slamon DJ, Clark GM, Wong SG, Levin WJ, Ullrich A, McGuire WL. Human breast cancer: correlation of relapse and survival with amplification of the HER-2/neu oncogene. *Science* (1987) 235(4785):177–82. doi: 10.1126/science.3798106
9. Toikkanen S, Helin H, Isola J, Joensuu H. Prognostic significance of HER-2 oncoprotein expression in breast cancer: a 30-year follow-up. *J Clin Oncol* (1992) 10(7):1044–8. doi: 10.1200/JCO.1992.10.7.1044
10. Gómez-Martin C, Garralda E, Echarri MJ, Ballesteros A, Arcediano A, Rodríguez-Peralto JL, et al. HER2/neu testing for antiHER2-based therapies in patients with unresectable and/or metastatic gastric cancer. *J Clin Pathol* (2012) 65(8):751–7. doi: 10.1136/jclinpath-2012-200774
11. Jain S, Filipe MI, Gullick WJ, Linehan J, Morris RW. c-erbB-2 proto-oncogene expression and its relationship to survival in gastric carcinoma: an immunohistochemical study on archival material. *Int J Cancer* (1991) 48 (5):668–71. doi: 10.1002/ijc.2910480506
12. Jorgensen JT, Hersom M. HER2 as a prognostic marker in gastric cancer-a systematic analysis of data from the literature. *J Cancer* (2012) 3(0):137–44. doi: 10.7150/jca.4090
13. Qiu M-Z, Li Q, Wang Z-Q, Liu T-S, Liu Q, Wei X-L, et al. HER2-positive patients receiving trastuzumab treatment have a comparable prognosis with HER2-negative advanced gastric cancer patients: a prospective cohort observation. *Int J Cancer* (2014) 134(10):2468–77. doi: 10.1002/ijc.28559
14. Liang J-W, Zhang J-J, Zhang T, Zheng Z-C. Clinicopathological and prognostic significance of HER2 overexpression in gastric cancer: a meta-analysis of the literature. *Tumour Biol* (2014) 35(5):4849–58. doi: 10.1007/s13277-014-1636-3
15. He C, Bian X-Y, Ni X-Z, Shen D-P, Shen Y-Y, Liu H, et al. Correlation of human epidermal growth factor receptor 2 expression with clinicopathological characteristics and prognosis in gastric cancer. *World J Gastroenterol* (2013) 19(14):2171–8. doi: 10.3748/wjg.v19.i14.2171
16. Janjigian YY, Werner D, Pauligk C, Steinmetz K, Kelsen DP, Jäger E, et al. Prognosis of metastatic gastric and gastroesophageal junction cancer by HER2 status: a European and USA Internationalcollaborative analysis. *Ann Oncol* (2012) 23(10):2656–62. doi: 10.1093/annonc/mds104
17. Kataoka Y, Okabe H, Yoshizawa A, Minamiguchi S, Yoshimura K, Haga H, et al. HER2 expression and its clinicopathological features in resectable gastric cancer. *Gastric Cancer* (2013) 16(1):84–93. doi: 10.1007/s10120-012-0150-9
18. Topalian SL, Drake CG, Pardoll DM. Targeting the PD-1/B7-H1 (PD-L1) pathway to activate anti-tumor immunity. *Curr Opin Immunol* (2012) 24 (2):207–12. doi: 10.1016/j.coi.2011.12.009
19. Garon EB, Rizvi NA, Hui R, Leighl N, Balmanoukian AS, Eder JP, et al. Pembrolizumab for the treatment of non-small-cell lung cancer. *N Engl J Med* (2015) 372(372):2018–28. doi: 10.1056/NEJMoa1501824
20. Antonia S, Goldberg SB, Balmanoukian A, Chaft JE, Sanborn RE, Gupta A, et al. Safety and antitumour activity of durvalumab plus tremelimumab in non-small cell lung cancer: a multicentre, phase 1b study. *Lancet Oncol* (2016) 17(3):299–308. doi: 10.1016/S1470-2045(15)00544-6
21. Borghaei H, Paz-Ares L, Horn L, Spigel DR, Steins M, Ready NE, et al. Nivolumab versus docetaxel in advanced nonsquamous non-small-cell lung cancer. *N Engl J Med* (2015) 373(17):1627–39. doi: 10.1056/NEJMoa1507643
22. Weber JS, D'Angelo SP, Minor D, Hodi FS, Gutzmer R, Neyns B, et al. Nivolumab versus chemotherapy in patients with advanced melanoma who progressed after anti-CTLA-4 treatment (CheckMate 037): a randomised, controlled, open-label, phase 3 trial. *Lancet Oncol* (2015) 16(4):375–84. doi: 10.1016/S1470-2045(15)70076-8
23. Powles T, Eder JP, Fine GD, Braiteh FS, Loriot Y, Cruz C, et al. MPDL3280A (anti-PD-L1) treatment leads to clinical activity in metastatic bladder cancer. *Nature* (2014) 515(7528):558–62. doi: 10.1038/nature13904
24. McDermott DF, Drake CG, Sznol M, Choueiri TK, Powderly JD, Smith DC, et al. Survival, Durable Response, and Long-Term Safety in Patients With Previously Treated Advanced Renal Cell Carcinoma Receiving Nivolumab. *J Clin Oncol* (2015) 33(18):2013–20. doi: 10.1200/JCO.2014.58.1041
25. Muro K, Chung HC, Shankaran V, Geva R, Catenacci D, Gupta S, et al. Pembrolizumab for patients with PD-L1-positive advanced gastric cancer (KEYNOTE-012): a multicentre, open-label, phase 1b trial. *Lancet Oncol* (2016) 17(6):717–26. doi: 10.1016/S1470-2045(16)00175-3
26. Kang YK. Nivolumab (ONO-4538/BMS-936558) as salvage treatment after second or later-line chemotherapy for advanced gastric or gastro-esophageal junction cancer (AGC): A double-blinded, randomized, phase III trial. *J Clin Oncol* (2017) 35(4_suppl):2–2. doi: 10.1200/JCO.2017.35.4_suppl.2
27. Sanmamed MF. Chen L. A Paradigm Shift in Cancer Immunotherapy: From Enhancement to Normalization. *Cell* (2018) 175(2):313–26. doi: 10.1016/j.cell.2018.09.035
28. Beer A, Taghizadeh H, Schiefer AI, Puhr HC, Karner AK, Jomrich G, et al. PD-L1 and HER2 Expression in Gastroesophageal Cancer: a Matched Case Control Study. *Pathol Oncol Res* (2020) 26(4):2225–35. doi: 10.1007/s12253-020-00814-2
29. Wang L, Zhang Q, Ni S, Tan C, Cai X, Huang D, et al. Programmed death-ligand 1 expression in gastric cancer: correlation with mismatch repair deficiency and HER2-negative status. *Cancer Med* (2018) 7(6):2612–20. doi: 10.1002/cam4.1502
30. Choueiri TK, Fishman MN, Escudier B, McDermott DF, Drake CG, Kluger H, et al. Immunomodulatory Activity of Nivolumab in Metastatic Renal Cell Carcinoma. *Clin Cancer Res* (2016) 22(22):5461–71. doi: 10.1158/1078-0432.CCR-15-2839
31. Pardoll DM. The blockade of immune checkpoints in cancer immunotherapy. *Nat Rev Cancer* (2012) 12(4):252–64. doi: 10.1038/nrc3239
32. Blank C, Kuball J, Voelkl S, Wiendl H, Becker B, Walter B, et al. Blockade of PD-L1 (B7-H1) augments human tumor-specific T cell responses in vitro. *Int J Cancer* (2006) 119(2):317–27. doi: 10.1002/ijc.21775
33. Boger C, Behrens HM, Mathiak M, Kruger S, Kalthoff H, Rocken C. PD-L1 is an independent prognostic predictor in gastric cancer of Western patients. *Oncotarget* (2016) 7(17):24269–83. doi: 10.18632/oncotarget.8169
34. Chang H, Jung WY, Kang Y, Lee H, Kim A, Kim HK, et al. Programmed death-ligand 1 expression in gastric adenocarcinoma is a poor prognostic factor in a high CD8+ tumor infiltrating lymphocytes group. *Oncotarget* (2016) 7(49):80426–34. doi: 10.18632/oncotarget.12603
35. Gu L, Chen M, Guo D, Zhu H, Zhang W, Pan J, et al. PD-L1 and gastric cancer prognosis: A systematic review and meta-analysis. *PloS One* (2017) 12(8): e0182692. doi: 10.1371/journal.pone.0182692
36. Zhao LN, Zhao HB, Wang Q, Li QZ, Yin TT. Correlation of HER2 and PD-L1 Expression in the Gastric Cancer Tissues with the Clinicopathological Features. *Prog Modern Biomed* (2019) 19:4324–400. doi: 10.13241/j.cnki.pmb.2019.22.027
37. Jiang Y, Zhang Q, Hu Y, Li T, Yu J, Zhao L, et al. ImmunoScore signature: a prognostic and predictive tool in gastric cancer. *Ann Surg* (2018) 267:504–13. doi: 10.1097/SLA.0000000000002116
38. Fridman WH, Zitvogel L, Sautès–Fridman C, Kroemer G. The immune contexture in cancer prognosis and treatment. *Nat Rev Clin Oncol* (2017) 14:717. doi: 10.1038/nrclinonc.2017.101
39. Kalluri R. The biology and function of fibroblasts in cancer. *Nat Rev Cancer* (2016) 16:582–98. doi: 10.1038/nrc.2016.73
40. Mariathasan S, Turley SJ, Nickles D, Castiglioni A, Yuen K, Wang Y, et al. TGF-beta attenuates tumour response to PD-L1 blockade by contributing to exclusion of T cells. *Nature* (2018) 554(7693):544–8. doi: 10.1038/nature25501

Conflict of Interest: JZ is an employee of Shanghai 3D Medicines Inc.

The remaining authors declare that the research was conducted in the absence of any commercial or financial relationships that could be construed as a potential conflict of interest.

frontiers in Oncology

REVIEW
published: 16 February 2021
doi: 10.3389/fonc.2020.598957

Therapeutic Strategies Against Cancer Stem Cells in Esophageal Carcinomas

Plabon Kumar Das[1], *Farhadul Islam*[1,2*], *Robert A. Smith*[3,4] *and Alfred K. Lam*[4,5*]

[1] Department of Biochemistry and Molecular Biology, University of Rajshahi, Rajshahi, Bangladesh, [2] Institute for Glycomics, Griffith University, Gold Coast, QLD, Australia, [3] Centre for Genomics and Personalised Health, Genomics Research Centre, School of Biomedical Sciences, Institute of Health and Biomedical Innovation, Queensland University of Technology (QUT), Kelvin Grove, QLD, Australia, [4] Cancer Molecular Pathology, School of Medicine, Griffith University, Gold Coast, QLD, Australia, [5] Faculty of Medicine, The University of Queensland, Brisbane, QLD, Australia

Cancer stem cells (CSCs) in esophageal cancer have a key role in tumor initiation, progression and therapy resistance. Novel therapeutic strategies to target CSCs are being tested, however, more in-depth research is necessary. Eradication of CSCs can result in successful therapeutic approaches against esophageal cancer. Recent evidence suggests that targeting signaling pathways, miRNA expression profiles and other properties of CSCs are important strategies for cancer therapy. Wnt/β-catenin, Notch, Hedgehog, Hippo and other pathways play crucial roles in proliferation, differentiation, and self-renewal of stem cells as well as of CSCs. All of these pathways have been implicated in the regulation of esophageal CSCs and are potential therapeutic targets. Interference with these pathways or their components using small molecules could have therapeutic benefits. Similarly, miRNAs are able to regulate gene expression in esophageal CSCs, so targeting self-renewal pathways with miRNA could be utilized to as a potential therapeutic option. Moreover, hypoxia plays critical roles in esophageal cancer metabolism, stem cell proliferation, maintaining aggressiveness and in regulating the metastatic potential of cancer cells, therefore, targeting hypoxia factors could also provide effective therapeutic modalities against esophageal CSCs. To conclude, additional study of CSCs in esophageal carcinoma could open promising therapeutic options in esophageal carcinomas by targeting hyper-activated signaling pathways, manipulating miRNA expression and hypoxia mechanisms in esophageal CSCs.

Keywords: esophageal cancer, esophageal cancer stem cells, cancer signaling, miRNAs, hypoxia, autophagy, therapeutic options

OPEN ACCESS

Edited by:
Hongjuan Cui,
Southwest University, China

Reviewed by:
Zhen Dong,
Southwest University, China
Shourong Wu,
Chongqing University, China
Jun Mi,
Shanghai Jiao Tong University, China

***Correspondence:**
Farhadul Islam
farhad_bio83@ru.ac.bd
Alfred K. Lam
a.lam@griffith.edu.au

Specialty section:
This article was submitted to Gastrointestinal Cancers, a section of the journal Frontiers in Oncology

Received: *26 August 2020*
Accepted: *29 December 2020*
Published: *16 February 2021*

Citation:
Das PK, Islam F, Smith RA and Lam AK (2021) Therapeutic Strategies Against Cancer Stem Cells in Esophageal Carcinomas. Front. Oncol. 10:598957. doi: 10.3389/fonc.2020.598957

INTRODUCTION

Esophageal cancer (EC) is the seventh most common malignancy around the world and the sixth most leading cause of cancer-related mortalities with an estimated 572,000 new incidences and 509,000 deaths in 2018 (1, 2). There are two histopathological subtypes of esophageal cancer such as esophageal squamous cell carcinoma (OSCC) and esophageal adenocarcinoma (OAC) (3–5). The incidence of OAC has been escalating in the Western world, whereas OSCC is more common in the

Asia-Pacific region (1). Currently, patients with either subtype receive similar treatment, which is a neoadjuvant chemo-radiotherapy followed by surgery (5). The clinical outcome of the standard therapeutic regimen is, however, limited, as much as 20% of tumors do not respond to chemo-radiotherapy at all, and more than 50% do not respond sufficiently. Furthermore, even after complete responses to adjuvant therapy, early and distant relapse occurs in most cases (5). Therefore, in-depth research is required to investigate the underlying mechanisms of therapy resistance and the subpopulation of cancer cells causing therapy failure needs to be thoroughly investigated.

Accumulating information from research has revealed that a subpopulation of cancer cells known as cancer stem cells (CSCs) are associated with clinical features such as drug resistance, self-renewal, and tumorigenicity in esophageal cancer (6–10). Several pathways *e.g.* Wnt/beta-catenin, Hedgehog, Notch, JAK-STAT3 and Hippo pathways are hyper-activated in both OSCC and OAC, especially in esophageal CSCs. These pathways drive proliferation, differentiation, stemness, and resistance to therapy in the tumors in which they are activated (11–16). For example, the Wnt/beta-catenin pathway was found to contribute to CSC renewal, whereas the Hedgehog pathway has been found to play profound roles in regulating proliferation, not only of normal embryonic cells, but also of cancer cells (11, 13). In addition, altered expression of micro-RNAs; tumor microenvironmental factors such as autophagy, and hypoxia; and reactivation of epithelial-mesenchymal transition (EMT) alone or in combination can trigger the pool of CSCs by aberrant activation of signaling pathways, resulting in the development of cancer recurrences and treatment resistance in esophageal cancer (17–19).Therefore, further investigation regarding the function of CSCs or their associated pathways could provide new potential therapeutic options against esophageal cancers.

Novel therapeutics targeting CSCs rather than bulk-cancer cells or later differentiated progenitors could provide many benefits in patients with esophageal cancer. Traditional cytotoxic agents cannot target CSCs properly as a majority of anti-tumor drugs at present are DNA damage inducing agents (20). They induce tumor cell death most effectively during cell division, while CSCs are usually dormant and do not enter the cell cycle. Thus, DNA damaging agents have little capacity to not induce the death of CSCs (20). Moreover, several mechanisms have been identified in CSCs to avoid DNA damage-induced cell death. For example, CSCs enhance ROS scavenging to inhibit oxidative DNA damage, promote DNA repair capability through ATM and CHK1/CHK2phosphorylation, and activate anti-apoptotic signaling pathways, such as PI3K/Akt, WNT/b-catenin, and Notch signaling pathways to escape DNA damaging agent mediated insults (21).

Interestingly, several therapies that specifically target CSCs or their components in the tumor microenvironment are making their way into clinics. Thus, in this review, we undertake a comprehensive overview of the literature regarding the role of CSCs in esophageal cancer. Moreover, the review also discusses potential therapies targeting aberrantly activated signaling pathways, miRNA expression and hypoxia regulated signaling in esophageal CSCs.

THE ROLE OF CANCER STEM CELLS IN ESOPHAGEAL CANCER

Cancer stem cells (CSCs) harbor unique properties, such as self-renewal, tumor maintenance (proliferation), invasion and migration, immune evasion, and therapy resistance (22, 23). Virchow and Conheim first proposed that CSCs exist as a subpopulation of cancer cells, which possess the traits of embryonic cells, including the ability to proliferate different lineages and renew themselves (24). They further assumed that cancer is derived from dormant stem-like cells of the same tissue (24). An experimental approach using leukemia stem cells provided the first evidence of the existence of a cell population having the capacity to initiate a secondary tumor, confirming the presence of CSCs (25). In general, there are two hypotheses that have been proposed regarding the origin of CSCs (5). Firstly, normal stem cells can be transformed into CSCs because of genetic and epigenetic alterations. Secondly, dedifferentiated cancer cells acquire the capabilities of CSCs by the process called cellular plasticity (22, 23, 25–27). CSCs often display resistance to therapy, the exact mechanisms of which are not clear, however, a number of underlying mechanisms have been identified *i.e.* enhanced DNA repair efficiency, increased expression of detoxification enzymes (ALDH), increased expression of drug resistance proteins, up-regulation of anti-apoptotic proteins (Bcl-2, Bcl-xL, Mcl-l, Bcl-w), mutations in key signaling molecules, and overexpression of drug efflux pumps (P glycoprotein 1, ABCG2) etc. in CSCs (28, 29).

Esophageal CSCs directly regulate cancer initiation, progression, metastasis, therapy resistance and recurrence both in esophageal adenocarcinomas (OAC) and esophageal squamous cell carcinomas (OSCC) (26, 30, 31). CSCs of esophageal cancer can be identified and isolated by specific cell surface and intracellular markers. For example, cell surface and intracellular markers such as CD44, ALDH, Pygo2, MAML1, Twist1, Musashi1, CD271, and CD90, are used to identify CSCs, whereas, stem cell markers including ALDH1, HIWI, Oct3/4, ABCG2, SOX2, SALL4, BMI-1, NANOG, CD133, and podoplanin were associated with the enrichment of CSCs in OSCC (26, 30, 31). In addition, isolation of side population (SP), a subpopulation of cells with the ability to exclude dyes such as Hoechst 33342, are enriched with stem cells and SP isolation can be used to identify CSCs in OSCC (31). According to several studies, side population has been utilized in the isolation of CSCs from esophageal cancer (32–34). For example, isolation of side population in different esophageal cancer cells such as OSCC (OE21) and OAC (OE19, OE33, PT1590, and LN1590) revealed that the proportions of side population cells are varied among the cell lines and they are resistant to chemotherapy (34). Also, SP cells exhibited stem-like cell phenomena such as epithelial-mesenchymal transition (EMT) (34). The stem-like esophageal cells also become more radio-resistant than parental cells (35). The radio-resistant property of esophageal CSCs is attributed to the overexpression of β-catenin, Oct3/4, and β1-integrin (36). Moreover, esophageal CSCs dictate intrinsic and acquired chemotherapy resistance to 5-fluorouracil (5-FU) and cisplatin in OAC (22). This therapy resistance is associated with changes in the regulation of EMT (22). Additionally, recent studies demonstrated a relationship between the expression of miRNAs, for example, miR-296 (37)

and miR-200c (38) and chemoresistance in esophageal CSCs. Furthermore, overexpression of *WNT10A*, a member of the *Wnt* gene family, increases self-renewal capabilities of CSCs and induces a larger population of CSCs in OSCC (39). Most importantly, CSCs with increased tumorigenicity were formed when tumors multiply and experience treatment threats such as targeted agents, cytotoxic agents or radiation (19). Therefore, it is plausible that eradication of CSCs or, alternatively, reduction of their malignant and stemness properties can result in more successful therapeutic approaches.

TARGETING SIGNALING PATHWAYS IN ESOPHAGEAL CANCER STEM CELLS

The signaling pathways which trigger embryogenesis also play a significant role in oncogenesis (40). The pathways highly associated with the maintenance of esophageal CSCs include Wnt/β-catenin, Notch, Hh, and Hippo pathways (39). These pathways are involved in maintaining tissue homeostasis and normal stem cell renewal and dysregulation of these signaling pathways drives esophageal CSCs formation (39). For example, a Wnt/β-catenin activator WNT10A is highly expressed in OSCC tissue. Consistently cells with the expression of WNT10A showed enrichment for CD44+/CD24–, and these cells showed increased self-renewal, invasive and metastatic potential (40, 41). Notch signaling is another prominent driver of cancer stemness in OAC. Experimental work shows, for example, that inhibiting Notch pathway by γ-secretase inhibitors reduces the size of patient-derived xenograft tumors of OAC in mice (42). Furthermore, aberrant activation of these pathways can result from autophagy, hypoxia, anti-cancer therapy and EMT, alone or in combination with each other, which subsequently leads to an enrichment of CSCs and development of recurrences, metastasis and increasing treatment resistance (39). These phenomena can be manipulated by novel therapeutics targeting specific components involving the stemness of cancer cells to offset their role in treatment resistance.

TARGETING THE WNT/β-CATENIN PATHWAY IN ESOPHAGEAL CANCER STEM CELLS

The Wnt/β-catenin signaling pathway plays a pivotal role in oncogenesis through different mechanisms (43). In normal physiological conditions, the Wnt/β-catenin pathway controls the expression of downstream genes, which are involved in basic cellular and biological functions including proliferation, differentiation, apoptosis, and cell death (44). Thus, in order to exert normal physiological functions, activation of Wnt/β-catenin signaling should be kept at the normal level. However, aberrant activation of this pathway is associated with many cancers including esophageal cancer. For instance, over-activation of the Wnt/β-catenin pathway can be an underlying factor of progression, metastasis, and invasion in OSCC by inducing a CSC phenotype (40). Therefore, targeting the Wnt/β-catenin pathway has potential for the inhibition of CSC growth. Though Wnt/β-catenin inhibitors are in clinical trials for various solid tumors, inhibitors are yet to reach clinical trials in esophageal cancer (39). Emerging molecules inhibiting Wnt/β-catenin signaling have provided promising preclinical outcome against esophageal cancer (**Figure 1**, **Table 1**). For example, Icaritin, an alkaloid extracted from *Herba epimedii*, was found to reduce the growth of CSCs derived from the OSCC cell line ECA109 by inhibiting Wnt/β-catenin and Hedgehog pathway (45). Icaritin inhibited proliferation, migration, and invasion of CD133+ esophageal CSCs in a dose-dependent manner and enhanced the apoptosis of these stem cells. In addition, Icaritin induced up-regulation of GSK3β and down-regulation of Wnt and β-catenin, Hedgehog, Smo, and Gli proteins in Wnt/β-catenin and Hedgehog pathways, respectively (45).

ABT-263, a potent Bcl-2 family inhibitor inhibits cell proliferation and induces apoptosis of human esophageal cells, especially CSCs derived from OAC cell lines (FLO-1, SKGT-4, BE3 and OE33) and OSCC cell lines (YES-6 and KATO-TN) (46, 55). ABT263 reduces the expression of many oncogenes, including genes associated with stemness pathways such as Wnt and YAP/SOX9 axes. Treatment of esophageal CSCs with ABT-263 alone and in combination with 5-FUresulted in the reduction of β-catenin and its target cyclinD1, as well asYAP-1 and its target SOX9 in a dose-dependent manner (46). In addition, ABT-263 selectively kills ABCG+ CSCs and inhibits tumor sphere formation of esophageal CSCs (both OSCC and OAC). Also, ABT-263 alone or in combination with 5-fluorouracil reduced tumor volume and tumor weight in a xenograft model. These treatments dramatically reduced the level of YAP1, SOX9 and the proliferation marker Ki-67 in xenotransplanted tumors of both OSCC and OAC cells (46).

Retinoic acids play a crucial role in embryogenesis, differentiation, and tumorigenesis, which are controlled by retinoic acid receptors (RARs) and retinoid X receptors (RXRs) (56). RARα knockdown suppresses the proliferation and metastasis of OSCC cells by minimizing the expression of proliferative markers (PCNA, Ki-67) and matrix metallo-proteinases (MMP7 and MMP9) (47). Not only that, RARα knockdown also enhances drug susceptibility of OSCC cells to 5-fluorouracil and cisplatin (47). On top of that, RARα knockdown results in inhibition of Wnt/β-catenin pathway by decreasing GSK3βphosphorylation at Ser-9 and inducing phosphorylation at Tyr-216, which subsequently results in reduced expression of its downstream targets such as MMP7, MMP9, and P-glycoprotein. Therefore, targeting Wnt/β-catenin or their components to inhibit the pathway should be effective to halt the growth of CSCs in OSCC (47). Moreover, a few Wnt inhibitors such as PRI-724, LGK-974, Vantictumab and OMP-54F28 are in clinical trials as a single agent or in combination with conventional therapy for many solid cancers (57).

TARGETING NOTCH SIGNALING IN ESOPHAGEAL CANCER STEM CELLS

Notch signaling is highly activated in less differentiated tumors and drives CSC phenotypes and carcinogenesis in both OSCC and OAC (39, 42). This signaling helps to maintain a robust population of

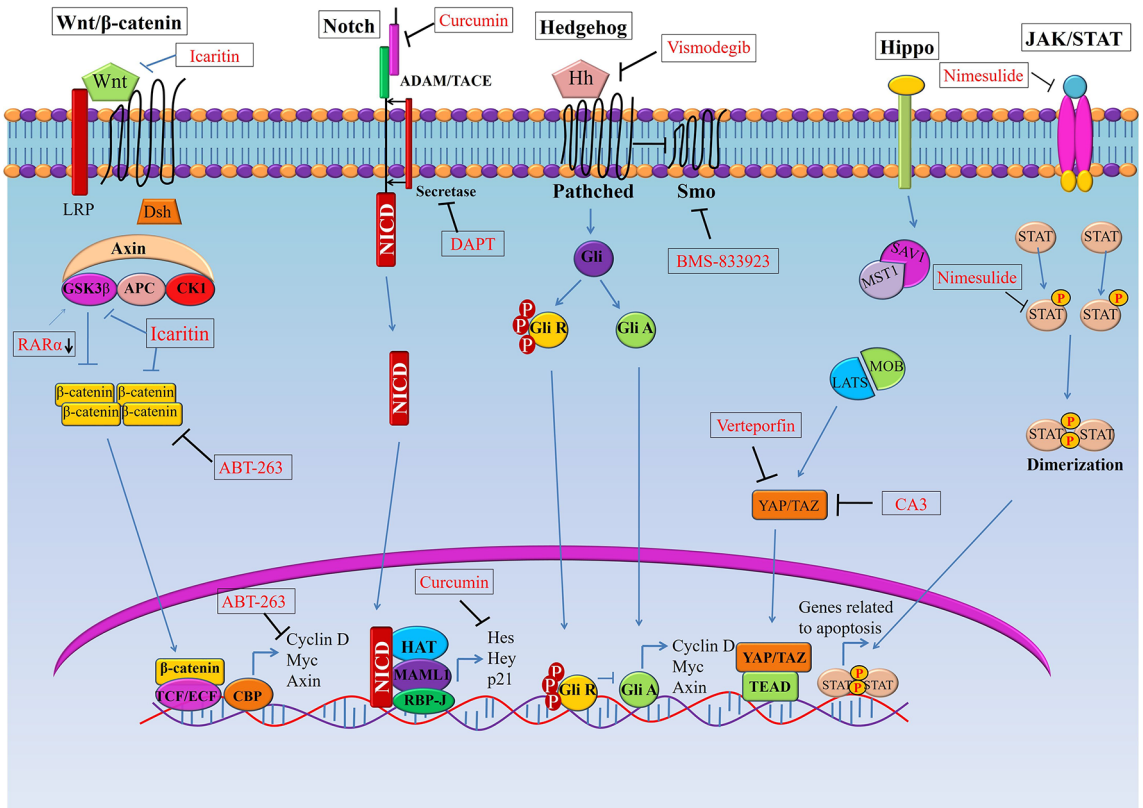

FIGURE 1 | Targeting signaling pathways in esophageal cancer stem cells (CSCs). Schematic representation of the Wnt, Notch, Hedgehog (Hh), and Hippo pathways in esophageal CSCs. Novel therapeutics (synthetic and natural) kill CSCs by targeting these signalling pathways or their components.GSK3β, Glycogen synthase kinase 3 beta; Dsh, Disheveled; APC, Adenomatous polyposis coli; CK1, Casein kinase 1; TCF, T-cell factor/lymphoid enhancer factor; SMO, Smoothened; YAP, (Yes-associated protein); TAZ, Transcriptional coactivator with PDZ-binding motif.

CSCs, thereby resulting in therapy resistance and cancer recurrence (38, 40). Notch inhibition depletes CSC populations in tumors and sensitizes cancer cells to chemotherapeutic agents, which leads to promising response toward neoadjuvant chemotherapy (NAC) in patients with both OSCC and OAC (**Figure 1**, **Table 1**). For example, blocking Notch pathway by DAPT (N-[N-(3, 5-difluorophenacetyl-L-alanyl)]-S-phenylglycine t-butyl ester), a commonly used gamma-secretase inhibitors (GSI), is effective in downsizing tumor growth of OAC. Efficacy of the treatment was shown by a dramatic reduction of the intracellular domain of the notch protein (NICD) in esophageal adenocarcinoma cells (OE33). There was also a reduction in Notch-mediated transcription and a subsequent decrease in the transcription of Notch target genes (42). Treatment of OAC cells with DAPT caused a decrease in cell viability, as well as reducing the number and size of colonies formed by OAC (OE33 and JH-EsoAd1) cells. The inhibition of the Notch pathway caused a significant reduction in transcription of several stem cell marker genes, including *ALDH*, *CD24*, *LGR5*, *SOX2* and *TWIST1*. Furthermore, patient-derived xenograft models clearly demonstrated that inhibition of Notch signaling by gamma-secretase inhibitors is efficacious in downsizing tumor growth (42). Thus, inhibition of Notch signaling by DAPT could impair the stemness of OAC cells *i.e.* esophageal CSCs, resulting in reduced tumor growth in both *in vitro* and *in vivo*.

Gene amplified in squamous cell carcinoma 1 (GASC1), plays a critical role in maintaining self-renewal and differentiation potential of embryonic stem cells (48). GASC1 epigenetically controls the stemness of OSCC by regulation of Notch1. Examination of the expression of GASC1 in OSCC cells and tissues indicated that GASC1 expression is increased in poorly differentiated OSCC (48). Consistent with this observation, patients with OSCCs expressing GASC1 presented a significantly worse survival rate than those without. Most importantly, GASC1 expression in purified CSCs (ALDH+) cells was higher than that in non-CSCs (ALDH−) cells. Several stemness phenotypes of CSCs from OSCC were dramatically decreased after GASC1 blockade, which subsequently resulted in reduced Notch1 expression *via* demethylation of Notch1 promoters (H3K9me2 and H3K9me3). However, the impaired stemness property of CSCs from OSCC followed by GASC1 inhibition was reversed with exogenous Notch1 overexpression (48). This finding suggested that GASC1 promoted stemness in OSCC CSCs cells *via* Notch1 promoter demethylation (48). Therefore, the GASC1/Notch1 signaling axis could be a potential therapeutic target against CSCs of OSCC.

TABLE 1 | Targeting signaling pathways in esophageal cancer stem cells.

Compounds/Drugs/Process	Carcinomas	Target Pathways	Functions	Reference
Icaritin	OSCC	Wnt/β-catenin	Inhibits the proliferation, migration, and invasion of CD133+ CSCs by up-regulating GSK3β and down-regulating Wnt and β-catenin proteins	(45)
ABT-263	OAC and OSCC	Wnt/β-catenin	Reduces the expression of β-catenin protein level, which subsequently results in downregulation of its target protein cyclinD1 in both OAC and OSCC Selectively kills ABCG+ CSCs and inhibits tumor sphere formation in both OAC and OSCC Reduces tumor volume and tumor weight alone or in combination with 5-flurouracil in both OAC and OSCC	(46)
Retinoic acid receptor α (RARα) knockdown	OSCC	Wnt/β-catenin	RARα knockdown inhibits the proliferation and metastasis of OSCC cells by minimizing the expression of PCNA, Ki-67, MMP7, and MMP9 It also enhances drug susceptibility of OSCC cells to 5-fuorouracil and cisplatin	(47)
*N-[N-(3, 5-difluorophenacetyl-L-alanyl)]-S-phenylglycine t-butyl ester (*DAPT)	OAC	Notch	Reduces Notch-mediated transcription and subsequently decreases transcription of Notch target genes Decreases cell viability, the number and size of colony formation	(42)
Blockade of Gene amplified in squamous cell carcinoma 1 (GASC1)	OSCC	Notch	Blockade of GASC1 results in inhibition of OSCC stemness property Reduces the expression of Notch1	(48)
Vismodegib	OAC	Hedgehog	Blocks the interaction between the Ptch-receptors and their ligands Reduces CSC pool in OAC	(49)
Silencing of ATPase family AAA domain containing protein 2 (ATAD2)	OSCC	Hedgehog	Silencing of ATAD2 or inhibiting the Hedgehog signaling decreased the proliferation, invasion and migration abilities along with colony formation of CSCs in OSCC	(50)
CA3	OAC	Hippo	Inhibits proliferation, induces apoptosis, reduces tumor sphere formation of ALDH1+ cells	(35)
Metformin	OAC and OSCCC	mTOR	Decreases the expression of stem cell signaling markers such as *Jagged1*, *Shh*, *YAP1* in both OAC and OSCC Effectively downregulates mTOR components including phospho-AKT, phospho-S6, phospho-70S6 in both OAC and OSCC Inhibits the growth of carcinoma cells *in vitro* and *in vivo* in both OAC and OSCC	(51)
Nimesulide	OSCC	JAK/STAT	Inhibits Cyclooxygenase-2 expression which subsequently diminishes JAK/STAT signaling leading to the suppression of OSCC cell growth and increase of apoptosis	(52)
Erlotinib and Cetuximab	OSCC	EGFR	Halts EMT by instigating differentiation in non-CSC populations	(53)
Pristimerin	OSCC	NF-kβ	Suppresses tumor necrosis factor α (TNFα)-induced Iκ Bα phosphorylation, p65 translocation, and the expression of NF-κB- dependent genes expression Inhibits proliferation, migration, invasion of OSCC cells and induces apoptosis, and eliminates CSCs like cells	(54)

OSCC, esophageal squamous cell carcinoma; OAC, esophageal adenocarcinoma; CSC, cancer stem cell.

TARGETING HEDGEHOG SIGNALING IN CANCER STEM CELLS OF ESOPHAGEAL CANCER

The Hedgehog (HH) signaling pathway plays a crucial role in growth and differentiation during embryonic development (58). However, abnormal activation of this pathway may also lead to cancer stemness along with stimulation of EMT, cancer metastasis and therapy resistance (59–61). Furthermore, activation of the Hedgehog pathway associated with distant metastases, advanced tumor stage in patients with esophageal cancers (both OSCC and OAC) (60, 62, 63). Although Hedgehog inhibitors have been extensively studied in clinical trials for different solid tumors, clinical trials on esophageal cancers are still limited (64). Vismodegib, also known as GDC-0449, is a small molecule inhibitor of Hedgehog signaling that blocks the interaction between the Ptch-receptors and their ligands (**Figure 1**, **Table 1**) (65). In addition, Vismodegib in combination with chemotherapy (FOLFOX) did not increase the survival of patients with gastroesophageal junction adenocarcinoma significantly (64).

Importantly, Vismodegib combined with neoadjuvant chemo-radiotherapy is under investigation in a clinical trial in Hedgehog activated OAC cells (49). Vismodegib treatment reduced the CSC pool derived in OSCC (OE21) and OAC (OE33) cells. Investigation of options for the suppression of the Hedgehog pathway may have additional importance, it has been suggested that neoadjuvant chemo-radiotherapy may activate the Hedgehog pathway, which in turn causes acquisition of more CSC features including the property of therapy resistance (49). For example, there is a subset of cancer cells with activated Hedgehog pathway prior to therapy that renders them able to survive chemo- and radiotherapy (66–69). By contrast, inhibiting the Hedgehog pathway resulted in a reduction of cells with CSC phenotype (CD44+/CD24–), inhibited sphere-forming capability and induced radio-sensitivity (70–72).

BMS-833923, an inhibitor of smoothened (SMO), another constituent of the Hedgehog pathway, combined with

chemotherapy (FOLFOX) is currently under investigation in patients with metastatic esophageal carcinoma (73). SMO brings about the translocation of Gli protein into nucleus which results in the transcription of downstream target genes. Other SMO inhibitors such as Sonidegib and Taladegib are being explored currently against gastroesophageal adenocarcinomas (73, 74). In addition, activation of Hedgehog signaling could be inhibited by targeting transcription factor ATPase family AAA domain-containing protein 2 (ATAD2) (73). ATAD2, a member of the AAA + ATPase family, which is involved in various cancers by regulating cell proliferation, apoptosis, invasion and migration, and its overexpression is associated with poor prognosis of patients with cervical and gastric cancer (75, 76). High expression of ATAD2 has been identified in various types of tumors, including OSCC (75, 77). Interestingly, inhibition of ATAD2 resulted in subsequent inhibition of the Hedgehog signaling pathway, which was confirmed by reduced expression of Gli1, SMO, and Ptch11 in OSCC (50). On top of that, silencing of ATAD2 or inhibiting the Hedgehog signaling decreased the proliferation, invasion and migration abilities along with colony formation of CSCs in OSCC. Furthermore, increased apoptosis followed by the suppression of Hedgehog signaling was noted in CSCs derived from OSCC cells (50). Moreover, *in vivo* experiments in nude mice further validated the suppressive effect of siRNA mediated ATAD2 silencing on tumor growth (50). Thus, down-regulation of ATAD2 can certainly restrict the malignant phenotypes of OSCC cells through inhibition of the Hedgehog signaling pathway in CSCs derived from OSCC cells. These findings suggest that targeting the Hedgehog pathway *via* any of a number of mechanisms could be an effective approach to control CSCs in esophageal carcinomas.

TARGETING HIPPO SIGNALING OF ESOPHAGEAL CELLS OF ESOPHAGEAL CANCER

The Hippo pathway has been implicated in the regulation of organ size, proliferation, and stem cell properties (78, 79). YAP1 plays a significant role in the maintenance of stemness of embryonic stem cells as well as contributing to the functions of CSCs (80–82).Therefore, deregulation of Hippo and activation of YAP1 in CSCs contributes many important properties of tumors, and thus, targeting YAP1 will be an effective strategy to target CSCs, thereby inhibiting tumor growth.

Several small-molecule inhibitors have been tested against the Hippo pathway in both OSCC and OAC cells (**Figure 1**, **Table 1**) (35, 80, 83–86). For example, a novel YAP inhibitor CA3 exhibited remarkable inhibitory activity on the transcriptional activity of YAP1/transcriptional enhanced associate domains (TEAD) (35). CA3 demonstrated strong inhibitory effects on the growth of OAC, especially on YAP1 overexpressing cancer cells both *in vitro* and *in vivo* (35). Most importantly, radio-resistant CSCs with aggressive phenotypes can be effectively suppressed by CA3 treatment. CA3inhibited proliferation, induced apoptosis and reduced tumor sphere formation of CSC (ALDH1+) cells derived from OSCC (35). Furthermore, CA3 in combination with 5-FU inhibited the growth of esophageal adenocarcinoma, especially in YAP1 overexpressing cancer cells (35). Taken together, these findings suggested that CA3 represents a new inhibitor of YAP1 and primarily targets YAP1 overexpressing and therapy-resistant CSCs generated from OAC.

Additionally, YAP1activity correlated with SOX9 expression in esophageal adenocarcinoma (35). SOX9 was found to be highly upregulated in various premalignant lesions and in tumor tissues and plays crucial roles in tumor development (83–85). The co-activator of Hippo pathway (YAP1) acts as a major determinant of CSC properties in non-transformed cells and as well as in OAC cells which directly upregulates the expression SOX9 (80). YAP1 regulates the transcription of SOX9 through a conserved TEAD binding site in the SOX9 promoter region. Exogenous expression of YAP1 or inhibition of its upstream negative regulators *in vivo* caused an increased SOX9 expression, which subsequently results in the acquisition of CSCs properties (80). On the other hand, shRNA-mediated knockdown of YAP1 or SOX9 in transformed cells inhibited CSC phenotypes *in vitro* and tumorigenicity *in vivo* (80). Furthermore, Verteporfin (VP), a small-molecule inhibitor of YAP1, significantly blocks CSCs (ALDH+ cells) properties in OAC cells overexpressingYAP1 (80). Thus, in the acquisition of CSC propertiesYAP1 driven SOX9 expression is critical, indicating that YAP1 inhibition might be an attractive option in targeting CSC population in esophageal cancer. For example, overexpression of YAP1 was positively associated with CDK6expression in radiation-resistant esophageal cancer tissues (both in OAC and OSCC) (86). CDK6 is a key regulator of the cell cycle. Induction of YAP1 expression in esophageal cancer cells up-regulated CDK6 expression, increased transcription, and consequently induced the resistance against radiotherapy (86). By blocking YAP1 and CDK6 with the YAP1 inhibitor CA3, and the CDK6 inhibitor LEE001 significantly suppressed esophageal cancer cell growth and CSC properties, particularly in radiation-resistant cells in both OAC and OSCC (86). The combination of LEE001 and CA3 exhibited the highest anti-tumor effects in radiation-resistant cells overexpressing YAP1 and CDK6 in both *in vitro* and *in vivo* by sensitizing resistant tumors to irradiation (86). Thus, it was implied that crosstalk between YAP1 and CDK6 seems to play a pivotal role in conferring radiation resistance and targeting both YAP1 and CDK6 could be a useful therapeutic strategy to treat both esophageal adenocarcinoma and squamous cell carcinoma.

TARGETING OTHER PATHWAYS IN ESOPHAGEAL CANCER STEM CELLS

The pathways discussed above may act alone or in crosstalk with other pathways to induce stem cell properties in cancer cells or can even participate in driving therapy resistance upon interacting with other pathways (51). For example, the mTOR pathway is often activated in cancers and may generate therapy resistance followed by Hedgehog pathway inhibition (87, 88). The mTOR pathway along with Hedgehog and other pathways are associated with the maintenance of CSC phenotypes (89–93).

Thus, interrupting mTOR with novel therapeutic could induce a reduction of stemness of cancer cells and sensitize them to the therapies. Metformin, an anti-diabetic agent, for instance, was found to significantly inhibit cell growth in both OSCC and OAC cells and sensitized them to 5-FU by targeting the mTOR signaling pathway in CSCs (80, 87–91). It increased the effectiveness of 5-FU against both OSCC and OAC cells and inhibited their growth *in vitro* and in a xenograft nude mouse model (51). Significant downregulation of mTOR pathway components including phospho-AKT, phospho-S6, phospho-70S6 was seen followed by metformin treatment, which are crucial to maintaining tumor cells' growth. Furthermore, metformin treatment strongly decreased the expression of stem cell markers such as *Jagged1*, *Shh*, and *YAP1* (51). Therefore, metformin-induced cell growth inhibition *in vitro* and *in vivo* in both OSCC and OAC cells by its ability to reduce the CSCs population as well as inhibition of the mTOR pathway. Furthermore, the synergistic effect of metformin with 5-FU was particularly of interest, because it would potentially provide an opportunity to treat both the CSCs and proliferating cell component at the same time, to effectively increase the sensitivity of chemo-radiation in patients with OSCC and OAC.

The JAK/STAT signaling pathway has been implicated in various physiological processes, and inhibition of this pathway could impede cancer cell growth and induce apoptosis in various cancers (94–96). Cyclooxygenase-2 (COX-2) together with JAK/STAT signaling has been found to be involved tumorigenesis. Specifically, the tumorigenesis pathway is associated with COX-2 upregulation (97, 98). Inhibition of COX-2 with nimesulide, a selective COX-2 inhibitor, results in suppression of the JAK/STAT signaling pathway, which subsequently inhibits the growth of Eca-109 human OSCC cells (52). Nimesulide induced apoptosis in Eca-109 cells by decreasing the expression of COX-2 and survivin and increasing caspase-3 expression (98). Also, nimesulide inhibited the JAK/STAT pathway by downregulating the phosphorylation of JAK2 and STAT3 (52). Inhibition of *in vivo* tumor growth of Eca-109 in xenotransplanted animals followed by a reduction inexpression of p-JAK2 and p-STAT3 were noted in Nimesulide treatment (52). Though Nimesulide could be used to inhibit JAK/STAT signaling pathway in OSCC cells, its effects on CSCs is yet to be evaluated. Thus, further studies are warranted to explore the effect of inhibition of JAK/STAT pathway in CSCs in esophageal cancers.

Epidermal growth factor receptors (EGFRs), a family of receptor kinases, are expressed in various cancers and contribute to a complex signaling cascade, which in turn controls growth, differentiation, adhesion, migration and survival of CSC and non-CSC cancer cells (53, 99). The wide range of roles for EGFRs in cancer progression makes them an attractive candidate for anti-cancer therapy. EGFRs are overexpressed in OSCC and play pivotal roles in the generation of stem-like cells *via* TGF-β (53). They induce EMT in CD44 overexpressing CSC cells derived from OSCC cells (53). CSCs (CD44+/CD24-) were significantly enriched in EPC2T and OKF6T cells (transformed keratinocyte cell lines) overexpressing EGFR, which could induce EMT by TGF-β1 in CSCs derived fromEPC2T and OKF6T cells (53). Interestingly, Erlotinib and Cetuximab (two EGFR inhibitors) significantly inhibited the enrichment of CSCs *via* inhibition of TGF-β1 mediated EMT (**Table 1**). Also, treatment with EGFR inhibitors resulted in increased expression of CD24 in the non-CSC population (CD44-/CD24+cells), indicating that EGFR inhibition could prompt differentiation in non-CSC populations as CD24 is a marker of keratinocyte differentiation (53). These results suggest that inhibition of EGFR may halt EMT by instigating differentiation in non-CSC populations, thereby suppressing enrichment of CSCs *via* inhibition of EMT. However, these EGFR inhibitors do not affect pre-existing CSCs. By contrast, some EGFR inhibitors suppress Zinc finger E-box binding proteins (ZEBs) and induce differentiation of CSCs in OSCC (53). These findings suggested that EGFR inhibition might suppress the expression of ZEBs and induce differentiation in a wider variety of cancers, thereby blocking EMT-mediated enrichment of CSCs.

NF-kβ, another prominent pathway, regulates various biological processes including apoptosis, proliferation, immune response, cell invasion, and cancer stem-like cells (CSCs) (100). The key proteins in the NF-κB pathway (e.g., p50, p52, and Rel) were overexpressed in patients with OSCC (101). In addition, the aberrant activation of the NF-κB signaling pathway is a significant predictor for prognosis and recurrence of OSCC, which makes it a potential target in the treatment of patients with OSCC (102). A natural quinonemethide triterpenoid compound has been isolated from traditional Chinese herbals known as pristimerin, potently inhibited the growth of OSCC xenograft in nude mice (**Table 1**) (54). Pristimerin demonstrated its anti-OSCC effects through the inhibition of NF-κB pathway by suppressing tumor necrosis factor α (TNFα)-induced Iκ Bα phosphorylation, p65 translocation, and the expression of NF-κB- dependent genes (e.g., *p50*, *p52*, and *Rel*).Furthermore, pristimerin inhibited cell proliferation, migration, invasion, induced apoptosis, and eliminated cancer stem-like cells (CSCs) derived from OSCC cells (54). In addition, pristimerin exhibited a synergistic effect on OSCC when combined with 5-FU (54). These results imply that pristimerin could increase chemo-sensitivity by suppressing the therapy-resistant CSC cell population in OSCCs.

TARGETING MICRORNA EXPRESSION IN ESOPHAGEAL CANCER STEM CELLS

MicroRNAs (miRNAs/miRs) are a class of small noncoding RNAs approximately 19–25 nucleotides in length, which regulate post-transcriptional gene expression by binding with their target mRNA transcripts (103, 104). Depending on the roles of their target genes, miRNAs can act either as tumor suppressors or oncogenes (105, 106). They are strongly involved in the formation of CSCs by regulating post transcriptional gene expressions in various cancer types (107).

Altered expression of particular cancer-associated miRNAs causes significant changes in the level of potential oncogenic and anti-oncogenic proteins, which suggests miRNAs as useful therapeutic targets in cancer (108). Thus, miRNA mediated changes in gene expression in cancer has become a subject undergoing intense research nowadays.

MicroRNAs could act as molecular markers of cancer stem-like cells in esophageal cancer. Thereby, novel therapeutic strategies targeting miRNAs in CSCs have the potential to eradicate CSCs population, resulting in the improved clinical outcomes for patients with esophageal squamous cell carcinoma or adenocarcinoma (**Table 2**, **Figure 2**) (109–111, 116–118). For example, miRNA-203 is downregulated in cancer stem-like cells (Side population generated from OSCC (EC9706) cells) and expression of miR-203 was inversely associated with the expression of stem cell self-renewal factor Bmi-1 (109). Comparison of expression ofBmi-1 between SP and non-SP cells revealed that Bmi-1 was highly expressed in SP cells and its expression was significantly diminished during the differentiation from SP to non-SP cells (109, 110, 118). Therefore, miR-203 and Bmi-1 appear to play important roles in the generation of cancer stem-like cells in OSCC. In addition, lentiviral mediated expression of miR-203 resulted in decreased colony formation ability of SP cells, which was associated with the resistance to chemotherapy and responsible for tumorigenesis in nude mice (109). Since miR-203 and Bmi-1 were inversely expressed in SP cells, Bmi-1 might be a direct target of miR-203, thus therapeutics targeting miR-203 or Bmi-1could have the potential to eradicate CSCs in OSCC.

Another miRNA, miR-181b in association with STAT3, plays a significant role in stem cell properties of esophageal squamous cell carcinoma stem-like cells (110). Isolating sphere-forming cells from OSCC cells (Eca109) exhibited proliferation and tumorigenicity characteristics of CSCs in a mouse xenograft model (110). The sphere-forming cells demonstrated cancer stem-like cell properties such as an enhanced population of CD44+/CD24- cells, increased stemness factors, mesenchymal marker expression, ATP-binding cassette (ABC) transporters and tumorigenicity *in vivo* when compared to that of parental cells (110). A mutual regulation between the signal transducer and activator transcription 3 (STAT3, a transcription factor) and miR-181b controls the sphere-forming cells' proliferation and apoptosis resistance in esophageal cancer stem-like cells. STAT3 directly activated miR-181b transcription in a sphere-forming cells, which in turn potentiated p-STAT3 activity (110). Mechanistically, miR-181b binds with 3′-untranslated region (UTR) of cylindromatosis (CYLD) mRNA and regulates CYLD expression, which in turn regulates sphere-forming cells *via* modulating the STAT3/miR-181b loop in esophageal CSCs.

MicroRNAs such asmiR-135a may regulate biological behaviors of CSCs in OSCC through the Hedgehog signaling pathway by targeting its component SMO (111). Expressions of hedgehog pathway proteins such as SMO, Gli1, Shh, and Gli2 were happened to be increased and the expression of miR-135a was decreased in in esophageal CSCs of squamous cell carcinoma. However, exogenous overexpression of miR-135a or silencing of SMO decreased the expression of Gli1, Gli2, and Shh, resulting in reduced proliferation migration, invasion and increased apoptosis of CSCs derived from esophageal cancer cells (111). Interestingly, silencing of miR-135a was associated with increased carcinogenic capability of miR-135a in CSCs derived from OSCC (111). These results suggest that miR-135a mediated inhibition of CSCs derived from esophageal squamous cell carcinoma cells through suppression of the SMO/Hedgehog axis may act as a potential therapeutic option for patients with the carcinoma.

Another example of a miRNA promoting stem cell-like characteristics is miR-942, which in OSCCs causes activation of the Wnt/β-catenin signaling pathway (112). miR-942 was significantly upregulated in OSCC and was correlated with poor prognosis in patients with OSCC. Upregulation of miR-942 promoted cancer stem-like cell (CD90+ cells) traits in OSCC, whereas inhibition of miR-942 decreased tumor sphere formation and inhibited the expression of pluripotency-associated markers in the stem-like cells (112). Moreover,

TABLE 2 | MicroRNAs associated with functions of esophageal cancer stem cells.

MicroRNAs	Expression pattern	Carcinoma (s)	Function	Reference
miRNA-203	Downregulated	OSCC	Expression of miR-203 results in decreased colony formation ability of SP cells by downregulating the expression of Bmi1	(109)
miR-181b	Upregulated	OSCC	miR-181b binds with 3′-untranslated region (UTR) of CYLD mRNA to positively regulate the stemness of esophageal cancer cells miR-181b together with STAT3 regulate stemness of esophageal cancer cells by maintaining feedback loop *via* CYLD pathway	(110)
miR-135a	Downregulated	OSCC	Overexpression of miR-135a decreases the expression of Gli1, Gli2, and Shh, which as a result reduces the proliferation, migration, and invasion of cancer cells and promotes apoptosis	(111)
miR-942	Up-regulated	OSCC	Upregulation of mir-942 promotes cancer stem cell-like traits and tumor sphere formation in OSCC	(112)
miR-455-3p	Up-regulated	OSCC	Promotes chemoresistance and tumorigenesis of OSCC cells	(113)
miR-17	Down-regulated	OAC	Expression of miR-17-5p significantly sensitizes radioresistant cells to X-ray radiation and enhanced the repression of genes such as *C6orf120*	(114)
miR-221	Up-regulated	OAC	Knockdown of miR-221 in 5-flurouracil resistant cells decreases cell proliferation, increases apoptosis, restores chemosensitivity, and leads to inactivation of the stem cell pathway Wnt/β-catenin by activation of DKK2 activity	(115)

OSCC, esophageal squamous cell carcinoma; OAC, esophageal adenocarcinoma.

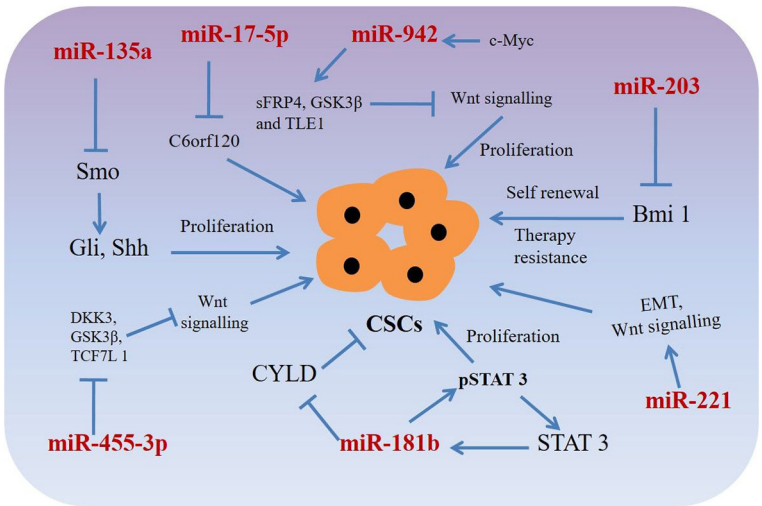

FIGURE 2 | miRNAs targeting phenotypic markers in esophageal cancer stem cells (CSCs). miRNAs upregulate or downregulate the genes related to proliferation, sphere-formation, and therapy resistance.

in vivo assays demonstrated thatmiR-942 overexpressing cells form larger tumors and display higher tumorigenesis capacity (112). miR-942 upregulates the Wnt/β-catenin signaling activity *via* directly targeting FRP4, GSK3β, and TLE1, which are prominent negative regulators of the Wnt/β-catenin signaling cascade (112). In addition, c-myc (a stem cell pluripotency-associated marker) directly binds to the miR-942 promoter and increased its expression, resulting in increased CSC mediated tumorigenesis (112). Considering the oncogenic role of miR-942 in OSCC, miR-942 might be an attractive therapeutic target for patients with OSCC.

Also, dysregulation of miR-455-3ppromoted chemoresistance and tumorigenesis of OSCC cells (113). Interestingly, treatment with a miR-455-3p antagomir significantly chemo-sensitized OSCC cells and decreased CD90+ and CD271 + cell populations (a CSC phenotype) through inhibition of various stemness-associated pathways including Wnt/β-catenin and TGF- β signaling (113). miR-455-3p targets several negative regulators e.g. DKK3, GSK3β, TCF7L 1, IGFBP4 etc. (Wnt/β-catenin pathway components) and Smurf2, NEDD4L, FKBP1A, BAMB I, etc. (TGF-β/Smad pathway components), resulting in inactivation of Wnt/β-catenin and TGF-β signaling in CSCs derived from OSCC cells (113). Association of miR-455-3p levels with chemoresistance and overall/relapse-free survival of patients with OSCC, indicating miR-455-3p antagonist could have potential as effective therapeutics for patients with OSCC. Another miRNA, miR-17 associated with the radio-resistant property of OAC cancer stem-like cells (114). An *in vitro* isogenic model using radio-resistantOE33 R cells derived from OE33 OAC cells demonstrated increased expression of CSC-associated markers and had enhanced tumorigenicity *in vivo* and increased holoclone forming capacity (114). Also, radio resistantOE33 R cells have increased ALDH activity. However, an *in vitro* study suggested that exogenous expression of miR-17-5p significantly sensitized radio-resistant cells to radiation therapy by repression of *chromosome 6 open reading frame 120* (*C6orf120)* expression (114). This study sheds novel insights into the role of miR-17-5p as a potential prognostic biomarker in patients with esophageal adenocarcinomas.

Additionally, miR-221 is another miRNA upregulated in 5-FU resistant esophageal cancer cells (OAC) as well as in human OAC tissues (115). DKK2, a putative inhibitor of Wnt signaling was identified as a potential target for miR-221. Importantly, miR-221 knockdown in 5-FU resistant cells resulted in decreased cell proliferation, increased apoptosis, restored chemo-sensitivity, and led to inactivation of the stem cell pathway Wnt/β-catenin by activation of DKK2 activity (115). In addition, reduction of miR-221 expression resulted in alteration of EMT-associated genes e.g. *E-cadherin* and *vimentin* and slowed xenograft tumor growth in nude mice (115). Furthermore, a substantial dysregulation of Wnt/β-catenin signaling and chemoresistance target genes such as *CDH1*, *CD44*, *MYC*, and *ABCG2* was reported as a result of miR-221 modulation in OAC (115). miR-221 may, therefore, could act as a prognostic marker and therapeutic target for patients with OAC.

TARGETING HYPOXIA-RELATED PATHWAYS IN ESOPHAGEAL CANCER TO ELIMINATE CANCER STEM CELLS

Hypoxia, resulting from low oxygen concentration and nutrition deprivation, is a very common scenario in locally advanced solid tumors (119, 120). It regulates hypoxia-inducible factor (HIF) 1 and 2, which in turn can play critical roles in cancer metabolism, stem cell proliferation, maintaining aggressiveness and metastatic potential of both OSCC and OAC cells

(**Figure 3**) (119, 120). Overexpression of HIFs also reduces radiosensitivity (121, 122) and induces EMT in cancer cells (123, 124). On the other hand, inhibition of HIF1α resulted in suppression of tumorigenicity of OSCC cells in both *in vitro* and *in vivo* (125). At tissue levels, hypoxia and HIF1α are associated with therapy resistance and poor prognosis in patients with OSCC and OAC (126–129). Moreover, hypoxia regulates EMT and cancer stemness in various cancers by targeting Notch, Wnt/β-catenin, Hedgehog, PI3K/mTOR and unfolded protein response (UPR) pathways (130).

In esophageal cancer, a lower level of oxygen increases the CSC population, suggesting the need to target hypoxia in order to eradicate all tumor cells, especially the CSC population (131). It was reported that the expression of HIF-1α and CSC-related genes conditions were upregulated under hypoxic condition. A significant reduction of cell proliferation, migration and tumor growth was occurred followed by HIF-1α knockdown in OSCC cells *in vivo* (131). In addition, knockdown of HIF-1α also inhibited spheroid formation, inhibited expression of CSC-related genes and Wnt/β-catenin target genes, thereby decreased Wnt/β-catenin activity CSCs derived from OSCC (131). Therefore, targeting hypoxia or its related factor and at the same time, inhibiting Wnt/β-catenin might be an attractive option against patients with both OSCC and OAC. There are two main strategies targeting tumor hypoxia. Firstly, by applying bioreductive prodrugs and secondly, inhibiting molecular targets associated with hypoxia using molecular inhibitors (132). A few prodrugs, for example, Tirapazamine, Apaziquone, TH-302, PR-104, Banoxantrone, and RH1 are effective in other solid cancers and are in clinical trials in minimizing tumor hypoxia (132). These prodrugs could be utilized against hypoxia in esophageal cancers. Interestingly, inhibition of the PI3K/mTOR pathway or a hypoxia may lead to activation of autophagy and could be used as an alternative therapeutic modality in esophageal cancers (130). The mTOR pathway negatively regulates autophagy in hypoxic conditions along with regulating cellular growth, proliferation, survival and metabolism (133). Thus, targeting the mTOR pathway mediated autophagy by Bafilomycin and Chloroquine could be useful against CSCs in both OAC and OSCC (73).

Finally, clinical trials targeting esophageal CSCs registered at https://clinicaltrials.gov/ were examined. To the best of our knowledge there is only a study using Fursultiamine, a nutrition supplement is undergoing a phase II clinical trial against OSCC patients in Taiwan in combination with concurrent chemo-radiation therapy to target CSCs (NCT02423811). Fursultiamine suppress OCT-4, SOX-2, NANOG expression and decreased ABCB1 and ABCG2 in tumor spheres. These findings encouraged the researchers to undertake a phase II trial to identify the effect of Fursultiamine combined with concurrent chemo-radiation therapy in ESCC patients. The outcome of the trial is not reported yet, however, they suggested that stem cell markers in clinical specimens collected before and after concurrent chemo-radiation therapy would be evaluated to identify whether Fursultiamine is effective against CSCs or not.

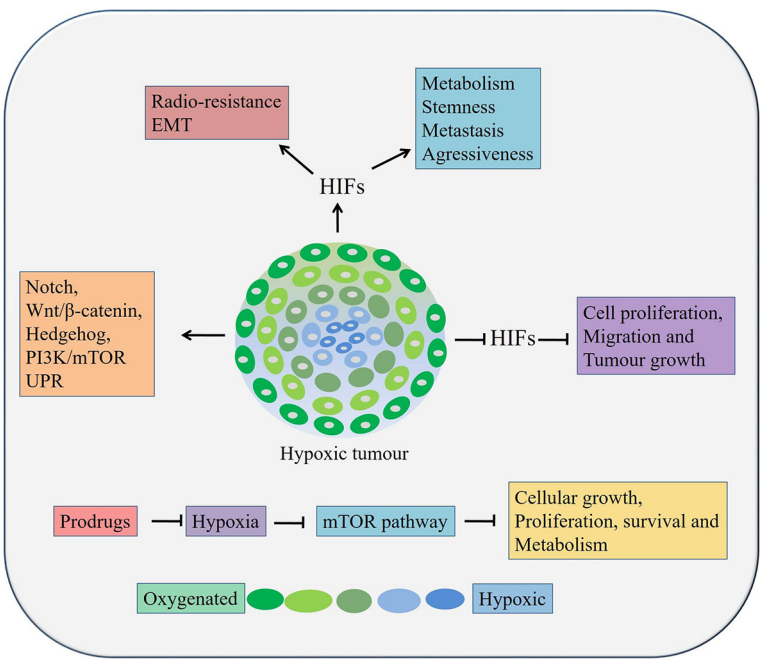

FIGURE 3 | Role of hypoxia in esophageal cancers. Hypoxia can lead to cancer cell growth, metastasis, stemness, and therapy resistance through aberrant activation of pathways, inducing EMT processes etc. HIFs, Hypoxia inducible factors.

CONCLUDING REMARKS

Current conventional anticancer therapies are unable to eliminate CSCs. Therefore, relapse can occur, and CSCs can enable tumors to develop with further resistance to treatment and with more biological aggressiveness. In esophageal cancer, accumulating information has led to the hypothesis that the CSC population could be the seeds of carcinogenesis and are associated with therapy resistance and cancer recurrence. Thus, targeted therapy against CSCs could offer new options approaches to eliminate the malignant phenotypes of cancer without causing any harm to normal stem cells. In addition, careful analysis of a patient's specific tumor may lead to a personalized approach, where both CSCs and the bulk tumor can potentially be eradicated. Eradicating both CSCs and bulk tumor should lead to a more promising outcome for patients with esophageal cancers. In some patients, conventional chemotherapy, surgical strategy along with targeted therapy will ultimately provide a more durable cure to this disease.

AUTHOR CONTRIBUTIONS

PD drafted the manuscript. FI synthesized the concept and edited the manuscript. AL supervised the project and edited the manuscript. RS edited the concept and did the English proofreading. All authors contributed to the article and approved the submitted version.

REFERENCES

1. Bray F, Ferlay J, Soerjomataram I, Siegel RL, Torre LA, Jemal A. Global cancer statistics 2018: GLOBOCAN estimates of incidence and mortality worldwide for 36 cancers in 185 countries. *CA Cancer J Clin* (2018) 68:394–424. doi: 10.3322/caac.21492
2. Global Burden of Disease Cancer Collaboration, Fitzmaurice C, Abate D, Abbasi N, Abbastabar H, Abd-Allah F, et al. Global, Regional, and National Cancer Incidence, Mortality, Years of Life Lost, Years Lived With Disability, and Disability-Adjusted Life-Years for 29 Cancer Groups, 1990 to 2017: A Systematic Analysis for the Global Burden of Disease Study. *JAMA Oncol* (2019) 5:1749–68. doi: 10.1001/jamaoncol.2019.2996
3. Codipilly DC, Qin Y, Dawsey SM, Kisiel J, Topazian M, Ahlquist D, et al. Screening for esophageal squamous cell carcinoma: recent advances. *Gastrointest Endosc* (2018) 88:413–26. doi: 10.1016/j.gie.2018.04.2352
4. Ajani JA, D'Amico TA, Almhanna K, Bentrem DJ, Besh S, Chao J, et al. National comprehensive cancer network. Esophageal and esophagogastric junction cancers, version 1.2015. *J Natl Compr Canc Netw* (2015) 13:194–227. doi: 10.6004/jnccn.2015.0028
5. van Hagen P, Hulshof MC, van Lanschot JJ, Steyerberg EW, van Berge Henegouwen MI, Wijnhoven BP, et al. Preoperative chemoradiotherapy for esophageal or junctional cancer. *N Engl J Med* (2012) 366:2074–84. doi: 10.1056/NEJMoa1112088
6. Das PK, Rakib MA, Khanam JA, Pillai S, Islam F. Novel therapeutics against breast cancer stem cells by targeting surface markers and signaling pathways. *Curr Stem Cell Res Ther* (2019) 14:669–82. doi: 10.2174/1574888X14666190628104721
7. Das PK, Islam F, Lam AK. The Roles of Cancer Stem Cells and Therapy Resistance in Colorectal Carcinoma. *Cells* (2020) 9:1392. doi: 10.3390/cells9061392
8. Islam F, Gopalan V, Lam AK. Identification of Cancer Stem Cells in Esophageal Adenocarcinoma. *Methods Mol Biol* (2018) 1756:165–76. doi: 10.1007/978-1-4939-7734-5_15
9. Islam F, Gopalan V, Smith RA, Lam AK. Translational potential of cancer stem cells: A review of the detection of cancer stem cells and their roles in cancer recurrence and cancer treatment. *Exp Cell Res* (2015) 335:135–47. doi: 10.1016/j.yexcr.2015.04.018
10. Islam F, Gopalan V, Wahab R, Smith RA, Lam AK. Cancer stem cells in oesophageal squamous cell carcinoma: Identification, prognostic and treatment perspectives. *Crit Rev Oncol Hematol* (2015) 96:9–19. doi: 10.1016/j.critrevonc.2015.04.007
11. Hoffmeyer K, Raggioli A, Rudloff S, Anton R, Hierholzer A, Del Valle I, et al. Wnt/β-catenin signaling regulates telomerase in stem cells and cancer cells. *Science* (2012) 336:1549–54. doi: 10.1126/science.1218370
12. Taniguchi H, Moriya C, Igarashi H, Saitoh A, Yamamoto H, Adachi Y, et al. Cancer stem cells in human gastrointestinal cancer. *Cancer Sci* (2016) 107:1556–62. doi: 10.1111/cas.13069
13. Wadhwa R, Wang X, Baladandayuthapani V, Liu B, Shiozaki H, Shimodaira Y, et al. Nuclear expression of Gli-1 is predictive of pathologic complete response to chemoradiation in trimodality treated oesophageal cancer patients. *Br J Cancer* (2017) 117:648–55. doi: 10.1038/bjc.2017.225
14. Wang Z, Chen J, Capobianco AJ. The Notch signaling pathway in esophageal adenocarcinoma. *Cell Mol Biol (Noisy-le-grand)* (2015) 61 (6):24–32.
15. You Z, Xu D, Ji J, Guo W, Zhu W, He J. JAK/STAT signal pathway activation promotes progression and survival of human oesophageal squamous cell carcinoma. *Clin Transl Oncol* (2012) 14:143–9. doi: 10.1007/s12094-012-0774-6
16. Zanconato F, Cordenonsi M, Piccolo S. YAP/TAZ at the Roots of Cancer. *Cancer Cell* (2016) 29:783–803. doi: 10.1016/j.ccell.2016.05.005
17. He B, Yin B, Wang B, Xia Z, Chen C, Tang J. MicroRNAs in esophageal cancer (review). *Mol Med Rep* (2012) 6:459–65. doi: 10.3892/mmr.2012.975
18. Bao B, Azmi AS, Ali S, Ahmad A, Li Y, Banerjee S, et al. Thebiological kinship of hypoxia with CSC and EMT and their relationship withderegulated expression of miRNAs and tumor aggressiveness. *Biochim Biophys Acta* (2012) 1826:272–96. doi: 10.1016/j.bbcan.2012.04.008
19. Gu J, Wang Y, Wu X. MicroRNA in the pathogenesis and prognosis of esophageal cancer. *Curr Pharm Des* (2013) 19:1292–300. doi: 10.2174/138161213804805775
20. Pan Y, Ma S, Cao K, Zhou S, Zhao A, Li M, et al. Therapeuticapproaches targeting cancer stem cells. *J Cancer Res Ther* (2018) 14:1469–75. doi: 10.4103/jcrt.JCRT_976_17
21. Wang QE. DNA damage responses in cancer stem cells: Implications for cancer therapeutic strategies. *World J Biol Chem* (2015) 6:57–64. doi: 10.4331/wjbc.v6.i3.57
22. Das PK, Pillai S, Rakib MA, Khanam JA, Gopalan V, Lam AKY, et al. Plasticity of cancer stem cell: origin and role in disease progression and therapy resistance. *Stem Cell Rev Rep* (2020) 16:397–412. doi: 10.1007/s12015-019-09942-y
23. Singh AK, Arya RK, Maheshwari S, Singh A, Meena S, Pandey P, et al. Tumor heterogeneity and cancer stem cell paradigm: updates in concept, controversies and clinical relevance. *Int J Cancer* (2015) 136:1991–2000. doi: 10.1002/ijc.28804
24. Cohnheim J. Congenitales, quergestreiftesmuskelsarkomdernieren. *Archivfürpathologische Anatomie und Physiologie und fürklinische Medicin* (1875) 65:64–9. doi: 10.1007/BF01978936
25. Huntly BJ, Gilliland DG. Leukaemia stem cells and the evolution of cancer-stem-cell research. *Nat Rev Cancer* (2005) 5:311–21. doi: 10.1038/nrc1592
26. Islam F, Qiao B, Smith RA, Gopalan V, Lam AK. Cancer stem cell: fundamental experimental pathological concepts and updates. *Exp Mol Pathol* (2015) 98:184–91. doi: 10.1016/j.yexmp.2015.02.002
27. Rassouli FB, Matin MM, Saeinasab M. Cancer stem cells in human digestive tract malignancies. *Tumour Biol* (2016) 37:7–21. doi: 10.1007/s13277-015-4155-y
28. Harada K, Pool Pizzi M, Baba H, Shanbhag ND, Song S, Ajani JA. Cancer stem cells in esophageal cancer and response to therapy. *Cancer* (2018) 124:3962–4. doi: 10.1002/cncr.31697

29. Steinbichler TB, Dudás J, Skvortsov S, Ganswindt U, Riechelmann H, Skvortsova II. Therapy resistance mediated by cancer stem cells. *Semin Cancer Biol* (2018) 53:156–67. doi: 10.1016/j.semcancer.2018.11.006
30. Islam F, Gopalan V, Law S, Tang JC, Lam AK. FAM134B promotes esophageal squamous cell carcinoma in vitro and its correlations with clinicopathologic features. *Hum Pathol* (2019) 87:1–10. doi: 10.1016/j.humpath.2018.11.033
31. Islam F, Gopalan V, Lam AK. Detention and Identification of Cancer Stem Cells in Esophageal Squamous Cell Carcinoma. *Methods Mol Biol* (2020) 2129:177–91. doi: 10.1007/978-1-0716-0377-2_14
32. Lu C, Xu F, Gu J, Yuan Y, Zhao G, Yu X, et al. Clinical and biological significance of stem-like CD133(+)CXCR4(+) cells in esophageal squamous cell carcinoma. *J Thorac Cardiovasc Surg* (2015) 150:386–95. doi: 10.1016/j.jtcvs.2015.05.030
33. Wu Q, Wu Z, Bao C, Li W, He H, Sun Y, et al. Cancer stem cells in esophageal squamous cell cancer. *Oncol Lett* (2019) 18:5022–32. doi: 10.3892/ol.2019.10900
34. Zhao Y, Bao Q, Schwarz B, Zhao L, Mysliwietz J, Ellwart J, et al. Stem cell-like side populations in esophageal cancer: a source of chemotherapy resistance and metastases. *Stem Cells Dev* (2014) 23:180–92. doi: 10.1089/scd.2013.0103
35. Song S, Xie M, Scott AW, Jin J, Ma L, Dong X, et al. A Novel YAP1 Inhibitor Targets CSC-Enriched Radiation-Resistant Cells and Exerts Strong Antitumor Activity in Esophageal Adenocarcinoma. *Mol Cancer Ther* (2018) 17:443–54. doi: 10.1158/1535-7163.MCT-17-0560
36. Zhang X, Komaki R, Wang L, Fang B, Chang JY. Treatment of radioresistant stem-like esophageal cancer cells by an apoptotic gene-armed, telomerase-specific oncolytic adenovirus. *Clin Cancer Res* (2008) 14:2813–23. doi: 10.1158/1078-0432.CCR-07-1528
37. Hong L, Han Y, Zhang H, Li M, Gong T, Sun L, et al. The prognostic and chemotherapeutic value of miR-296 in esophageal squamous cell carcinoma. *Ann Surg* (2010) 251:1056–63. doi: 10.1097/SLA.0b013e3181dd4ea9
38. Hamano R, Miyata H, Yamasaki M, Kurokawa Y, Hara J, Moon JH, et al. Overexpression of miR-200c induces chemoresistance in esophageal cancers mediated through activation of the Aktsignaling pathway. *Clin Cancer Res* (2011) 17:3029–38. doi: 10.1158/1078-0432.CCR-10-2532
39. Wang D, Plukker JTM, Coppes RP. Cancer stem cells with increased metastatic potential as a therapeutic target for esophageal cancer. *Semin Cancer Biol* (2017) 44:60–6. doi: 10.1016/j.semcancer.2017.03.010
40. Zhou C, Fan N, Liu F, Fang N, Plum PS, Thieme R, et al. Linking Cancer Stem Cell Plasticity to Therapeutic Resistance-Mechanism and Novel Therapeutic Strategies in Esophageal Cancer. *Cells* (2020) 9:1481. doi: 10.3390/cells9061481
41. Long A, Giroux V, Whelan KA, Hamilton KE, Tétreault MP, Tanaka K, et al. WNT10A promotes an invasive and self-renewing phenotype in esophageal squamous cell carcinoma. *Carcinogenesis* (2015) 36:598–606. doi: 10.1093/carcin/bgv025
42. Wang Z, Da Silva TG, Jin K, Han X, Ranganathan P, Zhu X, et al. Notch signaling drives stemness and tumorigenicity of esophageal adenocarcinoma. *Cancer Res* (2014) 74:6364–74. doi: 10.1158/0008-5472.CAN-14-2051
43. Katoh M. Canonical and non-canonical WNT signaling in cancer stem cells and their niches: Cellular heterogeneity, omics reprogramming, targeted therapy and tumor plasticity (Review). *Int J Oncol* (2017) 5:1357–69. doi: 10.3892/ijo.2017.4129
44. Clevers H, Nusse R. Wnt/β-catenin signaling and disease. *Cell* (2012) 149:1192–205. doi: 10.1016/j.cell.2012.05.012
45. Han S, Gou Y, Jin D, Ma J, Chen M, Dong X. Effects of Icaritin on thephysiological activities of esophageal cancer stem cells. *Biochem Biophys Res Commun* (2018) 504:792–6. doi: 10.1016/j.bbrc.2018.08.060
46. Chen Q, Song S, Wei S, Liu B, Honjo S, Scott A, et al. ABT-263 induces apoptosis and synergizes with chemotherapy by targeting stemness pathways in esophageal cancer. *Oncotarget* (2015) 6:25883–96. doi: 10.18632/oncotarget.4540
47. Mao XM, Li H, Zhang XY, Zhou P, Fu QR, Chen QE, et al. Retinoic Acid Receptor α Knockdown Suppresses the Tumorigenicity of Esophageal Carcinoma via Wnt/β-catenin Pathway. *Dig Dis Sci* (2018) 63:3348–58. doi: 10.1007/s10620-018-5254-6
48. Jia R, Yang L, Yuan X, Kong J, Liu Y, Yin W, et al. GASC1 Promotes Stemness of Esophageal Squamous Cell Carcinoma via NOTCH1 Promoter Demethylation. *J Oncol* (2019) 2019:1621054. doi: 10.1155/2019/1621054
49. Lee SY, Jeong EK, Ju MK, Jeon HM, Kim MY, Kim CH, et al. Induction of metastasis, cancer stem cell phenotype, and oncogenic metabolism in cancer cells by ionizing radiation. *Mol Cancer* (2017) 16:10. doi: 10.1186/s12943-016-0577-4
50. Cattaneo M, Morozumi Y, Perazza D, Boussouar F, Jamshidikia M, Rousseaux S, et al. Lessons from yeast on emerging roles of the ATAD2 protein family in gene regulation and genome organization. *Mol Cells* (2014) 37:851–6. doi: 10.14348/molcells.2014.0258
51. Honjo S, Ajani JA, Scott AW, Chen Q, Skinner HD, Stroehlein J, et al. Metformin sensitizes chemotherapy by targeting cancer stem cells and the mTOR pathway in esophageal cancer. *Int J Oncol* (2014) 45:567–74. doi: 10.3892/ijo.2014.2450
52. Liu JR, Wu WJ, Liu SX, Zuo LF, Wang Y, Yang JZ, et al. Nimesulide inhibits the growth of human esophageal carcinoma cells by inactivating the JAK2/STAT3pathway. *Pathol Res Pract* (2015) 211(6):426–34. doi: 10.1016/j.prp.2015.01.007
53. Sato F, Kubota Y, Natsuizaka M, Maehara O, Hatanaka Y, Marukawa K, et al. EGFR inhibitors prevent induction of cancer stem-like cells in esophageal squamous cell carcinoma by suppressing epithelial-\mesenchymal transition. *Cancer Biol Ther* (2015) 16:933–40. doi: 10.1080/15384047.2015.1040959
54. Tu Y, Tan F, Zhou J, Pan J. Pristimerin targeting NF-κB pathway inhibitsproliferation, migration, and invasion in esophageal squamous cell carcinomacells. *Cell Biochem Funct* (2018) 36:228–40. doi: 10.1002/cbf.3335
55. Harb JG, Neviani P, Chyla BJ, Ellis JJ, Ferenchak GJ, Oaks JJ, et al. Bcl-xL anti-apoptotic network is dispensable for development and maintenance of CML but is required for disease progression where it represents a new therapeutic target. *Leukemia* (2013) 27:1996–2005. doi: 10.1038/leu.2013.151
56. Gronemeyer H, Gustafsson JA, Laudet V. Principles for modulation of the nuclear receptor superfamily. *Nat Rev Drug Discovery* (2004) 3:950–64. doi: 10.1038/nrd1551
57. Krishnamurthy N, Kurzrock R. Targeting the Wnt/beta-catenin pathway in cancer: Update on effectors and inhibitors. *Cancer Treat Rev* (2018) 62:50–60. doi: 10.1016/j.ctrv.2017.11.002
58. Briscoe J, Thérond PP. The mechanisms of Hedgehog signalling and its roles in development and disease. *Nat Rev Mol Cell Biol* (2013) 14:416–29. doi: 10.1038/nrm3598
59. Yu Z, Pestell TG, Lisanti MP, Pestell RG. Cancer stem cells. *Int J Biochem Cell Biol* (2012) 44:2144–51. doi: 10.1016/j.biocel.2012.08.022
60. Das PK, Zahan T, AbdurRakib M, Khanam JA, Pillai S, Islam F. Naturalcompounds targeting cancer stem cells: a promising resource for chemotherapy. *Anticancer Agents Med Chem* (2019) 19(15):1796–808. doi: 10.2174/1871520619666190704111714
61. Isohata N, Aoyagi K, Mabuchi T, Daiko H, Fukaya M, Ohta H, et al. Hedgehog and epithelial-mesenchymal transition signaling in normal and malignant epithelial cells of the esophagus. *Int J Cancer* (2009) 125:1212–21. doi: 10.1002/ijc.24400
62. Yang Z, Cui Y, Ni W, Kim S, Xuan Y. Gli1, a potential regulator of esophageal cancer stem cell, is identified as an independent adverse prognostic factor in esophageal squamous cell carcinoma. *J Cancer Res Clin Oncol* (2017) 143:243–54. doi: 10.1007/s00432-016-2273-6
63. Ma X, Sheng T, Zhang Y, Zhang X, He J, Huang S, et al. Hedgehog signaling is activated in subsets of esophageal cancers. *Int J Cancer* (2006) 118:139–48. doi: 10.1002/ijc.21295
64. Fellner C. Vismodegib (erivedge) for advanced basal cell carcinoma. *P T* (2012) 37:670–82.
65. Cohen DJ, Christos PJ, Sparano JA, Kindler HL, Catenacci DV, Bekaii-Saab TB, et al. A randomized phase II study of vismodegib (V), a hedgehog (HH) pathway inhibitor, combined with FOLFOX in patients (pts) with advanced gastric and gastroesophageal junction (GEJ) carcinoma: a New York Cancer Consortium led study (abstract). *J Clin Oncol* (2013) 31(suppl 4):(abstr 67). doi: 10.1200/jco.2013.31.4_suppl.67
66. Katoh Y, Katoh M. Hedgehog target genes: mechanisms of carcinogenesis induced by aberrant hedgehog signaling activation. *Curr Mol Med* (2009) 9:873–86. doi: 10.2174/156652409789105570

67. Du FY, Zhou QF, Sun WJ, Chen GL. Targeting cancer stem cells in drug discovery: Current state and future perspectives. *World J Stem Cells* (2019) 11:398–420. doi: 10.4252/wjsc.v11.i7.398
68. Takebe N, Miele L, Harris PJ, Jeong W, Bando H, Kahn M, et al. Targeting Notch, Hedgehog, and Wnt pathways in cancer stem cells:clinical update. *Nat Rev Clin Oncol* (2015) 12:445–64. doi: 10.1038/nrclinonc.2015.61
69. Sari IN, Phi LTH, Jun N, Wijaya YT, Lee S, Kwon HY. Hedgehog signaling in cancer: a prospective therapeutic target for eradicating cancer stem cells. *Cells* (2018) 7:208. doi: 10.3390/cells7110208
70. Pan S, Wu X, Jiang J, Gao W, Wan Y, Cheng D, et al. Discovery of NVP-LDE225, a potent and selective smoothened antagonist. *ACS Med Chem Lett* (2010) 1:130–4. doi: 10.1021/ml1000307
71. Dummer R, Guminski A, Gutzmer R, Dirix L, Lewis KD, Combemale P, et al. The 12-month analysis from basal cell carcinoma outcomes with LDE225 Treatment (BOLT): A phase II, randomized, double-blind study of sonidegib in patients with advanced basal cell carcinoma. *J Am Acad Dermatol* (2016) 75:113–125.e5. doi: 10.1016/j.jaad.2016.02.1226
72. D'Amato C, Rosa R, Marciano R, D'Amato V, Formisano L, Nappi L, et al. Inhibition of Hedgehog signalling by NVP-LDE225 (Erismodegib) interferes with growth and invasion of human renal cell carcinoma cells. *Br J Cancer* (2014) 111:1168–79. doi: 10.1038/bjc.2014.421
73. Rimkus TK, Carpenter RL, Qasem S, Chan M, Lo HW. Targeting the Sonic Hedgehog Signaling Pathway: Review of Smoothened and GLI Inhibitors. *Cancers (Basel)* (2016) 8:22. doi: 10.3390/cancers8020022
74. Li N, Yu Y, Wang B. Downregulation of AAA-domain-containing protein 2 restrains cancer stem cell properties in esophageal squamous cell carcinoma via blockade of the Hedgehog signaling pathway. *Am J Physiol Cell Physiol* (2020) 319:C93–C104. doi: 10.1152/ajpcell.00133.2019
75. Zheng L, Li T, Zhang Y, Guo Y, Yao J, Dou L, et al. Oncogene ATAD2 promotes cell proliferation, invasion and migration in cervical cancer. *Oncol Rep* (2015) 33:2337–44. doi: 10.3892/or.2015.3867
76. Zhang M, Zhang C, Du W, Yang X, Chen Z. ATAD2 is overexpressed in gastric cancer and serves as an independent poor prognostic biomarker. *Clin Transl Oncol* (2016) 18:776–81. doi: 10.1007/s12094-015-1430-8
77. Wu G, Lu X, Wang Y, He H, Meng X, Xia S, et al. Epigenetic high regulation of ATAD2 regulates the Hh pathway in human hepatocellular carcinoma. *Int J Oncol* (2014) 45:351–61. doi: 10.3892/ijo.2014.2416
78. Tumaneng K, Russell RC, Guan KL. Organ size control by Hippo and TOR pathways. *Curr Biol* (2012) 22:R368–379. doi: 10.1016/j.cub.2012.03.003
79. Tumaneng K, Schlegelmilch K, Russell RC, Yimlamai D, Basnet H, Mahadevan N, et al. YAP mediates crosstalk between the Hippo and PI(3) K–TOR pathways by suppressing PTEN via miR-29. *Nat Cell Biol* (2012) 14:1322–9. doi: 10.1038/ncb2615
80. Song S, Ajani JA, Honjo S, Maru DM, Chen Q, Scott AW, et al. Hippo coactivator YAP1 upregulates SOX9 and endows esophageal cancer cells with stem-like properties. *Cancer Res* (2014) 74:4170–82. doi: 10.1158/0008-5472.CAN-13-3569
81. Gregorieff A, Liu Y, Inanlou MR, Khomchuk Y, Wrana JL. Yap-dependent reprogramming of Lgr5(+) stem cells drives intestinal regeneration and cancer. *Nature* (2015) 526:715–8. doi: 10.1038/nature15382
82. Bora-Singhal N, Nguyen J, Schaal C, Perumal D, Singh S, Coppola D, et al. YAP1 regulates OCT4 activity and SOX2 expression to facilitate self-renewal and vascular mimicry of stem-like cells. *Stem Cells* (2015) 33:1705–18. doi: 10.1002/stem.1993
83. Aguilar-Medina M, Avendaño-Félix M, Lizárraga-Verdugo E, Bermúdez M, Romero-Quintana JG, Ramos-Payan R, et al. SOX9 stem-cellfactor: clinical and functional relevance in cancer. *J Oncol* (2019) 2019:6754040. doi: 10.1155/2019/6754040
84. Thomsen MK, Ambroisine L, Wynn S, Cheah KS, Foster CS, Fisher G, et al. Transatlantic Prostate Group. SOX9 elevation in the prostate promotes proliferation and cooperates with PTEN loss to drive tumor formation. *Cancer Res* (2010) 70:979–87. doi: 10.1158/0008-5472.CAN-09-2370
85. Matheu A, Collado M, Wise C, Manterola L, Cekaite L, Tye AJ, et al. Oncogenicity of the developmental transcription factor Sox9. *Cancer Res* (2012) 72:1301–15. doi: 10.1158/0008-5472.CAN-11-3660
86. Li F, Xu Y, Liu B, Singh PK, Zhao W, Jin J, et al. YAP1-Mediated CDK6 Activation ConfersRadiation Resistance in Esophageal Cancer-Rationale for the Combination of YAP1 and CDK4/6 Inhibitors in Esophageal Cancer. *Clin Cancer Res* (2019) 25:2264–77. doi: 10.1158/1078-0432.CCR-18-1029
87. Wang Y, Ding Q, Yen CJ, Xia W, Izzo JG, Lang JY, et al. The crosstalk of mTOR/S6K1 and Hedgehog pathways. *Cancer Cell* (2012) 21:374–87. doi: 10.1016/j.ccr.2011.12.028
88. Jiang JH, Pi J, Jin H, Cai JY. Oridonin-induced mitochondria-dependent apoptosis in esophageal cancer cells by inhibiting PI3K/AKT/mTOR and Ras/Raf pathways. *J Cell Biochem* (2019) 120(3):3736–46. doi: 10.1002/jcb.27654
89. Bao B, Wang Z, Ali S, Ahmad A, Azmi AS, Sarkar SH, et al. Metformin inhibits cell proliferation, migration and invasion by attenuating CSC function mediated by deregulating miRNAs in pancreatic cancer cells. *Cancer Prev Res (Phila)* (2012) 5:355–64. doi: 10.1158/1940-6207.CAPR-11-0299
90. Hirsch HA, Iliopoulos D, Tsichlis PN, Struhl K. Metformin selectively targets cancer stem cells, and acts together with chemotherapy to block tumor growth and prolong remission. *Cancer Res* (2009) 69:7507–11. doi: 10.1158/0008-5472.CAN-09-2994
91. Iliopoulos D, Hirsch HA, Struhl K. Metformin decreases the dose of chemotherapy for prolonging tumor remission in mouse xenografts involvingmultiple cancer cell types. *Cancer Res* (2011) 71(9):3196–201. doi: 10.1158/0008-5472.CAN-10-3471
92. Bednar F, Simeone DM. Metformin and cancer stem cells: old drug, new targets. *Cancer Prev Res (Phila)* (2012) 5:351–4. doi: 10.1158/1940-6207.CAPR-12-0026
93. Vazquez-Martin A, Oliveras-Ferraros C, Cufi S, Del Barco S, Martin-Castillo B, Menendez JA. Metformin regulates breast cancer stem cell ontogeny by transcriptional regulation of the epithelial-mesenchymal transition (EMT) status. *Cell Cycle* (2010) 9:3807–14. doi: 10.4161/cc.9.18.13131
94. Buettner R, Mora LB, Jove R. Activated STAT signaling in human tumors provides novel molecular targets for therapeutic intervention. *Clin Cancer Res* (2002) 8(4):945–54.
95. Mora LB, Buettner R, Seigne J, Diaz J, Ahmad N, Garcia R, et al. Constitutive activation of Stat3 in human prostate tumors and cell lines: direct inhibition of Stat3 signaling induces apoptosis of prostate cancer cells. *Cancer Res* (2002) 62:6659–66.
96. Xiong H, Zhang ZG, Tian XQ, Sun DF, Liang QC, Zhang YJ, et al. Inhibition of JAK1, 2/STAT3 signaling induces apoptosis, cell cycle arrest, and reduces tumor cell invasion in colorectal cancer cells. *Neoplasia* (2008) 10:287–97. doi: 10.1593/neo.07971
97. Koon HW, Zhao D, Zhan Y, Rhee SH, Moyer MP, Pothoulakis C. Substance P stimulates cyclooxygenase-2 and prostaglandin E2 expression through JAK-STAT activation in human colonic epithelial cells. *J Immunol* (2006) 176:5050–9. doi: 10.4049/jimmunol.176.8.5050
98. Xuan YT, Guo Y, Zhu Y, Han H, Langenbach R, Dawn B, et al. Mechanism of cyclooxygenase-2 upregulation in late preconditioning. *J Mol Cell Cardiol* (2003) 35:525–37. doi: 10.1016/s0022-2828(03)00076-2
99. Mitchell RA, Luwor RB, Burgess AW. Epidermal growth factor receptor: structure-function informing the design of anticancer therapeutics. *Exp Cell Res* (2018) 371(1):1–19. doi: 10.1016/j.yexcr.2018.08.009
100. Soleimani A, Rahmani F, Ferns GA, Ryzhikov M, Avan A, Hassanian SM. Role of the NF-κB signaling pathway in the pathogenesis of colorectal cancer. *Gene* (2020) 726:144132. doi: 10.1016/j.gene.2019.144132
101. Kang MR, Kim MS, Kim SS, Ahn CH, Yoo NJ, Lee SH. NF-kappaB signalling proteins p50/p105, p52/p100, RelA, and IKKepsilon are over-expressed in oesophageal squamous cell carcinomas. *Pathology* (2009) 41:622–5. doi: 10.3109/00313020903257756
102. Peng Y, Zhou Y, Cheng L, Hu D, Zhou X, Wang Z, et al. The anti-esophageal cancer cell activity by a novel tyrosine/phosphoinositide kinase inhibitor PP121. *Biochem Biophys Res Commun* (2015) 465:137–44. doi: 10.1016/j.bbrc.2015.07.147
103. Yu SL, Chen HY, Chang GC, Chen CY, Chen HW, Singh S, et al. MicroRNA signature predicts survival and relapse in lung cancer. *Cancer Cell* (2008) 13:48–57. doi: 10.1016/j.ccr.2007.12.008
104. Das PK, Siddika MA, Asha SY, Aktar S, Rakib MA, Khanam JA, et al. MicroRNAs, a Promising Target for Breast Cancer Stem Cells. *Mol Diagn Ther* (2020) 24:69–83. doi: 10.1007/s40291-019-00439-5

105. Bertoli G, Cava C, Castiglioni I. MicroRNAs: New Biomarkers for Diagnosis, Prognosis, Therapy Prediction and Therapeutic Tools for Breast Cancer. *Theranostics* (2015) 5:1122–43. doi: 10.7150/thno.11543
106. Abdolvahabi Z, Nourbakhsh M, Hosseinkhani S, Hesari Z, Alipour M, Jafarzadeh M, et al. MicroRNA-590-3P suppresses cell survival and triggers breast cancer cell apoptosis via targeting sirtuin-1 and deacetylation of p53. *J Cell Biochem* (2018) 120:9356–68. doi: 10.1002/jcb.28211
107. Rahimi M, Sharifi-Zarchi A, Zarghami N, Geranpayeh L, Ebrahimi M, Alizadeh E. Down-Regulation of miR-200c and up-regulation of miR-30c target both stemness and metastasis genes in breast cancer. *Cell J* (2020) 21:467–78. doi: 10.22074/cellj.2020.6406
108. Carthew RW, Sontheimer EJ. Origins and mechanisms of miRNAs and siRNAs. *Cell* (2009) 136:642–55. doi: 10.1016/j.cell.2009.01.035
109. Yu X, Jiang X, Li H, Guo L, Jiang W, Lu SH. miR-203 inhibits the proliferation and self-renewal of esophageal cancer stem-like cells by suppressing stem renewal factor Bmi-1. *Stem Cells Dev* (2014) 23:576–85. doi: 10.1089/scd.2013.0308
110. Xu DD, Zhou PJ, Wang Y, Zhang L, Fu WY, Ruan BB, et al. Reciprocal activation between STAT3 and miR-181b regulates the proliferation of esophageal cancer stem-like cells via the CYLD pathway. *Mol Cancer* (2016) 15:40. doi: 10.1186/s12943-016-0521-7
111. Yang C, Zheng X, Ye K, Sun Y, Lu Y, Fan Q, et al. miR-135a inhibits the invasion and migration of esophageal cancer stem cells through the Hedgehog Signaling pathway by targeting Smo. *Mol Ther Nucleic Acids* (2020) 19:841–52. doi: 10.1016/j.omtn.2019.10.037
112. Ge C, Wu S, Wang W, Liu Z, Zhang J, Wang Z, et al. miR-942 promotes cancer stem cell-like traits in esophageal squamous cell carcinoma through activation of Wnt/β-catenin signalling pathway. *Oncotarget* (2015) 6:10964–77. doi: 10.18632/oncotarget.3696
113. Liu A, Zhu J, Wu G, Cao L, Tan Z, Zhang S, et al. Antagonizing miR-455-3p inhibits chemoresistance and aggressiveness in esophageal squamous cell carcinoma. *Mol Cancer* (2017) 16:106. doi: 10.1186/s12943-017-0669-9
114. Lynam-Lennon N, Heavey S, Sommerville G, Bibby BA, Ffrench B, Quinn J, et al. MicroRNA-17 is downregulated in esophageal adenocarcinoma cancer stem-like cells and promotes a radioresistant phenotype. *Oncotarget* (2017) 8:11400–13. doi: 10.18632/oncotarget.13940
115. Wang Y, Zhao Y, Herbst A, Kalinski T, Qin J, Wang X, et al. miR-221 Mediates Chemoresistance of Esophageal Adenocarcinoma by Direct Targeting of DKK2 Expression. *Ann Surg* (2016) 264:804–14. doi: 10.1097/SLA.0000000000001928
116. Sonkoly E, Wei T, Janson PC, Sääf A, Lundeberg L, Tengvall-Linder M, et al. MicroRNAs: novel regulators involved in the pathogenesis of psoriasis? *PloS One* (2007) 2:e610. doi: 10.1371/journal.pone.0000610
117. Feber A, Xi L, Luketich JD, Pennathur A, Landreneau RJ, Wu M, et al. MicroRNA expression profiles of esophageal cancer. *J Thorac Cardiovasc Surg* (2008) 135:255–60. doi: 10.1016/j.jtcvs.2007.08.055
118. Huang D, Gao Q, Guo L, Zhang C, Jiang W, Li H, et al. Isolation and identification of cancer stem-like cells in esophageal carcinoma cell lines. *Stem Cells Dev* (2009) 18:465–73. doi: 10.1089/scd.2008.0033
119. Carnero A, Lleonart M. The hypoxic microenvironment: A determinant of cancer stem cell evolution. *Bioessays* (2016) 38 Suppl 1:S65–74. doi: 10.1002/bies.201670911
120. Marie-Egyptienne DT, Lohse I, Hill RP. Cancer stem cells, the epithelial to mesenchymal transition (EMT) and radioresistance: potential role of hypoxia. *Cancer Lett* (2013) 341:63–72. doi: 10.1016/j.canlet.2012.11.019
121. Wang D, Qin Q, Jiang QJ, Wang DF. Bortezomib sensitizes esophageal squamous cancer cells to radiotherapy by suppressing the expression of HIF-1α and apoptosis proteins. *J Xray Sci Technol* (2016) 24:639–46. doi: 10.3233/XST-160571
122. Kato Y, Yashiro M, Fuyuhiro Y, Kashiwagi S, Matsuoka J, Hirakawa T, et al. Effects of acute and chronic hypoxia on the radiosensitivity of gastric and esophageal cancer cells. *Anticancer Res* (2011) 31:3369–75.
123. Wu X, Qiao B, Liu Q, Zhang W. Upregulation of extracellular matrix metalloproteinase inducer promotes hypoxia-induced epithelial-mesenchymal transition in esophageal cancer. *Mol Med Rep* (2015) 12:7419–24. doi: 10.3892/mmr.2015.4410
124. Jing SW, Wang YD, Kuroda M, Su JW, Sun GG, Liu Q, et al. HIF-1α contributes to hypoxia-induced invasion and metastasis of esophageal carcinoma via inhibiting E-cadherin and promoting MMP-2 expression. *Acta Med Okayama* (2012) 66:399–407. doi: 10.18926/AMO/48964
125. Zhu H, Feng Y, Zhang J, Zhou X, Hao B, Zhang G, et al. Inhibition of hypoxia inducible factor 1α expression suppresses the progression of esophageal squamous cell carcinoma. *Cancer Biol Ther* (2011) 11:981–7. doi: 10.4161/cbt.11.11.15707
126. Zhang HY, Wang ZQ, Li YY, Wang F, Zeng QR, Gao Y, et al. Transforming growth factor-β1-induced epithelial-mesenchymal transition in human esophageal squamous cell carcinoma via the PTEN/PI3K signaling pathway. *Oncol Rep* (2014) 32:2134–42. doi: 10.3892/or.2014.3453
127. Ping W, Sun W, Zu Y, Chen W, Fu X. Clinicopathological and prognostic significance of hypoxia-inducible factor-1α in esophageal squamous cell carcinoma: a meta-analysis. *Tumour Biol* (2014) 35:4401–9. doi: 10.1007/s13277-013-1579-0
128. Sohda M, Ishikawa H, Masuda N, Kato H, Miyazaki T, Nakajima M, et al. Pretreatment evaluation of combined HIF-1alpha, p53 and p21 expression is a useful and sensitive indicator of response to radiation and chemotherapy in esophageal cancer. *Int J Cancer* (2004) 110:838–44. doi: 10.1002/ijc.20215
129. Koukourakis MI, Giatromanolaki A, Skarlatos J, Corti L, Blandamura S, Piazza M, et al. Hypoxia inducible factor (HIF-1a and HIF-2a) expression in early esophageal cancer and response to photodynamic therapy and radiotherapy. *Cancer Res* (2001) 61:1830–2.
130. Wouters BG, Koritzinsky M. Hypoxia signalling through mTOR and the unfolded protein response in cancer. *Nat Rev Cancer* (2008) 8:851–64. doi: 10.1038/nrc2501
131. Lv Z, Liu RD, Chen XQ, Wang B, Li LF, Guo YS, et al. HIF−1α promotes the stemness of oesophageal squamous cell carcinoma by activating the Wnt/β−catenin pathway. *Oncol Rep* (2019) 42:726–34. doi: 10.3892/or.2019.7203
132. Wilson WR, Hay MP. Targeting hypoxia in cancer therapy. *Nat Rev Cancer* (2011) 11:393–410. doi: 10.1038/nrc3064
133. Laplante M, Sabatini DM. mTOR signalingat a glance. *J Cell Sci* (2009) 122:3589–94. doi: 10.1242/jcs.051011

Conflict of Interest: The authors declare that the research was conducted in the absence of any commercial or financial relationships that could be construed as a potential conflict of interest.

frontiers in Oncology

ORIGINAL RESEARCH
published: 11 March 2021
doi: 10.3389/fonc.2021.565676

Junctional Adhesion Molecule-Like Protein Promotes Tumor Progression and Metastasis *via* p38 Signaling Pathway in Gastric Cancer

Yuying Fang[1,2†], *Jianmin Yang*[3†], *Guohong Zu*[1,2], *Changsheng Cong*[1,2], *Shuai Liu*[1,2], *Fei Xue*[3], *Shuzhen Ma*[1,2], *Jie Liu*[1,2], *Yuping Sun*[1,2*] *and Meili Sun*[1,2,4*]

[1] *Department of Oncology, Jinan Central Hospital, Cheeloo College of Medicine, Shandong University, Jinan, China,* [2] *Department of Oncology, Central Hospital Affiliated to Shandong First Medical University, Jinan, China,* [3] *The Key Laboratory of Cardiovascular Remodeling and Function Research, Chinese Ministry of Education, Chinese Ministry of Health and Chinese Academy of Medical Sciences, The State and Shandong Province Joint Key Laboratory of Translational Cardiovascular Medicine, Department of Cardiology, Qilu Hospital, Cheeloo College of Medicine, Shandong University, Jinan, China,* [4] *Cardiovascular Disease Research Center of Shandong First Medical University, Central Hospital Affiliated to Shandong First Medical University, Jinan, China*

OPEN ACCESS

Edited by:
Jianjun Xie,
Shantou University, China

Reviewed by:
Yujun Dong,
Peking University First Hospital, China
Vera Kemp,
Leiden University Medical Center, Netherlands

***Correspondence:**
Meili Sun
smli1980@163.com
Yuping Sun
13370582181@163.com

[†]*These authors have contributed equally to this work*

Specialty section:
This article was submitted to Gastrointestinal Cancers, a section of the journal Frontiers in Oncology

Received: *25 May 2020*
Accepted: *01 February 2021*
Published: *11 March 2021*

Citation:
Fang Y, Yang J, Zu G, Cong C, Liu S, Xue F, Ma S, Liu J, Sun Y and Sun M (2021) Junctional Adhesion Molecule-Like Protein Promotes Tumor Progression and Metastasis via p38 Signaling Pathway in Gastric Cancer. Front. Oncol. 11:565676. doi: 10.3389/fonc.2021.565676

Junctional adhesion molecule-like protein (JAML), a newly discovered junctional adhesion molecule (JAM), mediates the adhesion and migration processes of various immune cells and endothelial/epithelial cells, ultimately regulating inflammation reaction. However, its role in tumors remains to be determined. The expression of JAML was examined in gastric cancer (GC) and peritumoral tissues from 63 patients. The relationship between JAML expression and clinical characteristics was also observed. *In vitro*, GC cell migration and proliferation were assessed by wound healing assay, transwell migration assay and EdU incorporation assay. Immunohistochemical staining results showed that JAML expression level was higher in GC tissues than in peritumoral tissues. High expression of JAML in cancer tissues was associated with worse cell differentiation, local lymph node involvement, deep infiltration, and advanced stage. *In vitro*, we found that JAML silencing inhibited GC cell migration and proliferation, while JAML overexpression promoted GC cell migration and proliferation, partially *via* p38 signaling. Taken together, our study revealed a critical role for JAML to promote GC cell migration and proliferation. JAML might be a novel diagnostic biomarker and therapeutic target for GC.

Keywords: junctional adhesion molecule-like protein (JAML), gastric cancer, p38, tumor progression, migration

INTRODUCTION

Gastric cancer (GC) is a malignant tumor originating from the gastric mucosa epithelium, which has high morbidity and mortality in worldwide. In 2018, there were an estimated 1,000,000 new GC cases and 783,000 deaths (1, 2). The main causes of GC death are rapid proliferation, invasion, metastasis, and anti-cancer drug resistance. However, because the symptoms of early GC are

Abbreviations: CAR, coxsackie and virus receptor; GC, gastric cancer; IHC, immunohistochemical; JAML, junctional adhesion molecule-like protein; JAMs, junctional adhesion molecules; JAM-A, junctional adhesion molecule A; JAM-C, junctional adhesion molecule C; MAPK, mitogen-activated protein kinase.

inconspicuous, the advanced stage at the diagnosis is an important factor in the gastric-cancer-related mortality (3). Therefore, it is necessary to search for effective targets for screening and diagnosing GC as early as possible, thus improving prognosis.

More and more studies have shown that complex steps such as adhesion, degradation, movement and blood vessel formation promote tumor cell infiltration and metastasis. Adhesion molecules are involved in the process of tumor metastasis (4). In recent years, the role of junctional adhesion molecules (JAMs) of immunoglobulin superfamily in cancer occurrence and progression has attracted extensive attentions (5, 6). Current research has found that tumorigenesis is associated with increased levels of JAM protein expression, and increased expression of JAM is associated with poor prognosis. The mechanism may involve the enhanced ability of tumor cells to migrate to the stroma and move across the vessel wall during local infiltration and metastatic spread (5–8).

Junctional adhesion molecule-like protein (JAML) is a new member of JAMs, which includes two extracellular immunoglobulin-like domains, a transmembrane fragment and a cytoplasmic tail. JAML has been found to be expressed in cells such as neutrophils, monocytes, some T cells, and acute promyelocytic leukemia cells. JAML mediates the adhesion and migration processes of various immune cells and endothelial/epithelial cells, ultimately regulating inflammation reaction (9–12). Although it has been found that JAML plays exact roles in the process of wound healing and atherosclerosis in recent years, its role in the tumor has been poorly investigated (13, 14). For this reason, in this study, we attempted to investigate the function of JAML in GC through *in vitro* and *in vivo* experiments.

MATERIALS AND METHODS

Human Samples

A total of 63 tissue specimens of GC from Jinan Central Hospital between 2014 and 2018 were collected, with a median age of 64 years (range: 36–88 years). There were 49 men (77.78%) and 14 women (22.22%). We analyzed the histopathological results of GC specimens using the eighth edition of AJCC/UICC (15). Each patient provided written informed consent. This study was approved by the evaluation committee of Jinan Central Hospital of Shandong University.

Immunohistochemical Staining

We cut the paraffin sections into 4 μM slices. The antigen was repaired with sodium citrate under high temperature and pressure. The sample was incubated with 3% H_2O_2 solution for 10 min to reduce endogenous peroxidase activity. It was sealed with 5% goat serum and 0.2% bovine serum albumin for 30 min. Rabbit anti-JAML polyclonal antibodies (Novus Biologicals, USA, NBP2-14286) were incubated overnight. After rewarming, the second antibody was incubated for 1 h. We then performed DAB staining and then hematoxylin staining. Two independent pathologists evaluated the results of immunohistochemistry at the same time. Scores were determined according to the degree of staining and the proportion of positive cells. The intensity score represents the average staining intensity of positive cells (0 = no staining; 1 = light yellow; 2 = buffy; 3 = brown). The proportion score represents the proportion of positively stained cells (0 = 0; 1 = less than 25%; 2 = 25–50%; 3 = 50–75%; 4 = more than 75%). The final score is the product of intensity score and proportion score: high expression ≥ 4 points; low expression < 4 points.

Cell Culture

The human GC cell lines (AGS, HGC-27 and MKN-28) were purchased from the cell resource center of Chinese Academy of Sciences (Beijing, China). HGC-27 and MKN-28 were cultured in RPMI-1640 medium (Gibco, USA) containing 10% fetal bovine serum (FBS; Gibco). AGS was cultured in F12k medium (Macgene, China) containing 10% fetal bovine serum (FBS; Gibco). The p38 inhibitor SB-203580 was purchased commercially (Selleck, Houston, TX, USA).

Cell Transfection

JAML plasmid (GenePharma, Shanghai, China) was formed using full length human JAML cDNA linked with the pcDNA3.1(+) vector to induce JAML over-expression in cultured GC cells. According to the manufacturer's product instructions, JAML plasmid was transfected into the cells using X-treme GENE HP Reagents (Roche, Basel, Switzerland). Cells transfected with pcDNA3.1(+) (NC) vector was used as a negative control group. Small interfering RNA against human JAML (siJAML) (GenePharma, Shanghai, China) was transfected within gastric cells to reduce JAML expression. siRNA sequences are: siJAML1, 5'-GGAAUUGUC UGUGCCACAATT-3', 5'-UUGUGGCACAGACAAUUCCTT-3'; siJAML2, 5'-CCAGAGCACAGAAGUGAAATT-3', 5'-UUUCACUUCUGUGCUCUGGTT-3'; siJAML3, 5'-CCAGAGCACAGAAGACAAATT-3', 5'-UUUGUCUUCU GUGCUCUGGTT-3'; negative control (siNC), 5'-UUCUCCG AACGUGUCACGUTT-3', 5'-ACGUGACACGUUCGG AGAATT-3'. Cell function experiments were performed after 72 h of treatment of cells with JAML plasmids or small interfering RNA. In order to ensure the continuous and effective transient transfection during the cell function test, western blot analysis was used to test the transfection efficiency at 72 h and 120 h after transient transfection.

Western Blot Analysis

Cells were acquired and prepared in RIPA buffer (Beyotime, China), 1% protease inhibitor cocktail 1, 1% phosphate inhibitor cocktail 2, and 1% phosphate inhibitor cocktail 3 (Sigma, USA). BCA protein assay kit (Beyotime, shanghai, China) was used to determine the protein concentration. The loading volume based on the cell concentration is calculated to ensure that the total number of loaded cells in each group is consistent. The protein extract was separated by 10% SDS-PAGE and added to the polyvinylidene difluoride membrane (Millipore, Boston, MA, USA). After electrophoresis and membrane transfer, the antibody was incubated overnight. The protein was visualized using chemiluminescence (ECL Plus Western Blot Detection System; Bio-Rad, USA). ImageJ was used to measure the gray value of bands to calibrate the expression of housekeeping gene (tubulin).The antibodies used include: rabbit anti-JAML monoclonal antibody (Abcam, USA, ab183714), rabbit anti-p-ERK1/2 monoclonal antibody (Cell signaling Technology, USA, 4370), rabbit anti-

ERK1/2 monoclonal antibody (Cell signaling Technology, USA, 4695), rabbit anti-p-JNK monoclonal antibody (Cell signaling Technology, USA, 4668), rabbit anti-JNK polyclonal antibody (Cell signaling Technology, USA, 9252), rabbit anti-p-p38 monoclonal antibody (Cell signaling Technology, USA, 4511), rabbit anti-p38 monoclonal antibody (Cell signaling Technology, USA, 8690), mouse anti-tubulin monoclonal antibody (Abcam, USA, ab210797). Tubulin was used as the loading control.

Wound Healing Assay

GC cells were covered in six-well plates (Corning Incorporated, Corning, NY, USA) and were scratched after sticking to the wall. RPMI-1640 medium (Gibco, USA) was used to culture cells, and the same field of vision was taken at 0 and 48 h respectively. Each experiment was performed in triplicate.

Transwell Migration Assay

Cell migration was measured in 24-well plates (Corning Incorporated, Corning, NY, USA) with 8μm-pore polycarbonate membranes. Cells were seeded at a density of 4×10^4 cells/well in the upper chamber with serum-free RPMI-1640 medium and incubated at 37°C for migration assay. After 48 h of culture, cells were fixed and stained with crystal violet, then observed under optical microscope (Nikon). Three fields were randomly selected for cell count. Each experiment was performed in triplicate.

Cell Proliferation Experiment

EdU (5-Ethynyl-2′-deoxyuridine) DNA cell proliferation Kit (Beyotime, Shanghai, China and RiboBio, Guangzhou, China) was chosen to determine cell proliferation. The cells after the required treatment are counted, resuspended in culture medium, and re-seeded on a 96-well plate with 4×10^4 cells per well. After incubation for 12 h, 10 μM EdU was added to the cultures and 2 h later cells were collected. According to the operation requirements of the kit, after fixation, washing, penetration and dye marking, observe and take photos with fluorescence microscope (Nikon). Each experiment was performed in triplicate.

Statistical Analysis

Statistical analysis was performed using SPSS version 20.0 (SPSS, Chicago, Illinois, USA) and GraphPad Prism 8.0 software (San Diego, CA, USA). Statistical significance was assessed by Student's t-test between two groups or by one-way ANOVA between three or more groups for continuous data. Chi-square test was used to analyze the association between JAML expression and clinicopathological variables. Experimental data were presented as mean ± standard deviation (SD). $P < 0.05$ was considered statistically significant.

RESULTS

Junctional Adhesion Molecule-Like Protein Was Highly Expressed in Human Gastric Cancer Tissues and High Junctional Adhesion Molecule-Like Protein Expression in Gastric Cancer Correlated With Advanced Clinicopathological Features

The detailed clinicopathological parameters and JAML expression of patients with gastric cancer were presented in the

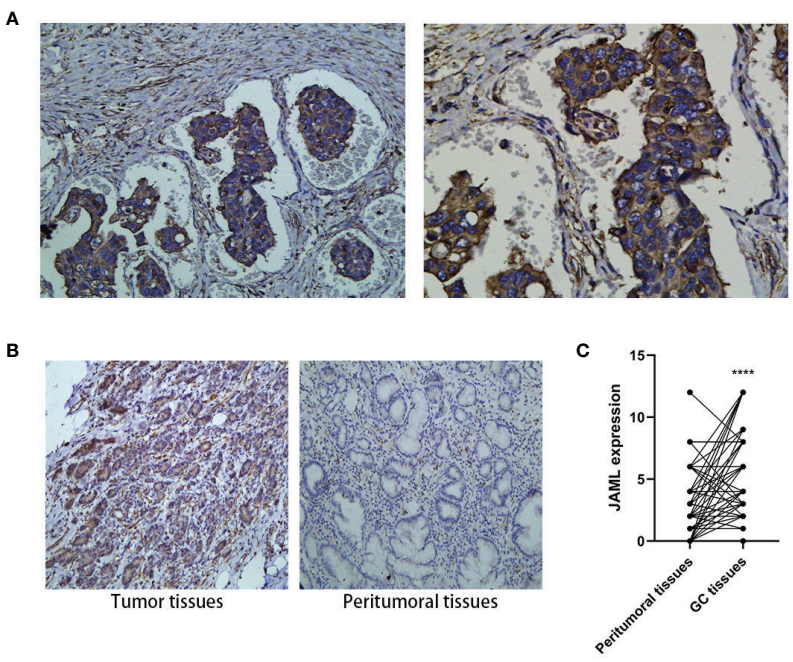

FIGURE 1 | Expression of JAML in human gastric cancer (GC) and peritumoral tissues. **(A)** JAML expression on cytoplasm and membrane of GC cells. **(B)** The JAML expression in GC and peritumoral tissues. **(C)** Quantitative analysis of JAML expression in GC and peritumoral tissues. n=63, paired t test, ****$P < 0.0001$, compared with peritumoral tissues.

Supplemental Data Sheet. The expression of JAML in 63 cases of GC was detected by IHC, and the relationship between JAML and clinicopathological parameters was also analyzed. JAML was expressed in the cytoplasm and membrane of cancer cells (**Figure 1A**). IHC analysis showed that JAML in GC tissue was significantly up-regulated compared with peritumoral tissues (**Figures 1B, C**). Thereafter, we investigated the relationship between JAML expression and various pathological parameters in GC tissues. We found that high expression of JAML in GC cells was associated with poor cell differentiation (P = 0.001), local lymph node involvement (P = 0.012), deeper infiltration (P = 0.026), and advanced stages (P = 0.021) (**Table 1**).

TABLE 1 | Correlation between JAML expression and clinicopathological parameters in human GC tissues.

Variables	JAML expression		
	high	low	p
Age (year)			
<60	12	4	0.609
≥60	30	17	
Gender			
Male	31	18	0.453
Female	11	3	
Primary tumor			
T0-T2	31	21	0.026
T3-T4	11	0	
Regional lymph node involvement			
N0-N1	18	16	0.012
N2-N3	24	5	
Histological grade			
G1-G2	11	15	0.001
G3	31	6	
TNM stage groupings			
I–II	22	18	0.021
III	20	3	

GC, gastric cancer; TNM, tumor, node, metastasis.

Junctional Adhesion Molecule-Like Protein Promoted Gastric Cancer Cell Proliferation and Migration

The result that high JAML levels were associated with higher tumor malignancy in GC patients encouraged us to assess whether JAML was related to oncogenic function. First, we examined JAML expression in GC cell lines (AGS, HGC-27, and MKN-28) (**Figures 2A, B**). The expression of JAML was

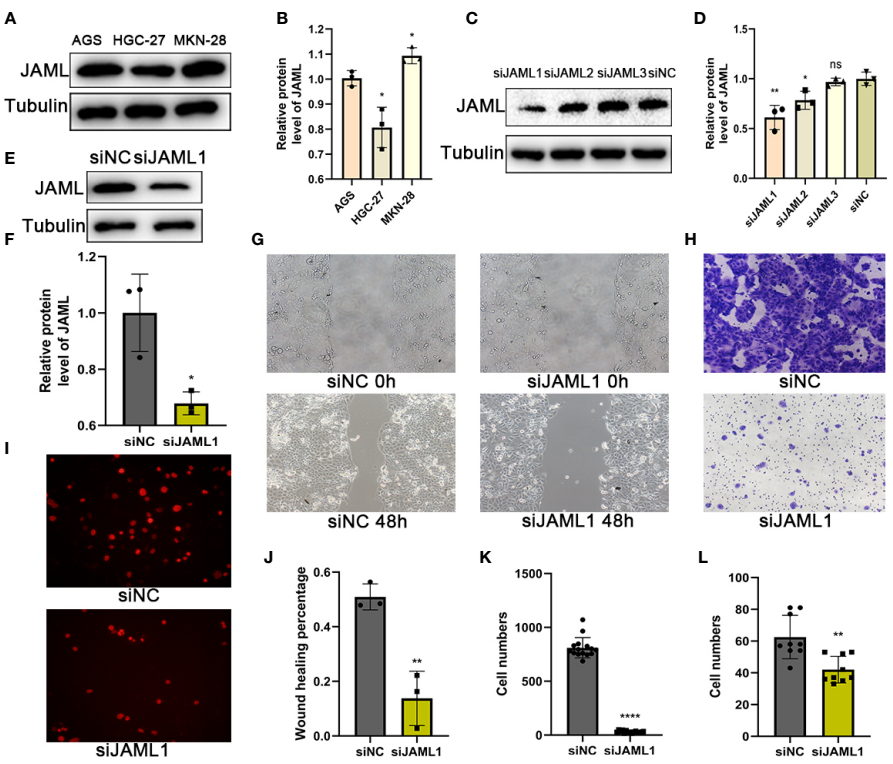

FIGURE 2 | JAML promoted GC cell proliferation and migration. **(A)** The expression of JAML in GC cell lines (AGS, HGC-27, MKN-28). **(B)** Quantitative analysis of **(A)** n=3, unpaired t test, *P < 0.05, compared with AGS group. **(C)** Knockdown efficiency of JAML was confirmed in MKN-28 cells after transient transfection of SiRNA for 72h by western blot. **(D)** Quantitative analysis of **(C)** n=3, unpaired t test, **P < 0.01, compared with siNC group; n=3, unpaired t test, *P < 0.05, compared with siNC group; n=3, unpaired t test, ns, P>0.05, compared with siNC group. **(E)** Knockdown efficiency of JAML in MKN-28 cells after transient transfection of siRNA for 120h by western blot. **(F)** Quantitative analysis of **(E)** n=3, unpaired t test, *P < 0.05, compared with siNC group. **(G)** Wound healing assay was performed in transfected MKN-28 cells treated with or without siRNA to evaluate cell migration. **(H)** Transwell migration assay to assess cell migration. **(I)** EdU incorporation assay to observe cell proliferation. **(J)** Quantitative analysis of **(G)** n=3, unpaired t test, **P < 0.01, compared with siNC group. **(K)** Quantitative analysis of **(H)** n=15, unpaired t test, ****P < 0.0001, compared with siNC group. **(L)** Quantitative analysis of **(I)** n=9, unpaired t test, **P < 0.01, compared with siNC group. siNC, negative control.

relatively higher in MKN-28 cells, while was lower in HGC-27 cells. Thus, small interfering RNA against human JAML (siJAML) was transfected to MKN-28 cells to reduce JAML expression. The results showed that the knockdown effect of siJAML1 was the most effective (**Figures 2C, D**) and was stable for 5 days (**Figures 2E, F**), so siJAML1 was used for the subsequent experiments. The wound healing and transwell migration assays showed that JAML deficiency significantly decreased migration in MKN-28 cells (**Figures 2G, H, J, K**). In addition, the EdU incorporation assay demonstrated the proliferation of MKN-28 cells was significantly inhibited after silencing of JAML (**Figures 2I, L**). Next, we transfected JAML plasmid to HGC-27 cells to increase the expression of JAML. Western blot analysis showed that the JAML plasmid transfection up-regulated the expression of JAML in HGC-27 cells (**Figures 3A, B**), and the effect was stable until the 5th day after transfection (**Figures 3C, D**). The wound healing and transwell migration assays showed that JAML overexpression significantly increased migration in HGC-27 cells (**Figures 3E–H**). In addition, the EdU incorporation assay showed that JAML overexpression enhanced HGC-27 cells proliferation (**Figures 3I, J**). These results suggested that JAML might facilitated GC migration and proliferation.

Junctional Adhesion Molecule-Like Protein Promoted Gastric Cancer Cell Migration and Proliferation by Activating p38 Signaling Pathway

In order to explore the underlying mechanism of JAML-mediated GC cells migration and proliferation, the activities of mitogen-activated protein kinases (MAPKs), including p38, JNK and ERK, were measured in GC cells by western blot. We found that JAML silencing significantly inhibited p38 phosphorylation, while did not affect the activities of ERK or JNK (**Figures 4A–D**). After that, we used SB-203580, a p38 inhibitor, to treat MKN-28 cells, which endogenously expresses high level of JAML. The results showed that the phosphorylation of p38 was effectively inhibited in MKN-28 cells treated with SB-203580 (**Figures 4E, F**). Then, the transwell migration and the EdU incorporation

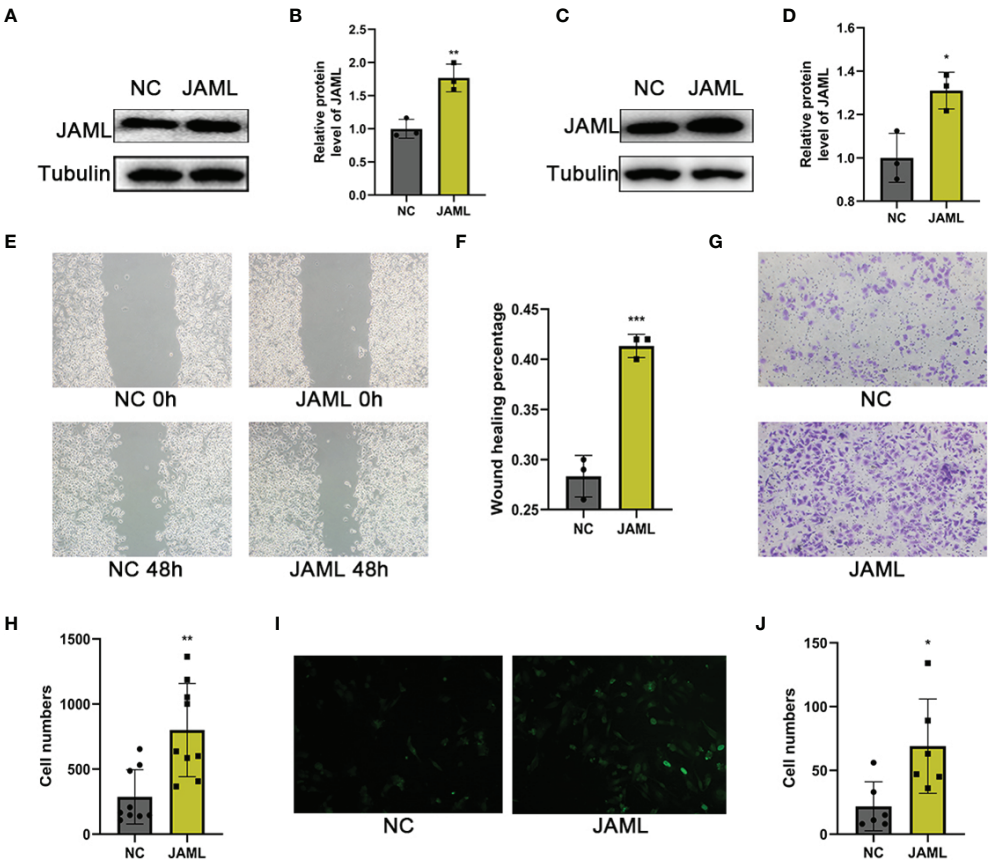

FIGURE 3 | **(A)** JAML expression in HGC-27 cells after transfection with JAML plasmid for 72h. **(B)** Quantitative analysis of **(A)** n=3, unpaired t test, $^{**}P < 0.01$, compared with NC group. **(C)** JAML expression in HGC-27 cells after transfection with JAML plasmid for 120h. **(D)** Quantitative analysis of **(C)** n=3, unpaired t test, $^{*}P < 0.05$, compared with NC group. **(E)** Wound healing assay to assess cell migration in HGC-27 cells. **(F)** Quantitative analysis of **(E)** n=3, unpaired t test, $^{***}P < 0.001$, compared with NC group. **(G)** Transwell migration assay to evaluated cell migration in HGC-27 cells. **(H)** Quantitative analysis of **(G)** n=9, unpaired t test, $^{**}P < 0.01$, compared with NC group. **(I)** EdU incorporation assay to observe cell proliferation in HGC-27 cells. **(J)** Quantitative analysis of **(I)** n=6, unpaired t test, $^{*}P < 0.05$, compared with NC group. NC, negative control.

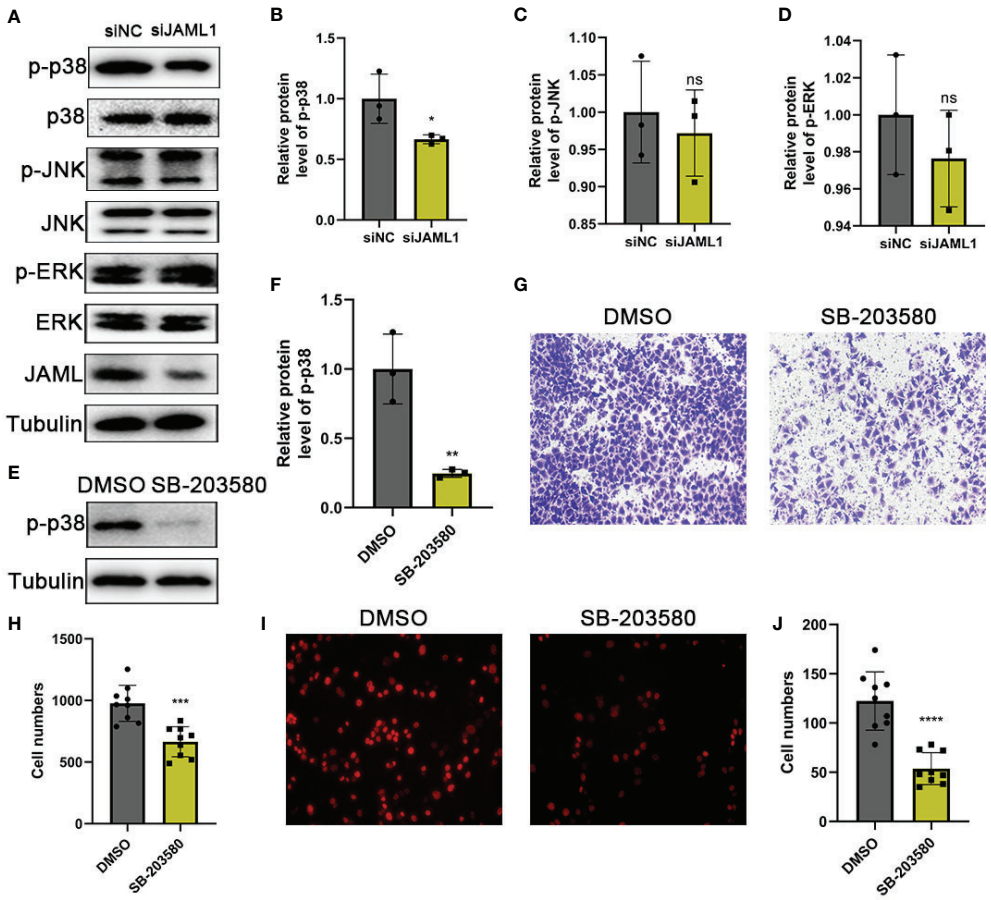

FIGURE 4 | JAML promoted GC cell migration and proliferation by activating p38 signaling pathway. **(A)** The effect of JAML silencing on the phosphorylation of p38, ERK and JNK. **(B–D)** Quantitative analysis of **(A)** n=3, unpaired t test, $^{*}P < 0.05$, compared with siNC group; ns, $P > 0.05$, compared with siNC group. **(E)** The effect of SB-203580 on p38 phosphorylation. **(F)** Quantitative analysis of **(E)** n=3, unpaired t test, $^{**}P < 0.01$, compared with DMSO group. **(G)** Transwell migration assay to evaluate the effect of SB-203580 on cell migration in MKN-28 cells. **(H)** Quantitative analysis of **(G)** n=9, unpaired t test, $^{***}P < 0.001$, compared with DMSO group. **(I)** EdU incorporation assay to assess the effect of SB-203580 on cell proliferation in MKN-28 cells. **(J)** Quantitative analysis of **(I)** n=9, unpaired t test, $^{****}P < 0.0001$, compared with DMSO group.

assays showed that SB-203580 significantly suppressed migration and proliferation in MKN-28 cells (**Figures 4G–J**). These results implied that the ability of JAML to promote GC cell migration and proliferation might be mediated by p38 signaling pathway.

DISCUSSION

Recently, the role of JAML in immune cell activation and inflammatory response has attracted researchers' attention. JAML, a newly discovered adhesion molecule, is a secretory type I transmembrane glycoprotein. It can both mediate intercellular interactions and bind to intracellular proteins to mediate downstream signaling pathways (16, 17). In recent years, the expression and role of JAML on other cell types have also been gradually explored. It has been found that JAML can promote the adhesion of leukocytes to endothelial cells in myeloid leukemia (10). Our recent study found that JAML silencing delayed the formation of atherosclerosis in mice (14). Although studies on JAML under various pathological conditions are becoming more common, the relationship between JAML and tumor development has never been reported. In our current study, we found that JAML was upregulated in GC tissues and JAML promoted the proliferation and migration of GC cells, partially by regulating p38 activation.

To investigate the relationship between JAML and tumor development, we selected gastric tumors as the research object. First, we found JAML was significantly upregulated in GC tissues by IHC and was associated with higher tumor malignancy. This study demonstrates for the first time that JAML is highly expressed in GC tissues and might be a diagnostic biomarker in GC. Then, we performed experiments *in vitro*. By regulating the expression of JAML, we found that upregulation of JAML promoted, while JAML deficiency attenuated GC cells proliferation and migration. The bidirectional regulation of JAML in different types of GC cells confirmed this conclusion.

In addition, we also discussed the primary mechanism by which JAML promotes GC progression. We found that JAML may play a tumor-promoting role by activating the p38 signaling pathway. The p38 signaling pathway is a key signal transduction pathway by which tumor cells to sense and adapt to a variety of environmental stimuli, and it plays an important role in the occurrence and maintenance of tumors (18–21). We found that the phosphorylation level of p38 decreased significantly after JAML expression was downregulated. After treatment with p38 classic inhibitors, the proliferation and migration of MKN-28 cells decreased significantly, suggesting that JAML promoted the growth and movement of GC cells by activating p38.

CONCLUSION

In summary, the present study revealed the high expression of JAML in GC, and results showed that JAML promoted GC proliferation and migration by regulating p38 pathway. Overall, the present data bring novel insights into the mechanisms by which JAML regulates GC and highlights the potential clinical significance of JAML in the pathogenesis of GC.

DATA AVAILABILITY STATEMENT

The raw data supporting the conclusions of this article will be made available by the authors, without undue reservation.

ETHICS STATEMENT

The studies involving human participants were reviewed and approved by Jinan Central Hospital. The patients/participants provided their written informed consent to participate in this study.

AUTHOR CONTRIBUTIONS

MS, JY, and YS designed the study. YF, JY, MS, and YS prepared the first draft of the paper. YF, MS, and YS performed the statistical analysis of the data. YF, CC, SL, FX, SM, JL, and GZ performed the data collection. All authors contributed to the article and approved the submitted version. All authors agreed to be responsible for this work and ensure that any issues related to the accuracy and completeness of the paper are investigated and resolved appropriately.

ACKNOWLEDGMENTS

This work was supported by the Academic Promotion Programme of Shandong First Medical University (2019QL025), the grants of Science and Technology Plan of Jinan Health and Family Planning Commission (No. 2018-1-01) and Jinan City's 2019 Science and Technology Development Plan (No. 201907031). We thank LetPub (www.letpub.com) for its linguistic assistance during the preparation of this manuscript.

SUPPLEMENTARY MATERIAL

The Supplementary Material for this article can be found online at: https://www.frontiersin.org/articles/10.3389/fonc.2021.565676/full#supplementary-material

REFERENCES

1. Bray F, Ferlay J, Soerjomataram I, Siegel RL, Torre LA, Jemal A. Global cancer statistics 2018: GLOBOCAN estimates of incidence and mortality worldwide for 36 cancers in 185 countries. *CA Cancer J Clin* (2018) 68:394–424. doi: 10.3322/caac.21492
2. Torre LA, Bray F, Siegel RL, Ferlay J, Lortet-Tieulent J, Jemal A. Global cancer statistics, 2012. *CA Cancer J Clin* (2015) 65:87–108. doi: 10.3322/caac.21262
3. Zhu M, Wang Q, Luo Z, Liu K, Zhang Z. Development and validation of a prognostic signature for preoperative prediction of overall survival in gastric cancer patients. *Onco Targets Ther* (2018) 11:8711–22. doi: 10.2147/OTT.S181741
4. Hamidi H, Ivaska J. Every step of the way: integrins in cancer progression and metastasis. *Nat Rev Cancer* (2018) 18:533–48. doi: 10.1038/s41568-018-0038-z
5. McSherry EA, McGee SF, Jirstrom K, Doyle EM, Brennan DJ, Landberg G, et al. JAM-A expression positively correlates with poor prognosis in breast cancer patients. *Int J Cancer* (2009) 125:1343–51. doi: 10.1002/ijc.24498
6. Garrido-Urbani S, Vonlaufen A, Stalin J, De Grandis M, Ropraz P, Jemelin S, et al. Junctional adhesion molecule C (JAM-C) dimerization aids cancer cell migration and metastasis. *Biochim Biophys Acta Mol Cell Res* (2018) 1865:638–49. doi: 10.1016/j.bbamcr.2018.01.008
7. Fuse C, Ishida Y, Hikita T, Asai T, Oku N. Junctional adhesion molecule-C promotes metastatic potential of HT1080 human fibrosarcoma. *J Biol Chem* (2007) 282:8276–83. doi: 10.1074/jbc.M608836200
8. Tenan M, Aurrand-Lions M, Widmer V, Alimenti A, Burkhardt K, Lazeyras F, et al. Cooperative expression of junctional adhesion molecule-C and -B supports growth and invasion of glioma. *Glia* (2010) 58:524–37. doi: 10.1002/glia.20941
9. Luissint AC, Lutz PG, Calderwood DA, Couraud PO, Bourdoulous S. JAM-L-mediated leukocyte adhesion to endothelial cells is regulated in cis by alpha4beta1 integrin activation. *J Cell Biol* (2008) 183:1159–73. doi: 10.1083/jcb.200805061
10. Moog-Lutz C, Cave-Riant F, Guibal FC, Breau MA, Di Gioia Y, Couraud PO, et al. JAML, a novel protein with characteristics of a junctional adhesion molecule, is induced during differentiation of myeloid leukemia cells. *Blood* (2003) 102:3371–8. doi: 10.1182/blood-2002-11-3462
11. Zen K, Liu Y, McCall IC, Wu T, Lee W, Babbin BA, et al. Neutrophil migration across tight junctions is mediated by adhesive interactions between epithelial coxsackie and adenovirus receptor and a junctional adhesion molecule-like protein on neutrophils. *Mol Biol Cell* (2005) 16:2694–703. doi: 10.1091/mbc.e05-01-0036
12. Guo YL, Bai R, Chen CX, Liu DQ, Liu Y, Zhang CY, et al. Role of junctional adhesion molecule-like protein in mediating monocyte transendothelial migration. *Arterioscler Thromb Vasc Biol* (2008) 29:75–83. doi: 10.1161/ATVBAHA.108.177717
13. Weber DA, Sumagin R, McCall IC, Leoni G, Neumann PA, Andargachew R, et al. Neutrophil-derived JAML inhibits repair of intestinal epithelial injury during acute inflammation. *Mucosal Immunol* (2014) 7:1221–32. doi: 10.1038/mi.2014.12
14. Sun Y, Guan J, Hou Y, Xue F, Huang W, Zhang W, et al. Silencing of junctional adhesion molecule-like protein attenuates atherogenesis and

enhances plaque stability in ApoE(-/-) mice. *Clin Sci (Lond)* (2019) 133:1215–28. doi: 10.1042/CS20180561
15. Amin MB, Greene FL, Edge SB, Compton CC, Gershenwald JE, Brookland RK, et al. The Eighth Edition AJCC Cancer Staging Manual: Continuing to build a bridge from a population-based to a more "personalized" approach to cancer staging. *CA Cancer J Clin* (2017) 67:93–9. doi: 10.3322/caac.21388
16. Witherden DA, Verdino P, Rieder SE, Garijo O, Mills RE, Teyton L, et al. The junctional adhesion molecule JAML is a costimulatory receptor for epithelial gammadelta T cell activation. *Science* (2010) 329:1205–10. doi: 10.1126/science.1192698
17. Verdino P, Witherden DA, Havran WL, Wilson IA. The molecular interaction of CAR and JAML recruits the central cell signal transducer PI3K. *Science* (2010) 329:1210–4. doi: 10.1126/science.1187996
18. Cuadrado A, Nebreda AR. Mechanisms and functions of p38 MAPK signalling. *Biochem J* (2010) 429:403–17. doi: 10.1042/BJ20100323
19. Dhillon AS, Hagan S, Rath O, Kolch W. MAP kinase signalling pathways in cancer. *Oncogene* (2007) 26:3279–90. doi: 10.1038/sj.onc.1210421
20. del Barco Barrantes I, Nebreda AR. Roles of p38 MAPKs in invasion and metastasis. *Biochem Soc Trans* (2012) 40:79–84. doi: 10.1042/BST20110676
21. Han J, Sun P. The pathways to tumor suppression via route p38. *Trends Biochem Sci* (2007) 32:364–71. doi: 10.1016/j.tibs.2007.06.007

Conflict of Interest: The authors declare that the research was conducted in the absence of any commercial or financial relationships that could be construed as a potential conflict of interest.

frontiers in Oncology

ORIGINAL RESEARCH
published: 11 March 2021
doi: 10.3389/fonc.2021.564270

Clinicopathological and Prognostic Characteristics of Esophageal Spindle Cell Squamous Cell Carcinoma: An Analysis of 43 Patients in a Single Center

Peng Li[1,2†], Yang Li[3†], Chao Zhang[1,2†], Yi-Hong Ling[1,2], Jie-Tian Jin[1,2], Jing-Ping Yun[1,2], Mu-Yan Cai[1,2] and Rong-Zhen Luo[1,2*]*

[1] State Key Laboratory of Oncology in South China, Collaborative Innovation Center for Cancer Medicine, Sun Yat-sen University Cancer Center, Guangzhou, China, [2] Department of Pathology, Sun Yat-sen University Cancer Center, Guangzhou, China, [3] Department of Pathology, The First Affiliated Hospital, Sun Yat-sen University, Guangzhou, China

OPEN ACCESS

Edited by:
Alfred King-yin Lam, Griffith University, Australia

Reviewed by:
Rupert Langer, University of Bern, Switzerland
Masato Yozu, Counties Manukau District Health Board, New Zealand

***Correspondence:**
Mu-Yan Cai
caimy@sysucc.org.cn
Rong-Zhen Luo
luorzh@sysucc.org.cn

†These authors have contributed equally to this work

Specialty section:
This article was submitted to Gastrointestinal Cancers, a section of the journal Frontiers in Oncology

Received: *21 May 2020*
Accepted: *18 January 2021*
Published: *11 March 2021*

Citation:
Li P, Li Y, Zhang C, Ling Y-H, Jin J-T, Yun J-P, Cai M-Y and Luo R-Z (2021) Clinicopathological and Prognostic Characteristics of Esophageal Spindle Cell Squamous Cell Carcinoma: An Analysis of 43 Patients in a Single Center. Front. Oncol. 11:564270. doi: 10.3389/fonc.2021.564270

Objective: Esophageal spindle cell squamous cell carcinoma (ESCSCC) is a distinct subtype of esophageal carcinoma with unique morphologic and clinicopathologic features. This study aimed to characterize the clinicopathologic manifestations and postoperative prognostic factors of ESCSCC.

Methods: In this study, 43 ESCSCC patients who underwent esophagectomy at Sun Yat-sen University Cancer Center between January 2001 and December 2014 were identified. 200 patients with conventional squamous cell carcinoma during the same period were sampled as a control. Hematoxylin and eosin-stained slides and available data were reviewed, and pertinent clinicopathologic features were retrospectively analyzed.

Results: Among the ESCSCC patients, the median age was 60.5 years, with a male-to-female ratio of 2.58:1. The five-year disease-free survival and cancer-specific survival rates were 51.6 and 55.5%, respectively. In the univariate analysis, drinking abuse, tumor size, macroscopic type, perineural invasion, pT, preoperative blood white blood cell count, preoperative blood neutrophil count, and preoperative blood neutrophil to lymphocyte ratio were significantly correlated with the cancer-specific survival and disease-free survival of the ESCSCC patients. The multivariate analysis showed that macroscopic type, perineural invasion, and preoperative blood neutrophil to lymphocyte ratio were independent prognostic factors for cancer-specific survival; macroscopic type, perineural invasion, tumor size, and pT were independent prognostic factors for disease-free survival. Moreover, the combined prognostic model for cancer-specific survival (including macroscopic type, perineural invasion, and preoperative blood neutrophil to lymphocyte ratio), the combined prognostic model for disease-free survival (including macroscopic type, perineural invasion, and tumor size) significantly stratified patients according to risk (low, intermediate, and high) to predict cancer-specific survival, disease-free survival, respectively. In terms of esophageal conventional squamous cell carcinoma

cohort, there was no significant difference in long-term outcome when compared with ESCSCC. Though five independent prognostic variables (macroscopic type, perineural invasion, preoperative blood neutrophil to lymphocyte ratio, tumor size, and pT) were indentified in ESCSCC, univariate analysis demonstrated that perineural invasion, preoperative blood neutrophil to lymphocyte ratio were correlated with esophageal conventional squamous cell carcinoma on cancer-specific survival; whereas only perineural invasion on disease-free survival.

Conclusions: The proposed two new prognostic models might aid in risk stratification and personalized management for patients with esophageal spindle cell squamous cell carcinoma who received radical surgery.

Keywords: esophageal spindle cell squamous cell carcinoma, clinicopathological characteristics, prognosis, macroscopic type, perineural invasion, preoperative blood neutrophil to lymphocyte ratio, tumor size

INTRODUCTION

Esophageal spindle cell squamous cell carcinoma (ESCSCC) is a rare subtype of esophageal squamous cell carcinoma, with unique morphology, histogenesis, and biological behavior. It accounts for 0.5–2.8% of all esophageal malignancies (1). Most ESCSCCs present as a gross intraluminal, polypoid mass. Histologically, ESCSCCs are composed of biphasic components of neoplastic squamous epithelium and spindle cells. The squamous part is always invasive and/or *in situ* squamous cell carcinoma, while the spindle cell element is usually malignant, which may show osseous, cartilaginous, or skeletal muscle differentiation (2, 3). Recent immunohistochemical, electron microscopic and genetic studies have provided support for the metaplastic concept, which states that the spindle cell component of ESCSCC exhibits various degrees of differentiation towards squamous cells and is a variant of poorly differentiated squamous cell carcinoma (4, 5). Therefore, ESCSCC was classified as subtype of esophageal squamous cell carcinoma in the current WHO classification (2019).

Radical esophagectomy with adequate lymph node dissection is the standard treatment for ESCSCC patients. Because of ESCSCC rarity, the long-term outcome of ESCSCC after radical surgery is controversial. Some investigators have suggested that ESCSCC treated with radical surgery has a comparatively better prognosis than that with esophageal conventional squamous cell carcinoma (6, 7). However, Sano et al. and Cavallin et al. have shown the opposite results (3, 8). During the past two decades, systemic adjuvant therapies, such as chemotherapy, radiotherapy, combination therapy, and targeted therapies, have been proposed to improve survival for ESCSCC patients with radical surgery (8–10). Minimizing the risk of overtreatment caused by non-selective use of these approaches, there is an urgent need to identify prognostic factors, especially for those with a high risk of tumor recurrence and poor prognosis. However, due to the controversy over ESCSCC's long-term outcome and lack of widely accepted prognostic factors, there is no consensus on the clinical management and adjuvant treatment for ESCSCC patients who received radical surgery.

In the present study, we retrospectively analyzed a series of 43 consecutive ESCSCC patients with radical surgery in our institute, focusing on the clinicopathological characteristics and postoperative prognostic factors, then compared the results with a cohort of esophageal conventional squamous cell carcinoma. The aim was to propose new prognostic models that might aid in risk stratification and personalized therapy for patients with ESCSCC.

PATIENTS AND METHODS

Patient Selection

The Institute Research Medical Ethics Committee of Sun Yat-sen University Cancer Center approved this study. We retrospectively collected a cohort of 43 ESCSCC patients who underwent radical esophagectomy between January 2001 and December 2014, from the pathological information system of the Department of Pathology of Sun Yat-sen University Cancer Center (Guangzhou, China). The cases were selected based on the following: (1) inclusion criteria: histologically confirmed primary esophageal spindle cell squamous cell carcinoma; complete follow-up data; (2) exclusion criteria: the percentage of spindle cell component was less than 10%; pTNM stage IV. Meanwhile, 200 patients with esophageal conventional squamous cell carcinoma during the same period were sampled. The inclusion criteria were shown as follows: histologically confirmed primary esophageal squamous cell carcinoma; complete follow-up data. The exclusion criterion was: pTNM stage IV.

For ESCSCC cohort, the clinicopathologic variables were obtained, including patient gender, age, smoking history, drinking history, tumor size, macroscopic type, tumor location, grade of conventional squamous cell carcinoma component, percentage of the spindle cell component, vascular invasion, perineural invasion, pT, pN, body mass index, level of serum alkaline phosphatase, level of serum lactic dehydrogenase, blood white blood cell count, blood neutrophil count, blood lymphocyte count, blood neutrophil to lymphocyte ratio, blood mononuclear cell count, blood eosinophil count, blood basophile count, hemoglobin, platelet count,

TABLE 1 | Baseline characteristics of the patients with esophageal spindle cell squamous cell carcinoma.

Characteristics	Patients (N = 43)
Gender	
Male	31 (72.1)
Female	12 (27.9)
Age (years)	
≤65	32 (74.4)
>65	11 (25.6)
Smoking abuse	
No	19 (44.2)
Yes	24 (55.8)
Drinking abuse	
No	33 (76.7)
Yes	10 (23.3)
Tumor size (cm)	
≤6	34 (79.1)
>6	9 (20.9)
Macroscopic type	
Polypoid type	36 (83.7)
Infiltrative type	7 (16.3)
Tumor location	
Upper portion	3 (6.9)
Middle portion	26 (60.5)
Lower portion-esophagogastric junction	14 (32.6)
Grade of conventional squamous cell carcinoma component	
G1	2 (4.7)
G2	24 (55.8)
G3	17 (39.5)
Percentage of the spindle cell component (%)	
Low (≤85)	31 (72.1)
High (>85)	12 (27.9)
Vascular invasion	
Absent	31 (72.1)
Present	12 (27.9)
Perineural invasion	
Absent	33 (76.7)
Present	10 (23.3)
pT	
T1	16 (37.2)
T2	15 (34.9)
T3	12 (27.9)
pN	
N0	24 (55.8)
N1	11(25.6)
N2	7 (16.3)
N3	1 (2.3)
Body mass index	
Normal (≤24)	36 (83.7)
High (>24)	7 (16.3)
Preoperative level of serum alkaline phosphatase (U/L)	
Low (<45)	2 (4.7)
Normal (45–125)	40 (93.0)
High (>125)	1 (2.3)
Preoperative level of serum lactic dehydrogenase(U/L)	
Low (<120)	4 (9.3)
Normal (120–250)	39 (90.7)
Preoperative blood white blood cell count (10^9/L)	
Normal (3.5–9.5)	30 (69.8)
High (>9.5)	13 (30.2)
Preoperative blood neutrophil count (10^9/L)	
Normal (1.8–6.3)	30 (69.8)
High (> 6.3)	13 (30.2)
Preoperative blood lymphocyte count (10^9/L)	
Low (<1.1)	3 (7.0)
Normal (1.1–3.2)	38 (88.4)
High (> 3.2)	2 (4.6)
Preoperative blood neutrophil to lymphocyte ratio	
Low (≤3.25)	26 (60.5)
High (>3.25)	17 (39.5)
Preoperative blood mononuclear cell count (10^9/L)	
Normal (0.1–0.6)	26 (60.5)
High (>0.6)	17 (39.5)
Preoperative blood eosinophil count (10^9/L)	
Normal (0.02–0.52)	40 (93.0)
High (>0.52)	3 (7.0)
Preoperative blood basophile count (10^9/L)	
Normal (0–0.06)	31 (72.1)
High (>0.06)	12 (27.9)
Preoperative blood hemoglobin (g/L)	
Low (<130)	24 (55.8)
Normal (130–175)	19 (44.2)
Preoperative blood platelet count (10^9/L)	
Normal (100–350)	31 (72.1)
High (>350)	12 (27.9)

disease-free survival time and cancer-specific survival time. According to the international criteria for the elderly, age was changed into a binary variable (≤65 year, or >65 year). Smoking abuse was defined as "consumption of tobacco for at least 6 months and at least one cigarette every three days". Similarly, drinking abuse refers to "consumption of alcohol for at least 6 months and at least once per week". With regard of body mass index, Chinese recommended standard (body mass index >24) was used for the criteria for overweight and obesity. According to the reference range of normal level, these blood variables involved in our study were classified as low, normal, or high. It is worth mentioning that the above blood cell-based markers were extracted from preoperative blood routine test. If there were multiple blood tests before the surgery, the one which was most close to surgery was adopted. The clinicopathological variables are detailed in **Table 1**. With regard to the cohort of esophageal conventional squamous cell carcinoma, only those variables indentified as independent prognostic factors in ESCSCC cohort were collected.

Follow-Up

The patients were followed up every three months for the first year and then every six months for the next two years and annually thereafter. Screening for recurrence was performed by a physical examination, endoscopy, esophageal barium

examination, CT, and MRI. Cancer-specific survival refers to the period from the date of diagnosis until death from ESCSCC, esophageal conventional squamous cell carcinoma, respectively. Disease-free survival refers to the period from the date of diagnosis until the date of first recurrence, locoregional or systemic; all other events were censored.

Pathological Evaluation

Tumor size was defined as the maximum diameter of the tumor. In terms of macroscopic type in ESCSCC, tumors which presented as a gross intraluminal and polypoid mass were classified as the polypoid type; while those with predominantly infiltrative growth pattern along esophageal wall were defined as the infiltrative type. In esophageal conventional squamous cell carcinoma, macroscopic appearance was classified as protruding type, ulcerative type, and diffusely infiltrative type.

All surgical specimens were processed according to standard pathological procedures. Two pathologists (PL and YL) independently reviewed all HE-stained slides of the primary tumors and regional lymph nodes without knowledge of the patient clinical parameters and the findings of the other reviewer. Any discrepancies were solved by simultaneous re-examination of the slides by both pathologists with a double-headed microscope. At least three slides per tumor were available for pathological evaluation, according to identical strict criteria.

The grade of conventional squamous cell carcinoma elements was determined based on the criteria proposed by the WHO Classification of Tumors of the Digestive System (2019); pT (tumor infiltration depth), and pN (lymph node status) were defined according to the 8th edition of the UICC/AJCC TNM (tumor-node-metastasis) Classification System (2017); vascular invasion was defined as the invasion of vessel walls by tumor cells and/or the existence of tumor emboli within an endothelium-lined space (11), and perineural invasion was defined as the presence of viable tumor cells in the perineural space (12).

Statistical Analysis

A receiver operating characteristic (ROC) curve analysis was used to determine the optimum cutoff point for continuous variables (tumor size, percentage of the spindle cell component, blood neutrophil to lymphocyte ratio). The cumulative cancer-specific survival and disease-free survival rates were calculated by the Kaplan–Meier method, and differences between the patient groups were tested by the log-rank test in univariate analysis. A Cox proportional hazard model was employed to determine independent prognostic factors. All tests were two-sided, and $P < 0.05$ was considered to be statistically significant. IBM SPSS 20.0 statistical software was used to perform the statistical analyses.

RESULTS

Patient Characteristics

A total of 43 patients with ESCSCC were included in the present study. The clinicopathological features for our ESCSCC cohort are presented in **Table 1**. Of the 43 patients, 31 (72.1%) were men, and 12 (27.9%) were women, with a male-to-female ratio of 2.58:1. The median age at the time of diagnosis was 60.5 years (range, 39.0 to 83.0 years). For the macroscopic type, 36 patients were defined as polypoid type (83.7%), and seven patients were defined as infiltrative type (16.3%). With regard to the pTNM stage, most patients were in early stages (stage I or II, 31 patients, 72.1%), whereas twelve patients (27.9%) were in stage III.

Radical esophagectomy with regional lymph node dissection was performed in all 43 ESCSCC patients. Postoperative therapy was given to five patients: four received radiotherapy, and one received concurrent chemoradiotherapy.

Pathologic Features

Microscopically, biphasic components of neoplastic squamous epithelium (invasive and/or *in situ* squamous cell carcinoma) and spindle-shaped sarcoma were observed in all 43 cases (**Figures 1A, B**). In addition, definite mesenchymal differentiation, including malignant peripheral nerve sheath tumor (one case), rhabdomyosarcoma/leiomyosarcoma (three cases, **Figure 1C**), or chondrosarcoma (one case, **Figure 1D**), was identified in the spindle cell components. The median percentage of spindle cell component was 65.5% (range, 10–95%). Regarding the depth of tumor invasion, sixteen tumors (37.2%) were superficial (T1), fifteen (34.9%) involved the muscular propria (T2), twelve (27.9%) involved the adventitia (T3). Lymph node metastasis was present in 19 of the patients (44.2%). Both the carcinomatous element and the spindle cell element have the potential for lymph node metastasis, with the predominance of a carcinomatous element. Vascular invasion and perineural invasion were detected in 12 patients (27.9%) and 10 patients (23.3%), respectively.

Prognostic Factor Analysis

To determine the optimal cutoff value for continuous variables involved in our study (tumor size, percentage of the spindle cell component, blood neutrophil to lymphocyte ratio), we utilized the ROC curve to identify the cutoff point. For example, according to the ROC curve analysis, the cutoff value for preoperative blood neutrophil to lymphocyte ratio was 3.25 (**Figure 2**).

Until October 2018, the median follow-up time was 45.3 months, with a range of 2.8 to 146.5 months. At the end of the follow-up, 22 patients (22/43, 51.2%) experienced tumor recurrence, which presented as anastomotic or esophageal remnant recurrence, hematogenous spread, and lymph node metastasis. Hematogenous spread mostly occurred in the lung, thoracic vertebra, liver, and brain. Lymph node recurrence was present in mediastinal and abdominal aortic lymph nodes.

As shown in **Table 2**, the univariate analysis for cancer-specific survival showed that the variables significantly associated with ESCSCC included drinking abuse ($P = 0.001$), tumor size ($P = 0.006$), macroscopic type ($P < 0.001$, **Figure 3A**), perineural invasion ($P = 0.004$, **Figure 3C**), pT ($P = 0.044$), preoperative blood white blood cell count ($P=0.011$), preoperative blood neutrophil count ($P = 0.001$), preoperative blood neutrophil to lymphocyte ratio ($P = 0.001$, **Figure 3E**). With regard to disease-

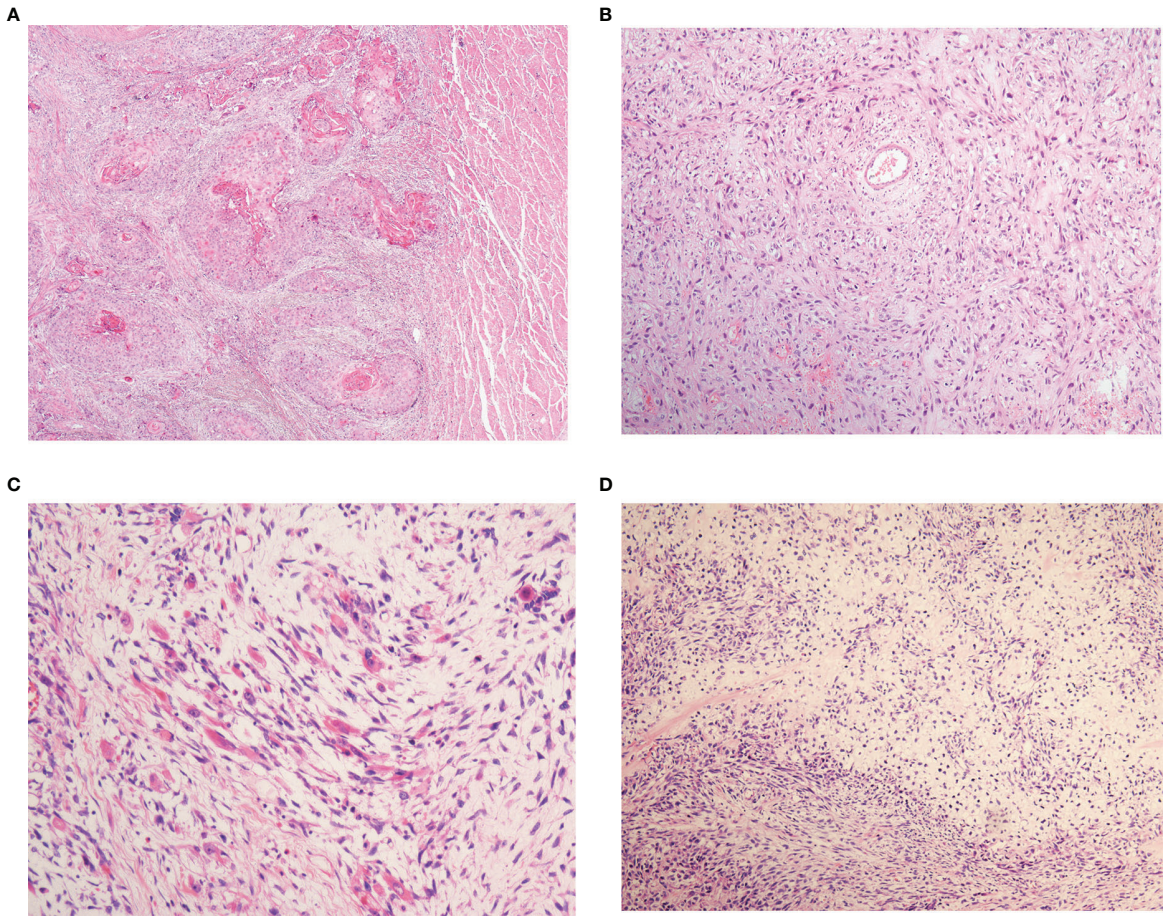

FIGURE 1 | The histopathological patterns of esophageal spindle cell squamous cell carcinoma. All patients in the present study were composed of neoplastic squamous epithelium **(A)** and spindle-shaped sarcoma **(B)**. Definite mesenchymal differentiation, such as that in rhabdomyosarcoma **(C)**, chondrosarcoma **(D)**, is occasionally observed in the spindle cell components.

free survival, the significant prognostic factors in univariate analysis included: drinking abuse (P = 0.004), macroscopic type (P < 0.001, **Figure 3B**), grade of conventional squamous cell carcinoma component (P = 0.044), perineural invasion (P = 0.001, **Figure 3D**), tumour size (P = 0.018, **Figure 3F**), pT (P = 0.019), preoperative blood white blood cell count (P = 0.037), preoperative blood neutrophil count (P = 0.003), preoperative blood neutrophil to lymphocyte ratio (P = 0.002).

Eventually, 20 patients (20/43, 46.5%) died of this tumor. The 1-, 3-, and 5-year cancer-specific survival rates were 79.1, 61.3, and 55.5% (**Figure 4A**), respectively. The 1-, 3-, and 5-year disease-free survival rates were 76.7, 54.5, and 51.6% (**Figure 4B**), respectively.

Multivariate Cox Regression Analysis

To determine independent prognostic factors, we performed multivariate analysis for cancer-specific survival using a Cox proportional hazard model. Both all statistically significant variables in univariate analysis and the variable with p value in the range of 0.05–0.1 (gender) were included in the multivariate analysis. The results confirmed that macroscopic type (HR = 0.047, 95% CI 0.004–0.592, P = 0.018), perineural invasion (HR = 0.088, 95% CI 0.008–0.969, P = 0.047), and preoperative blood neutrophil to lymphocyte ratio (HR = 0.208, 95% CI 0.052–0.835, P = 0.027) were independent prognostic factors for cancer-specific survival (**Table 3**). However, macroscopic type (P = 0.006), perineural invasion (P = 0.005), tumor size (P = 0.013), and pT (P = 0.049) were found to be associated with disease-free survival independent of other clinicopathological parameters (**Table 4**).

Two New Prognostic Models for Cancer-Specific Survival, Disease-Free Survival, Respectively

For cancer-specific survival, based on the three independent prognostic risk factors, macroscopic type, perineural invasion, and preoperative blood neutrophil to lymphocyte ratio, we built a new prognostic model to stratify the risk. The proposed model for cancer-specific survival confirmed that ESCSCC patients can be divided into a high-risk group (three risk factors), an intermediate-risk

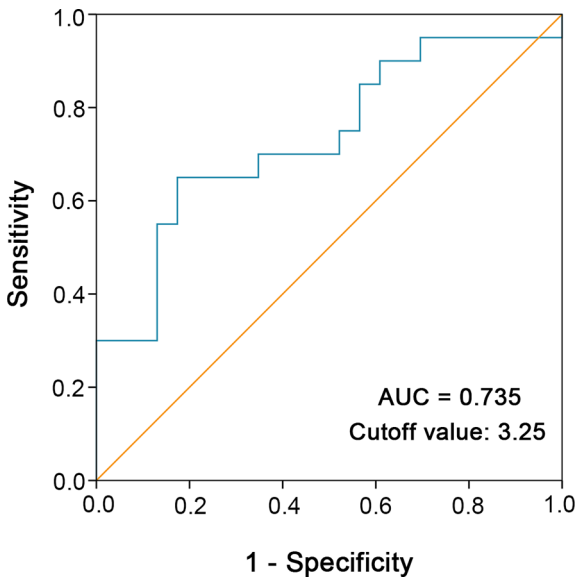

FIGURE 2 | ROC curve analysis was performed to determine the optimal cutoff value of preoperative blood neutrophil to lymphocyte ratio. The sensitivity and specificity for the status of cancer-specific survival were plotted.

group (one or two risk factors), and a low-risk group (none of the above risk factors). Similarly, in terms of disease-free survival, we proposed a new prognostic model including macroscopic type, perineural invasion, and tumor size. The prognostic model for disease-free survival could classify ESCSCC patients into a high-risk group (two or three risk factors), an intermediate-risk group (one risk factor), and a low-risk group (none of the above risk factors). The two combined models significantly stratified risk (low, intermediate, and high) for cancer-specific survival, disease-free survival prediction, respectively (both $P < 0.001$, **Figures 4C, D**). Further analysis revealed that the 5-year disease-free survival rate was 70.2% in the low-risk group, 38.9% in the intermediate-risk group, and 0% in the high-risk group. The 5-year cancer-specific survival rate was 88.5% in the low-risk group, 30.8% in the intermediate-risk group, and 0% in the high-risk group.

Comparison of Prognosis With Esophageal Conventional Squamous Cell Carcinoma

200 patients with conventional squamous cell carcinoma during the same period were sampled as a control. Five variables identified as independent prognostic factors in our cohort of ESCSC were collected, including macroscopic type, perineural invasion, preoperative blood neutrophil to lymphocyte ratio, tumor size, and pT. The clinicopathologic characteristics were detailed in **Supplemental Table 1**.

There were no significant difference between ESCSCC and esophageal conventional squamous cell carcinoma on the 5-year cancer-specific survival rate (55.5 *v* 42.0%, $P = 0.384$) and 5-year disease-free survival rate (51.6 *v* 41.5%, $P = 0.588$). Univariate analysis demonstrated that perineural invasion ($P < 0.001$), preoperative blood neutrophil to lymphocyte ratio ($P = 0.021$) were correlated with esophageal conventional squamous cell carcinoma on cancer-specific survival (**Supplemental Table 2**); whereas only perineural invasion on disease-free survival ($P < 0.001$, **Supplemental Table 3**). Two new prognostic models we proposed for ESCSCC failed to significantly stratified risk (low, intermediate, and high) on cancer-specific survival rate or disease-free survival rate in our cohort of esophageal conventional squamous cell carcinoma.

DISCUSSION

In the present study, based on a relatively large single-center cohort of 43 ESCSCC patients who underwent surgical treatment, we found that macroscopic type, perineural invasion, and preoperative blood neutrophil to lymphocyte ratio were independent prognostic factors for cancer-specific survival. However, macroscopic type, perineural invasion, tumor size, and pT were found to be associated with disease-free survival independent of other clinicopathological parameters. More importantly, two combined prognostic models we proposed can significantly stratify risk (low, intermediate, and high) to predict cancer-specific survival, disease-free survival, respectively.

Historically, ESCSCC is not a well-known entity. There are several synonyms, such as carcinosarcoma, sarcomatoid carcinoma, spindle cell carcinoma, metaplastic carcinoma, polypoid carcinoma, pseudosarcoma, squamous cell carcinoma with sarcomatous feature, squamous cell carcinoma with spindle cell features (3). These discrepancies in nomenclature reflect the limit knowledge of ESCSCC. In the WHO Classification of Tumors of the Digestive System (2019), ESCSCC is classified as the subtype of esophageal squamous cell carcinoma. Our findings support this classification. First, though it is companied by variable proportions of malignant spindle-shaped sarcoma element, there is no significant difference between ESCSCC and esophageal conventional squamous cell carcinoma in long-term outcome. Secondly, our research found several different prognostic factors only in ESCSCC, *e.g.* tumor size, macroscopic type, and pT. Thirdly, ESCSCC and esophageal conventional squamous cell carcinoma shared some common prognostic factors, such as perineural invasion, preoperative blood neutrophil to lymphocyte ratio. However, it is worth mentioning that in terms of preoperative blood neutrophil to lymphocyte ratio, the cutoff for esophageal conventional squamous cell carcinoma is 2.79 while it is 3.25 for ESCSCC. Lastly, two new prognostic models we proposed for ESCSCC failed to significantly stratified risk (low, intermediate, and high) in our cohort of esophageal conventional squamous cell carcinoma. Our findings demonstrated that the underlying molecular biological basis for ESCSCC might be at least in part different from that for esophageal conventional squamous cell carcinoma, supporting the notion that ESCSCC may be distinguished from esophageal conventional squamous cell carcinoma as a rare subtype.

TABLE 2 | Univariate analysis of clinicopathologic variables in patients with esophageal spindle cell squamous cell carcinoma for cancer-specific survival and disease-free survival (log-rank test).

Variables	Cases	Cancer-Specific Survival			Disease-Free Survival		
		Mean survival (months)	Median survival (months)	*P* value	Mean survival (months)	Median survival (months)	*P* value
Gender				0.062			0.129
Male	31	57. 7	50.0		54.7	49.5	
Female	12	114.7	NR		102.6	NR	
Age (years)				0.182			0.113
≤65	32	88.8	NR		85.3	73.5	
>65	11	35.0	27.1		29.3	27.1	
Smoking abuse							0.425
No	19	102.4	NR	0.125	88.9	NR	
Yes	24	55.7	50.0		55.4	49.5	
Drinking abuse				0.001			0.004
No	33	98.2	NR		90.8	NR	
Yes	10	29.7	8.7		29.4	8.7	
Tumor size (cm)				0.006			0.018
≤6	34	94.3	NR		87.4	NR	
>6	9	30.8	8.7		30.3	8.7	
Macroscopic type				<0.001			<0.001
Polypoid type	36	93.7	NR		90.8	NR	
Infiltrative type	7	18.0	6.5		8.4	3.8	
Tumor location				0.196			0.198
Upper portion	3	61.3	88.7		51.2	73.5	
Middle portion	26	95.6	NR		90.9	NR	
Lower portion-esophagogastric junction	14	34.9	21.6		30.1	21.6	
Grade of conventional squamous cell carcinoma component				0.114			0.044
G1	2	64.0	17.4		64.0	17.4	
G2	24	55.5	49.5		47.8	25.7	
G3	17	113.1	NR		113.4	NR	
Percentage of the spindle cell component(%)				0.533			0.844
Low (≤85)	31	74.1	NR		67.0	NR	
High (>85)	12	67.2	67.5		68.7	65.5	
Vascular invasion				0.240			0.119
Absent	31	89.3	88.7		85.8	NR	
Present	12	46.6	27.1		40.6	14.6	
Perineural invasion				0.004			0.001
Absent	33	93.6	NR		90.1	NR	
Present	10	34.5	8.70		28.1	6.5	
pT				0.044			0.019
T1	16	83.8	88.7		80.1	NR	
T2	15	81.8	49.5		81.8	49.5	
T3	12	40.9	8.7		34.5	6.9	
pN				0.158			0.078
N0	24	73.0	88.7		72.1	73.5	
N1	11	94.8	NR		85.3	65.5	
N2	7	47.9	20.2		36.4	6.9	
N3	1	8.7	8.7		8.7	8.7	
Body mass index				0.782			0.615
Low (≤24)	36	69.5	67.5		63.9	65.5	
High (>24)	7	89.0	NR		89.0	NR	
Preoperative level of serum alkaline phosphatase (U/L)				0.109			0.270
Low (<45)	2	28.0	6.5		28.0	6.5	
Normal (45–125)	40	87.2	88.7		81.7	73.5	
High (>125)	1	18.5	18.5		18.5	18.5	
Preoperative level of serum lactic dehydrogenase(U/L)				0.742			0.614
Low (<120)	4	66.3	67.5		68.8	65.5	

(Continued)

TABLE 2 | Continued

Variables	Cases	Cancer-Specific Survival			Disease-Free Survival		
		Mean survival (months)	Median survival (months)	*P* value	Mean survival (months)	Median survival (months)	*P* value
Normal (120–250)	39	82.2	88.7		76.2	49.5	
Preoperative blood white blood cell count (10^9/L)				0.011			0.037
Normal (3.5–9.5)	30	96.6	NR		89.2	NR	
High (>9.5)	13	41.7	19.8		41.8	18.5	
Preoperative blood neutrophil count (10^9/L)				0.001			0.003
Normal (1.8–6.3)	30	101.6	NR		93.9	NR	
High (>6.3)	13	23.1	19.8		22.8	16.9	
Preoperative blood lymphocyte count (10^9/L)				0.808			0.938
Low (<1.1)	3	58.0	NR		39.1	29.7	
Normal (1.1–3.2)	38	80.3	88.7		78.3	65.5	
High (>3.2)	2	73.9	27.1		73.9	27.1	
Preoperative blood neutrophil to lymphocyte ratio				0.001			0.002
Low (≤3.25)	26	107.8	NR		100.0	NR	
High (>3.25)	17	34.0	18.5		32.3	16.9	
Preoperative blood mononuclear cell count (10^9/L)				0.212			0.375
Normal (0.1–0.6)	26	73.2	NR		66.7	NR	
High (>0.6)	17	68.5	49.5		67.9	31.8	
Preoperative blood eosinophil count(10^9/L)				0.974			0.837
Normal (0.02–0.52)	40	83.4	88.7		77.7	65.5	
High (>0.52)	3	37.0	NR		37.0	NR	
Preoperative blood basophile count (10^9/L)				0.843			0.890
Normal (0–0.06)	31	85.9	NR		77.9	65.5	
High (>0.06)	12	66.7	88.7		64.5	73.5	
Preoperative blood haemoglobin (g/L)				0.655			0.966
Low (<130)	24	72.4	67.5		64.2	49.5	
Normal (130–175)	19	78.9	88.7		80.1	73.5	
Preoperative blood platelet count (10^9/L)				0.266			0.168
Normal (100–350)	31	74.0	67.5		68.1	29.7	
High (>350)	12	83.9	NR		84.1	NR	

NR indicates not reached.

Currently, the long-term clinical outcome of ESCSCC patients treated with radical surgery is controversial. Cavallin et al. found that the recurrence rate was 80%, leading to death within two years after surgery (8). The 5-year overall survival rate reported in other studies ranged from 44.8 to 61.9% (3, 6, 7, 13). Consistent with Sano et al. and Hashimoto et al.'s findings (3, 13), our study showed that the 5-year cancer-specific survival rate was 55.5%. Limited sample size, the quality of radical surgery, the percentage of patients in the early stage, and other prognostic factors might lead to these discrepancies in prognosis among different studies.

Our data showed that the percent of the spindle cell elements was not associated with cancer-specific survival and disease-free survival for ESCSCC patients who underwent radical surgery. These outcomes led us to speculate that both carcinomatous and spindle cell elements determine the malignant behavior of ESCSCCs. However, Natsugoe et al. found that cells in the sarcomatous and carcinomatous components were aneuploid and diploid, respectively, based on DNA flow cytometric analysis. They proposed the concept that the sarcomatous component in ESCSCC accounts for malignant behavior (14). Thus, which component in ESCSCC defines the degree of malignant behavior of this tumor is still controversial and needs further investigation.

In the current study, we paid special attention to the potential prognostic role of preoperative peripheral blood cell-based markers for ESCSCC. Currently, accumulating evidence has supported these blood cell-based markers as predictors of

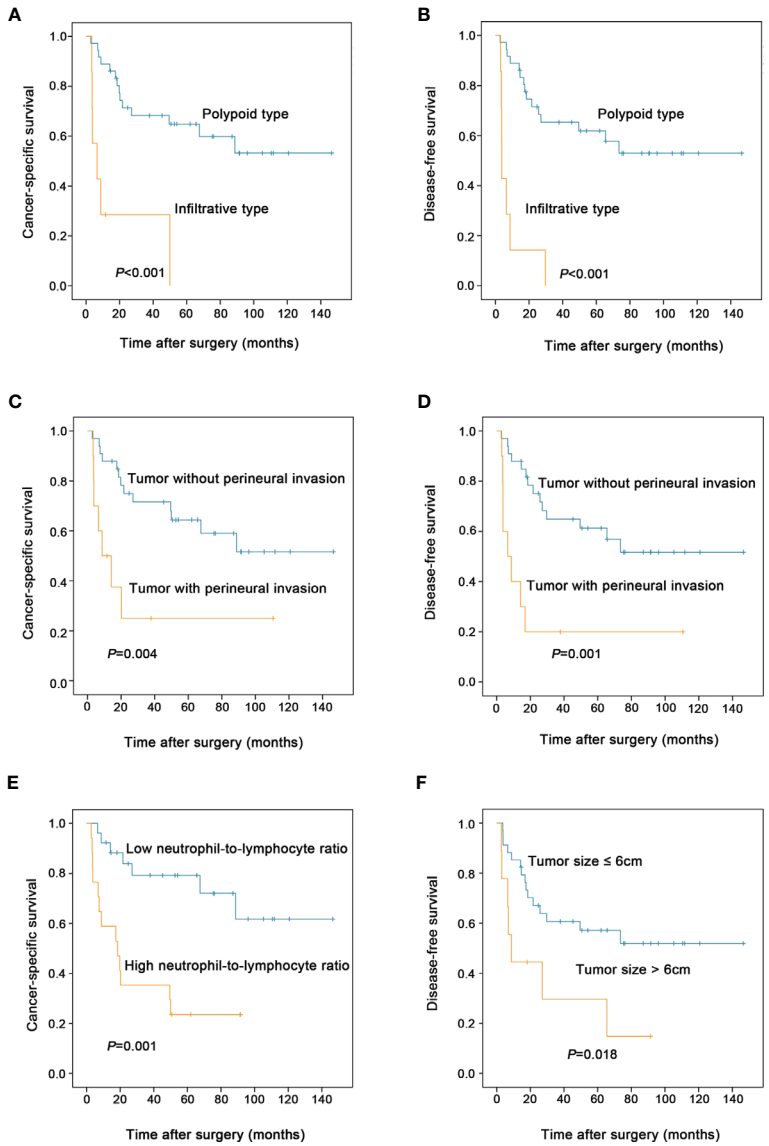

FIGURE 3 | Prognostic factors affecting the postoperative survival of patients with esophageal spindle cell squamous cell carcinoma (log-rank test). Compared to polypoid type, infiltrative tumor type was associated with decreased cancer-specific survival **(A)** and disease-free survival **(B)** of patients. Tumor with perineural invasion had worse cancer-specific survival **(C)** and disease-free survival **(D)** than those without perineural invasion. High preoperative blood neutrophil to lymphocyte ratio was associated with decreased cancer-specific survival **(E)** in patients. Patients with tumor size >6cm had worse disease-free survival than those with tumor size ≤6cm **(F)**.

outcome after an operation and treatment response to neoadjuvant chemotherapy in various types of malignancies (15–20). In terms of our research, the elevation of preoperative blood neutrophil to lymphocyte ratio was independent predictor of poor cancer-specific survival for patients with ESCSCC who underwent curative surgical resection. Our observations might suggest a potential impact of cancer-associated inflammation on the progression and metastasis of ESCSCC. In general, the inflammatory microenvironment established by the tumor promotes its further malignant behavior by producing DNA damage and genomic instability, enhancing proliferation and survival, stimulating angiogenesis, favoring invasion and metastasis, and inducing an immunosuppressive environment (21, 22). Moreover, our analysis highlighted the role of neutrophils in ESCSCC malignant behavior, suggesting the potential application of future therapies targeting the tumor inflammatory microenvironment for ESCSCC patients.

pTNM stage is the best-established risk factor for important aspects affecting the prognosis of patients with esophageal cancer. This parameter, based on specific clinicopathological

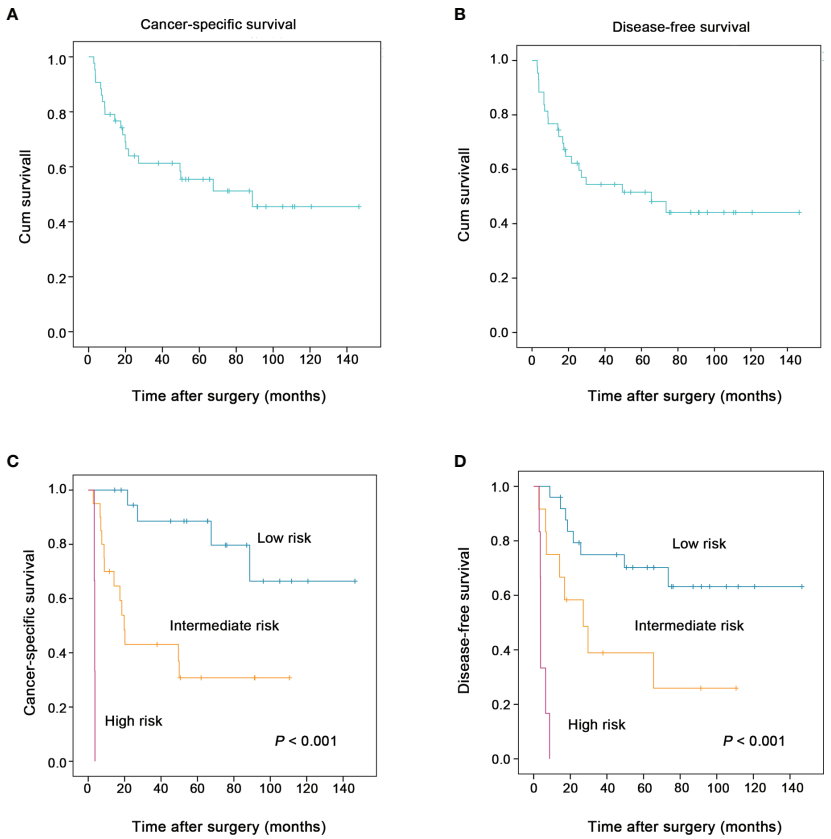

FIGURE 4 | The two proposed prognostic models successfully stratified the risk of patients with esophageal spindle cell squamous cell carcinoma to predict survival (log-rank test). The overall cancer-specific survival and disease-free survival of patients in the present study are presented in **(A, B)**, respectively. The new combined model for cancer-specific survival (including macroscopic type, perineural invasion, preoperative blood neutrophil to lymphocyte ratio), another model for disease-free survival (including macroscopic type, perineural invasion, tumor size) clearly stratified patients into groups according to risk (low, intermediate and high) and was used to predict the cancer-specific survival **(C)**, the disease-free survival **(D)** of esophageal spindle cell squamous cell carcinoma patients, respectively.

TABLE 3 | Cox multivariate analyses of prognostic factors on cancer-specific survival.

Variables	Hazard ratio	95% CI	*P* value
Gender (Male *v* Female)	1.499	0.283–7.944	0.634
Drinking abuse (No *v* Yes)	0.444	0.148–1.333	0.148
Tumor size (≤6 cm *v* >6 *cm*)	0.319	0.091–1.116	0.074
Macroscopic type (Polypoid *v* Infiltrative type)	0.047	0.004–0.592	0.018
Perineural invasion (Absent *v* Present)	0.088	0.008–0.969	0.047
pT			0.265
pT (T1 *v* T3)	10.973	0.568–211.839	0.113
pT (T2 *v* T3)	6.092	0.334–111.035	0.222
Preoperative blood white blood cell count (10^9/L) (Normal (3.5–9.5) *v* High (>9.5))	1.396	0.053–37.007	0.842
Preoperative blood neutrophil count (10^9/L) (Normal (1.8–6.3) *v* High(> 6.3))	0.159	0.005–4.846	0.292
Preoperative blood neutrophil to lymphocyte ratio (Low *v* High)	0.208	0.052–0.835	0.027

CI, confidence interval.

features and extent of disease, may have reached its limit in providing critical information in influencing patient prognosis and treatment strategies. Therefore, there is a need for new objective strategies that can effectively distinguish between patients with favorable and unfavorable outcomes. In our study, our data support the idea that macroscopic type, perineural invasion, preoperative blood neutrophil to lymphocyte ratio, and tumor size can effectively identify ESSC patients who may have aggressive clinical courses and adverse outcomes. Thus, macroscopic type, perineural invasion, preoperative blood neutrophil to lymphocyte ratio, and tumor size may become factors for predicting prognosis and render a more tailored treatment strategy in ESCSCC patients. Based on these interesting results, we propose two new prognostic models for cancer-specific survival, disease-free survival, respectively. The two proposed models may help to guide postoperative follow-up and individualized treatment.

Several limitations may affect the interpretation of this study due to the single-center retrospective design and the small sample size. However, given the rarity of the disease, larger prospective studies are difficult. In contrast, multi-center retrospective studies

TABLE 4 | Cox multivariate analyses of prognostic factors on disease-free survival.

Variables	Hazard ratio	95% CI	*P* value
Drinking abuse (No *v* Yes)	0.445	0.111–1.785	0.253
Tumor size (≤6 cm *v* >6 *cm*)	0.164	0.040–0.683	0.013
Macroscopic type (Polypoid *v* Infiltrative type)	0.003	0.000–0.189	0.006
Grade of conventional squamous cell carcinoma component			0.565
G1 *v* G3	2.066	0.059–72.178	
G2 *v* G3	2.153	0.526–8.815	
Perineural invasion (Absent *v* Present)	0.023	0.002–0.322	0.005
pT			0.049
pT (T1 *v* T3)	136.727	2.489–7511.031	
pT (T2 *v* T3)	48.208	0.976–2380.761	
pN			0.095
pN (N0 *v* N3*)*	30.286	1.021–898.548	
pN (N1 *v* N3*)*	18.062	0.727–448.554	
pN (N2 *v* N3*)*	114.165	2.574–5063.553	
Preoperative blood white blood cell count (10^9/L) (Normal (3.5–9.5) *v* High(>9.5))	1.116	0.016–78.718	0.960
Preoperative blood neutrophil count (10^9/L) (Normal (1.8–6.3) *v* High (>6.3))	0.218	0.003–16.492	0.490
Preoperative blood neutrophil to lymphocyte ratio (Low *v* High)	0.254	0.056–1.147	0.075

CI, confidence interval.

with a larger sample size should be encouraged. In addition, in our cohort of ESCSCC, five patients received postoperative therapy. Neoadjuvant treatment was not given in anyone patient with pTNM stage II or III. It was really disproportionately low compared to the current standard. Our cohort patients were retrospectively collected between January 2001 and December 2014. During this period, because of this tumor rarity, there was no consensus on the clinical management and adjuvant treatment for ESCSCC patients who received radical surgery.

DATA AVAILABILITY STATEMENT

The original contributions presented in the study are included in the article/**Supplementary Material**. Further inquiries can be directed to the corresponding authors. The authenticity of this article has been validated by uploading the key raw data onto the Research Data Deposit public platform (www.researchdata.org.cn), with the approval RDD number as RDDA2021001924.

ETHICS STATEMENT

The studies involving human participants were reviewed and approved by The Institute Research Medical Ethics Committee of Sun Yat-sen University Cancer Center. Written informed consent for participation was not required for this study in accordance with the national legislation and the institutional requirements.

AUTHOR CONTRIBUTIONS

M-YC and R-ZL designed the research. PL reviewed HE-stained slides, analyzed the data, and wrote the manuscript. YL reviewed HE-stained slides. CZ performed follow-up of patients after surgery. Y-HL and J-TJ acquired clinicopathological data. J-PY reviewed the manuscript. All authors contributed to the article and approved the submitted version.

FUNDING

This work was supported by grants from National Natural Science Foundation of China (81672407 and 81872001, to M-YC).

CONCLUSIONS

We proposed two new prognostic models based on macroscopic type, perineural invasion, preoperative blood neutrophil to lymphocyte ratio, and tumor size that can effectively identify ESCSCC patients with a high risk of tumor recurrence and poor prognosis. This may aid in personalized management for patients with ESCSCC.

ACKNOWLEDGMENTS

Part of our preliminary results in the research was presented in the conference proceedings of XXXI International Congress of the International Academy of Pathology and 28th Congress of the European Society of Pathology (Virchows Arch. 2016 Sep; 469 Suppl 1:1-346).

SUPPLEMENTARY MATERIAL

The Supplementary Material for this article can be found online at: https://www.frontiersin.org/articles/10.3389/fonc.2021.564270/full#supplementary-material

REFERENCES

1. Madan AK, Long AE, Weldon CB, Jaffe BM. Esophageal carcinosarcoma. *J Gastrointestinal Surg Off J Soc Surg Alimentary Tract* (2001) 5(4):414–7. doi: 10.1016/s1091-255x(01)80071-8

2. Chino O, Kijima H, Shimada H, Nishi T, Tanaka H, Oshiba G, et al. Clinicopathological studies of esophageal carcinosarcoma: analyses of its morphological characteristics using endoscopic, histological, and immunohistochemical procedures. *Endoscopy* (2000) 32(9):706–11. doi: 10.1055/s-2000-9026

3. Sano A, Sakurai S, Kato H, Sakai M, Tanaka N, Inose T, et al. Clinicopathological and immunohistochemical characteristics of esophageal carcinosarcoma. *Anticancer Res* (2009) 29(8):3375–80.
4. Wang ZY, Itabashi M, Hirota T, Watanabe H, Kato H. Immunohistochemical study of the histogenesis of esophageal carcinosarcoma. *Japan J Clin Oncol* (1992) 22(6):377–86.
5. Matsumoto T, Fujii H, Arakawa A, Yamasaki S, Sonoue H, Hattori K, et al. Loss of heterozygosity analysis shows monoclonal evolution with frequent genetic progression and divergence in esophageal carcinosarcoma. *Hum Pathol* (2004) 35(3):322–7. doi: 10.1016/j.humpath.2003.02.001
6. Wang L, Lin Y, Long H, Liu H, Rao H, He Y, et al. Esophageal carcinosarcoma: a unique entity with better prognosis. *Ann Surg Oncol* (2013) 20(3):997–1004. doi: 10.1245/s10434-012-2658-y
7. Zhang B, Xiao Q, Yang D, Li X, Hu J, Wang Y, et al. Spindle cell carcinoma of the esophagus: A multicenter analysis in comparison with typical squamous cell carcinoma. *Medicine* (2016) 95(37):e4768. doi: 10.1097/MD.0000000000004768
8. Cavallin F, Scarpa M, Alfieri R, Cagol M, Ruol A, Rugge M, et al. Esophageal carcinosarcoma: management and prognosis at a single Italian series. *Anticancer Res* (2014) 34(12):7455–9.
9. Yoshimoto T, Kobayashi S, Kanetaka K, Kobayashi K, Nagata Y, Morita M, et al. Preoperative chemotherapy with docetaxel, cisplatin, and 5-fluorouracil for locally advanced esophageal carcinosarcoma: a case report and review of the literature. *Surg Case Rep* (2018) 4(1):18. doi: 10.1186/s40792-018-0425-4
10. Lu H, Yang S, Zhu H, Tong X, Xie F, Qin J, et al. Targeted next generation sequencing identified clinically actionable mutations in patients with esophageal sarcomatoid carcinoma. *BMC Cancer* (2018) 18(1):251. doi: 10.1186/s12885-018-4159-2
11. Li P, He HQ, Zhu CM, Ling YH, Hu WM, Zhang XK, et al. The prognostic significance of lymphovascular invasion in patients with resectable gastric cancer: a large retrospective study from Southern China. *BMC Cancer* (2015) 15:370. doi: 10.1186/s12885-015-1370-2
12. Chen JW, Xie JD, Ling YH, Li P, Yan SM, Xi SY, et al. The prognostic effect of perineural invasion in esophageal squamous cell carcinoma. *BMC Cancer* (2014) 14:313. doi: 10.1186/1471-2407-14-313
13. Hashimoto M, Kitagami H, Niwa H, Kikkawa T, Ohuchi T, Takenouchi T, et al. Prognosis and prognostic factors of esophageal spindle cell carcinoma treated by esophagectomy: a retrospective single-institution analysis. *Esophagus Off J Japan Esophageal Soc* (2019) 16(3):292–9. doi: 10.1007/s10388-019-00667-y
14. Natsugoe S, Matsushita Y, Chuman Y, Kijima F, Haraguchi Y, Shimada M, et al. So-called carcinosarcoma of the esophagus: A clinicopathologic, immunohistochemical and DNA flow-cytometric analysis of 6 cases. *Oncology* (1999) 57(1):29–35. doi: 10.1159/000011997
15. Onesti CE, Josse C, Poncin A, Freres P, Poulet C, Bours V, et al. Predictive and prognostic role of peripheral blood eosinophil count in triple-negative and hormone receptor-negative/HER2-positive breast cancer patients undergoing neoadjuvant treatment. *Oncotarget* (2018) 9(72):33719–33. doi: 10.18632/oncotarget.26120
16. Yuan C, Li N, Mao X, Liu Z, Ou W, Wang SY. Elevated pretreatment neutrophil/white blood cell ratio and monocyte/lymphocyte ratio predict poor survival in patients with curatively resected non-small cell lung cancer: Results from a large cohort. *Thoracic Cancer* (2017) 8(4):350–8. doi: 10.1111/1759-7714.12454
17. Lin JX, Lin JP, Xie JW, Wang JB, Lu J, Chen QY, et al. Complete blood count-based inflammatory score (CBCS) is a novel prognostic marker for gastric cancer patients after curative resection. *BMC Cancer* (2020) 20(1):11. doi: 10.1186/s12885-019-6466-7
18. Bhindi B, Hermanns T, Wei Y, Yu J, Richard PO, Wettstein MS, et al. Identification of the best complete blood count-based predictors for bladder cancer outcomes in patients undergoing radical cystectomy. *Br J Cancer* (2016) 114(2):207–12. doi: 10.1038/bjc.2015.432
19. Takakura K, Ito Z, Suka M, Kanai T, Matsumoto Y, Odahara S, et al. Comprehensive assessment of the prognosis of pancreatic cancer: peripheral blood neutrophil-lymphocyte ratio and immunohistochemical analyses of the tumour site. *Scandinavian J Gastroenterol* (2016) 51(5):610–7. doi: 10.3109/00365521.2015.1121515
20. Kijima T, Arigami T, Uchikado Y, Uenosono Y, Kita Y, Owaki T, et al. Combined fibrinogen and neutrophil-lymphocyte ratio as a prognostic marker of advanced esophageal squamous cell carcinoma. *Cancer Sci* (2017) 108(2):193–9. doi: 10.1111/cas.13127
21. Galdiero MR, Garlanda C, Jaillon S, Marone G, Mantovani A. Tumor associated macrophages and neutrophils in tumor progression. *J Cell Physiol* (2013) 228(7):1404–12. doi: 10.1002/jcp.24260
22. Hanahan D, Weinberg RA. Hallmarks of cancer: the next generation. *Cell* (2011) 144(5):646–74. doi: 10.1016/j.cell.2011.02.013

Conflict of Interest: The authors declare that the research was conducted in the absence of any commercial or financial relationships that could be construed as a potential conflict of interest.

frontiers in Oncology

ORIGINAL RESEARCH
published: 08 April 2021
doi: 10.3389/fonc.2021.671180

Camptothecin Inhibits Neddylation to Activate the Protective Autophagy Through NF-κB/AMPK/mTOR/ULK1 Axis in Human Esophageal Cancer Cells

Yongqing Heng[1†], Yupei Liang[1†], Junqian Zhang[1], Lihui Li[1], Wenjuan Zhang[2], Yanyu Jiang[1], Shiwen Wang[3] and Lijun Jia[1]*

[1] Cancer Institute, Longhua Hospital, Shanghai University of Traditional Chinese Medicine, Shanghai, China, [2] Department of Breast Surgery, Key Laboratory of Breast Cancer in Shanghai, Fudan University Shanghai Cancer Center, Shanghai, China, [3] Department of Laboratory Medicine, Huadong Hospital, Affiliated to Fudan University, Shanghai, China

OPEN ACCESS

Edited by:
Bin Li,
Jinan University, China

Reviewed by:
Chun-Ping Cui,
Beijing Institute of Lifeomics, China
Lisha Zhou,
Taizhou University, China

***Correspondence:**
Lijun Jia
ljjia@shutcm.edu.cn

[†]These authors have contributed equally to this work

Specialty section:
This article was submitted to Gastrointestinal Cancers, a section of the journal Frontiers in Oncology

Received: 23 February 2021
Accepted: 15 March 2021
Published: 08 April 2021

Citation:
Heng Y, Liang Y, Zhang J, Li L, Zhang W, Jiang Y, Wang S and Jia L (2021) Camptothecin Inhibits Neddylation to Activate the Protective Autophagy Through NF-κB/AMPK/mTOR/ULK1 Axis in Human Esophageal Cancer Cells. Front. Oncol. 11:671180. doi: 10.3389/fonc.2021.671180

The neddylation pathway is overactivated in esophageal cancer. Our previous studies indicated that inactivation of neddylation by the NAE inhibitor induced apoptosis and autophagy in cancer cells. Camptothecin (CPT), a well-known anticancer agent, could induce apoptosis and autophagy in cancer cells. However, whether CPT could affect the neddylation pathway and the molecular mechanisms of CPT-induced autophagy in esophageal cancer remains elusive. We found that CPT induced apoptosis and autophagy in esophageal cancer. Mechanistically, CPT inhibited the activity of neddylation and induced the accumulation of p-IkBa to block NF-κB pathway. Furthermore, CPT induced the generation of ROS to modulate the AMPK/mTOR/ULK1 axis to finally promote protective autophagy. In our study, we elucidate a novel mechanism of the NF-κB/AMPK/mTOR/ULK1 pathway in CPT-induced protective autophagy in esophageal cancer cells, which provides a sound rationale for combinational anti-ESCC therapy with CPT and inhibition AMPK/ULK1 pathway.

Keywords: camptothecin, neddylation, p-IκBα, NF-κB/AMPK/mTOR/ULK1, autophagy, apoptosis, esophageal cancer

INTRODUCTION

Post-translational modification of proteins plays crucial roles in the regulation of tumorigenesis and tumor progression. Protein neddylation is an important post-translational modification that conjugates the ubiquitin-like molecule NEDD8 (neuronal precursor cell-expressed developmentally down-regulated protein 8) to substrate proteins (1–4). This process is catalyzed by NEDD8-activating enzyme (NAE, NAE1, and UBA3 heterodimer), transferred to NEDD8-conjugating enzymes E2 and

Abbreviations: NEDD8, neural precursor cell expressed developmentally down-regulated 8; CRL, Cullin-RING E3 ligase; ESCC, Esophageal squamous cell carcinoma; CQ, chloroquine; BafA1, Bafilomycin A1; 3MA, 3-methyladenine; IB, immunoblotting; Com.C, Compound C.

then conjugated to substrate-specific NEDD8-E3 ligases (1–4). The cullin subunits of Cullin-RING E3 ubiquitin ligase (CRL) are the best-characterized substrates of neddylation pathway (5, 6). Accumulated studies show that protein neddylation is elevated in multiple human cancers, and inhibition of this pathway has been developed as a promising anticancer strategy. Mechanistic studies showed that neddylation inhibition effectively induced DNA re-replication stress/DNA damage response, cell cycle arrest, apoptosis, or senescence in a cell-type-dependent manner (7–13). Moreover, neddylation inhibition also induced pro-survival autophagic responses in cancer cells partially *via* modulating the HIF1–REDD1–TSC1 or DEPTOR–mTORC1 pathways (14–16).

Camptothecin (CPT), a topoisomerase I inhibitor, was isolated from the Asian tree Camptotheca acuminate by Wall and Wani in 1966 (17). CPT can form a stable tertiary structure with DNA and topoisomerase I, thus resulting in the formation of the topoisomerase I-CPT complex, which induce DNA double-strand breakage to ultimately promote cell death (18–20). Recent studies have revealed that CPT and its derivatives have significant anticancer efficacy in lung cancer (21), colorectal cancer (22), ovarian cancer (23), and breast cancer (24) *in vitro* and *in vivo*. Mechanistic studies showed that CPT effectively induced cell cycle progression, apoptosis, and other cellular responses (25, 26). For example, CPT induces mitotic arrest through Mad2–Cdc20 complex by activating the JNK-mediated Sp1 pathway (27). In addition, CPT enhanced apoptosis in cancer cells by targeting the 3-UTR regions of Mcl1, Bak1, and p53 through the miR-125b-mediated mitochondrial pathways (20). Furthermore, previous study demonstrated that CPT inhibited the growth and invasion of prostate cancer cells *via* PI3K/AKT, αVβ3/αVβ5 and MMP-2/-9 signaling pathways (28). However, it is completely unknown whether CPT could induce autophagy in esophageal cancer cells.

Autophagy is a process of cellular stress response by which some cytosolic materials are engulfed into autophagosome, followed by lysosome-mediated degradation. Autophagy can be upregulated under different cellular stresses, such as nutrient starvation, ROS accumulation, and reduced cytokine signaling (29, 30). Increasing lines of evidence have confirmed that autophagy is a pro-survival signal in human disease prevention and therapy (31, 32). Targeting the neddylation pathway to inactivate CRL E3 ligases has been shown to induce autophagy (1, 14). In addition, CPT could induce autophagy in some cancer cells. However, the underlying mechanisms of CPT triggering autophagy in ESCC cells remain elusive. Here, for the first time, we reported that neddylation inhibition by CPT significantly induced the accumulation of p-IκBα to trigger pro-survival autophagy by modulating NF-κB/AMPK/mTOR/ULK1 axis in esophageal cancer cells, highlighting targeting autophagy as a potential strategy to enhance anti-ESCC therapy of CPT.

MATERIALS AND METHODS

Cell Lines, Culture, and Reagents

Human ESCC cell lines EC1 and EC109 were cultured in Dulbecco's Modified Eagle's Medium (Hyclone), containing 10% fetal bovine serum (Biochrom AG) and 1% penicillin–streptomycin solution, at 37°C with 5% carbon dioxide. Chloroquine (CQ), Bafilomycin A1 (BafA1), 3-methyladenine (3MA), and *N*-Acetyl-L-cysteine (NAC) were purchased from Sigma. Compound C (Com. C) was purchased from Selleck. (S)-(+)-camptothecin (CPT, 98%) was purchased from Aladdin Industrial Inc. For *in vitro* studies, CPT stock solution (5 mM) was prepared in dimethyl sulfoxide (DMSO) and stored at −20°C as small aliquots until needed. For *in vivo* studies, CPT was freshly dissolved in 10% 2-hydroxypropyl-b-cyclodextrin (HPBCD) and stored at room temperature before use.

Cell Viability and Clonogenic Survival Assay

Cells were seeded in 96-well plates (2×10^3 cells/well) and treated with DMSO or CPT. Cell proliferation was determined using the ATPLite Luminescence Assay Kit (PerkinElmer, Waltham, MA, USA) according to manufacturer's instructions. For the clonogenic assay, 500 cells were seeded in six-well plates and then were treated with DMSO or CPT and cultured for 10 days in six-well plates. The colonies were fixed, stained, and counted under an inverted microscope (Olympus, Tokyo, Japan). Colonies comprising 50 cells or more were counted under an inverted microscope. Three independent experiments were performed.

Immunoblotting

Cell lysates were prepared for immunoblotting analysis using antibodies against LC3, p62, NEDD8, AMPK, p-AMPKα (Thr172), ULK1, p-ULK1 (Ser317), p-H2AX, WEE1, p21, ORC1, Beclin1, ATG5, p-p70S6K (Thr389), p70S6K, 4EBP1, p-4EBP1 (Thr37/46), cleaved PARP, cleaved Caspase-3, IκBα, p-IκBα, p65, LaminA/C and Tublin (Cell Signaling Technology), Cullin1 (Abcam). ACTIN (Protein Tech) was used as the loading control.

Gene Silencing Using siRNA

EC1 and EC109 cells were transfected with siRNA oligonucleotides and synthesized by GenePharma (Shanghai, China) using Lipofectamine 2000 (Invitrogen, Carlsbad,CA, USA). The sequences of siRNA are as follows:

siIκBα: GCCAGAAATTGCTGAGGCA;
siULK1: CGCCTGTTCTACGAGAAGA;
siBeclin1: CAGTTTGGCACAATCAATA;
siATG5: GGATGAGATAACTGAAAGG.

Detection of Apoptosis

Cells were treated with CPT at a specified concentration for appointed time. Apoptosis was determined with the Annexin V-FITC/PI Apoptosis Kit (BD Biosciences, San Diego, CA, USA) according to the manufacturer's instructions.

Quantification of Reactive Oxygen Species

The quantification of reactive oxygen species (ROS) production was monitored by cell permeable ROS indicator, 2′, 7′-dichlorodihydrofluorescein diacetate (H2-DCFDA) (Sigma).

The functional role of ROS generation in autophagy was evaluated by free-radical scavenger NAC (Beyotime). Cells were pre-incubated with 50 μM NAC for 12 h, followed by co-incubation with the indicated chemicals and assessment of autophagy or ROS generation as described above.

Tumor Formation Assay

For tumor formation assay, five-week-old female athymic nude mice were purchased from the Shanghai Experimental Animal Center (Shanghai, China). 5×10^6 EC1 cells were subcutaneously injected into the right back. Tumor size was measured by a vernier caliper and calculated as (length × width^2)/2. All procedures were performed in accordance with the National Institutes of Health Guide for the Care and Use of Laboratory Animals.

Statistical Analysis

The statistical significance of differences between groups was assessed using the Graph Pad Prism 5 software. The unmatched two-tailed t-test was used for the comparison of parameters between two groups. The level of significance was set at $P < 0.05$.

RESULTS

CPT Induced Autophagy and Suppressed the Growth of Esophageal Cancer Cells *In Vitro* and *In Vivo*

To investigate whether CPT could induce autophagy in esophageal cancer cells, we detected the autophagy response after CPT treatment. Firstly, we determined the conversion of LC3-I to LC3-II, a classical marker of autophagy, and found that CPT dramatically induced the conversion of LC3-I to LC3-II and inhibited the expression of p62 in EC1 and EC109 cells (**Figure 1A**). In addition, we performed autophagic flux analysis by treating cells with classical autophagy inhibitors including Chloroquine (CQ), bafilomycin A1 (BafA1), and 3-methyladenine (3MA), respectively. As expected, 3MA inhibited, while BafA1 and CQ enhanced the accumulation of LC3 II, indicating that autophagic flux was intact and supraphysiological autophagic response was induced by CPT treatment (**Figure 1B**). These results convincingly demonstrated that CPT induced autophagy in esophageal cancer cells.

We next evaluated the antitumor activity after CPT treatment in ESCC cells. Firstly, we found that CPT significantly inhibited cell proliferation (**Figure 1C**) and colony formation (**Figure 1D**) in a dose-dependent manner in EC1 and EC109 cells. Next we found that CPT significantly induced apoptosis (**Figures 1E, F**), as best evidenced by the increase of Annexin V-positive cell populations and the accumulation of cleaved-PARP and cleaved-Caspase-3, two classical markers of apoptosis. These results convincingly demonstrated that CPT inhibited cell proliferation and induced apoptosis in esophageal cancer cells.

Having established that CPT induced autophagy and inhibited esophageal cancer cell growth *in vitro*, we next evaluated the antitumor activity and autophagy response after CPT treatment *in vivo*. CPT treatment significantly suppressed tumor growth over time while control tumors grew rapidly, as revealed by size of tumors, tumor growth curve, and tumor weight analysis. CPT-treated tumors progressed slowly, whereas control tumors grew rapidly over time, as shown by tumor growth curve (**Figure 1G**) and tumor weight analysis (**Figure 1H**). Consistently, the size of control tumors was much larger than that of CPT-treated tumors (**Figure 1I**) without obvious treatment-related toxicity, such as body weight loss (**Figure 1J**). In addition, as shown in **Figure 1K**, CPT significantly induced autophagy *in vivo*, as evidenced by the increase of conversion of LC3I to LC3II. Taken together, these findings demonstrated that CPT induced autophagy and inhibited esophageal tumor growth both *in vitro* and *in vivo*.

CPT-Induced Autophagy Was a Survival Signal in Esophageal Cancer Cells

In order to investigate the role of autophagy response induced by CPT in the growth of ESCC cells, we blocked autophagy pathway *via* siRNA silencing of autophagy essential genes Beclin1 or ATG5 and evaluated its effect on proliferation and apoptosis of esophageal cancer cells. As shown in **Figure 2A**, downregulation of Beclin1 expression effectively enhanced CPT-induced proliferation inhibition in EC1 and EC109 cells. Similarly, downregulation of ATG5 expression effectively enhanced CPT-induced proliferation inhibition in EC1 and EC109 cells (**Figure 2B**). Consistently, the inhibition of autophagic response by siBeclin1 and siATG5 significantly enhanced CPT-induced apoptosis, as best evidenced by the increase of Annexin V-positive cell populations (**Figures 2C, D**) and the accumulation of cleaved PARP, a classical marker of apoptosis (**Figures 2E, F**) in esophageal cancer cells. These results demonstrated that CPT induced autophagy as a prosurvival signal in esophageal cancer cells.

AMPK/mTOR/ULK1 Axis Contributes to CPT Induced Autophagy

Previous studies indicated that the activation of AMPK/ULK1 pathway induced autophagy, and inactivation of the mTOR pathway could promote autophagy in multiple human cancers (33). Based on these findings, we determined whether CPT-induced autophagy by modulating the AMPK/mTOR/ULK1 pathway. As shown in **Figure 3A**, we found that CPT activated the AMPK pathway, as best evidenced by the increase of phosphorylation of AMPK and ULK1. In addition, CPT inhibited the mTOR pathway, as best evidenced by the decrease of phosphorylation of p70S6K and 4EBP1. In order to determine the role of AMPK in CPT-induced expression of p-ULK1 and inhibition of p-p70S6K in EC1 and EC109 cells, we used Compound C (an AMPK inhibitor) to inactivate the AMPK pathway and found that inactivation of AMPK significantly reversed CPT-induced expression of p-ULK1 in ESCC cells. Consistently, inactivation of AMPK significantly reversed CPT-inhibited expression of p-p70S6K. Moreover, inactivation of AMPK *via* Compound C treatment significantly

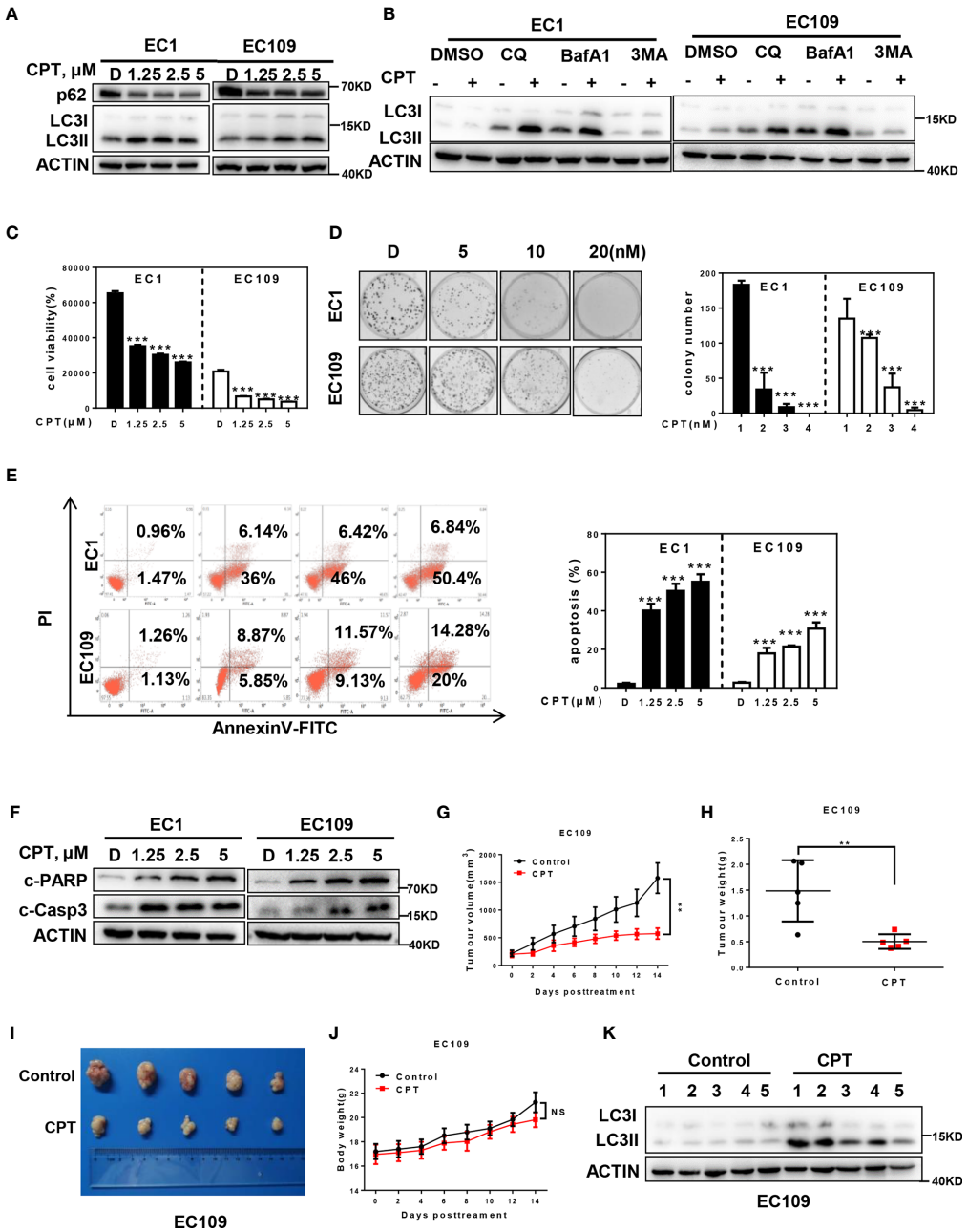

FIGURE 1 | CPT induced autophagy and suppressed the growth of esophageal cancer cells *in vitro* and *in vivo*. **(A)** Cells were treated with the indicated concentrations of CPT for 24 h, and cells were collected and subjected to IB analysis for the expression of LC3 and p62, Actin was used as an equal loading control. **(B)** Autophagic flux analysis. EC1 and EC109 cells treated with DMSO or CPT (2.5 μmol/L) for 24 h were incubated with or without CQ (50 μM), BafA1 (20 nM), or 3MA (5 mM) for 6 h. The treated cells were then collected and subjected to IB analysis with ACTIN as a loading control. **(C)** Cells were treated with the indicated concentrations of CPT for 72 h, and cell viability was assessed by the ATPLite assay (n = 4). **(D)** CPT inhibited clonogenic cell survival of ESCC cancer cells. EC1 and EC109 cells were seeded into 60 mm dishes in duplicate and then grown in the presence or absence of CPT for 10 days. The colonies with more than 50 cells were counted, following crystal violet staining (n = 3). **(E, F)** CPT induced apoptosis in ESCC cells. **(E)** Cells were treated with the indicated concentrations of CPT for 48 h and subjected to Annexin V-FITC/PI double-staining analysis (n = 3). **(F)** Cells were treated with the indicated concentrations of CPT for 24 h, and cell lysates were assessed by IB with specific antibodies against cleaved-Caspase-3 (c-Casp3) and cleaved-PARP (c-PARP). **(G–K)** CPT induced autophagy and suppressed the growth of esophageal cancer cells *in vivo*. Nude mice bearing esophageal cancer xenografts with EC109 cells were administered with CPT at 2.5 mg/kg. The treatments for the nude mice were carried out every 2 days and lasted for 14 days. **(G)** Tumor volumes were determined by caliper measurement, and the data were converted to tumor growth curves. Tumor tissues of mice were collected, photographed, weighed, and stored for further analysis (n = 5). **(H)** CPT significantly reduced tumor weight (n = 5). **(I)** Images of CPT-treated or control xenograft tumors at the end of experiment. **(J)** No obvious toxicity against body weight was observed during CPT treatment. Body weight of mice was measured twice a week during the treatment (n = 5). **(K)** Proteins extracted from tumor tissues were analyzed by IB using anti-LC3. Data were presented as mean ± S.E.M. $^{**}P < 0.01$ and $^{***}P < 0.001$.

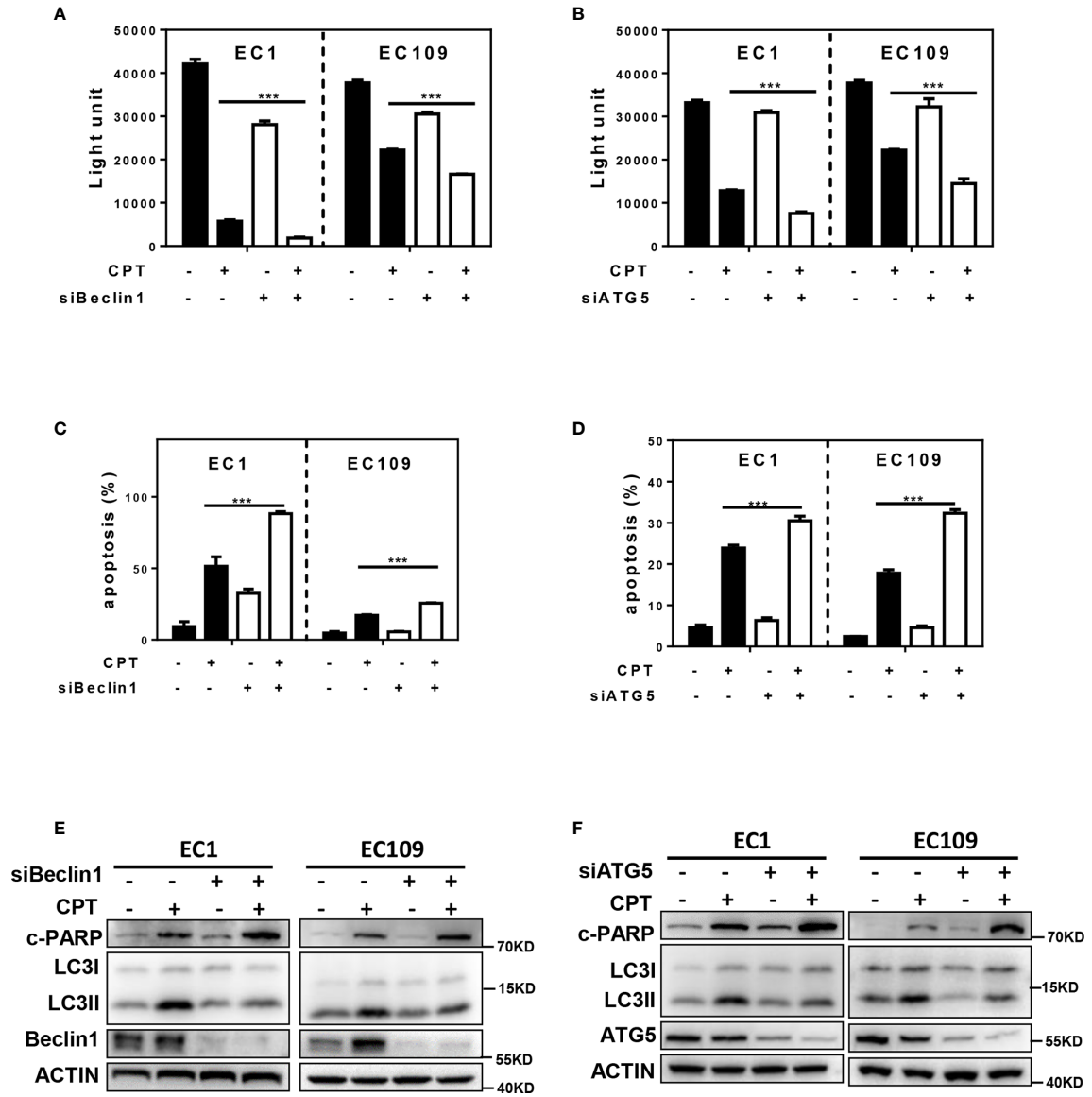

FIGURE 2 | CPT-induced autophagy was a survival signal in esophageal cancer cells. **(A, B)** The proliferation inhibition by CPT treatment was significantly increased by simultaneously blocking autophagy with siBeclin1 or siATG5. The combination of siBeclin1 or siATG5 with CPT in EC1 and EC109 cells significantly increased proliferation inhibition by ATPLite assay (n = 3). **(C, D)** Blocking of autophagy pathway by Beclin1 or ATG5 siRNA silencing amplified CPT-induced apoptosis. The combination of siBeclin1 or siATG5 with CPT in EC1 and EC109 cells significantly increased apoptosis by Annexin V-FITC/PI double-staining analysis (n = 3). **(E, F)** Beclin1 or ATG5 knockdown increased cleaved PARP expression induced by CPT. Cells were transferred with siRNAs against Beclin 1 **(E)** or ATG5 **(F)** for 48 h, and then treated with CPT at 2.5 μmol/L for 24 h. Knockdown efficiency and cleaved PARP were assessed by IB analysis. Data were presented as mean ± S.E.M. ***P < 0.001.

increased CPT-induced proliferation inhibition (**Figure 3B**). Additionally, inhibition of AMPK with Compound C significantly enhanced CPT-induced apoptosis, as evidenced by the accumulation of cleaved PARP (**Figure 3C**) and the increase of Annexin V-positive cell populations (**Figure 3D**). In order to determine the role of ULK1 in CPT-induced autophagy in EC1 and EC109 cells, we knockdown ULK1 and found that ULK1 knockdown markedly attenuated the conversion of LC3 I to LC3 II in ESCC cell (**Figures 3E, F**). These findings demonstrated that CPT induced protective autophagy by AMPK/mTOR/ULK1 axis in esophageal cancer cells.

CPT Induced ROS Generation to Promote Autophagy *via* AMPK/mTOR/ULK1 Axis

Given that ROS could activate the AMPK pathway to induce autophagy (34–36), we determined whether CPT-induced autophagy was mediated by ROS generation in esophageal cancer cells. We firstly detected cellular ROS level with the cell

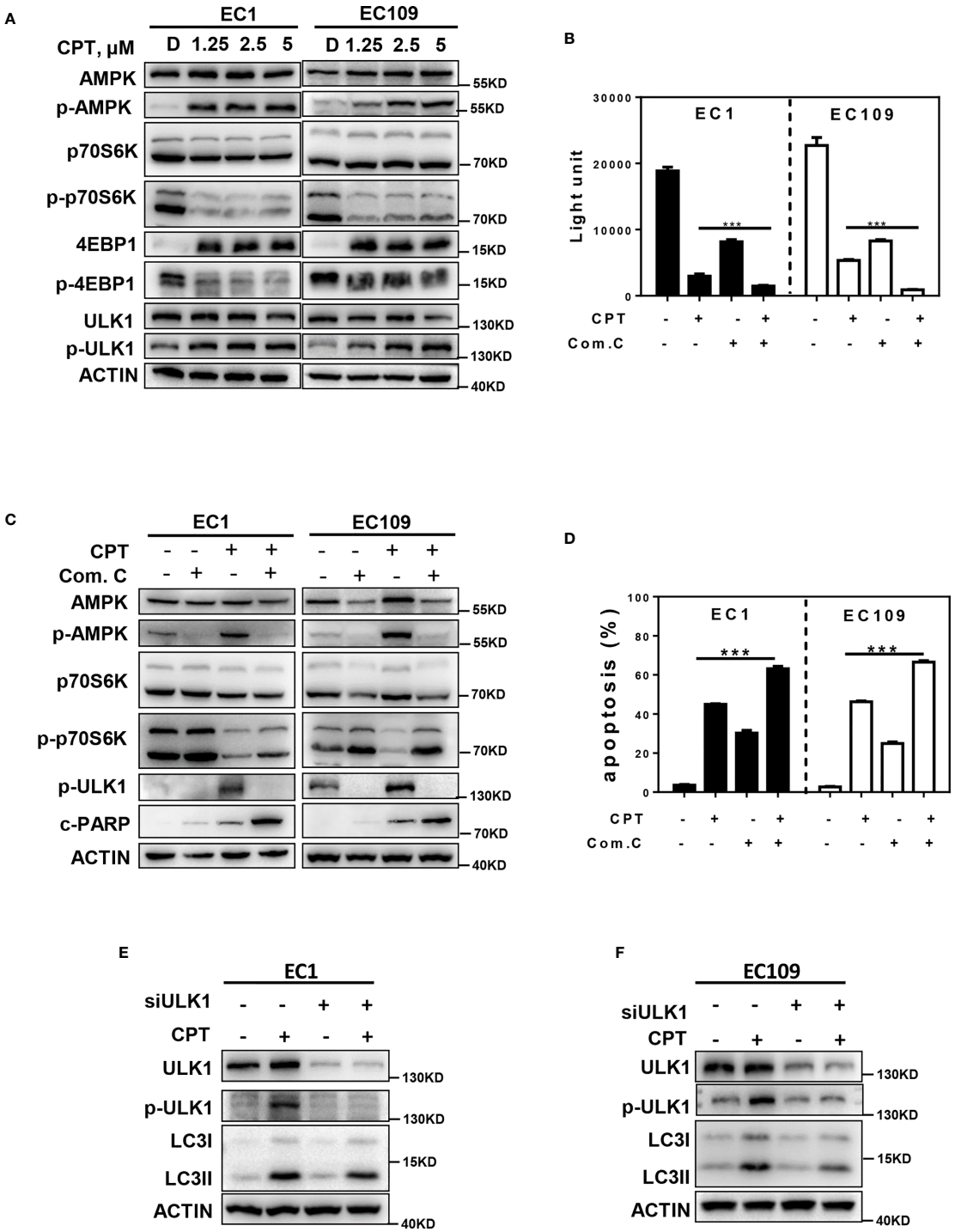

FIGURE 3 | AMPK/mTOR/ULK1 axis contributes to CPT induced autophagy. **(A)** EC1 and EC109 cells were treated with DMSO and 1.25, 2.5, 5 μmol/L CPT for 24 h and then collected and subjected to IB analysis for the expression of AMPK, p-AMPK, p-70S6K, p-p70S6K, 4EBP1, p-4EBP1, ULK1, and p-ULK1. **(B)** EC1 and EC109 cells were treated with 2.5 μmol/L CPT alone or CPT + Com.C (5 μmol/L) for 72 h and subjected to ATPLite assay (n = 3). **(C)** EC1 and EC109 cells were treated with 2.5 μmol/L CPT alone or CPT + Com.C (5 μmol/L) for 24 h and subjected to IB analysis for the expression of AMPK, p-AMPK, p-ULK1, p70S6K, p-p70S6K, and c-PARP. **(D)** EC1 and EC109 cells were treated with 2.5 μmol/L CPT alone or CPT + Com.C (5 μmol/L) for 48 h. Apoptosis induction was quantified by Annexin V-FITC/PI double-staining analysis (n = 3). **(E, F)** Autophagy was rescued by ULK1 siRNA silencing. ULK1 knockdown largely abrogated CPT-induced conversion of LC3-I to LC3-II in EC1 and EC109 cells. EC1 and EC109 cells were transfected with control or siULK1 for 48 h and then treated with 2.5 μmol/L CPT for 24 h. Knockdown efficiency and LC3 were assessed by IB analysis. Data were presented as mean ± S.E.M. ***$P < 0.001$.

permeable ROS indicator, 2′, 7-dichlorodihydrofuorescein diacetate (H2-DCFDA), and found that CPT significantly induced ROS production in both EC1 and EC109 cells (**Figures 4A–D**). Furthermore, we determined the role of ROS in CPT-induced AMPK/ULK1 pathway and CPT-inhibited mTOR pathway. We used NAC, a classical ROS scavenger, and found that NAC prevented CPT induced the generation of ROS (**Figures 4E, F**) and found that ROS reduction markedly attenuated CPT-induced the expression of p-AMPK, p-ULK1, LC3II and CPT-inhibited the expression of p-p70s6k (**Figures 4G, H**). Based on these observations, we concluded that CPT-induced ROS production modulated the AMPK/mTOR/ULK1 pathway to induce autophagy in esophageal cancer cells.

ROS-Mediated Autophagy Is Attributed to p-IκBα Accumulation by Neddylation Inactivation

Since the inactivation of NF-κB could induce ROS generation (37, 38), we next determined whether ROS/AMPK/mTOR/ULK1 axis-induced autophagy is mediated by the NF-κB pathway. Firstly, we found that pretreating cells with CPT prior to TNFα (an activator of NF-κB) stimulation significantly inhibited protein level of p65 NF-κB in the nuclear fraction of esophageal cancer cells, suggesting that CPT inhibited the activation of NF-κB pathway (**Figure 5A**). Furthermore, immunofluorescence staining demonstrated that cells stimulated with TNFα showed prominent p65 NF-κB accumulation in the nucleus (**Figure 5B**). Translocation of NF-κB to the nucleus is allowed by the phosphorylation of IκBα, resulting in its ubiquitination and degradation by CRL complex. Based on this, we hypothesized that CPT may induce p-IκBα accumulation due to the inactivation of CRL E3 ligase, and therefore activate ROS-mediated AMPK/mTOR/ULK1 axis to activate autophagy. As shown in **Figure 5C**, CPT significantly induced the expression of p-IκBα in both EC1 and EC109 cells. Interestingly, we found that CPT indeed suppressed the global protein neddylation and the neddylation levels of Cullin1 (**Figure 5D**). We further explored the mechanism of CPT-induced neddylation pathway in esophageal cancer cells. The key neddylation enzymes, NAE1, UBA3 and UBC12, were obviously suppressed upon CPT treatment in EC1 cells (**Figure 5E**). Furthermore, CRL substrates, including WEE1, p21, ORC1, and p-H2AX, were accumulated upon CPT treatment (**Figure 5E**). Having established that CPT inhibited neddylation pathway *in vitro*, we next evaluated whether CPT inactivated neddylation after CPT treatment *in vivo*. As shown in **Figure 5F**, CPT indeed suppressed the global protein neddylation, cullin1 neddylation, and the expression of the neddylation enzyme UBC12. These findings demonstrated that CPT inhibited the protein neddylation pathway *in vitro* and *in vivo*.

To further investigate the potential role of IκBα in CPT-induced ROS production and autophagy, we downregulated the IκBα expression in esophageal cancer cells. We found that IκBα knockdown markedly attenuated CPT-induced expression of p-AMPK, p-ULK1 (**Figure 5G**) and the generation of ROS (**Figures 5H, I**). Furthermore, we found that IκBα knockdown significantly enhanced CPT-induced proliferation inhibition (**Figure 5J**). In addition, IκBα knockdown significantly enhanced CPT-induced apoptosis, as evidenced by the accumulation of cleaved PARP (**Figure 5G**) and the increase of Annexin V-positive cell populations (**Figure 5K**). These findings collectively demonstrated that CPT inhibited NF-κB pathway to promote ROS generation, which modulated the AMPK/mTOR/ULK1 axis to eventually induce autophagy in esophageal cancer cells.

DISCUSSION

Esophageal cancer is one of the most human malignant tumors with high recurrence rate and poor long-term survival (39, 40). The severe threat of esophageal cancer to human health raises an urgent necessity to further elucidate the mechanisms for esophageal carcinogenesis and need novel effective therapeutic strategies. Recently, protein neddylation pathway has emerged as a potential anti-ESCC target, as supported by the discovery of overactivation of the neddylation pathway in esophageal cancer. Our present work demonstrated for the first time that CPT inhibited cullin neddylation, inactivated CRLs and induced the accumulation of classical CRL substrates p-IκBα. Mechanistic investigations further revealed that the neddylation inhibition by CPT induced the generation of ROS to modulate AMPK/mTOR/ULK1 axis to induce autophagy in esophageal cancer cells. Therefore, the neddylation pathway may serve as an important drug target for CPT to mediate cell death in ESCC cells.

Recently, the neddylation pathway, including its three enzymes NAE, UBC12 and NEDD8, has been reported to be overactivated in many kinds of cancer cells, indicating the neddylation pathway as a promising anticancer target (8, 9, 41–43). In our study, we discovered for the first time that CPT inhibited cullin neddylation to inactivate CRLs, as evidenced by the accumulation of CRLs substrate p-IκBα. Furthermore, we found that CPT reduced the expression of NAE1, UBA3, and BUC12. However, it is unclear how neddylation enzymes are downregulated by CPT in esophageal cancer. These findings establish the necessity to explore the mechanism by which CPT inhibits neddylation in future studies.

AMPK is an important cellular energy sensor and acts as a duplex molecule in cancer development and progression. In the early phase, AMPK may function as a tumor suppressor and its activation would lead to cell cycle arrest and tumor growth inhibition, thus playing a critical role in cancer prevention (44–47). However, it should be noted that AMPK might protect tumor cells from death-inducing events by maintaining intracellular homeostasis, once the tumors are established and finally lead to cancer drug resistance and metastasis (45, 48). For example, AMPK-deficient tumor cells were more susceptible to cell death induced by glucose deprivation, suggesting that AMPK activation is a pro-survival signal in cancer cells (49). In our study, we illustrated that CPT treatment induced AMPK activation to trigger autophagic response as a pro-survival signal in esophageal cancer cells, which provide a potential

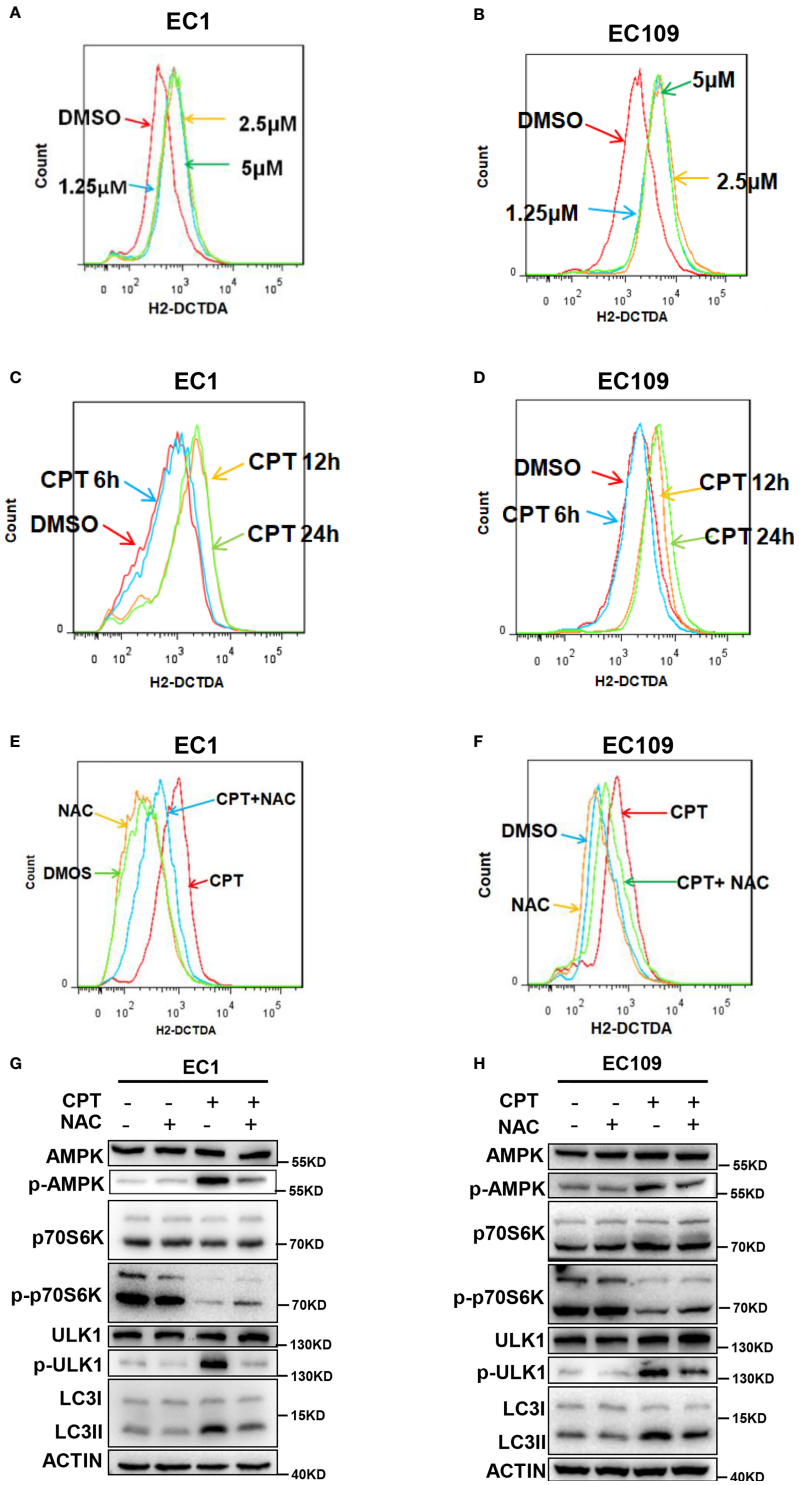

FIGURE 4 | CPT induced ROS generation to promote autophagy *via* AMPK/mTOR/ULK1 axis. **(A–D)** CPT elevated ROS levels in ESCC cells. **(A, B)** Cells were treated with various concentrations of CPT for 24 h. **(C, D)** Cells were treated with 1.25 μmol/L CPT for the indicated time periods. ROS generation was determined by H2-DCFDA staining and flow cytometry. **(E, F)** EC1 and EC109 cells were treated with 1.25 μmol/L CPT alone or CPT + NAC (50 μmol/L) for 12 h and subjected to H2-DCFDA staining analysis for the levels of ROS. **(G, H)** NAC inhibited CPT-induced autophagy and suppressed CPT-modulated AMPK/mTOR/ULK1 axis in ESCC cells. EC1 and EC109 cells were treated with 1.25 μmol/L CPT alone or CPT + NAC (50 μmol/L) for 12 h and subjected to IB analysis for the expression of AMPK, p-AMPK, ULK1, p-ULK1, p70S6K, p-p70S6K, and LC3.

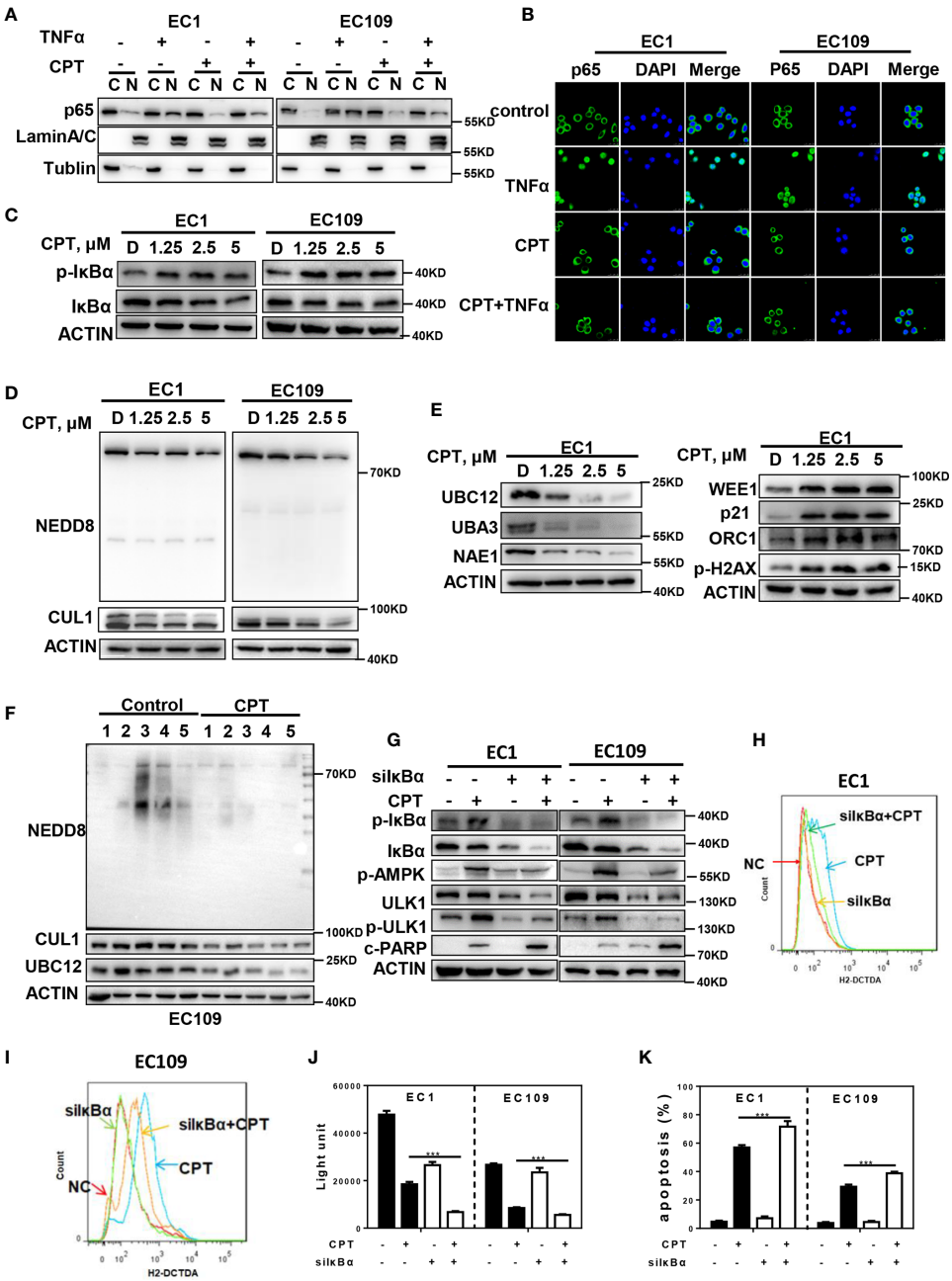

FIGURE 5 | ROS-mediated autophagy is attributed to p- IκBα accumulation by neddylation inactivation. **(A–C)** CPT inhibited the activation of NF-κB pathway. **(A, B)** CPT prevented p65 NF-κB translocation to the nucleus induced by TNFα. ESCC cells were cultured in the presence or absence of 2.5 μmol/L CPT (12 h) and stimulated concurrently with TNFα (100 ng/ml) for 30 min. **(A)** p65 isoform of NF-κB was determined by western blot analysis using nuclear (N) and cytosolic (C) fractions of ESCC cells treated as indicated. Lamin A/C and Tubulin were analyzed to demonstrate the presence of nuclear and cytosolic fractions, respectively. **(B)** p65 NF-κB subcellular localization was determined by immunofluorescence staining for endogenous p65 NF-κB (green). **(C)** EC1 and EC109 cells were treated with 2.5 μmol/L CPT for 24 h and cell lysates were assessed by IB with specific antibody against IκBα and p-IκBα. **(D, E)** CPT inhibited neddylation modification. **(D)** Immunoblotting was used to analyze the neddylation levels of cullin1 and global protein neddylation upon CPT treatment for 24 h with various concentrations. **(E)** ESCC cells were treated with CPT (0, 1.25, 2.5, and 5 μmol/L) for 24 h, followed by IB analysis using antibodies against NAE1, UBA3, UBC12, WEE1, p21, ORC1, p-H2AX, ACTIN as a loading control. **(F)** CPT inhibited neddylation pathway *in vivo*. Nude mice bearing esophageal cancer xenografts with EC109 cells were administered with CPT at 2.5 mg/kg. The treatments for the nude mice were carried out every 2 days and lasted for 14 days. Proteins extracted from tumor tissues were analyzed by IB using anti-NEDD8, cullin1, and UBC12. **(G, K)** ESCC cells were transfected with IκBα siRNA, then treated with 2.5 μmol/L CPT for 48 h. p-AMPK, p-ULK1, cleaved PARP activity were assessed by IB analysis **(G)**. ROS generation was determined by H2-DCFDA staining and flow cytometry **(H, I)**. Cell viability was measured using the ATPLite assay **(J)** and apoptosis was detected by annexin V and PI double staining **(K)** (n = 3). Data were presented as mean ± S.E.M. ***$P < 0.001$.

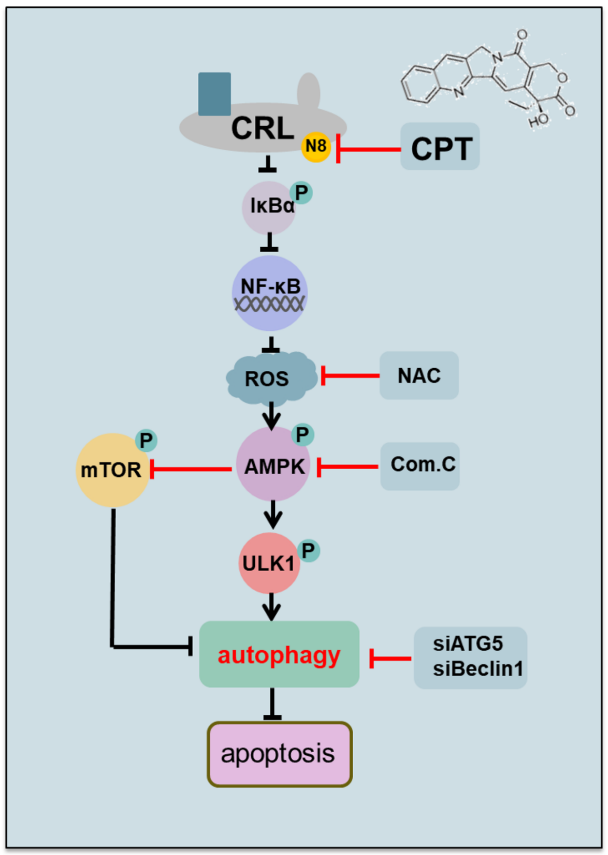

FIGURE 6 | Working model. CPT inhibited cullin neddylation, inactivated CRLs and induced the accumulation of classical CRL substrates p-IκBα. Mechanistic investigations further revealed that the neddylation inhibition by CPT induced the generation of ROS to modulate AMPK/mTOR/ULK1 axis to induce autophagy in esophageal cancer cells.

combination strategy of dually targeting AMPK and neddylation pathway for effective anti-ESCC therapy.

Our study suggested the following working model (**Figure 6**). We first time found that CPT promote autophagy in esophageal cancer cells. Mechanistically, CPT inactivates neddylation pathway, which induce the expression of p-IκBα to modulate AMPK/mTOR/ULK1 pathway to trigger pro-survival autophagy, whereas targeting this pathway blocks the autophagic response and thus sensitizes cancer cells to CPT-induced apoptosis. These findings provide a potential combination strategy of dually targeting AMPK/mTOR/ULK1 axis and neddylation pathway for effective anti-ESCC therapy.

DATA AVAILABILITY STATEMENT

The original contributions presented in the study are included in the article/supplementary material. Further inquiries can be directed to the corresponding author.

ETHICS STATEMENT

The animal study was reviewed and approved by Animal Experimental Ethics Committee of Shanghai University of Traditional Chinese Medicine.

AUTHOR CONTRIBUTIONS

YH, YL, and LJ conceived the general framework of this study and designed the experiments. YH, YL, JZ, and LL performed the experiments. WZ, YJ, and SW provided technical or material support. YH and YL prepared the manuscript. LJ supervised this study. All authors contributed to the article and approved the submitted version.

FUNDING

This work was supported by the following funds: The Chinese Minister of Science and Technology grant (2016YFA0501800), National Natural Science Foundation of China (Grants 81625018, 81820108022, 82002973), Program of Shanghai Academic/Technology Research Leader (18XD1403800), Innovation Program of Shanghai Municipal Education Commission (2019-01-07-00-10-E00056), and National Thirteenth Five-Year Science and Technology Major Special Project for New Drug and Development (2017ZX09304001).

REFERENCES

1. Zhou L, Zhang W, Sun Y, Jia L. Protein neddylation and its alterations in human cancers for targeted therapy. *Cell Signal* (2018) 44:92–102. doi: 10.1016/j.cellsig.2018.01.009
2. Soucy TA, Dick LR, Smith PG, Milhollen MA, Brownell JE. The NEDD8 Conjugation Pathway and Its Relevance in Cancer Biology and Therapy. *Genes Cancer* (2010) 1(7):708–16. doi: 10.1177/1947601910382898
3. Duncan K, Schafer G, Vava A, Parker MI, Zerbini LF. Targeting neddylation in cancer therapy. *Future Oncol* (2012) 8(11):1461–70. doi: 10.2217/fon.12.131
4. Xirodimas DP. Novel substrates and functions for the ubiquitin-like molecule NEDD8. *Biochem Soc Trans* (2008) 36(Pt 5):802–6. doi: 10.1042/BST0360802
5. Petroski MD, Deshaies RJ. Function and regulation of cullin-RING ubiquitin ligases. *Nat Rev Mol Cell Biol* (2005) 6(1):9–20. doi: 10.1038/nrm1547
6. Deshaies RJ, Joazeiro CA. RING domain E3 ubiquitin ligases. *Annu Rev Biochem* (2009) 78:399–434. doi: 10.1146/annurev.biochem.78.101807.093809
7. Godbersen JC, Humphries LA, Danilova OV, Kebbekus PE, Brown JR, Eastman A, et al. Correction: The Nedd8-Activating Enzyme Inhibitor MLN4924 Thwarts Microenvironment-Driven NF-kappaB Activation and Induces Apoptosis in Chronic Lymphocytic Leukemia B Cells. *Clin Cancer Res* (2016) 22(16):4274. doi: 10.1158/1078-0432.CCR-16-1475
8. Chen P, Hu T, Liang Y, Li P, Chen X, Zhang J, et al. Neddylation Inhibition Activates the Extrinsic Apoptosis Pathway through ATF4-CHOP-DR5 Axis in Human Esophageal Cancer Cells. *Clin Cancer Res* (2016) 22(16):4145–57. doi: 10.1158/1078-0432.CCR-15-2254

9. Li L, Wang M, Yu G, Chen P, Li H, Wei D, et al. Overactivated neddylation pathway as a therapeutic target in lung cancer. *J Natl Cancer Inst* (2014) 106 (6):dju083. doi: 10.1093/jnci/dju083
10. Lin JJ, Milhollen MA, Smith PG, Narayanan U, Dutta A. NEDD8-targeting drug MLN4924 elicits DNA rereplication by stabilizing Cdt1 in S phase, triggering checkpoint activation, apoptosis, and senescence in cancer cells. *Cancer Res* (2010) 70(24):10310–20. doi: 10.1158/0008-5472.CAN-10-2062
11. Milhollen MA, Narayanan U, Soucy TA, Veiby PO, Smith PG, Amidon B. Inhibition of NEDD8-activating enzyme induces rereplication and apoptosis in human tumor cells consistent with deregulating CDT1 turnover. *Cancer Res* (2011) 71(8):3042–51. doi: 10.1158/0008-5472.CAN-10-2122
12. Soucy TA, Smith PG, Milhollen MA, Berger AJ, Gavin JM, Adhikari S, et al. An inhibitor of NEDD8-activating enzyme as a new approach to treat cancer. *Nature* (2009) 458(7239):732–6. doi: 10.1038/nature07884
13. Zhao Y, Morgan MA, Sun Y. Targeting Neddylation pathways to inactivate cullin-RING ligases for anticancer therapy. *Antioxid Redox Signal* (2014) 21 (17):2383–400. doi: 10.1089/ars.2013.5795
14. Zhao Y, Xiong X, Jia L, Sun Y. Targeting Cullin-RING ligases by MLN4924 induces autophagy via modulating the HIF1-REDD1-TSC1-mTORC1-DEPTOR axis. *Cell Death Dis* (2012) 3:e386. doi: 10.1038/cddis.2012.125
15. Zhao Y, Sun Y. Targeting the mTOR-DEPTOR pathway by CRL E3 ubiquitin ligases: therapeutic application. *Neoplasia* (2012) 14(5):360–7. doi: 10.1593/neo.12532
16. Yang D, Zhao Y, Liu J, Sun Y, Jia L. Protective autophagy induced by RBX1/ROC1 knockdown or CRL inactivation via modulating the DEPTOR-MTOR axis. *Autophagy* (2012) 8(12):1856–8. doi: 10.4161/auto.22024
17. Wall ME, Wani MC, Cook CE, Palmer KH, Mcphail AT, Sim G. Plant Antitumor Agents. I. The Isolation and Structure of Camptothecin, a Novel Alkaloidal Leukemia and Tumor Inhibitor from Camptotheca acuminata1,2. *J Am Chem Soc* (1966) 88(16):3888–90. doi: 10.1021/ja00968a057
18. Eng WK, Faucette L, Johnson RK, Sternglanz R. Evidence that DNA topoisomerase I is necessary for the cytotoxic effects of camptothecin. *Mol Pharmacol* (1988) 34(6):755–60.
19. Wadkins RM, Bearss D, Manikumar G, Wani MC, Wall ME, Von Hoff DD. Topoisomerase I-DNA complex stability induced by camptothecins and its role in drug activity. *Curr Med Chem Anticancer Agents* (2004) 4(4):327–34. doi: 10.2174/1568011043352894
20. Zeng CW, Zhang XJ, Lin KY, Ye H, Feng SY, Zhang H, et al. Camptothecin induces apoptosis in cancer cells via microRNA-125b-mediated mitochondrial pathways. *Mol Pharmacol* (2012) 81(4):578–86. doi: 10.1124/mol.111.076794
21. Chiu YH, Hsu SH, Hsu HW, Huang KC, Liu W, Wu CY, et al. Human nonsmall cell lung cancer cells can be sensitized to camptothecin by modulating autophagy. *Int J Oncol* (2018) 53(5):1967–79. doi: 10.3892/ijo.2018.4523
22. Arakawa Y, Ozaki K, Okawa Y, Yamada H. Three missense mutations of DNA topoisomerase I in highly camptothecin-resistant colon cancer cell sublines. *Oncol Rep* (2013) 30(3):1053–8. doi: 10.3892/or.2013.2594
23. Shaikh IM, Tan KB, Chaudhury A, Liu Y, Tan BJ, Tan BM, et al. Liposome co-encapsulation of synergistic combination of irinotecan and doxorubicin for the treatment of intraperitoneally grown ovarian tumor xenograft. *J Control Release* (2013) 172(3):852–61. doi: 10.1016/j.jconrel.2013.10.025
24. Landgraf M, Lahr CA, Kaur I, Shafiee A, Sanchez-Herrero A, Janowicz PW, et al. Targeted camptothecin delivery via silicon nanoparticles reduces breast cancer metastasis. *Biomaterials* (2020) 240:119791. doi: 10.1016/j.biomaterials.2020.119791
25. Prasad Tharanga Jayasooriya RG, Dilshara MG, Neelaka Molagoda IM, Park C, Park SR, Lee S, et al. Camptothecin induces G2/M phase arrest through the ATM-Chk2-Cdc25C axis as a result of autophagy-induced cytoprotection: Implications of reactive oxygen species. *Oncotarget* (2018) 9(31):21744–57. doi: 10.18632/oncotarget.24934
26. Yin X, Sun H, Yu D, Liang Y, Yuan Z, Ge Y. Hydroxycamptothecin induces apoptosis of human tenon's capsule fibroblasts by activating the PERK signaling pathway. *Invest Ophthalmol Vis Sci* (2013) 54(7):4749–58. doi: 10.1167/iovs.12-11447
27. Dilshara MG, Jayasooriya R, Karunarathne W, Choi YH, Kim GY. Camptothecin induces mitotic arrest through Mad2-Cdc20 complex by activating the JNK-mediated Sp1 pathway. *Food Chem Toxicol* (2019) 127:143–55. doi: 10.1016/j.fct.2019.03.026
28. Sun LC, Luo J, Mackey LV, Fuselier JA, Coy DH. A conjugate of camptothecin and a somatostatin analog against prostate cancer cell invasion via a possible signaling pathway involving PI3K/Akt, alphaVbeta3/alphaVbeta5 and MMP-2/-9. *Cancer Lett* (2007) 246(1-2):157–66. doi: 10.1016/j.canlet.2006.02.016
29. Czarny P, Pawlowska E, Bialkowska-Warzecha J, Kaarniranta K, Blasiak J. Autophagy in DNA Damage Response. *Int J Mol Sci* (2015) 16(2):2641–62. doi: 10.3390/ijms16022641
30. Song X, Narzt MS, Nagelreiter IM, Hohensinner P, Terlecki-Zaniewicz L, Tschachler E, et al. Autophagy deficient keratinocytes display increased DNA damage, senescence and aberrant lipid composition after oxidative stress in vitro and in vivo. *Redox Biol* (2017) 11:219–30. doi: 10.1016/j.redox.2016.12.015
31. Deng S, Shanmugam MK, Kumar AP, Yap CT, Sethi G, Bishayee A. Targeting autophagy using natural compounds for cancer prevention and therapy. *Cancer* (2019) 125(8):1228–46. doi: 10.1002/cncr.31978
32. Galluzzi L, Bravo-San Pedro JM, Levine B, Green DR, Kroemer G. Pharmacological modulation of autophagy: therapeutic potential and persisting obstacles. *Nat Rev Drug Discovery* (2017) 16(7):487–511. doi: 10.1038/nrd.2017.22
33. Kim J, Kundu M, Viollet B, Guan KL. AMPK and mTOR regulate autophagy through direct phosphorylation of Ulk1. *Nat Cell Biol* (2011) 13(2):132–41. doi: 10.1038/ncb2152
34. Dewaele M, Maes H, Agostinis P. ROS-mediated mechanisms of autophagy stimulation and their relevance in cancer therapy. *Autophagy* (2014) 6(7):838–54. doi: 10.4161/auto.6.7.12113
35. Russell RC, Yuan H-X, Guan K-L. Autophagy regulation by nutrient signaling. *Cell Res* (2013) 24(1):42–57. doi: 10.1038/cr.2013.166
36. Rabinovitch RC, Samborska B, Faubert B, Ma EH, Gravel SP, Andrzejewski S, et al. AMPK Maintains Cellular Metabolic Homeostasis through Regulation of Mitochondrial Reactive Oxygen Species. *Cell Rep* (2017) 21(1):1–9. doi: 10.1016/j.celrep.2017.09.026
37. Morgan MJ, Liu Z-g. Crosstalk of reactive oxygen species and NF-κB signaling. *Cell Res* (2010) 21(1):103–15. doi: 10.1038/cr.2010.178
38. Nakajima S, Kitamura M. Bidirectional regulation of NF-κB by reactive oxygen species: A role of unfolded protein response. *Free Radical Biol Med* (2013) 65:162–74. doi: 10.1016/j.freeradbiomed.2013.06.020
39. Bray F, Ferlay J, Soerjomataram I, Siegel RL, Torre LA, Jemal A. Global cancer statistics 2018: GLOBOCAN estimates of incidence and mortality worldwide for 36 cancers in 185 countries. *CA: A Cancer J Clin* (2018) 68(6):394–424. doi: 10.3322/caac.21492
40. Lagergren J, Smyth E, Cunningham D, Lagergren P. Oesophageal cancer. *Lancet* (2017) 390(10110):2383–96. doi: 10.1016/S0140-6736(17)31462-9
41. Gao Q, Yu GY, Shi JY, Li LH, Zhang WJ, Wang ZC, et al. Neddylation pathway is up-regulated in human intrahepatic cholangiocarcinoma and serves as a potential therapeutic target. *Oncotarget* (2014) 5(17):7820–32. doi: 10.18632/oncotarget.2309
42. Hua W, Li C, Yang Z, Li L, Jiang Y, Yu G, et al. Suppression of glioblastoma by targeting the overactivated protein neddylation pathway. *Neuro Oncol* (2015) 17(10):1333–43. doi: 10.1093/neuonc/nov066
43. Xie P, Zhang M, He S, Lu K, Chen Y, Xing G, et al. The covalent modifier Nedd8 is critical for the activation of Smurf1 ubiquitin ligase in tumorigenesis. *Nat Commun* (2014) 5:3733. doi: 10.1038/ncomms4733
44. Mihaylova MM, Shaw RJ. The AMPK signalling pathway coordinates cell growth, autophagy and metabolism. *Nat Cell Biol* (2011) 13(9):1016–23. doi: 10.1038/ncb2329
45. Kim J, Yang G, Kim Y, Kim J, Ha J. AMPK activators: mechanisms of action and physiological activities. *Exp Mol Med* (2016) 48(4):e224–e. doi: 10.1038/emm.2016.16
46. Shackelford DB, Shaw RJ. The LKB1-AMPK pathway: metabolism and growth control in tumour suppression. *Nat Rev Cancer* (2009) 9(8):563–75. doi: 10.1038/nrc2676
47. Jones RG, Plas DR, Kubek S, Buzzai M, Mu J, Xu Y, et al. AMP-activated protein kinase induces a p53-dependent metabolic checkpoint. *Mol Cell* (2005) 18(3):283–93. doi: 10.1016/j.molcel.2005.03.027
48. Vara-Ciruelos D, Russell FM, Hardie DG. The strange case of AMPK and cancer: Dr Jekyll or Mr Hyde? *(dagger) Open Biol* (2019) 9(7):190099. doi: 10.1098/rsob.190099

49. Jeon S-M, Chandel NS, Hay N. AMPK regulates NADPH homeostasis to promote tumour cell survival during energy stress. *Nature* (2012) 485 (7400):661–5. doi: 10.1038/nature11066

Conflict of Interest: The authors declare that the research was conducted in the absence of any commercial or financial relationships that could be construed as a potential conflict of interest.

frontiers in Oncology

ORIGINAL RESEARCH
published: 14 June 2021
doi: 10.3389/fonc.2021.666549

Fangchinoline Inhibits Human Esophageal Cancer by Transactivating ATF4 to Trigger Both Noxa-Dependent Intrinsic and DR5-Dependent Extrinsic Apoptosis

Yunjing Zhang[1†], Shiwen Wang[1,2†], Yukun Chen[1], Junqian Zhang[1], Jing Yang[1], Jingrong Xian[1,2], Lihui Li[1], Hu Zhao[2], Robert M. Hoffman[3,4], Yanmei Zhang[2] and Lijun Jia[1*]*

[1] Cancer Institute, Longhua Hospital, Shanghai University of Traditional Chinese Medicine, Shanghai, China, [2] Department of Laboratory Medicine, Huadong Hospital Affiliated to Fudan University, Shanghai, China, [3] Department of Surgery, University of California, San Diego, San Diego, CA, United States, [4] Anticancer Inc., San Diego, CA, United States

OPEN ACCESS

Edited by:
Bin Li,
Jinan University, China

Reviewed by:
Jianxiang Chen,
Hangzhou Normal University, China
Tian Zhou,
Dongfang Hospital, China

***Correspondence:**
Yanmei Zhang
15618653286@163.com
Lijun Jia
ljjia@shutcm.edu.cn

[†]*These authors have contributed equally to this work*

Specialty section:
This article was submitted to Gastrointestinal Cancers, a section of the journal Frontiers in Oncology

Received: *10 February 2021*
Accepted: *12 May 2021*
Published: *14 June 2021*

Citation:
Zhang Y, Wang S, Chen Y, Zhang J, Yang J, Xian J, Li L, Zhao H, Hoffman RM, Zhang YM and Jia L (2021) Fangchinoline Inhibits Human Esophageal Cancer by Transactivating ATF4 to Trigger Both Noxa-Dependent Intrinsic and DR5-Dependent Extrinsic Apoptosis. Front. Oncol. 11:666549. doi: 10.3389/fonc.2021.666549

Esophageal squamous cell carcinoma (ESCC) is a recalcitrant cancer. The Chinese herbal monomer fangchinoline (FCL) has been reported to have anti-tumor activity in several human cancer cell types. However, the therapeutic efficacy and underlying mechanism on ESCC remain to be elucidated. In the present study, for the first time, we demonstrated that FCL significantly suppressed the growth of ESCC both *in vitro* and *in vivo*. Mechanistic studies revealed that FCL-induced G1 phase cell-cycle arrest in ESCC which is dependent on p21 and p27. Moreover, we found that FCL coordinatively triggered Noxa-dependent intrinsic apoptosis and DR5-dependent extrinsic apoptosis by transactivating ATF4, which is a novel mechanism. Our findings elucidated the tumor-suppressive efficacy and mechanisms of FCL and demonstrated FCL is a potential anti-ESCC agent.

Keywords: fangchinoline (FCL), esophageal squamous cell carcinoma (ESCC), cell cycle, intrinsic apoptosis, extrinsic apoptosis

INTRODUCTION

Esophageal squamous cell carcinoma (ESCC) is the major histologic subtype of esophageal cancer, and its incidence and fatality keep rising at an alarming rate worldwide (1). Despite the considerable progress in diagnosis and treatment of ESCC, the present therapeutic strategies, including chemotherapy, radiation and surgery, still have high recurrence and metastasis rates (2). Moreover, the developments of therapeutic targets and targeted drugs remain ineffective (3). Therefore, safe and effective therapeutic approaches for ESCC are urgently needed.

Currently, Chinese herbal medicinal agents have made great progress in the treatment of human cancers due to the relatively high efficacy and few side effects (4). The Chinese herbal monomer fangchinoline (FCL), extracted from the traditional Chinese herbal alkaloid tetrandrine root, characterizing as a new compound sharing structural features with tetrandrine (**Figure 1A**) (5). FCL has been shown to have a wide range of pharmacological activities such as anti-inflammation, anti-oxidation and anti-thrombosis activities (6–9). Remarkably, FCL exerts substantial anti-tumor

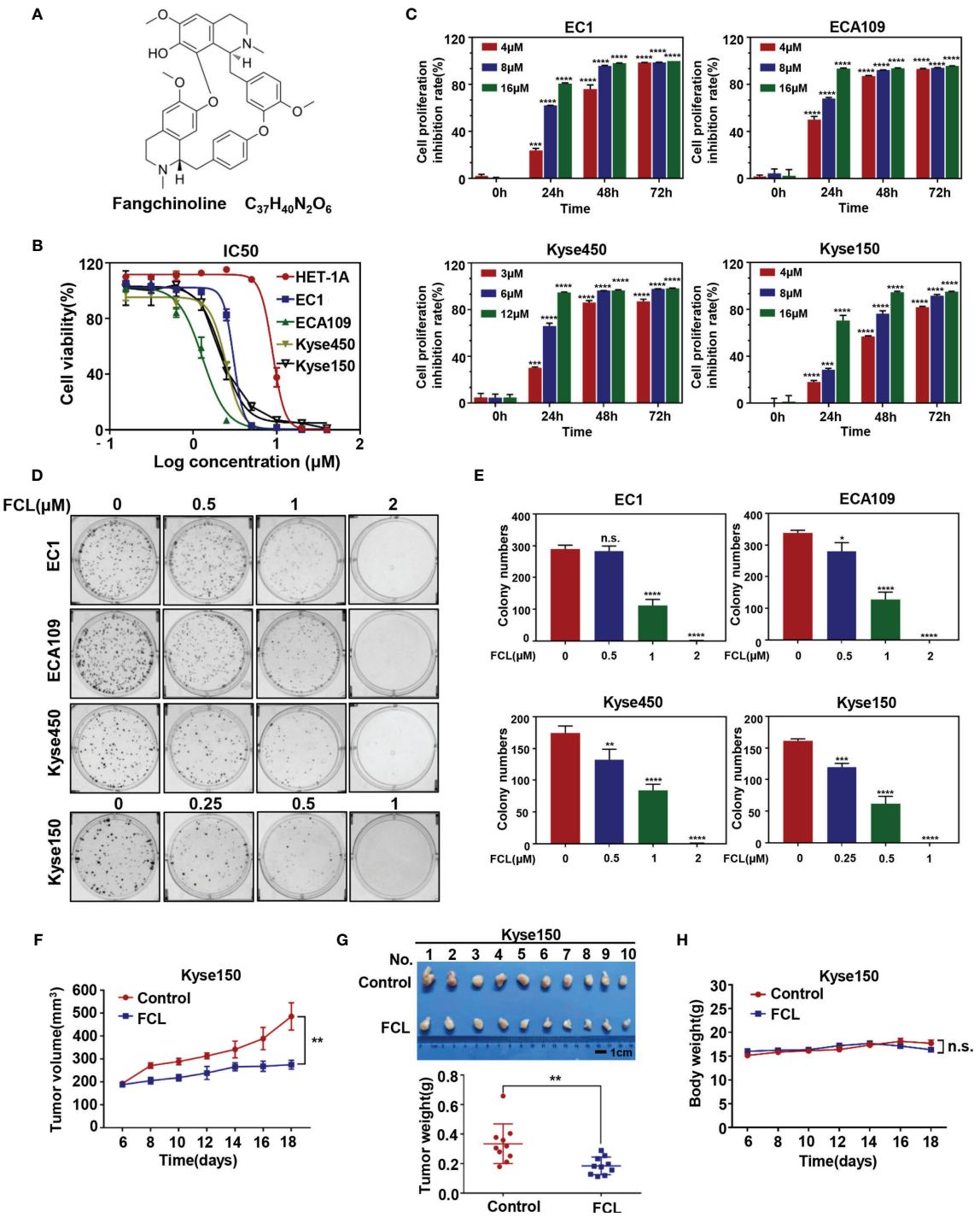

FIGURE 1 | Efficacy of Fangchinoline on ESCC *in vitro* and *in vivo*. **(A)** Chemical structure of FCL. **(B)** Human esophageal epithelial cell line HET-1A and ESCC cell lines EC1, ECA109, Kyse450, Kyse150 were treated with indicated concentrations of FCL for 72 hours, and cell viability was determined by ATPlite assay. Representative inhibitory curves for each cell line are shown. **(C)** ATPlite assay was used to determine the cell growth of different ESCC cell lines at the indicated concentrations of FCL for 0, 24, 48 and 72 hours. **(D)** Representative images of three independent experiments are shown for the inhibition of colony formation by FCL. **(E)** Graph of the relative number of colonies formed. **(F)** Nude mice were subcutaneously transplanted Kyse150 cells and treated with FCL as indicated in Materials and Methods. Tumor size was determined with caliper every other day, and the volume was calculated to construct a growth curve. **(G)** Mice were sacrificed, and tumor tissues were harvested and photographed. The tumor weight was measured with an electronic scale on the sacrificed day. **(H)** Mouse body weight was recorded every other day during the whole experiment. *denotes $P < 0.05$, **denotes $P < 0.01$, ***denotes $P < 0.001$, ****denotes $P < 0.0001$, n.s. denotes not significant.

efficacy on many types of human tumor cells by arresting cell cycle, inhibiting metastasis, as well as triggering apoptosis (10–12). For example, it was reported that FCL inhibited cell growth in lung cancer cells and melanoma cells by targeting the FAK pathway (13, 14). Furthermore, FCL induced apoptosis of breast cancer cells and glioblastoma cells by activating the PI3K/Akt/GSK-3β pathway (15, 16). However, the anti-tumor efficacy of FCL on ESCC and it's underlying mechanism has not been investigated.

In the present study, for the first time, we reported that FCL effectively suppressed the tumor progression of ESCC by triggering cell-cycle arrest and apoptosis. More importantly, we reported a novel mechanism by which FCL transactivated ATF4 to trigger both Noxa-dependent intrinsic and DR5-dependent extrinsic apoptosis. Our study revealed the tumor suppressive efficacy of FCL on ESCC, and validated FCL as a potential anti-ESCC agent.

MATERIALS AND METHODS

Reagents

Fangchinoline was purchased from MCE (MedChem Express, Shanghai, China), and the purity of the compounds was ≥99.92%. FCL was dissolved in dimethyl sulfoxide (DMSO) and stored at −80°C for the *in vitro* study. For the *in vivo* study, FCL was dissolved first in 5% DMSO and then in 10% 2-hydroxypropyl-β-cyclodextrin (Sangon Biotech, Shanghai, China).

Cell Culture

Human esophageal epithelial cell line HET-1A and human ESCC cell lines EC1, ECA109, Kyse450, Kyse150 were obtained from the Type Culture Collection of the Chinese Academy of Sciences (Shanghai, China) and cultured in Dulbecco's Modifed Eagle's Medium (DMEM, hyclone, Logan, UT), containing 10% fetal bovine serum (FBS, Biochrom AG, Berlin, Germany) and 1% penicillin–streptomycin solution (Gibco, USA) at 37°C with 5% CO_2.

Cell Viability and Clonogenic Survival Assay

Cells were seeded in black 96-well plates with 2×10^3 cells per well in triplicate and cultured overnight. Cells were treated with DMSO or FCL at the indicated concentrations for 0, 24, 48 and 72 hours. At the end of the incubation, the cell viability was measured by ATPlite luminescence assay (PerkinElmer, Norwalk, CT, USA) according to the manufacturer's protocol. For clonogenic survival assay, cells were plated into six-well plates (300 cells per well) in triplicate and allowed to adhere overnight. Cells were treated with the indicated concentrations of FCL and cultured for 12 days. Cells were stained with crystal violet and the colony number was counted. Colonies with more than 50 cells each were counted and photographed with a gel imager (GelDoc XR System, Bio-rad, USA).

Cell Cycle Analysis

For cell cycle analysis, cells were treated at the indicated concentrations of FCL for 24 hours. FCL-treated cells or control cells were harvested and fixed in 70% ethanol at -20°C overnight. Then, the fixed cells were stained with propidium iodide (PI, 36 μg/mL; Sigma, St. Louis, MO, USA) at 37°C for 15 min, and performed for fluorescence activated cell sorting (FACS) analysis by Flow Cytometry (BD FACSVerse™, New Jersey, USA). Data were analyzed with FlowJo 7.6 software.

Apoptosis Assay

For apoptosis analysis, cells were treated at the indicated concentrations of FCL for 24 hours. FCL-treated cells or control cells were collected and washed with cold PBS, and then stained with an AnnexinV-FITC and PI Apoptosis Kit according to manufacturer's instructions (Yuheng Biotechnology, Suzhou, China). Apoptotic cells were analyzed by Flow Cytometry (BD FACSVerse™, New Jersey, USA). Data were analyzed with FlowJo 7.6 software.

Western Blot Analysis

Total protein was collected using RIPA (Radio Immunoprecipitation Assay) lysis buffer and resolved by 7.5-15% SDS-PAGE, followed by transferring the proteins to an Immobilon-PVDF Membrane (Merck Millipore Ltd, Tullagreen, lreland). The membrane was then blocked with 5% skim milk for 1 hour followed by incubation with the primary antibodies overnight as follows, cleaved caspase-8 (c-CASP8), ATF4, CHOP, DR5, Noxa, p27, Bax, Bid (Cell Signaling Technology, Danvers, MA, USA), cleaved caspase-3 (c-CASP3), cleaved caspase-9 (c-CASP9), cleaved PARP(c-PARP), PARP, β-actin (HuaBio, China), p21(Proteintech, Chicago, USA), CyclinE, CDK2, CDK4, CDK6, Fas, DR3 (Santa Cruz Biotechnology, Santa Cruz, CA, USA). Corresponding second antibodies were incubated for 1 hour and membranes photographed by Tanon 5200 visualizer (Shanghai, China).

RNA Extraction and Real-Time PCR

Total RNA was isolated using the Ultrapure RNA Kit (Cwbiotech, Beijing, China) according to the manufacturer's instructions. The reverse transcription reaction was performed on 1 μg of total RNA per sample using the PrimerScript reverse transcription reagent kit (TaKaRa, Shiga, Japan) according to the manufacturer's instructions. After reverse transcription, the real-time polymerase chain reaction (PCR) was performed using the Power SYBR Green PCR MasterMix (Applied Biosystems, Foster City, CA) on the ABI 7500 thermocycler (Applied Biosystems) following the instrument instructions. For each sample, the mRNA abundance was normalized to the amount of β-actin. The sequences of the primers were as follows:

for β-actin, forward: 5′-CGTGCGTGACATTAAGGAGAAG-3′,
reverse: 5′-AAGGAAGGCTGGAAGAGTGC-3′;
for ATF4, forward: 5′-ATGACCGAAATGAGCTTCCTG-3′,
reverse: 5′-GCTGGAGAACCCATGAGGT-3′;
for DR5, forward: 5′-CCAGCAAATGAAGGTGATCC-3′,
reverse: 5′-GCACCAAGTCTGCAAAGTCA-3′;
for Noxa, forward: 5′-ACCAAGCCGGATTTGCGATT-3′,
reverse: 5′-ACTTGCACTTGTTCCTCGTGG-3′.

siRNA Silencing

The cells were transfected with siRNA oligonucleotides against the following genes using the Lipofectamine RNAiMAX Transfection Reagent (Invitrogen, USA), according to the manufacturer's instructions. The sequences of siRNA were as follows:

siControl: 5′-UUCUCCGAACGUGUCACGUTT-3′;
siATF4-1: 5′-CCAAAUAGGAGCCUCCCAUTT-3′;
siATF4-2: 5′-CCTCACTGGCGAGTGTAAA-3′;
siDR5: 5′-AAGACCCUUGUGCUCGUUGUC-3′;
siNoxa: 5′-GGUGCACGUUUCAUCAAUUUGTT-3′;
sip21: 5′-GACCAUGUGGACC UGUCAC-3′;
sip27: 5′-CCGACGATTCTTCTACTCA-3′.

Subcutaneous Transplantation Tumor Model

BALB/c nude female mice were purchased from Lingchang Biological Technology Co., Ltd. (Shanghai, China). All mice were kept and bred in a specific pathogen-free environment in the animal facility of Longhua hospital. The mice were maintained in a temperature–controlled room (22 ± 2°C) with a 12–hours light/12–hours dark cycle and a relative humidity of 40–60%, and were given free access to sterilized food and water. Animal experiments were performed in accordance with the National Guidelines for Experimental Animal Welfare, with approval from the Institutional Animal Care and Use Committee of Longhua hospital, Shanghai University of Traditional Chinese Medicine.

Briefly, 4×10^6 Kyse150 cells were subcutaneously injected into the bilateral flank of each mouse, and mice were randomly assigned to control and FCL-treatment groups (five mice per group). Each mouse was treated with either β-cyclodextrin crystalline (vehicle control) or FCL (100 mg/kg) *via* intraperitoneal injection once a day for 13 consecutive days. The day of tumor appearance was designated day 1 (6 days after xenografting). Tumor size was measured with a caliper and tumor volume was calculated using ellipsoid volume formula (length×width2)/2. The body weights of the mice were measured with an electronic scale every other day. Tumor tissues were harvested, photographed, and weighed at the end of the experiment.

Statistical Analysis

The statistical significance of differences between groups was assessed using GraphPad Prism7 software (GraphPad Software, Inc., San Diego, CA, USA). All data were presented as mean ± Standard Error of Mean. The student's t-test was used for the comparison of parameters between two groups. P-value of $P < 0.05$ was significant, n.s.=not significant. For all tests, four levels of significance (*$P < 0.05$, **$P < 0.01$, ***$P < 0.001$, ****$P < 0.0001$) were used.

RESULTS

Fangchinoline Suppressed the Tumor Growth of ESCC *In Vitro* and *In Vivo*

We first evaluated the efficacy of FCL on normal human esophageal epithelial cell and ESCC cells. Our results showed that the IC50 values of FCL for the normal human esophageal epithelial cell line HET-1A and ESCC cell lines EC1, ECA109, Kyse450, Kyse150 were 8.93, 3.042, 1.294, 2.471 and 2.22 μM, respectively (**Figure 1B**). Furthermore, we found a time and dose-dependent growth inhibition in the four ESCC cell lines (**Figure 1C**). FCL inhibited colony formation of ESCC cells in a dose-dependent manner (**Figures 1D, E**). These findings indicated that FCL suppressed the viability of ESCC cells. To further assess the efficacy of FCL, we established a subcutaneous-transplantation tumor model of human esophageal cancer in mice by using Kyse150 cells. As shown, FCL significantly inhibited tumor growth over time compared with the control group ($P < 0.01$, **Figure 1F**). Notably, FCL-treated group mice developed smaller tumors than the control group by tumor weight analysis ($P < 0.01$, **Figure 1G**). During the whole experiment, there was no substantial change in the body weights of mice between the control group and FCL treatment group, suggesting no general toxicity of FCL treatment (**Figure 1H**). Collectively, our findings indicated that FCL inhibited the tumor growth of ESCC both *in vitro* and *in vivo*.

Fangchinoline Induced G1-Phase Cell-Cycle Arrest of ESCC Cells

To further explore the inhibitory mechanism of FCL on the viability of ESCC cells, the effect of FCL on cell cycle was determined. We found that cell populations in G0/G1 phase of cell cycle were significantly increased in EC1, ECA109, Kyse150 and Kyse450 cells in a dose-dependent manner (**Figures 2A, B**). Owing to CyclinE and Cyclin-dependent kinases 2, 4 and 6 (CDK2/4/6) are key regulators in the G1 phase, we next determined the expression levels of indicated regulators in FCL-treated ESCC cells (17). Our data showed that FCL treatment obviously dropped the protein levels of CyclinE and CDK2/4/6 in both EC1 and ECA109 cells (**Figure 2C**), suggesting that FCL prevented G1 to S phase progression of ESCC cells.

In addition, we found that the cell cycle inhibitors p21 and p27, which inhibit CDK/Cyclin complexes (18, 19), were significantly accumulated upon FCL treatment in EC1 and ECA109 cells (**Figure 2C**). To further define the role of p21 and p27 in FCL-induced cell-cycle arrest, the expression of p21 or p27 was downregulated by siRNA silencing in FCL-treated EC1 cells. As shown in **Figures 2D, E**, p21 or p27 knockdown by siRNA significantly rescued the EC1 cells from FCL-induced G1 phase arrest. Taken together, our findings demonstrated that p21 and p27 played a crucial role in controlling G1 phase cell-cycle arrest elicited by FCL.

Fangchinoline Triggered Apoptosis in ESCC Cells

After revealing that FCL disturbed the ESCC cells in G1 phase, we next examined the cellular responses to FCL treatment. We observed that FCL-treated ESCC cells presented the notable feature of apoptosis-shrunk morphology (**Supplementary Figure 1A**). PI and Annexin-V-FITC staining analysis confirmed that the number of Annexin V-positive cells (apoptosis marker) increased significantly after FCL treatment (**Figures 3A, B**). Furthermore, FCL-treated ESCC cells had

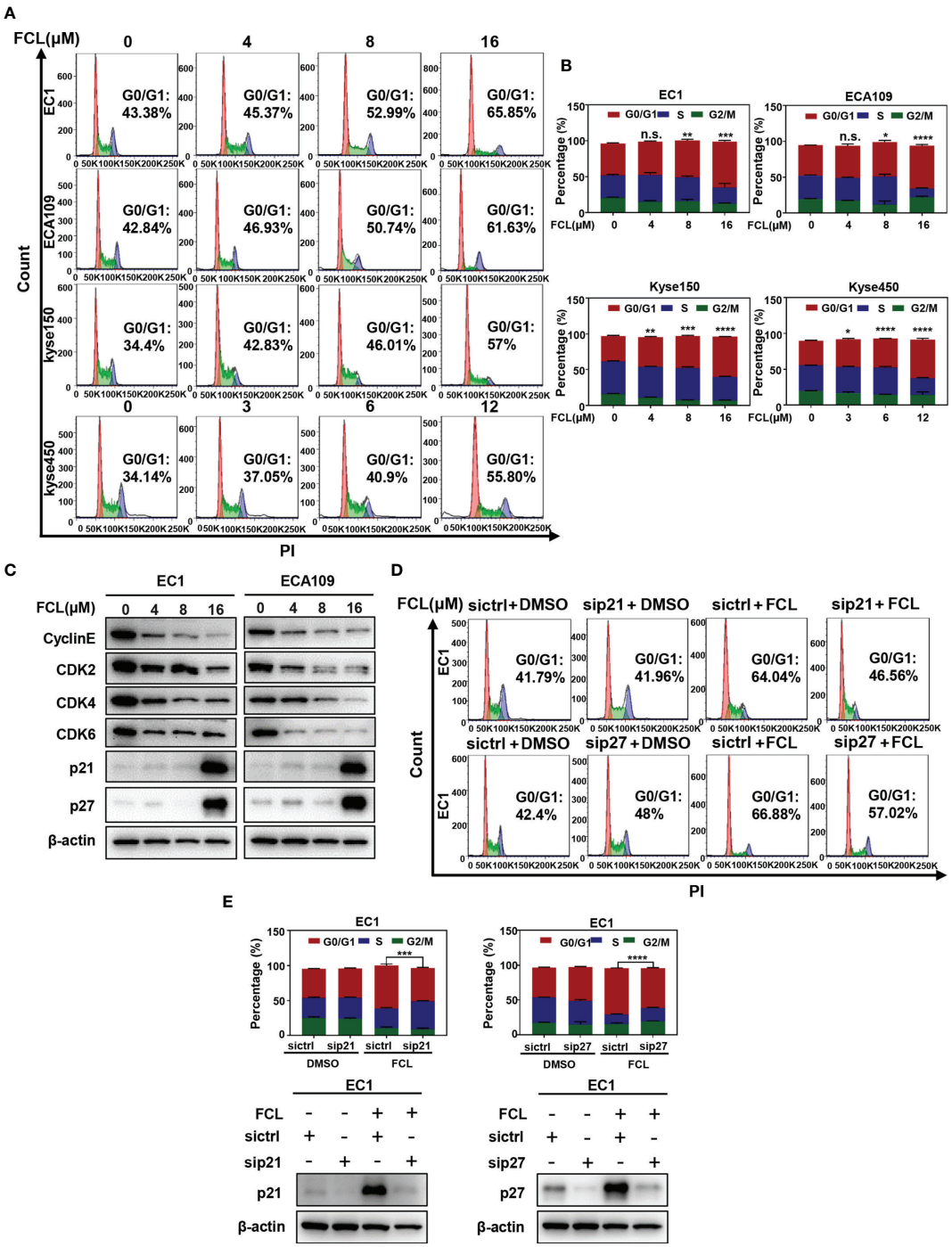

FIGURE 2 | Fangchinoline arrested ESCC cells in G1 phase. **(A, B)** ESCC cells were pre-incubated with DMSO or FCL for 24 hours, followed by PI staining and FACS analysis for cell-cycle profiling. **(C)** FCL-induced decrease of CyclinE, CDK2, CDK4, CDK6 was accompanied by the accumulation in p21 and p27. After 24 hours of FCL treatment at the indicated concentrations, EC1 and ECA109 cells were subjected to Western blotting using antibodies against Cyclin E, CDK2, CDK4, CDK6, p21 and p27 with β-actin as a loading control. **(D)** EC1 and ECA109 cells were transfected with control or p21 or p27 siRNA (72 hours), treated with 16 μmol/L FCL (24 hours), and subjected to PI staining and FACS analysis. **(E)** The percentage of cells at the G0/G1 phase was indicated. The protein levels of p21 or p27 were determined by Western blotting analysis with β-actin as a loading control. *denotes $P < 0.05$, **denotes $P < 0.01$, ***denotes $P < 0.001$, ****denotes $P < 0.0001$, n.s. denotes not significant.

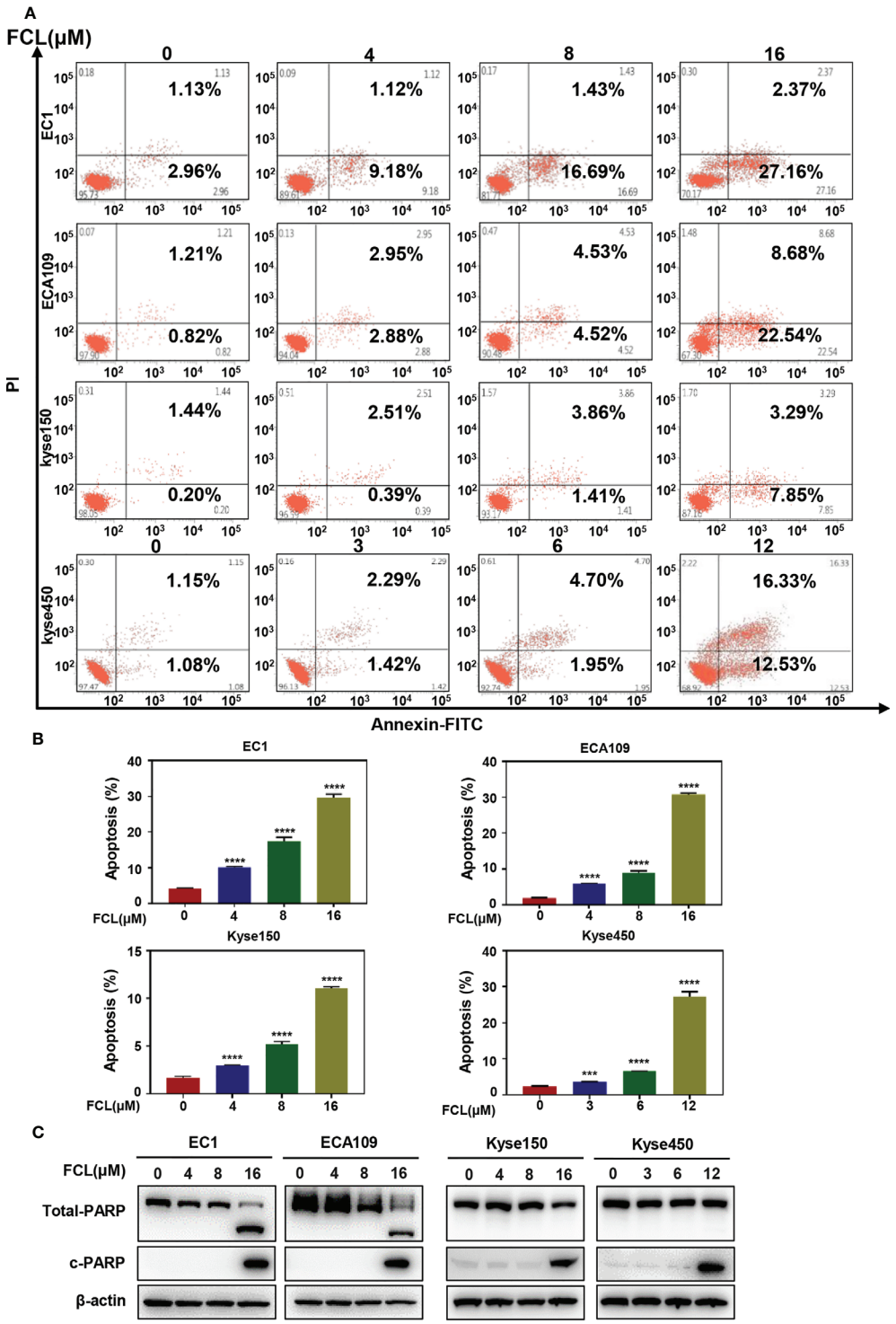

FIGURE 3 | Fangchinoline induced apoptosis in ESCC cells. **(A, B)** ESCC cells were pre-incubated with the indicated concentrations of FCL or DMSO for 24 hours, and then the cells were detected with an annexin-V-FITC apoptosis detection kit and analyzed with FCAS. **(C)** FCL increased the proteins level of c-PARP. ESCC cells were treated at the indicated concentrations of FCL or DMSO for 24 hours, and cell lysates were analyzed by Western blotting with an antibody against c-PARP. ***denotes $P < 0.001$, ****denotes $P < 0.0001$.

increased levels of cleaved PARP, a classical marker of apoptosis (**Figure 3C**). Therefore, our findings demonstrated that FCL triggered apoptosis in ESCC cells.

Fangchinoline-Induced Intrinsic Apoptosis Mediated by Noxa

To further characterize the mechanism underlying apoptosis in FCL-treated ESCC cells, we determined the expression of cleaved CASP9, a marker of intrinsic apoptosis. As shown in **Figure 4A**, FCL induced obvious accumulation of cleaved CASP9, as well as the upregulation of classical apoptotic hallmark cleaved CASP3 in EC1 and ECA109 cells, indicating that intrinsic apoptosis of ESCC cells was triggered by FCL. To explore the mechanism for activation of intrinsic apoptosis upon FCL treatment, we determined the expression of classical proapoptotic protein (Noxa, Bax and Bid). Strikingly, Noxa expression was obviously increased in both EC1 and ECA109 cells while Bax and Bid were downregulated (**Figure 4B**). Mechanistic studies showed that Noxa was transactivated by FCL (**Figure 4C**).

To further determine the potential role of Noxa in FCL-induced intrinsic apoptosis, the expression of Noxa was downregulated *via* siRNA silencing. Our data showed that Noxa knockdown with siRNA significantly suppressed FCL-induced intrinsic apoptosis, as evidenced by (i) the attenuated percentage of Annexin V-positive cells (**Figures 4D, E**), and (ii) the reduction of the cleaved fragments of PARP (**Figure 4F**), demonstrating that FCL induced Noxa-dependent intrinsic apoptosis in ESCC cells. Given that Noxa could be transactivated by ATF4 (20, 21), we, therefore tested the potential involvement of ATF4 in FCL-induced Noxa expression in ESCC cells. As shown in **Figures 4G, H**, downregulation of ATF4 significantly inhibited the induction of Noxa at both mRNA (**Figure 4G**) and protein levels (**Figure 4H**) in EC1 and ECA109 cells, indicating that ATF4 transactivated Noxa upon FCL treatment.

Fangchinoline Activated Extrinsic Apoptosis *via* the ATF4-DR5 Axis

Next, we examined the expression of cleaved CASP8, the initiator caspase of extrinsic apoptosis, to investigate whether FCL activated extrinsic apoptosis. Indeed, FCL stimulated the expression of cleaved CASP8 in both EC1 and ECA109 cells (**Figure 5A**). To further define the potential mechanism of FCL-induced extrinsic apoptosis, the expression of death receptor family members Fas, DR3, and DR5 were determined. Our results showed that FCL significantly induced the expression of death receptor DR5 both at protein and mRNA levels (**Figures 5B, C**), indicating that DR5 was involved in extrinsic apoptosis upon FCL treatment. To support this notion, the expression of DR5 was downregulated *via* siRNA silencing. We found downregulation of DR5 with siRNA significantly reduced the FCL-induced extrinsic apoptosis, along with a reduction in cleaved PARP expression (**Figures 5D–F**). These results highlighted the key role of DR5 in extrinsic apoptosis triggered by FCL.

Previous studies reported that transcription factor CHOP, a classical downstream target of ATF4, could transactivated DR5 (22–24). Therefore, we determined whether the induction of ATF4 and CHOP expression was responsible for the FCL-induced DR5 expression. Our study showed that FCL induced the obvious up-regulation of ATF4 and CHOP in EC1 and ECA109 cells (**Figure 5G**), along with an increase at the mRNA level of ATF4 (**Figure 5H**). To further examine whether DR5-induced extrinsic apoptosis upon FCL treatment was ATF4 dependent, ATF4 expression was downregulated by siRNA silencing. We found that downregulation of ATF4 significantly rescued the induction of DR5 both at the mRNA (**Figure 5I**) and protein levels (**Figure 5J**), demonstrating the crucial role of ATF4 in the induction of DR5 upon FCL stimulation. As a result, ATF4 siRNA dramatically diminished the expression of cleaved PARP and cleaved CASP8 (**Figure 5J**). Collectively, these results indicated that FCL activated the extrinsic apoptosis *via* ATF4-DR5 axis in ESCC cells.

DISCUSSION

ESCC is one of the most aggressive human malignancies with high incidence and mortality (25). However, few achievements have been achieved in the development of novel anti-ESCC strategies and effective drugs in the past few years (25). Recently, a variety of Chinese herbal extracts and isolated compounds exhibited the substantial anti-tumor efficacy in esophageal cancer cells, and some are candidates for clinical development (26). In the present study, FCL was shown to be a promising anti-ESCC agent with inhibited effects in four ESCC cell lines and in nude mouse xenograft. In mechanisms, FCL-treated ESCC cells arrested in the G1 phase of the cell cycle, which in a p21 and p27-induction manner. Furthermore, FCL transactivated ATF4 to coordinatively trigger Noxa-dependent intrinsic apoptosis and DR5-dependent extrinsic apoptosis (**Figure 6**).

The acceleration of cell cycle process contributes to sustained proliferation and rapid growth of cancer cells. Cyclin dependent kinases (CDKs), such as Cyclin D/E and CDK2/4/6, which are involved in promoting cell cycle progression, are often overexpressed, while cyclin-dependent kinases (CDKIs), such as p21 and p27, are generally downregulated in cancer cells (27). Therefore, suppressing cell cycle progression by controlling cell cycle regulators is considered as an effective strategy to halt tumor growth. FCL was demonstrated to induce G1-S arrest by suppressing the expression of Cyclin D/E and CDK2/4/6 in several human cancers (12, 16, 28). Furthermore, it was reported that FCL restrained the cell cycle progression by inducing the accumulation of p21 and p27 in most malignancies, such as breast cancer cells, prostate carcinoma cancer cells and glioblastoma cells (16, 28, 29). However, the potential role of p21 and p27 in FCL-elicited cell cycle inhibition was unclear. In our study, we found that FCL arrested cell cycle progression at G1 phase by inducing the accumulation of cell cycle inhibitors p21 and p27. Rescue experiments further revealed that additional p21 or p27 knockdown reversed the FCL-induced G1 phase arrest.

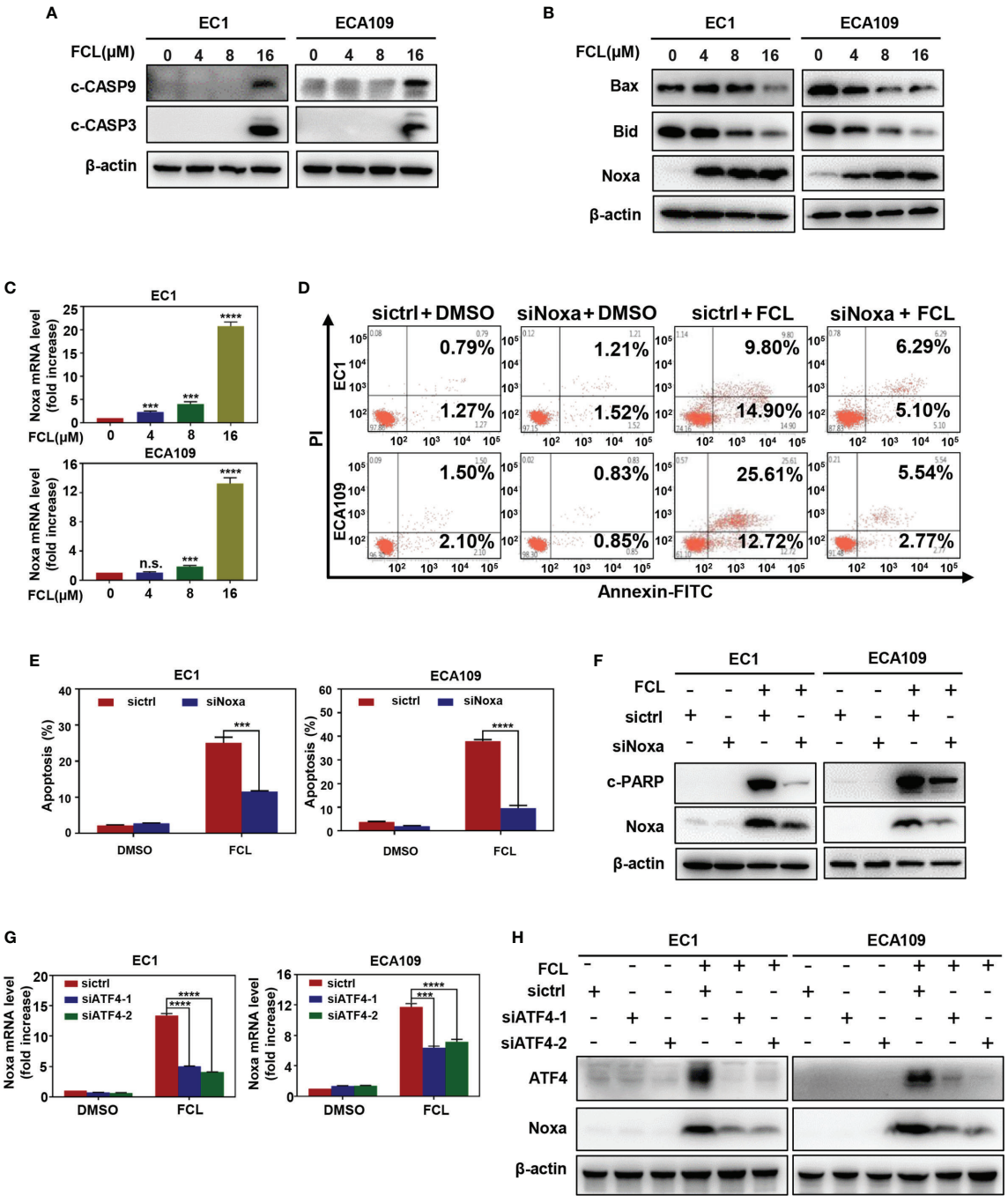

FIGURE 4 | Fangchinoline triggered intrinsic apoptosis *via* the up-regulation of Noxa. **(A)** FCL induced the activation of CASP9. EC1 and ECA109 cells were treated with FCL as described above and were subjected to Western blotting using antibodies against c-CASP9 and c-CASP3 with β-actin as a loading control. **(B)** The expression of classical pro-apoptotic proteins Noxa, Bax and Bid were determined after FCL treatment. EC1 and ECA109 cells were treated with FCL at the indicated concentrations for 24 hours, followed by Western blotting using the indicated antibodies with β-actin as a loading control. **(C)** FCL increased the mRNA level of Noxa. The mRNA level of Noxa was determined by real-time PCR in EC1 and ECA109 cells. **(D, E)** Knockdown of Noxa inhibited apoptosis induced by FCL. EC1 and ECA109 cells were transfected with control or Noxa siRNA (72 hours), treated with FCL (16 μmol/L) for 24 hours. Apoptosis induction was quantified by Annexin V–FITC/PI double-staining analysis. **(F)** Apoptosis induction was quantified by Western blotting using an antibody against c-PARP with β-actin as a loading control. **(G, H)** ATF4 is response for FCL-induced Noxa upregulation. EC1 and ECA109 cells were transfected (72 hours) with control or ATF4 siRNA, treated with FCL (16 μmol/L) for 24 hours. Expression of ATF4 and Noxa were assessed by Western blotting analysis. The effect of ATF4 on Noxa transcription was analyzed by real-time PCR. ***denotes $P < 0.001$, ****denotes $P < 0.0001$, n.s. denotes not significant.

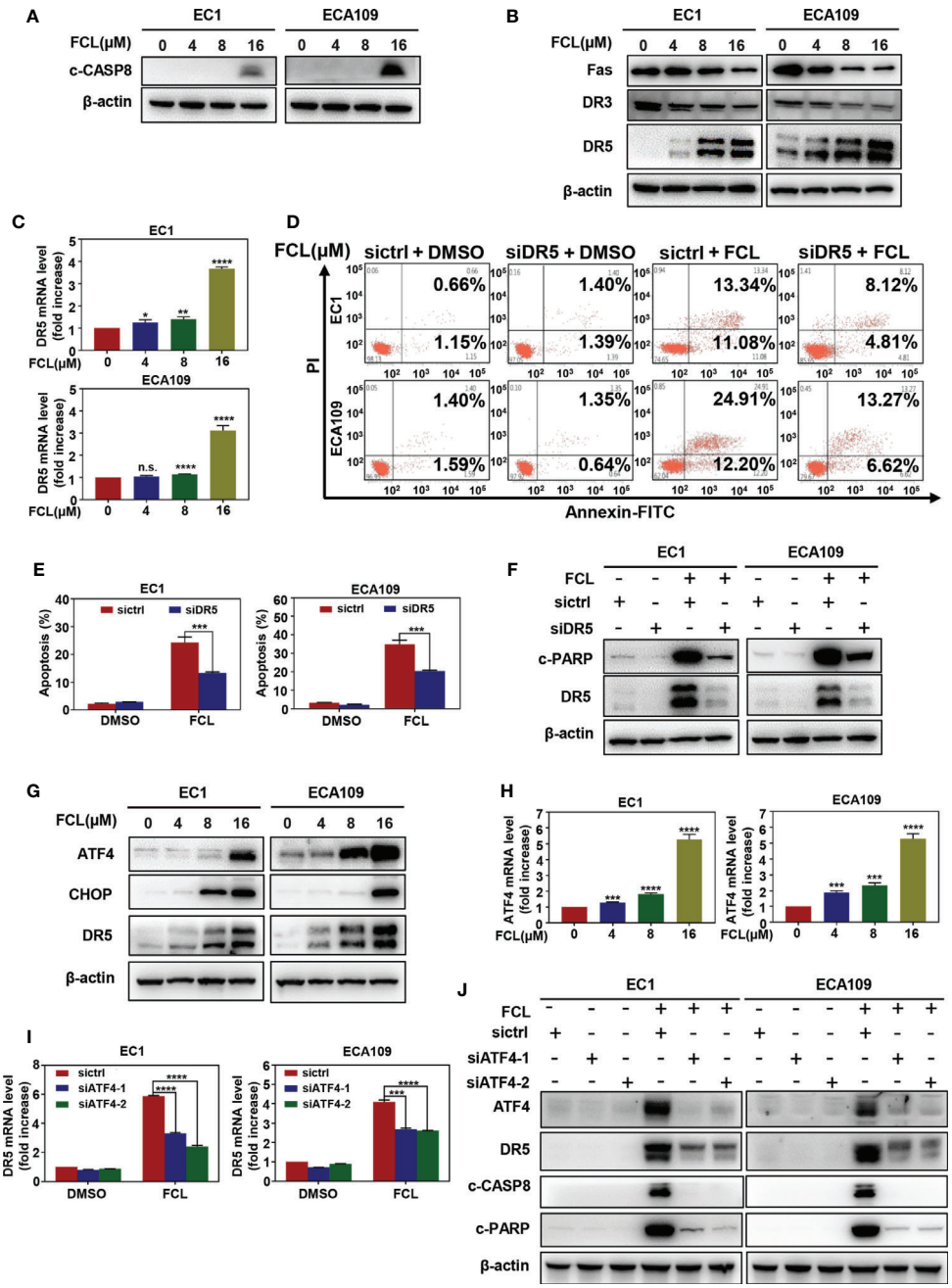

FIGURE 5 | Fangchinoline activated extrinsic apoptosis *via* the ATF4-DR5 axis. **(A)** FCL induced the activation of CASP8. EC1 and ECA109 cells were treated with FCL as described above and were subjected to Western blotting using the antibodies against c-CASP8 and c-CASP3 with β-actin as a loading control. **(B)** The expression of death receptors Fas, DR3 and DR5 was determined. EC1 and ECA109 cells treated with FCL at the indicated concentrations for 24 hours, followed by Western blotting using the indicated antibodies with β-actin as a loading control. **(C)** FCL increased the mRNA level of DR5. The mRNA level of DR5 was determined by the real-time PCR in EC1 and ECA109 cells. **(D, E)** Knockdown of DR5 inhibited apoptosis induced by FCL. EC1 and ECA109 cells were transfected with control or DR5 siRNA (72 hours), and then treated with FCL (16 μmol/L) for 24 hours. Apoptosis induction was quantified by Annexin V–FITC/PI double-staining analysis. **(F)** Apoptosis induction was quantified by Western blotting using an antibody against c-PARP with β-actin as a loading control. **(G)** FCL induced the accumulation of ATF4, CHOP and DR5. EC1 and ECA109 cells were treated with FCL at the indicated concentrations for 24 hours, followed by Western blotting using antibodies against ATF4, CHOP and DR5 with β-actin as a loading control. **(H)** The mRNA level of ATF4 was determined by real-time PCR in EC1 and ECA109 cells. **(I, J)** The expression of ATF4 mediated FCL-induced apoptosis in ESCC cells *via* ATF4-DR5 axis. ATF4 mediated FCL-induced DR5 upregulation. EC1 and ECA109 cells were transfected (72 hours) with control or ATF4 siRNA, treated with FCL (16 μmol/L) for 24 hours. Expression of ATF4, DR5, c-CASP8 and c-PARP was assessed by Western blotting. Transcriptional regulation of ATF4 on DR5 was analyzed by real-time PCR. *denotes $P < 0.05$, **denotes $P < 0.01$, ***denotes $P < 0.001$, **** denotes $P < 0.0001$, n.s. denotes not significant.

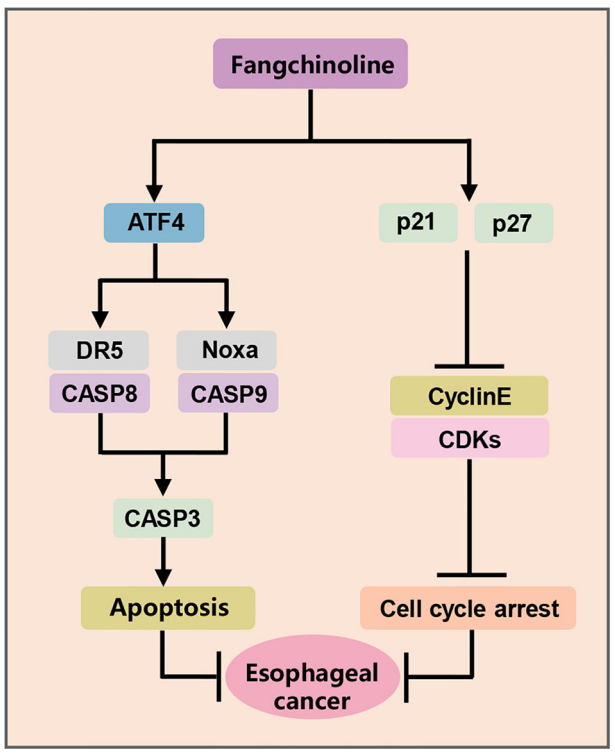

FIGURE 6 | The mechanism of FCL inhibiting the tumor growth of ESCC.

Therefore, for the first time, we demonstrated that FCL-induced cell-cycle arrest in ESCC is dependent on p21 and p27.

Endoplasmic reticulum (ER) stress, as the common trigger of apoptosis, has been reported to induce CHOP-mediated DR5 transcription and CASP8-mediated extrinsic apoptosis in human cancer cells (30, 31). Previous studies showed that FCL significantly upregulated the ER stress markers including CHOP and ATF4 (32). Therefore, we determined whether FCL activated apoptosis through ATF4-DR5 axis. In this study, we found that, in ESCC cells, FCL induced DR5-mediated extrinsic apoptosis. Moreover, DR5-induced extrinsic apoptosis is ATF4 dependent since downregulation of ATF4 significantly reduced FCL-induced apoptosis. In addition to extrinsic apoptosis, we showed that FCL triggered intrinsic apoptosis in a Noxa-dependent manner. FCL-induced Noxa up-regulation was also ATF4-dependent. However, knockdown of ATF4 did not completely rescue FCL-induced Noxa accumulation (**Figure 4G, H**). Considering several transcription factors (ATF3, p53, NF-κB, and c-Myc, etc) that are known to mediate Noxa gene expression, except for ATF4 (33, 34). The precise regulatory mechanism of Noxa induction elicited by FCL needs further exploration. Furthermore, our study showed that FCL transactivated ATF4 in ESCC cells. It has been reported that some Chinese herbal medicinal agents transactivate ATF4 by inducing ER stress. For example, Zerumbone and Parthenolide activated eIF2α through ER stress, thus inducing the transcription of ATF4 in human colon cancer cells and lung cells (35, 36). Therefore, FCL may also transactivate ATF4 through ER stress. Future studies will be performed to elucidate the mechanism by how FCL transactivates ATF4 in esophageal cancer cells.

In conclusion, our study highlighted a pivotal role of FCL in suppressing the tumor progression of ESCC both *in vitro* and *in vivo*, and discovered a novel mechanism of FCL induction of both intrinsic and extrinsic apoptosis in ESCC, suggesting that FCL was a potential anti-ESCC agent.

DATA AVAILABILITY STATEMENT

The original contributions presented in the study are included in the article/**Supplementary Material**. Further inquiries can be directed to the corresponding authors.

ETHICS STATEMENT

The animal study was reviewed and approved by Animal Experimental Ethics Committee of Longhua hospital, Shanghai University of Traditional Chinese Medicine.

AUTHOR CONTRIBUTIONS

YJZ, SW, and LJ designed the study. YJZ and SW conducted most of the experiments and wrote the manuscript. YJZ and SW analyzed the data and contributed to the manuscript completion. YC, JZ, JY, JX, and LL offered technical support. HZ and YMZ provided the reagents. RMH, YMZ, and LJ revised the manuscript. All authors contributed to the article and approved the submitted version.

FUNDING

This research was funded by the National Natural Science Foundation of China (Grant numbers 81820108022, 81625018, 81602072, 81902380), Innovation Program of Shanghai Municipal Education Commission (Grant number 2019-01-07-00-10-E00056), Program of Shanghai Academic/Technology Research Leader (Grant number 18XD1403800).

SUPPLEMENTARY MATERIAL

The Supplementary Material for this article can be found online at: https://www.frontiersin.org/articles/10.3389/fonc.2021.666549/full#supplementary-material

Supplementary Figure 1 | Fangchinoline inhibited ESCC proliferation *in vitro*. **(A)** ESCC cell lines EC1, ECA109, Kyse150 and Kyse450 were treated with indicated concentrations of FCL for 24 hours, and then for photographed under microcopy. Representative images are shown, scale bar = 100μm.

REFERENCES

1. Rustgi AK, El-Serag HB. Esophageal Carcinoma. *New Engl J Med* (2014) 371 (26):2499–509. doi: 10.1056/NEJMra1314530
2. Rustgi A, El-Serag HB. Esophageal Carcinoma. *New Engl J Med* (2015) 372 (15):1472–3. doi: 10.1056/NEJMc1500692
3. Jun Y, Tang Z, Luo C, Jiang B, Li X, Tao M, et al. LeukocyteMediated Combined Targeted Chemo and Gene Therapy for Esophageal Cancer. *ACS Appl Mater Interfacesa* (2020) 12(42):47330–41. doi: 10.1021/acsami.0c15419
4. Li FS, Weng JK. Demystifying Traditional Herbal Medicine With Modern Approach. *Nat Plants* (2017) 3:17109. doi: 10.1038/nplants.2017.109
5. Wang N, Pan W, Zhu M, Zhang M, Hao X, Liang G, et al. Fangchinoline Induces Autophagic Cell Death Via p53/sestrin2/AMPK Signalling in Human Hepatocellular Carcinoma Cells. *Br J Pharmacol* (2011) 164(2b):731–42. doi: 10.1111/j.1476-5381.2011.01349.x
6. Choi HS, Kim HS, Min KR, Kim Y, Lim HK, Chang YK, et al. Anti-Inflammatory Effects of Fangchinoline and Tetrandrine. *J ethnopharmacology* (2000) 69 (2):173–9. doi: 10.1016/s0378-8741(99)00141-5
7. Shen YC, Chou CJ, Chiou WF, Chen CF. Anti-Inflammatory Effects of the Partially Purified Extract of Radix Stephaniae Tetrandrae: Comparative Studies of Its Active Principles Tetrandrine and Fangchinoline on Human Polymorphonuclear Leukocyte Functions. *Mol Pharmacol* (2001) 60(5):1083–90. doi: 10.1124/mol.60.5.1083
8. Gülçin I, Elias R, Gepdiremen A, Chea A, Topal F. Antioxidant Activity of Bisbenzylisoquinoline Alkaloids From Stephania Rotunda: Cepharanthine and Fangchinoline. *J Enzyme Inhib Med Chem* (2010) 25(1):44–53. doi: 10.3109/14756360902932792
9. Kim HS, Zhang YH, Yun YP. Effects of Tetrandrine and Fangchinoline on Experimental Thrombosis in Mice and Human Platelet Aggregation. *Planta Med* (1999) 65(2):135–8. doi: 10.1055/s-1999-13974
10. Li X, Yang Z, Han W, Lu X, Jin S, Yang W, et al. Fangchinoline Suppresses the Proliferation, Invasion and Tumorigenesis of Human Osteosarcoma Cells Through the Inhibition of PI3K and Downstream Signaling Pathways. *Int J Mol Med* (2017) 40(2):311–8. doi: 10.3892/ijmm.2017.3013
11. Wang B, Xing Z, Wang F, Yuan X, Zhang Y. Fangchinoline Inhibits Migration and Causes Apoptosis of Human Breast Cancer MDA-MB-231 Cells. *Oncol Lett* (2017) 14(5):5307–12. doi: 10.3892/ol.2017.6831
12. Luo X, Peng JM, Su LD, Wang DY, Yu YJ. Fangchinoline Inhibits the Proliferation of SPC-A-1 Lung Cancer Cells by Blocking Cell Cycle Progression. *Exp Ther Med* (2016) 11(2):613–8. doi: 10.3892/etm.2015.2915
13. Guo B, Su J, Zhang T, Wang K, Li X. Fangchinoline as a Kinase Inhibitor Targets FAK and Suppresses FAK-Mediated Signaling Pathway in A549. *J Drug Targeting* (2014) 23(3):266–74. doi: 10.3109/1061186x.2014.992898
14. Shi J, Guo B, Hui Q, Chang P, Tao K. Fangchinoline Suppresses Growth and Metastasis of Melanoma Cells by Inhibiting the Phosphorylation of FAK. *Oncol Rep* (2017) 38(1):63–70. doi: 10.3892/or.2017.5678
15. Wang C-D, Yuan C-F, Bu Y-Q, Wu X-M, Wan J-Y, Zhang L, et al. Fangchinoline Inhibits Cell Proliferation Via Akt/GSK-3beta/cyclin D1 Signaling and Induces Apoptosis in MDA-MB-231 Breast Cancer Cells. *Asian Pacific J Cancer Prev* (2014) 15(2):769–73. doi: 10.7314/apjcp.2014.15.2.769
16. Guo B, Xie P, Su J, Zhang T, Li X, Liang G. Fangchinoline Suppresses the Growth and Invasion of Human Glioblastoma Cells by Inhibiting the Kinase Activity of Akt and Akt-Mediated Signaling Cascades. *Tumour Biol* (2016) 37 (2):2709–19. doi: 10.1007/s13277-015-3990-1
17. Donjerkovic D, Scott DW. Regulation of the G1 Phase of the Mammalian Cell Cycle. *Cell Res* (2000) 10(1):1–16. doi: 10.1038/sj.cr.7290031
18. Sherr CJ, Roberts JM. CDK Inhibitors: Positive and Negative Regulators of G1-phase Progression. *Genes Dev* (1999) 13:1501–12. doi: 10.1101/gad.13.12.1501
19. Marqués-Torrejón MA, Porlan E, Banito A, Gómez-Ibarlucea E, LopezContreras AJ, Fernández-Capetillo O, et al. Cyclin-Dependent Kinase Inhibitor p21 Controls Adult Neural Stem Cell Expansion by Regulating Sox2 Gene Expression. *Cell Stem Cell* (2013) 12:88–100. doi: 10.1016/j.stem.2012.12.001
20. Wang Q, Mora-Jensen H, Weniger MA, Perez-Galan P, Wolford C, Hai T, et al. ERAD Inhibitors Integrate ER Stress With an Epigenetic Mechanism to Activate BH3-Only Protein NOXA in Cancer Cells. *Proc Natl Acad Sci USA* (2009) 106(7):2200–5. doi: 10.1073/pnas.0807611106
21. Armstrong JL, Flockhart R, Veal GJ, Lovat PE, Redfern CP. Regulation of Endoplasmic Reticulum Stress-Induced Cell Death by ATF4 in Neuroectodermal Tumor Cells. *J Biol Chem* (2010) 285(9):6091–100. doi: 10.1074/jbc.M109.014092
22. Xu L, Su L, Liu X. Pkcδ Regulates Death Receptor 5 Expression Induced by PS-341 Through ATF4-ATF3/CHOP Axis in Human Lung Cancer Cells. *Mol Cancer Ther* (2012) 11(10):2174–82. doi: 10.1158/1535-7163.Mct-12-0602
23. Martín-Pérez R, Palacios C, Yerbes R, Cano-González A, Iglesias-Serret D, Gil J, et al. Activated ERBB2/HER2 Licenses Sensitivity to Apoptosis Upon Endoplasmic Reticulum Stress Through a PERK-Dependent Pathway. *Cancer Res* (2014) 74(6):1766–77. doi: 10.1158/0008-5472.Can-13-1747
24. Han J, Back SH, Hur J, Lin YH, Gildersleeve R, Shan J, et al. ER-Stress-Induced Transcriptional Regulation Increases Protein Synthesis Leading to Cell Death. *Nat Cell Biol* (2013) 15(5):481–90. doi: 10.1038/ncb2738
25. Torre LA, Bray F, Siegel RL, Ferlay J, Lortet-Tieulent J, Jemal A. Global Cancer Statistics, 2012. *CA Cancer J Clin* (2015) 65(2):87–108. doi: 10.3322/caac.21262
26. Chen X, Deng L, Jiang X, Wu T. Chinese Herbal Medicine for Oesophageal Cancer. *Cochrane Database Syst Rev* (2016) 1):Cd004520. doi: 10.1002/14651858.CD004520.pub7
27. Malumbres M, Barbacid M. Mammalian Cyclin-Dependent Kinases. *Trends Biochem Sci* (2005) 30(11):630–41. doi: 10.1016/j.tibs.2005.09.005
28. Xing Z, Zhang Y, Zhang X, Yang Y, Ma Y, Pang D. Fangchinoline Induces G1 Arrest in Breast Cancer Cells Through Cell-Cycle Regulation. *Phytother Res* (2013) 27(12):1790–4. doi: 10.1002/ptr.4936
29. Wang CD, Huang JG, Gao X, Li Y, Zhou SY, Yan X, et al. Fangchinoline Induced G1/S Arrest by Modulating Expression of P27, PCNA, and Cyclin D in Human Prostate Carcinoma Cancer PC3 Cells and Tumor Xenograft. *Biosci Biotechnol Biochem* (2010) 74(3):488–93. doi: 10.1271/bbb.90490
30. Wang G, Wang X, Yu H, Wei S, Williams N, Holmes DL, et al. Small-Molecule Activation of the TRAIL Receptor DR5 in Human Cancer Cells. *Nat Chem Biol* (2013) 9(2):84–9. doi: 10.1038/nchembio.1153
31. Lu M, Lawrence DA, Marsters S, Acosta-Alvear D, Kimmig P, Mendez AS, et al. Opposing Unfolded-Protein-Response Signals Converge on Death Receptor 5 to Control Apoptosis. *Science* (2014) 345(6192):98–101. doi: 10.1126/science.1254312
32. Lee HS, Safe S, Lee SO. Inactivation of the Orphan Nuclear Receptor NR4A1 Contributes to Apoptosis Induction by Fangchinoline in Pancreatic Cancer Cells. *Toxicol Appl Pharmacol* (2017) 332:32–9. doi: 10.1016/j.taap.2017.07.017
33. Sharma K, Vu TT, Cook W, Naseri M, Zhan K, Nakajima W, et al. P53-Independent Noxa Induction by Cisplatin Is Regulated by ATF3/ATF4 in Head and Neck Squamous Cell Carcinoma Cells. *Mol Oncol* (2018) 12(6):788–98. doi: 10.1002/1878-0261.12172
34. Sha B, Chen X, Wu H, Li M, Shi J, Wang L, et al. Deubiquitylatinase Inhibitor b-AP15 Induces c-Myc-Noxa-Mediated Apoptosis in Esophageal Squamous Cell Carcinoma. *Apoptosis an Int J programmed Cell Death* (2019) 24(9-10):826–36. doi: 10.1007/s10495-019-01561-9
35. Edagawa M, Kawauchi J, Hirata M, Goshima H, Inoue M, Okamoto T, et al. Role of Activating Transcription Factor 3 (ATF3) in Endoplasmic Reticulum (ER) Stress-Induced Sensitization of p53-Deficient Human Colon Cancer Cells to Tumor Necrosis Factor (TNF)-Related Apoptosis-Inducing Ligand (TRAIL)-Mediated Apoptosis Through Up-Regulation of Death Receptor 5 (DR5) by Zerumbone and Celecoxib. *J Biol Chem* (2014) 289(31):21544–61. doi: 10.1074/jbc.M114.558890
36. Zhao X, Liu X, Su L. Parthenolide Induces Apoptosis Via TNFRSF10B and PMAIP1 Pathways in Human Lung Cancer Cells. *J Exp Clin Cancer Res CR* (2014) 33(1):3. doi: 10.1186/1756-9966-33-3

Conflict of Interest: RMH was employed by Anticancer Inc.

The remaining authors declare that the research was conducted in the absence of any commercial or financial relationships that could be construed as a potential conflict of interest.

frontiers in Oncology

REVIEW
published: 18 June 2021
doi: 10.3389/fonc.2021.702510

Tetraspanins: Novel Molecular Regulators of Gastric Cancer

Yue Deng[1], *Sicheng Cai*[1], *Jian Shen*[2] *and Huiming Peng*[1]*

[1] Department of Human Anatomy, School of Basic Medicine, Tongji Medical College, Huazhong University of Science and Technology, Wuhan, China, [2] Department of Pancreatic Surgery, Union Hospital, Tongji Medical College, Huazhong University of Science and Technology, Wuhan, China

Gastric cancer is the fourth and fifth most common cancer worldwide in men and women, respectively. However, patients with an advanced stage of gastric cancer still have a poor prognosis and low overall survival rate. The tetraspanins belong to a protein superfamily with four hydrophobic transmembrane domains and 33 mammalian tetraspanins are ubiquitously distributed in various cells and tissues. They interact with other membrane proteins to form tetraspanin-enriched microdomains and serve a variety of functions including cell adhesion, invasion, motility, cell fusion, virus infection, and signal transduction. In this review, we summarize multiple utilities of tetraspanins in the progression of gastric cancer and the underlying molecular mechanisms. In general, the expression of TSPAN8, CD151, TSPAN1, and TSPAN4 is increased in gastric cancer tissues and enhance the proliferation and invasion of gastric cancer cells, while CD81, CD82, TSPAN5, TSPAN9, and TSPAN21 are downregulated and suppress gastric cancer cell growth. In terms of cell motility regulation, CD9, CD63 and CD82 are metastasis suppressors and the expression level is inversely associated with lymph node metastasis. We also review the clinicopathological significance of tetraspanins in gastric cancer including therapeutic targets, the development of drug resistance and prognosis prediction. Finally, we discuss the potential clinical value and current limitations of tetraspanins in gastric cancer treatments, and provide some guidance for future research.

Keywords: tetraspanins, gastric cancer, tumor proliferation, tumor invasion, tumor metastasis, targeted therapy, drug resistance

OPEN ACCESS

Edited by:
Jianjun Xie,
Shantou University, China

Reviewed by:
Peter Monk,
The University of Sheffield, United Kingdom
Prabhash Dadhich,
Cellf Bio LLC, United States

***Correspondence:**
Huiming Peng
hmpeng2003@hust.edu.cn

Specialty section:
This article was submitted to Gastrointestinal Cancers, a section of the journal Frontiers in Oncology

Received: *29 April 2021*
Accepted: *07 June 2021*
Published: *18 June 2021*

Citation:
Deng Y, Cai S, Shen J and Peng H (2021) Tetraspanins: Novel Molecular Regulators of Gastric Cancer. Front. Oncol. 11:702510. doi: 10.3389/fonc.2021.702510

Abbreviations: GC, gastric cancer; TM, transmembrane; N, amino; C, carboxyl; ECL, extracellular loop; TEMs, tetraspanin-enriched microdomains; HCC, hepatocellular carcinoma; GPVI, glycoprotein VI; MMP-9, matrix metalloproteinase-9; uPA, urokinase plasminogen activator; MRP-1, motility-related protein; CAFs, cancer-associated fibroblasts; GIA, gastrointestinal adenocarcinoma; MAPK, mitogen-activated protein kinase; JNK/SAPK, c-Jun N-terminal kinase/stress-activated protein kinase; MDR, multidrug resistance; NOTCH2, Notch Receptor 2; 5-FU, 5-Fluorouracil; PIK3R3, Phosphoinositide-3-Kinase Regulatory Subunit 3; mAb, monoclonal Antibody.

INTRODUCTION

Gastric cancer (GC) is the fourth most common cancer worldwide in men following lung, prostate, colorectal, and the fifth in women following breast, colorectal, cervical, lung. Risk factors for gastric cancer include Helicobacter pylori infection, age, high salt intake, and low-fruit and vegetables diets (1). About 70% of gastric cancer cases worldwide are in developing countries, including Eastern Asia, Central and Eastern Europe, and South America (2). The regional distribution variations suggest that the occurrence of gastric cancer is related to environmental factors and lifestyles (3). Patients with advanced gastric cancer usually start with a platinum and fluoropyrimidine doublet in the first line, and are treated with sequential lines of chemotherapy. Despite advances in treatment strategies recently, advanced gastric cancer patients still have a poor prognosis and the median survival is less than 1 year (1). Therefore, exploring the internal molecular mechanisms underlying gastric cancer development is conducive to generating more effective therapeutic targets and bringing hope to patients.

The tetraspanins belong to a protein superfamily with some common structural features. They have four hydrophobic transmembrane domains (TM1-TM4), short intracellular amino(N) and carboxyl(C) tails, a small intracellular loop, a small extracellular loop (ECL1), and a large extracellular loop (ECL2) (4). ECL2 is subdivided into a highly conserved region and a variable region. The conserved region has been revealed to mediate homodimerization, while the variable region is related to specific interactions with other proteins. Compared with ECL2, little is known about the function of ECL1. Within the intracellular regions, palmitoylation sites of cysteine residues work for tetraspanin web assembly, and the C-terminal tail contributes to specific functional links to cytoskeletal or signaling proteins. Four TM domains are important in 'tetraspanin web' biosynthesis and assembly as probable sites of intra- and inter-molecular interactions (5).

Currently, 33 mammalian tetraspanins have been reported and they are ubiquitously distributed in various cells and tissues (6). Some tetraspanins are detected to be abundantly expressed in specific tissues. For example, TSPAN32, CD37, and CD53 are tissue enhanced in blood and lymphoid tissue. TSPAN9, TSPAN5, and TSPAN7 are enriched in brain. TSPAN1, TSPAN11, and TSPAN8 are widely distributed in the intestine. TSPAN6 is in the salivary gland, TSPAN33 is in the kidney, while TSPAN21 is abundant in the prostate and urinary bladder. Other tetraspanins are low tissue specificity and are distributed in almost all tissues (7). On the cell membrane, tetraspanins interact with other membrane proteins to form tetraspanin-enriched microdomains (TEMs) and serve a variety of functions including cell adhesion, invasion, motility, cell fusion, virus infection, and signal transduction (8, 9). With a thorough study of tetraspanins, its role in multiple tumor development stages has been gradually revealed in recent years, such as early carcinogenesis, angiogenesis, proliferation, invasion, and metastasis (10). Accumulating studies found that tetraspanins play critical roles in gastric cancer development. Here, we review the current evidences on the function of tetraspanins in gastric cancer development and progression to provide some guidance for clinical treatment and future research.

ROLE OF TETRASPANINS IN GASTRIC CANCER CELL GROWTH

Tetraspanins have been confirmed to play an essential role in tumorigenesis and progression (10). Different tetraspanins contribute to diverse biological functions across cancer cells. Here, we summarize tetraspanins that enhance the proliferation and invasion of gastric cancer cells, including TSPAN8, CD151, TSPAN1, and TSPAN4 (**Figure 1**). We also discuss several tetraspanins, including CD81, CD82, TSPAN5, TSPAN9, and TSPAN21 that suppress gastric cancer cell growth (**Figure 2**).

Tetraspanins That Facilitate Gastric Cancer Cell Proliferation and Invasion

TSPAN8

TSPAN8, also known as CO-029 or TM4SF3, belongs to the tetraspanin family and has been reported to be associated with multiple cancer types, such as hepatocellular carcinoma (11), pancreatic adenocarcinoma (12), colon carcinoma (13), breast cancer (14). TSPAN8 expression in tumor cells is related to increased metastasis (10, 15), proliferation (16), induction of angiogenesis (17) and thrombosis (18). The mechanism by which TSPAN8 has emerged as a key molecular is attributed to its position in TEMs and is primarily related to integrins, proteases, and cytoplasmic signaling molecules (19). Besides, the effect of TSPAN8 on angiogenesis may be partially mediated by exosomes (20).

As for gastric cancer, several studies have revealed that TSPAN8 expression is increased in gastric cancer tissues compared to normal tissues. Matsumura et al. found TSPAN8 was up-regulated in gastric cancer using microarray analysis (21). Mottaghi-Dastjerdi et al. performed suppression subtractive hybridization (SSH) on gastric adenocarcinoma tissue and the corresponding normal gastric tissue, and found TSPAN8 was overexpressed in the tumor (22). These findings suggest that overexpressed TSPAN8 may be related to the occurrence and progression of gastric cancer.

Further, ZHU's lab showed TSPAN8 acts as an oncogene in gastric cancer and promotes gastric cancer cell proliferation and invasion partially through EGFR signaling (23). The authors demonstrated that the expression of TSPAN8 was affected by EGF in a concentration- and time-dependent manner by *in vitro* experiments. When TSPAN8 was knocked down, the effect of EGF on promoting gastric cancer cell proliferation and invasion was attenuated.

Later in 2015, Wei et al. reported that TSPAN8 promotes gastric cancer cell proliferation and growth partially by activating the ERK MAPK pathway (24). Through MTT and transwell-matrigel assay, the authors found that TSPAN8 overexpression promotes the cell survival and invasion while TSPAN8 silencing has the opposite effect. They also found the expression of phospho-MEK1/2 and phospho-ERK1/2 was increased

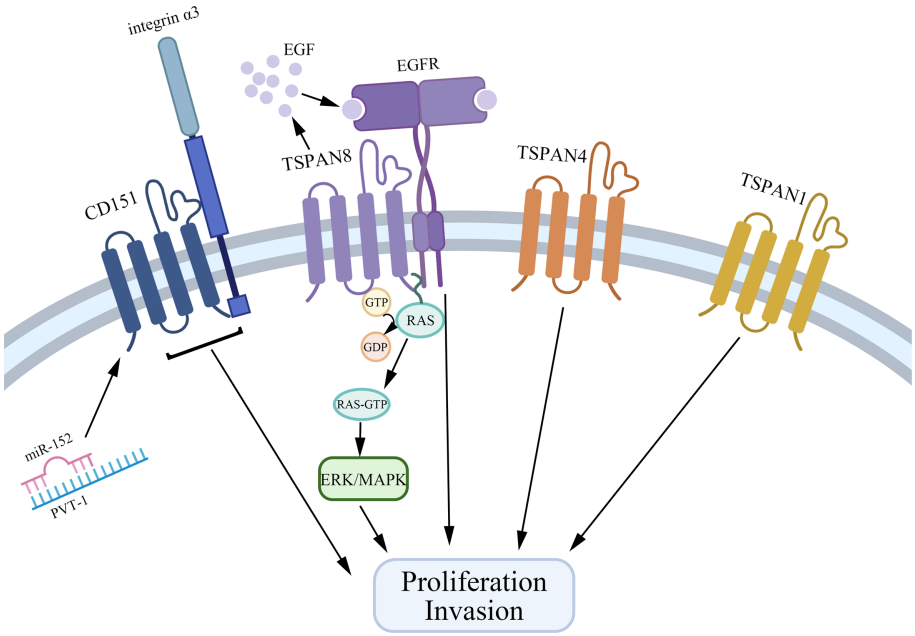

FIGURE 1 | Tetraspanins that promote gastric cancer cell proliferation and invasion. CD151, TSPAN8, TSPAN4, and TSPAN1 interact with other biomolecules in TEMs to facilitate the growth and invasion of gastric cancer cells. Especially, CD151 forms a complex with integrin α3, and on the other hand, PVT1 could bind to miR-152 to inhibit the expression of miR-152 to promote gastric cancer cell growth. TSPAN8 regulates gastric cancer cell proliferation *via* mediating the effect of EGF and activating the ERK MAPK pathway.

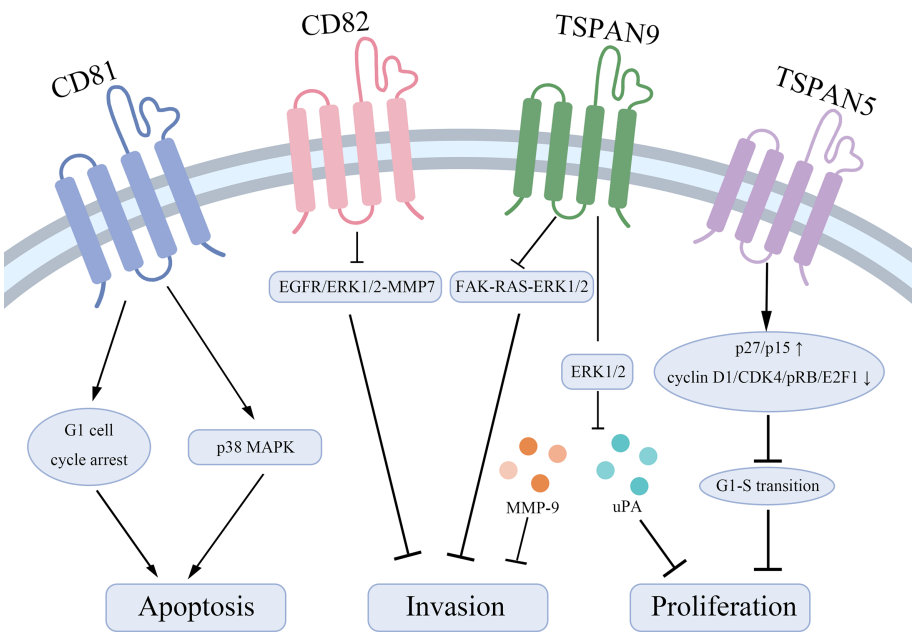

FIGURE 2 | Tetraspanins that suppress gastric cancer cell proliferation and lead to apoptosis. CD81 acts as a pro-apoptotic effector through inducing a G1 cell cycle arrest and inhibiting the phosphorylation of p38 MAPK. CD82 suppresses the EGFR/ERK1/2-MMP7 signaling pathway to represses gastric cancer invasion. TSPAN9 inhibits the ERK1/2 pathway to downregulate the expression of MMP-9 and uPA and inhibits the FAK-RAS-ERK1/2 signal pathway to repress invasion of gastric cancer cells. TSPAN5 suppresses the tumor proliferation *via* increasing the expression of p27/p15 and decreasing the expression of cyclin D1, CDK4, pRB, and E2F1 to control cell cycle transition.

dramatically in the TSPAN8 overexpression cells but decreased in the TSPAN8 suppressed cells. When MER-ERK was inhibited in TSPAN8 overexpression cells, the increased survival rate and migrated cell number caused by TSPAN8 overexpression were significantly reduced. Therefore, the research by Wei et al. suggested that the MAPK pathway was involved in the effects of TSPAN8 on gastric cancer cell proliferation and invasion.

Recently, a novel study indicated a negative relationship between the expression of TSPAN8 and miR-324-5p in gastric cancer cells. MiR-324-5p was demonstrated to repress the viability and induce the apoptosis of gastric cancer cells *via* down-regulating TSPAN8. They also proposed that the possible mechanism was the combination of TSPAN8 3'UTR and miR-324-5p (25). However, there are still few milestones on the treatment of gastric cancer targeting the above mechanisms.

CD151

CD151 has a broad distribution in the endothelium, epithelium, Schwann cells, and dendritic cells, as well as in skeletal, smooth, and cardiac muscle (26). It directly or indirectly interacts with abundant other transmembrane proteins to form TEMs and regulates integrin-dependent adhesion strengthening, cell morphology, and cell migration as a spectacular partner of laminin-binding integrins (8, 27). Karamatic Crew et al. revealed that CD151 was crucial for the proper assembly of the glomerular and tubular basement membrane in the kidney. In the skin, the inner ears, and erythropoiesis, CD151 also had functional significance. Therefore, it is not surprising that CD151 mutation is associated with end-stage kidney failure (28). As a major partner of laminin-binding integrins, CD151 modulates cancer cell motility, invasion, and metastasis together with $\alpha3\beta1$ and $\alpha6\beta4$ (15). For example, in hepatocellular carcinoma (HCC), CD151 was overexpressed compared with normal liver tissues and the expression level was positively related to the metastatic potential of HCC cell lines (29).

Evidences implicate that CD151 forms a complex with integrin $\alpha3$ in gastric cancer cells and is positively associated with the invasiveness of gastric cancer (30). In 2014, Zhai et al. demonstrated in gastric cancer, miR-152 was downregulated and overexpressed miR-152 inhibited the proliferation and motility of gastric cancer cells *via* targeting CD151 (31). Later, Li et al. found PVT1, a long noncoding RNA, highly expressed in human gastric cancer tissues and correlated with lymph node invasion of gastric cancer (32). PVT1 could increase the expression of CD151 through binding to miR-152 and inhibiting the expression of miR-152 to promote gastric cancer (33). The authors likened PVT1 to a "sponge" in gastric cancer to inhibit miR-152, and made it an emerging potential therapeutic target for gastric cancer (33).

Other Tetraspanins

TSPAN1

TSPAN1 (NET-1) is identified to express in epithelial cell lines and multiple tumor cell lines including cervical carcinoma, lung carcinoma, squamous carcinoma, colon carcinoma, and breast carcinoma (34). In gastric cancer, Chen et al. elaborated the clinicopathological significance of overexpressed TSPAN1. They found the expression level of TSPAN1 was positively related to the clinical stage and lymph node status of the tumor, while negatively associated with cancer cell differentiation and survival rates (35). Later, Lu et al. detected that the expression of TSPAN1 was dramatically increased in gastric cancer tissues, and clarified TSPAN1 as an oncogene to promote gastric cancer cell proliferation and invasion. Moreover, they identified that overexpressed miR-573 inhibited growth and invasion, induced G1/G0 arrest of gastric cancer cells through directly targeting 3'UTR of TSPAN1. This miR-573/TSPAN1 axis provides a novel perspective on the molecular mechanisms of gastric cancer (36).

TSPAN4

The role of TSPAN4 in gastric cancer was discovered through bioinformatics analysis. TSPAN4 was identified as one of the upregulated differentially expressed genes and the increased expression indicated a decreased survival rate. Moreover, the downregulation of TSPAN4 remarkably reduced the proliferation of gastric cancer cells (37). Therefore, TSPAN4 may be a biomarker and a potential therapeutic target for gastric cancer.

Together, TSPAN8, CD151, TSPAN1, and TSPAN4 are overexpressed in gastric cancer tissues and are related to a higher clinical stage and poorer prognosis *via* interacting with other molecules in TEMs. Specifically, TSPAN8 mediates the effect of EGF and actives the ERK MAPK pathway to promote gastric cancer cell proliferation. CD151 exerts its action by forming a complex with integrin $\alpha3$. Also, many microRNAs are reported to be bound with the expression of tetraspanins, which provides a new idea for gastric cancer therapy.

Tetraspanins That Repress Gastric Cancer Cell Proliferation

CD81

CD81 (TAPA-1), whose gene has been mapped to chromosomal region 11p15.5, is discovered as the target of an antiproliferative antibody initially (38, 39). As a protein widely distributed on the surface of various cell membranes, CD81 has been revealed to affect morphology, adhesion, activation, proliferation, and differentiation of B, T and other cells (40). On the surface of B cells, CD81 forms a complex with CD21, CD19, and Leu13. The complex reduces the signal transduction threshold for activating B cells mediated by B cell receptors (40, 41). Similarly, CD81 interacting with CD4 and CD8 on T cells provides CD3 a costimulatory signal (42). In nonimmune cells, CD81 assists in egg fusion with sperm (43), myoblasts fusion during muscle regeneration (44) and exerts as a cell surface receptor for hepatitis C virus entry into the cell (45). In human lymphomas, CD81 expresses differentially, with increased expression in diffuse large B-cell lymphomas, but decreased expression in multiple myeloma, Hodgkin lymphoma, myeloid leukemia, and leukemic blasts of precursor B-cell lymphoblastic leukemia (46, 47).

However, in gastric cancer, CD81 is assessed as a tumor suppressor gene and CD81 downregulation is related to the malignant progression of the tumors (48). Yoo et al. proposed that the decreased expression of CD81 mRNA was due to

aberrant CpG hypermethylation of its promoter but rarely due to genetic alterations. This downregulation facilitates the G1 to S transition of the cell cycle, while increased CD81 expression induces a G1 cell cycle arrest and promotes apoptosis. Moreover, downregulated CD81 significantly attenuates cellular responses to a variety of apoptotic stress signals, such as etoposide, 5-FU, doxorubicin, γ-irradiation, and hypoxia. Also, CD81 decreases the colony-forming ability of gastric tumor cells and inhibits the phosphorylation of p38 MAPK. Therefore, CD81 has anti-proliferative and pro-apoptotic functions in gastric cancer cells and acts as a tumor suppressor gene.

Other Tetraspanins

CD82

As a metastasis suppressor gene, CD82 is also closely related to the gastric tumor cell invasion and metastasis. Xu's lab disclosed that CD82 downregulates the expression of phosphorylated(p)-EGFR, p-ERK1/2, and MMP7 to suppress the EGFR/ERK1/2-MMP7 signaling pathway. Therefore, CD82 inhibits the invasion of gastric cancer (49). Meanwhile, in gastric tumor cells, nuclear Drosha, an enzyme of endonuclease RNase III, promotes miR-197 biosynthesis. The increased miR-197 downregulates CD82 to activate EGFR-ERK1/2-MMP7 signaling pathway, thus having an effect on promoting gastric tumor cells invasion and metastasis.

TSPAN5

TSPAN5 (NET-4, TMS4SF9) is shown to be highly expressed in the neocortex, the hippocampus, the amygdala, and murine cerebellar Purkinje cells, suggesting that TSPAN5 is of importance in the maintenance of brain activity in mice (50). It is also reported that TSPAN5 contributes to osteoclast formation and differentiation (51). In gastric cancer, the expression of TSPAN5 is significantly reduced and inversely correlated with tumor size and TNM stage, which indicates that TSPAN5 works as a tumor suppressor to inhibit the tumor proliferation, colony formation, and migration. Further, TSPAN5 increases the expression of p27/p15 and decreases the expression of cyclin D1, CDK4, pRB and E2F1, especially cyclin D1/CDK4, to control cell cycle transition from G1-S phase (52).

TSPAN9

TSPAN9 (NET-5, PP1057) is elucidated to regulate the platelet function through synergy with the collagen receptor GPVI (glycoprotein VI) and integrin α6β1 (53). Li et al. reported that overexpressed TSPAN9 inhibited the proliferation, migration, and invasion of human gastric cancer SGC7901 cells. TSPAN9 suppresses the ERK1/2 pathway to downregulate the proteins associated with tumor metastasis including matrix metalloproteinase-9 (MMP-9) and urokinase plasminogen activator (uPA) (54). Recently, Qi et al. found TSPAN9 inhibited migration and invasion of gastric cancer cells *via* inhibiting the FAK-RAS-ERK1/2 signal pathway. Furthermore, they confirmed EMILIN1, an extracellular secretory protein, exerted an anti-tumor effect by increasing the expression of TSPAN9 (55).

TSPAN21

TSPAN21 (UPK1A) is highly specifically expressed in normal urothelium, and can be observed in normal genitourinary tract, uterus and prostate (4). Kar et al. found TSPAN21 inhibited the down-regulation of MMP7 to regulate cell metastasis, invasion and survival. Loss the expression of TSPAN21 can lead to cell proliferation, metastasis and invasion (56). In gastric cancer, Zheng et al. reported that the protein level of TSPAN21 was significantly reduced, and the low expression of TSPAN21 was related to the poor prognosis of gastric cancer. When TSPAN21 was overexpressed, the invasion and migration of gastric cancer cell lines was inhibited (57). This indicates that TSPAN21 has a potential tumor suppressor effect in gastric cancer, but the mechanism remains to be fully explored.

Taken together, CD81, CD82, TSPAN5, TSPAN9, and TSPAN21 are regarded as tumor suppressors in gastric cancer to inhibit tumor cell growth and invasion, and enhance the sensitivity to apoptotic stress signals. Mechanically, CD82 represses the EGFR/ERK1/2-MMP7 signaling pathway and TSPAN9 suppresses the ERK1/2 pathway and the FAK-RAS-ERK1/2 signal pathway to play biological roles.

ROLE OF TETRASPANINS IN GASTRIC CANCER CELL METASTASIS

Tetraspanins regulate cell motility, adhesion, and migration by interacting with integrins, signal molecules and other transmembrane proteins in TEMs. However, different tetraspanins can achieve even totally opposing functions in cancer cell metastasis. Here, we focus on the insights into the roles and molecular mechanisms of three tetraspanins involved in gastric cancer cell metastasis, CD9, CD63, and CD82 (also known as KAI1).

CD9 and CD63

CD9 was initially identified as a 24-kDa surface protein specific for acute lymphoblastic leukemic cells. However, CD9 is also widely expressed on normal platelets and several non-hematopoietic tissues such as fibroblasts (58, 59). Later in 1991, CD9 was identified as a motility-related protein (MRP-1) to suppress motility and metastasis of multiple cancerous cell lines (60, 61). A significant feature of CD9 is that it tends to interact with various integrins including α1β1, α2β1, α3β1, α4β1, α5β1, α6β1, α6β4, αIIbβ3, and other transmembrane proteins including the EWI family, EGFR and DDR1 within TEMs (62, 63). Therefore, the potential of CD9 to regulate the motility is attributed to the association with these molecules.

CD63, mapped to chromosome region 12p12→12q13, was initially reported as an early stage-specific marker of melanoma progression because of the strong-expression in dysplastic nevi and radial growth phase primary melanoma (64). In histological studies, CD63 is related to melanoma malignancy and is differentially expressed in primary and metastatic lesions (65). However, another report has shown no significant difference in the expression of CD63 between primary and metastatic melanoma (66). Moreover, CD63 is involved in phagocytic and intracellular lysosome-phagosome fusion events (67).

Chen's lab found the expression level of CD9 and CD63 was decreased in gastric cancer. They proposed that CD9 protein level

was inversely associated with lymph node metastasis and the reduction of CD9 was strongly associated with an increasing recurrence risk. Furthermore, the downregulation of CD63 also promotes metastasis and CD63 may serve as a marker for metastatic potential of gastric cancer (67). The mechanism of CD63 and CD9 on regulating motility is reported to be similar and both associate with β1 and β3 integrins (8).

However, in 2018, Miki et al. confirmed that CD9-positive exosomes from cancer-associated fibroblasts (CAFs) increased the migration and invasion abilities of scirrhous-type gastric cancer cells through activating MMP2 (68). And the prognosis of patients with positive CD9 in cancer and/or stromal cells was worse than the patients with dual CD9-negative expression. Their experiments revealed the unique role of CD9 in scirrhous-type gastric cancer.

CD82/KAI1

CD82 was originally discovered from T cell activation study in 1991 (69). In the same year, Ichikawa et al. found CD82 as a metastasis suppressor gene in prostatic cancer (70). Later in 1995, Dong, Isaacs, and Barrett isolated a metastasis suppressor gene from human chromosome 11 p11.2 and designated it as KAI1 which is identical to CD82 (71). CD82/KAI1 associates with the proteins related to cell migration such as cell adhesion molecule, growth factor receptor, and signaling molecule in TEMs (72). Therefore, CD82 suppresses multiple metastasis stages, including cell motility and invasion, proliferation, apoptosis, and senescence (73). Moreover, CD82 promotes homotypic cell-cell adhesion, which plays an important role in suppressing metastasis. For example, overexpressed CD82 promotes E-cadherin-mediated intercellular adhesion in non-small cell lung carcinoma *via* stabilizing E-cadherin/β-catenin complex formation (74). In various solid tumors, many studies have demonstrated that CD82 is a wide-spectrum invasion- and metastasis-suppressor *via* regulating the functions of associated proteins, redistributing the plasma membrane components, post-translational modifications, and inducing apoptosis (72).

The metastasis suppression effect of CD82/KAI1 has also been confirmed in gastric cancer. As early as 1998, Hinoda et al. found CD82 expressed in normal fundic glands and intestinal metaplasia of the stomach but a decreased or lost expression in intestinal-type gastric cancer, especially the less differentiated type. They suggested an inversely relationship between CD82 expression and the progression of gastric cancer. However, whether CD82 is a metastasis suppressor gene in gastric cancer was not verified at that time (75). Later in 2007, decreased expression of CD82 in lymph node and liver metastases of gastric cancer compared with the primary tumors was shown by Yu's lab. Their studies indicated CD82 as a metastasis suppressor in gastric cancer and higher expression of CD82 reduced the metastatic potential (76).

In the same year, Zheng et al. obtained a similar conclusion that the expression of CD82 is negatively associated with liver metastasis of gastrointestinal adenocarcinoma (GIA) (77). However, Zheng's lab found that CD82 was expressed in the gastric hyperplastic gland and up-regulated in GIA, thereby proposing that CD82 was related to a physiological process in the gastrointestinal mucosa. And the overexpression was due to malignant transformation of mucosal epithelial cells or the upregulation of transcriptional regulators of CD82 (77).

In summary, the dominant view is that CD9, CD63, CD82 are metastasis suppressors and are negatively correlated with gastric cancer progression and lymph node metastasis. But interestingly, several recent studies suggest diverse perspectives in this regard. CD9-positive exosomes from CAFs increase the migration abilities of scirrhous-type gastric cancer cells and the prognosis is worse in patients with positive CD9 in cancer cells. In GIA, the expression level of CD82 is upregulated and this overexpression may be attributed to malignant transformation of mucosal epithelial cells. Although these studies are relatively superficial, we have a new understanding of tetraspanins, especially the role in gastric cancer metastasis.

CLINICOPATHOLOGICAL SIGNIFICANCE OF TETRASPANINS IN GASTRIC CANCER

Therapeutics of Gastric Cancer That Target CD9

As mentioned earlier, CD9 has an inhibitory effect on gastric cancer cell migration, and it plays a vital role in the development of gastric cancer, so CD9 may be a potential therapeutic target for gastric cancer. Nakamoto et al. revealed that ALB6, an anti-CD9 mAb, significantly inhibited gastric cancer proliferation, angiogenesis, and promoted apoptosis *in vivo* in a mouse xenograft model of human gastric cancer (78). This anti-CD9 mAb ALB6 could be used to treat gastric cancer for the following reasons. First, the ligation of CD9 with ALB6 enhances the function of CD9 (79). Mechanically, ALB6 treatment-mediated apoptosis is achieved through activating the c-Jun N-terminal kinase/stress-activated protein kinase (JNK/SAPK), p38 mitogen-activated protein kinase (MAPK) and Caspase-3. However, ALB6 induced tyrosines phosphorylation of the p46 Shc isoform and the overexpression of its dominant-negative form inhibit ALB6-induced activation of JNK/SAPK, p38 MAPK, and Caspase-3, which leads to apoptosis suppression (80). Therefore, ALB6 can only limitedly activate p46 Shc isoform to induce apoptotic signals. Moreover, CD9 expression in gastric cancer is higher than non-cancerous tissues, thereby the adverse effects of anti-CD9 mAb therapy might be tolerable (81). In summary, CD9 maybe a powerful potential molecular target for gastric cancer therapy, but there is still a long way to go in improving the effectiveness of the treatment and overcoming the side effects.

Tetraspanins Promote Gastric Cancer Drug Resistance

TSPAN8

A major obstacle in treating gastric cancer is the development of multidrug resistance (MDR) to chemotherapy in cancer cells (82). It is reported that MDR in tumor cells associates with

several signaling pathways, including the Wnt/β-catenin signal pathway in pancreatic cancer (83), the IL-6/STAT3/Jagged-1/Notch axis in gastric cancer (84) and so on. TSPAN8 is a pro-drug resistance protein in gastric cancer cells, while the silencing of TSPAN8 enhances the sensitivity of cancer cells to the cisplatin, 5-FU and adriamycin (85). TSPAN8 activates the Wnt/β-catenin pathway *via* binding to NOTCH2 and increases β-catenin expression and accumulation in the nucleus to form MDR (85). Overall, TSPAN8 inhibitors may be developed as an adjuvant therapy of gastric cancer to reduce the resistance of cancer cells.

TSPAN9

5-Fluorouracil (5-FU) is a chemotherapeutic agent used for various malignant tumors, especially gastrointestinal cancers such as colorectal cancer, gastric adenocarcinoma and pancreatic cancer (86). However, the resistance to 5-FU has become a significant obstacle to the treatment of gastric cancer (87). Recently, Qi et al. demonstrated that 5-FU resistant gastric cancer cells had a high expression of TSPAN9 and TSPAN9 bound to PIK3R3 (p55) to suppress PI3K/Akt/mTOR pathway activation, which promoted autophagy and resulted in 5-FU resistance (88). Therefore, TSPAN9 inhibitors are shedding light for 5-FU-resistant gastric cancer patients.

TSPAN20/UPK1B

It is identified that UPK1B can be used as a biomarker to predict the chemotherapeutic outcomes of capecitabine and oxaliplatin in gastric cancer patients (89). The high expression of UPK1B in adjuvant capecitabine and oxaliplatin treated patients with GC was associated with poor outcomes. Some studies have shown that after knocking down UPK1B in cancer cells, the expression of key genes in the Wnt/β-catenin signaling pathway is inhibited (90). Thus, it is speculated that UPK1B regulates oxaliplatin drug sensitivity through the Wnt/β-catenin signaling pathway.

Tetraspanins Predict the Prognosis of Gastric Cancer

Tetraspanins have important significance in the occurrence, proliferation, invasion, and metastasis of gastric cancer. Different tetraspanins with increased or decreased expression level in cancer tissues can serve as the prognosis factor of gastric cancer (**Table 1**). The expression of TSPAN20/UPK1B (91), TSPAN1 (35), TSPAN8 (92), CD9 (93) and CD151 (30, 94–96) is positively associated with the clinical stage of gastric cancer and indicate a poor prognosis, while TSPAN5 (52), TSPAN21/UPK1A (57), CD82/KAI1 (97–100) are opposite. Especially, TSPAN9 expression is significantly decreased in gastric cancer tissues compared with the adjacent non-cancerous tissues but the high expression of TSPAN9 is associated with a poor prognosis (101). These tetraspanins, as biomarkers, have guiding significance in the diagnosis and prognosis prediction of gastric cancer. It is noteworthy that in previous studies, the overexpression of UPK1B mRNA is associated with laryngeal cancer recurrence (102), but Dai et al. found that UPK1B is negatively correlated with the prognosis of gastric cancer through bioinformatics analysis (91). This suggests that we can make full use of the database and data mining to further explore the functions of other tetraspanins in gastric cancer.

CONCLUSIONS AND FUTURE PROSPECTS

Tetraspanins interact with diverse other molecules and transmembrane proteins in TEMs, as well as in gastric cancer cells. Tetraspanin family can be seen in each stage of the occurrence and development of gastric cancer, from the growth, apoptosis, invasion and metastasis to the molecular targeted therapy and prognosis. Nonetheless, very little was found in the literature on the underlying molecular mechanisms of tetraspanins in gastric

TABLE 1 | Tetraspanins with prognosis prediction of gastric cancer.

		Clinicopathological Factors						
Tetraspanin	**Expression level in GC**	**Tumor size**	**Tumor Differentiation**	**Lymph node Metastasis**	**TNM Stage**	**Clinical Stage (I/II and III/IV)**	**Survival Rate**	**Reference**
TSPAN20	Upregulated						Negative	(91)
TSPAN1	Upregulated		Negative(***)	Positive(***)		Positive (**)	Negative(within 3 years **; within 5 years ***)	(35)
TSPAN8	Upregulated				NS	NS	Negative(***)	(92)
CD9	Upregulated		NS	Positive(***)		Positive (***)		(93)
CD151	Upregulated	NS (94); Positive(**) (30)	Negative(**) (94); Negative(*) (30)		NS (95); Positive(***) (30)		Negative(***) (30, 94–96)	(30, 94–96)
TSPAN5	Downregulated	Negative (***)	NS	Negative(**)	Negative(***)		Positive(***)	(52)
TSPAN21	Downregulated		Positive(**)	Negative(***)	Negative(***)		Positive(**)	(57)
CD82	Downregulated	NS (97, 98)	Positive(***) (97); Positive(*) (99)	Negative(**) (98); Negative(***) (97, 99)	Negative(***) (97, 98)	Negative(***) (99)	Positive(***) (98–100)	(97–100)
TSPAN9	Downregulated	Positive(**)	Negative(**)	Positive(***)	Positive(**)		Negative(***)	(101)

*$p < 0.10$; **$p < 0.05$; ***$p < 0.01$; NS, Not Significant. Positive means a higher expression level of tetraspanins indicating a larger tumor size, higher tumour differentiation, more lymph node metastasis, more advanced TNM stage and clinical stage, a better survival rate. Negative is opposite.*

cancer, increasing the difficulty of its clinical application and targeted therapy. Thus far, the potential candidate therapeutic targets of tetraspanins in gastric cancer have mainly involved mAbs and mRNAs. Animal experiments have shown that ALB6, a mAb targeting CD9, can significantly inhibit the progression of gastric cancer (79, 80). The overexpression of some miRNAs also inhibits the proliferation and invasion of gastric cancer cell *via* targeting tetraspanins [for example, miR-324-5p and TSPAN8 (25), miR-152 and CD151 (31), miR-573 and TSPAN1 (36)]. Therefore, using these mAbs or upregulating the expression level of these miRNAs might be beneficial for the treatment of gastric cancer. Tetraspanins can also be used as therapeutic targets to overcome drug resistance or to increase drug sensitivity. However, research in clinical application is in its infancy, and there is still a long way to go before biological agents targeting tetraspanins are applied in clinical practice. Though the clinical researches of tetraspanins and gastric cancer are a drop in the bucket, we are still looking forward to more studies to reveal deep connection between tetraspanin family and gastric cancer, so as to find more potential and powerful therapeutic targets of gastric cancer.

AUTHOR CONTRIBUTIONS

YD and SC designed and wrote all the sections of the manuscript. JS contributed to the data collection. HP supervised and revised the review. All authors contributed to the article and approved the submitted version.

FUNDING

This study was conducted with the support by the National Natural Science Foundation of China (Grant Nos. 82073400).

ACKNOWLEDGMENTS

We would like to thank Jun Zhao for his support and discussion of the manuscript, and Wei Wang for discussion of manuscript preparations.

REFERENCES

1. Smyth EC, Nilsson M, Grabsch HI, van Grieken NC, Lordick F. Gastric Cancer. *Lancet (London England)* (2020) 396:635–48. doi: 10.1016/s0140-6736(20)31288-5
2. Jemal A, Bray F, Center MM, Ferlay J, Ward E, Forman D. Global Cancer Statistics. *CA Cancer J Clin* (2011) 61:69–90. doi: 10.3322/caac.20107
3. Torre LA, Bray F, Siegel RL, Ferlay J, Lortet-Tieulent J, Jemal A. Global Cancer Statistics, 2012. *CA Cancer J Clin* (2015) 65:87–108. doi: 10.3322/caac.21262
4. Maecker HT, Todd SC, Levy S. The Tetraspanin Superfamily: Molecular Facilitators. *FASEB J* (1997) 11:428–42. doi: 10.1007/s007920050022
5. Stipp CS, Kolesnikova TV, Hemler ME. Functional Domains in Tetraspanin Proteins. *Trends Biochem Sci* (2003) 28:106–12. doi: 10.1016/s0968-0004(02)00014-2
6. Charrin S, le Naour F, Silvie O, Milhiet PE, Boucheix C, Rubinstein E. Lateral Organization of Membrane Proteins: Tetraspanins Spin Their Web. *Biochem J* (2009) 420:133–54. doi: 10.1042/bj20082422
7. The Human Protein Atlas. (2021). Available at: https://www.proteinatlas.org/search/tetraspanin (Accessed May 29, 2021).
8. Hemler ME. Tetraspanin Functions and Associated Microdomains. *Nat Rev Mol Cell Biol* (2005) 6:801–11. doi: 10.1038/nrm1736
9. Yáñez-Mó M, Barreiro O, Gordon-Alonso M, Sala-Valdés M, Sánchez-Madrid F. Tetraspanin-Enriched Microdomains: A Functional Unit in Cell Plasma Membranes. *Trends Cell Biol* (2009) 19:434–46. doi: 10.1016/j.tcb.2009.06.004
10. Hemler ME. Tetraspanin Proteins Promote Multiple Cancer Stages. *Nat Rev Cancer* (2014) 14:49–60. doi: 10.1038/nrc3640
11. Kanetaka K, Sakamoto M, Yamamoto Y, Yamasaki S, Lanza F, Kanematsu T, et al. Overexpression of Tetraspanin CO-029 in Hepatocellular Carcinoma. *J Hepatol* (2001) 35:637–42. doi: 10.1016/s0168-8278(01)00183-0
12. Gesierich S, Paret C, Hildebrand D, Weitz J, Zgraggen K, Schmitz-Winnenthal FH, et al. Colocalization of the Tetraspanins, CO-029 and CD151, With Integrins in Human Pancreatic Adenocarcinoma: Impact on Cell Motility. *Clin Cancer Res* (2005) 11:2840–52. doi: 10.1158/1078-0432.ccr-04-1935
13. Greco C, Bralet MP, Ailane N, Dubart-Kupperschmitt A, Rubinstein E, Le Naour F, et al. E-Cadherin/p120-Catenin and Tetraspanin Co-029 Cooperate for Cell Motility Control in Human Colon Carcinoma. *Cancer Res* (2010) 70:7674–83. doi: 10.1158/0008-5472.can-09-4482
14. Voglstaetter M, Thomsen AR, Nouvel J, Koch A, Jank P, Navarro EG, et al. Tspan8 Is Expressed in Breast Cancer and Regulates E-Cadherin/Catenin Signalling and Metastasis Accompanied by Increased Circulating Extracellular Vesicles. *J Pathol* (2019) 248:421–37. doi: 10.1002/path.5281
15. Zoller M. Tetraspanins: Push and Pull in Suppressing and Promoting Metastasis. *Nat Rev Cancer* (2009) 9:40–55. doi: 10.1038/nrc2543
16. Bonnet M, Maisonial-Besset A, Zhu Y, Witkowski T, Roche G, Boucheix C, et al. Targeting the Tetraspanins With Monoclonal Antibodies in Oncology: Focus on TSPAN8/Co-029. *Cancers* (2019) 11:179. doi: 10.3390/cancers11020179
17. Gesierich S, Berezovskiy I, Ryschich E, Zoller M. Systemic Induction of the Angiogenesis Switch by the Tetraspanin D6.1A/CO-029. *Cancer Res* (2006) 66:7083–94. doi: 10.1158/0008-5472.can-06-0391
18. Claas C, Seiter S, Claas A, Savelyeva L, Schwab M, Zoller M. Association Between the Rat Homologue of CO-029, A Metastasis-Associated Tetraspanin Molecule and Consumption Coagulopathy. *J Cell Biol* (1998) 141:267–80. doi: 10.1083/jcb.141.1.267
19. Yue S, Zhao K, Erb U, Rana S, Zöller M. Joint Features and Complementarities of TSPAN8 and CD151 Revealed in Knockdown and Knockout Models. *Biochem Soc Trans* (2017) 45:437–47. doi: 10.1042/bst20160298
20. Andreu Z, Yanez-Mo M. Tetraspanins in Extracellular Vesicle Formation and Function. *Front Immunol* (2014) 5:442. doi: 10.3389/fimmu.2014.00442
21. Matsumura N, Zembutsu H, Yamaguchi K, Sasaki K, Tsuruma T, Nishidate T, et al. Identification of Novel Molecular Markers for Detection of Gastric Cancer Cells in the Peripheral Blood Circulation Using Genome-Wide Microarray Analysis. *Exp Ther Med* (2011) 2:705–13. doi: 10.3892/etm.2011.252
22. Mottaghi-Dastjerdi N, Soltany-Rezaee-Rad M, Sepehrizadeh Z, Roshandel G, Ebrahimifard F, Setayesh N. Identification of Novel Genes Involved in Gastric Carcinogenesis by Suppression Subtractive Hybridization. *Hum Exp Toxicol* (2015) 34:3–11. doi: 10.1177/0960327114532386
23. Zhu H, Wu Y, Zheng W, Lu S. Co-029 Is Overexpressed in Gastric Cancer and Mediates the Effects of EGF on Gastric Cancer Cell Proliferation and Invasion. *Int J Mol Med* (2015) 35:798–802. doi: 10.3892/ijmm.2015.2069
24. Wei L, Li Y, Suo Z. TSPAN8 Promotes Gastric Cancer Growth and Metastasis Via ERK MAPK Pathway. *Int J Clin Exp Med* (2015) 8:8599–607.
25. Lin H, Zhou AJ, Zhang JY, Liu SF, Gu JX. MiR-324-5p Reduces Viability and Induces Apoptosis in Gastric Cancer Cells Through Modulating TSPAN8. *J Pharm Pharmacol* (2018) 70:1513–20. doi: 10.1111/jphp.12995

26. Sincock PM, Mayrhofer G, Ashman LK. Localization of the Transmembrane 4 Superfamily (TM4SF) Member PETA-3 (CD151) in Normal Human Tissues: Comparison With CD9, CD63, and alpha5beta1 Integrin. *J Histochem Cytochem* (1997) 45:515–25. doi: 10.1177/002215549704500404
27. Wang HX, Li Q, Sharma C, Knoblich K, Hemler ME. Tetraspanin Protein Contributions to Cancer. *Biochem Soc Trans* (2011) 39:547–52. doi: 10.1042/bst0390547
28. Karamatic Crew V, Burton N, Kagan A, Green CA, Levene C, Flinter F, et al. CD151, the First Member of the Tetraspanin (TM4) Superfamily Detected on Erythrocytes, Is Essential for the Correct Assembly of Human Basement Membranes in Kidney and Skin. *Blood* (2004) 104:2217–23. doi: 10.1182/blood-2004-04-1512
29. Ke AW, Shi GM, Zhou J, Wu FZ, Ding ZB, Hu MY, et al. Role of Overexpression of CD151 and/or c-Met in Predicting Prognosis of Hepatocellular Carcinoma. *Hepatol (Baltimore Md)* (2009) 49:491–503. doi: 10.1002/hep.22639
30. Yang YM, Zhang ZW, Liu QM, Sun YF, Yu JR, Xu WX. Overexpression of CD151 Predicts Prognosis in Patients With Resected Gastric Cancer. *PloS One* (2013) 8:e58990. doi: 10.1371/journal.pone.0058990
31. Zhai R, Kan X, Wang B, Du H, Long Y, Wu H, et al. miR-152 Suppresses Gastric Cancer Cell Proliferation and Motility by Targeting CD151. *Tumour Biol* (2014) 35:11367–73. doi: 10.1007/s13277-014-2471-2
32. Ding J, Li D, Gong M, Wang J, Huang X, Wu T, et al. Expression and Clinical Significance of the Long Non-Coding RNA PVT1 in Human Gastric Cancer. *Onco Targets Ther* (2014) 7:1625–30. doi: 10.2147/ott.s68854
33. Li T, Meng XL, Yang WQ. Long Noncoding RNA PVT1 Acts as a "Sponge" to Inhibit microRNA-152 in Gastric Cancer Cells. *Dig Dis Sci* (2017) 62:3021–8. doi: 10.1007/s10620-017-4508-z
34. Serru V, Dessen P, Boucheix C, Rubinstein E. Sequence and Expression of Seven New Tetraspans. *Biochim Biophys Acta* (2000) 1478:159–63. doi: 10.1016/s0167-4838(00)00022-4
35. Chen L, Li X, Wang GL, Wang Y, Zhu YY, Zhu J. Clinicopathological Significance of Overexpression of TSPAN1, Ki67 and CD34 in Gastric Carcinoma. *Tumori* (2008) 94:531–8. doi: 10.1177/030089160809400415
36. Lu Z, Luo T, Nie M, Pang T, Zhang X, Shen X, et al. TSPAN1 Functions as an Oncogene in Gastric Cancer and Is Downregulated by miR-573. *FEBS Lett* (2015) 589:1988–94. doi: 10.1016/j.febslet.2015.05.044
37. Qi W, Sun L, Liu N, Zhao S, Lv J, Qiu W. Tetraspanin Family Identified as the Central Genes Detected in Gastric Cancer Using Bioinformatics Analysis. *Mol Med Rep* (2018) 18:3599–610. doi: 10.3892/mmr.2018.9360
38. Andria ML, Hsieh CL, Oren R, Francke U, Levy S. Genomic Organization and Chromosomal Localization of the TAPA-1 Gene. *J Immunol (Baltimore Md 1950)* (1991) 147:1030–6. doi: 10.1515/crll.1993.442.91
39. Oren R, Takahashi S, Doss C, Levy R, Levy S. TAPA-1, the Target of an Antiproliferative Antibody, Defines a New Family of Transmembrane Proteins. *Mol Cell Biol* (1990) 10:4007–15. doi: 10.1128/mcb.10.8.4007
40. Levy S, Todd SC, Maecker HT. CD81 (TAPA-1): A Molecule Involved in Signal Transduction and Cell Adhesion in the Immune System. *Annu Rev Immunol* (1998) 16:89–109. doi: 10.1146/annurev.immunol.16.1.89
41. Tedder TF, Inaoki M, Sato S. The CD19-CD21 Complex Regulates Signal Transduction Thresholds Governing Humoral Immunity and Autoimmunity. *Immunity* (1997) 6:107–18. doi: 10.1016/s1074-7613(00)80418-5
42. Todd SC, Lipps SG, Crisa L, Salomon DR, Tsoukas CD. CD81 Expressed on Human Thymocytes Mediates Integrin Activation and Interleukin 2-Dependent Proliferation. *J Exp Med* (1996) 184:2055–60. doi: 10.1084/jem.184.5.2055
43. Rubinstein E, Ziyyat A, Prenant M, Wrobel E, Wolf JP, Levy S, et al. Reduced Fertility of Female Mice Lacking CD81. *Dev Biol* (2006) 290:351–8. doi: 10.1016/j.ydbio.2005.11.031
44. Charrin S, Latil M, Soave S, Polesskaya A, Chretien F, Boucheix C, et al. Normal Muscle Regeneration Requires Tight Control of Muscle Cell Fusion by Tetraspanins CD9 and CD81. *Nat Commun* (2013) 4:1674. doi: 10.1038/ncomms2675
45. Pileri P, Uematsu Y, Campagnoli S, Galli G, Falugi F, Petracca R, et al. Binding of Hepatitis C Virus to CD81. *Science (New York NY)* (1998) 282:938–41. doi: 10.1126/science.282.5390.938
46. Luo RF, Zhao S, Tibshirani R, Myklebust JH, Sanyal M, Fernandez R, et al. CD81 Protein Is Expressed at High Levels in Normal Germinal Center B Cells and in Subtypes of Human Lymphomas. *Hum Pathol* (2010) 41:271–80. doi: 10.1016/j.humpath.2009.07.022
47. Muzzafar T, Medeiros LJ, Wang SA, Brahmandam A, Thomas DA, Jorgensen JL. Aberrant Underexpression of CD81 in Precursor B-Cell Acute Lymphoblastic Leukemia: Utility in Detection of Minimal Residual Disease by Flow Cytometry. *Am J Clin Pathol* (2009) 132:692–8. doi: 10.1309/ajcp02rpvoktnwec
48. Yoo TH, Ryu BK, Lee MG, Chi SG. CD81 Is a Candidate Tumor Suppressor Gene in Human Gastric Cancer. *Cell Oncol (Dordr)* (2013) 36:141–53. doi: 10.1007/s13402-012-0119-z
49. Xu L, Hou Y, Tu G, Chen Y, Du YE, Zhang H, et al. Nuclear Drosha Enhances Cell Invasion Via an EGFR-ERK1/2-MMP7 Signaling Pathway Induced by Dysregulated miRNA-622/197 and Their Targets LAMC2 and CD82 in Gastric Cancer. *Cell Death Dis* (2017) 8:e2642. doi: 10.1038/cddis.2017.5
50. Garcia-Frigola C, Burgaya F, Calbet M, de Lecea L, Soriano E. Mouse Tspan-5, a Member of the Tetraspanin Superfamily, Is Highly Expressed in Brain Cortical Structures. *Neuroreport* (2000) 11:3181–5. doi: 10.1097/00001756-200009280-00027
51. Iwai K, Ishii M, Ohshima S, Miyatake K, Saeki Y. Expression and Function of Transmembrane-4 Superfamily (Tetraspanin) Proteins in Osteoclasts: Reciprocal Roles of Tspan-5 and NET-6 During Osteoclastogenesis. *Allergol Int* (2007) 56:457–63. doi: 10.2332/allergolint.O-07-488
52. He P, Wang S, Zhang X, Gao Y, Li J-L. TSPAN5 Is an Independent Favourable Prognostic Factor and Suppresses Tumour Growth in Gastric Cancer. *Oncotarget* (2016) 7:40160–73. doi: 10.18632/oncotarget.9514
53. Protty MB, Watkins NA, Colombo D, Thomas SG, Heath VL, Herbert JM, et al. Identification of TSPAN9 as a Novel Platelet Tetraspanin and the Collagen Receptor GPVI as a Component of Tetraspanin Microdomains. *Biochem J* (2009) 417:391–400. doi: 10.1042/bj20081126
54. Li PY, Lv J, Qi WW, Zhao SF, Sun LB, Liu N, et al. Tspan9 Inhibits the Proliferation, Migration and Invasion of Human Gastric Cancer SGC7901 Cells Via the ERK1/2 Pathway. *Oncol Rep* (2016) 36:448–54. doi: 10.3892/or.2016.4805
55. Qi Y, Lv J, Liu S, Sun L, Wang Y, Li H, et al. TSPAN9 and EMILIN1 Synergistically Inhibit the Migration and Invasion of Gastric Cancer Cells by Increasing TSPAN9 Expression. *BMC Cancer* (2019) 19:630. doi: 10.1186/s12885-019-5810-2
56. Kong KL, Kwong DL, Fu L, Chan TH, Chen L, Liu H, et al. Characterization of a Candidate Tumor Suppressor Gene Uroplakin 1A in Esophageal Squamous Cell Carcinoma. *Cancer Res* (2010) 70:8832–41. doi: 10.1158/0008-5472.Can-10-0779
57. Zheng Y, Wang DD, Wang W, Pan K, Huang CY, Li YF, et al. Reduced Expression of Uroplakin 1A Is Associated With the Poor Prognosis of Gastric Adenocarcinoma Patients. *PloS One* (2014) 9:e93073. doi: 10.1371/journal.pone.0093073
58. Jones NH, Borowitz MJ, Metzgar RS. Characterization and Distribution of a 24,000-Molecular Weight Antigen Defined by a Monoclonal Antibody (DU-ALL-1) Elicited to Common Acute Lymphoblastic Leukemia (cALL) Cells. *Leuk Res* (1982) 6:449–64. doi: 10.1016/0145-2126(82)90002-9
59. Morrish DW, Shaw AR, Seehafer J, Bhardwaj D, Paras MT. Preparation of Fibroblast-Free Cytotrophoblast Cultures Utilizing Differential Expression of the CD9 Antigen. *In Vitro Cell Dev Biol* (1991) 27a:303–6. doi: 10.1007/bf02630907
60. Miyake M, Koyama M, Seno M, Ikeyama S. Identification of the Motility-Related Protein (MRP-1), Recognized by Monoclonal Antibody M31-15, Which Inhibits Cell Motility. *J Exp Med* (1991) 174:1347–54. doi: 10.1084/jem.174.6.1347
61. Ikeyama S, Koyama M, Yamaoko M, Sasada R, Miyake M. Suppression of Cell Motility and Metastasis by Transfection With Human Motility-Related Protein (MRP-1/CD9) DNA. *J Exp Med* (1993) 177:1231–7. doi: 10.1084/jem.177.5.1231
62. Berditchevski F. Complexes of Tetraspanins With Integrins: More Than Meets the Eye. *J Cell Sci* (2001) 114:4143–51. doi: 10.1038/embor.2012.135

63. Powner D, Kopp PM, Monkley SJ, Critchley DR, Berditchevski F. Tetraspanin CD9 in Cell Migration. *Biochem Soc Trans* (2011) 39:563–7. doi: 10.1042/bst0390563
64. Hotta H, Ross AH, Huebner K, Isobe M, Wendeborn S, Chao MV, et al. Molecular Cloning and Characterization of an Antigen Associated With Early Stages of Melanoma Tumor Progression. *Cancer Res* (1988) 48:2955–62.
65. Atkinson B, Ernst CS, Ghrist BF, Herlyn M, Blaszczyk M, Ross AH, et al. Identification of Melanoma-Associated Antigens Using Fixed Tissue Screening of Antibodies. *Cancer Res* (1984) 44:2577–81.
66. Barrio MM, Bravo AI, Portela P, Hersey P, Mordoh J. A New Epitope on Human Melanoma-Associated Antigen CD63/ME491 Expressed by Both Primary and Metastatic Melanoma. *Hybridoma* (1998) 17:355–64. doi: 10.1089/hyb.1998.17.355
67. Chen Z, Gu S, Trojanowicz B, Liu N, Zhu G, Dralle H, et al. Down-Regulation of TM4SF Is Associated With the Metastatic Potential of Gastric Carcinoma TM4SF Members in Gastric Carcinoma. *World J Surg Oncol* (2011) 9:43. doi: 10.1186/1477-7819-9-43
68. Miki Y, Yashiro M, Okuno T, Kitayama K, Masuda G, Hirakawa K, et al. CD9-Positive Exosomes From Cancer-Associated Fibroblasts Stimulate the Migration Ability of Scirrhous-Type Gastric Cancer Cells. *Br J Cancer* (2018) 118:867–77. doi: 10.1038/bjc.2017.487
69. Gaugitsch HW, Hofer E, Huber NE, Schnabl E, Baumruker T. A New Superfamily of Lymphoid and Melanoma Cell Proteins With Extensive Homology to Schistosoma Mansoni Antigen Sm23. *Eur J Immunol* (1991) 21:377–83. doi: 10.1002/eji.1830210219
70. Ichikawa T, Ichikawa Y, Isaacs JT. Genetic Factors and Suppression of Metastatic Ability of Prostatic Cancer. *Cancer Res* (1991) 51:3788–92. doi: 10.1002/1097-0142(19910715)68:2<451::AID-CNCR2820680241>3.0.CO;2
71. Dong JT, Lamb PW, Rinker-Schaeffer CW, Vukanovic J, Ichikawa T, Isaacs JT, et al. KAI1, A Metastasis Suppressor Gene for Prostate Cancer on Human Chromosome 11p11.2. *Science (New York NY)* (1995) 268:884–6. doi: 10.1126/science.7754374
72. Liu WM, Zhang XA. KAI1/CD82, a Tumor Metastasis Suppressor. *Cancer Lett* (2006) 240:183–94. doi: 10.1016/j.canlet.2005.08.018
73. Tsai YC, Weissman AM. Dissecting the Diverse Functions of the Metastasis Suppressor CD82/KAI1. *FEBS Lett* (2011) 585:3166–73. doi: 10.1016/j.febslet.2011.08.031
74. Abe M, Sugiura T, Takahashi M, Ishii K, Shimoda M, Shirasuna K. A Novel Function of CD82/KAI-1 on E-Cadherin-Mediated Homophilic Cellular Adhesion of Cancer Cells. *Cancer Lett* (2008) 266:163–70. doi: 10.1016/j.canlet.2008.02.058
75. Hinoda Y, Adachi Y, Takaoka A, Mitsuuchi H, Satoh Y, Itoh F, et al. Decreased Expression of the Metastasis Suppressor Gene KAI1 in Gastric Cancer. *Cancer Lett* (1998) 129:229. doi: 10.1016/S0304-3835(98)00112-8
76. Guan-Zhen Y, Ying C, Can-Rong N, Guo-Dong W, Jian-Xin Q, Jie-Jun W. Reduced Protein Expression of Metastasis-Related Genes (nm23, KISS1, KAI1 and p53) in Lymph Node and Liver Metastases of Gastric Cancer. *Int J Exp Pathol* (2007) 88:175–83. doi: 10.1111/j.1365-2613.2006.00510.x
77. Zheng H, Tsuneyama K, Cheng C, Takahashi H, Cui Z, Nomoto K, et al. Expression of KAI1 and Tenascin, and Microvessel Density Are Closely Correlated With Liver Metastasis of Gastrointestinal Adenocarcinoma. *J Clin Pathol* (2007) 60:50–6. doi: 10.1136/jcp.2006.036699
78. Nakamoto T, Murayama Y, Oritani K, Boucheix C, Rubinstein E, Nishida M, et al. A Novel Therapeutic Strategy With Anti-CD9 Antibody in Gastric Cancers. *J Gastroenterol* (2009) 44:889–96. doi: 10.1007/s00535-009-0081-3
79. Murayama Y, Oritani K, Tsutsui S. Novel CD9-Targeted Therapies in Gastric Cancer. *World J Gastroenterol* (2015) 21:3206–13. doi: 10.3748/wjg.v21.i11.3206
80. Murayama Y, Miyagawa J, Oritani K, Yoshida H, Yamamoto K, Kishida O, et al. CD9-Mediated Activation of the P46 Shc Isoform Leads to Apoptosis in Cancer Cells. *J Cell Sci* (2004) 117:3379–88. doi: 10.1242/jcs.01201
81. Liu LX, Liu ZH, Jiang HC, Qu X, Zhang WH, Wu LF, et al. Profiling of Differentially Expressed Genes in Human Gastric Carcinoma by cDNA Expression Array. *World J Gastroenterol* (2002) 8:580–5. doi: 10.3748/wjg.v8.i4.580
82. Zhang D, Fan D. Multidrug Resistance in Gastric Cancer: Recent Research Advances and Ongoing Therapeutic Challenges. *Expert Rev Anticancer Ther* (2007) 7:1369–78. doi: 10.1586/14737140.7.10.1369
83. Cui J, Jiang W, Wang S, Wang L, Xie K. Role of Wnt/beta-catenin Signaling in Drug Resistance of Pancreatic Cancer. *Curr Pharm Des* (2012) 18:2464–71. doi: 10.2174/13816128112092464
84. Yang Z, Guo L, Liu D, Sun L, Chen H, Deng Q, et al. Acquisition of Resistance to Trastuzumab in Gastric Cancer Cells Is Associated With Activation of IL-6/STAT3/Jagged-1/Notch Positive Feedback Loop. *Oncotarget* (2015) 6:5072–87. doi: 10.18632/oncotarget.3241
85. Li L, Yang D, Cui D, Li Y, Nie Z, Wang J, et al. Quantitative Proteomics Analysis of the Role of Tetraspanin-8 in the Drug Resistance of Gastric Cancer. *Int J Oncol* (2018) 52:473–84. doi: 10.3892/ijo.2017.4231
86. Leelakanok N, Geary S, Salem A. Fabrication and Use of Poly(d,l-lactide-co-glycolide)-Based Formulations Designed for Modified Release of 5-Fluorouracil. *J Pharm Sci* (2018) 107:513–28. doi: 10.1016/j.xphs.2017.10.012
87. Park JB, Lee JS, Lee MS, Cha EY, Kim S, Sul JY. Corosolic Acid Reduces 5FU Chemoresistance in Human Gastric Cancer Cells by Activating AMPK. *Mol Med Rep* (2018) 18:2880–8. doi: 10.3892/mmr.2018.9244
88. Qi Y, Qi W, Liu S, Sun L, Ding A, Yu G, et al. TSPAN9 Suppresses the Chemosensitivity of Gastric Cancer to 5-Fluorouracil by Promoting Autophagy. *Cancer Cell Int* (2020) 20:4. doi: 10.1186/s12935-019-1089-2
89. Zhang Y, Yuan Z, Shen R, Jiang Y, Xu W, Gu M, et al. Identification of Biomarkers Predicting the Chemotherapeutic Outcomes of Capecitabine and Oxaliplatin in Patients With Gastric Cancer. *Oncol Lett* (2020) 20:290. doi: 10.3892/ol.2020.12153
90. Wang FH, Ma XJ, Xu D, Luo J. UPK1B Promotes the Invasion and Metastasis of Bladder Cancer Via Regulating the Wnt/β-Catenin Pathway. *Eur Rev Med Pharmacol Sci* (2018) 22:5471–80. doi: 10.26355/eurrev_201809_15807
91. Dai J, Li ZX, Zhang Y, Ma JL, Zhou T, You WC, et al. Whole Genome Messenger RNA Profiling Identifies a Novel Signature to Predict Gastric Cancer Survival. *Clin Trans Gastroenterol* (2019) 10:e00004. doi: 10.14309/ctg.0000000000000004
92. Anami K, Oue N, Noguchi T, Sakamoto N, Sentani K, Hayashi T, et al. TSPAN8, Identified by Escherichia Coli Ampicillin Secretion Trap, Is Associated With Cell Growth and Invasion in Gastric Cancer. *Gastric Cancer* (2016) 19:370–80. doi: 10.1007/s10120-015-0478-z
93. Hori H, Yano S, Koufuji K, Takeda J, Shirouzu K. CD9 Expression in Gastric Cancer and its Significance. *J Surg Res* (2004) 117:208–15. doi: 10.1016/j.jss.2004.01.014
94. Ha SY, Do IG, Lee J, Park SH, Park JO, Kang WK, et al. CD151 Overexpression Is Associated With Poor Prognosis in Patients With pT3 Gastric Cancer. *Ann Surg Oncol* (2014) 21:1099–106. doi: 10.1245/s10434-013-3339-1
95. Kang BW, Lee D, Chung HY, Han JH, Kim YB. Tetraspanin CD151 Expression Associated With Prognosis for Patients With Advanced Gastric Cancer. *J Cancer Res Clin Oncol* (2013) 139:1835–43. doi: 10.1007/s00432-013-1503-4
96. Zeng P, Wang YH, Si M, Gu JH, Li P. Tetraspanin CD151 as an Emerging Potential Poor Prognostic Factor Across Solid Tumors: A Systematic Review and Metaanalysis. *Oncotarget* (2015) 8:5592–602. doi: 10.18632/oncotarget.13532
97. Ilhan O, Celik SY, Han U, Onal B. Use of KAI-1 as a Prognostic Factor in Gastric Carcinoma. *Eur J Gastroenterol Hepatol* (2009) 21:1369–72. doi: 10.1097/MEG.0b013e328323aac9
98. Lu G, Zhou L, Zhang X, Zhu B, Wu S, Song W, et al. The Expression of Metastasis-Associated in Colon Cancer-1 and KAI1 in Gastric Adenocarcinoma and Their Clinical Significance. *World J Surg Oncol* (2016) 14:276. doi: 10.1186/s12957-016-1033-z
99. Knoener M, Krech T, Puls F, Lehmann U, Kreipe H, Christgen M. Limited Value of KAI1/CD82 Protein Expression as a Prognostic Marker in Human Gastric Cancer. *Dis Markers* (2012) 32:337–42. doi: 10.3233/DMA-2012-0896
100. Lee HS, Lee HK, Kim HS, Yang HK, Kim WH. Tumour Suppressor Gene Expression Correlates With Gastric Cancer Prognosis. *J Pathol* (2003) 200:39–46. doi: 10.1002/path.1288
101. Feng T, Sun L, Qi W, Pan F, Lv J, Guo J, et al. Prognostic Significance of Tspan9 in Gastric Cancer. *Mol Clin Oncol* (2016) 5:231–6. doi: 10.3892/mco.2016.961

102. Su J, Zhang Y, Su H, Zhang C, Li W. A Recurrence Model for Laryngeal Cancer Based on SVM and Gene Function Clustering. *Acta Otolaryngol* (2017) 137:557–62. doi: 10.1080/00016489.2016.1247984

Conflict of Interest: The authors declare that the research was conducted in the absence of any commercial or financial relationships that could be construed as a potential conflict of interest.

frontiers in Oncology

ORIGINAL RESEARCH
published: 27 October 2021
doi: 10.3389/fonc.2021.605894

miR-17-5p and miR-4443 Promote Esophageal Squamous Cell Carcinoma Development by Targeting TIMP2

Xiaojun Wang[1†], Jiayi Han[2†], Yatian Liu[3†], Jingwen Hu[1†], Ming Li[1], Xi Chen[4*] and Lin Xu[1*]*

[1] Department of Thoracic Surgery, Nanjing Medical University Affiliated Cancer Hospital and Jiangsu Cancer Hospital and Jiangsu Institute of Cancer Research, Cancer Institute of Jiangsu Province, Nanjing, China, [2] Tianjin Medical University Cancer Institute and Hospital, National Clinical Research Center for Cancer, Tianjin's Clinical Research Center for Cancer, Key Laboratory of Cancer Prevention and Therapy, Tianjin Medical University, Tianjin, China, [3] Department of Radiotherapy, The Affiliated Cancer Hospital of Nanjing Medical University & Jiangsu Cancer Hospital & Jiangsu Institute of Cancer Research, Nanjing, China, [4] State Key Laboratory of Pharmaceutical Biotechnology, Collaborative Innovation Center of Chemistry for Life Sciences, Jiangsu Engineering Research Center for MicroRNA Biology and Biotechnology, NJU Advanced Institute for Life Sciences (NAILS), School of Life Sciences, Nanjing University, Nanjing, Jiangsu, China

Background: Esophageal squamous cell carcinoma (ESCC) is one of the most frequently diagnosed cancers in the world with a high mortality rate. The mechanism about ESCC development and whether miRNAs play a critical role remains unclear and needs carefully elucidated.

Materials and Methods: High-throughput miRNA sequencing was used to identify the different expression miRNAs between the ESCC tissues and paired adjacent normal tissues. Next, both CCK-8, Transwell and apotosis assay were used to evaluate the role of miRNA in ESCCcells. In addition, we used bioinformatic tools to predict the potential target of the miRNAs and verified by Western Blot. The function of miRNA-target network was further identified in xenograft mice model.

Results: In ESCC, we identified two miRNAs, miR-17-5p and miR-4443, were significantly upregulated in ESCC tissues than adjacent normal tissues. TIMP2 was proved to be the direct target of both two miRNAs. The miR-17-5p/4443- TIMP2 axis was shown to promote the tumor progression *in vitro* and *in vivo* experiments.

Conclusions: This study highlights two oncomiRs, miR-17-5p and miR-4443, and its potential role in ESCC progression by regulating TIMP2 expression, suggesting miR-17-5p and miR-4443 may serve as a novel molecular target for ESCC treatment.

Keywords: miR-17-5p, miR-4443, ESCC, TIMP2, cancer development

OPEN ACCESS

Edited by:
Wen Wen Xu,
Jinan University, China

Reviewed by:
Mingxin Zhang,
First Affiliated Hospital of Xi'an Medical University, China
Yan Xin,
Nanjing Drum Tower Hospital, China
Yanbo Wang,
Nanjing University, China
Suna Zhou,
Wenzhou Medical University, China

***Correspondence:**
Lin Xu
xulin83cn@gmail.com
Xi Chen
xichen@nju.edu.cn
Xiaojun Wang
doctorwxj326@hotmail.com

†These authors have contributed equally to this work

Specialty section:
This article was submitted to Gastrointestinal Cancers, a section of the journal Frontiers in Oncology

Received: *13 September 2020*
Accepted: *05 October 2021*
Published: *27 October 2021*

Citation:
Wang X, Han J, Liu Y, Hu J, Li M, Chen X and Xu L (2021) miR-17-5p and miR-4443 Promote Esophageal Squamous Cell Carcinoma Development by Targeting TIMP2. Front. Oncol. 11:605894. doi: 10.3389/fonc.2021.605894

INTRODUCTION

Esophageal cancer (EC), one of the most frequently diagnosed cancers in the world, has the highest incidence rate in Eastern Asia (1). It has two main components: esophageal squamous cell carcinoma (ESCC, for about 80% of all ECs), and esophageal adenocarcinoma (for about 20% of all ECs). Due to the development of diagnosis and treatment techniques, the prognosis of ECs has been improved in the past decades. But it's still far from satisfactory for its high recurrence rate and poor 5-year survival rate. Research indicates that over 80% of EC patients were dead within 5 years (2). Thus, exploring the key factors that cause the occurrence and development of EC may give evidence to the clinical treatment and improve the prognosis of EC.

MicroRNAs (miRNAs), which consisting of 18-22 nucleotide base pairs, has been verified to play important roles in regulating gene expression (3). The abnormal expression of miRNAs has been found in almost all kinds of tumors including EC (4). miRNA can play an oncogenic role or a tumor-suppressive role to affect the proliferation, migration or apoptosis of tumor cells. Among them, overexpression of miR-17-5p has been reported in various human cancers, including breast cancer (5), prostate cancer (6), hepatocellular carcinoma (7), pancreatic cancer (8), gastric cancer (9) and so on. Besides, miR-4443 was also shown to be upregulated in lung cancer (10) and breast cancer (11). It's has also been reported that miR-17-5p can directly target ETV resulting in suppressing cell proliferation and invasion in triple-negative breast cancer (12), while it can also enhance cell proliferation in pancreatic cancer by targeting RBL2/E2F4 (13). However, the precise role of miR-17-5p and miR-4443 in EC has not been fully understood.

In this study, we identified the overexpression of miR-17-5p and miR-4443 in EC tissues compared to their paired adjacent tissues. Overexpression of miR-17-5p and miR-4443 promote EC cells' proliferation and migration as well as reduces the expression of TIMP2, while down-regulation of miR-17-5p and miR-4443 got the opposite effect. We testified the important roles of miR-17-5p and miR-4443 in the development of EC and these results may provide new strategies for ESCC treatment.

MATERIAL AND METHODS

Tissues Specimens and Cell Lines

20 ESCC tissue samples and their paired adjacent paratumor normal tissues were collected from Jiangsu Cancer Hospital (Nanjing, Jiangsu, China). All patients signed the informed consents and the Ethics Committee of the Jiangsu Cancer Hospital approves the whole study. The protocol used in this study was based on approved guidelines by Ethics Committee of the Jiangsu Cancer Hospital. All patients were diagnosed ESCC by histopathology examination, and none of them had diagnosed other malignant tumor or received neoadjuvant chemotherapy or radiotherapy. All samples were immediately cut into small pieces after surgical resection and keep in liquid nitrogen until use.

The human esophageal cancer cell line, TE-10, and ECA-109 were purchased from Cell Bank of Chinese Academy of Science, Shanghai, China. All cells were cultured in RPMI-1640 (Gibco Life Technologies, Waltham, MA USA) containing 10% fetal bovine serum (FBS), 100 units/mL penicillin, and 100ug/mL streptomycin. The humidified incubator was set at 37°C containing 5% CO2.

High-Throughput miRNA Sequencing

Total RNA extracted from 3 ESCC tissues and its paired adjacent normal tissues were used for high-throughput miRNA sequencing. The detailed procedure was the same as previously described (14).

RNA Extraction and Real-Time qRT-PCR

Total RNA was extracted from cells or tissues by TRIzol reagent (Invitrogen) and quantified by NanoDrop spectrophotometer. TaqMan miRNA probes (Applied Biosystems, Foster City, CA) were used to quantify the miRNAs. All procedures were performed as previously described (15). And all of the experiments were run in triplicate. The miRNA internal control was U6 small nuclear RNA. After the completion of the reactions, the $2^{-\triangle\triangle CT}$ method was used to compare the relative quantification of each miRNA between every group.

Cell Transfection

All of the miRNA mimics, inhibitors and scrambled negative control used in this research were designed and synthesized by GenePharma (Shanghai, China). The sequence of mature miR-17-5p and miR-4443 are 5'-CAAAGUGCUUACAGUGCAGGUAG-3' and 5'-UUGGAGGCGUGGGUUUU-3', respectively. Lipofectamine 2000 (Invitrogen, USA) was used as the cell transfection reagent and performed according to the manufacturer's instructions.

Cell Proliferation Assay

TE-10 and ECA-109 cells were seeded in the 6-well plate. 6h after transfection, the cells were reseeded to a 96-well plate at a density of 5×10^3 cells per well. A Cell Counting Kit-8 assay (CCK-8) was performed at 0, 24h, 48h, and 72h respectively. The absorbance of the 450nm laser was measured after 2-hour incubation of cells and CCK-8. Each group had at least 5 repeats and all experiments were performed in triplicate.

Cell Migration and Apoptosis Assay

Transwell assay was used to test the cells migration ability. In brief, the transwell chamber with 8μm pore polycarbonate membranes was put into a 24-well plate. A total number of 1×10^5 cells suspended with serum-free RPMI-1640 were added into the upper chamber and 500μl RPMI-1640 with 10% FBS was added to the lower chamber. After 16h incubation, the cells in the upper chamber was wiped with a cotton swab and the cells migrated to the lower surface were fixed with 4% paraformaldehyde and stained with 0.05% crystal violet. The stained cells were then quantified by a spectrophotometer at 3

random areas. The apoptosis of cancer cells was tested by Annexin V-FITC/PI staining kit (BD Biosciences, San Diego, CA, USA). Besides, the total apoptotic cells were counted as the sum of early apoptotic (PI− AV+) and late apoptotic (PI+ AV+) cells.

Luciferase Reporter Assay

The 3′-UTR of human TIMP2 containing putative binding sites was cloned into the p-MIR-REPORT plasmid (Ambion), and efficient insertion was confirmed by sequencing. To test the binding specificity, the sequences in human TIMP2 3′-UTR that interact with miRNA seed sequence were mutated. 293T cells were co-transfected with β-galactosidase (β-gal) expression plasmid (Ambion), a firefly luciferase reporter plasmid, and miRNA mimics or negative control. The β-gal plasmid was used as a transfection control. Luciferase activity was measured 24 h after transfection using a luciferase assay kit (Promega, Madison, WI, USA).

Western Blot Analysis

The expression of TIMP2, as well as internal control GAPDH in cells and tissues, was assessed by western blot analysis. Homogenate tissues and cultured cells were lysed in RIPA buffer containing protease inhibitor cocktail. We used the 10% SDS-PAGE gels to separate the protein lysates, which was then electrically transferred to a polyvinylidene difluoride (PVDF) membranes. The membranes were then blocked by 5% skimmed milk for at least 1h at room temperature and followed on incubating with primary antibody (anti-TIMP2, 1:2000, Abcam, and anti-GAPDH, 1:3000, Abcam). After incubating with their specific second antibody at room temperature for 1h, the membranes were then visualized by ECL (Thermo Scientific, Rockford, USA) detection assay.

Tumor Xenografts in Mice

All animals used in this study were approved by the ethics committee of Jiangsu Cancer Hospital and complied with NIH Guidelines. TE-10 cells were treated with miR-17-5p/miR-4443 overexpressing lentivirus or control lentivirus and were then injected subcutaneously into the inguinal folds of the nude mice at the concentration of 10^6 cells per 0.2ml PBS. 28 days later, the mice were sacrificed and removed the xenografted tumors. The tumors were then measured the volumes and weights and then extracted protein for the TIMP2 expression detection.

Statistical Analysis

All western blot images are representative of at least three independent experiments. Quantitative RT-PCR, luciferase reporter assay, cell proliferation, migration assay and cell apoptosis assay were performed in triplicate, and each experiment was repeated several times. Statistical analysis was calculated by SPSS 16.0. Presented data was carried out by at least 3 separate experiments and showed as mean ± SD. $P<0.05$ was considered statistically significant in this study by using the student's t-test. *P<0.05, **P<0.01, ***P<0.001.

RESULTS

High Expression of miR-17-5p and miR-4443 Was Observed in ESCC Tissue

To explore the significantly expressed miRNAs in ESCC, we first use the high-throughput miRNA sequencing to identify the expression profiles of all miRNAs in the ESCC tissues and paired adjacent normal tissues. As shown in **Figure 1A**, among total 1295 miRNAs, 23 miRNAs were shown to be significantly dysregulated ($P<0.05$ and fold change > 2 or <0.5; 18 miRNAs were up-regulated and 5 miRNAs were down-regulated). We further validated all these 23 miRNAs levels by qRT-PCR in 13 ESCC tissues and their paired adjacent normal tissues (**Figure 1B**). And we found that two miRNAs (miR-17-5p and miR-4443) were stably up-regulated in ESCC (**Figure 1C**). So, the two miRNAs were selected as candicates for further investigation. Then we investigated the association between the two miRNAs expression and various clinicopathological variables in all samples. High correlation between miRNAs and tumor TNM stages was shown in **Figure 1D**, indicating that the two miRNAs signature is closely associated with ESCC progression.

miR-17-5p and miR-4443 Promote Proliferation and Migration, and Inhibit Apoptosis *In Vitro*

To further explore the specific role of miR-17-5p and miR-4443 in the ESCC, we transfected the TE-10 and ECA-109 cells with miRNA mimics, inhibitors, and negative control then checked their effects on tumor behavior. As shown in **Figure 2A**, miR-17-5p or miR-4443 overexpression significantly promoted cell proliferation in both TE-10 and ECA-109, while downregulation showed the opposite effect (**Figure 2B**). In addition, transwell assay showed miR-17-5p and miR-4443 promoted cell migration ability in both cells (**Figures 2C, D**). Also, downregulation of miR-17-5p and miR-4443 reduced cell migration ability (**Figures 2E, F**). In the cell apoptosis assay, the percentage of apoptotic cells was significantly lower in TE-10 cells transfected with miR-17-5p or miR-4443 mimic (**Figure 2G**) and higher in cells transfected with miR-17-5p or miR-4443 inhibitor (**Figure 2H**). Taken together, these results suggest that miR-17-5p and miR-4443 may act as oncomiRs to promote ESCC progression.

TIMP2 Is Identified as a Direct Target Gene to Both miR-17-5p and miR-4443

To identify the direct target genes of miR-17-5p and miR-4443 in ESCC, we used two bioinformatics tools (TargetScan http://www.targetscan.org/vert_72/ and miRDB http://mirdb.org/). Because of miR-17-5p and miR-4443 having a similar effect on ESCC, we hypothesize if they could target the same protein. As shown in **Figure 3A**, TIMP2, the inhibitor of matrix metalloproteinases (MMPs), was considered to be a potential target with a high confidence level among all predicted common targets of miR-17-5p and miR-4443. The predicted site and their interaction

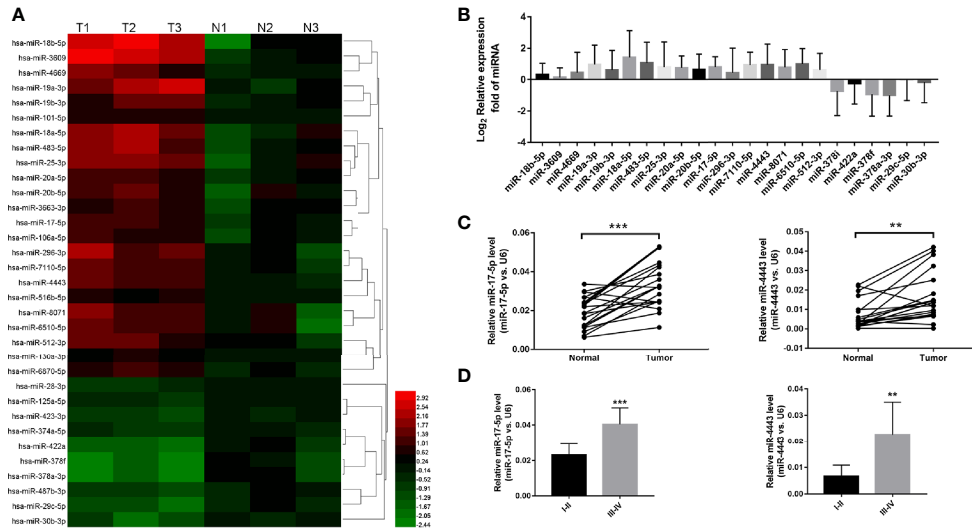

FIGURE 1 | The expression level of miR-17-5p and miR-4443 in ESCC tissues. **(A)** high-throughput miRNA sequencing results. 23 miRNAs were statistically dysregulated, P<0.05, fold change>2 or <0.5. **(B)** Q-PCR analysis of all 23 screened miRNAs in 20 ESCC tissues and normal adjacent tissues. **(C)** Q-PCR analysis of the relative expression levels of miR-17-5p and miR-4443 in 20 pairs tissues. **(D)** The two miRNAs concentrations in different TNM stages (I–IV) of all 20 ESCC tissues. **P < 0.01, ***P < 0.001.

between miR-17-5p, miR-4443 and 3'-UTR of TIMP2 was shown in **Figure 3B**.

miRNAs are known to play their role by inhibiting their target protein. We first investigated whether TIMP2 was down-regulated in ESCC tissues than paired adjacent normal tissues. As shown in **Figures 3C, D**, TIMP2 protein levels was significantly downregulated in ESCC tissues. To further clarify the relationship between miR-17-5p, miR-4443 and TIMP2, we performed a correlation analysis between miR- miR-17-5p, miR-4443 and TIMP2. According to the results, both the expression levels of miR-17-5p, miR-4443 are significantly and negatively correlated with TIMP2 protein level (**Figures 3E, F**). Moreover, in TE-10 cells, transfection of mimics-miR-17-5p or mimics-miR-4443-5p significantly inhibit TIMP2 expression, while downregulation of miR-17-5p or miR-4443 expression showed increased expression of TIMP2 (**Figure 3G**). These results were further verified in ECA-109 cells (**Figure 3H**).

To further confirm whether miR-17-5p and miR-4443 could directly target the predicted binding sites in the 3'-UTR of TIMP2, we performed luciferase reporter assays. The presumed binding sites of TIMP2 3'-UTR was designed to be inserted into a reporter plasmid which has a downstream firefly luciferase gene. We next transfected this recombined plasmid into 293T cells together with miRNA mimics or antisenses. As expected, transfection of mimics-miR-17-5p and mimics-miR-4443 significantly reduced the luciferase activity in A549 cells, while transfection their antisenses induced an increase in reporter activity (**Figure 3I**). Furthermore, we mutated the predicted binding sites in TIMP2 3'-UTR of both miRNAs and the luciferase activity resulting in not changing after either miRNAs overexpression. Thus, the results indicated that TIMP2 mRNA was the direct target of miR-17-5p and miR-4443.

TIMP2 Attenuates the Effects of the miR-17-5p and miR-4443 in ESCC Cells

To test whether miR-17-5p and miR-4443 may suppress TIMP2 expression to affect cell proliferation, apoptosis and invasion, we transfected TE-10 cells with both mixture of mimic-miR-17-5p and mimic-miR-4443 and a plasmid designed to specially express the full-length ORF of TIMP2 without the miR-17-5p and miR-4443–responsive 3′-UTR. Proliferation, apoptosis and invasion assays revealed that ectopic expression of TIMP2 dramatically attenuated the inhibitory effect of the miR-17-5p and miR-4443 on cell apoptosis, and stimulatory effect on cell proliferation an invasion (**Figures 4A–C**).

miR-17-5p and miR-4443 Promote ESCC Progression *In Vivo*

We next investigated whether miR-17-5p and miR-4443 has an influence on tumor growth *in vivo*. TE-10 cells were pretreated with miR-17-5p lentivirus, miR-4443 lentivirus or control lentivirus. These pretreated cells were subcutaneously injected into the inguinal folds of the nude mice. The flowchart of the whole experiment was shown in **Figure 5A**. 28 days after the implantation, the implanted tumors were completely harvested and measured the weight and diameter. As shown in **Figures 5B, C**, miR-17-5p and miR-4443 overexpression group have a relatively high rate of tumor growth comparing to the control group. We then examined the effect of miR-17-5p and miR-4443 on TIMP2 expression and ESCC malignancy. QRT-PCR and Western blot shows that the

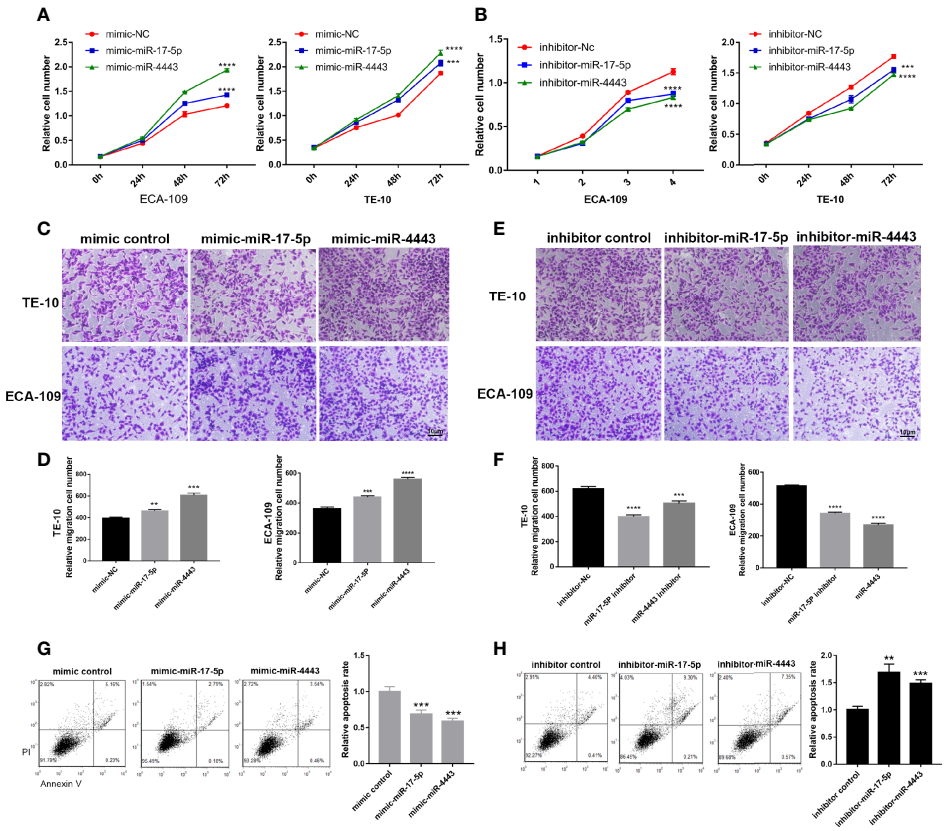

FIGURE 2 | Effect of miR-17-5p and miR-4443 in the regulation of proliferation and migration of ESCC cells. **(A, B)** CCK8 assays were performed at 0h, 24h, 48h and 72h after the transfection of the ECA-109 cells and TE-10 cells with mimic-NC, mimic-miR-17-5p, mimic-miR-4443, inhibitor-NC, inhibitor-miR-17-5p and inhibitor-miR-4443. **(C, D)** Transwell analysis of the migration rate of ECA-109 and TE-10 cells transfected with an equal dose of mimic-NC, mimic-miR-17-5p, mimic-miR-4443. **(C)**, representative image; **(D)**, quantitative analysis. **(E, F)** Transwell analysis of the migration rate of ECA-109 and TE-10 cells transfected with equal dose of inhibitor-NC, inhibitor-miR-17-5p and inhibitor-miR-4443. **(E)**, representative image; **(F)**, quantitative analysis. **(G, H)** Analysis of apoptosis in TE-10 cells treated with mimic control, mimic-miR-17-5p, mimic-miR-4443, inhibitor control, inhibitor-miR-17-5p and inhibitor-miR-4443. The total apoptotic cells were counted as the sum of early apoptotic (PI– AV+) and late apoptotic (PI+ AV+) cells (left: representative image; right: quantitative analysis). **P < 0.01, ***P < 0.001, ****P < 0.0001.

overexpression of miR-17-5p and miR-4443 significantly down-regulated TIMP2 expression in xenografted tumor tissues (**Figures 5D, E**). These tumor tissues were then embedded in paraffin for H&E staining and immunohistochemical examination. H&E staining showed increased mitosis ratio in both miR-17-5p and miR-4443 overexpressing group compared to control group (**Figure 5F**). As shown in **Figures 5F-H**, higher level of miR-17-5p or miR-4443 resulted in decreased TIMP2 level and higher Ki-67 level. Taken together, these results further confirmed that miR-17-5p and miR-4443 acted as oncomiRs to regulate the progression of ESCC cells by targeting TIMP2.

DISCUSSION

Esophagus cancer is one of the most lethiferous malignant tumors all over the world, especially in East Asia like China. ESCC accounts for most of the EC patients. With the advancement of diagnostic techniques and the development of surgery as well as the application of molecular targeted drug and immunotherapy, the survival rate of ESCC patients has been greatly extended. However, the specific mechanism of the development of ESCC remains unknown. The quality of life of ESCC patients will seriously be degraded if tumor recurrence occurred. Current clinical treatment lacks effective therapy to inhibit metastasis. Our research provides a new potential way to inhibit ESCC metastasis.

Recent studies have shown the importance of miRNA in carcinogenesis and cancer development. For example, miR-148a might play its oncogenic role by targeting AVR1 in ESCC (16). miR-1224-5p inhibits tumor progression by targeting the TNS4/EGFR axis (17). There are also several types of research confirmed the oncogenetic roles of miR-17-5p. For example, in pancreatic cancer miR-17-5p enhance its proliferation by disrupting RBL2/E2F2-repressing complexes (13). And

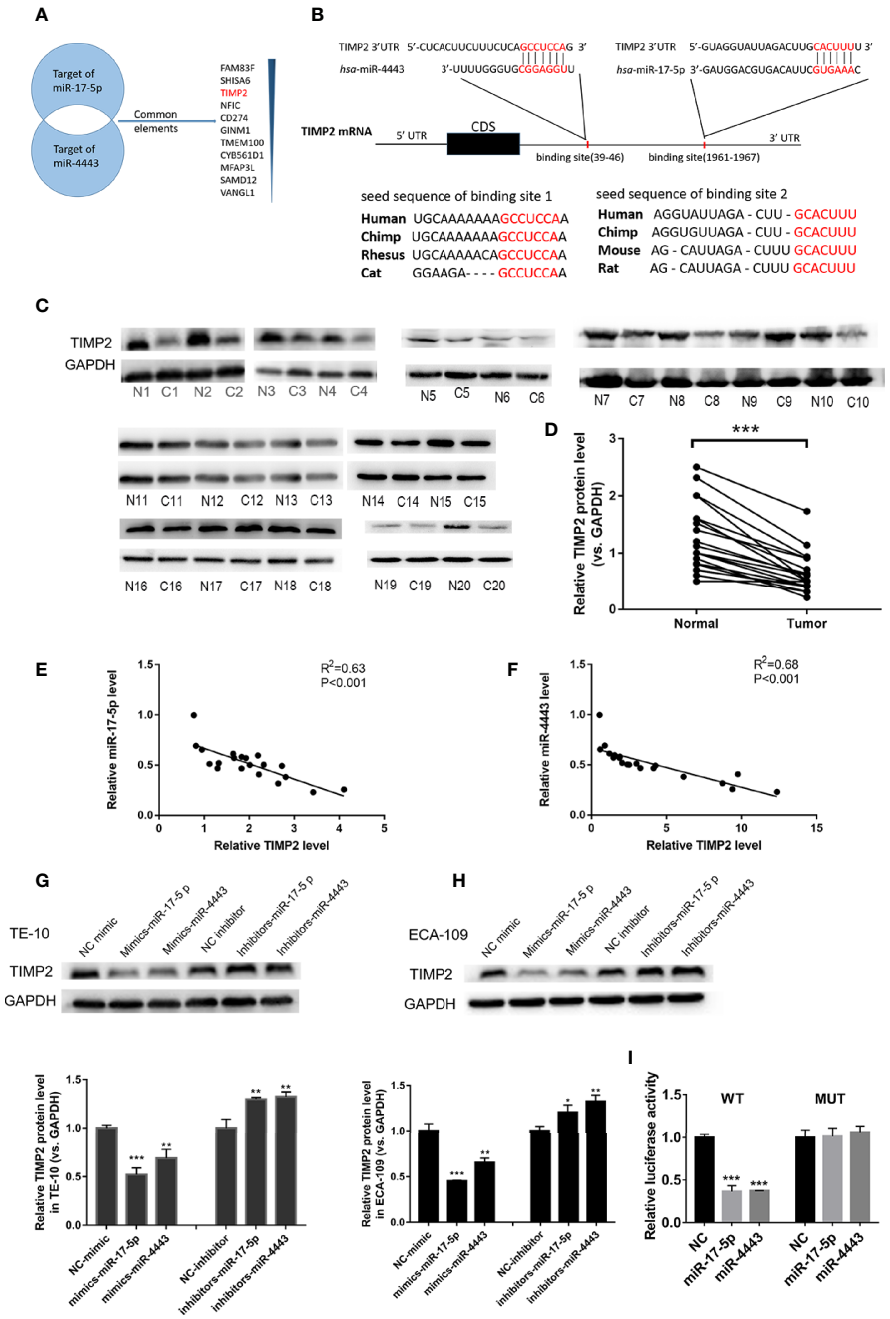

FIGURE 3 | TIMP2 is the target of miR-17-5p and miR-4443 in ESCC cells. **(A)** The common targets of miR-4443 and miR-17-5p. All targets are predicted by two bioinformatics tools and the common targets are arranged by the confidence level. **(B)** Graphic description of the base-pairing interaction between miR-17-5p, miR-4443 and TIMP2 3'UTR and their exact position in the TIMP2 mRNA. **(C)** Western blot analysis of TIMP2 in 20 pairs of ESCC tissues. (N=Normal, C=Cancer). **(D)** Quantification of TIMP2 levels in ESCC tissues. **(E, F)** Pearson's correlation scatter plot of the fold changes of miR-17-5p, miR-4443 and TIMP2 protein ESCC tissues. **(G, H)** The effect of transfection of inhibitor-miR or mimic-miR or their negative control on the expression of TIMP2 in two cell lines, TE-10 **(G)** and ECA-109 **(H)**. **(I)** Dual luciferase activity assay was used to detect the binding affinity between miR-17-5p, miR-4443 and TIMP2. All results were shown as mean ± SD (n = 3). *p < 0.05, **P < 0.01, ***P < 0.001.

miR-17-5p can modulate NF-κB signaling in gastric cancer (18). Although there are few researches showed the opposite role of miR-17-5p in certain cancers (12, 19), it is reported that miR-17-5p can serve as prognostic indicators in ESCC (20). But the exact mechanism of miR-17-5p in ESCC remains unclear. miR-4443 is a rarely studied miRNA. It showed an oncogenetic role in breast cancer (21) and non-small cell lung cancer (10), and showed an opposite effect in ovarian cancer

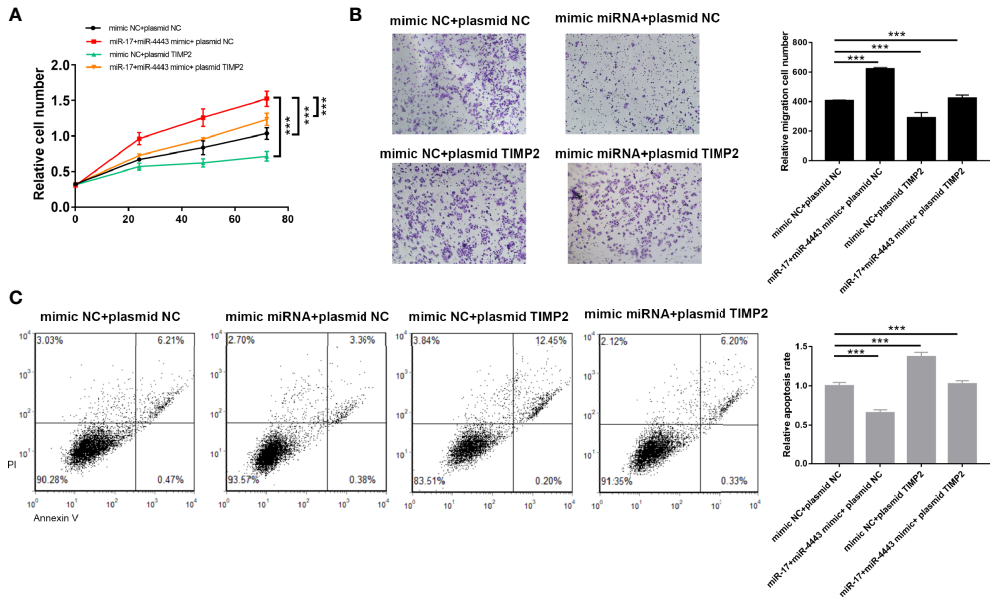

FIGURE 4 | TIMP2 attenuates the effects of the miR-17-5p and miR-4443 in ESCC cells. **(A)** Analysis of proliferation **(A)**, migration **(B)** and apoptosis **(C)** in TE-10 cells treated with mimic-control plus plasmid control, mimic-miR-17-5p and mimic-miR-4443 mixture plus control vector, mimic-control plus TIMP2 plasmid, or mimic-miR-17-5p and mimic-miR-4443 mixture plus HIC1 TIMP2 plasmid. All results were shown as mean ± SD (n = 3). ***P < 0.001.

(22) and colon cancer (23). There is no research about miR-4443 in ESCC has been reported yet. In our study, we demonstrated that miR-17-5p and miR-4443 are stably up-regulated in ESCC tissues than in adjacent non-carcinoma tissues among all up-regulated miRNAs in the high-throughput miRNA sequencing. Both *in vitro* and *in vivo* experiments demonstrated the tumor-promoting effect of miR-17-5p and miR-4443 in ESCC. Because of the similar effect of miR-17-5p and miR-4443, we hypothesized that they may target the same protein. Then two independent bioinformatic tools were used to predict the potential target of the two miRNAs we studied. 11 genes were predicted to be targeted by both miR-17-5p and miR-4443. Among them, TIMP2, the inhibitor of matrix metalloproteinases (MMPs), was considered to be a potential target due to the known functions in cell proliferation and migration. Other target genes may also contribute to the effect of miR-17-5p and miR-4443 in ESCC cells. Among all results, TIMP2 was experimentally validated to be down-regulated by both of the miRNAs. Clinical ESCC tissues also showed lower expression of TIMP2 than adjacent non-carcinoma tissues. These results suggested that TIMP2 may serve as a tumor suppressor and be down-regulated during tumorigenesis, as has been shown by other researches (24–27). And targeting miR-17-5p and miR-4443 may be a potential therapy to control ESCC development. In the future, the mechanism of the up-regulation of miR-17-5p and miR-4443 in the ESCC patients need further studying.

TIMP2 (tissue inhibitor of metallopeptidase-2) is a member of the tissue inhibitor of metallopeptidases (TIMPs). The metastasis of cancer cells should invade into the extracellular matrix (ECM) firstly, and matrix metalloproteinases (MMPs) are essential and play core effect to degrade the ECM, paving a road for tumor cells to migrate into cycle system for distant metastasis (28). On the other hand, TIMPs, the inhibitor of MMPs, can reduce the degradation of ECM and therefore inhibit the invade of the primary tumor cells. There have been identified 4 members in the TIMP family (TIMP1-4) with different effects against different MMPs (29). TIMP2 has been reported to regulate the activity of MMP-2 (30), a significant factor to promote collagen degradation and lead to cancer cells' dissemination (31). Researchers have found that MMP-2 is over-expressed in ESCC tumor tissues (32), and TIMP2 is down-regulated in both tissues and serum (33). Our research indicates that miR-17-5p and miR-4443 may be the reason and play a critical role to break the dynamic balance between TIMP2 and MMP-2 during ESCC development.

Taken together, our research demonstrated that miR-17-5p and miR-4443 are significantly upregulated in ESCC tissues, and serve as a tumor promoter by directly targeting TIMP2. Ectopic expression of miR-17-5p and miR-4443 may be one of the reasons for the up-regulation of MMP-2 in ESCC tissues. And the unbalanced state between TIMP2 and MMP-2 promote ESCC development and distant metastasis. Our research develops a new approach for understanding ESCC development and miR-17-5p and miR-4443 may serve as a potential target for ESCC therapy in future.

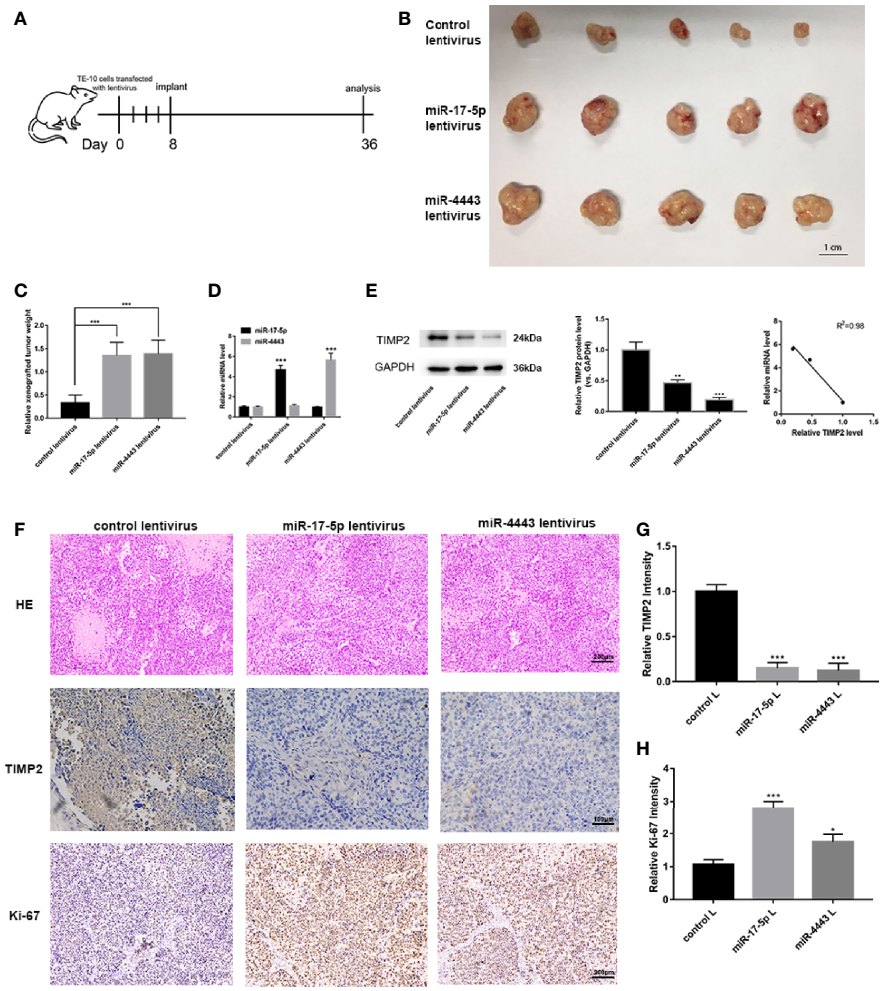

FIGURE 5 | *In vivo* experiments to verify the effects of miR-17-5p and miR-4443 on ESCC cells. **(A)** The flow chart of the whole *in vivo* experiments. **(B)** The morphology of the isolated tumors in each group (n = 5). **(C)** Quantitative analysis of the xenografted tumor weight. **(D, E)** qRT-PCR analysis of miR-17-5p/4443 **(D)** and western blot analysis of TIMP2 expression **(E)**, left and middle) in each group and their quantification; Pearson's correlation scatter plot of the fold changes of miR-17-5p, miR-4443 and TIMP2 protein tumor tissues. **(F)** HE staining and immunohistochemical analyses of Ki-67 and TIMP2 in primary tumors (n = 5) derived from the different groups. **(G, H)** Quantification of Ki-67 and TIMP2 intensity in figure. All data are represented as mean ± SD. *P < 0.05, ***P < 0.001.

DATA AVAILABILITY STATEMENT

The original contributions presented in the study are included in the article/**Supplementary Material**, further inquiries can be directed to the corresponding authors.

ETHICS STATEMENT

The studies involving human participants were reviewed and approved by Ethics Committee of the Jiangsu Cancer Hospital. The patients/participants provided their written informed consent to participate in this study. The animal study was reviewed and approved by Ethics Committee of the Jiangsu Cancer Hospital.

AUTHOR CONTRIBUTIONS

XC and LX planned the study. XW, JYH, and YL carried out the experiments. JWH and ML performed the data analysis and helped to draft the manuscript. XW wrote the manuscript. All authors contributed to the article and approved the submitted version.

SUPPLEMENTARY MATERIAL

The Supplementary Material for this article can be found online at: https://www.frontiersin.org/articles/10.3389/fonc.2021.605894/full#supplementary-material

Supplementary Table 1 | Raw microRNA array data.

REFERENCES

1. Bray F, et al. Global Cancer Statistics 2018: GLOBOCAN Estimates of Incidence and Mortality Worldwide for 36 Cancers in 185 Countries. *CA Cancer J Clin* (2018) 68:394–424. doi: 10.3322/caac.21492
2. Chen JG, Chen HZ, Zhu J, Yang YL, Zhang YH, Huang PX, et al. Cancer Survival in Patients From a Hospital-Based Cancer Registry, China. *J Cancer* (2018) 9:851–60. doi: 10.7150/jca.23039
3. Schickel R, Boyerinas B, Park SM, Peter ME. MicroRNAs: Key Players in the Immune System, Differentiation, Tumorigenesis and Cell Death. *Oncogene* (2008) 27:5959–74. doi: 10.1038/onc.2008.274
4. Jang HJ, Lee HS, Burt BM, Lee GK, Yoon KA, Park YY, et al. Integrated Genomic Analysis of Recurrence-Associated Small non-Coding RNAs in Oesophageal Cancer. *Gut* (2017) 66:215–25. doi: 10.1136/gutjnl-2015-311238
5. Li HL, Bian CJ, Liao LM, Li J, Zhao RC. miR-17-5p Promotes Human Breast Cancer Cell Migration and Invasion Through Suppression of HBP1. *Breast Cancer Res Treat* (2011) 126:565–75. doi: 10.1007/s10549-010-0954-4
6. Yang XL, Du WW, Li HR, Liu FQ, Khorshidi A, Rutnam ZJ, et al. Both Mature miR-17-5p and Passenger Strand miR-17-3p Target TIMP3 and Induce Prostate Tumor Growth and Invasion. *Nucleic Acids Res* (2013) 41:9688–704. doi: 10.1093/nar/gkt680
7. Shan SW, Fang L, Shatseva T, Rutnam ZJ, Yang XL, Du WW, et al. Mature miR-17-5p and Passenger miR-17-3p Induce Hepatocellular Carcinoma by Targeting PTEN, GalNT7 and Vimentin in Different Signal Pathways. *J Cell Sci* (2013) 126:1517–30. doi: 10.1242/jcs.122895
8. Yu J, Ohuchida K, Mizumoto K, Fujita H, Nakata K, Tanaka M. MicroRNA miR-17-5p is Overexpressed in Pancreatic Cancer, Associated With a Poor Prognosis and Involved in Cancer Cell Proliferation and Invasion. *Cancer Biol Ther* (2010) 10:748–57. doi: 10.4161/cbt.10.8.13083
9. Li XS, Zhang ZC, Yu M, Li LQ, Du GS, Xiao WD, et al. Involvement of miR-20a in Promoting Gastric Cancer Progression by Targeting Early Growth Response 2 (Egr2). *Int J Mol Sci* (2013) 14:16226–39. doi: 10.3390/ijms140816226
10. Zhang WG, Qiao B, Fan JL. Overexpression of miR-4443 Promotes the Resistance of non-Small Cell Lung Cancer Cells to Epirubicin by Targeting INPP4A and Regulating the Activation of JAK2/STAT3 Pathway. *Pharmazie* (2018) 73:386–92. doi: 10.1691/ph.2018.8313
11. Wang J, Wang J, Gu Q, Yang Y, Ma Y, Zhu J, et al. MiR-4443 Promotes Migration and Invasion of Breast Cancer Cells by Inhibiting PEBP1 Expression. *Nan Fang Yi Ke Da Xue Xue Bao = J South Med Univ* (2020) 40:1712–9. doi: 10.12122/j.issn.1673-4254.2020.12.03
12. Li J, Lai Y, Ma J, Liu Y, Bi J, Zhang L, et al. miR-17-5p Suppresses Cell Proliferation and Invasion by Targeting ETV1 in Triple-Negative Breast Cancer. *BMC Cancer* (2017) 17:745. doi: 10.1186/s12885-017-3674-x
13. Zhu Y, Gu J, Li Y, Peng C, Shi M, Wang X, et al. MiR-17-5p Enhances Pancreatic Cancer Proliferation by Altering Cell Cycle Profiles *via* Disruption of RBL2/E2F4-Repressing Complexes. *Cancer Lett* (2018) 412:59–68. doi: 10.1016/j.canlet.2017.09.044
14. Chen T, Wang C, Yu H, Ding M, Zhang C, Lu X, et al. Increased Urinary Exosomal microRNAs in Children With Idiopathic Nephrotic Syndrome. *EBioMedicine* (2019) 39:552–61. doi: 10.1016/j.ebiom.2018.11.018
15. Zhang H, Deng T, Liu R, Bai M, Zhou L, Wang X, et al. Exosome-Delivered EGFR Regulates Liver Microenvironment to Promote Gastric Cancer Liver Metastasis. *Nat Commun* (2017) 8:15016. doi: 10.1038/ncomms15016
16. Tan Y, Lu X, Cheng Z, Pan G, Liu S, Apiziaji P, et al. miR-148a Regulates the Stem Cell-Like Side Populations Distribution by Affecting the Expression of ACVR1 in Esophageal Squamous Cell Carcinoma. *Onco Targets Ther* (2020) 13:8079–94. doi: 10.2147/OTT.S248925
17. Shi ZZ, Wang WJ, Chen YX, Fan ZW, Xie XF, Yang LY, et al. The miR-1224-5p/TNS4/EGFR Axis Inhibits Tumour Progression in Oesophageal Squamous Cell Carcinoma. *Cell Death Dis* (2020) 11:597. doi: 10.1038/s41419-020-02801-6
18. Liu F, Cheng L, Xu J, Guo F, Chen W. miR-17-92 Functions as an Oncogene and Modulates NF-kappaB Signaling by Targeting TRAF3 in MGC-803 Human Gastric Cancer Cells. *Int J Oncol* (2018) 53:2241–57. doi: 10.3892/ijo.2018.4543
19. Gong C, Yang Z, Wu F, Han L, Liu Y, Gong W. miR-17 Inhibits Ovarian Cancer Cell Peritoneal Metastasis by Targeting ITGA5 and ITGB1. *Oncol Rep* (2016) 36:2177–83. doi: 10.3892/or.2016.4985
20. Xu XL, Jiang YH, Feng JG, Su D, Chen PC, Mao WM. MicroRNA-17, microRNA-18a, and microRNA-19a are Prognostic Indicators in Esophageal Squamous Cell Carcinoma. *Ann Thorac Surg* (2014) 97:1037–45. doi: 10.1016/j.athoracsur.2013.10.042
21. Chen X, Zhong SL, Lu P, Wang DD, Zhou SY, Yang SJ, et al. miR-4443 Participates in the Malignancy of Breast Cancer. *PloS One* (2016) 11:e0160780. doi: 10.1371/journal.pone.0160780
22. Ebrahimi SO, Reiisi S. Downregulation of miR-4443 and miR-5195-3p in Ovarian Cancer Tissue Contributes to Metastasis and Tumorigenesis. *Arch Gynecol Obstet* (2019) 299:1453–8. doi: 10.1007/s00404-019-05107-x
23. Meerson A, Yehuda H. Leptin and Insulin Up-Regulate miR-4443 to Suppress NCOA1 and TRAF4, and Decrease the Invasiveness of Human Colon Cancer Cells. *BMC Cancer* (2016) 16:882. doi: 10.1186/s12885-016-2938-1
24. Kai AK, Chan LK, Lo RC, Lee JM, Wong CC, Wong JC, et al. Down-Regulation of TIMP2 by HIF-1alpha/miR-210/HIF-3alpha Regulatory Feedback Circuit Enhances Cancer Metastasis in Hepatocellular Carcinoma. *Hepatology* (2016) 64:473–87. doi: 10.1002/hep.28577
25. Yi X, Guo J, Guo J, Sun S, Yang P, Wang J, et al. EZH2-Mediated Epigenetic Silencing of TIMP2 Promotes Ovarian Cancer Migration and Invasion. *Sci Rep* (2017) 7:3568. doi: 10.1038/s41598-017-03362-z
26. Zhu M, Zhang N, He S, Lui Y, Lu G, Zhao L. MicroRNA-106a Targets TIMP2 to Regulate Invasion and Metastasis of Gastric Cancer. *FEBS Lett* (2014) 588:600–7. doi: 10.1016/j.febslet.2013.12.028
27. Guan H, Li W, Li Y, Wang J, Li Y, Tang Y, et al. MicroRNA-93 Promotes Proliferation and Metastasis of Gastric Cancer *via* Targeting TIMP2. *PloS One* (2017) 12:e0189490. doi: 10.1371/journal.pone.0189490
28. Stetler-Stevenson WG. Tissue Inhibitors of Metalloproteinases in Cell Signaling: Metalloproteinase-Independent Biological Activities. *Sci Signal* (2008) 1:re6. doi: 10.1126/scisignal.127re6
29. Stetler-Stevenson WG. The Tumor Microenvironment: Regulation by MMP-Independent Effects of Tissue Inhibitor of Metalloproteinases-2. *Cancer Metastasis Rev* (2008) 27:57–66. doi: 10.1007/s10555-007-9105-8
30. Bourboulia D, Stetler-Stevenson WG. Matrix Metalloproteinases (MMPs) and Tissue Inhibitors of Metalloproteinases (TIMPs): Positive and Negative Regulators in Tumor Cell Adhesion. *Semin Cancer Biol* (2010) 20:161–8. doi: 10.1016/j.semcancer.2010.05.002
31. Brooks PC, Stromblad S, Sanders LC, von Schalscha TL, Aimes RT, Stetler-Stevenson WG, et al. Localization of Matrix Metalloproteinase MMP-2 to the Surface of Invasive Cells by Interaction With Integrin Alpha V Beta 3. *Cell* (1996) 85:683–93. doi: 10.1016/S0092-8674(00)81235-0
32. Li Y, Ma J, Guo Q, Duan F, Tang F, Zheng P, et al. Overexpression of MMP-2 and MMP-9 in Esophageal Squamous Cell Carcinoma. *Dis Esophagus* (2009) 22:664–7. doi: 10.1111/j.1442-2050.2008.00928.x
33. Groblewska M, Mroczko B, Kozlowski M, Niklinski J, Laudanski J, Szmitkowski M, et al. Serum Matrix Metalloproteinase 2 and Tissue Inhibitor of Matrix Metalloproteinases 2 in Esophageal Cancer Patients. *Folia Histochem Cytobiol* (2012) 50:590–8. doi: 10.5603/20327

Conflict of Interest: The reviewers YW and YX declared a shared affiliation with author XC, to the handling editor at time of review.

The remaining authors declare that the research was conducted in the absence of any commercial or financial relationships that could be construed as a potential conflict of interest.

Publisher's Note: All claims expressed in this article are solely those of the authors and do not necessarily represent those of their affiliated organizations, or those of the publisher, the editors and the reviewers. Any product that may be evaluated in this article, or claim that may be made by its manufacturer, is not guaranteed or endorsed by the publisher.

Advantages of publishing in Frontiers

OPEN ACCESS
Articles are free to read for greatest visibility and readership

FAST PUBLICATION
Around 90 days from submission to decision

HIGH QUALITY PEER-REVIEW
Rigorous, collaborative, and constructive peer-review

TRANSPARENT PEER-REVIEW
Editors and reviewers acknowledged by name on published articles

Frontiers
Avenue du Tribunal-Fédéral 34
1005 Lausanne | Switzerland

Visit us: www.frontiersin.org
Contact us: frontiersin.org/about/contact

REPRODUCIBILITY OF RESEARCH
Support open data and methods to enhance research reproducibility

DIGITAL PUBLISHING
Articles designed for optimal readership across devices

FOLLOW US
@frontiersin

IMPACT METRICS
Advanced article metrics track visibility across digital media

EXTENSIVE PROMOTION
Marketing and promotion of impactful research

LOOP RESEARCH NETWORK
Our network increases your article's readership